frontiers | Research Topics

Altered expression of proteins in cancer: Function and potential therapeutic targets, volume II

Edited by
João Pessoa, Maria Teresa Valenti, Tamrat Abebe Zeleke, Lorenzo Gerratana, Paula Chiarella, Julia Kzhyshkowska, Carlos Pérez-Plasencia and Nadège Bellance

Published in
Frontiers in Oncology

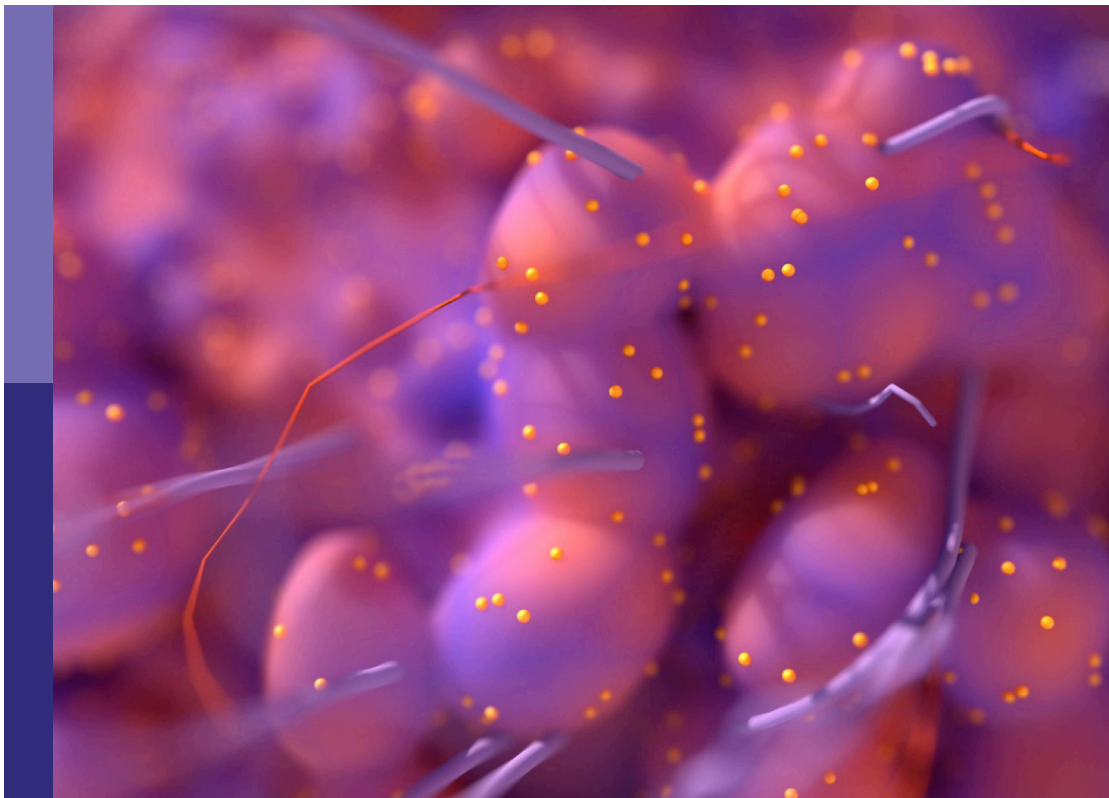

ISSN 1664-8714
ISBN 978-2-8325-3144-0
DOI 10.3389/978-2-8325-3144-0

About Frontiers

Frontiers is more than just an open access publisher of scholarly articles: it is a pioneering approach to the world of academia, radically improving the way scholarly research is managed. The grand vision of Frontiers is a world where all people have an equal opportunity to seek, share and generate knowledge. Frontiers provides immediate and permanent online open access to all its publications, but this alone is not enough to realize our grand goals.

Frontiers journal series

The Frontiers journal series is a multi-tier and interdisciplinary set of open-access, online journals, promising a paradigm shift from the current review, selection and dissemination processes in academic publishing. All Frontiers journals are driven by researchers for researchers; therefore, they constitute a service to the scholarly community. At the same time, the *Frontiers journal series* operates on a revolutionary invention, the tiered publishing system, initially addressing specific communities of scholars, and gradually climbing up to broader public understanding, thus serving the interests of the lay society, too.

Dedication to quality

Each Frontiers article is a landmark of the highest quality, thanks to genuinely collaborative interactions between authors and review editors, who include some of the world's best academicians. Research must be certified by peers before entering a stream of knowledge that may eventually reach the public - and shape society; therefore, Frontiers only applies the most rigorous and unbiased reviews. Frontiers revolutionizes research publishing by freely delivering the most outstanding research, evaluated with no bias from both the academic and social point of view. By applying the most advanced information technologies, Frontiers is catapulting scholarly publishing into a new generation.

What are Frontiers Research Topics?

Frontiers Research Topics are very popular trademarks of the *Frontiers journals series*: they are collections of at least ten articles, all centered on a particular subject. With their unique mix of varied contributions from Original Research to Review Articles, Frontiers Research Topics unify the most influential researchers, the latest key findings and historical advances in a hot research area.

Find out more on how to host your own Frontiers Research Topic or contribute to one as an author by contacting the Frontiers editorial office: frontiersin.org/about/contact

Altered expression of proteins in cancer: Function and potential therapeutic targets, volume II

Topic editors

João Pessoa — University of Coimbra, Portugal
Maria Teresa Valenti — University of Verona, Italy
Tamrat Abebe Zeleke — Addis Ababa University, Ethiopia
Lorenzo Gerratana — University of Udine, Italy
Paula Chiarella — Instituto de Medicina Experimental del CONICET, Academia Nacional de Medicina, Argentina
Julia Kzhyshkowska — Heidelberg University, Germany
Carlos Pérez-Plasencia — National Autonomous University of Mexico, Mexico
Nadège Bellance — Université de Bordeaux, France

Citation

Pessoa, J., Valenti, M. T., Zeleke, T. A., Gerratana, L., Chiarella, P., Kzhyshkowska, J., Pérez-Plasencia, C., Bellance, N., eds. (2023). *Altered expression of proteins in cancer: Function and potential therapeutic targets, volume II*. Lausanne: Frontiers Media SA. doi: 10.3389/978-2-8325-3144-0

Table of contents

frontiers | Frontiers in Oncology

TYPE Editorial
PUBLISHED 18 July 2023
DOI 10.3389/fonc.2023.1242855

OPEN ACCESS

EDITED AND REVIEWED BY
Luisa Lanfrancone,
European Institute of Oncology (IEO), Italy

*CORRESPONDENCE
João Pessoa
joao.pessoa@cnc.uc.pt

RECEIVED 19 June 2023
ACCEPTED 29 June 2023
PUBLISHED 18 July 2023

CITATION
Pessoa J, Valenti MT, Bellance N, Chiarella P, Abebe T, Gerratana L, Pérez-Plasencia C and Kzhyshkowska J (2023) Editorial: Altered expression of proteins in cancer: function and potential therapeutic targets, volume II. *Front. Oncol.* 13:1242855. doi: 10.3389/fonc.2023.1242855

Editorial: Altered expression of proteins in cancer: function and potential therapeutic targets, volume II

João Pessoa[1,2]*, Maria Teresa Valenti[3], Nadège Bellance[4], Paula Chiarella[5], Tamrat Abebe[6], Lorenzo Gerratana[7], Carlos Pérez-Plasencia[8,9] and Julia Kzhyshkowska[10,11,12,13]

[1]CNC - Center for Neuroscience and Cell Biology, University of Coimbra, Coimbra, Portugal, [2]CIBB - Center for Innovative Biomedicine and Biotechnology, University of Coimbra, Coimbra, Portugal, [3]Department of Neurosciences, Biomedicine and Movement Sciences, University of Verona, Verona, Italy, [4]INSERM U1211, Rare Diseases: Genetic and Metabolism, University of Bordeaux, Bordeaux, France, [5]Department of Experimental Oncology, Instituto de Medicina Experimental, Academia Nacional de Medicina de Buenos Aires, Ciudad Autónima de Buenos Aires, Argentina, [6]Department of Microbiology, Immunology and Parasitology, School of Medicine, Addis Ababa University, Addis Ababa, Ethiopia, [7]Department of Medical Oncology, CRO Aviano, National Cancer Institute, IRCCS, Aviano, Italy, [8]Laboratorio de Genómica, Instituto Nacional de Cancerología, Tlalpan, Mexico, [9]Laboratorio de Genómica Funcional, Unidad de Biomedicina, FES-IZTACALA, Universidad Nacional Autónoma de México, Tlalnepantla, Mexico, [10]Institute of Transfusion Medicine and Immunology, Mannheim Institute for Innate Immunosciences (MI3), Medical Faculty Mannheim, Heidelberg University, Mannheim, Germany, [11]German Red Cross Blood Service Baden-Württemberg – Hessen, Mannheim, Germany, [12]Laboratory for Translational Cellular and Molecular Biomedicine, Tomsk State University, Tomsk, Russia, [13]Laboratory for Gene Technology, Siberian State Medical University, Tomsk, Russia

KEYWORDS

cancer, protein expression levels, up-regulation, down-regulation, therapeutic target

Editorial on the Research Topic
Altered expression of proteins in cancer: function and potential therapeutic targets, volume II

Introduction

Cancer cells and cells of the tumor microenvironment (TME) show extensive biochemical alterations, which provide multiple opportunities for developing innovative strategies for diagnosis, therapy, and prognosis. The disrupted metabolism of cancer cells (1) and immune cells of the TME (2) is controlled by several protein families. As such, it is not surprising that many of them have their cellular levels significantly increased or decreased. In the first volume of the Research Topic "*Altered expression of proteins in cancer: function and potential therapeutic targets*", we provided an update on proteins whose cellular levels are altered in cancer, highlighting their promise for diagnosis and therapy. The second volume of this Research Topic complements the first one. It contains 9 original research articles and 5 review articles. In the following sections, we summarize the main concepts and findings of these studies, grouped according to the main physiological or pathological role of each protein.

Gene expression

Proteins with altered cellular levels in cancer cells include those regulating gene expression. In prostate cancer, Yang et al. investigated the interactions of the competitive endogenous RNA regulatory network associated with the forkhead box A1 transcription factor. Its up-regulation correlated with the down-regulation of the dual specificity phosphatase 2 (DUSP2). DUSP2 overexpression reduced cell proliferation and migration. Alterations in gene expression can cross-talk with environmental factors, including hypoxia (decreased oxygen availability) (3). Guo et al. reviewed the mechanistic interactions between the hypoxic response and the Notch signaling pathways, proposing a combinatorial therapeutic strategy targeting both pathways. Depending on the cancer type, the Notch pathway can be oncogenic or tumor-suppressive. Gene expression can also be influenced by nuclear pore proteins, the nucleoporins. Singh et al. demonstrated that the Nup88 and Nup62 nucleoporins were up-regulated in head and neck cancer samples and cell lines. Nup88 was stabilized by Nup62 and enhanced cell proliferation, through gene expression alterations mediated by the NF-κB transcription factor.

These studies exemplify the multiple direct and indirect players involved in gene expression and their complex regulation, whose disruption in cancer cells affects the levels of messenger RNA (mRNA) and translated proteins.

Protein phosphorylation and degradation

Cellular levels of functional proteins are also determined by the equilibrium between their phosphorylation and degradation. These processes, also governed by proteins, can be disrupted in cancer cells. Pidkovka and Belkhiri reviewed the impact of the up-regulated transmembrane AXL receptor tyrosine kinase in gastrointestinal cancers and its potential role as a therapeutic target. Inhibition of this protein with small molecules or antibodies is currently being investigated in several clinical trials. In addition, Tang et al. reviewed the relevance of intracellular non-receptor protein tyrosine phosphatases across multiple cancer histologies. Some of these proteins seem to play a dual role in specific cancer types. They are also emerging as targets for immunotherapy and specific inhibitors have shown promising activity. Alterations in protein degradation levels are also found in cancer cells (4). Zhou et al. demonstrated the impact and suggested the therapeutic role of up-regulated MMP1 zinc-dependent endopeptidase in the progression and dedifferentiation of papillary thyroid cancer into poorly differentiated or anaplastic thyroid cancer. Another essential proteolytic mechanism disrupted in cancer involves ubiquitin ligation, which targets proteins for proteasomal degradation (5). Guo et al. reviewed the dual role of tripartite motif 31 (an E3 ubiquitin ligase) in different cancer types. Its oncogenic or tumor-suppressive roles (depending on the histology) could result from differential cellular levels in its isoforms that could be involved in different functions. In addition, Jin et al. demonstrated that the ubiquitin-specific peptidase 20 (a deubiquitinating enzyme) was down-regulated in colorectal cancer. Nevertheless, inducing its overexpression in representative cell lines increased cell migration and invasion, suggesting a potential therapeutic strategy.

These studies confirm that proteostasis is deregulated in cancer cells. The same regulatory protein can be oncogenic or tumor-suppressive across cancer types, underlining the complexity of these regulatory mechanisms.

Cell division and apoptosis

Altered protein levels can change cell homeostasis through several processes, including cell division and programmed cell death. One of the critical stages in cell division is chromosome segregation during the anaphase stage of mitosis, in which sister chromatids are attached to microtubules *via* kinetochores (6). Leng at al. investigated the mechanism causing up-regulation of the NDC80 kinetochore complex component in epithelial ovarian cancer. Its knockdown decreased proliferation, invasion, and migration in cell lines and decreased tumor growth in mice. Together with cell division blockade, apoptosis induction is, despite its limitations, a promising emerging anticancer strategy (7). Delgado-Waldo et al. used a combination of three small molecules for inducing apoptosis in three cervical cancer-derived cell lines. The approach involved the simultaneous inhibition of complex I of the mitochondrial respiratory chain, lactate dehydrogenase A, and DNA topoisomerase II, affecting multiple metabolic pathways. In addition, Pandey et al. characterized the non-apoptotic function of SMAC/diablo in lung cancer. Although this mitochondrial protein is generally pro-apoptotic, its knockout in lung cancer cells activated apoptosis and inhibited proliferation and migration. It also decreased tumor growth in mice.

These studies introduce novel strategies to interfere with cell division or to induce apoptosis, which provide promising outcomes against uncontrolled proliferation, the most distinctive feature of cancer cells.

Tumor microenvironment, angiogenesis, and metastasis

The effects of altered protein levels can reach beyond their cell of origin. Through proteomics, Akhtar et al. identified differentially expressed proteins in early-stage gallbladder cancer. These proteins were mostly associated with neutrophil degranulation and extracellular matrix remodeling, which might promote cell invasion. Alterations in the TME are correlated with enhanced angiogenesis. In the major types of solid tumors, most noncancerous cells are tumor-associated macrophages (TAMs), which control both cancer cell proliferation and tumor angiogenesis (8, 9). In our Research Topic, Kazakova et al.

studied the impact, in colon and rectal cancer, of the pro-angiogenic S100A4 calcium-binding protein and the integrin-binding secreted phosphoprotein 1, as well as the anti-angiogenic SPARC calcium-binding protein, expressed by TAMs. Although their up-regulation indicated poor prognosis, neoadjuvant chemotherapy/chemoradiotherapy converted S100A4 into a more favorable prognosis marker. Moreover, Ali et al. reviewed the impact of the TME and exosomes in the formation of metastases in the brain. Despite their harmful impact, exosomes could be exploited as a liquid biopsy technology, for the non-invasive diagnosis of brain metastases.

These studies demonstrate that proteins related to the propagation of cancer features are promising tools for diagnosis and prognosis.

Concluding remarks

The data reported in the present Research Topic provide novel data about regulatory proteins expressed in cancer cells and in immune cells of the TME. These regulatory proteins can control not only primary tumor growth and metastasis but also the efficiency of anti-cancer therapies. These proteins include transcription factors, which affect the levels of transcribed mRNA and translated protein. They also include enzymes involved in protein phosphorylation, dephosphorylation, and degradation, whose altered expression deregulates the levels of functional proteins (Figure 1A). These alterations can affect processes including cell division and apoptosis (Figure 1B). Altered protein levels can exert effects on a larger scale, by modifying the TME and promoting tumor angiogenesis

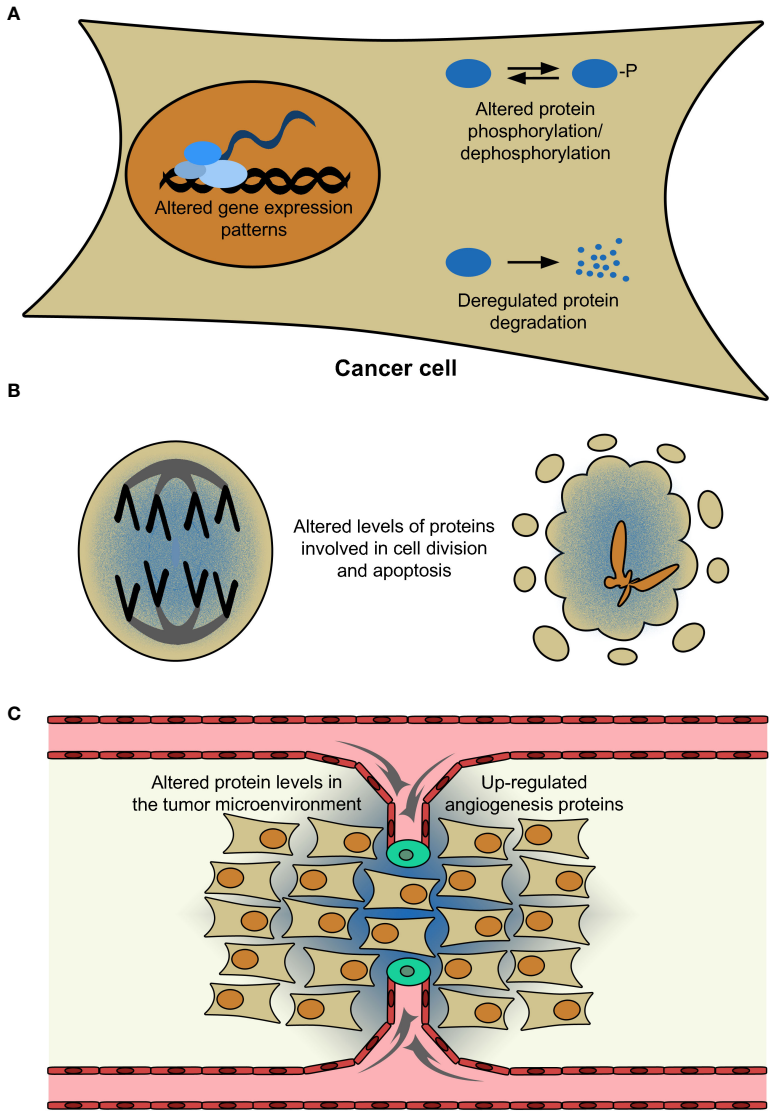

FIGURE 1
Causes and consequences of altered protein levels in cancer cells. **(A)** In the nucleus of a cancer cell (orange), up-/down-regulated transcription factors (light-blue) modify the levels of transcribed messenger RNA (dark-blue). The resulting proteins (blue) can be phosphorylated or degraded, in an equilibrium whose disruption affects their functional levels. **(B)** Altered protein levels can deregulate cell division and apoptosis (whose therapeutic induction up-regulates pro-apoptotic proteins). **(C)** They can also affect the tumor microenvironment and enhance angiogenesis (represented by gray arrows), which will promote cancer cell proliferation. For simplicity, only tumor (dark-yellow), endothelial (red), and tip (green) cells are represented. In panels **(B, C)**, protein up-regulation is represented as a blue gradient.

(Figure 1C). Since these alterations are responsible for cancer development and progression, they are also potential new molecular tools for its diagnosis and therapy.

Author contributions

JP, MV, and JK wrote the article with input from all authors, who contributed insight and approved the final manuscript.

Funding

This work was financed by the European Regional Development Fund (ERDF), through the COMPETE 2020 – Operational Programme for Competitiveness and Internationalization and Portuguese national funds via FCT – Fundação para a Ciência e a Tecnologia, under the projects UIDB/04539/2020, UIDP/04539/2020, and LA/P/0058/2020 (to JP); by Fondi Universitari di Ricerca (FUR; to MV); by Programa de financiamiento para la Investigación, UNAM, PAPIIT-IN231420, México, under the project UNAM-DGAPA: IN231420 (to CP-P); and by the state contract of the Ministry of Science and Higher Education of the Russian Federation "Genetic and epigenetic editing of tumor cells and microenvironment in order to block metastasis" (075-15-2021-1073) and by the Tomsk State University Development Programme (Priority 20-30; to JK).

Acknowledgments

We thank all contributing researchers and the respective reviewers for ensuring the success of the second volume of the present Research Topic. We are also thankful to all the patients whose biological sample donations were instrumental in the studies mentioned herein.

Conflict of interest

The authors declare that the research was conducted in the absence of any commercial or financial relationships that could be construed as a potential conflict of interest.

Publisher's note

References

1. Morrison AJ. Cancer cell metabolism connects epigenetic modifications to transcriptional regulation. *FEBS J* (2022) 289:1302–14. doi: 10.1111/febs.16032

2. Larionova I, Kazakova E, Patysheva M, Kzhyshkowska J. Transcriptional, epigenetic and metabolic programming of tumor-associated macrophages. *Cancers (Basel)* (2020) 12(6):1411. doi: 10.3390/cancers12061411

3. Lee P, Chandel NS. And Simon, M.C. 2020. cellular adaptation to hypoxia through hypoxia-inducible factors and beyond. *Nat Rev Mol Cell Biol* (2020) 21:268–83. doi: 10.1038/s41580-020-0227-y

4. Vizovisek M, Ristanovic D, Menghini S, Christiansen MG, Schuerle S. The tumor proteolytic landscape: a challenging frontier in cancer diagnosis and therapy. *Int J Mol Sci* (2021) 22(5):2514. doi: 10.3390/ijms22052514

5. Sun T, Liu Z. And yang, q. 2020. the role of ubiquitination and deubiquitination in cancer metabolism. *Mol Cancer* (2020) 19:146. doi: 10.1186/s12943-020-01262-x

6. Musacchio A, Desai A. A molecular view of kinetochore assembly and function. *Biol (Basel)* (2017) 6(1):5. doi: 10.3390/biology6010005

7. Morana O, Wood W, Gregory CD. The apoptosis paradox in cancer. *Int J Mol Sci* (2022) 23(3):1328. doi: 10.3390/ijms23031328

8. Larionova I, Kazakova E, Gerashchenko T, Kzhyshkowska J. New angiogenic regulators produced by TAMs: perspective for targeting tumor angiogenesis. *Cancers (Basel)* (2021) 13(13):3253. doi: 10.3390/cancers13133253

9. Kloosterman DJ, Akkari L. Macrophages at the interface of the co-evolving cancer ecosystem. *Cell* (2023) 186:1627–51. doi: 10.1016/j.cell.2023.02.020

frontiers | Frontiers in Oncology

TYPE Review
PUBLISHED 26 July 2022
DOI 10.3389/fonc.2022.972906

OPEN ACCESS

EDITED BY
João Pessoa,
University of Coimbra, Portugal

REVIEWED BY
Ulrike Lorenz,
University of Virginia, United States
Bonsu Ku,
Korea Research Institute of Bioscience and Biotechnology (KRIBB), South Korea

*CORRESPONDENCE
Honghong Zhou
zhouhonghong@ibp.ac.cn
Yongshuo Liu
liuyongshuo@pku.edu.cn

†These authors have contributed equally to this work

SPECIALTY SECTION
This article was submitted to Cancer Molecular Targets and Therapeutics, a section of the journal Frontiers in Oncology

RECEIVED 19 June 2022
ACCEPTED 04 July 2022
PUBLISHED 26 July 2022

CITATION
Tang X, Qi C, Zhou H and Liu Y (2022) Critical roles of PTPN family members regulated by non-coding RNAs in tumorigenesis and immunotherapy. *Front. Oncol.* 12:972906. doi: 10.3389/fonc.2022.972906

Critical roles of PTPN family members regulated by non-coding RNAs in tumorigenesis and immunotherapy

Xiaolong Tang[1†], Chumei Qi[2†], Honghong Zhou[3*] and Yongshuo Liu[4*]

[1]Department of Clinical Laboratory Diagnostics, Binzhou Medical University, Binzhou, China, [2]Department of Clinical Laboratory, Dazhou Women and Children's Hospital, Dazhou, China, [3]Key Laboratory of RNA Biology, Center for Big Data Research in Health, Institute of Biophysics, Chinese Academy of Sciences, Beijing, China, [4]Biomedical Pioneering Innovation Center (BIOPIC), Beijing Advanced Innovation Center for Genomics, Peking-Tsinghua Center for Life Sciences, Peking University Genome Editing Research Center, State Key Laboratory of Protein and Plant Gene Research, School of Life Sciences, Peking University, Beijing, China

Since tyrosine phosphorylation is reversible and dynamic *in vivo*, the phosphorylation state of proteins is controlled by the opposing roles of protein tyrosine kinases (PTKs) and protein tyrosine phosphatase (PTPs), both of which perform critical roles in signal transduction. Of these, intracellular non-receptor PTPs (PTPNs), which belong to the largest class I cysteine PTP family, are essential for the regulation of a variety of biological processes, including but not limited to hematopoiesis, inflammatory response, immune system, and glucose homeostasis. Additionally, a substantial amount of PTPNs have been identified to hold crucial roles in tumorigenesis, progression, metastasis, and drug resistance, and inhibitors of PTPNs have promising applications due to striking efficacy in antitumor therapy. Hence, the aim of this review is to summarize the role played by PTPNs, including PTPN1/PTP1B, PTPN2/TC-PTP, PTPN3/PTP-H1, PTPN4/PTPMEG, PTPN6/SHP-1, PTPN9/PTPMEG2, PTPN11/SHP-2, PTPN12/PTP-PEST, PTPN13/PTPL1, PTPN14/PEZ, PTPN18/PTP-HSCF, PTPN22/LYP, and PTPN23/HD-PTP, in human cancer and immunotherapy and to comprehensively describe the molecular pathways in which they are implicated. Given the specific roles of PTPNs, identifying potential regulators of PTPNs is significant for understanding the mechanisms of antitumor therapy. Consequently, this work also provides a review on the role of non-coding RNAs (ncRNAs) in regulating PTPNs in tumorigenesis and progression, which may help us to find effective therapeutic agents for tumor therapy.

KEYWORDS

PTPNs, cancer, immunotherapy, miRNAs, lncRNAs, circRNAs

Introduction

Protein tyrosine phosphatases (PTPs) are a wide class of enzymes that oppose protein tyrosine kinases (PTKs) (1). PTPs can be categorized into four families based on the amino acid sequence of its catalytic structural domain, each with different substrate specificities (2). Of these, 17 intracellular non-receptor PTPs, belonging to the largest class I cysteine PTP family, are designated as PTPNs (2). Extensive evidence suggests that PTPNs are involved in a range of physiological and pathological processes, including but not limited to hematopoiesis, inflammatory response, immune system, cell proliferation and differentiation, and glucose homeostasis (3–6). Furthermore, PTPNs hold a critical role in tumor progression by dephosphorylating various substrate proteins to activate or inhibit oncogenic pathways (7, 8). More notably, several PTPNs are implicated in resistance to chemotherapy and radiotherapy, and numerous studies have demonstrated that targeting certain PTPNs can boost anti-tumor immunity and efficacy, which stimulates the immune system to attack tumors (9). Therefore, PTPNs are remarkably promising therapeutic targets to combat tumors.

Non-coding RNAs (ncRNAs) are a type of RNA transcript found in many eukaryotic genomes that function as a regulator of cellular processes, including chromatin remodeling, transcription, post-transcriptional modifications and signal transduction (10, 11). In recent years, ncRNAs have been linked to the development and progression of cancer, particularly microRNAs (miRNAs), long-stranded non-coding RNAs (lncRNAs), and circular RNAs (circRNAs) (11, 12). Of these, miRNAs are defined as short ncRNAs of approximately 22 nt, lncRNAs are ncRNAs with transcripts longer than 200 nt, and circRNAs are closed continuous loop structures lacking a terminal 5' cap and a 3' polyadenylated tail (11). Interestingly, lncRNAs and circRNAs can perform as miRNA sponges, binding to miRNAs and altering their function. Here, ncRNAs act as tumor promoters and suppressors, depending on targeting PTPNs.

In this review, we elaborate on the roles played by PTPN family members and provide a comprehensive summary of the molecular pathways in which PTPNs are involved in various human cancers. Subsequently, the essential position occupied by PTPNs in the immune system and cancer immunotherapy is further described. Furthermore, we characterize how ncRNAs modulate PTPNs in tumorigenesis and hypothesize that ncRNA regulation in combination with immunotherapy may lead to more precise and effective efficacy.

The physiological role of PTPNs

PTPNs, belonging to the PTP family, share the common property of possessing phosphatase activity that dephosphorylates a series of proteins, thereby governing cellular signal transduction and biological processes. Several studies have shown that PTPN2 and PTPN6 are highly expressed in hematopoietic cells and act as negative signaling regulators (13, 14). For instance, PTPN2 dephosphorylates and inactivates signal transducer and activator of transcription (STAT) protein, which is required to maintain cellular homeostasis in the hematopoietic system (15). Furthermore, PTPN2 also holds an essential role in glucose homeostasis. For example, PTPN2 negatively regulates the insulin receptor (INSR) signaling pathway through dephosphorylation of INSR and controls gluconeogenesis and hepatic glucose production through negative regulation of the interleukin-6 (IL-6) signaling pathway (16, 17). PTPN14 is required for the regulation of lymphangiogenesis (18). In addition, PTPNs perform crucial roles in the regulation of immune cell development and inflammatory responses, which will be described in later sections. Overall, the PTPN family members act as a "brake" and are essential for the maintenance of homeostasis in the body.

Role of PTPNs in the context of cancer

Members of the PTPN family hold crucial roles in cancer genesis, progression, metastasis, and drug resistance by dephosphorylating a variety of substrate proteins to execute oncogenic or tumor suppressive functions in various cancers (Figure 1).

Breast cancer

PTPN family members have been extensively investigated in breast cancer, with PTPN1 and PTPN11 driving the progression of breast cancer. PTPN1, which is required for invadopodia formation (19), promotes invasiveness of breast cancer cells by negatively regulating PTEN and facilitates human epidermal growth factor receptor 2 (HER2)-induced breast tumorigenesis with lung metastasis (20, 21). PTPN11 is essential for HER2, IL-6, and platelet-derived growth factor-B (PDGF-B)-induced tumorigenesis and epithelial-to-mesenchymal transition (EMT) (22–24). Mechanistically, PTPN11 enhances the oncogenic activity of β-catenin and activates Src family kinases, as well as regulates focal adhesion kinase (FAK) to promote epidermal growth factor (EGF)-induced lamellipodia persistence and migration of triple-negative breast cancer (TNBC) cells (25–27).

However, most PTPN family members function as tumor suppressors in breast cancer, including PTPN2, PTPN4, PTPN6, PTPN9, PTPN13, PTPN14, and PTPN23. Specifically, PTPN2 is implicated in the subtype specificity of breast cancer, and low expression in patients with Luminal A and HER2-positive

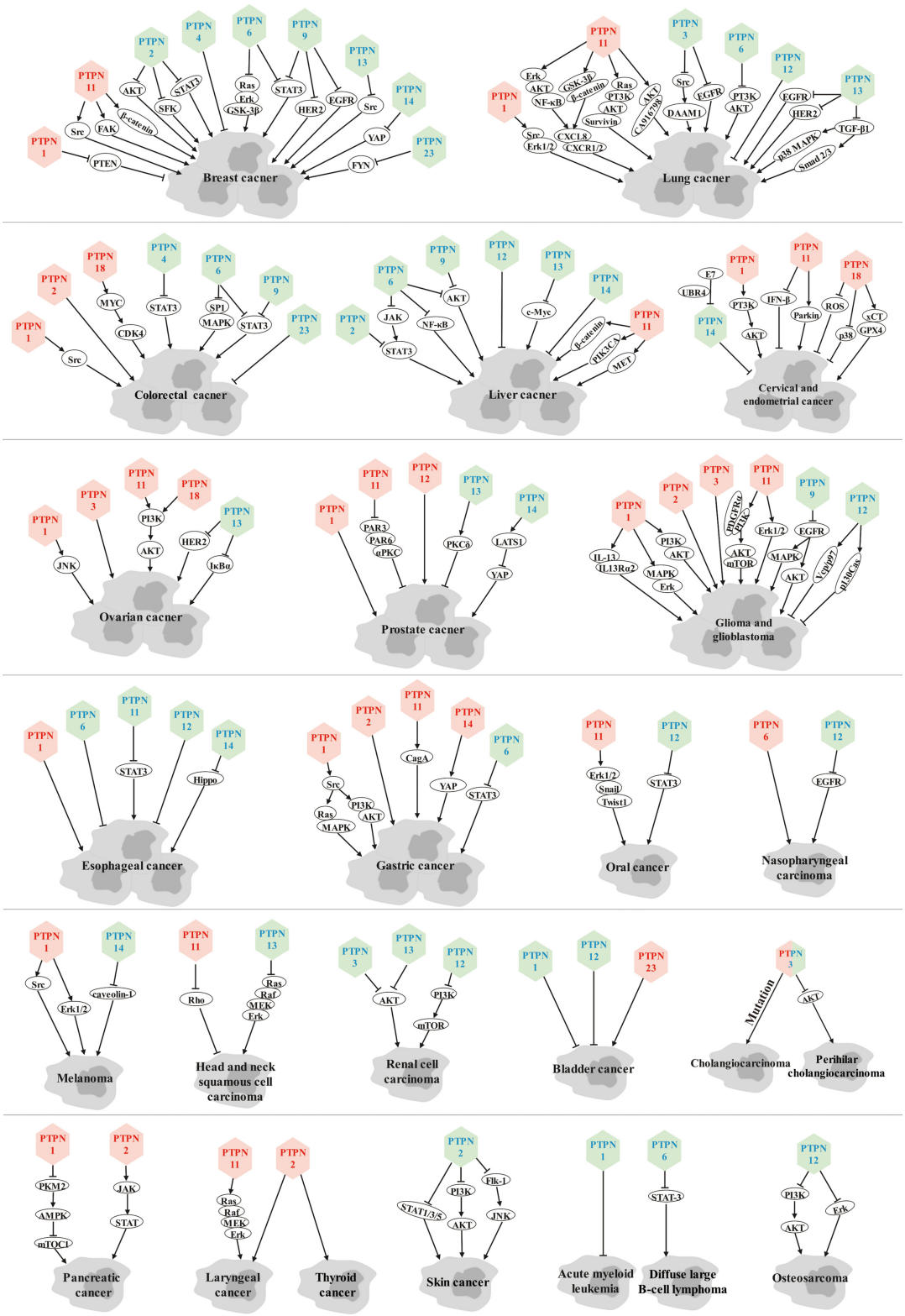

FIGURE 1
Role of PTPN family members in various cancers. Red font represents tumor promoters and blue font represents tumor suppressors.

tumors is linked to a higher recurrence rate, but not in patients with triple-negative tumors (28). More importantly, loss of PTPN2 is coupled with activation of oncogenic signaling pathways, such as protein kinase B (AKT), Src family kinase (SFK) and STAT3 signaling pathways, and also with resistance to tamoxifen (29, 30). PTPN6 dampens the oncogenic characteristics of breast cancer by dephosphorylating STAT3 and inactivating the Ras/extracellular signal-regulated kinase (Erk)/glycogen synthase kinase-3beta (GSK-3β) signaling pathway (31, 32). PTPN9 suppresses the growth and invasion of breast cancer cells by negatively regulating HER2 and epidermal growth factor receptor (EGFR) and suppressing STAT3 activation (33, 34). Furthermore, PTPN4 and PTPN13 are favorable prognostic biomarkers for breast cancer patients (35, 36), in which PTPN13 induces apoptosis of breast cancer cells and inhibits breast tumor aggressiveness by directly inactivating Src kinase and stabilizing intercellular adhesion and promoting desmosome formation (37–39). PTPN14 negatively regulates the oncogenic function of yes-associated protein (YAP) by modulating the subcellular localization of YAP and suppressing its transcriptional co-activator activity (40), and also inhibits breast cancer metastasis by altering protein transport (41). PTPN23 is identified as a suppressor of cell motility and invasion in breast cancer cells by inhibiting FYN kinase (42).

Lung cancer

As with breast cancer, PTPN1 and PTPN11 also serve as oncogenic factors in lung cancer. PTPN1 contributes to the proliferation and metastasis of non-small cell lung cancer (NSCLC) cells by enhancing the Erk1/2 signaling pathway and diminishing the expression of p-Src (Tyr527), which activates Src (43). Of note, PTPN11 is not only essential for lung cancer cell growth, but also confers chemotherapy resistance (44). Mechanistically, overexpression of PTPN11 increases resistance to tyrosine kinase inhibitors (TKI) in either EGFR mutant or EGFR wild-type NSCLC cells through Erk-AKT-nuclear factor kappa B (NF-κB) and GSK3β-β-Catenin signaling pathway-mediated C-X-C motif chemokine ligand 8 (CXCL8)-chemokine receptor 1/2 (CXCR1/2) feedback loop that promotes stemness and tumorigenesis (45, 46). Moreover, PTPN11 confers cisplatin resistance to lung cancer cells through activation of the AKT-CA916798 pathway and the Ras/phosphoinositide 3-kinase (PI3K)/AKT1/survivin pathway, respectively (47, 48). Consequently, PTPN11 inhibitors in combination with chemotherapy may be a promising therapy strategy for patients with lung cancer.

Furthermore, PTPN3, PTPN6, PTPN12 and PTPN13 play tumor suppressor roles in lung cancer. PTPN3 suppresses lung cancer cell proliferation and migration by counteracting Src-mediated disheveled-associated activator of morphogenesis 1 (DAAM1) activation and actin polymerization and by promoting EGFR endocytic degradation (49, 50). Similarly, PTPN6 inactivates PI3K/AKT signaling pathway (51). PTPN12 is a valuable prognostic biomarker for patients with NSCLC (52). PTPN13 negatively regulates the growth and migration of lung cancer cells *in vitro* and inhibits tumorigenicity *in vivo* by controlling tyrosine phosphorylation of EGFR and HER2 and by inhibiting transforming growth factor beta1 (TGF-β1)-induced activation of p38 mitogen-activated protein kinase (MAPK) and Smad 2/3 pathways, respectively (53, 54).

Colorectal cancer

In colorectal cancer, PTPN1, PTPN2 and PTPN18 undoubtedly drive its progression. Among them, PTPN1 expression is related to poor prognosis in colorectal cancer patients through dephosphorylation of the Tyr530 site of Src, which activates the Src signaling pathway and enhances the oncogenicity of colon cancer (55, 56). Similarly, high expression of PTPN2 is implicated in the incidence of colorectal cancer (57), and specific deletion of PTPN2 in bone marrow cells and macrophages prevents the development of colorectal cancer, although it promotes inflammation in the intestine (58). PTPN18 activates myelocytomatosis oncogene (MYC) signaling pathway and further potentiates cyclin-dependent kinase 4 (CDK4) expression to promote colorectal cancer progression (59).

PTPN4, PTPN6 and PTPN9, as tumor suppressors, suppress the progression of colorectal cancer by dephosphorylating pSTAT3 at the Tyr705 residue and restraining the transcriptional activity of STAT3 (60–62). Moreover, PTPN6 also facilitates chemosensitivity of colorectal cancer cells by inhibiting specificity protein 1 (SP1)/MAPK signaling pathway (63). Additionally, PTPN23 also suppresses the proliferation and EMT of human intestinal cancer cells (64).

Liver cancer

The vast majority of the reported PTPN family members hold an inhibitory role in hepatocellular carcinoma (HCC), with the exception of PTPN11, which drives HCC progression by potentiating oncogenic proteins such as β-Catenin, PIK3CA and MET, and is associated with chemoresistance in HCC patients (65, 66).

PTPN2 can prevent hepatocyte progression to HCC by inactivating STAT3 signaling and suppressing T-cell recruitment in obese C57BL/6 mice (67). Consistently, PTPN6 overexpression inhibits the proliferation, migration, invasion and tumorigenicity of HCC cells by suppressing multiple oncogenic pathways, including janus kinase (JAK)/STAT, NF-

κB and AKT signaling pathways (68). Likewise, PTPN9 contributes to the inhibition of HCC growth and metastasis by repressing the AKT pathway (69). In addition, PTPN12 and PTPN13 are associated with a favorable prognosis in HCC patients. Mechanistically, PTPN13 suppresses HCC progression by directly and competitively binding insulin-like growth factor 2 mRNA-binding protein 1 (IGF2BP1) to diminish the intracellular concentration of functional IGF2BP1, thereby promoting c-Myc mRNA degradation (70). Furthermore, PTPN14 significantly represses the proliferation, migration, and invasion of HCC cells *in vitro* and tumor growth and metastasis *in vivo* (71).

Cervical and endometrial cancer

Currently, most PTPN family members perform oncogenic roles in cervical and endometrial cancers, with the exception of PTPN14. In detail, PTPN1 expression is linked to poor prognosis in cervical cancer possibly through activation of the PI3K/AKT pathway (72). Importantly, PTPN11 contributes to the growth and migration of cervical cancer cells and decreases the sensitivity of cells to cisplatin (73). Specifically, PTPN11 facilitates cervical cancer cell proliferation by suppressing interferon-β (IFN-β) production and restricts chemotherapeutic drug-induced apoptosis of cervical cancer cells through Parkin-dependent autophagy (74, 75). Likewise, PTPN18 promotes proliferation and metastasis and restrains apoptosis in endometrial cancer (76). Mechanistically, silencing of PTPN18 induced ferroptosis in endometrial cancer cells by increasing intracellular reactive oxygen species (ROS) levels and p-p38 expression as well as decreasing the expression of glutathione peroxidase 4 (GPX4) and system xc(-) cystine/glutamate antiporter (xCT) (72).

What's more, the deletion of PTPN14 contributes to human papillomavirus (HPV)-mediated cervical carcinogenesis, while the major transforming activity of high-risk HPV is linked to the E7 oncoprotein. Mechanistically, the crystal structure of the terminal structural domain of E7 C binds to the catalytic structural domain of PTPN14 and induces proteasome-mediated degradation of PTPN14 *via* the ubiquitin ligase UBR4 (77, 78), thereby restricting keratin-forming cell differentiation and contributing to HPV-mediated tumorigenesis (79).

Ovarian cancer

PTPN family members almost contribute to the progression of ovarian cancer, except for PTPN13. PTPN1 and PTPN6 are highly expressed in ovarian cancer cell lines (80, 81), in which PTPN1 accelerates ovarian cancer progression in a c-Jun N-terminal kinase (JNK)-dependent mechanism (80). Strikingly, PTPN3 confers chemoresistance and tumor stem cell-like characteristics to ovarian cancer cells (82). Furthermore, PTPN11 and PTPN18 potentiate ovarian cancer invasion and metastasis through activation of PI3K/AKT axis (83, 84).

However, high PTPN13 expression in patients with high-grade plasma ovarian cancer is related to better prognosis (85). Mechanistically, PTPN13 dephosphorylates the signaling domain of HER2 and the phosphorylation of tyrosine 42 on IκBα (IκBα-pY42), respectively, thereby attenuating the invasiveness and metastasis of ovarian cancer (86, 87).

Prostate cancer

In prostate cancer, PTPN1 and PTPN12 are linked to poor prognosis in patients (88, 89). Importantly, PTPN11 promotes prostate cancer metastasis by attenuating the PAR3/PAR6/atypical protein kinase C (aPKC) polarity protein complex, resulting in disruption of cell polarity, dysregulation of cell-cell junctions, and increased EMT (90).

In contrast, PTPN13 and PTPN14 function as tumor suppressors in prostate cancer. Specifically, PTPN13 suppresses the proliferation and migration of prostate cancer cells and stimulates apoptosis mediated by PKCδ (91). Furthermore, PTPN14 restrains cell proliferation and invasion by enhancing phosphorylation of YAP through activation of large tumor suppressor 1 (LATS1), an effect that leads to a significant decrease in YAP-mediated transcriptional activity (92).

Glioma and glioblastoma

PTPN1 and PTPN2 can be used as predictors of poor prognosis in glioma patients (93, 94). Mechanistically, PTPN1 promotes glioma progression through activation of MAPK/Erk and PI3K/AKT pathways as well as IL-13-mediated adhesion, migration and invasion of IL13Rα2-expressing cancer cells (93, 95). Up-regulation of PTPN2 expression induced by inflammatory response and oxidative stress contributes to glioma progression (96). Furthermore, PTPN11 regulates proliferation and tumorigenicity of glioma stem cells (97).

Likewise, PTPN2 and PTPN3 are correlated with poor patient prognosis in glioblastoma (GBM) (94, 98). In Ink4a/Arf-deficient glioblastomas, PTPN11 regulates the interaction of PI3K with PDGFRα and activates the downstream AKT/mTOR pathway, ultimately promoting tumorigenesis (99). In addition, the multivariate signaling regulatory function of PTPN11 holds a crucial role in GBM cellular decision-making. PTPN11-driven Erk1/2 activity is dominant in driving cellular proliferation and PTPN11-mediated antagonism of STAT3 phosphorylation prevails in the promotion of GBM cell death in response to EGFR and c-MET co-inhibition (100).

But for PTPN9, which appears to be a tumor suppressor, leads to decreased glioma cell viability by reducing the phosphorylation of EGFR and cooperating with BRAF (V600E) inhibitors to restrain MAPK and AKT signaling (101). Furthermore, PTPN12 controls GBM cell growth and invasion by interacting with the ATP-dependent ubiquitin segregase valosin-containing protein (Vcp)/p97 and regulating phosphorylation and stability of the focal adhesion protein p130Cas (Crk-associated substrate) (102).

Esophageal cancer

Interestingly, PTPN1 expression is implicated in the incidence of esophageal cancer (57), while PTPN6 is down-regulated in esophageal cancer and PTPN12 is a favorable prognostic biomarker for patients with esophageal squamous cell carcinoma (103, 104). What's more, PTPN11 and PTPN14 suppress malignant progression and chemoresistance in esophageal cancer through dephosphorylation of STAT3 and negative regulation of the Hippo signaling pathway, respectively (105, 106).

Gastric cancer

PTPN1 significantly promotes gastric cancer (GC) cell proliferation *in vitro* and tumor growth *in vivo* by regulating Src-related signaling pathways, such as the Src/Ras/MAPK and Src/PI3K/AKT pathways (107–109). Furthermore, PTPN1 is implicated in the poor prognosis of gastric cancer, and PTPN2 is linked to the incidence of gastric cancer (57, 109). It is well known that *Helicobacter pylori* is a high risk factor for gastric cancer. Jing Jiang et al. reveals that PTPN11 expression is elevated in gastric cancer with *H. pylori* infection (110). In the early stages of gastric carcinogenesis, CagA from *H. pylori* translocates into gastric epithelial cells, undergoes tyrosine phosphorylation, and binds to PTPN11 in the human gastric mucosa *in vivo* to form a complex which is thought to contribute to the development of gastric cancer (111). SHIP2, similar to PTPN11, also binds to CagA in a tyrosine phosphorylation-dependent manner and increases CagA delivery into gastric epithelial cells (112). Of note, PTPN14 enhances the proliferation and migration of GC cells by promoting YAP phosphorylation in the Hippo signaling pathway (113). On the contrary, PTPN6 attenuates the invasion and migration of GC cells by dephosphorylating STAT3 (114).

Other cancers

In oral cancer, PTPN11 is significantly up-regulated and promotes cell invasion and metastasis through the Erk1/2-Snail/Twist1 pathway (115). In contrast, PTPN12 suppresses oral cancer cell proliferation and invasion through induction of STAT3 dephosphorylation (116). In nasopharyngeal carcinoma (NPC), PTPN6 potentiates radioresistance and restrains cellular senescence (117). However, PTPN12, a favorable prognostic biomarker for NPC patients, suppresses the proliferation and migration of NPC cells through negative regulation of EGFR (118). In melanoma, PTPN1 promotes melanoma progression by activating the Src signaling pathway through dephosphorylating the Tyr530 site of Src as well as by enhancing the Erk1/2 signaling pathway, respectively (119, 120). Moreover, PTPN14 blocks caveolin-1-induced cancer cell metastasis by decreasing phosphorylation at the Tyr14 site of caveolin-1 (121). In the head and neck squamous cell carcinoma, PTPN11 promotes invadopodia formation through suppression of Rho signaling, leading to cancer metastasis (122). Yet, PTPN13 controls the progression of spontaneous or HPV-induced squamous cell carcinoma by inhibiting Ras/Raf/MEK/Erk signaling (123). In clear cell renal cell carcinoma, PTPN3 and PTPN13 act as tumor suppressors by inactivating the AKT signaling pathway (124, 125), whereas PTPN12 restrains the proliferation of renal cell carcinoma by inhibiting PI3K/mechanistic target of rapamycin (mTOR) pathway activity (126). In bladder cancer, PTPN1 and PTPN12 function as tumor suppressors to attenuate the growth, invasion and migration of cancer cells (127, 128). However, PTPN23 can regulate the motility of bladder cancer cells (129). In cholangiocarcinoma more than 40% of PTPN3 somatic mutations, activation of PTPN3 mutations promotes cancer cell proliferation and migration and is linked to cancer recurrence (130). Strikingly, PTPN3 suppresses proliferation through inhibition of AKT phosphorylation and is correlated with a favorable prognosis in patients with perihilar cholangiocarcinoma (131). In pancreatic cancer, PTPN1 and PTPN2 are highly expressed and associated with poor survival. Specifically, PTPN1 directly decreases pyruvate kinase M2 (PKM2) Tyr105 phosphorylation, which further leads to AMP-activated protein kinase (AMPK) inactivation, thereby increasing mTOC1 activity. PTPN2 activates the JAK-STAT signaling pathway to promote cancer progression (132, 133). Furthermore, inflammatory response and oxidative stress induce up-regulation of PTPN2, which accelerates the progression of laryngeal and thyroid cancers (134, 135). PTPN11 also promotes laryngeal cancer growth through the Ras/Raf/Mek/Erk pathway and serves as a prognostic indicator for laryngeal cancer (136). Several studies have shown that PTPN2, which exerts tumor suppressive effects in skin carcinogenesis, suppresses proliferation and induces apoptosis by negatively regulating multiple oncogenic signaling pathways, including STAT1, STAT3, STAT5, PI3K/AKT, and fetal liver kinase 1 (Flk-1)/JNK signaling pathways (137–139). In hematologic tumors, specific deficiency of PTPN1 in mouse bone marrow accelerates the development of acute myeloid leukemia (140), and PTPN6 inhibits the progression of diffuse large B-cell

lymphoma by dephosphorylating STAT3 (141). Finally, PTPN12 inhibits tumor progression in osteosarcoma cells probably by inactivating PI3K/AKT and Erk pathways (142).

In summary, we have comprehensively described the role of PTPN family members in human cancers and observed that various PTPN family members are implicated in almost all oncogenic phenotypes, such as tumor proliferation, metastasis, and drug resistance, through unique molecular pathways. Interestingly, the majority of PTPN family members perform oncogenic or tumor suppressive functions depending on the tumor in which they are located. Nevertheless, a small number of PTPN family members exert more specific functions, for instance, PTPN11 as a tumor promoter whereas PTPN13 as a tumor suppressor in almost all cancers.

Dual role of PTPNs in specific cancers

Strikingly, we observed that a portion of the PTPN family members have dual roles in the same cancer. For instance, PTPN1 in hepatocellular carcinoma, PTPN11 in colon cancer and PTPN12 in breast cancer can be both tumor promoters and tumor suppressors based on different molecular pathways (Figure 2). Elucidating the dual roles of certain PTPN may lead to better understanding of its exact functions in tumorigenesis.

Dual-sidedness of PTPN1 in hepatocellular carcinoma

Leukocyte-derived chemotoxin 2 (LECT2), a tumor suppressor in HCC, contributes to blocking vascular invasion and metastasis in HCC by recruiting PTPN1 to antagonize MET receptor activation (143). However, Wei-Tien Tai et al. and Fang Yuan et al. proposed that PTPN1 exerts a carcinogenic role in HCC. Specifically, Pituitary homeobox 1 (PITX1) exerts a tumor suppressive effect in hepatocarcinogenesis through regulation of Ras guanosine triphosphatase-activating protein (p120RasGAP) expression levels, but PTPN1 attenuates the protein stability of PITX by directly dephosphorylating PITX1 at residues Y160, Y175 and Y179 (144). Furthermore, down-regulation of PTPN1 expression inhibits HCC progression possibly by inactivating the PI3K/AKT pathway and activating the AMPK pathway (145).

Two faces of PTPN11 in colon cancer

Controversially, Wang Y et al. (146) and Yu M et al. (147) demonstrated that PTPN11 promotes vascular growth and proliferation of colon cancer cells as well as resistance to oxaliplatin through AKT and Erk signaling pathways. However,

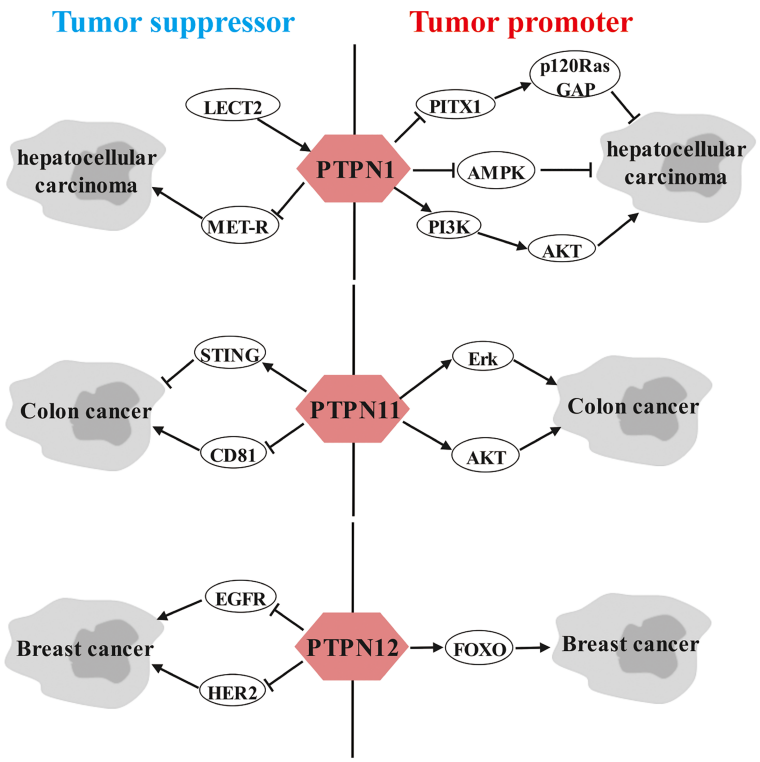

FIGURE 2
Dual role of PTPNs in specific cancers.

Yuan H et al. (148) and Wei B et al. (149) argued that PTPN11 possesses anticancer activity in colon cancer. Mechanistically, the anticancer effects of PTPN11 are achieved by interacting with CD81 and inhibiting its expression and by inhibiting DNA repair and enhancing stimulator of interferon genes (STING) pathway-mediated antitumor immunity, respectively.

Dual role of PTPN12 in breast cancer

In addition, several studies have shown that PTPN12 is linked to a favorable prognosis in TNBC patients by suppressing multiple oncogenic tyrosine kinases, including HER2 and EGFR, thereby dampening breast cancer cell survival, migration and EMT (150–152). However, Harris IS et al. noted that PTPN12 is highly expressed in TNBC and promotes resistance to oxidative stress and supports tumorigenesis by regulating forkhead box O (FOXO) signaling (153).

Regarding the controversy of the three PTPN members mentioned above in specific cancers, we have speculated the following three reasons. First, there may be some differences in various experimental settings and tumor cell lines. Second, there are also differences in molecular mutation profiles in tumor cell lines. If mutations occur in the regulator of PTPN, it might lead to a change in the function of PTPN so that the exact opposite function appears in the same cancer. Furthermore, mutations in PTPN itself can result in opposite functions, as previously described, where PTPN3 inhibits the progression of cholangiocarcinoma by suppressing the AKT signaling pathway, whereas mutated PTPN3 promotes the oncogenic properties of cholangiocarcinoma (130, 131). Likewise, mutations occurring in PTPN11 significantly potentiate its function, producing oncogenes that facilitate the proliferation of leukemic cells (154). Third, PTPNs possess phosphatase active structural domains that regulate the dephosphorylation of many substrate proteins, including tumor promoters or suppressors, so focusing on only one molecular pathway may introduce bias for the overall role of PTPNs in a particular cancer.

Therefore, the study of PTPNs in combination with cell lines *in vitro* and mouse genetic studies *in vivo*, by knocking out specific regulators and effectors, will contribute to a better understanding of the specific signaling pathways regulated by PTPNs.

PTPNs are crucial targets for regulating immune cells development and cancer immunotherapy

Given that PTPNs occupy important roles in human tumors, in addition to achieving pro- or anti-tumor effects by modulating multiple oncogenic pathways, perhaps they also reshape the tumor microenvironment by inducing tumor cells to secrete various cytokines and chemokines. It is well known that immune cells are an essential component of the tumor microenvironment (TME) (155). There is growing evidence that some PTPN family members can negatively regulate the development and differentiation of immune cells to achieve an anti-inflammatory response and prevent the onset of autoimmune diseases, but on the other hand provide an opportunity for tumors to evade surveillance by the immune system. Since the immunosuppressive tumor microenvironment creates the appropriate conditions for tumor proliferation and metastasis, an accumulating number of studies indicate that targeting PTPNs could activate the body's immune system, thereby enhancing the efficacy of anti-tumor immunity (Figure 3).

PTPNs mediate the physiological functions of immune cells

During development and maturation, various inhibitory receptors linked with phosphatases are expressed by subsets of T cells. Phosphatases, in turn, dephosphorylate key players in receptor signaling pathways. Several studies have shown that PTPN family members are crucial for suppressing T cell activation, with PTPN2, PTPN3, PTPN4, PTPN7, PTPN11 and PTPN22 negatively regulating T-cell receptor (TCR) signaling (156–163). Specifically, PTPN2 dephosphorylates and inactivates Src family kinases to regulate T cell responses (162). PTPN22 functions in a synergistic manner when forming a complex with C-terminal Src kinase (CSK), and dissociation of this complex is necessary to recruit PTPN22 to the plasma membrane, where it down-regulates TCR signaling and inhibits T cell activation (164). However, end-binding protein 1 (EB1) specifically binds to the P1 structural domain of PTPN22 by competing with CSK, which contributes to the regulation of TCR signaling (165). Another essential purpose of PTPN11 is to prevent T cells from differentiating into the T-helper 2 (Th2) phenotype (166). However, phosphatase activities of PTPN3 and PTPN4 are now dispensable for T cell development and T cell effector function (156, 157, 167). PTPN12, although not required for T cell development or primary responses, promotes secondary T cell responses by dephosphorylating the protein tyrosine kinase Pyk2 (168).

Likewise, PTPN1 and PTPN6 are also negative regulators of B-cell receptor (BCR) signaling and hold a vital role in modulating B cell activation and immunological tolerance (169, 170). Mechanistically, PTPN1 restricts B cell activation *via* negatively regulating CD40, B cell activating factor receptor (BAFF-R), and toll-like Receptor 4 (TLR4) signaling in B cells (169).

In Dendritic cells (DCs), ablation of PTPN1 and PTPN12 impairs motility *in vivo* and prevents efficient antigen presentation to T cells (171, 172). These results indicate that PTPN1 and PTPN12 hold a significant regulatory role in

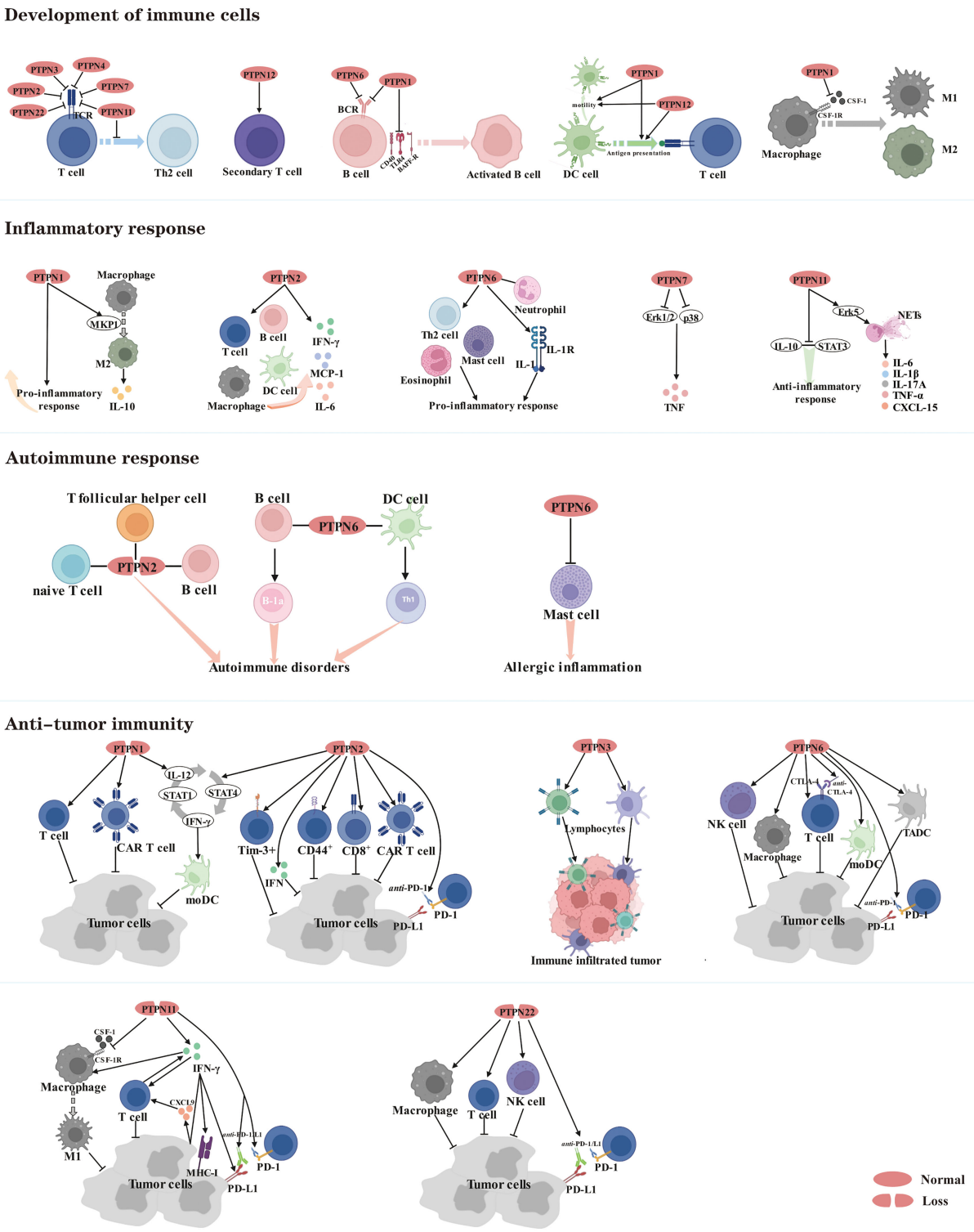

FIGURE 3
Members of the PTPN family are involved in regulating the development of immune cells and serve as therapeutic targets for inflammatory diseases, autoimmune diseases and cancer.

modulating a central DC function of initiating adaptive immune responses in response to innate immune cell activation.

Pro-inflammatory macrophages M1 and tolerance-inducible macrophages M2 are the two major subpopulations of macrophages, the former mediating host defense and the latter undertaking homeostatic and tissue regeneration functions (173). PTPN1 negatively regulates macrophage development through macrophage-colony stimulating factor 1 (CSF-1) signaling. Mechanistically, PTPN1 deficiency tends to make cells more sensitive to CSF-1, resulting in increased phosphorylation of the CSF-1 receptor (CSF-1R) in bone marrow-derived macrophages and increased inflammatory activity, implying that PTPN1 is a critical regulator of bone marrow differentiation and macrophage activation *in vivo* (174, 175).

PTPNs perform pivotal roles in the regulation of inflammatory and autoimmune responses

Currently, several studies place PTPN family members as a double-edged sword in the regulation of inflammatory responses. PTPN1 deletion displays enhanced inflammatory activity *in vitro* and *in vivo* through constitutive overexpression of activation markers as well as greater sensitivity to endotoxins (174). However, PTPN1 deletion increases Mitogen-activated protein kinase phosphatase-1 (MKP1) expression in mouse macrophages, facilitating M2 macrophage polarization, which promotes the production of anti-inflammatory cytokine (IL-10) according to another study (176).

PTPN2 is a negative regulator of cytokine signaling, and its loss-of-function carriers have increased susceptibility to the development of inflammatory diseases (173). For instance, $PTPN2^{-/-}$ mice develop progressive systemic inflammatory diseases with dermatitis, liver inflammation, chronic myocarditis, gastritis, nephritis, and salpingitis, as well as elevated serum interferon-γ (IFN-γ) (177). Mechanistically, PTPN2 deficiency promotes increased infiltration of B and T lymphocytes, macrophages and DCs (178, 179), and up-regulated IFN-γ induces STAT signaling and secretion of IL-6 and monocyte chemoattractant protein-1 (MCP-1) (180).

PTPN6 is a key regulatory protein in the control of inflammatory cell signaling, and its knockdown not only increases systemic inflammation in mice, but more importantly, is also implicated in human inflammatory diseases (181). For instance, Th2 cell production and mast cell-specific cytokine production are potentiated in Motheaten mice with a natural mutation in PTPN6. In an OVA-induced model of allergic airway inflammation, eosinophil inflammation, mucus hypersecretion, and airway hyperresponsiveness are enhanced in Motheaten mice, all of which contribute to the development of allergic disease (182). Furthermore, conditional deletion of PTPN6 in neutrophils is sufficient to initiate IL-1 receptor-dependent inflammatory skin diseases. Mechanistically, PTPN6 prevents caspase-8- and Ripk3-Mlkl-dependent cell death and concomitant IL-1α/β release (183).

PTPN7 exerts an anti-inflammatory function by negatively regulating Erk1/2 and p38, which enhance pro-inflammatory tumor necrosis factor (TNF)-production (184).

Intriguingly, PTPN11 holds many functions in distinct cells. PTPN11 protects mice from intestinal inflammation in epithelial cells (185), while promotes colitis and colitis-driven colon cancer in macrophages (186). Mechanistically, PTPN11 impairs IL-10-STAT3 signaling and its dependent anti-inflammatory response in human and mouse macrophages (186). Additionally, PTPN11 promotes the formation of neutrophil extracellular traps (NETs) through the Erk5 pathway, leading to pro-inflammatory cytokines such as TNF-α, IL-1β, IL-6, IL-17A, and CXCL-15, which exacerbate the inflammatory response (187).

Currently, despite extensive research on the mechanisms underlying autoimmune diseases, the fundamental causes remain unknown. Here, the main focus is on the regulatory mechanisms by which PTPN2 and PTPN6 can be involved in autoimmunity. Autoimmunity is characterized by a significant increase associated with antinuclear antibodies, inflammatory cytokines and immunoglobulins. Autoimmunity is exacerbated by PTPN2 deficits in numerous immune lineages, including naive T cells, T follicular helper cells (Tfh), and B cells (188). PTPN6 deficiency in B cells and DC cells promotes B-1a cell development and Th1 cell differentiation, respectively, leading to autoimmune disorders (189, 190). In addition, PTPN6 acts as a key negative regulator in allergic inflammation and allergen-induced anaphylaxis by regulating the function of mast cells (191).

PTPNs are emerging targets for cancer immunotherapy

In recent years, significant progress has been made in the immunotherapy of cancer. With the intensive exploration of immune checkpoints, several PTPN family members have been revealed to possess essential roles in anti-tumor immunity and are promising therapeutic targets.

PTPN1 is elevated in intra-tumor T cells, and knocking it out promotes T cell antitumor activity and chimeric antigen receptor (CAR) T cell efficacy against solid tumors (192). Furthermore, deletion of PTPN1 and PTPN2 in DCs stimulated the growth of IL-12 and IFN-γ, which amplified the IL-12/STAT4/IFN-γ/STAT1/IL-12 positive autocrine loop, boosting the therapeutic potential of mature monocyte-derived dendritic cells (moDCs) in tumor-bearing mice (193).

In several studies, PTPN2 has been proven to be a negative regulator of interferon signaling (194, 195). Lack of PTPN2 in tumor cells enhances immunotherapy efficacy through

augmenting interferon-mediated antigen presentation and growth inhibition (196). What's more, PTPN2 deficiency in T cells boosts the generation of Tim-3$^+$ cells, CD44$^+$ effector/memory T cells, and CD8$^+$ T cell infiltration and cytotoxicity in tumors, as well as the efficacy of *anti-* programmed cell death protein 1 (PD-1) and CAR T cells in solid tumors by promoting activation of Src family kinase LCK and cytokine-induced STAT-5 signaling (195, 197–199), which can actually facilitate tumor control and improve immunotherapy potency.

Furthermore, inhibition of PTPN3 in lymphocytes expands the proportion of tumor-infiltrating lymphocytes and activated lymphocyte cytotoxicity, as well as the anticancer effect on small cell lung cancer (SCLC) and large cell neuroendocrine carcinoma (LCNEC) (200, 201).

PTPN6 shows a negative regulatory effect on the activation of T cells, natural killer (NK) cells and macrophages. However, deletion of PTPN6 significantly strengthens the capacity of these immune cells for tumor killing and promotes anti-tumor immunity (202–204). Of note, a considerable and durable T cell-mediated suppression of tumor growth was observed when PTPN6 knockdown of OT-I T cells was combined with *anti*-PD-1 and cytotoxic T-lymphocyte-associated protein 4 (CTLA-4) immunotherapy (205). And the ability of tumor-associated DCs (TADCs) and MoDCs to take up and process immune complexes (IC) containing tumor antigens bound to antitumor antibody, ultimately inducing anti-tumor immunity *in vivo*, was augmented by simultaneous inhibition of PTPN6 and phosphatases regulating AKT activation (206).

PTPN11, involved in the regulation of tumor and immune cell signaling, is a critical modulator of PD-1 and B and T lymphocyte attenuator (BTLA) immune checkpoint pathways and promising drug target in tumor immunotherapy (207). Inhibition of PTPN11 activity enhances tumor-intrinsic IFN-γ signaling, resulting in increased chemoattractant cytokine release and cytotoxic T cell recruitment, as well as increased expression of major histocompatibility complex (MHC) class I and programmed cell death ligand 1 (PD-L1) on the surface of cancer cells, along with decreased differentiation and suppression of immunosuppressive myeloid cells in the tumor microenvironment (208, 209). In highly aggressive mouse models of breast cancer and melanoma, simultaneous suppression of CSF-1R and PTPN11 to activate macrophages and promote phagocytosis may be an effective strategy for macrophage-based immunotherapy (210). Mechanistically, PTPN11 deletion attenuates CSF-1 receptor signaling, which depletes pro-tumor M2 macrophages while increasing anti-tumor M1 macrophages (211). On the other hand, deletion of PTPN11 enhances macrophage response to IFN-γ and increases production of the tumor cell-derived cytokine CXCL9, thereby promoting tumor infiltration of IFN-γ-producing T cells (212). More importantly, PTPN11 inhibitors combined with immunotherapies, such as *anti*-PD-1/L1, would reverse immunosuppression in the tumor microenvironment (TME) and potentiate the systemic antitumor effect in NSCLC cancer (213, 214).

Currently, research on PTPN22 is not only limited to autoimmune diseases, but more evidence indicates a considerable importance in tumor immunity. Implantation of syngeneic tumors in PTPN22$^{-/-}$ mice resulted in greater infiltration and activation of macrophages, NK cells and T cells, which in turn led to spontaneous tumor regression. More importantly, the combination with anti-PD-1/L1 therapy in the presence of PTPN22 inhibition significantly enhanced the antitumor efficacy (215, 216).

Based on the above findings, PTPN family members still serve as negative regulators in the immune system by restricting the development and differentiation of immune cells to achieve anti-inflammatory and anti-autoimmune responses. But on the other hand, PTPNs could make tumor cells evade immune surveillance.

Non-coding RNAs regulate the role of PTPNs in cancers

A substantial body of evidence has demonstrated that inhibition of some PTPN family members can considerably improve the efficacy of antitumor immunity, and the availability of small molecule inhibitors has given hope. However, drug discovery is an extremely long process, so the search for new therapeutic tools is urgent. The presence of a large number of non-protein-coding RNAs in the human genome and the potential for these non-coding RNAs to affect normal gene expression and disease progression make them a new class of targets for drug discovery (217). Therefore, we present here a comprehensive summary of ncRNAs, including miRNAs, lncRNAs and circRNAs, involved in the regulation of PTPNs in tumors and other diseases (Figure 4).

MicroRNAs are implicated in the regulation of tumorigenesis, progression, metastasis, and drug resistance by targeting PTPNs

Currently, it is widely reported that miRNAs can influence the disease process, especially in cancer, by regulating the expression of PTPN1. In hepatocellular carcinoma, miR-122 and miR-206 target the 3' untranslated region (3' UTR) of PTPN1 mRNA and induce its degradation (218, 219), while miR-125a-5p suppresses PTPN1 expression *via* the MAPK signaling pathway (220), both of which ultimately alleviated the progression of hepatocellular carcinoma. Interestingly, miR-14b reverses the EMT phenotype of cisplatin-resistant lung adenocarcinoma cells by targeting PTPN1 (221). PTPN1 has also been discovered to be a target of numerous miRNAs in

various malignancies. PTPN1 is targeted by miR-542-5p and miR-34c in glioma (222, 223), miR-146b and miR-338-3p in gastric cancer (224, 225), and miR-193a-3p in breast cancer (226). By regulating PTPN1, the miRNAs described above serve as tumor suppressors in cancers. Conversely, by targeting PTPN1, a tumor suppressor in bladder cancer, the miR-130 family (miR-130b, miR-301a, and miR-301b) contributes to cancer development (127).

The previously mentioned PTPN3 can confer chemotherapy resistance and tumor stem cell-like characteristics to ovarian cancer cells, but its expression is regulated by miR-199 (82). What's more, miR-574-5p facilitates phosphorylation of p44/42 MAPKs by targeting PTPN3, thereby promoting angiogenesis in gastric cancer (227).

PTPN4 appears to function as a tumor suppressor in cancer, miR-15b-5p activates STAT3 signaling by targeting PTPN4 to promote oral squamous cell carcinoma progression (228). And miR-183 promotes migration and invasion of $CD133^{+}/CD326^{+}$ lung adenocarcinoma initiating cells by inhibiting PTPN4 (229). Furthermore, miR-34a-5p inhibits ROS-mediated apoptosis in papillary thyroid cancer cells through down-regulation of PTPN4 (230).

The regulation of PTPN6 is primarily mediated by a tiny proportion of miRNAs. Among them, miR-152 indirectly promotes PTPN6 expression to suppress lymphoma growth through down-regulation of DNA methyltransferase 1 (DNMT1) (231). But in nasopharyngeal carcinoma, miR-4649-3p inhibits cell proliferation and miR-378g partially enhances the radiosensitivity of NPC cells both by targeting PTPN6 (232, 233).

PTPN9 exhibits various functions depending on the type of tumor. PTPN9 promotes proliferation and invasion of esophageal cancer cells and non-small cell lung cancer and is negatively regulated by miR-126 and miR-126-3p, respectively (234, 235). But in cervical, breast, colorectal and gastric cancers, PTPN9 functions as a tumor suppressor with an essential role in suppressing tumor proliferation, invasion and migration. However, PTPN9 is targeted by miR-613 and miR-96 in cervical cancer (236–238), miR-96 and miR-24 in breast cancer (239, 240), miR-21 in colorectal cancer (241), and miR-181a-5p in gastric cancer (242).

PTPN11, which is considered an oncogenic factor and a key target for cancer immunotherapy according to several studies, is mediated by several miRNAs. MiR-124 and miR-489 inhibited the progression of renal cell carcinoma and hypopharyngeal squamous cell carcinoma by suppressing the expression of PTPN11, respectively (243, 244). In cutaneous squamous cell carcinoma, miR-204 inhibits STAT3 and facilitates the MAPK signaling pathway, possibly through PTPN11, a direct target of miR-204 (245). In oral squamous cell carcinoma, miR-186 directly binds to 3' UTR of PTPN11 mRNA and inhibits the expression, which suppresses the signaling activity of Erk and AKT that is required for cancer cell growth (246). In hepatocellular carcinoma, miR-186 inhibits self-renewal of hepatocellular carcinoma stem cells and is more sensitive to cisplatin treatment by binding to 3'-UTR of PTPN11 mRNA and

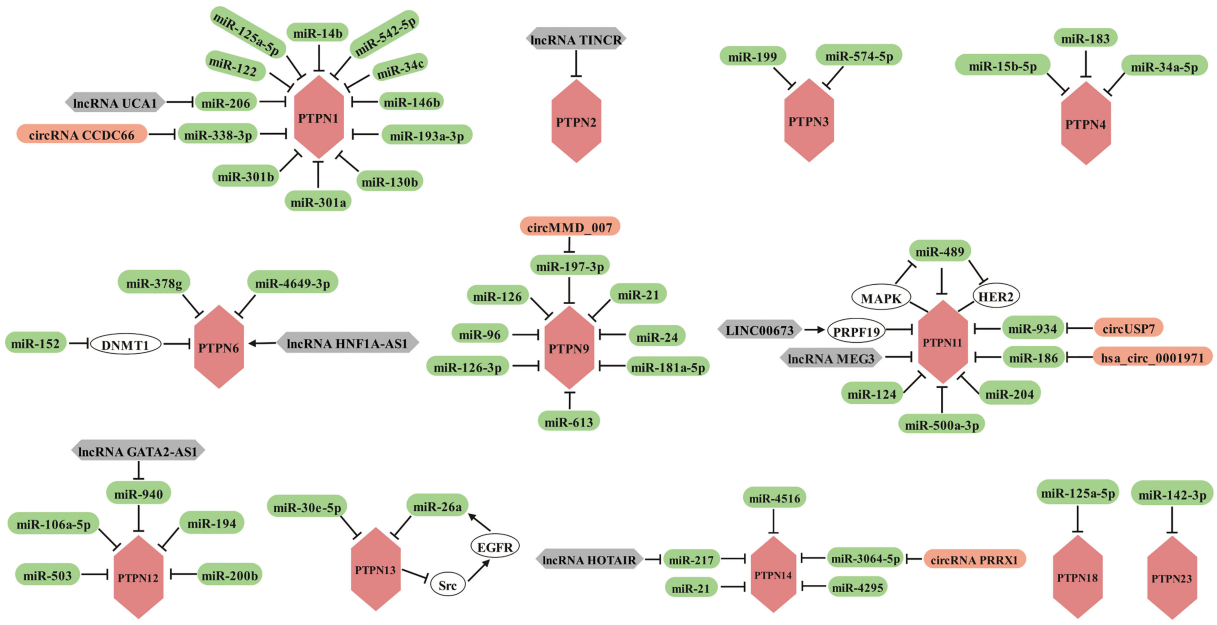

FIGURE 4
Members of the PTPN family are regulated by miRNAs, lncRNAs and circRNAs in various cancers.

reducing its expression (247). However, miR-500a-3p promotes HCC cancer stem cell properties by targeting PTPN11, a negative regulator of the JAK/STAT3 signaling pathway (248). Moreover, HER2 is a direct target of miR-489, overexpression of miR-489 suppresses breast cancer invasion by attenuating HER2-PTPN11-MAPK signaling, which in turn inhibits miR-489, producing a mutually inhibitory loop (249).

PTPN12 suppresses progression of multiple cancers and is negatively controlled by miR-106a-5p in hepatocellular carcinoma (250), miR-503 in retinoblastoma (251), miR-194 in ovarian cancer (252), and miR-200b in colon cancer (253).

MiR-30e-5p promotes lung adenocarcinoma cell growth by targeting PTPN13 and is detrimental to the survival of LUAD patients (254). What's more, miR-26a desensitizes NSCLC cells to tyrosine kinase inhibitors by targeting PTPN13. Mechanistically, miR-26a, which is downstream of EGFR signaling, directly targets and silences PTPN13 to maintain activation of Src, the dephosphorylated substrate of PTPN13, thereby enhancing the EGFR pathway in regulatory circuits (255).

By targeting PTPN14, miR-21 promotes intrahepatic cholangiocarcinoma proliferation and growth *in vitro* and *in vivo* (256), miR-4295 and miR-4516 contribute to the progression of osteosarcoma and glioblastoma, respectively (257, 258). But miR-217 inhibits EMT in gastric cancer (259).

In addition, miR-125a-5p is implicated in imatinib resistance in gastrointestinal stromal tumor (GIST). Mechanistically, overexpression of miR-125a-5p suppresses PTPN18 expression and subsequently enhances phosphorylated FAK (pFAK) expression in GIST cells, which contributes to imatinib resistance in GIST (260, 261).

PTPN23, which features a tumor suppressor function in testicular germ cell tumors, is regulated by miR-142-3p (262).

In light of the fact that almost all miRNAs target and suppress the expression of PTPNs, miRNA modulation combined with immunotherapy may be a novel therapeutic strategy.

LncRNAs and circRNAs regulate the role of PTPNs in cancers in part by sponging miRNAs

In recent years, a growing review of the literature revealed that lncRNA and circRNA appear to play a pivotal role in cancer and hold considerable promise as novel biomarkers and therapeutic targets (263). Next, we illustrate the mechanisms by which lncRNAs and circRNAs modulate PTPN family members, respectively.

PTPN family members have been shown to be regulated by different lncRNAs, including but not limited to lncRNA UCA1, TINCR, HNF1A-AS1, LINC00673, MEG3, GATA2-AS1, and HOTAIR. Specifically, lncRNA UCA1 accelerates the proliferation of breast cancer cells based on the miR-206/PTPN1 axis (264). In hepatocellular carcinoma, lncRNA TINCR interacts directly with and inhibits PTPN2 to promote the proliferation and invasion through activating STAT3 signaling (265). However, lncRNA HNF1A-AS1 reverses the malignancy of hepatocellular carcinoma by enhancing the phosphatase activity of PTPN6 (266). Furthermore, LINC00673 can strengthen the interaction of PTPN11 with PRPF19, an E3 ubiquitin ligase, and promote PTPN11 degradation through ubiquitination, resulting in reduced Src-Erk oncogenic signaling and enhanced STAT1-dependent antitumor response activation (267). PTPN11 can be targeted by lncRNA MEG3, thereby suppressing the proliferation and metastasis of renal cell carcinoma (243). On the basis of the miR-940/PTPN12 axis, lncRNA GATA2-AS1 restrains esophageal squamous cell carcinoma progression (268). In contrast, ectopic expression of lncRNA HOTAIR promotes drug resistance and augments GC cell proliferation and migration by inhibiting miR-217 expression and enhancing PTPN14 expression (269).

CircRNAs with similar regulatory mechanisms to lncRNAs are implicated in the regulation of PTPN family members, namely circRNA CCDC66, circMMD 007, circUSP7, has_circ_0001971, and circPRRX1. CircRNA CCDC66, in particular, promotes osteosarcoma proliferation and metastasis by sponging miR-338-3p to increase PTPN1 expression (270). Likewise, circMMD_007 promotes oncogenic effects in lung adenocarcinoma progression *via* the miR-197-3p/PTPN9 axis (271). CircUSP7 renders NSCLC patients resistant to *anti*-PD1 immunotherapy. Mechanistically, circUSP7 suppresses $CD8^+$ T cell function by sponging miR-934 to up-regulate PTPN11 expression (272). Moreover, hsa_circ_0001971 promotes the proliferation of oral squamous carcinoma cells *via* miR-186/PTPN11 axis (273). Finally, circPRRX1 strengthens doxorubicin resistance in gastric cancer by regulating miR-3064-5p/PTPN14 signaling (274).

Taken together, lncRNAs and circRNAs serve as oncogenic or tumor suppressors and regulate the expression of PTPNs overwhelmingly through sponging miRNA, thereby dominating cancer progression.

Conclusion and perspective

Over the last three decades, a growing series of investigations have been able to conclude that PTPNs perform an essential role in almost all phenotypes of tumor cells. As described previously, there are numerous members of the PTPN family that all exert distinct functions in various malignancies, although they share the same catalytic structural domain. Some PTPNs exploit their structural domains with phosphatase activity to dephosphorylate a variety of oncogenic substrate proteins to achieve activation or inactivation, thereby participating in the regulation of cancer progression. Importantly, some members confer stem cell-like

and EMT characteristics to tumor cells. The functions and signaling pathways regulated by PTPN family members are tissue- and cell-specific, so most PTPNs exert their functions still depend on the type of tumor in which they are located, but a small proportion of members still serve more specific functions, for instance, PTPN11 exerts oncogenic effects, while PTPN13 holds a tumor suppressive role in almost all cancers. Currently, although part of the mechanisms underlying the engagement of PTPN family members in tumors have been elucidated, the understanding of their operational mechanisms is even more challenging and urgent. In the future, a better understanding of the multifunctional and sophisticated regulatory mechanisms of PTPNs may be significant for the development of more specific targeted therapeutic strategies.

What's more, PTPNs also hold critical role in cancer treatment, growing evidence suggested that PTPNs are implicated in chemotherapy and radiotherapy resistance. For instance, PTPN11 confers cisplatin resistance in small cell lung cancer, while PTPN6 promotes radiation resistance in nasopharyngeal carcinoma. Furthermore, inhibiting PTPNs, regardless of immune checkpoint inhibitors or CAR T therapies, can significantly improve the efficacy of immunotherapy. Currently, PTPN11 is the most reported to be associated with tumor immunotherapy and has spawned multiple inhibitors, including but not limited to SHP099 and TN0155, which in combination with *anti*-PD-1 and *anti*-PD-L1 therapies can significantly improve the malignant characteristics of tumors (209, 213, 275). Accordingly, further development of novel PTPNs inhibitors and investigation of the safety of these compounds is urgently need for conquering cancer in future.

Given the special role of PTPNs in cancer progression and immunotherapy, the question about how PTPNs inhibitors can move from the laboratory to rational clinical application should be the next thing to consider. As previously described, PTPNs perform a negative regulatory role in the immune system. Inhibition of PTPNs can activate a variety of immune cells involved in the killing of tumor cells, and also significantly potentiate the efficacy of cancer immunotherapy. In brief, PTPN inhibitors are positive modulators of antitumor immunotherapy. Then regarding the rational use of PTPNs inhibitors there are three situations: first, if PTPN plays a carcinogenic role, the usage of PTPN inhibitors will dramatically enhance the antitumor efficacy by suppressing the carcinogenic properties of PTPN while activating the immune system to combat tumors. Second, if PTPN exerts a tumor suppressive function, the use of PTPN inhibitors needs to be more cautious because it is not clear whether the anti-cancer effect of PTPN itself or the anti-tumor immune effect of PTPN inhibition is stronger, which needs to be further studied in mouse models. Third, there is the issue of the dual-sidedness of PTPN in specific cancers that we mentioned earlier, which requires even more *in vivo* experiments to further explore. Therefore, the rational and accurate clinical use of these inhibitors depends on the individual situation.

As we all know, the inhibitors applied in the clinic must be with high specificity. For the development of PTPN inhibitors, there is still a thorny issue of specificity. Furthermore, designing drug-like inhibitors for PTPNs is challenging due to their highly conserved and positively charged active site structures (276). Hence, the elucidation of the mechanisms regulating PTPNs may become a new therapeutic strategy. Here, we systematically summarize the ncRNAs involved in the regulation of PTPNs as an alternative to developing new inhibitors and propose that ncRNAs, especially miRNAs, in combination with immunotherapy, which may be a promising therapeutic approach to combat tumors.

Author contributions

XT and CQ participated in consolidation of information and writing. HZ and YL guided and supervised this study. All authors contributed to the article and approved the submitted version.

Funding

This work was supported by National Natural Science Foundations of China (81802400, 81902519) and China Postdoctoral Science Foundation (2020M670053). This work was also supported in part by the Postdoctoral Fellowship of Peking-Tsinghua Center for Life Sciences.

Conflict of interest

The authors declare that the research was conducted in the absence of any commercial or financial relationships that could be construed as a potential conflict of interest.

Publisher's note

References

1. Gurzov EN, Stanley WJ, Brodnicki TC, Thomas HE. Protein tyrosine phosphatases: molecular switches in metabolism and diabetes. *Trends Endocrinol Metab* (2015) 26:30–9. doi: 10.1016/j.tem.2014.10.004

2. Alonso A, Sasin J, Bottini N, Friedberg I, Friedberg I, Osterman A, et al. Protein tyrosine phosphatases in the human genome. *CELL* (2004) 117:699–711. doi: 10.1016/j.cell.2004.05.018

3. Hao F, Wang C, Sholy C, Cao M, Kang X. Strategy for leukemia treatment targeting SHP-1,2 and SHIP. *Front Cell Dev Biol* (2021) 9:730400. doi: 10.3389/fcell.2021.730400

4. Spalinger MR, Schwarzfischer M, Scharl M. The role of protein tyrosine phosphatases in inflammasome activation. *Int J Mol Sci* (2020) 21(15):5481. doi: 10.3390/ijms21155481

5. Abdelsalam SS, Korashy HM, Zeidan A, Agouni A. The role of protein tyrosine phosphatase (PTP)-1B in cardiovascular disease and its interplay with insulin resistance. *Biomolecules* (2019) 9(7):286. doi: 10.3390/biom9070286

6. Mustelin T, Vang T, Bottini N. Protein tyrosine phosphatases and the immune response. *Nat Rev Immunol* (2005) 5:43–57. doi: 10.1038/nri1530

7. Pike KA, Tremblay ML. TC-PTP and PTP1B: Regulating JAK-STAT signaling, controlling lymphoid malignancies. *CYTOKINE* (2016) 82:52–7. doi: 10.1016/j.cyto.2015.12.025

8. Roskoski RJ. Src kinase regulation by phosphorylation and dephosphorylation. *Biochem Biophys Res Commun* (2005) 331:1–14. doi: 10.1016/j.bbrc.2005.03.012

9. Kerr DL, Haderk F, Bivona TG. Allosteric SHP2 inhibitors in cancer: Targeting the intersection of RAS, resistance, and the immune microenvironment. *Curr Opin Chem Biol* (2021) 62:1–12. doi: 10.1016/j.cbpa.2020.11.007

10. Anastasiadou E, Jacob LS, Slack FJ. Non-coding RNA networks in cancer. *Nat Rev Cancer* (2018) 18:5–18. doi: 10.1038/nrc.2017.99

11. Wang J, Zhu S, Meng N, He Y, Lu R, Yan GR. ncRNA-encoded peptides or proteins and cancer. *Mol Ther* (2019) 27:1718–25. doi: 10.1016/j.ymthe.2019.09.001

12. Li Y, Li G, Guo X, Yao H, Wang G, Li C. Non-coding RNA in bladder cancer. *Cancer Lett* (2020) 485:38–44. doi: 10.1016/j.canlet.2020.04.023

13. Duval R, Bui LC, Mathieu C, Nian Q, Berthelet J, Xu X, et al. Benzoquinone, a leukemogenic metabolite of benzene, catalytically inhibits the protein tyrosine phosphatase PTPN2 and alters STAT1 signaling. *J Biol Chem* (2019) 294:12483–94. doi: 10.1074/jbc.RA119.008666

14. Yuan T, Ma H, Du Z, Xiong X, Gao H, Fang Z, et al. Shp1 positively regulates EGFR signaling by controlling EGFR protein expression in mammary epithelial cells. *Biochem Biophys Res Commun* (2017) 488:439–44. doi: 10.1016/j.bbrc.2017.04.072

15. Baker SJ, Rane SG, Reddy EP. Hematopoietic cytokine receptor signaling. *ONCOGENE* (2007) 26:6724–37. doi: 10.1038/sj.onc.1210757

16. Dodd GT, Lee-Young RS, Bruning JC, Tiganis T. TCPTP regulates insulin signaling in AgRP neurons to coordinate glucose metabolism with feeding. *DIABETES* (2018) 67:1246–57. doi: 10.2337/db17-1485

17. Fukushima A, Loh K, Galic S, Fam B, Shields B, Wiede F, et al. T-Cell protein tyrosine phosphatase attenuates STAT3 and insulin signaling in the liver to regulate gluconeogenesis. *DIABETES* (2010) 59:1906–14. doi: 10.2337/db09-1365

18. Au AC, Hernandez PA, Lieber E, Nadroo AM, Shen YM, Kelley KA, et al. Protein tyrosine phosphatase PTPN14 is a regulator of lymphatic function and choanal development in humans. *Am J Hum Genet* (2010) 87:436–44. doi: 10.1016/j.ajhg.2010.08.008

19. Cortesio CL, Chan KT, Perrin BJ, Burton NO, Zhang S, Zhang ZY, et al. Calpain 2 and PTP1B function in a novel pathway with src to regulate invadopodia dynamics and breast cancer cell invasion. *J Cell Biol* (2008) 180:957–71. doi: 10.1083/jcb.200708048

20. Liu X, Chen Q, Hu XG, Zhang XC, Fu TW, Liu Q, et al. PTP1B promotes aggressiveness of breast cancer cells by regulating PTEN but not EMT. *Tumour Biol* (2016) 37:13479–87. doi: 10.1007/s13277-016-5245-1

21. Julien SG, Dube N, Read M, Penney J, Paquet M, Han Y, et al. Protein tyrosine phosphatase 1B deficiency or inhibition delays ErbB2-induced mammary tumorigenesis and protects from lung metastasis. *Nat Genet* (2007) 39:338–46. doi: 10.1038/ng1963

22. Zhao H, Martin E, Matalkah F, Shah N, Ivanov A, Ruppert JM, et al. Conditional knockout of SHP2 in ErbB2 transgenic mice or inhibition in HER2-amplified breast cancer cell lines blocks oncogene expression and tumorigenesis. *ONCOGENE* (2019) 38:2275–90. doi: 10.1038/s41388-018-0574-8

23. Sun X, Zhang J, Wang Z, Ji W, Tian R, Zhang F, et al. Shp2 plays a critical role in IL-6-Induced EMT in breast cancer cells. *Int J Mol Sci* (2017) 18(2):395. doi: 10.3390/ijms18020395

24. Zhang L, Yuan C, Peng J, Zhou L, Jiang Y, Lin Y, et al. SHP-2-Mediated upregulation of ZEB1 is important for PDGF-B-Induced cell proliferation and metastatic phenotype in triple negative breast cancer. *Front Oncol* (2020) 10:1230. doi: 10.3389/fonc.2020.01230

25. Martin E, Agazie YM. SHP2 potentiates the oncogenic activity of beta-catenin to promote triple-negative breast cancer. *Mol Cancer Res* (2021) 19:1946–56. doi: 10.1158/1541-7786.MCR-21-0060

26. Sausgruber N, Coissieux MM, Britschgi A, Wyckoff J, Aceto N, Leroy C, et al. Tyrosine phosphatase SHP2 increases cell motility in triple-negative breast cancer through the activation of SRC-family kinases. *ONCOGENE* (2015) 34:2272–8. doi: 10.1038/onc.2014.170

27. Hartman ZR, Schaller MD, Agazie YM. The tyrosine phosphatase SHP2 regulates focal adhesion kinase to promote EGF-induced lamellipodia persistence and cell migration. *Mol Cancer Res* (2013) 11:651–64. doi: 10.1158/1541-7786.MCR-12-0578

28. Veenstra C, Karlsson E, Mirwani SM, Nordenskjold B, Fornander T, Perez-Tenorio G, et al. The effects of PTPN2 loss on cell signalling and clinical outcome in relation to breast cancer subtype. *J Cancer Res Clin Oncol* (2019) 145:1845–56. doi: 10.1007/s00432-019-02918-y

29. Karlsson E, Veenstra C, Emin S, Dutta C, Perez-Tenorio G, Nordenskjold B, et al. Loss of protein tyrosine phosphatase, non-receptor type 2 is associated with activation of AKT and tamoxifen resistance in breast cancer. *Breast Cancer Res Treat* (2015) 153:31–40. doi: 10.1007/s10549-015-3516-y

30. Shields BJ, Wiede F, Gurzov EN, Wee K, Hauser C, Zhu HJ, et al. TCPTP regulates SFK and STAT3 signaling and is lost in triple-negative breast cancers. *Mol Cell Biol* (2013) 33:557–70. doi: 10.1128/MCB.01016-12

31. Liu CY, Chen KF, Chao TI, Chu PY, Huang CT, Huang TT, et al. Sequential combination of docetaxel with a SHP-1 agonist enhanced suppression of p-STAT3 signaling and apoptosis in triple negative breast cancer cells. *J Mol Med (Berl)* (2017) 95:965–75. doi: 10.1007/s00109-017-1549-x

32. Geng Q, Xian R, Yu Y, Chen F, Li R. SHP-1 acts as a tumor suppressor by interacting with EGFR and predicts the prognosis of human breast cancer. *Cancer Biol Med* (2021) 19(4):468–485. doi: 10.20892/j.issn.2095-3941.2020.0501

33. Yuan T, Wang Y, Zhao ZJ, Gu H. Protein-tyrosine phosphatase PTPN9 negatively regulates ErbB2 and epidermal growth factor receptor signaling in breast cancer cells. *J Biol Chem* (2010) 285:14861–70. doi: 10.1074/jbc.M109.099879

34. Su F, Ren F, Rong Y, Wang Y, Geng Y, Wang Y, et al. Protein tyrosine phosphatase Meg2 dephosphorylates signal transducer and activator of transcription 3 and suppresses tumor growth in breast cancer. *Breast Cancer Res* (2012) 14:R38. doi: 10.1186/bcr3134

35. Wang D, Wang S, Chen L, He D, Han S, Huang B, et al. The correlation of PTPN4 expression with prognosis in breast cancer. *Int J Clin Exp Pathol* (2018) 11:4845–53.

36. Revillion F, Puech C, Rabenoelina F, Chalbos D, Peyrat JP, Freiss G. Expression of the putative tumor suppressor gene PTPN13/PTPL1 is an independent prognostic marker for overall survival in breast cancer. *Int J Cancer* (2009) 124:638–43. doi: 10.1002/ijc.23989

37. Bompard G, Puech C, Prebois C, Vignon F, Freiss G. Protein-tyrosine phosphatase PTPL1/FAP-1 triggers apoptosis in human breast cancer cells. *J Biol Chem* (2002) 277:47861–9. doi: 10.1074/jbc.M208950200

38. Glondu-Lassis M, Dromard M, Lacroix-Triki M, Nirde P, Puech C, Knani D, et al. PTPL1/PTPN13 regulates breast cancer cell aggressiveness through direct inactivation of src kinase. *Cancer Res* (2010) 70:5116–26. doi: 10.1158/0008-5472.CAN-09-4368

39. Hamyeh M, Bernex F, Larive RM, Naldi A, Urbach S, Simony-Lafontaine J, et al. PTPN13 induces cell junction stabilization and inhibits mammary tumor invasiveness. *THERANOSTICS* (2020) 10:1016–32. doi: 10.7150/thno.38537

40. Liu X, Yang N, Figel SA, Wilson KE, Morrison CD, Gelman IH, et al. PTPN14 interacts with and negatively regulates the oncogenic function of YAP. *ONCOGENE* (2013) 32:1266–73. doi: 10.1038/onc.2012.147

41. Belle L, Ali N, Lonic A, Li X, Paltridge JL, Roslan S, et al. The tyrosine phosphatase PTPN14 (Pez) inhibits metastasis by altering protein trafficking. *Sci Signal* (2015) 8:a18. doi: 10.1126/scisignal.2005547

42. Zhang S, Fan G, Hao Y, Hammell M, Wilkinson JE, Tonks NK. Suppression of protein tyrosine phosphatase N23 predisposes to breast tumorigenesis *via* activation of FYN kinase. *Genes Dev* (2017) 31:1939–57. doi: 10.1101/gad.304261.117

43. Liu H, Wu Y, Zhu S, Liang W, Wang Z, Wang Y, et al. PTP1B promotes cell proliferation and metastasis through activating src and ERK1/2 in non-small cell lung cancer. *Cancer Lett* (2015) 359:218–25. doi: 10.1016/j.canlet.2015.01.020

44. Mainardi S, Mulero-Sanchez A, Prahallad A, Germano G, Bosma A, Krimpenfort P, et al. SHP2 is required for growth of KRAS-mutant non-small-cell lung cancer *in vivo*. *Nat Med* (2018) 24:961–7. doi: 10.1038/s41591-018-0023-9

45. Sun YJ, Zhuo ZL, Xian HP, Chen KZ, Yang F, Zhao XT. Shp2 regulates migratory behavior and response to EGFR-TKIs through ERK1/2 pathway activation in non-small cell lung cancer cells. *Oncotarget* (2017) 8:91123–33. doi: 10.18632/oncotarget.20249

46. Xia L, Yang F, Wu X, Li S, Kan C, Zheng H, et al. SHP2 inhibition enhances the anticancer effect of osimertinib in EGFR T790M mutant lung adenocarcinoma by blocking CXCL8 loop mediated stemness. *Cancer Cell Int* (2021) 21:337. doi: 10.1186/s12935-021-02056-x

47. Yang X, Tang C, Luo H, Wang H, Zhou X. Shp2 confers cisplatin resistance in small cell lung cancer *via* an AKT-mediated increase in CA916798. *Oncotarget* (2017) 8:23664–74. doi: 10.18632/oncotarget.15641

48. Tang C, Luo H, Luo D, Yang H, Zhou X. Src homology phosphotyrosyl phosphatase 2 mediates cisplatin-related drug resistance by inhibiting apoptosis and activating the Ras/PI3K/Akt1/survivin pathway in lung cancer cells. *Oncol Rep* (2018) 39:611–8. doi: 10.3892/or.2017.6109

49. Li MY, Peng WH, Wu CH, Chang YM, Lin YL, Chang GD, et al. PTPN3 suppresses lung cancer cell invasiveness by counteracting src-mediated DAAM1 activation and actin polymerization. *ONCOGENE* (2019) 38:7002–16. doi: 10.1038/s41388-019-0948-6

50. Li MY, Lai PL, Chou YT, Chi AP, Mi YZ, Khoo KH, et al. Protein tyrosine phosphatase PTPN3 inhibits lung cancer cell proliferation and migration by promoting EGFR endocytic degradation. *ONCOGENE* (2015) 34:3791–803. doi: 10.1038/onc.2014.312

51. Chi D, Wang D, Zhang M, Ma H, Chen F, Sun Y. CLEC12B suppresses lung cancer progression by inducing SHP-1 expression and inactivating the PI3K/AKT signaling pathway. *Exp Cell Res* (2021) 409:112914. doi: 10.1016/j.yexcr.2021.112914

52. Cao X, Chen YZ, Luo RZ, Zhang L, Zhang SL, Zeng J, et al. Tyrosine-protein phosphatase non-receptor type 12 expression is a good prognostic factor in resectable non-small cell lung cancer. *Oncotarget* (2015) 6:11704–13. doi: 10.18632/oncotarget.3588

53. Scrima M, De Marco C, De Vita F, Fabiani F, Franco R, Pirozzi G, et al. The nonreceptor-type tyrosine phosphatase PTPN13 is a tumor suppressor gene in non-small cell lung cancer. *Am J Pathol* (2012) 180:1202–14. doi: 10.1016/j.ajpath.2011.11.038

54. Zhu N, Zhang XJ, Zou H, Zhang YY, Xia JW, Zhang P, et al. PTPL1 suppresses lung cancer cell migration *via* inhibiting TGF-beta1-induced activation of p38 MAPK and smad 2/3 pathways and EMT. *Acta Pharmacol Sin* (2021) 42:1280–7. doi: 10.1038/s41401-020-00596-y

55. Hoekstra E, Das AM, Swets M, Cao W, van der Woude CJ, Bruno MJ, et al. Increased PTP1B expression and phosphatase activity in colorectal cancer results in a more invasive phenotype and worse patient outcome. *Oncotarget* (2016) 7:21922–38. doi: 10.18632/oncotarget.7829

56. Zhu S, Bjorge JD, Fujita DJ. PTP1B contributes to the oncogenic properties of colon cancer cells through src activation. *Cancer Res* (2007) 67:10129–37. doi: 10.1158/0008-5472.CAN-06-4338

57. Chen J, Zhao X, Yuan Y, Jing JJ. The expression patterns and the diagnostic/prognostic roles of PTPN family members in digestive tract cancers. *Cancer Cell Int* (2020) 20:238. doi: 10.1186/s12935-020-01315-7

58. Spalinger MR, Manzini R, Hering L, Riggs JB, Gottier C, Lang S, et al. PTPN2 regulates inflammasome activation and controls onset of intestinal inflammation and colon cancer. *Cell Rep* (2018) 22:1835–48. doi: 10.1016/j.celrep.2018.01.052

59. Li C, Li SZ, Huang XC, Chen J, Liu W, Zhang XD, et al. PTPN18 promotes colorectal cancer progression by regulating the c-MYC-CDK4 axis. *Genes Dis* (2021) 8:838–48. doi: 10.1016/j.gendis.2020.08.001

60. Zhang BD, Li YR, Ding LD, Wang YY, Liu HY, Jia BQ. Loss of PTPN4 activates STAT3 to promote the tumor growth in rectal cancer. *Cancer Sci* (2019) 110:2258–72. doi: 10.1111/cas.14031

61. Fan LC, Teng HW, Shiau CW, Lin H, Hung MH, Chen YL, et al. SHP-1 is a target of regorafenib in colorectal cancer. *Oncotarget* (2014) 5:6243–51. doi: 10.18632/oncotarget.2191

62. Wang D, Cheng Z, Zhao M, Jiao C, Meng Q, Pan H, et al. PTPN9 induces cell apoptosis by mitigating the activation of Stat3 and acts as a tumor suppressor in colorectal cancer. *Cancer MANAG Res* (2019) 11:1309–19. doi: 10.2147/CMAR.S187001

63. Fang H, Ma W, Guo X, Wang J. PTPN6 promotes chemosensitivity of colorectal cancer cells via inhibiting the SP1/MAPK signalling pathway. *Cell Biochem Funct* (2021) 39:392–400. doi: 10.1002/cbf.3604

64. van der Lely L, Hafliger J, Montalban-Arques A, Babler K, Schwarzfischer M, Sabev M, et al. Loss of PTPN23 promotes proliferation and epithelial-to-Mesenchymal transition in human intestinal cancer cells. *Inflammation Intest Dis* (2019) 4:161–73. doi: 10.1159/000502861

65. Xiang D, Cheng Z, Liu H, Wang X, Han T, Sun W, et al. Shp2 promotes liver cancer stem cell expansion by augmenting beta-catenin signaling and predicts chemotherapeutic response of patients. *HEPATOLOGY* (2017) 65:1566–80. doi: 10.1002/hep.28919

66. Liu JJ, Li Y, Chen WS, Liang Y, Wang G, Zong M, et al. Shp2 deletion in hepatocytes suppresses hepatocarcinogenesis driven by oncogenic beta-catenin, PIK3CA and MET. *J Hepatol* (2018) 69:79–88. doi: 10.1016/j.jhep.2018.02.014

67. Grohmann M, Wiede F, Dodd GT, Gurzov EN, Ooi GJ, Butt T, et al. (2018) 175:1289–306.

68. Wen LZ, Ding K, Wang ZR, Ding CH, Lei SJ, Liu JP, et al. SHP-1 acts as a tumor suppressor in hepatocarcinogenesis and HCC progression. *Cancer Res* (2018) 78:4680–91. doi: 10.1158/0008-5472.CAN-17-3896

69. Ying D, Ruan Y, Zhou X. MEG2 inhibits the growth and metastasis of hepatocellular carcinoma by inhibiting AKT pathway. *GENE* (2019) 687:1–8. doi: 10.1016/j.gene.2018.11.003

70. Yan Y, Huang P, Mao K, He C, Xu Q, Zhang M, et al. Anti-oncogene PTPN13 inactivation by hepatitis b virus X protein counteracts IGF2BP1 to promote hepatocellular carcinoma progression. *ONCOGENE* (2021) 40:28–45. doi: 10.1038/s41388-020-01498-3

71. Zhang D, Wu F, Song J, Meng M, Fan X, Lu C, et al. A role for the NPM1/PTPN14/YAP axis in mediating hypoxia-induced chemoresistance to sorafenib in hepatocellular carcinoma. *Cancer Cell Int* (2022) 22:65. doi: 10.1186/s12935-022-02479-0

72. Wang H, Peng S, Cai J, Bao S. Silencing of PTPN18 induced ferroptosis in endometrial cancer cells through p-P38-Mediated GPX4/xCT down-regulation. *Cancer MANAG Res* (2021) 13:1757–65. doi: 10.2147/CMAR.S278728

73. Cao M, Gao D, Zhang N, Duan Y, Wang Y, Mujtaba H, et al. Shp2 expression is upregulated in cervical cancer, and Shp2 contributes to cell growth and migration and reduces sensitivity to cisplatin in cervical cancer cells. *Pathol Res Pract* (2019) 215:152621. doi: 10.1016/j.prp.2019.152621

74. Meng F, Zhao X, Zhang S. SHP-2 phosphatase promotes cervical cancer cell proliferation through inhibiting interferon-beta production. *J Obstet Gynaecol Res* (2013) 39:272–9. doi: 10.1111/j.1447-0756.2012.01952.x

75. Yan D, Zhu D, Zhao X, Su J. SHP-2 restricts apoptosis induced by chemotherapeutic agents *via* parkin-dependent autophagy in cervical cancer. *Cancer Cell Int* (2018) 18:8. doi: 10.1186/s12935-018-0505-3

76. Cai J, Huang S, Yi Y, Bao S. Downregulation of PTPN18 can inhibit proliferation and metastasis and promote apoptosis of endometrial cancer. *Clin Exp Pharmacol Physiol* (2019) 46:734–42. doi: 10.1111/1440-1681.13098

77. Yun HY, Kim MW, Lee HS, Kim W, Shin JH, Kim H, et al. Structural basis for recognition of the tumor suppressor protein PTPN14 by the oncoprotein E7 of human papillomavirus. *PloS Biol* (2019) 17:e3000367. doi: 10.1371/journal.pbio.3000367

78. White EA, Munger K, Howley PM. High-risk human papillomavirus E7 proteins target PTPN14 for degradation. *MBIO* (2016) 7(5):e01530-16. doi: 10.1128/mBio.01530-16

79. Hatterschide J, Bohidar AE, Grace M, Nulton TJ, Kim HW, Windle B, et al. PTPN14 degradation by high-risk human papillomavirus E7 limits keratinocyte differentiation and contributes to HPV-mediated oncogenesis. *Proc Natl Acad Sci U.S.A.* (2019) 116:7033–42. doi: 10.1073/pnas.1819534116

80. Wang W, Cao Y, Zhou X, Wei B, Zhang Y, Liu X. PTP1B promotes the malignancy of ovarian cancer cells in a JNK-dependent mechanism. *Biochem Biophys Res Commun* (2018) 503:903–9. doi: 10.1016/j.bbrc.2018.06.094

81. Mok SC, Kwok TT, Berkowitz RS, Barrett AJ, Tsui FW. Overexpression of the protein tyrosine phosphatase, nonreceptor type 6 (PTPN6), in human epithelial ovarian cancer. *GYNECOL Oncol* (1995) 57:299–303. doi: 10.1006/gyno.1995.1146

82. Li S, Cao J, Zhang W, Zhang F, Ni G, Luo Q, et al. Protein tyrosine phosphatase PTPN3 promotes drug resistance and stem cell-like characteristics in ovarian cancer. *Sci Rep* (2016) 6:36873. doi: 10.1038/srep36873

83. Hu Z, Li J, Gao Q, Wei S, Yang B. SHP2 overexpression enhances the invasion and metastasis of ovarian cancer *in vitro* and in vivo. *Onco Targets Ther* (2017) 10:3881–91. doi: 10.2147/OTT.S138833

84. Mao N, Li H, Yang H, Su J, Liang Z, He G. PTPN18 stimulates the development of ovarian cancer by activating the PI3K/AKT signaling. *Evid Based Complement Alternat Med* (2022) 2022:1091042. doi: 10.1155/2022/1091042

85. D'Hondt V, Lacroix-Triki M, Jarlier M, Boissiere-Michot F, Puech C, Coopman P, et al. High PTPN13 expression in high grade serous ovarian carcinoma is associated with a better patient outcome. *Oncotarget* (2017) 8:95662–73. doi: 10.18632/oncotarget.21175

86. Zhu JH, Chen R, Yi W, Cantin GT, Fearns C, Yang Y, et al. Protein tyrosine phosphatase PTPN13 negatively regulates Her2/ErbB2 malignant signaling. *ONCOGENE* (2008) 27:2525–31. doi: 10.1038/sj.onc.1210922

87. Wang Y, Li M, Huang T, Li J. Protein tyrosine phosphatase L1 inhibits high-grade serous ovarian carcinoma progression by targeting IkappaBalpha. *Onco Targets Ther* (2018) 11:7603–12. doi: 10.2147/OTT.S167106

88. Lessard L, Labbe DP, Deblois G, Begin LR, Hardy S, Mes-Masson AM, et al. PTP1B is an androgen receptor-regulated phosphatase that promotes the progression of prostate cancer. *Cancer Res* (2012) 72:1529–37. doi: 10.1158/0008-5472.CAN-11-2602

89. Weidemann SA, Sauer C, Luebke AM, Moller-Koop C, Steurer S, Hube-Magg C, et al. High-level expression of protein tyrosine phosphatase non-receptor 12 is a strong and independent predictor of poor prognosis in prostate cancer. *BMC Cancer* (2019) 19:944. doi: 10.1186/s12885-019-6182-3

90. Zhang K, Zhao H, Ji Z, Zhang C, Zhou P, Wang L, et al. Shp2 promotes metastasis of prostate cancer by attenuating the PAR3/PAR6/aPKC polarity protein complex and enhancing epithelial-to-mesenchymal transition. *ONCOGENE* (2016) 35:1271–82. doi: 10.1038/onc.2015.184

91. Castilla C, Chinchon D, Medina R, Torrubia FJ, Japon MA, Saez C. PTPL1 and PKCdelta contribute to proapoptotic signalling in prostate cancer cells. *Cell Death Dis* (2013) 4:e576. doi: 10.1038/cddis.2013.90

92. Wang R, Du Y, Shang J, Dang X, Niu G. PTPN14 acts as a candidate tumor suppressor in prostate cancer and inhibits cell proliferation and invasion through modulating LATS1/YAP signaling. *Mol Cell Probes* (2020) 53:101642. doi: 10.1016/j.mcp.2020.101642

93. Jin T, Li D, Yang T, Liu F, Kong J, Zhou Y. PTPN1 promotes the progression of glioma by activating the MAPK/ERK and PI3K/AKT pathways and is associated with poor patient survival. *Oncol Rep* (2019) 42:717–25. doi: 10.3892/or.2019.7180

94. Wang PF, Cai HQ, Zhang CB, Li YM, Liu X, Wan JH, et al. Molecular and clinical characterization of PTPN2 expression from RNA-seq data of 996 brain gliomas. *J Neuroinflamm* (2018) 15:145. doi: 10.1186/s12974-018-1187-4

95. Bartolome RA, Martin-Regalado A, Jaen M, Zannikou M, Zhang P, de Los RV, et al. Protein tyrosine phosphatase-1B inhibition disrupts IL13Ralpha2-promoted invasion and metastasis in cancer cells. *Cancers (Basel)* (2020) 12 (2):500. doi: 10.3390/cancers12020500

96. Wu L, Wang F, Xu J, Chen Z. PTPN2 induced by inflammatory response and oxidative stress contributed to glioma progression. *J Cell Biochem* (2019) 120:19044–51. doi: 10.1002/jcb.29227

97. Roccograndi L, Binder ZA, Zhang L, Aceto N, Zhang Z, Bentires-Alj M, et al. SHP2 regulates proliferation and tumorigenicity of glioma stem cells. *J Neurooncol* (2017) 135:487–96. doi: 10.1007/s11060-017-2610-x

98. Wang Y, Su Y, Ji Z, Lv Z. High expression of PTPN3 predicts progression and unfavorable prognosis of glioblastoma. *Med Sci Monit* (2018) 24:7556–62. doi: 10.12659/MSM.911531

99. Liu KW, Feng H, Bachoo R, Kazlauskas A, Smith EM, Symes K, et al. SHP-2/PTPN11 mediates gliomagenesis driven by PDGFRA and INK4A/ARF aberrations in mice and humans. *J Clin Invest* (2011) 121:905–17. doi: 10.1172/JCI43690

100. Furcht CM, Buonato JM, Skuli N, Mathew LK, Munoz RA, Simon MC, et al. Multivariate signaling regulation by SHP2 differentially controls proliferation and therapeutic response in glioma cells. *J Cell Sci* (2014) 127:3555–67. doi: 10.1242/jcs.150862

101. Yao TW, Zhang J, Prados M, Weiss WA, James CD, Nicolaides T. EGFR blockade prevents glioma escape from BRAFV600E targeted therapy. *Oncotarget* (2015) 6:21993–2005. doi: 10.18632/oncotarget.4014

102. Chen Z, Morales JE, Guerrero PA, Sun H, McCarty JH. PTPN12/PTP-PEST regulates phosphorylation-dependent ubiquitination and stability of focal adhesion substrates in invasive glioblastoma cells. *Cancer Res* (2018) 78:3809–22. doi: 10.1158/0008-5472.CAN-18-0085

103. Liu L, Zhang S, Liu X, Liu J. Aberrant promoter 2 methylationmediated downregulation of protein tyrosine phosphatase, nonreceptor type 6, is associated with progression of esophageal squamous cell carcinoma. *Mol Med Rep* (2019) 19:3273–82. doi: 10.3892/mmr.2019.9971

104. Cao X, Li Y, Luo RZ, He LR, Yang J, Zeng MS, et al. Tyrosine-protein phosphatase nonreceptor type 12 is a novel prognostic biomarker for esophageal squamous cell carcinoma. *Ann Thorac Surg* (2012) 93:1674–80. doi: 10.1016/j.athoracsur.2011.12.056

105. Qi C, Han T, Tang H, Huang K, Min J, Li J, et al. Shp2 inhibits proliferation of esophageal squamous cell cancer *via* dephosphorylation of Stat3. *Int J Mol Sci* (2017) 18(1):134. doi: 10.3390/ijms18010134

106. Lu Y, Wang Z, Zhou L, Ma Z, Zhang J, Wu Y, et al. FAT1 and PTPN14 regulate the malignant progression and chemotherapy resistance of esophageal cancer through the hippo signaling pathway. *Anal Cell Pathol (Amst)* (2021) 2021:9290372. doi: 10.1155/2021/9290372

107. Wang J, Chen X, Liu B, Zhu Z. Suppression of PTP1B in gastric cancer cells *in vitro* induces a change in the genome-wide expression profile and inhibits gastric cancer cell growth. *Cell Biol Int* (2010) 34:747–53. doi: 10.1042/CBI20090447

108. Wang J, Liu B, Chen X, Su L, Wu P, Wu J, et al. PTP1B expression contributes to gastric cancer progression. *Med Oncol* (2012) 29:948–56. doi: 10.1007/s12032-011-9911-2

109. Wang N, She J, Liu W, Shi J, Yang Q, Shi B, et al. Frequent amplification of PTP1B is associated with poor survival of gastric cancer patients. *Cell Cycle* (2015) 14:732–43. doi: 10.1080/15384101.2014.998047

110. Jiang J, Jin MS, Kong F, Wang YP, Jia ZF, Cao DH, et al. Increased expression of tyrosine phosphatase SHP-2 in helicobacter pylori-infected gastric cancer. *World J Gastroenterol* (2013) 19:575–80. doi: 10.3748/wjg.v19.i4.575

111. Yamazaki S, Yamakawa A, Ito Y, Ohtani M, Higashi H, Hatakeyama M, et al. The CagA protein of helicobacter pylori is translocated into epithelial cells and binds to SHP-2 in human gastric mucosa. *J Infect Dis* (2003) 187:334–7. doi: 10.1086/367807

112. Fujii Y, Murata-Kamiya N, Hatakeyama M. Helicobacter pylori CagA oncoprotein interacts with SHIP2 to increase its delivery into gastric epithelial cells. *Cancer Sci* (2020) 111:1596–606. doi: 10.1111/cas.14391

113. Han X, Sun T, Hong J, Wei R, Dong Y, Huang D, et al. Nonreceptor tyrosine phosphatase 14 promotes proliferation and migration through regulating phosphorylation of YAP of hippo signaling pathway in gastric cancer cells. *J Cell Biochem* (2019) 120:17723–30. doi: 10.1002/jcb.29038

114. Kim SH, Yoo HS, Joo MK, Kim T, Park JJ, Lee BJ, et al. Arsenic trioxide attenuates STAT-3 activity and epithelial-mesenchymal transition through induction of SHP-1 in gastric cancer cells. *BMC Cancer* (2018) 18:150. doi: 10.1186/s12885-018-4071-9

115. Wang HC, Chiang WF, Huang HH, Shen YY, Chiang HC. Src-homology 2 domain-containing tyrosine phosphatase 2 promotes oral cancer invasion and metastasis. *BMC Cancer* (2014) 14:442. doi: 10.1186/1471-2407-14-442

116. Su Z, Tian H, Song HQ, Zhang R, Deng AM, Liu HW. PTPN12 inhibits oral squamous epithelial carcinoma cell proliferation and invasion and can be used as a prognostic marker. *Med Oncol* (2013) 30:618. doi: 10.1007/s12032-013-0618-4

117. Sun Z, Pan X, Zou Z, Ding Q, Wu G, Peng G. Increased SHP-1 expression results in radioresistance, inhibition of cellular senescence, and cell cycle redistribution in nasopharyngeal carcinoma cells. *Radiat Oncol* (2015) 10:152. doi: 10.1186/s13014-015-0445-1

118. Lin Q, Wang H, Lin X, Zhang W, Huang S, Zheng Y. PTPN12 affects nasopharyngeal carcinoma cell proliferation and migration through regulating EGFR. *Cancer Biother Radiopharm* (2018) 33:60–4. doi: 10.1089/cbr.2017.2254

119. Wang Q, Pan Y, Zhao L, Qi F, Liu J. Protein tyrosine phosphatase 1B (PTP1B) promotes melanoma cells progression through src activation. *Bioengineered* (2021) 12:8396–406. doi: 10.1080/21655979.2021.1988376

120. Liu J, Luan W, Zhang Y, Gu J, Shi Y, Yang Y, et al. HDAC6 interacts with PTPN1 to enhance melanoma cells progression. *Biochem Biophys Res Commun* (2018) 495:2630–6. doi: 10.1016/j.bbrc.2017.12.145

121. Diaz-Valdivia NI, Diaz J, Contreras P, Campos A, Rojas-Celis V, Burgos-Ravanal RA, et al. The non-receptor tyrosine phosphatase type 14 blocks caveolin-1-enhanced cancer cell metastasis. *Oncogene* (2020) 39:3693–709. doi: 10.1038/s41388-020-1242-3

122. Tsai WC, Chen CL, Chen HC. Protein tyrosine phosphatase SHP2 promotes invadopodia formation through suppression of rho signaling. *Oncotarget* (2015) 6:23845–56. doi: 10.18632/oncotarget.4313

123. Hoover AC, Strand GL, Nowicki PN, Anderson ME, Vermeer PD, Klingelhutz AJ, et al. Impaired PTPN13 phosphatase activity in spontaneous or HPV-induced squamous cell carcinomas potentiates oncogene signaling through the MAP kinase pathway. *Oncogene* (2009) 28:3960–70. doi: 10.1038/onc.2009.251

124. Peng XS, Yang JP, Qiang YY, Sun R, Cao Y, Zheng LS, et al. PTPN3 inhibits the growth and metastasis of clear cell renal cell carcinoma *via* inhibition of PI3K/AKT signaling. *Mol Cancer Res* (2020) 18:903–12. doi: 10.1158/1541-7786.MCR-19-1142

125. Long Q, Sun J, Lv J, Liang Y, Li H, Li X. PTPN13 acts as a tumor suppressor in clear cell renal cell carcinoma by inactivating akt signaling. *Exp Cell Res* (2020) 396:112286. doi: 10.1016/j.yexcr.2020.112286

126. Piao YR, Jin ZH. Protein tyrosine phosphatase nonreceptor type 12 suppresses the proliferation of renal cell carcinoma by inhibiting the activity of the PI3K/mTOR pathway. *J Buon* (2015) 20:1258–66.

127. Monoe Y, Jingushi K, Kawase A, Hirono T, Hirose R, Nakatsuji Y, et al. Pharmacological inhibition of miR-130 family suppresses bladder tumor growth by targeting various oncogenic pathways *via* PTPN1. *Int J Mol Sci* (2021) 22(9):4751. doi: 10.3390/ijms22094751

128. Piao Y, Liu X, Lin Z, Jin Z, Jin X, Yuan K, et al. Decreased expression of protein tyrosine phosphatase non-receptor type 12 is involved in the proliferation and recurrence of bladder transitional cell carcinoma. *Oncol Lett* (2015) 10:1620–6. doi: 10.3892/ol.2015.3454

129. Mariotti M, Castiglioni S, Maier JA. Inhibition of T24 human bladder carcinoma cell migration by RNA interference suppressing the expression of HD-PTP. *Cancer Lett* (2009) 273:155–63. doi: 10.1016/j.canlet.2008.08.017

130. Gao Q, Zhao YJ, Wang XY, Guo WJ, Gao S, Wei L, et al. Activating mutations in PTPN3 promote cholangiocarcinoma cell proliferation and migration

and are associated with tumor recurrence in patients. *Gastroenterology* (2014) 146:1397–407. doi: 10.1053/j.gastro.2014.01.062

131. Sun R, Chen T, Li M, Liu Z, Qiu B, Li Z, et al. PTPN3 suppresses the proliferation and correlates with favorable prognosis of perihilar cholangiocarcinoma by inhibiting AKT phosphorylation. *BioMed Pharmacother* (2020) 121:109583. doi: 10.1016/j.biopha.2019.109583

132. Xu Q, Wu N, Li X, Guo C, Li C, Jiang B, et al. Inhibition of PTP1B blocks pancreatic cancer progression by targeting the PKM2/AMPK/mTOC1 pathway. *Cell Death Dis* (2019) 10:874. doi: 10.1038/s41419-019-2073-4

133. Kuang W, Wang X, Ding J, Li J, Ji M, Chen W, et al. PTPN2, a key predictor of prognosis for pancreatic adenocarcinoma, significantly regulates cell cycles, apoptosis, and metastasis. *Front Immunol* (2022) 13:805311. doi: 10.3389/fimmu.2022.805311

134. Yang HJ, Yu G, Wang Y, Guo X. Inflammatory response or oxidative stress induces upregulation of PTPN2 and thus promotes the progression of laryngocarcinoma. *Eur Rev Med Pharmacol Sci* (2020) 24:4314–9. doi: 10.26355/eurrev_202004_21012

135. Zhang Z, Xu T, Qin W, Huang B, Chen W, Li S, et al. Upregulated PTPN2 induced by inflammatory response or oxidative stress stimulates the progression of thyroid cancer. *Biochem Biophys Res Commun* (2020) 522:21–5. doi: 10.1016/j.bbrc.2019.11.047

136. Gu J, Han T, Ma RH, Zhu YL, Jia YN, Du JJ, et al. SHP2 promotes laryngeal cancer growth through the Ras/Raf/Mek/Erk pathway and serves as a prognostic indicator for laryngeal cancer. *Int J Oncol* (2014) 44:481–90. doi: 10.3892/ijo.2013.2191

137. Kim M, Morales LD, Lee CJ, Olivarez SA, Kim WJ, Hernandez J, et al. Overexpression of TC-PTP in murine epidermis attenuates skin tumor formation. *Oncogene* (2020) 39:4241–56. doi: 10.1038/s41388-020-1282-8

138. Baek M, Kim M, Lim JS, Morales LD, Hernandez J, Mummidi S, et al. Epidermal-specific deletion of TC-PTP promotes UVB-induced epidermal cell survival through the regulation of flk-1/JNK signaling. *Cell Death Dis* (2018) 9:730. doi: 10.1038/s41419-018-0781-9

139. Lee H, Kim M, Baek M, Morales LD, Jang IS, Slaga TJ, et al. Targeted disruption of TC-PTP in the proliferative compartment augments STAT3 and AKT signaling and skin tumor development. *Sci Rep* (2017) 7:45077. doi: 10.1038/srep45077

140. Le Sommer S, Morrice N, Pesaresi M, Thompson D, Vickers MA, Murray GI, et al. Deficiency in protein tyrosine phosphatase PTP1B shortens lifespan and leads to development of acute leukemia. *Cancer Res* (2018) 78:75–87. doi: 10.1158/0008-5472.CAN-17-0946

141. Demosthenous C, Han JJ, Hu G, Stenson M, Gupta M. Loss of function mutations in PTPN6 promote STAT3 deregulation *via* JAK3 kinase in diffuse large b-cell lymphoma. *Oncotarget* (2015) 6:44703–13. doi: 10.18632/oncotarget.6300

142. Wang X, Wang X, Lai J, Xu W, Zhu W, Chen G. Protein tyrosine phosphatase non-receptor type 12 suppresses tumor progression in osteosarcoma cells. *J Orthop Sci* (2022) S0949-2658(22)00007-0. doi: 10.1016/j.jos.2021.12.018

143. Chen CK, Yang CY, Hua KT, Ho MC, Johansson G, Jeng YM, et al. Leukocyte cell-derived chemotaxin 2 antagonizes MET receptor activation to suppress hepatocellular carcinoma vascular invasion by protein tyrosine phosphatase 1B recruitment. *Hepatology* (2014) 59:974–85. doi: 10.1002/hep.26738

144. Tai WT, Chen YL, Chu PY, Chen LJ, Hung MH, Shiau CW, et al. Protein tyrosine phosphatase 1B dephosphorylates PITX1 and regulates p120RasGAP in hepatocellular carcinoma. *Hepatology* (2016) 63:1528–43. doi: 10.1002/hep.28478

145. Yuan F, Gao Q, Tang H, Shi J, Zhou Y. OphiopogoninB targets PTP1B to inhibit the malignant progression of hepatocellular carcinoma by regulating the PI3K/AKT and AMPK signaling pathways. *Mol Med Rep* (2022) 25(4):122. doi: 10.3892/mmr.2022.12638

146. Wang Y, Salvucci O, Ohnuki H, Tran AD, Ha T, Feng JX, et al. Targeting the SHP2 phosphatase promotes vascular damage and inhibition of tumor growth. *EMBO Mol Med* (2021) 13:e14089. doi: 10.15252/emmm.202114089

147. Yu M, Xu C, Zhang H, Lun J, Wang L, Zhang G, et al. The tyrosine phosphatase SHP2 promotes proliferation and oxaliplatin resistance of colon cancer cells through AKT and ERK. *Biochem Biophys Res Commun* (2021) 563:1–7. doi: 10.1016/j.bbrc.2021.05.068

148. Yuan H, Zhao J, Yang Y, Wei R, Zhu L, Wang J, et al. SHP-2 interacts with CD81 and regulates the malignant evolution of colorectal cancer by inhibiting epithelial-mesenchymal transition. *Cancer Manag Res* (2020) 12:13273–84. doi: 10.2147/CMAR.S270813

149. Wei B, Xu L, Guo W, Wang Y, Wu J, Li X, et al. SHP2-mediated inhibition of DNA repair contributes to cGAS-STING activation and chemotherapeutic sensitivity in colon cancer. *Cancer Res* (2021) 81:3215–28. doi: 10.1158/0008-5472.CAN-20-3738

150. Wu MQ, Hu P, Gao J, Wei WD, Xiao XS, Tang HL, et al. Low expression of tyrosine-protein phosphatase nonreceptor type 12 is associated with lymph node metastasis and poor prognosis in operable triple-negative breast cancer. *Asian Pac J Cancer Prev* (2013) 14:287–92. doi: 10.7314/APJCP.2013.14.1.287

151. Sun T, Aceto N, Meerbrey KL, Kessler JD, Zhou C, Migliaccio I, et al. Activation of multiple proto-oncogenic tyrosine kinases in breast cancer via loss of the PTPN12 phosphatase. *Cell* (2011) 144:703–18. doi: 10.1016/j.cell.2011.02.003

152. Li J, Davidson D, Martins SC, Zhong MC, Wu N, Park M, et al. Loss of PTPN12 stimulates progression of ErbB2-dependent breast cancer by enhancing cell survival, migration, and epithelial-to-Mesenchymal transition. *Mol Cell Biol* (2015) 35:4069–82. doi: 10.1128/MCB.00741-15

153. Harris IS, Blaser H, Moreno J, Treloar AE, Gorrini C, Sasaki M, et al. PTPN12 promotes resistance to oxidative stress and supports tumorigenesis by regulating FOXO signaling. *Oncogene* (2014) 33:1047–54. doi: 10.1038/onc.2013.24

154. Chan RJ, Feng GS. PTPN11 is the first identified proto-oncogene that encodes a tyrosine phosphatase. *Blood* (2007) 109:862–7. doi: 10.1182/blood-2006-07-028829

155. Hinshaw DC, Shevde LA. The tumor microenvironment innately modulates cancer progression. *Cancer Res* (2019) 79:4557–66. doi: 10.1158/0008-5472.CAN-18-3962

156. Bauler TJ, Hughes ED, Arimura Y, Mustelin T, Saunders TL, King PD. Normal TCR signal transduction in mice that lack catalytically active PTPN3 protein tyrosine phosphatase. *J Immunol* (2007) 178:3680–7. doi: 10.4049/jimmunol.178.6.3680

157. Bauler TJ, Hendriks WJ, King PD. The FERM and PDZ domain-containing protein tyrosine phosphatases, PTPN4 and PTPN3, are both dispensable for T cell receptor signal transduction. *PloS One* (2008) 3:e4014. doi: 10.1371/journal.pone.0004014

158. Oh-hora M, Ogata M, Mori Y, Adachi M, Imai K, Kosugi A, et al. Direct suppression of TCR-mediated activation of extracellular signal-regulated kinase by leukocyte protein tyrosine phosphatase, a tyrosine-specific phosphatase. *J Immunol* (1999) 163:1282–8.

159. Wu Y, Deng W, McGinley EC, Klinke DN. Melanoma exosomes deliver a complex biological payload that upregulates PTPN11 to suppress T lymphocyte function. *Pigment Cell Melanoma Res* (2017) 30:203–18. doi: 10.1111/pcmr.12564

160. Saito T. Molecular dynamics of Co-signal molecules in T-cell activation. *Adv Exp Med Biol* (2019) 1189:135–52. doi: 10.1007/978-981-32-9717-3_5

161. Takehara T, Wakamatsu E, Machiyama H, Nishi W, Emoto K, Azuma M, et al. PD-L2 suppresses T cell signaling via coinhibitory microcluster formation and SHP2 phosphatase recruitment. *Commun Biol* (2021) 4:581. doi: 10.1038/s42003-021-02111-3

162. Wiede F, Shields BJ, Chew SH, Kyparissoudis K, van Vliet C, Galic S, et al. T Cell protein tyrosine phosphatase attenuates T cell signaling to maintain tolerance in mice. *J Clin Invest* (2011) 121:4758–74. doi: 10.1172/JCI59492

163. Salmond RJ, Brownlie RJ, Zamoyska R. Multifunctional roles of the autoimmune disease-associated tyrosine phosphatase PTPN22 in regulating T cell homeostasis. *Cell Cycle* (2015) 14:705–11. doi: 10.1080/15384101.2015.1007018

164. Vang T, Liu WH, Delacroix L, Wu S, Vasile S, Dahl R, et al. LYP inhibits T-cell activation when dissociated from CSK. *Nat Chem Biol* (2012) 8:437–46. doi: 10.1038/nchembio.916

165. Zhang X, Yu Y, Bai B, Wang T, Zhao J, Zhang N, et al. PTPN22 interacts with EB1 to regulate T-cell receptor signaling. *FASEB J* (2020) 34:8959–74. doi: 10.1096/fj.201902811RR

166. Salmond RJ, Huyer G, Kotsoni A, Clements L, Alexander DR. The src homology 2 domain-containing tyrosine phosphatase 2 regulates primary T-dependent immune responses and Th cell differentiation. *J Immunol* (2005) 175:6498–508. doi: 10.4049/jimmunol.175.10.6498

167. Young JA, Becker AM, Medeiros JJ, Shapiro VS, Wang A, Farrar JD, et al. The protein tyrosine phosphatase PTPN4/PTP-MEG1, an enzyme capable of dephosphorylating the TCR ITAMs and regulating NF-kappaB, is dispensable for T cell development and/or T cell effector functions. *Mol Immunol* (2008) 45:3756–66. doi: 10.1016/j.molimm.2008.05.023

168. Davidson D, Shi X, Zhong MC, Rhee I, Veillette A. The phosphatase PTP-PEST promotes secondary T cell responses by dephosphorylating the protein tyrosine kinase Pyk2. *Immunity* (2010) 33:167–80. doi: 10.1016/j.immuni.2010.08.001

169. Medgyesi D, Hobeika E, Biesen R, Kollert F, Taddeo A, Voll RE, et al. The protein tyrosine phosphatase PTP1B is a negative regulator of CD40 and BAFF-r signaling and controls b cell autoimmunity. *J Exp Med* (2014) 211:427–40. doi: 10.1084/jem.20131196

170. Yam-Puc JC, Zhang L, Maqueda-Alfaro RA, Garcia-Ibanez L, Zhang Y, Davies J, et al. Enhanced BCR signaling inflicts early plasmablast and germinal center b cell death. *iScience* (2021) 24:102038. doi: 10.1016/j.isci.2021.102038

171. Martin-Granados C, Prescott AR, Le Sommer S, Klaska IP, Yu T, Muckersie E, et al. A key role for PTP1B in dendritic cell maturation, migration, and T cell activation. *J Mol Cell Biol* (2015) 7:517–28. doi: 10.1093/jmcb/mjv032

172. Rhee I, Zhong MC, Reizis B, Cheong C, Veillette A. Control of dendritic cell migration, T cell-dependent immunity, and autoimmunity by protein tyrosine phosphatase PTPN12 expressed in dendritic cells. *Mol Cell Biol* (2014) 34:888–99. doi: 10.1128/MCB.01369-13

173. Spalinger MR, Crawford M, Bobardt SD, Li J, Sayoc-Becerra A, Santos AN, et al. Loss of protein tyrosine phosphatase non-receptor type 2 reduces IL-4-driven alternative macrophage activation. *Mucosal Immunol* (2022) 15:74–83. doi: 10.1038/s41385-021-00441-3

174. Heinonen KM, Dube N, Bourdeau A, Lapp WS, Tremblay ML. Protein tyrosine phosphatase 1B negatively regulates macrophage development through CSF-1 signaling. *Proc Natl Acad Sci U.S.A.* (2006) 103:2776–81. doi: 10.1073/pnas.0508563103

175. Heinonen KM, Tremblay ML. Protein tyrosine phosphatase 1B in hematopoiesis. *Cell Cycle* (2006) 5:1053–6. doi: 10.4161/cc.5.10.2735

176. Xu X, Wang X, Guo Y, Bai Y, He S, Wang N, et al. Inhibition of PTP1B promotes M2 polarization *via* MicroRNA-26a/MKP1 signaling pathway in murine macrophages. *Front Immunol* (2019) 10:1930. doi: 10.3389/fimmu.2019.01930

177. Heinonen KM, Nestel FP, Newell EW, Charette G, Seemayer TA, Tremblay ML, et al. T-Cell protein tyrosine phosphatase deletion results in progressive systemic inflammatory disease. *Blood* (2004) 103:3457–64. doi: 10.1182/blood-2003-09-3153

178. Hering L, Katkeviciute E, Schwarzfischer M, Niechcial A, Riggs JB, Wawrzyniak M, et al. Macrophages compensate for loss of protein tyrosine phosphatase N2 in dendritic cells to protect from elevated colitis. *Int J Mol Sci* (2021) 22(13):6820. doi: 10.3390/ijms22136820

179. Hering L, Katkeviciute E, Schwarzfischer M, Busenhart P, Gottier C, Mrdjen D, et al. Protein tyrosine phosphatase non-receptor type 2 function in dendritic cells is crucial to maintain tissue tolerance. *Front Immunol* (2020) 11:1856. doi: 10.3389/fimmu.2020.01856

180. Scharl M, Hruz P, McCole DF. Protein tyrosine phosphatase non-receptor type 2 regulates IFN-gamma-induced cytokine signaling in THP-1 monocytes. *Inflammation Bowel Dis* (2010) 16:2055–64. doi: 10.1002/ibd.21325

181. Kiratikanon S, Chattipakorn SC, Chattipakorn N, Kumfu S. The regulatory effects of PTPN6 on inflammatory process: Reports from mice to men. *Arch Biochem Biophys* (2022) 721:109189. doi: 10.1016/j.abb.2022.109189

182. Kamata T, Yamashita M, Kimura M, Murata K, Inami M, Shimizu C, et al. Src homology 2 domain-containing tyrosine phosphatase SHP-1 controls the development of allergic airway inflammation. *J Clin Invest* (2003) 111:109–19. doi: 10.1172/JCI15719

183. Speir M, Nowell CJ, Chen AA, O'Donnell JA, Shamie IS, Lakin PR, et al. Ptpn6 inhibits caspase-8- and Ripk3/Mlkl-dependent inflammation. *Nat Immunol* (2020) 21:54–64. doi: 10.1038/s41590-019-0550-7

184. Seo H, Lee IS, Park JE, Park SG, Lee DH, Park BC, et al. Role of protein tyrosine phosphatase non-receptor type 7 in the regulation of TNF-alpha production in RAW 264.7 macrophages. *PloS One* (2013) 8:e78776. doi: 10.1371/journal.pone.0078776

185. Coulombe G, Leblanc C, Cagnol S, Maloum F, Lemieux E, Perreault N, et al. Epithelial tyrosine phosphatase SHP-2 protects against intestinal inflammation in mice. *Mol Cell Biol* (2013) 33:2275–84. doi: 10.1128/MCB.00043-13

186. Xiao P, Zhang H, Zhang Y, Zheng M, Liu R, Zhao Y, et al. Phosphatase Shp2 exacerbates intestinal inflammation by disrupting macrophage responsiveness to interleukin-10. *J Exp Med* (2019) 216:337–49. doi: 10.1084/jem.20181198

187. Ding Y, Ouyang Z, Zhang C, Zhu Y, Xu Q, Sun H, et al. Tyrosine phosphatase SHP2 exacerbates psoriasis-like skin inflammation in mice *via* ERK5-dependent NETosis. *MedComm* (2020) 2022) 3:e120. doi: 10.1002/mco2.120

188. Wiede F, Sacirbegovic F, Leong YA, Yu D, Tiganis T. PTPN2-deficiency exacerbates T follicular helper cell and b cell responses and promotes the development of autoimmunity. *J Autoimmun* (2017) 76:85–100. doi: 10.1016/j.jaut.2016.09.004

189. Pao LI, Lam KP, Henderson JM, Kutok JL, Alimzhanov M, Nitschke L, et al. B cell-specific deletion of protein-tyrosine phosphatase Shp1 promotes b-1a cell development and causes systemic autoimmunity. *Immunity* (2007) 27:35–48. doi: 10.1016/j.immuni.2007.04.016

190. Kaneko T, Saito Y, Kotani T, Okazawa H, Iwamura H, Sato-Hashimoto M, et al. Dendritic cell-specific ablation of the protein tyrosine phosphatase Shp1 promotes Th1 cell differentiation and induces autoimmunity. *J Immunol* (2012) 188:5397–407. doi: 10.4049/jimmunol.1103210

191. Zhou L, Oh SY, Zhou Y, Yuan B, Wu F, Oh MH, et al. SHP-1 regulation of mast cell function in allergic inflammation and anaphylaxis. *PloS One* (2013) 8: e55763. doi: 10.1371/journal.pone.0055763

192. Wiede F, Lu KH, Du X, Zeissig MN, Xu R, Goh PK, et al. PTP1B is an intracellular checkpoint that limits T-cell and CAR T-cell antitumor immunity. *Cancer Discovery* (2022) 12:752–73. doi: 10.1158/2159-8290.CD-21-0694

193. Penafuerte C, Feldhammer M, Mills JR, Vinette V, Pike KA, Hall A, et al. Downregulation of PTP1B and TC-PTP phosphatases potentiate dendritic cell-based immunotherapy through IL-12/IFNgamma signaling. *Oncoimmunology* (2017) 6:e1321185. doi: 10.1080/2162402X.2017.1321185

194. Lawson KA, Sousa CM, Zhang X, Kim E, Akthar R, Caumanns JJ, et al. Functional genomic landscape of cancer-intrinsic evasion of killing by T cells. *Nature* (2020) 586:120–6. doi: 10.1038/s41586-020-2746-2

195. LaFleur MW, Nguyen TH, Coxe MA, Miller BC, Yates KB, Gillis JE, et al. PTPN2 regulates the generation of exhausted CD8(+) T cell subpopulations and restrains tumor immunity. *Nat Immunol* (2019) 20:1335–47. doi: 10.1038/s41590-019-0480-4

196. Manguso RT, Pope HW, Zimmer MD, Brown FD, Yates KB, Miller BC, et al. *In vivo* CRISPR screening identifies Ptpn2 as a cancer immunotherapy target. *Nature* (2017) 547:413–8. doi: 10.1038/nature23270

197. Katkeviciute E, Hering L, Montalban-Arques A, Busenhart P, Schwarzfischer M, Manzini R, et al. Protein tyrosine phosphatase nonreceptor type 2 controls colorectal cancer development. *J Clin Invest* (2021) 131(1):e140281. doi: 10.1172/JCI140281

198. Wiede F, Lu KH, Du X, Liang S, Hochheiser K, Dodd GT, et al. PTPN2 phosphatase deletion in T cells promotes anti-tumour immunity and CAR T-cell efficacy in solid tumours. *EMBO J* (2020) 39:e103637. doi: 10.15252/embj.2019103637

199. Goh PK, Wiede F, Zeissig MN, Britt KL, Liang S, Molloy T, et al. PTPN2 elicits cell autonomous and non-cell autonomous effects on antitumor immunity in triple-negative breast cancer. *Sci Adv* (2022) 8:k3338. doi: 10.1126/sciadv.abk3338

200. Koga S, Onishi H, Masuda S, Fujimura A, Ichimiya S, Nakayama K, et al. PTPN3 is a potential target for a new cancer immunotherapy that has a dual effect of T cell activation and direct cancer inhibition in lung neuroendocrine tumor. *Transl Oncol* (2021) 14:101152. doi: 10.1016/j.tranon.2021.101152

201. Fujimura A, Nakayama K, Imaizumi A, Kawamoto M, Oyama Y, Ichimiya S, et al. PTPN3 expressed in activated T lymphocytes is a candidate for a non-antibody-type immune checkpoint inhibitor. *Cancer Immunol Immunother* (2019) 68:1649–60. doi: 10.1007/s00262-019-02403-y

202. Watson HA, Dolton G, Ohme J, Ladell K, Vigar M, Wehenkel S, et al. Purity of transferred CD8(+) T cells is crucial for safety and efficacy of combinatorial tumor immunotherapy in the absence of SHP-1. *Immunol Cell Biol* (2016) 94:802–8. doi: 10.1038/icb.2016.45

203. Ben-Shmuel A, Sabag B, Puthenveetil A, Biber G, Levy M, Jubany T, et al. Inhibition of SHP-1 activity by PKC-theta regulates NK cell activation threshold and cytotoxicity. *Elife* (2022) 11:e73282. doi: 10.7554/eLife.73282

204. Myers DR, Abram CL, Wildes D, Belwafa A, Welsh A, Schulze CJ, et al. Shp1 loss enhances macrophage effector function and promotes anti-tumor immunity. *Front Immunol* (2020) 11:576310. doi: 10.3389/fimmu.2020.576310

205. Snook JP, Soedel AJ, Ekiz HA, O'Connell RM, Williams MA. Inhibition of SHP-1 expands the repertoire of antitumor T cells available to respond to immune checkpoint blockade. *Cancer Immunol Res* (2020) 8:506–17. doi: 10.1158/2326-6066.CIR-19-0690

206. Carmi Y, Prestwood TR, Spitzer MH, Linde IL, Chabon J, Reticker-Flynn NE, et al. Akt and SHP-1 are DC-intrinsic checkpoints for tumor immunity. *JCI Insight* (2016) 1:e89020. doi: 10.1172/jci.insight.89020

207. Chen YN, LaMarche MJ, Chan HM, Fekkes P, Garcia-Fortanet J, Acker MG, et al. Allosteric inhibition of SHP2 phosphatase inhibits cancers driven by receptor tyrosine kinases. *Nature* (2016) 535:148–52. doi: 10.1038/nature18621

208. Wang Y, Mohseni M, Grauel A, Diez JE, Guan W, Liang S, et al. SHP2 blockade enhances anti-tumor immunity *via* tumor cell intrinsic and extrinsic mechanisms. *Sci Rep* (2021) 11:1399. doi: 10.1038/s41598-021-80999-x

209. Zhao M, Guo W, Wu Y, Yang C, Zhong L, Deng G, et al. SHP2 inhibition triggers anti-tumor immunity and synergizes with PD-1 blockade. *Acta Pharm Sin B* (2019) 9:304–15. doi: 10.1016/j.apsb.2018.08.009

210. Ramesh A, Kumar S, Nandi D, Kulkarni A. CSF1R- and SHP2-Inhibitor-Loaded nanoparticles enhance cytotoxic activity and phagocytosis in tumor-associated macrophages. *Adv Mater* (2019) 31:e1904364. doi: 10.1002/adma.201904364

211. Quintana E, Schulze CJ, Myers DR, Choy TJ, Mordec K, Wildes D, et al. Allosteric inhibition of SHP2 stimulates antitumor immunity by transforming the immunosuppressive environment. *Cancer Res* (2020) 80:2889–902. doi: 10.1158/0008-5472.CAN-19-3038

212. Xiao P, Guo Y, Zhang H, Zhang X, Cheng H, Cao Q, et al. Myeloid-restricted ablation of Shp2 restrains melanoma growth by amplifying the reciprocal promotion of CXCL9 and IFN-gamma production in tumor microenvironment. *Oncogene* (2018) 37:5088–100. doi: 10.1038/s41388-018-0337-6

213. Chen D, Barsoumian HB, Yang L, Younes AI, Verma V, Hu Y, et al. SHP-2 and PD-L1 inhibition combined with radiotherapy enhances systemic antitumor effects in an anti-PD-1-Resistant model of non-small cell lung cancer. *Cancer Immunol Res* (2020) 8:883–94. doi: 10.1158/2326-6066.CIR-19-0744

214. Li J, Jie HB, Lei Y, Gildener-Leapman N, Trivedi S, Green T, et al. PD-1/SHP-2 inhibits Tc1/Th1 phenotypic responses and the activation of T cells in the tumor microenvironment. *Cancer Res* (2015) 75:508–18. doi: 10.1158/0008-5472.CAN-14-1215

215. Cubas R, Khan Z, Gong Q, Moskalenko M, Xiong H, Ou Q, et al. Autoimmunity linked protein phosphatase PTPN22 as a target for cancer immunotherapy. *J Immunother Cancer* (2020) 8(2):e001439. doi: 10.1136/jitc-2020-001439

216. Ho WJ, Croessmann S, Lin J, Phyo ZH, Charmsaz S, Danilova L, et al. Systemic inhibition of PTPN22 augments anticancer immunity. *J Clin Invest* (2021) 131(17):e146950. doi: 10.1172/JCI146950

217. Matsui M, Corey DR. Non-coding RNAs as drug targets. *Nat Rev Drug Discovery* (2017) 16:167–79. doi: 10.1038/nrd.2016.117

218. Li H, Li B, Larose L, CELL SIGNAL. (2017) 36:79–90.

219. Yang Q, Zhang L, Zhong Y, Lai L, Li X. miR-206 inhibits cell proliferation, invasion, and migration by down-regulating PTP1B in hepatocellular carcinoma. *Biosci Rep* (2019) 39(5):BSR20181823. doi: 10.1042/BSR20181823

220. Xu X, Tao Y, Niu Y, Wang Z, Zhang C, Yu Y, et al. miR-125a-5p inhibits tumorigenesis in hepatocellular carcinoma. *Aging (Albany NY)* (2019) 11:7639–62. doi: 10.18632/aging.102276

221. Han Q, Cheng P, Yang H, Liang H, Lin F. miR-146b reverses epithelial-mesenchymal transition via targeting PTP1B in cisplatin-resistance human lung adenocarcinoma cells. *J Cell Biochem* (2019) 10.1002/jcb.29554. doi: 10.1002/jcb.29554

222. Li Z, Hu C, Zhen Y, Pang B, Yi H, Chen X. Pristimerin inhibits glioma progression by targeting AGO2 and PTPN1 expression *via* miR-542-5p. *Biosci Rep* (2019) 39(5):BSR20182389. doi: 10.1042/BSR20182389

223. Shu Y, Yao S, Cai S, Li J, He L, Zou J, et al. miR-34c inhibits proliferation of glioma by targeting PTP1B. *Acta Biochim Biophys Sin (Shanghai)* (2021) 53:325–32. doi: 10.1093/abbs/gmaa178

224. Xu J, Zhang Z, Chen Q, Yang L, Yin J. miR-146b regulates cell proliferation and apoptosis in gastric cancer by targeting PTP1B. *Dig Dis Sci* (2020) 65:457–63. doi: 10.1007/s10620-019-05771-8

225. Sun F, Yu M, Yu J, Liu Z, Zhou X, Liu Y, et al. miR-338-3p functions as a tumor suppressor in gastric cancer by targeting PTP1B. *Cell Death Dis* (2018) 9:522. doi: 10.1038/s41419-018-0611-0

226. Yu M, Liu Z, Liu Y, Zhou X, Sun F, Liu Y, et al. PTP1B markedly promotes breast cancer progression and is regulated by miR-193a-3p. *FEBS J* (2019) 286:1136–53. doi: 10.1111/febs.14724

227. Zhang S, Zhang R, Xu R, Shang J, He H, Yang Q. MicroRNA-574-5p in gastric cancer cells promotes angiogenesis by targeting protein tyrosine phosphatase non-receptor type 3 (PTPN3). *Gene* (2020) 733:144383. doi: 10.1016/j.gene.2020.144383

228. Liu X, Dong Y, Song D. Inhibition of microRNA-15b-5p attenuates the progression of oral squamous cell carcinoma via modulating the PTPN4/STAT3 axis. *Cancer Manag Res* (2020) 12:10559–72. doi: 10.2147/CMAR.S272498

229. Zhu C, Deng X, Wu J, Zhang J, Yang H, Fu S, et al. MicroRNA-183 promotes migration and invasion of CD133(+)/CD326(+) lung adenocarcinoma initiating cells *via* PTPN4 inhibition. *Tumour Biol* (2016) 37:11289–97. doi: 10.1007/s13277-016-4955-8

230. Tang Y, Yang H, Yu J, Li Z, Xu Q, Ding B, et al. Crocin induces ROS-mediated papillary thyroid cancer cell apoptosis by modulating the miR-34a-5p/PTPN4 axis *in vitro*. *Toxicol Appl Pharmacol* (2022) 437:115892. doi: 10.1016/j.taap.2022.115892

231. Wang QM, Lian GY, Song Y, Peng ZD, Xu SH, Gong Y. Downregulation of miR-152 contributes to DNMT1-mediated silencing of SOCS3/SHP-1 in non-Hodgkin lymphoma. *Cancer Gene Ther* (2019) 26:195–207. doi: 10.1038/s41417-018-0057-7

232. Pan X, Peng G, Liu S, Sun Z, Zou Z, Wu G. MicroRNA-4649-3p inhibits cell proliferation by targeting protein tyrosine phosphatase SHP-1 in nasopharyngeal carcinoma cells. *Int J Mol Med* (2015) 36:559–64. doi: 10.3892/ijmm.2015.2245

233. Lin T, Zhou F, Zhou H, Pan X, Sun Z, Peng G. MicroRNA-378g enhanced radiosensitivity of NPC cells partially by targeting protein tyrosine phosphatase SHP-1. *Int J Radiat Biol* (2015) 91:859–66. doi: 10.3109/09553002.2015.1096028

234. Zhu J, Li H, Ma J, Huang H, Qin J, Li Y. PTPN9 promotes cell proliferation and invasion in Eca109 cells and is negatively regulated by microRNA-126. *Oncol Lett* (2017) 14:1419–26. doi: 10.3892/ol.2017.6315

235. Chen J, Ding C, Yang X, Zhao J. BMSCs-derived exosomal MiR-126-3p inhibits the viability of NSCLC cells by targeting PTPN9. *J BUON* (2021) 26:1832–41.

236. Li WT, Wang BL, Yang CS, Lang BC, Lin YZ. MiR-613 promotes cell proliferation and invasion in cervical cancer *via* targeting PTPN9. *Eur Rev Med Pharmacol Sci* (2018) 22:4107–14. doi: 10.26355/eurrev_201807_15402

237. Ma X, Shi W, Peng L, Qin X, Hui Y. MiR-96 enhances cellular proliferation and tumorigenicity of human cervical carcinoma cells through PTPN9. *Saudi J Biol Sci* (2018) 25:863–7. doi: 10.1016/j.sjbs.2017.10.020

238. Chen X, Liu W, Guo X, Huang S, Song X. Ropivacaine inhibits cervical cancer cell growth via suppression of the miR96/MEG2/pSTAT3 axis. *Oncol Rep* (2020) 43:1659–68. doi: 10.3892/or.2020.7521

239. Hong Y, Liang H, Uzair-Ur- R, Wang Y, Zhang W, Zhou Y, et al. miR-96 promotes cell proliferation, migration and invasion by targeting PTPN9 in breast cancer. *Sci Rep* (2016) 6:37421. doi: 10.1038/srep37421

240. Du WW, Fang L, Li M, Yang X, Liang Y, Peng C, et al. MicroRNA miR-24 enhances tumor invasion and metastasis by targeting PTPN9 and PTPRF to promote EGF signaling. *J Cell Sci* (2013) 126:1440–53. doi: 10.1242/jcs.118299

241. Bao Z, Gao S, Zhang B, Shi W, Li A, Tian Q. The critical role of the miR-21-MEG2 axis in colorectal cancer. *Crit Rev Eukaryot Gene Expr* (2020) 30:509–18. doi: 10.1615/CritRevEukaryotGeneExpr.2020036484

242. Liu Z, Sun F, Hong Y, Liu Y, Fen M, Yin K, et al. MEG2 is regulated by miR-181a-5p and functions as a tumour suppressor gene to suppress the proliferation and migration of gastric cancer cells. *Mol Cancer* (2017) 16:133. doi: 10.1186/s12943-017-0695-7

243. Zhou H, Tang K, Liu H, Zeng J, Li H, Yan L, et al. Regulatory network of two tumor-suppressive noncoding RNAs interferes with the growth and metastasis of renal cell carcinoma. *Mol Ther Nucleic Acids* (2019) 16:554–65. doi: 10.1016/j.omtn.2019.04.005

244. Kikkawa N, Hanazawa T, Fujimura L, Nohata N, Suzuki H, Chazono H, et al. miR-489 is a tumour-suppressive miRNA target PTPN11 in hypopharyngeal squamous cell carcinoma (HSCC). *Br J Cancer* (2010) 103:877–84. doi: 10.1038/sj.bjc.6605811

245. Toll A, Salgado R, Espinet B, Diaz-Lagares A, Hernandez-Ruiz E, Andrades E, et al. MiR-204 silencing in intraepithelial to invasive cutaneous squamous cell carcinoma progression. *Mol Cancer* (2016) 15:53. doi: 10.1186/s12943-016-0537-z

246. Cai Z, Hao XY, Liu FX. MicroRNA-186 serves as a tumor suppressor in oral squamous cell carcinoma by negatively regulating the protein tyrosine phosphatase SHP2 expression. *Arch Oral Biol* (2018) 89:20–5. doi: 10.1016/j.archoralbio.2018.01.016

247. Yao H, Yang Z, Lou Y, Huang J, Yang P, Jiang W, et al. miR-186 inhibits liver cancer stem cells expansion *via* targeting PTPN11. *Front Oncol* (2021) 11:632976. doi: 10.3389/fonc.2021.632976

248. Jiang C, Long J, Liu B, Xu M, Wang W, Xie X, et al. miR-500a-3p promotes cancer stem cells properties *via* STAT3 pathway in human hepatocellular carcinoma. *J Exp Clin Cancer Res* (2017) 36:99. doi: 10.1186/s13046-017-0568-3

249. Patel Y, Shah N, Lee JS, Markoutsa E, Jie C, Liu S, et al. A novel double-negative feedback loop between miR-489 and the HER2-SHP2-MAPK signaling axis regulates breast cancer cell proliferation and tumor growth. *Oncotarget* (2016) 7:18295–308. doi: 10.18632/oncotarget.7577

250. Liang Z, Li X, Duan F, Song L, Wang Z, Li X, et al. Protein tyrosine phosphatase non-receptor type 12 (PTPN12), negatively regulated by miR-106a-5p, suppresses the progression of hepatocellular carcinoma. *Hum Cell* (2022) 35:299–309. doi: 10.1007/s13577-021-00627-8

251. Cheng Y, Liu W. MicroRNA-503 serves an oncogenic role in retinoblastoma progression by directly targeting PTPN12. *Exp Ther Med* (2019) 18:2285–92. doi: 10.3892/etm.2019.7795

252. Liang T, Li L, Cheng Y, Ren C, Zhang G. MicroRNA-194 promotes the growth, migration, and invasion of ovarian carcinoma cells by targeting protein tyrosine phosphatase nonreceptor type 12. *Onco Targets Ther* (2016) 9:4307–15. doi: 10.2147/OTT.S90976

253. Rossi L, Bonmassar E, Faraoni I. Modification of miR gene expression pattern in human colon cancer cells following exposure to 5-fluorouracil *in vitro*. *Pharmacol Res* (2007) 56:248–53. doi: 10.1016/j.phrs.2007.07.001

254. Zhuang L, Shou T, Li K, Gao CL, Duan LC, Fang LZ, et al. MicroRNA-30e-5p promotes cell growth by targeting PTPN13 and indicates poor survival and recurrence in lung adenocarcinoma. *J Cell Mol Med* (2017) 21:2852–62. doi: 10.1111/jcmm.13198

255. Xu S, Wang T, Yang Z, Li Y, Li W, Wang T, et al. miR-26a desensitizes non-small cell lung cancer cells to tyrosine kinase inhibitors by targeting PTPN13. *Oncotarget* (2016) 7:45687–701. doi: 10.18632/oncotarget.9920

256. Wang LJ, He CC, Sui X, Cai MJ, Zhou CY, Ma JL, et al. MiR-21 promotes intrahepatic cholangiocarcinoma proliferation and growth in vitro and *in vivo* by targeting PTPN14 and PTEN. *Oncotarget* (2015) 6:5932–46. doi: 10.18632/oncotarget.3465

257. Liang G, Duan C, He J, Ma W, Dai X. PTPN14, a target gene of miR-4295, restricts the growth and invasion of osteosarcoma cells through inactivation of YAP1 signalling. *Clin Exp Pharmacol Physiol* (2020) 47:1301–10. doi: 10.1111/1440-1681.13296

258. Cui T, Bell EH, McElroy J, Becker AP, Gulati PM, Geurts M, et al. miR-4516 predicts poor prognosis and functions as a novel oncogene via targeting PTPN14 in human glioblastoma. *ONCOGENE* (2019) 38:2923–36. doi: 10.1038/s41388-018-0601-9

259. Liu YP, Sun XH, Cao XL, Jiang WW, Wang XX, Zhang YF, et al. MicroRNA-217 suppressed epithelial-to-mesenchymal transition in gastric cancer metastasis through targeting PTPN14. *Eur Rev Med Pharmacol Sci* (2017) 21:1759–67.

260. Huang WK, Akcakaya P, Gangaev A, Lee L, Zeljic K, Hajeri P, et al. miR-125a-5p regulation increases phosphorylation of FAK that contributes to imatinib resistance in gastrointestinal stromal tumors. *Exp Cell Res* (2018) 371:287–96. doi: 10.1016/j.yexcr.2018.08.028

261. Akcakaya P, Caramuta S, Ahlen J, Ghaderi M, Berglund E, Ostman A, et al. microRNA expression signatures of gastrointestinal stromal tumours: associations with imatinib resistance and patient outcome. *Br J Cancer* (2014) 111:2091–102. doi: 10.1038/bjc.2014.548

262. Tanaka K, Kondo K, Kitajima K, Muraoka M, Nozawa A, Hara T. Tumor-suppressive function of protein-tyrosine phosphatase non-receptor type 23 in testicular germ cell tumors is lost upon overexpression of miR142-3p microRNA. *J Biol Chem* (2013) 288:23990–9. doi: 10.1074/jbc.M113.478891

263. Bhan A, Soleimani M, Mandal SS. Long noncoding RNA and cancer: A new paradigm. *Cancer Res* (2017) 77:3965–81. doi: 10.1158/0008-5472.CAN-16-2634

264. Li Y, Zeng Q, Qiu J, Pang T, Xian J, Zhang X. Long non-coding RNA UCA1 promotes breast cancer by upregulating PTP1B expression via inhibiting miR-206. *Cancer Cell Int* (2019) 19:275. doi: 10.1186/s12935-019-0958-z

265. Tang C, Feng W, Bao Y, Du H. Long non-coding RNA TINCR promotes hepatocellular carcinoma proliferation and invasion *via* STAT3 signaling by direct interacting with T-cell protein tyrosine phosphatase (TCPTP). *Bioengineered* (2021) 12:2119–31. doi: 10.1080/21655979.2021.1930336

266. Ding CH, Yin C, Chen SJ, Wen LZ, Ding K, Lei SJ, et al. The HNF1alpha-regulated lncRNA HNF1A-AS1 reverses the malignancy of hepatocellular carcinoma by enhancing the phosphatase activity of SHP-1. *Mol Cancer* (2018) 17:63. doi: 10.1186/s12943-018-0813-1

267. Zheng J, Huang X, Tan W, Yu D, Du Z, Chang J, et al. Pancreatic cancer risk variant in LINC00673 creates a miR-1231 binding site and interferes with PTPN11 degradation. *Nat Genet* (2016) 48:747–57. doi: 10.1038/ng.3568

268. Niu Y, Guo Y, Li Y, Shen S, Liang J, Guo W, et al. LncRNA GATA2-AS1 suppresses esophageal squamous cell carcinoma progression *via* the mir-940/PTPN12 axis. *Exp Cell Res* (2022) 416(2):113130. doi: 10.1016/j.yexcr.2022.113130

269. Wang H, Qin R, Guan A, Yao Y, Huang Y, Jia H, et al. HOTAIR enhanced paclitaxel and doxorubicin resistance in gastric cancer cells partly through inhibiting miR-217 expression. *J Cell Biochem* (2018) 119:7226–34. doi: 10.1002/jcb.26901

270. Xiang D, Li Y, Lin Y. Circular RNA circCCDC66 contributes to malignant phenotype of osteosarcoma by sponging miR-338-3p to upregulate the expression of PTP1B. *BioMed Res Int* (2020) 2020:4637109. doi: 10.1155/2020/4637109

271. Zhu L, Guo T, Chen W, Lin Z, Ye M, Pan X. CircMMD_007 promotes oncogenic effects in the progression of lung adenocarcinoma through microRNA-197-3p/protein tyrosine phosphatase non-receptor type 9 axis. *Bioengineered* (2022) 13:4991–5004. doi: 10.1080/21655979.2022.2037956

272. Chen SW, Zhu SQ, Pei X, Qiu BQ, Xiong D, Long X, et al. Cancer cell-derived exosomal circUSP7 induces CD8(+) T cell dysfunction and anti-PD1 resistance by regulating the miR-934/SHP2 axis in NSCLC. *Mol Cancer* (2021) 20:144. doi: 10.1186/s12943-021-01448-x

273. Jun W, Shaobo O, Xianhua Z, Siyu Z, Mingyang C, Xin F, et al. Deregulation of hsa_circ_0001971/miR-186 and hsa_circ_0001874/miR-296 signaling pathways promotes the proliferation of oral squamous carcinoma cells by synergistically activating SHP2/PLK1 signals. *Sci Rep* (2021) 11:20561. doi: 10.1038/s41598-021-99488-2

274. Wang S, Ping M, Song B, Guo Y, Li Y, Jia J. Exosomal CircPRRX1 enhances doxorubicin resistance in gastric cancer by regulating MiR-3064-5p/PTPN14 signaling. *Yonsei Med J* (2020) 61:750–61. doi: 10.3349/ymj.2020.61.9.750

275. Liu C, Lu H, Wang H, Loo A, Zhang X, Yang G, et al. Combinations with allosteric SHP2 inhibitor TNO155 to block receptor tyrosine kinase signaling. *Clin Cancer Res* (2021) 27:342–54. doi: 10.1158/1078-0432.CCR-20-2718

276. Lee C, Rhee I. Important roles of protein tyrosine phosphatase PTPN12 in tumor progression. *Pharmacol Res* (2019) 144:73–8. doi: 10.1016/j.phrs.2019.04.011

frontiers | Frontiers in Oncology

TYPE Original Research
PUBLISHED 14 September 2022
DOI 10.3389/fonc.2022.992260

OPEN ACCESS

EDITED BY
João Pessoa,
University of Coimbra, Portugal

REVIEWED BY
Mark A. Miles,
RMIT University, Australia
Panagis Polykretis,
National Research Council (CNR), Italy
Irene Diaz-Moreno,
Sevilla University, Spain

*CORRESPONDENCE
Varda Shoshan-Barmatz
vardasb@bgu.ac.il

SPECIALTY SECTION
This article was submitted to Molecular and Cellular Oncology, a section of the journal Frontiers in Oncology

RECEIVED 12 July 2022
ACCEPTED 10 August 2022
PUBLISHED 14 September 2022

CITATION
Pandey SK, Shteinfer-Kuzmine A, Chalifa-Caspi V and Shoshan-Barmatz V (2022) Non-apoptotic activity of the mitochondrial protein SMAC/Diablo in lung cancer: Novel target to disrupt survival, inflammation, and immunosuppression.
Front. Oncol. 12:992260.
doi: 10.3389/fonc.2022.992260

Non-apoptotic activity of the mitochondrial protein SMAC/Diablo in lung cancer: Novel target to disrupt survival, inflammation, and immunosuppression

Swaroop Kumar Pandey[1], Anna Shteinfer-Kuzmine[1], Vered Chalifa-Caspi[2] and Varda Shoshan-Barmatz[1,3]*

[1]The National Institute for Biotechnology in the Negev, Ben-Gurion University of the Negev, Beer-Sheva, Israel, [2]Ilse Katz Institute for Nanoscale Science & Technology, Ben-Gurion University of the Negev, Beer-Sheva, Israel, [3]Department of Life Sciences, Ben-Gurion University of the Negev, Beer-Sheva, Israel

Mitochondrial SMAC/Diablo induces apoptosis by binding the inhibitor of apoptosis proteins (IAPs), thereby activating caspases and, subsequently, apoptosis. Previously, we found that despite its pro-apoptotic activity, SMAC/Diablo is overexpressed in cancer, and demonstrated that in cancer it possesses new essential and non-apoptotic functions that are associated with regulating phospholipid synthesis including modulating mitochondrial phosphatidylserine decarboxylase activity. Here, we demonstrate additional functions for SMAC/Diablo associated with inflammation and immunity. CRISPR/Cas9 SMAC/Diablo-depleted A549 lung cancer cells displayed inhibited cell proliferation and migration. Proteomics analysis of these cells revealed altered expression of proteins associated with lipids synthesis and signaling, vesicular transport and trafficking, metabolism, epigenetics, the extracellular matrix, cell signaling, and neutrophil-mediated immunity. SMAC-KO A549 cell-showed inhibited tumor growth and proliferation and activated apoptosis. The small SMAC-depleted "tumor" showed a morphology of alveoli-like structures, reversed epithelial-mesenchymal transition, and altered tumor microenvironment. The SMAC-lacking tumor showed reduced expression of inflammation-related proteins such as NF-kB and TNF-α, and of the PD-L1, associated with immune system suppression. These results suggest that SMAC is involved in multiple processes that are essential for tumor growth and progression. Thus, targeting SMAC's non-canonical function is a potential strategy to treat cancer.

KEYWORDS

SMAC, cell proliferation, inflammation, lung cancer, immunosuppression

Introduction

SMAC/Diablo, the second mitochondrial-derived activator of caspases (SMAC) is also known as a direct inhibitor of apoptosis-binding low pI (DIABLO). SMAC is produced and a precursor and resides within the intermembranous space (IMS) of the mitochondria (1). Upon apoptosis initiation, proteolytical cleavage of the SMAC/DIABLO (SMAC) mitochondrial targeting signal takes place before its translocation from the mitochondria into the cytosol. SMAC, as other proapoptotic proteins (Cyto *c*, AIF, Htra2, Endo-G), is released to the cytosol *via* a protein-conducting channel assembled in the outer mitochondrial membrane in response to an apoptotic signal (2). The released SMAC interacts with inhibitors of apoptosis proteins (IAPs) and competes with caspase-3 and -9 for binding to IAPs, allowing the activation of the caspase cascade, and thereby, induction of apoptosis (3–5). XIAP, an important member of IAPs, was shown to interact with SMAC with a stoichiometric inhibitory interaction of one XIAP homodimer binds to one tetramer of SMAC, forming a 201.5 kDa complex (6).

Thus, SMAC, by inhibiting IAPs' anti-apoptotic function promotes apoptotic cell death.

One of the hallmarks of cancer is deregulated apoptosis (7), involving several mechanisms including overexpression of IAP and failure of the IAP antagonist SMAC to translocate from the mitochondria to the cytosol (8). IAPs expression levels were increased in a number of human tumor and their overexpression has been correlated with tumor growth, and poor prognosis or low response to treatment (9).

However, IAPs not only regulate caspases and apoptosis, but also modulate inflammatory signaling and immunity, mitogenic kinase signaling, proliferation and mitosis, as well as cell invasion and metastasis (10). Expressing full-length SMAC (11), pro-SMAC (8), or cytosol-targeted SMAC (tSMAC), (12) showed that SMAC plays a pivotal role in the onset of cancer cell apoptosis. However, another study demonstrated that SMAC does not induce apoptosis by itself, even when expressed as a mature form in the cytosol of mammalian cells (4). Moreover, disruption of the *Smac* gene in mice produces no obvious phenotype—the mice are viable, and grow and mature normally, without any histological abnormalities, and exhibit wild-type responses to all types of apoptotic stimuli (13). However, it has been suggested that the role of SMAC can vary depending on the cell type (14).

Despite SMAC pro-apoptotic function, it is expressed in a wide range of normal tissues and in some tumor cells lines. It is overexpressed in different types of cancer (15–17), such as breast, lung, bladder, cervical, pancreas, prostate, and colorectal cancer, as well as melanoma and glioma (18). This SMAC overexpression in primary human tumors suggests that it possesses additional non-apoptotic functions.

Recently, we explored this non-apoptotic function of SMAC by silencing its expression using specific siRNA in cells in culture or in sub-cutaneous lung cancer xenografts in mice (19, 20). We demonstrated that SMAC regulates mitochondrial phosphatidylserine decarboxylase (PSD) activity that catalyzes the synthesis of phosphatidylethanolamine (PE) from phosphatidylserine (PS), with SMAC depletion leading to increased PE in the mitochondria, while decreasing the level of all phospholipids in the cell (20). Moreover, inhibition of PSD by specific peptides targeted to the mitochondria or to the nucleus resulted in inhibiting cell growth. These results suggest that SMAC and its associated protein PSD (20) are necessary to promote neoplastic metaplasia.

In this study, we further evaluated the function of SMAC in cancer using CRISPR/Cas9-mediated SMAC knockout (SMAC-KO) lung cancer A549 cells. Our results show that tumors comprising SMAC-lacking cells show reversed epithelial-mesenchymal transition (EMT), altered microenvironment and highly reduced expression of inflammation-related proteins and of the programmed death-ligand 1 (PD-L1), associated with suppression of the adaptive immune system. In addition, a proteomics analysis showed a larger number of the differentially expressed proteins between SMAC expressing and non-expressing cells. These include proteins associated with lipids and lipid-signaling molecules, metabolism, DNA- and RNA-associated processes, transport and intracellular trafficking, cellular signaling, immunity, and more, pointing to SMAC's multiple functions in cancer.

Materials and methods

Materials, the TUNEL assay, the Sulforhodamine B (SRB) cell proliferation assay, the migration and wound-healing assay, and protein extraction and immunoblots are presented in the Supplementary Materials.

Cell culture and CRISPR/Cas9 SMAC knockout

A549 (human lung adenocarcinoma epithelial cell) cell line was purchased from the American Type Culture Collection (ATCC) (Manassas, VA). Cells were maintained in DMEM medium provided with 10% FBS at 37°C in an incubator with 5% CO_2. Cell line was routinely tested for mycoplasma contamination.

SMAC CRISPR/Cas9 Knockout Plasmid with GFP marker (sc-402009) was purchased from Santa Cruz Biotechnology (Dallas, TX). A549 cells were seeded in 6-well cell culture plates (200,000 cells/well) and allowed to attach overnight. Cells were transfected with SMAC CRISPR/Cas9 Knockout Plasmid as per manufacturers' instructions using JetPRIME

transfection reagent. GFP-positive cells were sorted using FACS (SY3200 cell sorter; Synergy) and plated in 96-well plates (1 cell/well). Cells grew for 10 days, and each colony was transferred to a separate well of 12-well cell culture plates. Individual colonies having SMAC-KO were selected for maintenance after immunoblotting for SMAC.

Xenograft mouse models

Female athymic nude mice (7–8 weeks old) (weight ~20–25g) were procured from Envigo and allowed a week of acclimatization to their new surroundings. Lung cancer A549 cells or SMAC CRISPR/Cas9 Knockout A549 cells ($3x10^6$) were implanted subcutaneously on the dorsal flanks of the mice. The size of the developed tumors was monitored twice a week for a period of 33 days in two dimensions using a digital caliper, and volumes were calculated using the formula $(\pi/6)^*(L \times W^2)$ (L = length; W = width). At the end point of the experiment, i.e., when the mice were sacrificed using CO_2 gas, the tumors were excised and *ex-vivo* weight was determined. Half of each tumor was either fixed and processed for IHC or frozen in liquid nitrogen for later immunoblotting and RNA isolation. Approval for the experimental protocol was obtained from the Institutional Animal Care and Use Committee of the Soroka University Medical Center.

Immunohistochemistry and Immunofluorescence

IF staining of cells was performed in cells plated on sterile glass coverslips placed in 12-well cell culture plates (30,000 cells/well) and incubated overnight in a CO_2 incubator, washed with PBS, and fixed with 4% paraformaldehyde. To reduce non-specific binding, cells were incubated with 5% normal goat serum for 2 h, then incubated with primary antibodies (Table S1) overnight at 4° C. Following overnight incubation with the primary antibodies, PBST (PBS containing 0.1% Triton-X100)-washed samples were incubated with fluorescent-tagged secondary antibodies for 2 h at room temperature in the dark. Following a wash with PBS, samples were incubated with DAPI for 15 min in the dark, washed, mounted with mounting medium (Immuno bio science, Mukilteo, Washington, USA Fluoroshield). and viewed by confocal microscopy (Olympus 1X81).

IHC and IF of tumor sections was performed on formalin-fixed and paraffin-embedded tumor sections that were deparaffinized using xylene and a series of ethanol treatments. Sections were then incubated with 3% H_2O_2 for 10 min to block endogenous peroxidase activity. Antigen retrieval was done in 0.01 M citrate buffer (pH 6.0) at 95–98° C for 30 min, followed by PBST wash. In order to reduce non-specific binding, sections were incubated in 10% normal goat serum for 2 h, and then incubated with primary antibodies (Table S1) overnight at 4°C. For IHC, after washing with PBST, sections were incubated for 2 h at room temperature with HRP-conjugated secondary antibodies, washed well with PBST, and incubated with the substrate DAB. Sections were washed with water, counterstained with hematoxylin, and mounted with mounting medium (ORSAtec GmbH, Bobingem). Sections were observed under a microscope (Leica DM2500), and images were collected at 20× magnification with the same light intensity and exposure time. For IF, following overnight incubation with the primary antibodies, PBST-washed sections were incubated with fluorescent-tagged secondary antibodies for 2 h at room temperature in the dark. Following a wash with PBST, sections were incubated with DAPI for 15 min in the dark, washed, mounted with mounting medium Fluoroshield (Immuno bio science, Mukilteo, Washington, USA), and viewed by confocal microscopy (Olympus 1X81).

RNA preparation, qRT-PCRanalysis

Total RNA was isolated from cells and tumor tissues using an RNeasy mini kit (Qiagen), according to the manufacturer's instructions. Complementary DNA (cDNA) was synthesized with a PCRBio cDNA synthesis kit (PCR Biosystems, Wayne, PA, USA) and used for real-time q-RT-PCR using specific primers (Table S2) with Power SYBER green master mix (Applied Biosystems, Foster City, CA). Levels of target genes were normalized relative to β-actin mRNA levels. Samples were amplified by a 7300 Real Time PCR System (Applied Biosystems) for 40 cycles using the following PCR parameters: 95° C for 15 s, 60° C for 1 min, and 72°C for 1 min. Relative expression levels for each gene in each sample were calculated by the ddCT-based calibrated standard curve method. The mean fold changes (± SEM) of the three replicates were calculated.

Liquid chromatography–high-resolution mass spectrometry and proteomics analysis

For the LC-HR MS/MS analysis, proteins were extracted from CRISPR/Cas9 SMAC knockout cells using lysis buffer [100 mM Tris-HCl, pH 8.0, 5 mM DTT 4% SDS, and a protease inhibitor cocktail (Calbiochem)], followed by homogenization, incubation for 3 min at 95° C, and centrifugation (10 min, 15,000 g). The protein concentration of each lysate was determined using a Lowry assay. Samples were stored at -80° C until LC-HR-

MS/MS analysis. Samples were subjected to tryptic digestion, alkylation, detergent removal, and desalting, and then to LC-HR MS/MS analysis, described in the Supplementary Materials section. Mass spectrometry (MS)-based proteomics profiling and initial processing of the results were carried out at the de Botton Institute for Protein Profiling, G-INCPM at the Weizmann Institute of Science.

Statistical analyses for identification of differentially expressed proteins

MS/MS raw data were processed with MaxQuant v1.6.6.0. The data were searched with the Andromeda search engine against the human SwissProt proteome database and appended with common lab protein contaminants. Quantification and normalization were performed using the LFQ method, yielding a total of 4,968 identified proteins. This data analysis was carried out by de the Botton Institute. A subsequent bioinformatic analysis was carried out at the Bioinformatics Core Facility at Ben-Gurion University, using the R and Partek Genomics Suite.

Proteins marked as "contaminant" were filtered out. In an additional filtering step, only proteins in which at least one of the groups (SMAC KO, Control) had two non-zero replicates were retained (n=4636). LFQ intensities were Log_2 transformed, and zero intensities were imputed (replaced) by random numbers derived from a normal distribution in the low expression range (width = 0.2, downshift = 1.8). Imputation was repeated ten times to avoid relying too heavily on fabricated numbers. Each of the ten imputed datasets was submitted for hypothesis testing for differential protein expressions using Limma (21). The statistical model tested the contrast: SMAC-KO *vs*. Control. A protein was considered differentially expressed (DE) if it had a nominal p-value < 0.05 and an absolute fold change (in linear scale) > 1.6 in at least eight of the ten imputed datasets. The analyzed proteins were selected based on human proteins for which at least one unique peptide was identified.

Hierarchical clustering of the DE proteins was performed in Partek, using Pearson's dissimilarity and complete linkage. For hierarchical clustering, Log_2-transformed LFQ values were z-scored after the zero values were replaced by the global minimum (19.443). Enrichment analysis versus the gene ontology (GO) biological process and GO cellular component was performed in Enrich R (22) using a Fisher's exact test.

Statistics

Results are presented as the means ± SEM of results obtained from independent experiments. A difference was considered statistically significant when the p-value was deemed <0.05 (*), < 0.01 (**), <0.001 (***), or ****p ≤ 0.0001 assessed through an unpaired Student's two-tailed t-test.

Results

SMAC-KO A549 cells show inhibited proliferation and migration

Here, we studied the function of SMAC on cancer cell growth and tumor oncogenic properties using CRISPR/Cas9-mediated SMAC knockout (SMAC-KO) lung cancer A549 cells tested in culture and as a xenograft in nude mice. As expected, SMAC-KO cells showed no SMAC expression and reduced cell proliferation, as assayed by the SRB method (Figures 1A, B). The reduced proliferation of SMAC-KO cells was also reflected in the decreased expression of Ki-67, a proliferation marker (Figures 1C, D).

The expression levels of XIAP and survivin in SMAC-KO were highly decreased (Figure 1E). Survivin, also known as baculoviral inhibitor of apoptosis repeat-containing 5 (BIRC5), is a member of the IAP family. It binds to SMAC/Diablo and prevents caspase activation, thereby leading to negative regulation of apoptosis with inhibition of this interaction promoting apoptosis (23).

We also assessed the effect of SMAC-KO on cell migration by comparing control and SMAC-KO A549 cells using a wound-healing assay (Figures 1F, G). A fixed-width scratch was created in a cell monolayer, and the progress of the cell migrating front was monitored using a digital camera coupled with a microscope. In comparison to control cells, which closed 81% of the gap after 24 h, SMAC-KO cells showed attenuated migration, closing only 25% of the gap (Figures 1F, G). Finally, we analyzed whether apoptosis is activated in SMAC-KO cells (Figure 1H) and found no significant different in the apoptotic cells between SMAC-expressing and SMAC-KO cells.

SMAC-KO cells produce very small tumors with inhibited proliferation and activated apoptosis

Next, we tested whether SMAC-KO A549 cells could form tumors in nude mice, with tumor growth followed for about 35 days. While the tumor volume of control A549 cells grew exponentially and increased over 22-fold to a volume of 1110 mm^3, the SMAC-KO cell-derived tumor increased to a volume of 250 mm^3, 78% smaller than the tumors in the control cells (Figures 2A, B), with a 70% decrease in weight (Figure 2C). Immunoblot, IHC, and IF analyses of the tumors indicated, as expected, that SMAC was not expressed in the tumors derived from SMAC-KO cells (Figures 2D–F). The inhibited cell proliferation in the SMAC-KO-derived tumors was reflected in an 80% decrease in the expression level of the cell proliferation factor, KI-67, as shown by IF staining (Figures 2G, H) and qRT-PCR analysis (Figure 2I).

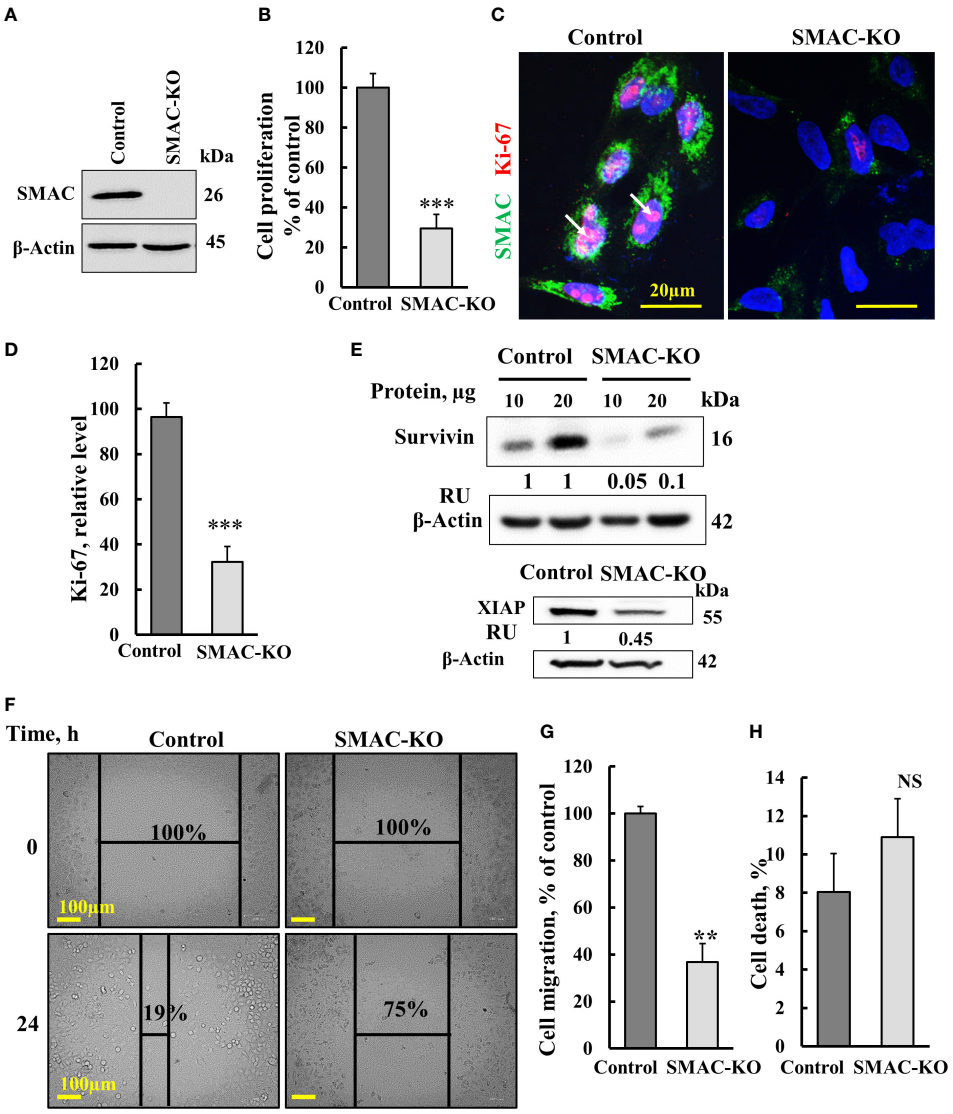

FIGURE 1
Crispr/Cas-9 SMAC knockout in A549 cells inhibits cell proliferation and migration. **(A)** Immunoblot of CRISPR/Cas9-generated SMAC-deficient A549 cells. **(B)** Cell proliferation in SMAC-KO A549 cells as analyzed using the SRB method. **(C, D)** A549 cells expressing SMAC and SMAC-KO A549 cells were IF co-stained with anti-SMAC and anti-Ki-67 antibodies **(C)** with quantitative analysis of Ki-67 expression levels **(D)**. **(E)** Immunoblot analysis of survivin and XIAP in protein extracts from SMAC-expressing and SMAK-KO cells. **(F, G),** A549 cells expressing SMAC and SMAC-KO A549 cells were allowed to grow to 80% confluence. The cell layer was scraped using a 200-μl sterile pipette tip to create a scratch/wound devoid of cells. Migration was assessed after 24 h. Representative photomicrographs are shown **(F)** (n=3). Quantification of the results describes the change in percentage of the scratch size at the indicated times (n=3) **(G)**. **(H)** Control and SMAC-KO A549 cells were analyzed for cell death using propidium iodine staining and FACS analysis. Results are the means± SEM, **p ≤ 0.01; ***p < 0.001, NS, non-significant.

The marked inhibition of tumor growth in the SMAC-KO-cell xenograft resulted from inhibition of cell proliferation, as reflected in the highly reduced Ki-67 expression (Figures 2G–I). However, it may also be the result of cell death activation. Accordingly, apoptotic cells were analyzed *in situ*, by TUNEL staining of tumor sections derived from control and SMAC-KO cells (Figures 3A, B). While only a few TUNEL-positive cells were apparent in the control tumors, the majority of the cells in the SMAC-KO tumors were TUNEL-positive, with staining co-localized with propidium iodide (PI) nucleus staining (Figures 3A, B).

Activated apoptosis is also shown by the increased levels of cleaved/activated caspase-3, analyzed by immunoblotting (Figures 3C, D) and IF staining (Figures 3E, F) and q-RT-PCR (Figure 3G.) In addition, the expression levels of the anti-apoptotic protein Bcl-2, as assayed using IF staining, and Finally, the

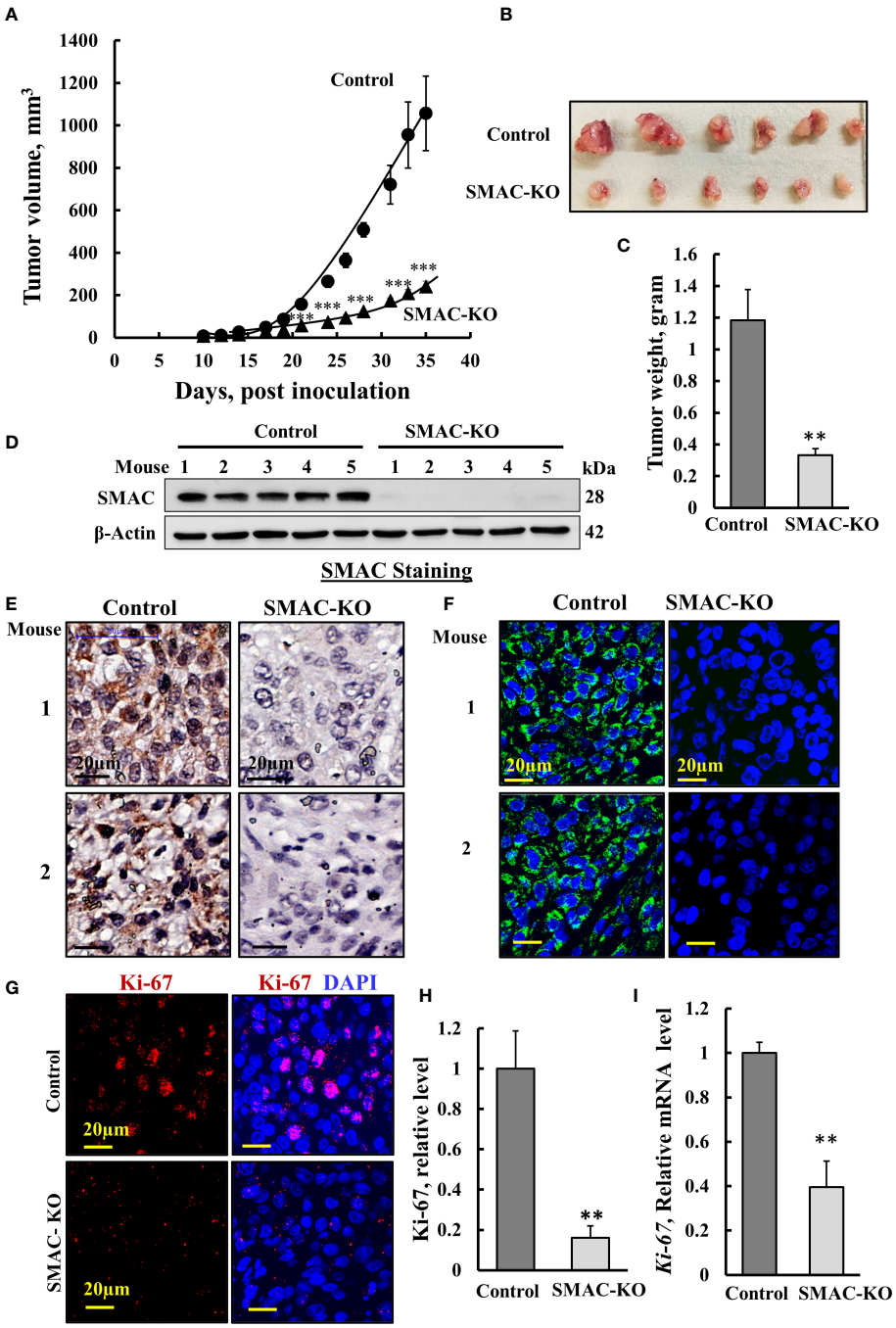

FIGURE 2
Inhibited cell proliferation in SMAC-KO A549-cell lung cancer xenograft. Control or SMAC-KO A549 cells (3x10^{6}cells/mouse) were inoculated into athymic female mice (6 mice/group). Tumor volumes were monitored (using a digital caliper) for 35 days. In **(A)**, xenograft sizes were measured on the indicated days, and the calculated average tumor volumes are presented as means ± SEM, *** p > 0.001; a two tailed Student's t-test was performed to calculate the statistical significance. Tumors from mouse A549 cell xenografts were dissected, photographed **(B)**, and weighed **(C)**. Immunoblot analysis of SMAC in protein extracts from tumors derived from control and SMAC-KO A549 cells **(D)**. Sections of paraffin-embedded control and SMAC-KO A549 cell-derived tumors were immunostained using specific antibodies for SMAC expression using IHC **(E)** or IF **(F)** and for the nuclear proliferation marker Ki-67 using IF **(G)** and its quantification **(H)**. q-RT-PCR analysis of Ki-67 mRNA **(I)**. Results represent the means ± SEM (n = 3) **p ≤ 0.01; ***p ≤ 0.001.

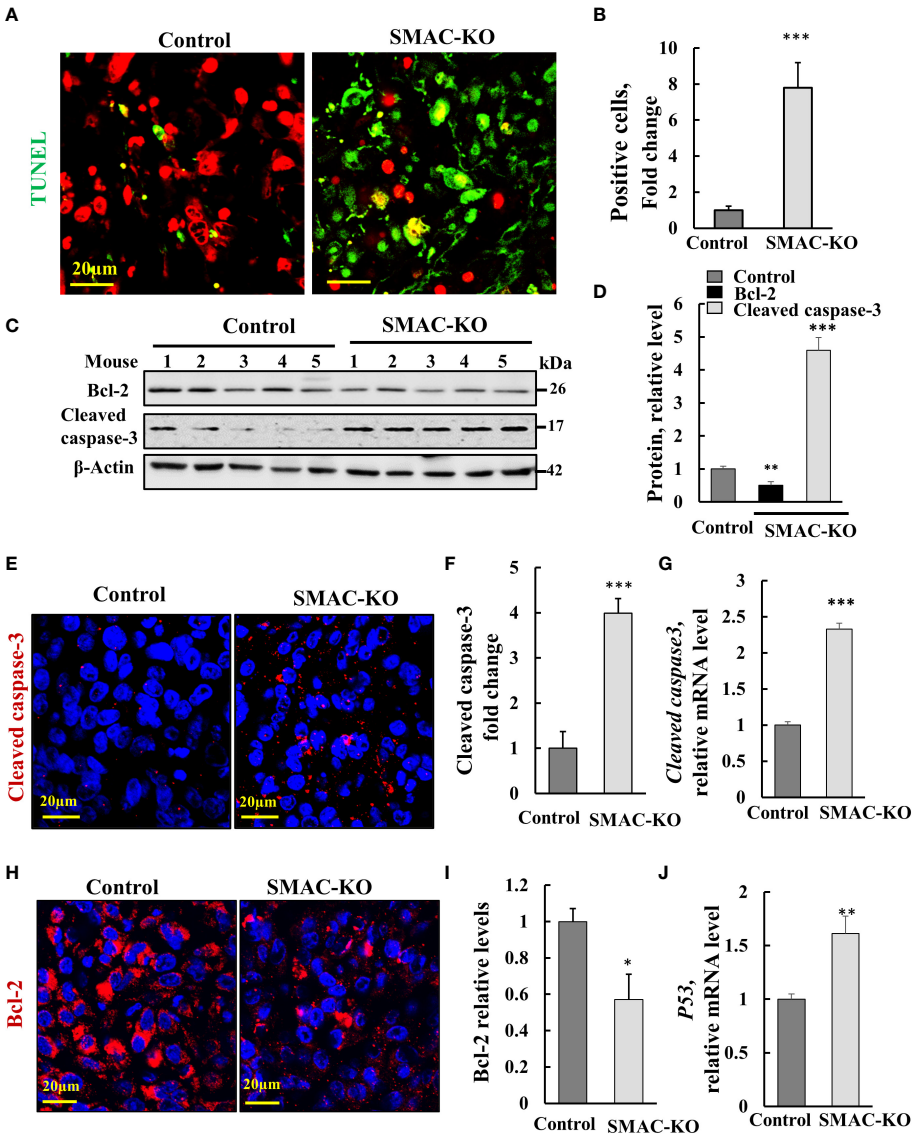

FIGURE 3
SMAC-KO-derived tumors showed apoptotic cell death. Sections of paraffin-embedded control and SMAC-KO A549 cell-derived tumors were stained with TUNEL with propidium iodide used as counter stain **(A)**, and quantified **(B)**. Immunoblot analysis of Bcl-2 and cleaved caspase-3 in protein extracts from tumors derived from control and SMAC-KO A549 cells **(C)** and their quantification **(D)**. Sections were also IF stained for cleaved caspases-3 (E,F) or Bcl-2 **(H, I)**. Cleaved caspase-3 **(G)** and p53 **(J)** mRNA levels were also analyzed by q-RT-PCR. Results represent the means ± SEM (n = 3) *p ≤ 0.05, **p ≤ 0.01; ***p ≤ 0.001.

expression levels of the multifaceted function, tumor suppressor p53 increased (Figure 3J). The results suggest that apoptosis is activated in tumors derived from cells lacking SMAC.

SMAC-depletion altered tumor morphology and the microenvironment

Hematoxylin and eosin (H&E) staining of sections from control- and SMAC-KO cell-derived tumors demonstrated that SMAC-depleted tumors showed a different morphology with cell-free areas that may resemble alveolar-like clusters of lung tissue (Figure 4A). As the tumor is derived from A549 cells, considered as alveolar epithelial type II (AT2) cells (24), it can trans-differentiate into alveolar epithelial type I (AT1) (25). We analyzed the expression of the AT1 cell marker podoplanin, a membranal mucin-type sialoglycoprotein (25). A massive increase (400-fold) in the podoplanin expression level was observed in the SMAC-KO tumors (Figures 4B, C). This may suggest that the AT2 A549 cells in the SMAC-KO-derived tumors had undergone differentiation into AT1-like cells.

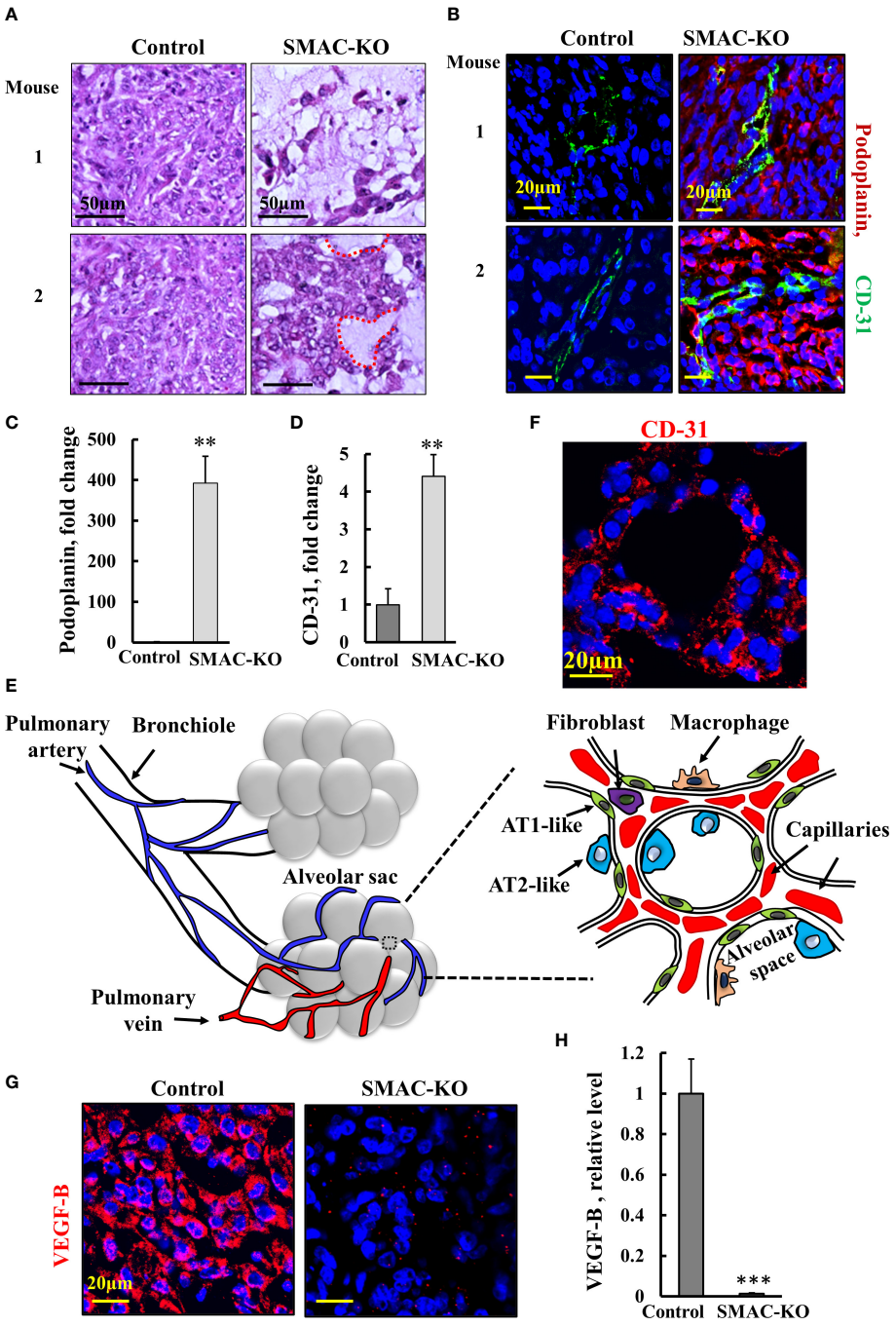

FIGURE 4
Morphology alterations in SMAC-KO-derived tumors. Representative sections from control and SMAC-KO A549 cell-derived tumors stained with H&E with cell-free areas circled **(A)**. Representative IF staining and quantification of sections of control and SMAC-KO A549 cell-derived tumors stained with specific antibodies against podoplanin **(B, C)** or CD-31 **(B-D, F)**. A schematic presentation of the morphological changes in the SMAC-KO tumors showing reorganization into alveoli-like structures with organized blood capillary and AT2-and AT1-like cells **(E)**. IF staining control and SMAC-KO A549 cell-derived tumors for VEGF-B **(G)** and its quantification **(H)**. Results represent the means ± SEM (n = 3) **p ≤ 0.01, ***p ≤ 0.001.

Staining for the endothelial cell marker CD-31, as present in blood vessels, revealed over 4-fold higher staining in the SMAC-KO tumors relative to the SMAC-expressing tumors (Figures 4B-D). Importantly, the cells positively stained for CD-31 created a chain around the podoplanin-expressing cells. The CD-31-positive cell organization seems to closely resemble the normal physiological alveolar endothelial arrangement and not tumor angiogenesis.

Analysis of the pulmonary-associated surfactant proteins (SFTP-C) C expressed by AT2 cells in the SMAC-expressing and depleted tumors, showed non-homogenous expression of SETP-B, exhibiting low, medium, and high levels of SFTP-C (Figure S1). Generally, there was no major difference in the expression levels of SFTP-C between SMAC-expressing and -depleted tumors, although the percentage of the three sub-groups was slightly changed.

The changes in SMAC-KO tumor morphology, along with the differentiation of AT2-like cells into AT1-like cells and the blood capillary organization, suggest the formation of glandular/alveoli-like structures (Figure 4E, F).

Tumors often express angiogenic factors at high levels to induce neovascularization (26). Among all known angiogenic factors, vascular endothelial growth factor B (VEGF-B), *via* binding to its receptor (VEGFR), a tyrosine kinase receptor, modulates angiogenesis, vascular permeability, vessel survival, and vascular remodeling. As found for many cancers, VEGF was highly expressed in SMAC-expressing tumors, but its levels were dramatically decreased by about 100-fold in the SMAC-KO-derived tumors (Figures 4G, H)).

The tumor metastatic potential is attenuated by the epithelial to mesenchymal transition (EMT) (27). To follow EMT, we analyzed the expression of epithelial and mesenchymal cell markers N-cadherin (type I cell–cell adhesion glycoproteins), vimentin (intermediate filaments), and E-cadherin, an epithelial cell marker (28) (Figures 5A–E). As expected, for reversed EMT, IF staining showed that vimentin and N-cadherin expression levels were highly decreased, while those of E-cadherin was increased 4-fold in the SMAC-KO tumors relative to their expression in the control tumors (Figures 5A–E). Similar results were obtained by immunoblotting (Figures 5F, G).

Finally, IF-staining of SMAC-expressing tumors for the alpha smooth muscle actin (α-SMA) showed strong staining of cells, exhibiting the long, spindle-shaped morphology characteristic of fibroblasts. This staining was decreased by about 70% in the SMAC-KO tumors (Figures 5H, I). The results clearly show that SMAC-depleted tumors underwent morphological and microenvironment modulation.

SMAC depletion reduced tumor inflammation and immunosuppression

Inflammation is often associated with the development of cancer and promotes all stages of tumorigenesis [24]. Cancer cells in the tumor are surrounding stromal and inflammatory cells that are engaged in well-orchestrated reciprocal interactions to form an inflammatory tumor microenvironment (TME) (29). To test whether SMAC deletion affects tumor inflammation and immunity, we analyzed the expression of several inflammation- and immunity-related proteins (Figure 6).

Nuclear factor kappa B (NF-κB) is a network hub that consists of homo- and heterodimers of five distinct proteins: RelA (p65), RelB, c-Rel, p105 (NF-kB1), and p100 (NF-kB2) (30, 31), It coordinates many signals that drive proliferation, inflammation, oncogenesis (32), and innate immunity (33). The expression levels of the phosphorylated NF-κB/RelA (p65) and (p-NF-κB) in the SMAC-KO tumors were highly reduced by 70% (immunoblotting), and IF analysis showed an over 90% decrease relative to its levels in SMAC-expressing tumors (Figures 6A–D).

The decrease in p-NF-κB levels in SMAC-KO tumors may also be associated with an increased expression level of p53 (Figure 3J) with its transcriptional antagonism with NF-kB (34, 35). NF-κB regulates the expression of many inflammatory cytokines including tumor necrosis factor-α TNF-α. The results indicate that the levels of TNF-α were high in the control mice, but reduced in the SMAC-KO tumors (Figures 6E, F).

The transcription factor HIF-1α orchestrates the expression of a vast number of essential cellular functions in genes, affecting cancer progression associated with angiogenesis (as VEGF), metabolism (hexokinase, glucose transporters), cell survival, and proliferation (TGF-α, C-Myc). In SMAC-KO tumors, the levels of HIF-1α, as revealed by IF and immunoblotting, were reduced by about 70%, relative to its levels in SMAC-expressing tumors (Figures 6E, G, H).

Finally, we compared the expression of programmed cell death ligand 1 (PD-L1) in control- and SMAC-KO cell-derived tumors (Figures 6I, J). IF staining of PD-L1 using specific antibodies demonstrated a decrease of about 50% in PD-L1 expression levels in the SMAC-KO cell-derived tumors. PD-L1 interaction with its receptor, PD-1, compromises T-cell-mediated immune surveillance, promoting cancer cell progression. Thus, the decreased expression of PD-L1 in SMAC-lacking tumors was expected to decrease immunosuppression of the cancer.

The overall results suggest that SMAC is required for tumor-associated inflammation and immunity, and reduction in PD-L1 in its absence can advance immunotherapeutic strategies.

Mass spectrometry analysis of the differentially expressed protein in SMAC-KO cells

To identify proteins showing different expression levels in A549 cells depleted of SMAC, and their association with

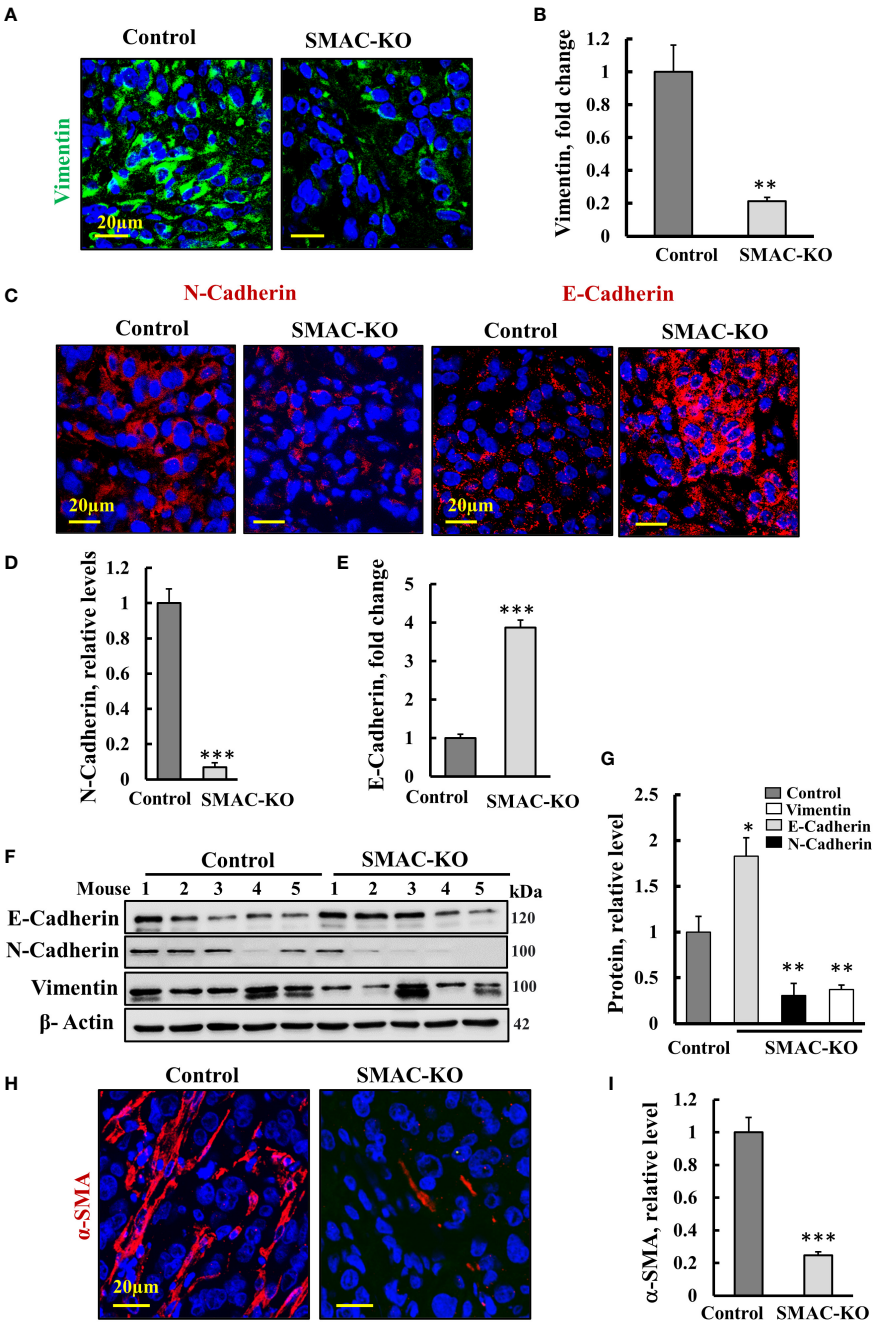

FIGURE 5
Microenvironment alterations in SMAC-KO-derived tumors. Representative IF staining and quantification of sections from control and SMAC-KO A549 cell-derived tumors stained with specific antibodies against vimentin **(A)**, N-cadherin and E-cadherin **(C)** and their quantification **(B, D, E)**. Immunoblotting of E-cadherin, N-cadherin, and vimentin **(F)** and their quantification **(G)**. IF staining of α-SMA and its quantification **(H, I)**. Results represent the means ± SEM (n = 3) *p ≤ 0.05, **p ≤ 0.01; ***p ≤ 0.001.

inhibited cancer cell proliferation and altered tumor TME, inflammation, and immunity, CRISPR/Cas9 SMAC/Diablo-depleted cells and cells expressing SMAC were subjected to LC-HR MS/MS, proteomics, and functional enrichment analyses (Figures 7, 8).

After filtering for human proteins, which had at least one unique peptide, about 4,636 proteins were submitted for subsequent analysis. Of the differentially expressed proteins (p-value < 0.05 and fold change |FC| > 1.6) between cells expressing and depleted of SMAC, 115 proteins were

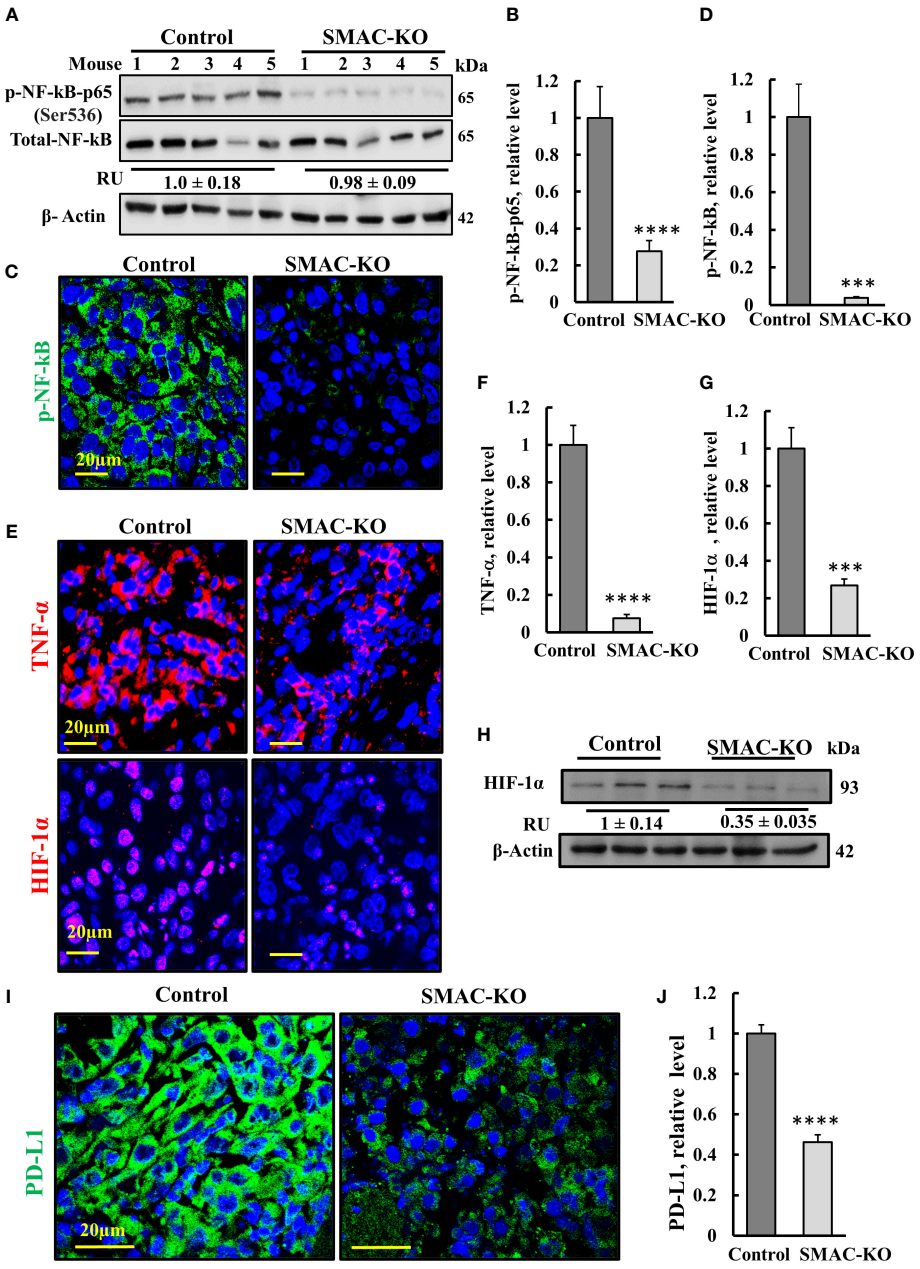

FIGURE 6
SMAC-KO-derived tumors showed altered expression of decreased inflammation and immunity-related proteins. Immunoblot of protein extracts from control and SMAC-KO A549 cell-derived tumors for NF-kB and p-NF-kB(p65) **(A)** and quantification (**B**). Average relative levels of NF-kB are presented as relative units (RUs) at the bottom of the blot. Sections of control and SMAC-KO A549 cell-derived tumors were subjected to IF staining with specific antibodies against p-NF-kB(p65) **(C)** and its quantified staining intensity **(D)**. IF staining of control and SMAC-KO tumors for TNF-α and HIF-1α **(E)** and their quantified staining intensity **(F, G)**. Immunoblotting of HIF-1α, with average relative levels presented as RUs at the bottom of the blot **(H)**. IF staining for PD-L1 **(I)** and its quantification **(J)**. Results represent the means ± SEM (n = 3) ***p ≤ 0.001. ****p ≤ 0.0001.

upregulated and 116 were downregulated. As expected, SMAC/Diablo was detected in the control cells, but not in the SMAC-KO cells (Table S3).

The hierarchical clustering of the differently expressed proteins in cells expressing and depleted of SMAC (Figure 7A) and the volcano plots (Figure 7B) showed that larger numbers of the differentially expressed proteins were down- or upregulated.

An enrichment analysis of the proteins differentially expressed between cells expressing and depleted of SMAC was performed using the Gene Ontology (GO) databases for

biological processes (Figure 7C) (36, 37). The proteins with altered expression upon SMAC depletion were sub-grouped according to cellular functions. These included proteins associated with lipids and lipid-signaling molecules (Table S3, Figure 8A), transport and intracellular trafficking (Table S4, Figure 8B), metabolism (Table S5, Figure 8C), extracellular matrix (ECM) and structural proteins (Table S6, Figure 8D), cellular signaling (Table S7, Figure 8E), immune response including neutrophil-mediated immunity and neutrophil degradation (Table S8, Figure 8F), DNA- and RNA-associated processes (Table S9), protein synthesis and degradation (Table S10), and epigenetics (Table S11, Figure 8G).

Selected proteins from the various groups are presented in Figure 8A. The lipid and lipid-signaling molecules (Table S3, Figure 7A) included increased expression of ethanolamine kinase 1 (ETNK1), mediating ethanolamine phosphorylation, a rate-controlling step in PE biosynthesis (38). All other proteins in this group were downregulated (Table S3, Figure 8A). These included: phospholipid phosphatase 3 (PLPP3) and 2, a phospholipid phosphatase that catalyzes the conversion of phosphatidic acid (PA) to diacylglycerol (DG); mono-glyceride lipase (MGLL), which converts mono-acylglycerides to free fatty acids and glycerol; and glycosylphosphatidylinositol anchor attachment 1 protein (GPAA1), which is involved in the glycosylphosphatidylinositol-anchor biosynthesis pathway that is part of glycolipid biosynthesis. Annexin A8-like protein 1 (ANXA8L1) functions as an anticoagulant, and indirectly inhibits the thromboplastin-specific complex.

The expression levels of several intracellular trafficking-related proteins and transporters were mostly reduced (Table S4, Figure 8B). These included: signal sequence receptor 3 (SSR3) a subunit of the translocon-associated protein (TRAP) complex which facilitates the translocation of proteins across the ER membrane; solute carrier family 2; glucose transporter member 3 (SLC2A3); apolipoprotein L2 (APOL2), which is involved in the movement of lipids in the cytoplasm and allows the binding of lipids to organelles; solute carrier family 35 member B1 (SLC35B1) which facilitates UDP-galactose transmembrane transport; intracellular cholesterol transporter 1 (NPC1); vacuolar protein sorting-associated protein 52 homolog (VPS52), which is involved in retrograde transport from early and late endosomes to the trans-Golgi network; synaptotagmin-like protein 2 (SYTL2), a protein required for cytotoxic granule docking at the immunologic synapse; and secretory carrier-associated membrane protein 4 (SCAMP4), a membrane protein, with components of regulated secretory carriers in exocrine, neural, and endocrine cells, all are which downregulated 6–8 fold in SMAC-KO cells compared with wild-type A549 cells.

The expression of several metabolism-related proteins was altered in the SMAC-depleted cells (Table S5, Figure 8C). These include the carbonic anhydrase-related protein (CA8), a non-active isoform with the only known biochemical function is affecting IP3 binding to its receptor IP3R1 on the ER, thereby modulating Ca^{2+} signaling (39). Mitochondrial glycine dehydrogenase (GLDC), catalyzing the degradation of glycine, is also upregulated in SMAC-KO cells, while glycolytic enzyme.

Phosphoglycerate kinase 1 (PGK1), microsomal NADPH-cytochrome P450 reductase (POR), and protein mono-ADP-ribosyltransferase (PARP14), which mediates mono-ADP-ribosylation of glutamate residues on target proteins, were significantly downregulated.

Another group of proteins whose expression was modified is associated with the organization and functions of extra-cellular matrix (ECM) and structural proteins (Table S6, Figure 8D), which were found to be significantly reduced (3–17-fold), while others increased 2–6 fold. The downregulated proteins included tensin-4 (TNS4), which is involved in cell migration and links the signal transduction pathways to the cytoskeleton; and protein-glutamine gamma-glutamyltransferase 2 (TGM2), catalyzing the cross-linking of proteins between Gln and Lys residues (40). Several cell adhesion proteins such as G-protein coupled receptor G1 (ADGRG1), plakophilin-2 (PKP2), and claudin-2 (CLDN2) were also significantly reduced.

Some proteins were found to be upregulated in SMAK-KO cells, such as fibronectin (FN1) which is involved in cell adhesion and motility, the wound healing process, the collagen alpha-2(V) chain (COL5A2), a connective tissue component that binds to DNA, heparan sulfate, heparin, thrombospondin, and insulin. Unconventional myosin-IXb (MYO9B) and microtubule-stabilizing protein ensconsin (MAP7) expression levels were also increased upon SMAC depletion (Figure 8D, Table S6).

The proteomics data explored proteins related to signaling pathways, development, and differentiation whose expression levels were altered in SMAC-KO cells (Table S7, Figure 8E). ADP-ribosyl cyclase/cyclic ADP-ribose hydrolase 1 (CD38) synthesizes the second messenger cyclic ADP-ribose and nicotinate-adenine dinucleotide phosphate decreasing it by about 8-fold. Protein strawberry notch homolog 1 (SBNO1) and high mobility group protein (HMGI-C) were increased over 3-fold. The p100 subunit of NF-kB, a master transcription factor, and the melanoma-associated antigen D1 (MAGED1), a cell cycle inhibitor and inducer of NGFR-mediated apoptosis were also upregulated. Other proteins such as catenin beta-1 (CTNNB1), a key downstream component of the canonical Wnt signaling pathway; cyclin-dependent kinase 6 (CDK6) which functions as a cell cycle and differentiation regulator; and sushi domain-containing protein 2 (SUSD2) that negatively regulates cell cycle G1/S phase transition were decreased 3–7-fold. SMAC-KO also altered the expression of immune response-related proteins, including neutrophil-mediated immunity (Table S8, Figure 8F).

Among the proteins whose expression levels were decreased upon SMAC depletion was ferritin light chain (FTL), a subunit

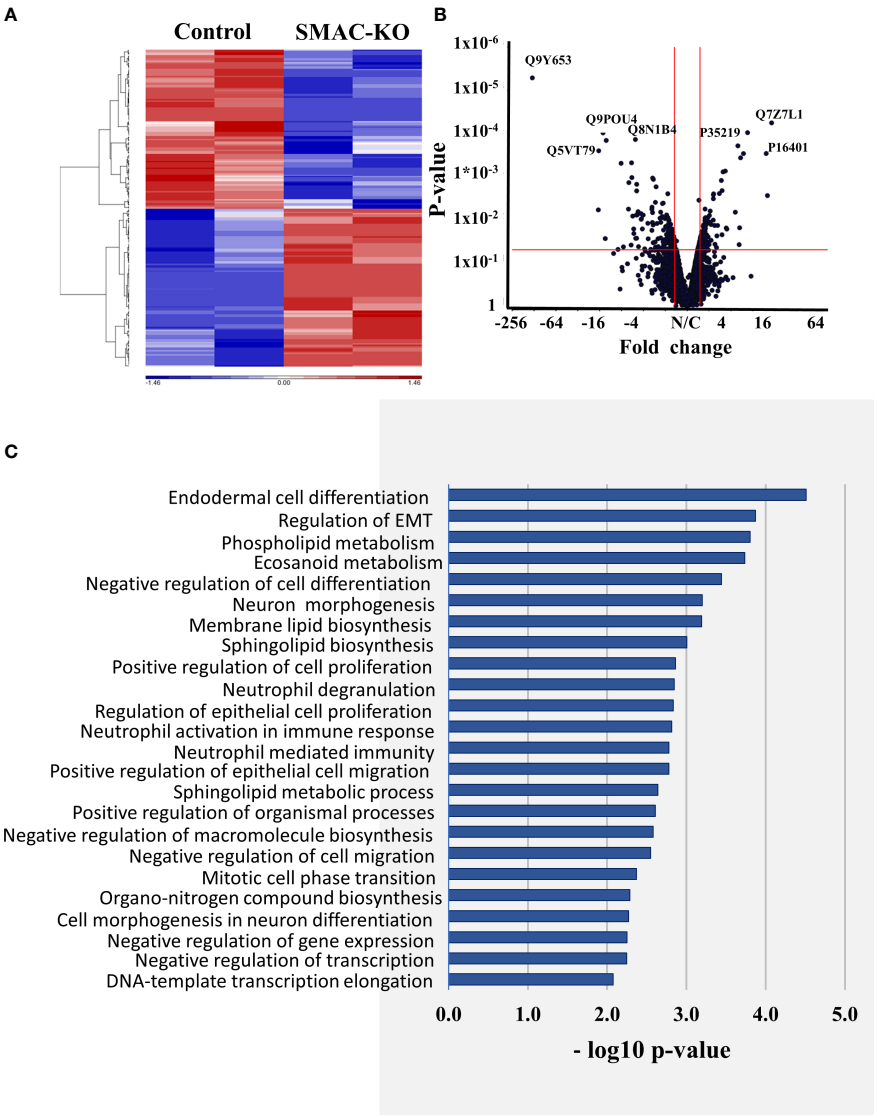

FIGURE 7
Differentially expressed proteins in SMAC-KO- and SMAC-expressing cells. Human proteins differentially expressed between SMAC-expressing and SMAC-depleted A549 cells, as analyzed by LC-HR-MS/MS. Human proteins presenting at least one unique peptide, those with a p-value of 0.05 and linear fold change of +/- 1.6 are presented. **(A)** Hierarchical clustering of the 231 proteins found to be differentially expressed between SMAC-expressing and SMAC-depleted cells. The color scale of the standardized expression values is shown. **(B)** Volcano plots showing p-values as a function of fold change in SMAC-KO- relative to SMAC-expressing cells. Significantly enriched functional groups in the proteins showing changed expression based on the David Gene Ontology system **(C)**.

of ferritin that is the main form of iron storage protein and is known to influence tumor immunity (41), which decreased over 5-fold. Similarly, CD55 decreased about 5-fold when overexpressed in tumors, resulting in immune escape adopted to avoid recognition by the immune system or of survival from antibody-mediated immunotherapy (42) (Fig. 8F, Table S8). CTSD (cathepsin D), a lysosomal aspartic, has been related to immune response and regulation of programmed cell death. The aldehyde dehydrogenase 3 family, member B1 ALDH3B1 is proposed to play a significant role in the tumor immune landscape by modulating immunocytes (43) Table S8.

The expression of proteins related to DNA and RNA (Table S9) also was modified in SMAC-KO cells as schlafen family member 11 (SLFN11), an inhibitor of DNA replication, was increased about 14-fold, while the expression levels of protein bicaudal C homolog 1, an ARNA binding protein that acts as a negative regulator of Wnt signaling and is upregulated in oral cancer tissues, was decreased over 2-fold.

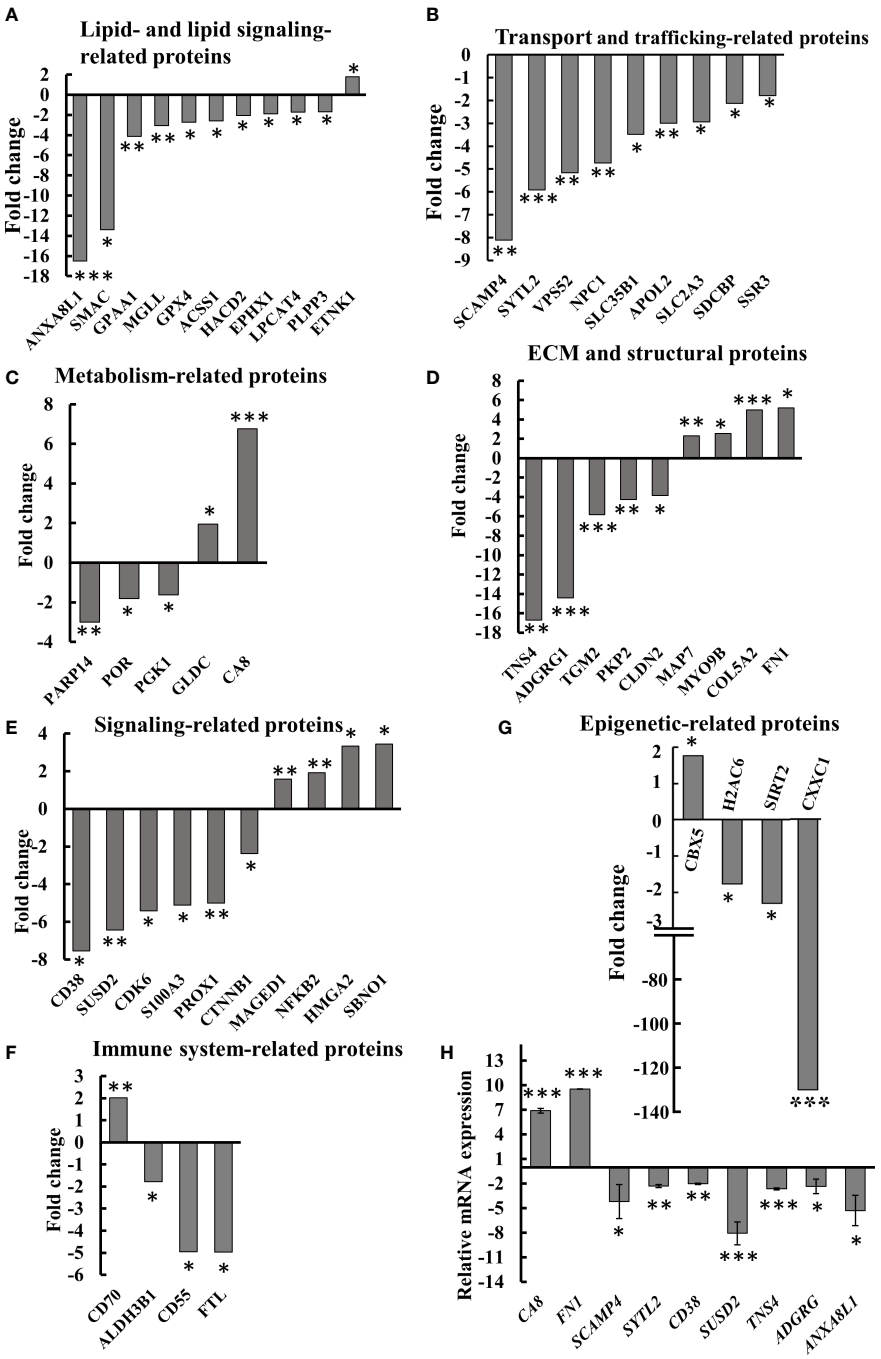

FIGURE 8
Differential expression of lipid-, metabolism-, transport- and trafficking-, ECM- and signaling-related proteins in SMAC-KO A549 cells. Quantitative analysis of the LC-HR MS/MS data. Differentially expressed lipid-related proteins **(A)** transport- and trafficking-related proteins **(B)** metabolism-related proteins **(C)** ECM and structural proteins **(D)**, cell signaling related proteins **(E)**, immune-response-related proteins **(F)** and epigenetics-related proteins **(G)** are presented in terms of fold change of expression in SMAC-KO A549, relative to A549 cells. q-RT-PCR analysis of mRNA levels of selected proteins **(H)**. *p ≤ 0.05, **p ≤ 0.001, ***p ≤ 0.0001.

Finally, expression of proteins associated with epigenetics (Table S11, Figure 8G) was also modified as Histone H1.5, a regulator of individual gene transcription and overexpression in prostate cancer, increased about 12-fold, while the expression of CXXC-type zinc finger protein 1, a transcriptional activator was reduced by 135-fold in SMAC-KO cells.

Alterations in the expression of selected proteins at the mRNA level were analyzed using q- RT-PCR (Figure 8H). The obtained results validated the proteomic results.

These results point to the involvement of SMAC in many cell-signaling pathways and activities, as mediated *via* its interaction and modulation of key proteins in cellular pathways.

Discussion

Mice lacking the pro-apoptotic protein SMAC/Diablo are viable, and grow and mature normally, without any histological abnormalities, and exhibit responses to all types of apoptotic stimuli such as SMAC-expressing mice, suggesting that this protein is not essential for apoptosis (13). Interestingly, we showed that in spite of being a pro-apoptotic protein, SMAC is overexpressed in many cancer types (19), suggesting that it possesses an additional non-apoptotic function that is important in tumor development.

Indeed, we demonstrated that SMAC depletion in cancer cells using specific si-RNA led to multiple effects, including reduced cell proliferation and decreased phospholipid levels, and in tumor silencing, SMAC expression inhibited tumor growth, and the residual "tumor" showed cell differentiation and reorganization to alveoli-like structures (19, 20). Moreover, CRISPR/Cas9 SMAC depleted cells showed inhibited proliferation of cancer cells, but not non-cancerous cells (20). This further points to the importance of SMAC for the cancer cell. Here, using CRISPR/Cas9 SMAC-depleted cells, we further explored the non-apoptotic functions of SMAC using proteomic analysis and a lung cancer mouse model.

The results show that SMAC is also involved in regulating lipid synthesis, cell proliferation, the TME, inflammation, and immunity. The involvement of SMAC in these processes is summarized in Figure 9, suggesting that targeting SMAC would result in attacking many cancer properties.

SMAC, as a pro-apoptotic protein that interacts and antagonizes IAPs activity, allows the activation of caspases and apoptosis. SMAC-derived peptides, peptidomimetics, to target IAPs and induce apoptosis were produced and applied as cancer therapy (44–48). However, SMAC-mimetic treatment increases resistance to DNA-damaging chemotherapeutic agents rather than reducing it (49). In addition, IAP antagonists have been shown to interact with tumor necrosis factor receptor-associated factor 2 (TRAF2), shown to interact with SMAC (19, 20).The resulting complex reportedly antagonizes the activation of caspase-8, hence, inhibiting TNF receptor-mediated apoptosis (14). Moreover, SMAC-mimetics clinical trials for hematological and solid cancers showed variable and limited results (50). The SMAC mimetics may modulate other SMAC-interacting protein activities reflected in the SMAC non-apoptotic activities and may explain their lack of effectiveness on tumor growth. Thus, they are not approved for clinical treatment of cancer (50).

It should be noted that, in this study, we used A549 lung cancer-derived xenografts that were developed in nude mice, and that the tumors were analyzed for microenvironment, inflammation and immunity. Therefore, the properties of these mice should be considered. Nude mice carry a FOXN1 mutation that leads to athymic phenotype lacking αβ-T cells, Th1, Th2, Th17, and Treg cells, but they also have cells of myeloid origin, such as macrophages, granulocytes, antigen presenting cells (APCs), natural killer (NK) cells, B cells and T cells, such as NK T and γδ-T cells (51).

These nude mice, however, were used in various studies related to the TME including in A549 lung cancer- or MDA-MB231 breast cancer-derived tumors, as well as other cancer types which showed that, in these mice, the TME including tumor-associated fibroblasts, immune cells, and cellular components (e.g., cytokines, chemokines, growth factors) are present in the TME and can be modulated by various treatments (52, 53). In addition, these mice were used in several studies using A549 cells xenograft and analyzed PD-L1 expression (54–56).

SMAC depletion inhibited tumor growth and induced apoptosis

SMAC-depleted A549 lung cancer-derived xenografts in mice showed a low capacity to develop tumors, as expected from their reduced proliferation (Figure 2G). However, the inhibition of tumor growth could also be due to activation of apoptosis. Interestingly, while SMAC/-KO cells in culture, showed no significant apoptosis (Figure 1G), the SMA-KO-derived tumors showed massive apoptosis, as revealed using TUNEL staining, increased activated caspase-3, and reduced expression of the anti-apoptotic protein Bcl-2, XIAP and increased p53 (Figure 3).

Moreover, survivin/BIRC5, overexpressed in cancers and a prognostic marker of several cancers (57), was highly reduced in the SMAC-KO cells (Figure 1). As survivin/BIRC5 binds to SMAC/Diablo and prevents caspase activation thereby leading to negative regulation of apoptosis (23), its decreased levels would promote apoptosis. Survivin/BIRC5 silencing leads to apoptosis *via* activation of p53, which was found to increase in SMAC-KO cells (58).

Survivin, however, is functionally important not only for apoptosis, but also in mitochondrial metabolism, mitosis, autophagy, promotion of cell proliferation regulation of cell division, and cell survival (59). Thus, its reduction in SMAC-

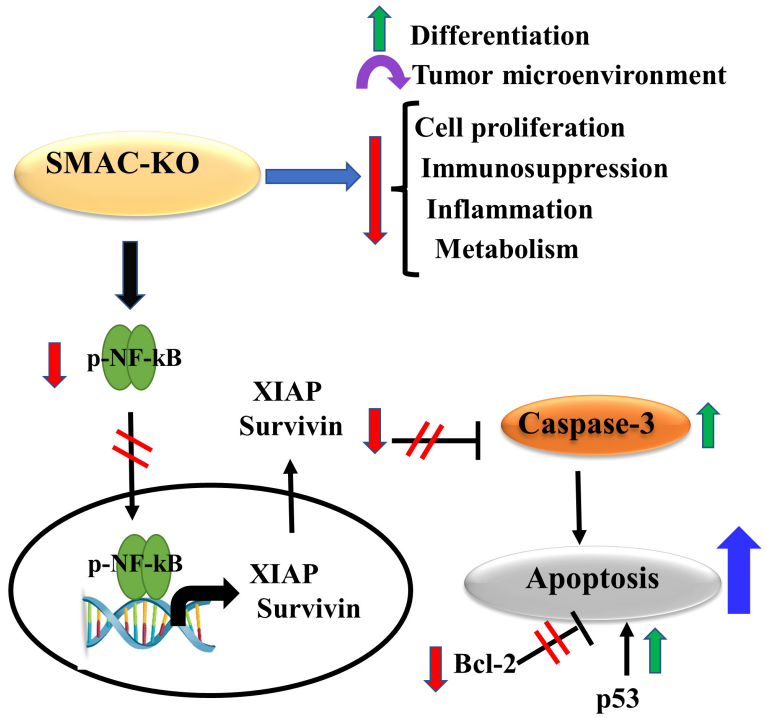

FIGURE 9
Proposed model for SMAC multifunction's in cancer. The small tumors formed by the SMAC-KO cells showed reversal of the unique properties of the tumor. These include inhibited cell proliferation, reduced metabolism, inflammation and immunosuppression, altered TME, and induced differentiation. In addition, they lead to apoptosis induction due to several factors that include increased caspase activity and p53 expression, and reduced expression levels of Bc-l2, survivin, and XIAP.

lacking cells impacts not only in apoptosis regulating, but also multi-tasking, and it is an onco-therapeutic target (60).

This apoptosis may also be associated with p-NF-kB/p65. Our results show very high expression levels of p-NF-kB/p65 in tumors derived from SMAC expressing A549 cells that were highly reduced in tumors lacking SMAC. This decrease in p-NF-kB/p65 can induce apoptosis as found in other studies where apoptosis was induced when NF-kB activation was inhibited by different means (61, 62).

SMAC depletion induced morphological changes and cell differentiation

The non-apoptotic function of SMAC is reflected in the spectrum of proteins whose expression levels were altered in the SMAC-KO cells. This includes proteins related to lipids and lipid-signaling molecules, metabolism, DNA- and RNA-associated processes, transport and intracellular trafficking, cellular signaling, ECM and structural proteins, epigenetics, protein synthesis and degradation, and immune response (Tables S3–S11, Figure 8). The proteins with altered expression in the SMAC-KO cells, presented in detail in the Results section, show a network of key regulators of cell function whose altered expression can lead to cancer cell differentiation.

Here, we focus on the morphological changes and the differentiation observed in the SMAC-KO tumors. Moreover, the inoculated A549 cells, considered as alveolar epithelial type II (AT2)-type cells (19) are considered to be not fully differentiated alveolar epithelial type II (AT2) cells (24). AT2 cells are surfactant-producing cells expressing the pulmonary-associated surfactant proteins (SFTP) A, B. Yet, in the tumors derived from SMAC-KO A549 cells, we detected AT1 cell marker podoplanin (also known as T1α or PDPN), a membranal mucin-type sialoglycoprotein, suggesting that in the absence of SMAC, AT2 cells differentiated into AT1 cells, as reported for cells in culture under certain conditions (25). PDPN is present in many types of normal cells, such as in endothelial cells in lymphatic vessels, and not only in AT1 cells (63).

The morphological changes found in the SMAC-KO cell-derived tumors resembled alveolar-like clusters of lung cancer tissue (Figure 4). This agrees with our previous study, in which we used si-RNA against SMAC, demonstrating that the residual tumors showed morphological changes, including cell differentiation and reorganization into glandular/alveoli-like structures (19, 20). The morphology reorganization into these structures was also reflected in

the arrangement of the blood capillaries in the periphery of the alveolus to allow gas exchange.

SMAC depletion altered the tumor microenvironment

Tumors lacking SMAC also showed an altered TME which included ECM, fibroblasts, inflammatory cells, and endothelial cells. All are important in promoting tumor progression.

Angiogenesis is the consequence of interactions between the tumor and its environment with many factors such as VEGF secreted by tumor cells and surrounding stroma stimulating the proliferation and survival of endothelial cells, leading to the formation of new blood vessels (64). Consequently, treatment strategies have focused on angiogenesis inhibition such as using anti-VEGF in non-small cell lung cancer (NSCLC) patients. However, it has been shown that anti-angiogenic therapy elicits malignant progression of tumors and increases local invasion and metastasis (65–67). Here, we demonstrated that, in contrast to the highly expressed VEGF in SMAC-expressing cells, almost no VEGF was found in the tumors derived from SMAC-lacking cells.

Epithelial-to-mesenchymal transition (EMT) is considered to be one of the steps involved in normal cells becoming cancerous (68). Using the markers for EMT, such as α-SMA, vimentin, E-cadherin, and N-cadherin, our results show that in SMAC-KO cell-derived tumors, the process of EMT was reversed (MET). Vimentin, a type III intermediate filament, normally expressed in mesenchymal cells, is considered a biomarker for EMT, and it is upregulated during cancer metastasis (69). Vimentin expression levels were highly reduced in SMAC-KO cell-derived tumors (Figures 5A, B, F). This is important for vimentin to be considered as a therapeutic target to inhibit cancer growth and spread (69). EMT hallmarks also include upregulated N-cadherin and downregulated E-cadherin. This is reversed in SMAC-depleted tumors (Figures 5C–G), suggesting that induction of MET thereby inhibited migration and metastasis.

The reversal of EMT is also reflected in altered expression of α-SMA produced by the cancer-associated fibroblasts (CAFs), most often associated with poor patient survival/outcome (70). Our results showed a high decrease in α-SMA levels in SMAC-depleted tumors when compared to control tumors (Figures 5H, I). This suggests decreased infiltration of CAFs. Tumor cells expressing α-SMA are predicted to have an invasive nature. These cells tend to metastasize and have a poorer prognosis (70).

Finally, alterations in the TME are also shown in the altered expression of ECM and in structural proteins in SMAC-KO A549 cancer cells (Table S6, Figure 8D). ECM is extremely versatile and performs many functions in addition to its structural role, taking part in most basic cell behaviors from cell proliferation, adhesion and migration to cell differentiation, cell death, and tissue remodeling (71, 72). Thus, these functions of the ECM are modified in the absence of SMAC.

As cancer cells utilize EMT to acquire the ability to migrate, resist therapeutic agents, and escape immunity, reversing EMT by depleting SMAC is a promising strategy for targeting cancer.

SMAC is involved in inflammation and immunity

Our results show that in SMAC-KO cells, and in tumors established from these cells, the expression of many proteins involved in the regulation of tumor inflammation and immunity were altered, suggesting reduced inflammation and activating an immune response.

SMAC association with the immune system is reflected in the proteomic analysis of SMAC-expression and SMAC-KO cells, revealing that the expression levels of many proteins of the immune system were altered (Table S8, Figure 8F). SMAC-KO cells showed altered neutrophil-mediated immunity such as decreased expression, ferritin light chain (FTL), and CD55. Neutrophils play an essential role during an inflammatory response and participate in the initiation and regulation of the adaptive immune response at the inflammation site through interaction with antigen-presenting cells and lymphocytes (72–76). Moreover, neutrophils play a major role in the pathogenesis of cancer, including in tumor initiation, development, and progression (77, 78). The role of neutrophils in cancer is dependent on various factors and may result in a pro-tumoral or an antitumoral effect (79), with most studies indicating that neutrophils promote tumorigenesis (80, 81).

NF-κB coordinates hundreds of gene expressions involved in cell proliferation and apoptosis, stress responses to a variety of stimuli, and an innate immune response (30). Our results show very high expression levels of the activated p-NF-kB/p65 in tumors derived from SMAC-expressing A549 cells, that was highly reduced (over 90%) in SMAC-lacking tumors. This decrease in p-NF-kB/p65 led to reduced inflammation (Figure 6) and apoptosis (Figure 3), as also obtained when NF-kB activation was induced by different means (61, 62).

Pro-inflammatory NF-κB signaling is activated by at least three pathways (82). Among them is TNF-α, a pro-inflammatory cytokine that results in activating p65 that regulates inflammatory responses (83). TNF-α, acting *via* specific cell-surface receptors, can induce both apoptosis and inflammation, and can modulate the innate and adaptive immune system (84). Our results show deceased expression of TNF-α in SMAC-lacking tumors (Figure 6). Thus, the decreased inflammation and induced apoptosis in these tumors suggests that in cancer, SMAC is involved in TNF-α/NF-kB signaling.

In this respect, as SMAC binds IAPs, which were shown to also regulate the activation of NF-κB, and, thereby, inflammation, immunity, cell migration and cell survival, the absence of SMAC and the decrease in XIP and survivn may affect these IAP activities (10, 85).

Another player in inflammation and immunity is transcription factor HIF-1α. It influences many aspects of innate immune cells and regulates M1 macrophage polarization, dendritic-cell maturation and migration, and neutrophil NET formation and survival, and modulates various EMT transcription factors (86) [64]. HIF-1α expression level was highly reduced in SMAC-lacking tumors (Figures 6E, G, H), and, as discussed above, EMT and the neutrophil-associated inflammatory response and regulation of adaptive immune response regulation were altered (Table S8, Figure 8F).

Different types of cancers develop immune escape mechanisms such as the expression of high levels of PD-L1 protein. PD-L1 and its receptor PD-1 are two typical immune checkpoints (ICs) whose interaction concedes T-cell-mediated immune surveillance, thus, promoting cancer cell progression (87). The binding of PD-L1 to PD-1 inhibits T-cell proliferation and activity, leading to tumor immunosuppression (88). Accordingly, cancer immunotherapy, with IC inhibitors (ICIs), such as antibodies against PD-1 or PD-L1 to block PD-L1 or PD-1 on activated T cell membranes, were developed (89, 90), with ICIs significantly enhancing antitumor immunity and prolonging survival (91). However, response rates of patients are less than 40% (92), and they develop adaptive resistance and treatment toxicity (93). NSCLC is one of several tumors in which there are significant atypically upregulated expression levels of PD-L1 and PD-L2, yet the response to immunotherapy of NSCLC patients is about 30% (94).

Our results demonstrate that SMAC-KO tumors express reduced PD-L1 levels (Figures 6I, J). ICIs such as PD-L1 or PD-1 monoclonal antibodies have been used for cancer treatment, including for melanoma, non-small-cell lung cancer, gastric cancer, and breast cancer (95).

The expression of PD-L1 in cancer cells is regulated by multiple signaling pathways that include NF-κB, (96), which induce PD-L1 gene expression, which is abolished by NF-κB inhibitors (97, 98). It has also been reported that TNF-α upregulates PD-L1 expression in cancer cells (99). Thus, the decrease in p-NF-kB and TNF-α levels demonstrated in SMAC-depleted tumors can explain the observed decrease in PD-L1. In addition, inhibition of PD-L1 expression promotes apoptosis in cancer cells (100), in agreement with the increased apoptosis in the SMAC-lacking tumors.

The decrease in EMT in SMAC-KO tumors observed here may also be induced by the decrease in PD-L1 shown to promote EMT (101, 102). It should be noted that chemotherapy or radiation could decrease the response rates to the PD-L1/PD-1 blockade by increasing PD-L1 expression in cancer cells (103).

Interestingly, in a previous study it was shown that expression of a lentiviral vector encoding the cytosolic form of SMAC (tSMAC) elicits proinflammatory cell death that is sufficient to activate adaptive anti-tumor immune responses in cancer (12). Moreover, the infiltration of effector T cells within tumors treated with tSMAC show low expression of PD-1 (12). It was also shown that SMAC mimetics, which competitively inhibit SMAC-cIAP-1/2 interaction and thus repress anti-apoptotic functions of IAP proteins, elicit proinflammatory cell death in cancer cells that engages an adaptive antitumor immune response (104). These finding support our results proposing an additional function for SMAC related to anti-tumor immunity. Taken together, our finding that SMAC depletion significantly reduced the level of PD-L1, suggests that the combination of si-RNA against SMAC with ICIs may be a more effective treatment for cancer than ICIs alone. Moreover, si-SMAC also inhibits cell proliferation, modulates EMT, promotes tumor tissue reorganization, and increases immunogenicity; thus, its combination with anti-PD-L1 therapy could effectively treat tumors.

In summary, for the first time, we demonstrated that, in cancer, SMAC/Diablo possesses several functions distinguished from its well-known activation apoptosis *via* binding the XIAP. Proteomics analysis of SMAC-KO cells revealed that the absence of SMAC resulted in altered expression of proteins associated with a verity of cell functions from lipid transport and intracellular trafficking to metabolism, DNA- and RNA-associated processes, cellular signaling, and immunity. Moreover, SMAC-lacking tumors showed inhibited proliferation and altered oncogenic properties. These include reduced tumor growth and angiogenesis, microenvironment re-modulation, switching from EMT to MET, reduced inflammation, and inducing cell differentiation/arrangement to alveoli-like structures. In addition, the expression of PD-L1, TNF-α, and NF-kB were reduced, resulting in suppressed inflammation, enhanced immunogenicity, and apoptosis promotion.

These results suggest that in cancer cells, SMAC is involved in multiple processes that are essential for tumor growth and progression. Thus, SMAC should be considered as a potential target for the development of new approaches to treat cancer.

Data availability statement

The original contributions presented in the study are included in the article/Supplementary Material. Further inquiries can be directed to the corresponding author.

Ethics statement

All experiments were approved by the Animal Care and Use Committee of Ben-Gurion University of the Negev, as required by Israeli legislation, and all efforts were taken to minimize animal suffering.

Author contributions

Methodology: SP and AS-K; visualization: VS-B, SP, and AS-K; formal analysis: VC-C; conceptualization: VS-B; writing -

review and editing: VS-B; supervision: VS-B. All authors contributed to the article and approved the submitted version.

Funding

This research was supported by a grant from the National Institute for Biotechnology in the Negev (NIBN).

Conflict of interest

The authors declare that the research was conducted in the absence of any commercial or financial relationships that could be construed as a potential conflict of interest.

Publisher's note

Supplementary material

The Supplementary Material for this article can be found online at: https://www.frontiersin.org/articles/10.3389/fonc.2022.992260/full#supplementary-material

References

1. Martinez-Ruiz G, Maldonado V, Ceballos-Cancino G, Grajeda JP, Melendez-Zajgla J. Role of Smac/DIABLO in cancer progression. *J Exp Clin Cancer Res* (2008) 27:48. doi: 10.1186/1756-9966-27-48

2. Shoshan-Barmatz V, Ben-Hail D, Admoni L, Krelin Y, Tripathi SS. The mitochondrial voltage-dependent anion channel 1 in tumor cells. *Biochim Biophys Acta* (2015) 1848:2547–75. doi: 10.1016/j.bbamem.2014.10.040

3. Du C, Fang M, Li Y, Li L, Wang X. Smac, a mitochondrial protein that promotes cytochrome c-dependent caspase activation by eliminating IAP inhibition. *Cell* (2000) 102:33–42. doi: 10.1016/S0092-8674(00)00008-8

4. Verhagen AM, Ekert PG, Pakusch M, Silke J, Connolly LM, Reid GE, et al. Identification of DIABLO, a mammalian protein that promotes apoptosis by binding to and antagonizing IAP proteins. *Cell* (2000) 102:43–53. doi: 10.1016/S0092-8674(00)00009-X

5. Yang QH, Du C. Smac/DIABLO selectively reduces the levels of c-IAP1 and c-IAP2 but not that of XIAP and livin in HeLa cells. *J Biol Chem* (2004) 279:16963–70. doi: 10.1074/jbc.M401253200

6. Polykretis P, Luchinat E. Biophysical characterization of the interaction between the full-length XIAP and Smac/DIABLO. *Biochem Biophys Res Commun* (2021) 568:180–5. doi: 10.1016/j.bbrc.2021.06.077

7. Hanahan D, Weinberg RA. Hallmarks of cancer: The next generation. *Cell* (2011) 144:646–74. doi: 10.1016/j.cell.2011.02.013

8. Ruttinger D, Li R, Poehlein CH, Haley D, Walker EB, Hu HM, et al. Increased susceptibility to immune destruction of B16BL6 tumor cells engineered to express a novel pro-smac fusion protein. *J Immunother.* (2008) 31:43–51. doi: 10.1097/CJI.0b013e318158fd16

9. Dubrez L, Berthelet J, Glorian V. IAP proteins as targets for drug development in oncology. *Onco Targets Ther* (2013) 9:1285–304. doi: 10.2147/OTT.S33375

10. Gyrd-Hansen M, Meier P. IAPs: From caspase inhibitors to modulators of NF-kappaB, inflammation and cancer. *Nat Rev Cancer* (2010) 10:561–74. doi: 10.1038/nrc2889

11. McNeish IA, Bell S, Mckay T, Tenev T, Marani M, Lemoine NR. Expression of Smac/DIABLO in ovarian carcinoma cells induces apoptosis *via* a caspase-9-mediated pathway. *Exp Cell Res* (2003) 286:186–98. doi: 10.1016/S0014-4827(03)00073-9

12. Emeagi PU, Van Lint S, Goyvaerts C, Maenhout S, Cauwels A, Mcneish IA, et al. Proinflammatory characteristics of SMAC/DIABLO-induced cell death in antitumor therapy. *Cancer Res* (2012) 72:1342–52. doi: 10.1158/0008-5472.CAN-11-2400

13. Okada H, Suh WK, Jin J, Woo M, Du C, Elia A, et al. Generation and characterization of Smac/DIABLO-deficient mice. *Mol Cell Biol* (2002) 22:3509–17. doi: 10.1128/MCB.22.10.3509-3517.2002

14. Varfolomeev E, Blankenship JW, Wayson SM, Fedorova AV, Kayagaki N, Garg P, et al. IAP antagonists induce autoubiquitination of c-IAPs, NF-kappaB activation, and TNFalpha-dependent apoptosis. *Cell* (2007) 131:669–81. doi: 10.1016/j.cell.2007.10.030

15. Yoo NJ, Kim HS, Kim SY, Park WS, Park CH, Jeon H, et al. Immunohistochemical analysis of Smac/DIABLO expression in human carcinomas and sarcomas. *APMIS* (2003) 111:382–8. doi: 10.1034/j.1600-0463.2003.t01-1-1110202.x

16. Bao ST, Gui SQ, Lin MS. Relationship between expression of smac and survivin and apoptosis of primary hepatocellular carcinoma. *Hepatobiliary Pancreat. Dis Int* (2006) 5:580–3.

17. Kempkensteffen C, Hinz S, Christoph F, Krause H, Magheli A, Schrader M, et al. Expression levels of the mitochondrial IAP antagonists Smac/DIABLO and Omi/HtrA2 in clear-cell renal cell carcinomas and their prognostic value. *J Cancer Res Clin Oncol* (2008) 134:543–50. doi: 10.1007/s00432-007-0317-7

18. Mohamed MS, Bishr MK, Almutairi FM, Ali AG. Inhibitors of apoptosis: Clinical implications in cancer. *Apoptosis* (2017) 22:1487–509. doi: 10.1007/s10495-017-1429-4

19. Paul A, Krelin Y, Arif T, Jeger R, Shoshan-Barmatz V. A new role for the mitochondrial pro-apoptotic protein SMAC/Diablo in phospholipid synthesis associated with tumorigenesis. *Mol Ther* (2018) 26:680–94. doi: 10.1016/j.ymthe.2017.12.020

20. Pandey SK, Paul A, Shteinfer-Kuzmine A, Zalk R, Bunz U, Shoshan-Barmatz V. SMAC/Diablo controls proliferation of cancer cells by regulating phosphatidylethanolamine synthesis. *Mol Oncol* (2021) 15:3037–61. doi: 10.1002/1878-0261.12959

21. Ritchie ME, Phipson B, Wu D, Hu Y, Law CW, Shi W, et al. Limma powers differential expression analyses for RNA-sequencing and microarray studies. *Nucleic Acids Res* (2015) 43:e47. doi: 10.1093/nar/gkv007

22. Kuleshov MV, Jones MR, Rouillard AD, Fernandez NF, Duan Q, Wang Z, et al. Enrichr: A comprehensive gene set enrichment analysis web server 2016 update. *Nucleic Acids Res* (2016) 44:W90–97. doi: 10.1093/nar/gkw377

23. Park SH, Shin I, Park SH, Kim ND, Shin I. An inhibitor of the interaction of survivin with smac in mitochondria promotes apoptosis. *Chem Asian J* (2019) 14:4035–41. doi: 10.1002/asia.201900587

24. Mao P, Wu S, Li J, Fu W, He W, Liu X, et al. Human alveolar epithelial type II cells in primary culture. *Physiol Rep* (2015) 3. doi: 10.14814/phy2.12288

25. Barkauskas CE, Cronce MJ, Rackley CR, Bowie EJ, Keene DR, Stripp BR, et al. Type 2 alveolar cells are stem cells in adult lung. *J Clin Invest* (2013) 123:3025–36. doi: 10.1172/JCI68782

26. Jubb AM, Pham TQ, Hanby AM, Frantz GD, Peale FV, Wu TD, et al. Expression of vascular endothelial growth factor, hypoxia inducible factor 1alpha, and carbonic anhydrase IX in human tumours. *J Clin Pathol* (2004) 57:504–12. doi: 10.1136/jcp.2003.012963

27. Mani SA, Guo W, Liao MJ, Eaton EN, Ayyanan A, Zhou AY, et al. The epithelial-mesenchymal transition generates cells with properties of stem cells. *Cell* (2008) 133:704–15. doi: 10.1016/j.cell.2008.03.027

28. Zhang TJ, Xue D, Zhang CD, Zhang ZD, Liu QR, Wang JQ. Cullin 4A is associated with epithelial to mesenchymal transition and poor prognosis in perihilar cholangiocarcinoma. *World J Gastroenterol* (2017) 23:2318–29. doi: 10.3748/wjg.v23.i13.2318

29. Greten FR, Grivennikov SI. Inflammation and cancer: Triggers, mechanisms, and consequences. *Immunity* (2019) 51:27–41. doi: 10.1016/j.immuni.2019.06.025

30. Hayden MS, Ghosh S. Signaling to NF-kappaB. *Genes Dev* (2004) 18:2195–224. doi: 10.1101/gad.1228704

31. Mitchell S, Vargas J, Hoffmann A. Signaling *via* the NFkappaB system. *Wiley Interdiscip Rev Syst Biol Med* (2016) 8:227–41. doi: 10.1002/wsbm.1331

32. Karin M. Nuclear factor-kappaB in cancer development and progression. *Nature* (2006) 441:431–6. doi: 10.1038/nature04870

33. Baltimore D. Discovering NF-kappaB. *Cold Spring Harb Perspect Biol* (2009) 1:a000026. doi: 10.1101/cshperspect.a000026

34. Komarova EA, Krivokrysenko V, Wang K, Neznanov N, Chernov MV, Komarov PG, et al. p53 is a suppressor of inflammatory response in mice. *FASEB J* (2005) 19:1030–2. doi: 10.1096/fj.04-3213fje

35. Schwitalla S, Ziegler PK, Horst D, Becker V, Kerle I, Begus-Nahrmann Y, et al. Loss of p53 in enterocytes generates an inflammatory microenvironment enabling invasion and lymph node metastasis of carcinogen-induced colorectal tumors. *Cancer Cell* (2013) 23:93–106. doi: 10.1016/j.ccr.2012.11.014

36. Ashburner M, Ball CA, Blake JA, Botstein D, Butler H, Cherry JM, et al. Gene ontology: tool for the unification of biology. the gene ontology consortium. *Nat Genet* (2000) 25:25–9. doi: 10.1038/75556

37. Gene Ontology C. Gene ontology consortium: Going forward. *Nucleic Acids Res* (2015) 43:D1049–1056. doi: 10.1093/nar/gku1179

38. Lasho TL, Finke CM, Zblewski D, Patnaik M, Ketterling RP, Chen D, et al. Novel recurrent mutations in ethanolamine kinase 1 (ETNK1) gene in systemic mastocytosis with eosinophilia and chronic myelomonocytic leukemia. *Blood Cancer J* (2015) 5:e275. doi: 10.1038/bcj.2014.94

39. Hirota J, Ando H, Hamada K, Mikoshiba K. Carbonic anhydrase-related protein is a novel binding protein for inositol 1,4,5-trisphosphate receptor type 1. *Biochem J* (2003) 372:435–41. doi: 10.1042/bj20030110

40. Maeda A, Nishino T, Matsunaga R, Yokoyama A, Suga H, Yagi T, et al. Transglutaminase-mediated cross-linking of WDR54 regulates EGF receptor-signaling. *Biochim Biophys Acta Mol Cell Res* (2019) 1866:285–95. doi: 10.1016/j.bbamcr.2018.11.009

41. Hu ZW, Chen L, Ma RQ, Wei FQ, Wen YH, Zeng XL, et al. Comprehensive analysis of ferritin subunits expression and positive correlations with tumor-associated macrophages and T regulatory cells infiltration in most solid tumors. *Aging (Albany NY)* (2021) 13:11491–506. doi: 10.18632/aging.202841

42. Kolev M, Towner L, Donev R. Complement in cancer and cancer immunotherapy. *Arch Immunol Ther Exp (Warsz)* (2011) 59:407–19. doi: 10.1007/s00005-011-0146-x

43. Bazewicz CG, Dinavahi SS, Schell TD, Robertson GP. Aldehyde dehydrogenase in regulatory T-cell development, immunity and cancer. *Immunology* (2019) 156:47–55. doi: 10.1111/imm.13016

44. Chen DJ, Huerta S. Smac mimetics as new cancer therapeutics. *Anticancer Drugs* (2009) 20:646–58. doi: 10.1097/CAD.0b013e32832ced78

45. Petersen SL, Peyton M, Minna JD, Wang X. Overcoming cancer cell resistance to smac mimetic induced apoptosis by modulating cIAP-2 expression. *Proc Natl Acad Sci U S A* (2010) 107:11936–41. doi: 10.1073/pnas.1005667107

46. Fulda S. Smac mimetics to therapeutically target IAP proteins in cancer. *Int Rev Cell Mol Biol* (2017) 330:157–69. doi: 10.1016/bs.ircmb.2016.09.004

47. Baggio C, Gambini L, Udompholkul P, Salem AF, Aronson A, Dona A, et al. Design of potent pan-IAP and lys-covalent XIAP selective inhibitors using a thermodynamics driven approach. *J Med Chem* (2018) 61:6350–63. doi: 10.1021/acs.jmedchem.8b00810

48. Boddu P, Carter BZ, Verstovsek S, Pemmaraju N. SMAC mimetics as potential cancer therapeutics in myeloid malignancies. *Br J Haematol* (2019) 185:219–31. doi: 10.1111/bjh.15829

49. Hagenbuchner J, Oberacher H, Arnhard K, Kiechl-Kohlendorfer U, Ausserlechner MJ. Modulation of respiration and mitochondrial dynamics by SMAC-mimetics for combination therapy in chemoresistant cancer. *Theranostics* (2019) 9:4909–22. doi: 10.7150/thno.33758

50. Morrish E, Brumatti G, Silke J. Future therapeutic directions for smac-mimetics. *Cells* (2020) 9. doi: 10.3390/cells9020406

51. Harris B, Fairfield. He., Berry Ml., Bergstrom De., Bronson Rt., Donahue Lr. Nude 2 Jackson: A new spontaneous mutation in Foxn1 MGI direct data submission. (2013). Available at: http://www.informatics.jax.org/reference/J:192383

52. Zhang B, Jin K, Jiang T, Wang L, Shen S, Luo Z, et al. Celecoxib normalizes the tumor microenvironment and enhances small nanotherapeutics delivery to A549 tumors in nude mice. *Sci Rep* (2017) 7:10071. doi: 10.1038/s41598-017-09520-7

53. Worner PM, Schachtele DJ, Barabadi Z, Srivastav S, Chandrasekar B, Izadpanah R, et al. Breast tumor microenvironment can transform naive mesenchymal stem cells into tumor-forming cells in nude mice. *Stem Cells Dev* (2019) 28:341–52. doi: 10.1089/scd.2018.0110

54. Li F, Zhu T, Yue Y, Zhu X, Wang J, Liang L. Preliminary mechanisms of regulating PDL1 expression in nonsmall cell lung cancer during the EMT process. *Oncol Rep* (2018) 40:775–82. doi: 10.3892/or.2018.6474

55. Liu Q, Wang X, Yang Y, Wang C, Zou J, Lin J, et al. Immuno-PET imaging of PD-L1 expression in patient-derived lung cancer xenografts with [(68)Ga]Ga-NOTA-Nb109. *Quant. Imaging Med Surg* (2022) 12:3300–13. doi: 10.21037/qims-21-991

56. Zhong B, Zheng J, Wen H, Liao X, Chen X, Rao Y, et al. NEDD4L suppresses PD-L1 expression and enhances anti-tumor immune response in A549 cells. *Genes Genomics* (2022) 44:1071–79 . doi: 10.1007/s13258-022-01238-9

57. Li D, Hu C, Li H. Survivin as a novel target protein for reducing the proliferation of cancer cells. *BioMed Rep* (2018) 8:399–406. doi: 10.3892/br.2018.1077

58. Lamers F, van der Ploeg I, Schild L, Ebus ME, Koster J, Hansen BR, et al. Knockdown of survivin (BIRC5) causes apoptosis in neuroblastoma *via* mitotic catastrophe. *Endocr Relat Cancer* (2011) 18:657–68. doi: 10.1530/ERC-11-0207

59. Caldas H, Jiang Y, Holloway MP, Fangusaro J, Mahotka C, Conway EM, et al. Survivin splice variants regulate the balance between proliferation and cell death. *Oncogene* (2005) 24:1994–2007. doi: 10.1038/sj.onc.1208350

60. Wheatley SP, Altieri DC. Survivin at a glance. *J Cell Sci* (2019) 132. doi: 10.1242/jcs.223826

61. Zhang XA, Zhang S, Yin Q, Zhang J. Quercetin induces human colon cancer cells apoptosis by inhibiting the nuclear factor-kappa b pathway. *Pharmacogn. Mag.* (2015) 11:404–9. doi: 10.4103/0973-1296.153096

62. Anaya-Eugenio GD, Eggers NA, Ren Y, Rivera-Chavez J, Kinghorn AD, Carcache D.E.B.E.J. Apoptosis induced by (+)-betulin through NF-kappaB inhibition in MDA-MB-231 breast cancer cells. *Anticancer Res* (2020) 40:6637–47. doi: 10.21873/anticanres.14688

63. Ugorski M, Dziegiel P, Suchanski J. Podoplanin - a small glycoprotein with many faces. *Am J Cancer Res* (2016) 6:370–86.

64. Ferrara N. VEGF and intraocular neovascularization: From discovery to therapy. *Transl Vis Sci Technol* (2016) 5:10. doi: 10.1167/tvst.5.2.10

65. Ebos JM, Lee CR, Cruz-Munoz W, Bjarnason GA, Christensen JG, Kerbel RS. Accelerated metastasis after short-term treatment with a potent inhibitor of tumor angiogenesis. *Cancer Cell* (2009) 15:232–9. doi: 10.1016/j.ccr.2009.01.021

66. Paez-Ribes M, Allen E, Hudock J, Takeda T, Okuyama H, Vinals F, et al. Antiangiogenic therapy elicits malignant progression of tumors to increased local invasion and distant metastasis. *Cancer Cell* (2009) 15:220–31. doi: 10.1016/j.ccr.2009.01.027

67. Cortes-Santiago N, Hossain MB, Gabrusiewicz K, Fan X, Gumin J, Marini FC, et al. Soluble Tie2 overrides the heightened invasion induced by anti-angiogenesis therapies in gliomas. *Oncotarget* (2016) 7:16146–57. doi: 10.18632/oncotarget.7550

68. Kalluri R, Weinberg RA. The basics of epithelial-mesenchymal transition. *J Clin Invest* (2009) 119:1420–8. doi: 10.1172/JCI39104

69. Usman S, Waseem NH, Nguyen TKN, Mohsin S, Jamal A, Teh MT, et al. Vimentin is at the heart of epithelial mesenchymal transition (EMT) mediated metastasis. *Cancers (Basel)* (2021) 13. doi: 10.3390/cancers13194985

70. Parikh JG, Kulkarni A, Johns C. Alpha-smooth muscle actin-positive fibroblasts correlate with poor survival in hepatocellular carcinoma. *Oncol Lett* (2014) 7:573–5. doi: 10.3892/ol.2013.1720

71. Hynes RO. The extracellular matrix: Not just pretty fibrils. *Science* (2009) 326:1216–9. doi: 10.1126/science.1176009

72. Leliefeld PH, Koenderman L, Pillay J. How neutrophils shape adaptive immune responses. *Front Immunol* (2015) 6:471. doi: 10.3389/fimmu.2015.00471

73. Rosales C, Demaurex N, Lowell CA, Uribe-Querol E. Neutrophils: Their role in innate and adaptive immunity. *J Immunol Res* (2016) 2016:1469780. doi: 10.1155/2016/1469780

74. Yang F, Feng C, Zhang X, Lu J, Zhao Y. The diverse biological functions of neutrophils, beyond the defense against infections. *Inflammation* (2017) 40:311–23. doi: 10.1007/s10753-016-0458-4

75. Wang X, Qiu L, Li Z, Wang XY, Yi H. Understanding the multifaceted role of neutrophils in cancer and autoimmune diseases. *Front Immunol* (2018) 9:2456. doi: 10.3389/fimmu.2018.02456

76. Li Y, Wang W, Yang F, Xu Y, Feng C, Zhao Y. The regulatory roles of neutrophils in adaptive immunity. *Cell Commun Signal* (2019) 17:147. doi: 10.1186/s12964-019-0471-y

77. Kim J, Bae JS. Tumor-associated macrophages and neutrophils in tumor microenvironment. *Mediators Inflamm* (2016) 2016:6058147. doi: 10.1155/2016/6058147

78. Shaul ME, Fridlender ZG. Neutrophils as active regulators of the immune system in the tumor microenvironment. *J Leukoc Biol* (2017) 102:343–9. doi: 10.1189/jlb.5MR1216-508R

79. Coffelt SB, Wellenstein MD, De Visser KE. Neutrophils in cancer: neutral no more. *Nat Rev Cancer* (2016) 16:431–46. doi: 10.1038/nrc.2016.52

80. Sionov RV, Fridlender ZG, Granot Z. The multifaceted roles neutrophils play in the tumor microenvironment. *Cancer Microenviron.* (2015) 8:125–58. doi: 10.1007/s12307-014-0147-5

81. Vols S, Sionov RV, Granot Z. Always look on the bright side: Anti-tumor functions of neutrophils. *Curr Pharm Des* (2017) 23:4862–92. doi: 10.2174/1381612823666170704125420

82. Hoesel B, Schmid JA. The complexity of NF-kappaB signaling in inflammation and cancer. *Mol Cancer* (2013) 12:86. doi: 10.1186/1476-4598-12-86

83. Lawrence T. The nuclear factor NF-kappaB pathway in inflammation. *Cold Spring Harb Perspect Biol* (2009) 1:a001651. doi: 10.1101/cshperspect.a001651

84. Dinarello CA. Historical insights into cytokines. *Eur J Immunol* (2007) 37 Suppl 1:S34–45. doi: 10.1002/eji.200737772

85. Vince JE, Wong WW, Khan N, Feltham R, Chau D, Ahmed AU, et al. IAP antagonists target cIAP1 to induce TNFalpha-dependent apoptosis. *Cell* (2007) 131:682–93. doi: 10.1016/j.cell.2007.10.037

86. McGettrick AF, O'Neill L. The role of HIF in immunity and inflammation. *Cell Metab* (2020) 32:524–36. doi: 10.1016/j.cmet.2020.08.002

87. Chen L, Han X. Anti-PD-1/PD-L1 therapy of human cancer: past, present, and future. *J Clin Invest* (2015) 125:3384–91. doi: 10.1172/JCI80011

88. Topalian SL, Drake CG, Pardoll DM. Targeting the PD-1/B7-H1(PD-L1) pathway to activate anti-tumor immunity. *Curr Opin Immunol* (2012) 24:207–12. doi: 10.1016/j.coi.2011.12.009

89. Sharma P, Allison JP. The future of immune checkpoint therapy. *Science* (2015) 348:56–61. doi: 10.1126/science.aaa8172

90. Hahn AW, Gill DM, Pal SK, Agarwal N. The future of immune checkpoint cancer therapy after PD-1 and CTLA-4. *Immunotherapy* (2017) 9:681–92. doi: 10.2217/imt-2017-0024

91. Akinleye A, Rasool Z. Immune checkpoint inhibitors of PD-L1 as cancer therapeutics. *J Hematol Oncol* (2019) 12:92. doi: 10.1186/s13045-019-0779-5

92. Yarchoan M, Hopkins A, Jaffee EM. Tumor mutational burden and response rate to PD-1 inhibition. *N Engl J Med* (2017) 377:2500–1. doi: 10.1056/NEJMc1713444

93. Sharma P, Hu-Lieskovan S, Wargo JA, Ribas A. Primary, adaptive, and acquired resistance to cancer immunotherapy. *Cell* (2017) 168:707–23. doi: 10.1016/j.cell.2017.01.017

94. Karachaliou N, Gonzalez-Cao M, Sosa A, Berenguer J, Bracht JWP, Ito M, et al. The combination of checkpoint immunotherapy and targeted therapy in cancer. *Ann Transl Med* (2017) 5:388. doi: 10.21037/atm.2017.06.47

95. Iwai Y, Hamanishi J, Chamoto K, Honjo T. Cancer immunotherapies targeting the PD-1 signaling pathway. *J BioMed Sci* (2017) 24:26. doi: 10.1186/s12929-017-0329-9

96. Ritprajak P, Azuma M. Intrinsic and extrinsic control of expression of the immunoregulatory molecule PD-L1 in epithelial cells and squamous cell carcinoma. *Oral Oncol* (2015) 51:221–8. doi: 10.1016/j.oraloncology.2014.11.014

97. Bi XW, Wang H, Zhang WW, Wang JH, Liu WJ, Xia ZJ, et al. PD-L1 is upregulated by EBV-driven LMP1 through NF-kappaB pathway and correlates with poor prognosis in natural killer/T-cell lymphoma. *J Hematol Oncol* (2016) 9:109. doi: 10.1186/s13045-016-0341-7

98. Lim W, Jeong M, Bazer FW, Song G. Curcumin suppresses proliferation and migration and induces apoptosis on human placental choriocarcinoma cells *via* ERK1/2 and SAPK/JNK MAPK signaling pathways. *Biol Reprod* (2016) 95:83. doi: 10.1095/biolreprod.116.141630

99. Wang X, Yang L, Huang F, Zhang Q, Liu S, Ma L, et al. Inflammatory cytokines IL-17 and TNF-alpha up-regulate PD-L1 expression in human prostate and colon cancer cells. *Immunol Lett* (2017) 184:7–14. doi: 10.1016/j.imlet.2017.02.006

100. Li J, Chen L, Xiong Y, Zheng X, Xie Q, Zhou Q, et al. Knockdown of PD-L1 in human gastric cancer cells inhibits tumor progression and improves the cytotoxic sensitivity to CIK therapy. *Cell Physiol Biochem* (2017) 41:907–20. doi: 10.1159/000460504

101. Dong P, Xiong Y, Yue J, Hanley SJB, Watari H. Tumor-intrinsic PD-L1 signaling in cancer initiation, development and treatment: Beyond immune evasion. *Front Oncol* (2018) 8:386. doi: 10.3389/fonc.2018.00386

102. Escors D, Gato-Canas M, Zuazo M, Arasanz H, Garcia-Granda MJ, Vera R, et al. The intracellular signalosome of PD-L1 in cancer cells. *Signal Transduct. Target Ther* (2018) 3:26. doi: 10.1038/s41392-018-0022-9

103. Sun LL, Yang RY, Li CW, Chen MK, Shao B, Hsu JM, et al. Inhibition of ATR downregulates PD-L1 and sensitizes tumor cells to T cell-mediated killing. *Am J Cancer Res* (2018) 8:1307–16.

104. Ali H, Caballero R, Dong SXM, Gajnayaka N, Vranjkovic A, Ahmed D, et al. Selective killing of human M1 macrophages by smac mimetics alone and M2 macrophages by smac mimetics and caspase inhibition. *J Leukoc Biol* (2021) 110:693–710. doi: 10.1002/JLB.4A0220-114RR

frontiers | Frontiers in Oncology

TYPE Review
PUBLISHED 20 October 2022
DOI 10.3389/fonc.2022.983878

OPEN ACCESS

EDITED BY
Nadège Bellance,
Université de Bordeaux,
France

REVIEWED BY
Beth Coyle,
University of Nottingham,
United Kingdom
Rafael Roesler,
Federal University of Rio Grande do Sul, Brazil

*CORRESPONDENCE
Zengliang Wang
wzl3ng@126.com
Yongxin Wang
xjdwyx2000@sohu.com

†These authors have contributed equally to this work

SPECIALTY SECTION
This article was submitted to Molecular and Cellular Oncology, a section of the journal Frontiers in Oncology

RECEIVED 01 July 2022
ACCEPTED 28 September 2022
PUBLISHED 20 October 2022

CITATION
Aili Y, Maimaitiming N, Qin H, Ji W, Fan G, Wang Z and Wang Y (2022) Tumor microenvironment and exosomes in brain metastasis: Molecular mechanisms and clinical application.
Front. Oncol. 12:983878.
doi: 10.3389/fonc.2022.983878

Tumor microenvironment and exosomes in brain metastasis: Molecular mechanisms and clinical application

Yirizhati Aili[1†], Nuersimanguli Maimaitiming[2†], Hu Qin[1], Wenyu Ji[1], Guofeng Fan[1], Zengliang Wang[1,3,4*] and Yongxin Wang[1*]

[1]Department of Neurosurgery, First Affiliated Hospital of Xinjiang Medical University, Urumqi, China, [2]Department of Four Comprehensive Internal Medicine, The First Affiliated Hospital of Xinjiang Medical University, Xinjiang, China, [3]School of Health Management, Xinjiang Medical University, Urumqi, China, [4]Department of Neurosurgery, Xinjiang Bazhou People's Hospital, Xinjiang, China

Metastasis is one of the important biological features of malignant tumors and one of the main factors responsible for poor prognosis. Although the widespread application of newer clinical technologies and their continuous development have significantly improved survival in patients with brain metastases, there is no uniform standard of care. More effective therapeutic measures are therefore needed to improve prognosis. Understanding the mechanisms of tumor cell colonization, growth, and invasion in the central nervous system is of particular importance for the prevention and treatment of brain metastases. This process can be plausibly explained by the "seed and soil" hypothesis, which essentially states that tumor cells can interact with various components of the central nervous system microenvironment to produce adaptive changes; it is this interaction that determines the development of brain metastases. As a novel form of intercellular communication, exosomes play a key role in the brain metastasis microenvironment and carry various bioactive molecules that regulate receptor cell activity. In this paper, we review the roles and prospects of brain metastatic tumor cells, the brain metastatic tumor microenvironment, and exosomes in the development and clinical management of brain metastases.

KEYWORDS

brain tumor, metastases, tumor cell, tumor microenvironment, exosomes

Introduction

In the natural course, brain metastases occur in approximately 20–40% of patients with malignancies. Lung cancers are the most common source of brain metastases (40%–50%), and are followed by cancers of the breast (15%–20%), skin (mainly melanoma; 5%–10%), and gastrointestinal system (4%–6%) (Figure 1) (1). The survival and quality of life of patients with cancer have improved considerably in recent years due to the advent of newer treatment methods, and especially precision therapy. However, owing to the anatomical and physiological peculiarities of the central nervous system (CNS), it is difficult to achieve the desired effect of various treatments; brain metastases are therefore known as the last refuge of malignant tumors (2, 3). The median survival period in patients with untreated brain metastases is 1-2 months, while that of those who have been treated is approximately 6 months (4). The currently available treatments for brain metastases mainly include radiotherapy, systemic chemotherapy, and surgery. In this context, the widespread use of targeted drugs has improved the prognosis of these patients to a certain extent (5). However, the overall prognosis remains unsatisfactory.

Metastasis of tumor cells is one of the most important features of malignant tumors, and the intra- and inter-cellular molecular mechanisms involved in the metastasis process are considerably complex. These include epithelial-mesenchymal transition, survival of circulating tumor cells in blood vessels, tumor cell dormancy, and tumor cell heterogeneity and stemness, among others. The interaction between tumor and stromal cells, tumor-related angiogenesis, and a series of events related to the tumor microenvironment are also involved (6). The seed and soil hypothesis suggests that a specific tumor cell can only survive in a suitable tumor microenvironment; this explains the occurrence and development of tumor-specific metastasis (7). In this context, exosomes (a type of extracellular vesicles loaded with proteins, nucleic acids, and other signaling molecules) are involved in multiple processes leading to the development of brain metastases (8). Metastatic lesions to the CNS are unique compared to those in other organs (9). Evaluation of the biological characteristics of tumor cells that metastasize to the

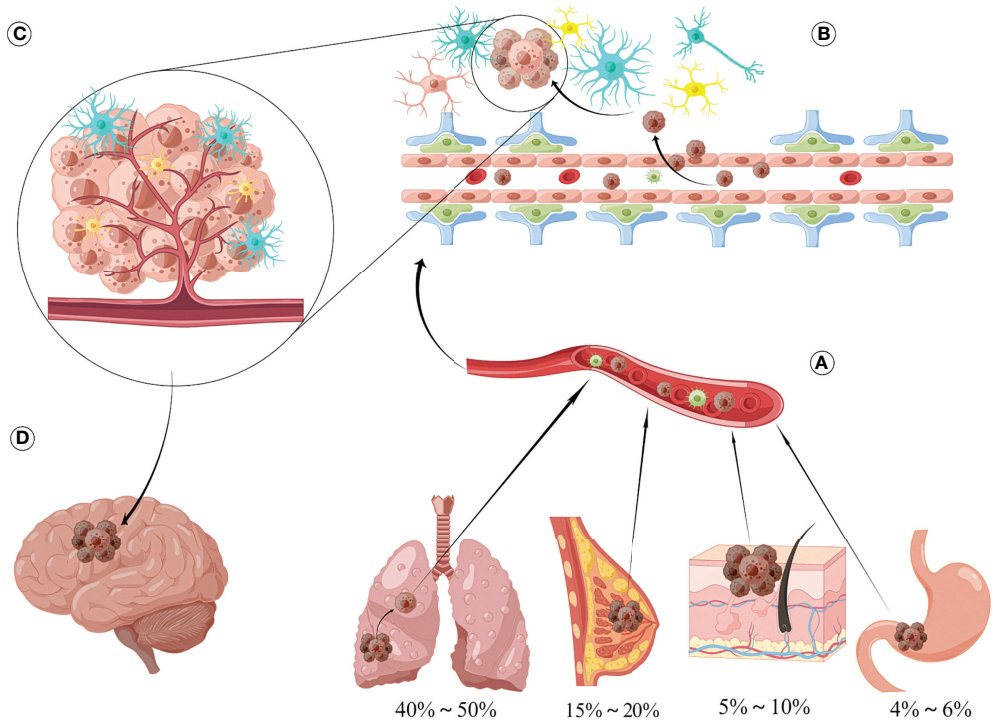

FIGURE 1
Sources and formation processes of brain metastases. **(A)** The most common sources of brain metastases are lung cancer (40%-50%), followed by breast cancer (15%-20%), skin cancer (mainly melanoma) accounting for 5%-10%, and gastrointestinal malignancy (4%-6%). **(B)** Tumor cells and secreted vesicle contents can disrupt the integrity of BBB, thereby promoting tumor metastasis to intracranial, interacting with surrounding astrocytes, microglia/macrophages, and then influencing the biological behavior of brain metastasis through various pathways such as secreting cytokine networks, direct contact and exosomes, and establishing complex networks. **(C)** Tumor cells can produce mutual adaptive changes with the components of the central nervous system microenvironment, and it is this interaction that determines the occurrence and development of brain metastatic lesions. **(D)** Metastatic foci appear in the skull, producing obvious mass and edematic effects, which seriously affects the quality of life of patients.

brain and their interaction with the microenvironment is therefore essential for the prevention and treatment of brain metastases.

Proposal of the tumor microenvironment

The tumor microenvironment was first proposed in 1979, and has been variably termed as the tumor niche or tumor stem cell niche, among others (10). The tumor microenvironment refers to the local homeostatic milieu associated with tumorigenesis and metastasis, and is composed of tumor and non-tumor cells. It mainly includes tumor cells, tumor stem cells, endothelial cells, fibroblasts, immune cells, extracellular matrix structural components (such as collagen and elastin, among others) locally secreted cytokines, peptide growth factors, and other soluble substances (11, 12). It is widely accepted that the tumor microenvironment is a necessary functional unit for protecting and supporting tumorigenesis, development, metastasis, and recurrence; studies are also increasingly demonstrating the vital role of the tumor microenvironment in the evolution of tumors (13). Normal cells reside in a relatively stable internal environment (homeostatic milieu), and follow regulated processes for proliferation, differentiation, apoptosis, and the secretion and expression of related factors (14). Tumorigenesis involves a process that persistently disrupts this balance to alter the equilibrium in the local microenvironment, making it more suitable for tumor cell proliferation (15). Tumor cells proliferate indefinitely, and need to constantly shape an external tissue environment suitable for their growth. This involves the creation of tissue hypoxia and acidosis; formation of interstitial hypertension; and the production of a large number of growth factors, proteolytic enzymes, and immune inflammatory responses (16, 17). The tumor microenvironment provides shelter for metastatic tumor cells, protecting them from differentiation stimulation, apoptosis stimulation, and immune surveillance, thereby improving resistance to radiotherapy and chemotherapy (18). The tumor microenvironment can also induce tumor cell metastasis *via* secretion of cyclooxygenase-2 (COX2) and epidermal growth factor receptor (EGFR), the factors responsible for the organophilic nature of tumor cell metastasis. Tumor growth may therefore be inhibited by altering the local microenvironment of the tumor (19, 20).

Characteristics of the microenvironment of brain metastases

The microenvironment of brain metastases has the following unique properties compared with that of other tissues (1): the presence of two biological barriers, namely, the blood-brain barrier (BBB) and blood-cerebrospinal fluid barrier (2), lack of immune cells such as lymphocytes and macrophages (microglia play an important role in the immune response) (3), lack of mesenchymal tissues such as fibroblasts (but is rich in astrocytes and oligodendrocytes), and (4) high expression of CNS-specific molecules such as CXCL-12 and neuroserpin (with neutropenia) (21–23). However, the role of the intracranial microenvironment in the development of brain metastases is debated. Previous studies have shown that tumor cells isolated from brain metastases models or co-cultured *in vitro* in the CNS microenvironment have stronger proliferation, invasion, and metastasis capabilities than the protocellular line (24). However, other studies have shown that astrocytes can secrete plasminogen activators to promote apoptosis of tumor cells; this is not conducive to tumor cell growth (Figure 1) (25). The impact of the intracranial microenvironment on tumor cells (based on the components that constitute the CNS microenvironment and their interaction with tumor cells) has been described below.

Astrocytes

Astrocytes are the most abundant glial cells in the CNS. They are activated on stimulation, and appear morphologically hypertrophied; this is accompanied by increased expression of glial fibrillary acidic protein, a marker specific for astrocyte activation (26). Astrocytes perform a variety of functions, which include supporting nerve cells, nourishing nerve tissue, maintaining CNS homeostasis, forming a BBB, and repairing damaged CNS tissue (27). As the most important component of the CNS microenvironment, astrocytes play an important role in the formation of brain metastases (28). Following activation, astrocytes secrete a variety of cytokines that affect the proliferation, invasion, and metastatic ability of tumor cells (29). Studies have suggested that astrocytes can secrete matrix metalloproteinase (MMP)-2 and MMP-9, remove matrix components on the surface of tumor cells and the surrounding matrix, and promote the invasion and metastasis of tumor cells. In this context, MMP-2 and MMP-9 can activate transforming growth factor-β (TGF-β) (30), which in turn regulates cell growth, angiogenesis, and other functions through vascular endothelial growth factor (VEGF). Related clinical data show that patients with MMP-2-positive *in situ* or metastatic tumors of the brain have shorter survival times (31). A study on melanoma brain metastases found that astrocytes can produce interleukin (IL)-3, CD40L, CXCL 12, interferon-γ, and other cytokines that stimulate melanoma cells; in this context, IL-23 stimulates tumor cells to produce MMP-2, thereby promoting tumor cell proliferation (32). The mechanism of interaction between tumor cells and astrocytes (via cytokine networks) is considerably complex. Studies have shown that tumor cells in

the CNS can secrete macrophage migration inhibitory factor, IL-8, and plasminogen activator inhibitor 1, thereby activating astrocytes; activated astrocytes can secrete IL-6 and tumor necrosis factor-α (TNF-α). TNF-α and IL-1β promote tumor cell growth; however, IL-6 receptor expression is down-regulated in these tumors (33, 34). However, as demonstrated by Sierra et al. (35), astrocytes also inhibit the growth of tumor cells. This is mainly mediated by fibrinolytic enzymes in the CNS that cause shedding of Fas ligand from astrocyte membranes; the secreted Fas ligand triggers apoptosis of tumor cells (36).

Astrocytes also protect tumor cells from the cytotoxic effects of chemotherapy. This protection may be mediated by direct contact with tumor cells and gap junctions (GJs); however, fibroblasts do not play a similar role (37–39). In this context, direct connexin 43-mediated intercellular communication between astrocytes and melanoma cells protects the latter against chemotherapy-induced apoptosis (40). Direct contact between astrocytes and tumor cells can also promote the secretion of IL-6 and IL-8 by tumor cells. Astrocytes then produce endothelin 1, which binds to the endothelin receptor of tumor cells to activate the AKT and mitogen-activated protein kinase pathways; this affects the downstream expression of Bcl-2-like protein 1, twist family basic helix-loop-helix transcription factor 1, and glutathione s-transferase alpha 5, thereby protecting the cells against chemotherapy drugs (41). Murphy et al. (42) found that connexin 43 can induce resistance to temozolomide by activating the AKT/AMP-activated protein kinase/mammalian target of rapamycin signaling pathway in malignant gliomas. However, studies have shown that connexin 43-mediated intercellular communication can enhance the cytotoxic effect of chemotherapy drugs in testicular cancer cells; in this context, studies suggest that GJs can transmit certain small molecules to induce tumor cell apoptosis (43). These findings suggest that specific GJ signaling molecules in tumor cells and the microenvironment can affect tumor cell sensitivity to chemotherapy in the CNS; they may block or activate signaling between GJs and offer clinically significant enhancement of chemotherapy drug effects.

As a key factor in the microenvironment, astrocytes can interact with tumor cells to influence the biological behavior of brain metastases *via* various channels such as cytokine networks and direct contact. The interaction between the two is complex and some mechanisms have not been fully understood; this needs further evaluation (44–46).

Microglia/macrophages

Microglia play an important role in the CNS immune response (47). They belong to the monocyte-macrophage system, and it is difficult to distinguish them from circulating macrophages based on morphological and molecular markers after activation (48). Animal experiments have shown that in metastatic tumor models, microglia/macrophages are mostly derived from circulating monocytes; original intracranial microglia represent a minority. Certain studies therefore refer to activated microglia as microglia/macrophages (49).

The immune system plays an important role in tumorigenesis and development. Tumor macrophages can be divided into two types, namely, M1 and M2; the M2 mononuclear macrophage surface antigens CD163 and CD204 lead to secretion of arginase, IL-10, lipopolysaccharide, interferon γ, and transforming growth factor-β1. Cytokines such as transforming growth factor-β1 promote tumor growth. Conversely, M1 macrophages show high levels of inducible nitric oxide synthase expression and secrete IL-1, IL-12, nitric oxide, and TNF-α, all of which have tumoricidal effect (50). Wei et al. (48) studied the role of microglia/macrophages in glioma. They found that the M2 macrophages in the tumor microenvironment promoted glioma cell invasion, angiogenicity, and the formation of an inhibitory immune microenvironment, resulting in poor prognosis. Microglia/macrophages serve as the most important link for immune function in the CNS. It is therefore essential to identify the types of microglia/macrophages and the mechanisms of their production in brain metastatic tumors; this may help to confirm the relationship between the immune system and tumor cells in the CNS (51).

Data regarding the phenotypic changes of microglia/macrophages in brain metastases and the related mechanisms are lacking. Data regarding their impact on the treatment of tumors are also considerably scarce compared to those on current popular immunotherapy (52). *In vitro* experiments have shown that zoledronic acid can promote phenotypic changes in CNS microglia/macrophages to inhibit tumor invasion; clinical data also suggest that zoledronic acid can reduce the risk of recurrence in patients with breast cancer (53). However, sufficient clinical evidence is lacking for patients with brain metastases. Further trials are needed to evaluate the effect of microglia/macrophages in the treatment of brain metastasis (52, 54).

Recent research suggests that in addition to astrocytes and microglia, neurons and neurotransmitters play an important role in the occurrence and development of metastases (55). Zeng et al. (56) found that elevated N-methyl-D-aspartic acid (NMDA) receptor expression promotes the development of intracranial metastasis in breast cancer. The process is mediated by a protein subunit of the NMDA receptor, namely, GIuN2B, which is required for synapse formation and alteration of synaptic junction intensity; it is highly expressed in both human and mouse breast cancer cells. NMDA receptors allow calcium ions to enter the cells; this may be involved in the development of some human cancers. Zeng et al. (56) also found that human breast cancer cells express a protein known as neuroligin, which contributes to intercellular adhesion; it typically promotes the formation of synapes between neurons. This suggests that similar to human glioma cells, human breast

cancer cells may exploit neuronal machinery to establish synaptic connections. Microscopy of mouse brain tissue samples containing human breast cancer cells has shown that the proteins that pack glutamate into vesicles are in close proximity to NMDA receptors; it also demonstrated the formation of synaptic structures between cancer cells and neurons. Compared with the mice that were injected with breast cancer cells having normal GIuN2B levels, the modified mice produced smaller brain tumors; they also had longer survival times with lower GIuN2B expression. This suggests that GIuN2B-mediated NMDA receptor signaling occurs through the formation of "pseudo" three-way synapses, which promote tumor cell colonization and growth in the brain. Several subsequent studies have shown that brain metastatic tumor cells can establish synaptic connections with neurons by using the molecular mechanisms involved in synapse formation between neurons. Synaptic activity causes depolarization in neurons and facilitates calcium ion flow, which is necessary for cell differentiation, proliferation, and survival. In cancer cells, this process promotes tumor colonization and progression (57, 58).

Blood-brain barrier

The BBB is the structure with which tumor cells first come into contact during the development of brain metastases. It is composed of capillary endothelial cells and the tight connections between them, basal membranes, and dendrites of astrocytes (59). Under physiological circumstances, the BBB maintains CNS homeostasis and has an isolating effect on drugs, toxins, ions, and other substances (60). The tight connections of the BBB are the key to maintaining its integrity. These are composed of transmembrane proteins and surrounding proteins; the transmembrane proteins which constitute the connection between cells comprise occludin, junctional adhesion molecules, and the tight junction protein, claudin (mainly claudin-5 on BBB). The surrounding proteins are distributed on both sides of the tight junction (52, 61–63). Proteins such as the atresia band (zonula occludin [ZO]) and the filamentous actin-binding protein (afadin) maintain BBB stability (64). Animal experiments have shown that a variety of tumor cell lines can successfully pass through the BBB (65), and that the passage of tumor cells through the BBB is the first step in the formation of brain metastatic foci; however, the specific mechanism is not fully understood. On comparing differences in gene expression between brain metastatic lesions and protocellular cells, Bos et al. (66) found that COX2, α2,6-sialyltransferase (ST6Gal-I), and EGF can mediate passage of breast cancer cells through the BBB; they speculated that ST6Gal-I can specifically mediate brain metastasis by promoting acidification of endothelial cell surfaces (67). In patients with colon cancer, a single-nucleotide polymorphism of ST6Gal-I RS1736858 is highly associated with the risk of brain metastasis. The COX2 produced by tumor cells can induce the production of prostaglandins, which promote high expression of MMP-1 in tumor cells and degrade claudin and ZO-1 on the BBB (68). However, Lee et al. (69) suggested that the main source of COX2 was not the tumor cells, but the endothelial cells of the BBB. The neuropeptide, substance P, can also facilitate the passage of tumor cells through the BBB by changing the distribution and location of ZO-1 and claudin-5. *In vitro* studies have shown that small cell lung cancer cells can secrete placental growth factor after binding to VEGF-1 receptors, activate the extracellular signal-regulated kinase 1/2 pathway, promote occludin phosphorylation, and change the tight connections of the BBB, all of which eventually aid the easy transport of these cancer cells through the BBB (70).

Cell-secreted vesicle contents can also mediate tumor cell-induced destruction of the BBB. Studies have shown that miR-105 secreted by breast cancer cells can be transported across tight junctions *via* exosomes to destroy the integrity of the BBB; this promotes intracranial metastasis of tumor cells (71). However, some studies suggest that the destruction of the BBB does not only involve the ZO-1 tight junction protein. Tominaga and others found that breast cancer cell-secreted extracellular vesicles can be specifically taken up by endothelial cells of the BBB; miRNA-181c in the extracellular vesicles can inhibit the expression of phosphoinositide-dependent protein kinase 1 on endothelial cells of the BBB. Down-regulation of phosphoinositide-dependent protein kinase 1 can reduce actinin phosphorylation levels and activate cofilin; this causes conformational changes in actin, disrupts the tight connections of the BBB, and prompts breast cancer cells to pass through the BBB. Given the diversity and fragility of the mechanisms by which tumor cells cross the BBB, it may not be a good therapeutic target for resistance to tumor invasion (72, 73). Previous research on the mechanisms of tumor cell penetration of the BBB has mainly focused on breast cancer; studies on other cancers are relatively lacking. The presence of different mechanisms in various tumor cell types therefore warrants further exploration.

Another component of the BBB, namely, vascular endothelial cells, mainly interact with metastatic tumor cells by intercellular adhesion. In the early stages of brain metastasis in non-small cell lung cancer, tumor cells adhere with endothelial cells through VLA-4/VCAM-1, ALCAM/ALCAM, and LFA-1/ICAM-1 binding; these early adhesion molecules can therefore be used as targets to prevent brain metastasis (74). Other studies have shown that non-small cell lung cancer cells that metastasize to the brain have high levels of CD15 expression; they interact with TNF-α-activated CD62E on endothelial cells to mediate adhesion of tumor cells to microvessels (74). In addition, the interaction between tumor and endothelial cells can also promote tumor invasion and angiogenesis. Activation of the Janus kinase-signal transducer and activator of transcription pathway in tumor cells can cause

them to secrete VEGF. In the vascular endothelium, this pathway is activated after VEGFR2 binding; this increases MMP-9 secretion and enhances the invasion ability of tumor cells (75).

The BBB limits antigen presentation and immune cell infiltration in the normal resting state. In order to enter the CNS parenchymal space in an inflammatory environment, T cells must first pass through the endothelial layer followed by the glial boundary (76). The vascular structure loses its integrity in patients with brain metastases, and may therefore promote other restrictions on the entry of peripheral immune cells. However, the more modern conceptual framework is that the BBB does not break down, but forms a blood-tumor barrier (BTB) instead; lymphocytes can pass through the intact BBB *via* the chemokine axis and multi-step adhesion process (77). In this context, the BTB has been shown to have heterogeneous permeability (regulated by reactive astrocytes); this may drive variable immune cell infiltration (78). The process of thrombotic inflammation, which has been recently studied in mouse models of acute stroke, provides new insights into the possibility of biological overlap between brain metastases and BBB/BTB immune interfaces. Studies have shown that clots form preferentially in cerebral microvasculature and tumor cells form large metastases at the site of stagnation in blood vessels; cancer cells embedded in the clot have a higher rate of successful extravasation (79). To date, minimal progress has been made on transformation strategies involving the development of BBB/BTB destruction methods, receptor agonists that alter permeability, radiosensitizing nanoparticles, and novel delivery platforms, all of which have been evaluated in phase I clinical trials (80). These focus areas for future research will not only require increased understanding on the BBB/BTB itself, but also specific knowledge of its role in regulating CNS anti-tumor immunity.

Microvasculature in brain metastasis

Adequate blood supply is indispensable for tumor growth. The microvasculature therefore plays an important role in the metastasis and growth of tumor cells (81). Pathological findings from animal models of brain metastases have shown that tumor cells are mostly distributed around the microvasculature within a radial distance of 75 μm; tumor cells located 100 μm away from the microvasculature cannot not survive (82, 83). Kienast et al. (84) traced the fate of all tumor cells in a brain metastases model using fluorescence tracing; they found that the tumor cells that were separated from blood vessels had all died. In this context, Fidler et al. (85) found that the microvasculature of brain metastases has low microvessel density. However, the lumen is characterized by numerous abnormally dilated segments.

VEGF is a key factor in angiogenesis. Earlier experiments have shown that although it is necessary, its presence is not sufficient for the formation of brain metastases (86). Studies have shown VEGF levels in brain metastases tend to be higher than those of primary lesions; the levels also correlate positively with microvessel density (87). In addition to angiogenesis, VEGF can activate a proportion of dormant cells during brain metastasis, prompting proliferation to micrometastases (84). A retrospective analysis showed that the use of bevacizumab can effectively reduce the development of brain metastases in patients with lung cancer without increasing the risk of CNS bleeding (88). However, it should be noted that tumor vasculature formation is affected by many factors; the regulatory role of other factors therefore need to be considered (89).

Other cellular components of the brain metastases microenvironment

Interactions of tumor cells with other cellular components such as oligodendrocytes, circulating immune cells, and CNS interstitial components have been less studied (90). Studies using natural killer cells in animal models of breast cancer or glioma showed that they inhibited the growth of glioma cells and human epidermal growth factor receptor (HER)-positive breast cancer cells. However, in animal models of breast cancer with brain metastases, CD11b-positive myeloid cells have been found to aggregate and form the "soil" for early tumor metastasis; this further releases the inflammatory factors S100A8 and S100A9, inducing tumor cell chemotaxis (91). Cancer associated fibroblasts have been found in human tumors of the CNS; research suggests that these fibroblasts promote tumor cell invasion (7).

Biological characteristics of tumor cells in the brain metastases microenvironment

In the process of tumor metastasis, a series of biological changes occur in cells of distant metastatic foci to enable adaptation to the microenvironment (92–94). The alterations may manifest at the deoxyribonucleic acid (DNA) or epigenetic levels, thereby influencing phenotypic changes in tumor cells (Figure 1). The biological characteristics of brain metastatic tumor cells have been explained from the aspects of genetic alteration, post-translational modification, and metabolic characteristics of brain metastatic tumors (95).

Gene changes in brain metastatic tumor cells

Brastianos et al. (96) examined 86 metastatic brain lesions and their matching primary lesions based on focal point

mutations and copy number variations (CNVs), which map the evolutionary tree of tumor cells by calculating the individual cancer cell fraction. They estimated the homology between cells by measuring the number of gene copies near the mutation at the checkpoint, and found that although the tumor cells from the metastases and primary lesion originated from the same ancestor, they had different subclones. They also found homology between subclonal tumor cells from multiple intracranial foci. A series of other related studies (Table 1) have confirmed different genotypic changes such as single nucleotide variations, CNVs, deletion, and amplification, among others, between the primary and metastatic brain lesions. The changes mainly involve activation of multiple cell signaling pathways, apoptosis, and cell adhesion, and partially explain the mechanism of development of brain metastases (100, 101, 103, 104).

Studying the patterns of change and the mechanisms by which they arise may provide promising therapeutic targets for brain metastases (99). In this context, a study on 86 patients with breast cancer showed the presence of clinically relevant therapeutic mutations in metastatic lesions from the brain; these included mutations of HER2, EGFR, the B-Raf proto-oncogene, and AKT. These genes were not detected in the primary lesion. The CNVs of HER1 and HER2 were higher in the metastatic brain lesions than in the primary lesion; however, the CNVs of hormone receptors including the estrogen and progesterone receptors had decreased (105). Genetic alterations such as fibroblast growth factor receptor amplification and B-Raf proto-oncogene and neuroblastoma RAS hotspot mutations can also be detected in brain metastases (Table 1) (98, 106).

Epigenetic changes in the brain metastases microenvironment

A study had compared the whole genome methylation levels of tumor cells in brain metastases of nude mice with

TABLE 1 Gene profile changes in brain metastasis tumor Microenvironment.

Study	Primary tumor (number)	Matched brain metastasis	Gene profiles	Implication
Sherise D.Ferguson et al. (97)	lung cancer (8178) Breast cancer(7064) Melanoma(757)	293 99 101	Mutation: RRM1,TS,ERCC1,TOPO1	DNA synthesis and repair and implicated in chemotherapy resistance
Brastianos PK et al. (94)	Lung cancer (38) Breast cancer (21) Renal carcinoma (10) Others (17)	15 12 3 8	Mutation : CDK,MLC1,HER2,EGFR,BRAF,MEK	Cell cycle proteins; PI3K/AKT/mTOR pathway; HER family; RAF/MEK/ERK pathway;
Bollig-Fischer et al. (98)	Breast cancer (10)	4	Amplification : HER2	HER family
Li F et al. (95)	Breast cancer(1)	1	CNV : Gain:Gain: 1p33-p34, 1q22, 5p13, 14q11 Loss:3p, 4q31, 5q, 11p15, Xp21-22, Xq21	CNV Gain: leukocyte migration and organ development; CNV Loss: proteolysis, negative regulation of cell proliferation and cell adhesion
Preusser M et al. (99)	Lung cancer(175)	175	Amplification : FGFR1	FGF/FGFR pathway;
Chen G et al. (96)	Melanoma (74)	30	CNV:generally identical BRAF,NRAF,CTNNB1 hot spot; Mutation : TP53;Loss : PTEN	CNV and hot spot mutations: generally identical
Lo Nigro C et al. (100)	Breast cancer (23)	23	Mutation : TP53	Anti-oncogene mutation
Wikman H et al. (37)	Breast cancer (128)	15	Loss : PTEN	PI3K/AKT/mTOR pathway
Ding L et al. (93)	Breast cancer (1)	1	WWTR1, SNV : NRK, PTPRJ,CNV:80.65% overlaps	SNV missense mutation; 19.35% of CNV difference
Gaedcke J et al. (101)	Breast cancer (102)	85	CNV : Gain:EGFR,HER2;Loss : ER,PR	HER pathway; Estrogen and progesterone receptors
Arai T et al. (103)	Lung cancer (11) Gastric cancer (9) Esophageal cancer (1) Breast cancer (1)	7 6 1 1	Amplification : HER2,EGFR	HER family

those of subcutaneous tumor models of melanoma, lung cancer, stomach cancer, and other cell lines; the methylation levels of a series of transcription factors such as transcription factor 4, purine rich element binding protein B, one cut homeobox 2, estrogen related receptor gamma, nuclear factor IB, and myocyte enhancer factor 2C were found to differ significantly in the brain metastases model. In particular, the difference in transcription factor 4, a transcription factor related to neurodevelopment, was the most obvious (107). Tumor cells that metastasize to the brain have unique gene expression profiles owing to these changes (108). Marzese et al. (109) also observed an inconsistency in methylation levels between brain metastases and extracranial lesions of human melanoma; methylation levels were significantly increased in the promoter range of the homeobox A9 gene (among members of the homeobox family), a transcription component that encodes multiple genes and induces changes in neuro development-related genes (110). In a study on breast cancer, the methylation levels of genes such as polypeptide N-acetylgalactosaminyltransferase 9, coiled-coil domain containing 8, and basonuclin 1 were significantly higher in brain metastases than in the primary lesions; *in vitro* silencing of the mentioned genes could enhance the invasion ability of tumor cells (Table 1) (111). Changes in methylation levels of tumor cells in the CNS may be responsible for changes in tumor phenotype; however, the mechanism for the changes is not fully understood.

Recent studies have confirmed that micro ribonucleic acids (miRNAs) are one of the key factors affecting protein expression after transcription (112). By comparing miRNA levels between the primary lesion and brain metastases, Zhao et al. (113) identified a group of down-regulated miRNAs in patients with lung cancer; these included miR-145, miR-214, miR-9, and miR-1471. Among these, miR-145 was the most obviously down-regulated. In this context, the down-regulation of miR-145 may promote the proliferation of the A549 and SPC-A1 cell lines in lung cancer. Previous studies have shown that miR-145 can affect the proliferation and invasion of lung cancer cells by participating in the regulation of c-Myc, EGFR, and nudix hydrolase 1 expression (114). MiR-145-5p, another member of the miR-145 family, was also found to be significantly down-regulated in patients with brain metastases from lung cancer; this increased the expression levels of downstream EGFR, octamer-binding transcription factor 4, mucin 1, c-Myc, and tumor protein D52. In this context, the down-regulation of miR-145-5p was caused by initiation of interval methylation (115). MiR-141-3p and miR-200b-3p of the miR-200 family have also been found to be significantly up-regulated in metastatic brain lesions than in primary tumors; they down-regulate zinc finger E-Box binding homeobox 2 expression, thereby affecting the proliferation and invasion ability of tumor cells (116).

Characteristics of tumor cell metabolism in the microenvironment of brain metastases

The CNS has an abundant blood supply, with a blood flow that accounts for 1/5 of the total body volume; blood and energy supplies to the CNS are therefore relatively sufficient (117). Due to the presence of the BBB, the levels of glucose in the interstitial fluid of the CNS are lower than those in the blood. However, it has abundant levels of branched-chain amino acids such as leucine, valine, isoleucine, and glutamic acid (118).

Compared to the invasion and proliferation characteristics of brain metastases, the metabolic characteristics of tumor cells in the CNS have been relatively underexplored (119). Chen et al. (120) compared the levels of protein expression related to energy metabolism between tumor cells in brain and bone metastasis models; they found that unlike common tumor cells which rely predominantly on anaerobic metabolism, tumor cells in the CNS actively demonstrate tricarboxylic acid cycle-oxidative phosphorylation with activation of the pentose phosphate pathway. This may induce resistance of tumor cells to certain antimetabolite chemotherapy drugs such as D-2-deoxyglucose (121). Chen et al. (122) found that breast cancer cells that metastasize to the brain have greater tolerance to low sugar levels than their parent cells; they also express more glutamate dehydrogenase and α-ketoacid dehydrogenase to use the glutamic acid and branched-chain amino acids available in the environment.

In terms of lipid metabolism, Chen et al. (120) found fatty acid-β oxidation-related enzyme profile expression to be higher in the animal brain metastases model than in the bone metastases model. However, the human breast cancer brain metastases tissue chip showed the expression levels of acetyl-CoA oxidase-1 and fatty acid synthase to be higher than those of metastases to other sites. This suggests that the processes of lipid synthesis and catabolism were more active in the metastatic brain lesions (123).

Tumor cells in the brain metastases microenvironment acquire nerve cell properties

Park et al. (107) found that tumor cells in animal models of brain metastasis from lung cancer, melanoma, and colon cancer showed certain characteristics of neuronal cells; the levels of glutamate signaling pathway proteins and neurotransmitter complex proteins such as synaptosomal-associated protein 25 and synaptosomal-associated protein 91 were significantly increased. Similarly, brain metastases models of human breast cancer showed the expression of γ-aminobutyric acid (GABA) receptors and transaminase

sources to have increased; this allows tumor cells to use the available GABA in the CNS for various metabolic activities (124, 125). Nygaard et al. (126) found the expression of glutamate-related signaling pathway signaling proteins, glutamate receptor ionotropic AMPA 2 and glutamate metabotropic receptor 4, to have increased in patients with melanoma brain metastases and animal models; this promotes the growth of tumor cells. Studies have also shown that plasmin found in the CNS can induce apoptosis of tumor cells; however, breast and lung cancer cell lines highly express neuroserpin, a neuronal inhibitor of plasminogen activator, thereby evading the pro-apoptotic effect of plasmin (127). This finding may be based on the fact that high levels of chloride in the interstitial fluid have a damaging effect on non-neuronal cells; coupled with the abundant neurotrophic factors, glutamate, and other substances in the CNS, this may induce certain neuronal properties in tumor cells to make them more suitable for survival in the CNS microenvironment (128).

Role of exosomes in the brain metastases microenvironment

Exosomes are membranous vesicles with a diameter of between 30-100 nm; they have a lipid bilayer; can be secreted from all kinds of cells; are present in serum, urine, saliva, and other human body fluids; and can be separated and purified by ultracentrifugation, density gradient centrifugation, and other methods (129). Exosomes have a considerably complex composition, and include a variety of lipids, proteins, mRNAs, miRNAs, long non-coding RNAs, circular RNAs, and DNA. Advances in exosome-related research in recent years is gradually revealing the causes for organ propensity of metastatic tumors (102). Hoshino et al. (130) found that tumor exosome integrin expression profiles determine the organ propensity of tumor metastasis; they also found that ingestion of exosomes in the brain can create a pre-metastatic microenvironment for tumor metastasis. This suggests that exosomes can alter the pre-metastatic microenvironment to help target tumor localization (Figure 1). Studies also suggest that CD46 found on endothelial cells of human cerebral microvasculature is a receptor that mediates melanoma exosome uptake; this further confirms the role of exosomes in tumor targeting (131). Exosomes can also help target the localization of tumors by altering the manner by which energy is metabolized. Fong et al. (130) found that cancer cells inhibit glucose uptake by non-tumor cells; they down-regulate pyruvate kinase, and thereby glycolysis, in the pre-metastatic microenvironment by secreting high levels of exosomal miR-122. This suggests that exosomes can also promote tumor brain metastasis by changing glucose uptake in the pre-metastatic microenvironment (Table 2) (134).

TABLE 2 The role of exosomes in brain metastasis.

Study	Exosomal original	Exosomal cargo	Role in brain metastatic process
Umeze et al. (132)	Multiple myeloma	miR-135b	promotes neoangiogenesis
Fong et al. (130)	Breast cancer	miR-122	Reduces glucose uptake in normal brain cells
Wu et al. (133)	Non-small cell lung cancer	Lnc-MMP2-2	Destroys the tight junctions of the BBB
Tominaga et al. (72)	Breast cancer	miR-181c	Destroys the BBB by modulating the actin dynamics
Zhang et al. (134)	Normal astrocytic cells	PTEN targeting miR-19a	Reduces PTEN expression in brain metastatic tumor cells
Lu et al. (65)	Breast cancer	Lnc GS1-600G8.5	Disrupts the BBB by targeting the tight junction proteins
Zhou et al. (133)	Breast cancer	miR-105	Destroys the endothelial cell barrier by down-regulating ZO-1 tight junctions
Satelli et al. (135)	Lung cancer	Vimentin	promotes vimentin expression in the brain metastatic and induces EMT
Xing et al. (136)	Breast cancer	miR-503	Induces the release of tumoral growth factors and microglial reprograming leading to immune suppression microenvironment
Zhi et al. (137)	Lung cancer	S100A16	Improves the survival of SCLC metastatic cells in cerebrum
Rodrigues et al. (138)	Lung and breast cancer	CEMIP	Induces a proinflammatory vascular niche, promoting metastasis
Puigdelloses et al. (139)	Lung cancer, breast cancer, colorectal cancer, melanoma, pancreatic cancer, gastroesophageal cancer, bladder cancer	RNU6-1	Regulates tumoral growth rate

The role of exosomes in the proliferation of brain metastases

Stromal cell exosomes promote the proliferation of brain metastases

Phosphatase and Tensin homolog deleted on chromosome ten is a tumor suppressor gene with phosphorylation activity, that regulates the apoptosis and proliferation of tumor cells (140). Zhang et al. (141) found that exosomal miRNA-19 produced by astrocytes can target the inhibition of Phosphatase and Tensin homolog tumor suppressor genes, resulting in increased secretion of chemokine ligand-2 and nuclear factor kappa-B; this promotes the growth of brain metastases. This shows that stromal cell exosomes found in the microenvironment can promote tumor cell growth by carrying miRNAs to influence tumor cell proliferation and inhibit apoptosis (Table 2; Figure 2).

Exosome-regulated immune mechanisms promote tumor cell proliferation

Metastatic exosomes can change the microenvironment to promote tumor cell proliferation (142). A study on breast cancer brain metastases found that X-inactive specific transcript deletion increased the secretion of exosomal miR-503, which was transmitted to microglia; this led to M1-M2 transformation and inhibition of T cell proliferation, enabling tumor immune evasion (136, 137). This confirms that tumor cell exosomes can regulate immune cells to enable tumor cell immune escape mechanisms and provide conditions for tumor cell proliferation (Table 2; Figure 2).

Exosomes regulate the stability of tumor cells

A variety of apoptotic mechanisms are often accompanied by a decrease in mitochondrial membrane potential (143). Xu et al. (144) found that exosomes can prevent the loss of mitochondrial membrane potentials through the prohibitin 1 protein present on mitochondrial membranes; tumor cells can therefore tolerate apoptosis in a stressed environment. This indicates that exosomes can regulate tumor cell stability and promote tumor cell proliferation by influencing mitochondrial membrane potential (Figure 2).

Diagnostic significance of exosomes in brain metastases

Liquid biopsy technologies are rapidly gaining attention because of their rapid and non-invasive characteristics.

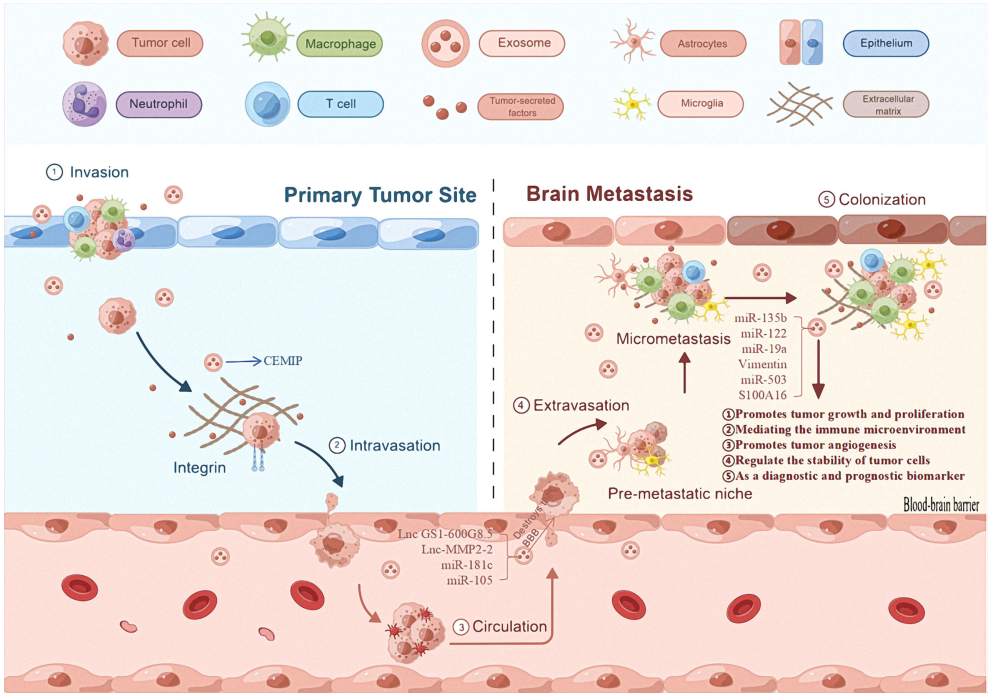

FIGURE 2
The role of exosomes in brain metastases. The first mechanism of primary tumor exosomes is that they can promote their own progression and metastasis. The second general mechanism is that exosomes derived from primary tumor cells promote the proliferation of brain metastases, regulated immune mechanism to promote tumor cell proliferation, and regulate the stability of tumor cells, and can be useful diagnostic and/or prognostic biomarkers.

Common techniques for tumor fluid biopsy include traditional circulating tumor cell detection, circulating tumor DNA detection, and tumor cell exosome detection (144, 145).

Advantages of exosomes in diagnosis

Exosome-based diagnosis offers the following advantages: (1) exosomes exist in almost all body fluids, are easier to enrich, and are more sensitive to current detection methods, and (2) they have high stability, allowing a large number of specific proteins to be isolated at temperatures as low as -80°C. However, exosome-related research has started recently and there is a paucity of cumulative data from studies; further in-depth research and analysis is required (146).

Prospects of exosomes in the diagnosis of brain metastases

In recent years, studies have focused on the role of exosomes in brain metastases (147). Camacho et al. studied the miRNA and protein profiles of brain metastasis-competent exosomes (148). Multiple proteins pertaining to cell communication, the cell cycle, and key signaling pathways involved in cell invasion and metastasis are promising biomarkers for brain metastases. Although exosomes are still in their infancy as biomarkers for the diagnosis of brain metastases, they are already in use for the diagnosis of lung cancer. Exosome Diagnostics made a major breakthrough in 2016 with the ExoDx^{TM} Lung (ALK) technology for detection of exosomal miRNA by analysis of blood samples; this is being widely used. Combining exosomal miRNA and circulating tumor DNA analysis can increase diagnostic sensitivity by approximately 3-fold compared to circulating tumor DNA-based diagnosis alone (149).

Exosomes can be used as targets and tools for the treatment of brain metastases

Exosomes are involved in almost all processes of brain metastasis including cell genesis, metastasis, and proliferation. It is possible to target exosomes and the corresponding nucleic acids and proteins to treat the corresponding tumors; this provides new concepts for the treatment of brain metastases (150). In a recent study, Yang et al. (151) found that exosomes secreted by tumor cells contain functional programmed death-1 (PD-L1) protein, which can be transferred to other cells to inhibit T-cell resistance; binding of PD-1 to T cells inhibits anti-tumor immunity and protects the tumor cells. Inhibiting the secretion of PD-L1-containing exosomes by knocking down Rab27a or applying the inhibitor GW4869 can lead to meaningful anti-cancer effects. This offers a major step towards precision and individualized treatment of brain metastases (152).

The BBB has always been the greatest challenge in the treatment of brain metastases. Most traditional chemotherapeutic drugs and large molecule targeted drugs are denied entry by the BBB, thus making the CNS a sanctuary for survival and multiplication of metastatic cells (153). As a drug delivery system, exosomes may effectively address the issue BBB permeability to chemotherapy drugs (154). There are two main types of drug delivery methods for exosomes: exogenous and endogenous (155). Exogenous drug delivery requires the extraction of exosomes from donor cells and the delivery of small molecules (paclitaxel, adriamycin, and curcumin, among others) or gene-based drugs (e.g., small interfering RNA) into the exosome by electroporation (156). The endogenous drug delivery method carries the drug out of the cell *via* exosome secretion after the drug enters the donor cell; the drug-loaded exosome is finally extracted (157). Reversible protein-protein interaction molecules have been designed for large molecule proteins; these are controlled by blue light to allow integration into the endogenous pathway of exosome production, and are successfully loaded as "cargo proteins" into the new exosomes. This provides an important method for carriage of large molecule proteins by exosomes (158). Yang et al. (159) reported that exosomes derived from endothelial cells of mouse brain microvasculature can effectively deliver antitumor drugs *in vivo* across the BBB to inhibit tumor growth. This is indicates the advantages and possibilities of exosome treatment for brain metastases.

Discussion

Changes in the biological properties of brain metastatic tumor cells and the interaction between tumor cells and their microenvironment may explain the relatively inefficient metastatic process of tumor cell colonization and growth in the intracranial "soil." However, it is unclear whether the cranial microenvironment plays a screening or inducing role in the altered biological behavior of tumor cells in metastatic lesions (160). A study that examined genome-wide methylation levels of lung cancer and melanoma cells co-cultured with astrocytes partially replicated the altered methylation profile in animal models of brain metastasis; this suggests that astrocytes can cause changes in methylation levels in tumor cells (161). However, McDermott (162) proposed a model in which CNS microenvironment components such as astrocytes and microglia interacted with tumor cells to produce certain cytokines; these cytokines altered miRNA levels in tumor cells, which in turn affected the expression of the corresponding target genes.

Several studies have shown that tumor cell exosomes are closely related to tumor metastasis. The alteration of the cranial microenvironment and targeted migration of cancer cell exosomes are particularly important for the development of lung cancer brain metastases. In this context, exosomes play an important role in the tumor microenvironment and are directly or indirectly involved in intercellular signal transduction, tumorigenesis, and progression in the tumor microenvironment (163). For example, exosomes secreted by lung cancer cells contain oncogenes and

they target the tumor microenvironment, thus promoting tumor progression (164). Exosomes are involved in DNA methylation, histone modification, post-transcriptional regulation, and RNA regulation. The relevant substances delivered by exosomes reflect the state of the cell, and exosomes originating from tumor cells may alter the tumor and promote the expression of tumor suppressor genes in recipient cells. Thus, exosomes in body fluids (including blood) may serve as biomarkers of cancer, and the detection of these biomarkers may be used for diagnosis or prognostic assessment of cancer.

As a target system, exosomes are expected to effectively promote the development of medical oncology. The relationship between exosomes and brain metastases needs to be explored further to understand the intrinsic mechanisms of exosome structure and their interactions with regulatory proteins (165–167). Along with the in-depth study of exosomes in brain metastases, their monitoring can aid the screening of susceptible or high-risk groups, clinical diagnosis, molecular staging, prognosis assessment, recurrence or metastasis prediction, and efficacy evaluation. In particular, the monitoring of exosomes may aid the formulation of brain metastases prevention strategies and the establishment of a risk evaluation system.

Conclusion

In conclusion, the metastatic tumor microenvironment is a complex biological system. The mechanisms of metastasis formation and regulation that are associated with the microenvironment are areas of particular interest in cancer research. Findings indicate that the factors in the microenvironment that promote the formation of metastases are interrelated and interdependent. The proposed "seed and soil" hypothesis provides a broad framework for addressing the growth of brain metastases. As metastasis is almost always closely related to the formation and alteration of the microenvironment in a large number of cancers, continuous research on the microenvironment will improve understanding on the mechanisms of metastasis development and provide new targets for their diagnosis and treatment. Finally, as new therapeutic tools, exosomes are expected to be ideal markers for the early diagnosis of brain metastases and new targets for their treatment.

Author contributions

ZW and YW designed the study; YA and NM wrote the first draft of the manuscript; HQ and WJ prepared the figure; GF prepared the Tables. All authors approved the final version of the manuscript for submission.

Funding

This study was supported by The Xinjiang Uygur Autonomous Regional Cooperative Innovation ProgramGrant (NO. 2021D01A02), Regional Collaborative Innovation Special Project of Xinjiang Uygur Autonomous Region (No.2021E01013).

Conflict of interest

The authors declare that the research was conducted in the absence of any commercial or financial relationships that could be construed as a potential conflict of interest.

Publisher's note

References

1. Steeg PS, Camphausen KA, Smith QR. Brain metastases as preventive and therapeutic targets. *Nat Rev Cancer*. (2011) 11(5):352–63. doi: 10.1038/nrc3053

2. Lowery FJ, Yu D. Brain metastasis: Unique challenges and open opportunities. *Biochim Biophys Acta Rev Cancer*. (2017) 1867(1):49–57. doi: 10.1016/j.bbcan.2016.12.001

3. Valiente M, Ahluwalia MS, Boire A, Brastianos PK, Goldberg SB, Lee EQ, et al. The evolving landscape of brain metastasis. *Trends Cancer*. (2018) 4(3):176–96. doi: 10.1016/j.trecan.2018.01.003

4. Eichler AF, Chung E, Kodack DP, Loeffler JS, Fukumura D, Jain RK, et al. The biology of brain metastases-translation to new therapies. *Nat Rev Clin Oncol* (2011) 8(6):344–56. doi: 10.1038/nrclinonc.2011.58

5. Lee HH, Chen CH, Chuang HY, Huang YW, Huang MY. Brain surgery in combination with tyrosine kinase inhibitor and whole brain radiotherapy for epidermal growth factor receptor-mutant non-small-cell lung cancer with brain metastases. *Sci Rep* (2019) 9(1):16834. doi: 10.1038/s41598-019-53456-z

6. Fares J, Fares MY, Khachfe HH, Salhab HA, Fares Y. Molecular principles of metastasis: a hallmark of cancer revisited. *Signal Transduct Target Ther* (2020) 5 (1):28. doi: 10.1038/s41392-020-0134-x

7. Valastyan S, Weinberg RA. Tumor metastasis: Molecular insights and evolving paradigms. *Cell* (2011) 147(2):275–92. doi: 10.1016/j.cell.2011.09.024

8. Ono M, Kosaka N, Tominaga N, Yoshioka Y, Takeshita F, Takahashi RU, et al. Exosomes from bone marrow mesenchymal stem cells contain a microRNA

that promotes dormancy in metastatic breast cancer cells. *Sci Signal* (2014) 7(332): ra63. doi: 10.1126/scisignal.2005231

9. Zhang C, Yu D. Advances in decoding breast cancer brain metastasis. *Cancer Metastasis Rev* (2016) 35(4):677–84. doi: 10.1007/s10555-016-9638-9

10. Whiteside TL. The tumor microenvironment and its role in promoting tumor growth. *Oncogene* (2008) 27(45):5904–12. doi: 10.1038/onc.2008.271

11. Witz IP. The tumor microenvironment: the making of a paradigm. *Cancer Microenviron.* (2009) 2 Suppl 1(Suppl 1):9–17. doi: 10.1007/s12307-009-0025-8

12. Neophytou CM, Panagi M, Stylianopoulos T, Papageorgis P. The role of tumor microenvironment in cancer metastasis: Molecular mechanisms and therapeutic opportunities. *Cancers (Basel).* (2021) 13(9):2053. doi: 10.3390/cancers13092053

13. Whipple CA. Tumor talk: Understanding the conversation between the tumor and its microenvironment. *Cancer Cell Microenviron.* (2015) 2:e773. doi: 10.14800/ccm.773

14. Merrell AJ, Stanger BZ. Adult cell plasticity *in vivo*: de-differentiation and transdifferentiation are back in style. *Nat Rev Mol Cell Biol* (2016) 17(7):413–25. doi: 10.1038/nrm.2016.24

15. Shalapour S, Karin M. Pas de deux: Control of anti-tumor immunity by cancer-associated inflammation. *Immunity* (2019) 51(1):15–26. doi: 10.1016/j.immuni.2019.06.021

16. Seimiya T, Otsuka M, Iwata T, Shibata C, Tanaka E, Suzuki T, et al. Emerging roles of exosomal circular RNAs in cancer. *Front Cell Dev Biol* (2020) 8:568366. doi: 10.3389/fcell.2020.568366

17. Greten FR, Grivennikov SI. Inflammation and cancer: Triggers, mechanisms, and consequences. *Immunity* (2019) 51(1):27–41. doi: 10.1016/j.immuni.2019.06.025

18. Quail DF, Joyce JA. Molecular pathways: Deciphering mechanisms of resistance to macrophage-targeted therapies. *Clin Cancer Res* (2017) 23(4):876–84. doi: 10.1158/1078-0432.CCR-16-0133

19. Li F, Liu Y, Chen H, Liao D, Shen Y, Xu F, et al. EGFR and COX-2 protein expression in non-small cell lung cancer and the correlation with clinical features. *J Exp Clin Cancer Res* (2011) 30(1):27. doi: 10.1186/1756-9966-30-27

20. Sasaki T, Hiroki K, Yamashita Y. The role of epidermal growth factor receptor in cancer metastasis and microenvironment. *BioMed Res Int* (2013) 2013:546318. doi: 10.1155/2013/546318

21. Luo L, Liu P, Zhao K, Zhao W, Zhang X. The immune microenvironment in brain metastases of non-small cell lung cancer. *Front Oncol* (2021) 11:698844. doi: 10.3389/fonc.2021.698844

22. Li M, Ransohoff RM. Multiple roles of chemokine CXCL12 in the central nervous system: a migration from immunology to neurobiology. *Prog Neurobiol* (2008) 84(2):116–31. doi: 10.1016/j.pneurobio.2007.11.003

23. Srinivasan ES, Deshpande K, Neman J, Winkler F, Khasraw M. The microenvironment of brain metastases from solid tumors. *Neurooncol Adv* (2021) 3(Suppl 5):v121–32. doi: 10.1093/noajnl/vdab121

24. Xing F, Liu Y, Sharma S, Wu K, Chan MD, Lo HW, et al. Activation of the c-met pathway mobilizes an inflammatory network in the brain microenvironment to promote brain metastasis of breast cancer. *Cancer Res* (2016) 76(17):4970–80. doi: 10.1158/0008-5472.CAN-15-3541

25. Toshniwal PK, Firestone SL, Barlow GH, Tiku ML. Characterization of astrocyte plasminogen activator. *J Neurol Sci* (1987) 80(2-3):277–87. doi: 10.1016/0022-510x(87)90162-6

26. Ye P, Popken GJ, Kemper A, McCarthy K, Popko B, D'Ercole AJ. Astrocyte-specific overexpression of insulin-like growth factor-I promotes brain overgrowth and glial fibrillary acidic protein expression. *J Neurosci Res* (2004) 78(4):472–84. doi: 10.1002/jnr.20288

27. Quist E, Trovato F, Avaliani N, Zetterdahl OG, Gonzalez-Ramos A, Hansen MG, et al. Transcription factor-based direct conversion of human fibroblasts to functional astrocytes. *Stem Cell Rep* (2022). doi: 10.1016/j.stemcr.2022.05.015. S2213-6711(22)00268-5.

28. Sirkisoon SR, Wong GL, Aguayo NR, Doheny DL, Zhu D, Regua AT, et al. Breast cancer extracellular vesicles-derived miR-1290 activates astrocytes in the brain metastatic microenvironment *via* the FOXA2→CNTF axis to promote progression of brain metastases. *Cancer Lett* (2022) 540:215726. doi: 10.1016/j.canlet.2022.215726

29. Deng J, Zhang Q, Lu L, Fan C. Long noncoding RNA DLGAP1-AS1 promotes the aggressive behavior of gastric cancer by acting as a ceRNA for microRNA-628-5p and raising astrocyte elevated gene 1 expression. *Cancer Manag Res* (2020) 12:2947–60. doi: 10.2147/CMAR.S246166

30. Shi G, Zhang Z. Rap2B promotes the proliferation and migration of human glioma cells *via* activation of the ERK pathway. *Oncol Lett* (2021) 21(4):314. doi: 10.3892/ol.2021.12575

31. Thanabalasundaram G, Schneidewind J, Pieper C, Galla HJ. The impact of pericytes on the blood-brain barrier integrity depends critically on the pericyte differentiation stage. *Int J Biochem Cell Biol* (2011) 43(9):1284–93. doi: 10.1016/j.biocel.2011.05.002

32. Klein A, Schwartz H, Sagi-Assif O, Meshel T, Izraely S, Ben Menachem S, et al. Astrocytes facilitate melanoma brain metastasis via secretion of IL-23. *J Pathol* (2015) 23(6):116–27. doi: 10.1002/path.4509

33. Seike T, Fujita K, Yamakawa Y, Kido MA, Takiguchi S, Teramoto N, et al. Interaction between lung cancer cells a nd astrocytes *via* specific in flammatory cytokines in the microenvironment of brain metastasis. *Clin Exp Metastasis* (2011) 28(1):13–25. doi: 10.1007/s10585-010-9354-8

34. Noda M, Seike T, Fujita K, Yamakawa Y, Kido M, Iguchi H. Role of immune cells in brain metastasis of lung cancer cells and neuron-tumor cell interaction., 243–51. doi: 10.1007/s11055-011-9406-9

35. Sierra A, Price JE, García-Ramirez M, Méndez O, López L, Fabra A, et al. Astrocyte-derived cytokines contribute to the metastatic brain specificity of breast cancer cells. *Lab Invest* (1997) 77(4):357–68.

36. Xiao Y, Liu T, Liu X, Zheng L, Yu D, Zhang Y, et al. Total astragalus saponins attenuates CVB3-induced viral myocarditis through inhibiting expression of tumor necrosis factor α and fas ligand. *Cardiovasc Diagn Ther* (2019) 9(4):337–45. doi: 10.21037/cdt.2019.07.11

37. Wikman H, Lamszus K, Detels N, Uslar L, Wrage M, Benner C, et al. Relevance of PTEN loss in brain metastasis formation in breast cancer patients. *Breast Cancer Res* (2012) 14(2):R49. doi: 10.1186/bcr3150

38. Lin Q, Balasubramanian K, Fan D, Kim SJ, Guo L, Wang H, et al. Reactive astrocytes protect melanoma cells from chemotherapy by sequestering intracellular calcium through gap junction communication channels. *Neoplasia Int J Oncol Res* (2010) 12(9):748–54. doi: 10.1593/neo.10602

39. Kim SJ, Kim JS, Park ES, Lee JS, Lin Q, Langley RR, et al. Astrocytes upregulate survival genes in tumor cells and induce protection from chemotherapy. *Neoplasia* (2011) 13(3):286–98. doi: 10.1158/1538-7445.am10-3428

40. Jung HS, Verwilst P, Sharma A, Shin J, Sessler JL, Kim JS. Organic molecule-based photothermal agents: an expanding photothermal therapy universe. *Chem Soc Rev* (2018) 47(7):2280–97. doi: 10.1039/c7cs00522a

41. Kim SJ, Lee HJ, Kim MS, Choi HJ, He J, Wu Q, et al. Macitentan, a dual endothelin receptor antagonist, in combination with temozolomide leads to glioblastoma regression and long-term survival in mice. *Clin Cancer Res* (2015) 21(20):4630–41. doi: 10.1158/1078-0432.CCR-14-3195

42. Murphy SF, Varghese RT, Lamouille S, Guo S, Pridham KJ, Kanabur P, et al. Connexin 43 inhibition sensitizes chemoresistant glioblastoma cells to temozolomide. *Cancer Res* (2016) 76(1):139–49. doi: 10.1158/0008-5472.CAN-15-1286

43. Hong X, Wang Q, Yang Y, Zheng S, Tong X, Zhang S, et al. Gap junctions propagate opposite effects in normal and tumor testicular cells in response to cisplatin. *Cancer Lett* (2012) 317(2):165–71. doi: 10.1016/j.canlet.2011.11.019

44. Shipman L. Microenvironment: Astrocytes silence PTEN to promote brain metastasis. *Nat Rev Cancer* (2015) 15(12):695. doi: 10.1038/nrc4045

45. Yu D. PTEN loss by exosomal microRNA primes brain metastasis outgrowth. *Cancer Res* (2017) 77:BS2–2-BS2-2. doi: 10.1158/1538-7445.SABCS16-BS2-2

46. Uslar L. Clinical relevance of allelic imbalances on chromosome 10q in brain metastases formation in breast cancer patients. (2012) 10:4707.

47. Watters JJ, Schartner JM, Badie B. Microglia function in brain tumors. *J Neurosci Res* (2005) 81(3):447–55. doi: 10.1002/jnr.20485

48. Wei J, Gabrusiewicz K, Heimberger A. The controversial role of microglia in malignant gliomas. *Clin Dev Immunol* (2013) 2013:285246. doi: 10.1155/2013/285246

49. Perry VH, Teeling J. Microglia and macrophages of the central nervous system: the contribution of microglia priming and systemic inflammation to chronic neurodegeneration. *Semin Immunopathol* (2013) 35(5):601–12. doi: 10.1007/s00281-013-0382-8

50. Allavena P, Sica A, Garlanda C. The yin-yang of tumor-associated macrophages in neoplastic progression and immune sur veillance. *Immunol Rev* (2008) 222:155–61. doi: 10.1111/j.1600-065x.2008.00607.x

51. Whiteside TL, Demaria S, Rodriguez-Ruiz ME, Zarour HM, Melero I. Emerging opportunities and challenges in cancer immunotherapy. *Clin Cancer Res* (2016) 22(8):1845–55. doi: 10.1158/1078-0432.CCR-16-0049

52. Herz J, Filiano AJ, Smith A, Yogev N, Kipnis J. Myeloid cells in the central nervous system. *Immunity* (2017) 46(6):943–56. doi: 10.1016/j.immuni.2017.06.007

53. Rietkotter E, Menck K, Bleckmann A, Farhat K, Schaffrinski M, Schulz M, et al. Zoledronic acid inhibits macrophage/microglia-assisted breast cancer cell invasion. *Oncotarget* (2013) 4(9):1449–60. doi: 10.18632/oncotarget.1201

54. Gnant M. Bisphosphonates in the prevention of disease recurrence: current results and ongoing trials. *Curr Cancer Drug Targets* (2009) 9(7):824–33. doi: 10.2174/156800909789760267

55. Venkataramani V, Tanev DI, Strahle C, Studier-Fischer A, Fankhauser L, Kessler T, et al. Glutamatergic synaptic input to glioma cells drives brain tumour progression. *Nature* (2019) 573(7775):532–8. doi: 10.1038/s41586-019-1564-x

56. Zeng Q, Michael IP, Zhang P, Saghafinia S, Knott G, Jiao W, et al. Synaptic proximity enables NMDAR signalling to promote brain metastasis. *Nature* (2019) 573(7775):526–31. doi: 10.1038/s41586-019-1576-6

57. Barria A. Dangerous liaisons as tumour cells form synapses with neurons. *Nature* (2019) 573(7775):499–501. doi: 10.1038/d41586-019-02746-7

58. Venkatesh HS, Johung TB, Caretti V, Noll A, Tang Y, Nagaraja S, et al. Neuronal activity promotes glioma growth through neuroligin-3 secretion. *Cell* (2015) 161(4):803–16. doi: 10.1016/j.cell.2015.04.012

59. Jassam YN, Izzy S, Whalen M, McGavern DB, El Khoury J. Neuroimmunology of traumatic brain injury: Time for a paradigm shift. *Neuron* (2017) 95(6):1246–65. doi: 10.1016/j.neuron.2017.07.010

60. Tominaga N, Hagiwara K, Kosaka N, Honma K, Nakagama H, Ochiya T. RPN2-mediated glycosylation of tetraspanin CD63 regulates breast cancer cell malignancy. *Mol Cancer.* (2014) 13:134. doi: 10.1186/1476-4598-13-134

61. Aldape K, Brindle KM, Chesler L, Chopra R, Gajjar A, Gilbert MR, et al. Challenges to curing primary brain tumours. *Nat Rev Clin Oncol* (2019) 16(8):509–20. doi: 10.1038/s41571-019-0177-5

62. Ribeiro DE, Oliveira-Giacomelli Á, Glaser T, Arnaud-Sampaio VF, Andrejew R, Dieckmann L, et al. Hyperactivation of P2X7 receptors as a culprit of COVID-19 neuropathology. *Mol Psychiatry* (2021) 26(4):1044–59. doi: 10.1038/s41380-020-00965-3

63. Sweeney MD, Sagare AP, Zlokovic BV. Blood-brain barrier breakdown in Alzheimer disease and other neurodegenerative disorders. *Nat Rev Neurol* (2018) 14(3):133–50. doi: 10.1038/nrneurol.2017.188

64. Jia W, Lu R, Martin TA, Jiang WG. The role of claudin-5 in blood-brain barrier (BBB) and brain metastases (review). *Mol Med Rep* (2014) 9(3):779–85. doi: 10.3892/mmr.2013.1875

65. Lu W, Bucana CD, Schroit AJ. Pathogenesis and vascular integrity of breast cancer brain metastasis. *Int J Cancer* (2007) 120(5):1023–6. doi: 10.1002/ijc.22388

66. Bos PD, Zhang XH, Nadal C, Shu W, Gomis RR, Nguyen DX, et al. Genes that mediate breast cancer metastasis to the brain. *Nature* (2009) 459(7249):1005–9. doi: 10.1038/NATURE08021

67. Cardinal T, Pangal D, Strickland BA, Newton P, Mahmoodifar S, Mason J, et al. Anatomical and topographical variations in the distribution of brain metastases based on primary cancer origin and molecular subtypes: a systematic review. *Neurooncol Adv* (2021) 4(1):vdab170. doi: 10.1093/noajnl/vdab170

68. Wu K, Fukuda K, Xing F, Zhang Y, Sharma S, Liu Y, et al. Roles of the cyclooxygenase 2 matrix metalloproteinase 1 pathway in brain metastasis of breast cancer. *J Biol Chem* (2015) 290(15):9842–54. doi: 10.1074/jbc.M114.602185

69. Lee KY, Kim YJ, Yoo H, Lee SH, Park JB, Kim HJ, et al. Human brain endothelial cell-derived COX-2 facilitates extravasation of breast cancer cells across the bloodbrain barrier. *Anticancer Res* (2011) 31(12):4307–13. doi: 10.1016/j.canrad.2011.03.008

70. Li B, Wang C, Zhang Y, Zhao XY, Huang B, Wu PF, et al. Elevated PLGF contributes to small-cell lung cancer brain metastasis. *Oncogene* (2013) 32 (24):2952–62. doi: 10.1038/onc.2012.313

71. Zhou W, Fong MY, Min Y, Somlo G, Liu L, Palomares MR, et al. Cancer-secreted miR-105 destroys vascular endothelial barriers to promote metastasis. *Cancer Cell* (2014) 25(4):501–15. doi: 10.1016/j.ccr.2014.03.007

72. Tominaga N, Kosaka N, Ono M, Katsuda T, Yoshioka Y, Tamura K, et al. Brain metastatic cancer cells release microR NA-181c-containing extracellular vesicles capable of destructing blood-brain barrier. *Nat Commun* (2015) 6:6716. doi: 10.1038/ncomms7716

73. Erickson MA, Banks WA. Neuroimmune axes of the blood-brain barriers and blood-brain interfaces: Bases for physiological regulation, disease states, and pharmacological interventions. *Pharmacol Rev* (2018) 70(2):278–314. doi: 10.1124/pr.117.014647

74. Soto MS, Serres S, Anthony DC, Sibson NR. Functional role of endothelial adhesion molecules in the early stages of brain metastasis. *Neuro Oncol* (2014) 16 (4):540–51. doi: 10.1093/neuonc/not222

75. Jassam SA, Maherally Z, Smith JR, Ashkan K, Roncaroli F, Fillmore HL, et al. TNF-α enhancement of CD62E mediates adhesion of non–small cell lung cancer cells to brain endothelium *via* CD15 in lung-brain metastasis. *Neuro-Oncology* (2016) 18(5):679–90. doi: 10.1093/neuonc/nov248

76. Xie J, Shen Z, Anraku Y, Kataoka K, Chen X. Nanomaterial-based blood-brain-barrier (BBB) crossing strategies. *Biomaterials* (2019) 224:119491. doi: 10.1016/j.biomaterials.2019.119491

77. Lee HT, Xue J, Chou PC, Zhou A, Yang P, Conrad CA, et al. Stat3 orchestrates interaction between endothelial and tumor cells and inhibition of Stat3 suppresses brain metastasis of breast cancer cells. *Oncotarget* (2015) 6 (12):10016–29. doi: 10.18632/oncotarget.3540

78. Mehrabian H, Detsky J, Soliman H, Sahgal A, Stanisz GJ. Advanced magnetic resonance imaging techniques in management of brain metastases. *Front Oncol* (2019) 9:440. doi: 10.3389/fonc.2019.00440

79. de Vries NA, Buckle T, Zhao J, Beijnen JH, Schellens JH, et al. Restricted brain penetration of the tyrosine kinase inhibitor erlotinib due to the drug transporters p-gp and BCRP. *Invest New Drugs* (2012) 30(2):443–9. doi: 10.1007/s10637-010-9569-1

80. Pardridge WM. Drug transport across the blood-brain barrier. *J Cereb Blood Flow Metab* (2012) 32(11):1959–72. doi: 10.1038/jcbfm.2012.126

81. Hulin JA, Gubareva EA, Jarzebska N, Rodionov RN, Mangoni AA, Tommasi S. Inhibition of dimethylarginine dimethylaminohydrolase (DDAH) enzymes as an emerging therapeutic strategy to target angiogenesis and vasculogenic mimicry in cancer. *Front Oncol* (2020) 9:1455. doi: 10.3389/fonc.2019.01455

82. Al Tameemi W, Dale TP, Al-Jumaily RMK, Forsyth NR. Hypoxia-modified cancer cell metabolism. *Front Cell Dev Biol* (2019) 7:4. doi: 10.3389/fcell.2019.00004

83. Langley RR, Fidler IJ. The biology of brain metastasis. *Clin Chem* (2013) 59 (1):180–9. doi: 10.1097/ppo.0000000000000126

84. Kienast Y, von Baumgarten L, Fuhrmann M, Klinkert WE, Goldbrunner R, Herms J, et al. Real-time imaging reveals the single steps of brain metastasis formation. *Nat Med* (2010) 16(1):116–22. doi: 10.1038/nm.2072

85. Fidler IJ, Yano S, Zhang RD, Fujimaki T, Bucana CD. The seed and soil hy pothesis: vascularisation and brain metastases. *Lancet Oncol* (2002) 3(1):53–7. doi: 10.1016/s1470-2045(01)00622-2

86. Yano S, Shinohara H, Herbst RS, Kuniyasu H, Bucana CD, Ellis LM, et al. Expression of vascular endothelial growth factor is necessary but not sufficient for production and growth of brain metastasis. *Cancer Res* (2000) 60(17):4959–67.

87. Jubb AM, Cesario A, Ferguson M, Congedo MT, Gatter KC, Lococo F, et al. Vascular phenotypes in primary non-small cell lung carcinomas and matched brain metastases. *Br J Cancer* (2011) 104(12):1877–81. doi: 10.1038/bjc.2011.147

88. Fu Y, Hu J, Du N, Jiao S, Li F, Li X, et al. Bevacizu mab plus chemot herapy versus chemotherapy alone for preventing brain metastasis derived from advanced lung cancer. *J Chemother* (2015) 28(3):218–24. doi: 10.1179/1973947815Y.0000000045

89. Sandler A, Hirsh V, Reck M, von Pawel J, Akerley W, Johnson DH, et al. A n evidence-based review of the incidence of CNS bleeding with anti-VEGF therapy in non-small cell lung cancer patients with brain metastases. *Lung Cancer* (2012) 78 (1):1–7. doi: 10.1016/j.lungcan.2012.07.004

90. Lee SJ, Kang WY, Yoon Y, Jin JY, Song HJ, Her JH, et al. Natural killer (NK) cells inhibit systemic metastasis of glioblastoma cells and have therapeutic effects against glioblastomas in the brain. *BMC Cancer* (2015) 15(1):1011. doi: 10.1186/s12885-015-2034-y

91. Chisari A, Golán I, Campisano S, Gélabert C, Moustakas A, Sancho P, et al. Glucose and amino acid metabolic dependencies linked to stemness and metastasis in different aggressive cancer types. *Front Pharmacol* (2021) 12:723798. doi: 10.3389/fphar.2021.723798

92. Rondeau G, Abedinpour P, Desai P, Baron VT, Borgstrom P, Welsh J. Effects of different tissue microenvironments on gene expression in breast cancer cells. *PloS One* (2014) 9(7):e101160. doi: 10.1371/journal.pone.0101160

93. Ding L, Ellis MJ, Li S, Larson DE, Chen K, Wallis JW, et al. Genome remodelling in a basal-like breast cancer metastasis and xenograft. *Nature* (2010) 464(7291):999–1005. doi: 10.1038/nature08989

94. Brastianos PK, Carter SL, Santagata S, Cahill DP, Taylor-Weiner A, Jones RT, et al. Genomic characterization of brain metastases reveals branched evolution and potential therapeutic targets. *Cancer Discovery* (2015) 5(11):1164–77. doi: 10.1158/2159-8290.CD-15-0369

95. Li F, Sun L, Zhang S. Acquirement of DNA copy number variations in non-small cell lung cancer metastasis to the brain. *Oncol Rep* (2015) 34(4):1701–7. doi: 10.3892/or.2015.4188

96. Chen G, Chakravarti N, Aardalen K, Lazar AJ, Tetzlaff MT, Wubbenhorst B, et al. Molecular profiling of patient-matched brain and extracranial melanoma metastases implicates the PI3K pathway as a therapeutic target. *Clin Cancer Res* (2014) 20(21):5537–46. doi: 10.1158/1078-0432.CCR-13-3003

97. Ferguson SD, Zheng S, Xiu J, Zhou S, Khasraw M, Brastianos PK, et al. Profiles of brain metastases: Prioritization of therapeutic targets. *Int J Cancer.* (2018) 143(11):3019–26. doi: 10.1002/ijc.31624

98. Bollig-Fischer A, Michelhaugh SK, Wijesinghe P, Dyson G, Kruger A, Palanisamy N, et al. Cytogenomic profiling of breast cancer brain metastases reveals potential for repurposing targeted the rapeutics. *Oncotarget* (2015) 6 (16):14614–24. doi: 10.18632/oncotarget.3786

99. Preusser M, Berghoff AS, Berger W, Ilhan-Mutlu A, Dinhof C, Widhalm G, et al. High rate of FGFR1 amplifications in brain metastases of squamous and non-squamous lung cancer. *Lung Cancer.* (2014) 83(1):83–9. doi: 10.1016/j.lungcan.2013.10.004

100. Lo Nigro C, Vivenza D, Monteverde M, Lattanzio L, Gojis O, Garrone O, et al. High frequency of complex TP53 mutations in CNS metastases from breast cancer. *Br J Cancer* (2012) 106(2):397–404. doi: 10.1038/bjc.2011.464

101. Gaedcke J, Traub F, Milde S, Wilkens L, Stan A, Ostertag H, et al. Predominance of the basal type and HER-2/neu type in brain metastasis from breast cancer. *Mod Pathol* (2007) 20(8):864–70. doi: 10.1038/modpathol.3800830

102. Kuroda H, Tachikawa M, Yagi Y, Umetsu M, Nurdin A, Miyauchi EY, et al. Cluster of differentiation 46 is the major receptor in human blood-brain barrier endothelial cells for uptake of exosomes derived from brain-metastatic melanoma cells (SK-Mel-28). *Mol Pharm* (2019) 16(1):292–304. doi: 10.1021/acs.molpharmaceut.8b00985

103. Arai T, Ichimura K, Hirakawa K, Yuasa Y. DNA Amplifications and elevated expression of proto-oncogene in addition to altered DNA ploidy in metastatic brain tumors. *Clin Exp Metastasis* (1994) 12(4):267–75. doi: 10.1007/BF01753833

104. . doi: 10.18632/oncotarget.3786

105. Park ES, Kim SJ, Kim SW, Yoon SL, Leem SH, Kim SBC, et al. Cross-species hybridization of microarrays for studying tumor transcriptome of brain metastasis. *Proc Natl Acad Sci U S A.* (2011) 108(42):17456–61. doi: 10.1073/pnas.1114210108

106. Bleckmann A, Siam L, Klemm F, Rietkötter E, Wegner C, Kramer F, et al. Nuclear LEF1/TCF4 correlate with poor prognosis but not with nuclear β-catenin in cerebral metastasis of lung adenocarcinomas. *Clin Exp Metastasis.* (2013) 30(4):471–82. doi: 10.1007/s10585-012-9552-7

107. Marzese DM, Scolyer RA, Huynh JL, Huang SK, Hirose H, Chong KK, et al. Epigenome-wide DNA methylation landscape of melanoma progression to brain metastasis reveals aberrations on homeobox d cluster associated with prognosis. *Hum Mol Genet* (2014) 23(1):226–38. doi: 10.1093/hmg/ddt420

108. Pangeni RP, Channathodiyil P, Huen DS, Eagles LW, Johal BK, Pasha D, et al. The GALNT9, BNC1 and CCDC8 genes are frequently epigenetically dysregulated in breast tumours that metastasise to the brain. *Clin Epigenetics.* (2015) 7(1):57. doi: 10.1186/s13148-015-0089-x

109. Li T, Lian H, Li H, Xu Y, Zhang H. HY5 regulates light-responsive transcription of microRNA163 to promote primary root elongation in arabidopsis seedlings. *J Integr Plant Biol* (2021) 63(8):1437–50. doi: 10.1111/jipb.13099

110. Zhao C, Xu Y, Zhang Y, Tan W, Xue J, Yang Z, et al. Downregulation of miR-145 contributes to lung adenocarcinoma cell growth to form brain metastases. *Oncol Rep* (2013) 30(5):2027–34. doi: 10.3892/or.2013.2728

111. Cho WC, Chow AS, Au JS. Restoration of tumour suppressor hsa-miR-145 inhibits cancer cell growth in lung adenocarcinoma patients with epidermal growth factor receptor mutation. *Eur J Cancer.* (2009) 45(12):2197–206. doi: 10.1016/j.ejca.2009.04.039

112. Cho WC, Chow AS, Au JS. MiR-145 inhibits cell proliferation of human lung adenocarcinoma by targeting EGFR and NUDT1. *RNA Biol* (2011) 8(1):125–31. doi: 10.4161/rna.8.1.14259

113. Donzelli S, Mori F, Bellissimo T, Sacconi A, Casini B, Frixa T, et al. Epigenetic silencing of miR-145-5p contributes to brain metastasis. *Oncotarget* (2015) 6(34):35183–201. doi: 10.18632/oncotarget.5930

114. Minn YK, Lee DH, Hyung WJ, Kim JE, Choi J, Yang SH, et al. MicroRNA-200 family members and ZEB2 are associated with brain metastasis in gastric adenocarcinoma. *Int J Oncol* (2014) 45(6):2403–10. doi: 10.3892/ijo.2014.2680

115. Fellows LK, Boutelle MG, Fillenz M. Extracellular brain glucose levels reflect local neuronal activity: a microdialysis study in awake, freely moving rats. *J Neurochem* (1992) 59(6):2141–7. doi: 10.1111/j.1471-4159.1992.tb10105.x

116. Daikhin Y, Yudkoff M. Compartmentation of brain glutamate metabolism in neurons and glia. *J Nutr* (2000) 130(4S Suppl):1026S–31S. doi: 10.1093/jn/130.4.1026S

117. Lau D, Wadhwa H, Sudhir S, Chang AC, Jain S, Chandra A, et al. Role of c-Met/β1 integrin complex in the metastatic cascade in breast cancer. *JCI Insight* (2021) 6(12):e138928. doi: 10.1172/jci.insight.138928

118. Chen EI, Hewel J, Krueger JS, Tiraby C, Weber MR, Kralli A, et al. Adaptation of energy metabolism in breast cancer brain metastases. *Cancer Res* (2007) 67(4):1472–86. doi: 10.1158/0008-5472.CAN-06-3137

119. Gurung RB, Gong SY, Dhakal D, Le TT, Jung NR, Jung HJ, et al. Synthesis of curcumin glycosides with enhanced anticancer properties using one-pot multienzyme glycosylation technique. *J Microbiol Biotechnol* (2017) 27(9):1639–48. doi: 10.4014/jmb.1701.01054

120. Chen J, Lee HJ, Wu X, Huo L, Kim SJ, Xu L, et al. Gain of glucose-independent growth upon metastasis of breast cancer cells to the brain. *Cancer Res* (2015) 75(3):554–65. doi: 10.1158/0008-5472.CAN-14-2268

121. Jung YY, Kim HM, Koo JS. Expression of lipid metabolism-related proteins in metastatic breast cancer. *PloS One* (2015) 10(9):e0137204. doi: 10.1371/journal.pone.0137204

122. Dahn ML, Walsh HR, Dean CA, Giacomantonio MA, Fernando W, Murphy JP, et al. Metabolite profiling reveals a connection between aldehyde dehydrogenase 1A3 and GABA metabolism in breast cancer metastasis. *Metabolomics* (2022) 18(1):9. doi: 10.1007/s11306-021-01864-6

123. Ran L, Hong T, Xiao X, Xie L, Zhou J, Wen G. GABARAPL1 acts as a potential marker and promotes tumor proliferation and metastasis in triple negative breast cancer. *Oncotarget* (2017) 8(43):74519–26. doi: 10.18632/oncotarget.20159

124. Nygaard V, Prasmickaite L, Vasiliauskaite K, Clancy T, Hovig E. Melanoma brain colonization involves the emergence of a brain-adaptive phenotype. *Oncoscience* (2014) 1(1):82–94. doi: 10.18632/oncoscience.11

125. Beasley KD, Toms SA. The molecular pathobiology of metastasis to the brain: a review. *Neurosurg Clin N Am* (2011) 22(1):7–v. doi: 10.1016/j.nec.2010.08.009

126. Termini J, Neman J, Jandial R. Role of the neural niche in brain metastatic cancer. *Cancer Res* (2014) 74(15):4011–5. doi: 10.1158/0008-5472.CAN-14-1226

127. Aili Y, Maimaitiming N, Mahemuti Y, Qin H, Wang Y, Wang Z. Liquid biopsy in central nervous system tumors: the potential roles of circulating miRNA and exosomes. *Am J Cancer Res* (2020) 10(12):4134–50. doi: 10.3389/fonc.2021.686369

128. Aili Y, Maimaitiming N, Mahemuti Y, Qin H, Wang Y, Wang Z. The role of exosomal miRNAs in glioma: Biological function and clinical application. *Front Oncol* (2021) 11:686369. doi: 10.3389/fonc.2021.686369

129. Hoshino A, Costa-Silva B, Shen TL, Rodrigues G, Hashimoto A, Tesic Mark M, et al. Tumour exosome integrins determine organotropic metastasis. *Nature* (2015) 527(7578):329–35. doi: 10.1038/nature15756

130. Fong MY, Zhou W, Liu L, Alontaga AY, Chandra M, Ashby J, et al. Breast-cancer-secreted miR-122 reprograms glucose metabolism in premetastatic niche to promote metastasis. *Nat Cell Biol* (2015) 17(2):183–94. doi: 10.1038/ncb3094

131. Cao M, Isaac R, Yan W, Ruan X, Jiang L, Wan Y, et al. Cancer-cell-secreted extracellular vesicles suppress insulin secretion through miR-122 to impair systemic glucose homeostasis and contribute to tumour growth. *Nat Cell Biol* (2022) 24(6):954–67. doi: 10.1038/s41556-022-00919-7

132. Umezu T, Tadokoro H, Azuma K, Yoshizawa S, Ohyashiki K, Ohyashiki JH, et al. Exosomal miR-135b shed from hypoxic multiple myeloma cells enhances angiogenesis by targeting factor-inhibiting HIF-1. *Blood* (2014) 124(25):3748. doi: 10.1182/blood-2014-05-576116

133. Wu D, Shihua D, Li L, Liu T, Zhang T, Li J, et al. TGF-β1-mediated exosomal lnc-MMP2-2 increases blood–brain barrier permeability *via* the miRNA-1207-5p/EPB41L5 axis to promote non-small cell lung cancer brain metastasis. *Cell Death Dis* (2021) 12(10):1–1. doi: 10.1038/s41419-021-04072-1

134. Zhang L, Zhang S, Yao J, Lowery FJ, Zhang Q, Huang WC. Microenvironment-induced PTEN loss by exosomal microRNA primes brain metastasis outgrowth. *Nature* (2015) 527(7576):100–4. doi: 10.1038/nature15376

135. Satelli A, Li S. Vimentin in cancer and its potential as a molecular target for cancer therapy. *Cell Mol Life Sci* (2011) 68(18):3033–46. doi: 10.1007/s00018-011-0735-1

136. Xing F, Liu Y, Wu SY, Wu K, Sharma S, Mo YY, et al. Loss of XIST in breast cancer activates MSN-c-Met and reprograms microglia *via* exosomal miRNA to promote brain metastasis. *Cancer Res* (2018) 78(15):4316–30. doi: 10.1158/0008-5472.CAN-18-1102

137. Xu Z-H, Miao Z-W, Jiang QZ, Gan DX, Wei XG, Xue XZ, et al. Brain microvascular endothelial cell exosome-mediated S100A16 up-regulation confers small-cell lung cancer cell survival in brain. *FASEB J Off Publ Fed Am Societies Exp Biol* (2018) 33(2):1742–54. doi: 10.1096/fj.201800428R

138. Rodrigues G, Hoshino A, Kenific CM, Matei IR, Steiner L, Freitas D, et al. Tumour exosomal CEMIP protein promotes cancer cell colonization in brain metastasis. *Nat Cell Biol* (2019) 21:1403–12. doi: 10.1038/s41556-019-0404-4

139. Tămaş F, Bălaşa R, Manu D, Gyorki G, Chinezu R, Tămaş C, et al. The importance of small extracellular vesicles in the cerebral metastatic process. *Int J Mol Sci* (2022) 23(3):1449. doi: 10.3390/ijms23031449

140. Zhu Y, Tao Z, Chen Y, Lin S, Zhu M, Ji W, et al. Exosomal MMP-1 transfers metastasis potential in triple-negative breast cancer through PAR1-mediated EMT. *Breast Cancer Res Treat* (2022) 193(1):65–81. doi: 10.1007/s10549-022-06514-6

141. Meng L, Song K, Li S, Kang Y. Exosomes: Small vesicles with important roles in the development, metastasis and treatment of breast cancer. *Membranes (Basel).* (2022) 12(8):775. doi: 10.3390/membranes12080775

142. Ingenito F, Roscigno G, Affinito A, Nuzzo S, Scognamiglio I, Quintavalle C, et al. The role of exo-miRNAs in cancer: A focus on therapeutic and diagnostic applications. *Int J Mol Sci* (2019) 20(19):4687. doi: 10.3390/ijms20194687

143. Penfornis P, Vallabhaneni KC, Whitt J, Pochampally RJ, et al. Extracellular vesicles as carriers of microRNA, proteins andlipids in tumor microenvironment. *Int J Cancer* (2016) 138(1):14–21. doi: 10.1002/ijc.29417

144. Maroto R, Zhao Y, Jamaluddin M, Popov VL, Wang H, Kalubowilage M, et al. Effects of storage temperature on airway exosome integrity for diagnostic and functional analyses. *J Extracell Vesicles* (2017) 6(1):1359478. doi: 10.1080/20013078.2017.1359478

145. Zhang N, He F, Li T, Chen J, Jiang L, Ouyang XP. Role of exosomes in brain diseases. *Front Cell Neurosci* (2021) 15:743353. doi: 10.3389/fncel.2021.743353

146. Camacho L, Guerrero P, Marchetti D. MicroRNA and protein profiling of brain metastasis competent cellderived exosomes. *PloS One* (2013) 8(9):e73790. doi: 10.1371/journal.pone.0073790

147. Yu W, Hurley J, Roberts D, Chakrabortty SK, Enderle D, Noerholm M, et al. Exosome-based liquid biopsies in cancer: opportunities and challenges. *Ann Oncol* (2021) 32(4):466–77. doi: 10.1016/j.annonc.2021.01.074

148. Sheridan C. Exosome cancer diagnostic reaches market. *Nat Biotechnol* (2016) 34(4):359–60. doi: 10.1038/nbt0416-359

149. Yang Y, Li CW, Chan LC, Wei Y, Hsu JM, Xia W, et al. Exosomal PD-L1harbors active defense function to suppress T cell killing ofbreast cancer cells and promote tumor growth. *Cell Res* (2018) 28(8):862–4. doi: 10.1038/s41422-018-0060-4

150. Li J, Liu K, Liu Y, Xu Y, Zhang F, Yang H, et al. Exosomes mediate the cell-to-cell transmission of IFN-a-induced antiviral activity. *Nat Immunol* (2013) 14 (8):793–803. doi: 10.1038/ni.2647

151. Toyokawa G, Seto T, Takenoyama M, Ichinose Y. Insights into brain metastasis in patients with ALK+ lung cancer: is the brain truly a sanctuary? *Cancer Metastasis Rev* (2015) 34(4):797–805. doi: 10.1007/s10555-015-9592-y

152. Arab S. Exosomes: Novel bio-inspired nanocarriers for efficient targeting of glioblastoma tumor cells. *J Babol Univ Med Sci* (2020) 23(1):16–22.

153. Alvarez-erviti L, Seow Y, Yin HF, Betts C, Lakhal S, Wood MJ, et al. Deliveryof siRNA to the mouse brain by systemic injection of targeted exosomes. *Nat Biotechnol* (2011) 29(4):341–5. doi: 10.1038/nbt.1807

154. Pascucci L, Cocce V, Bonomi A, Ami D, Ceccarelli P, Ciusani E, et al. Paclitaxel is incorporated by mesenchymal stromal cells and released in exosomes that inhibit *in vitro* tumor growth: a new approach for drug delivery. *J Control Release* (2014) 192:262–70. doi: 10.1016/j.jconrel.2014.07.042

155. Yim N, Ryu SW, Choi K, Lee KR, Lee S, Choi H, et al. Exosome engineering forefficient intracellular delivery of soluble proteins usingoptically reversible protein-protein interaction module. *Nat Commun* (2016) 7:12277. doi: 10.1038/ncomms12277

156. , Saari HLisitsyna ERautaniemi KRojalin TNiemi LNivaro O, et al. FLIM reveals alternative EV-mediated cellular up-take pathways of paclitaxel. *J Control Release* (2018) 284:133ş143. doi: 10.1016/j.jconrel.2018.06.015

157. Yu M, Gai C, Li Z, Ding D, Zheng J, Zhang W, et al. Targeted exosome-encapsulated erastin induced ferroptosis in triple negative breast cancer cells. *Cancer Sci* (2019) 110(10). doi: 10.1111/cas.14181

158. Yang T, Martin P, Fogarity B, Brown A, Schurman K, Phipps R, et al. Exosome delivered anticancer drugs across the blood-brain barrier for brain cancer therapy in danio rerio. *Pharm Res* (2015) 32(6):2003–14. doi: 10.1007/s11095-014-1593-y

159. Winkler F. The brain microenvironment: friend or foe for metastatic tumor cells? *Neuro-oncology* (2014) 16(12):1565–6. doi: 10.1093/neuonc/nou308

160. O'Brien ER, Clare H, Sibson NR. The role of astrocytes in CNS tumors: pre-clinical models and novel imaging approaches. *Front Cell Neurosci* (2013) 7:40. doi: 10.3389/fncel.2013.00040

161. McDermott R, Gabik ian P, Sar vaiya P, Ulasov I, Lesniak MS. MicroRNA s in brain metastases: big things come in small packages. *J Mol Med (Berl)* (2013) 91 (1):5–13. doi: 10.1007/s00109-012-0971-3

162. Li I, Nabet BY. Exosomes in the tumor microenvironment as mediators of cancer therapy resistance. *Mol Cancer* (2019) 18:32. doi: 10.1186/s12943-019-0975-5

163. Sandúa A, Alegre E, González Á. Exosomes in lung cancer: Actors and heralds of tumor development. *Cancers (Basel).* (2021) 13(17):4330. doi: 10.3390/cancers13174330

164. Oliveira FD, Castanho MARB, Neves V. Exosomes and brain metastases: A review on their role and potential applications. *Int J Mol Sci* (2021) 22(19):10899. doi: 10.3390/ijms221910899

165. Catelan S, Olioso D, Santangelo A, Scapoli C, Tamanini A, Pinna G, et al. miRNAs in serum exosomes for differential diagnosis of brain metastases. *Cancers (Basel).* (2022) 14(14):3493. doi: 10.3390/cancers14143493

166. Sweeney MD, Kisler K, Montagne A, Toga AW, Zlokovic BV. The role of brain vasculature in neurodegenerative disorders. *Nat Neurosci* (2018) 21 (10):1318–31. doi: 10.1038/s41593-018-0234-x

167. Catelan S, Olioso D, Santangelo A, Scapoli C, Tamanini A, Pinna G, et al. Emerging role of exosomes in cancer progression and tumor microenvironment remodeling. *J Hematol Oncol* (2022) 15(1):83. doi: 10.1186/s13045-022-01305-4

frontiers | Frontiers in Oncology

TYPE Original Research
PUBLISHED 21 November 2022
DOI 10.3389/fonc.2022.1030590

OPEN ACCESS

EDITED BY
Maria Teresa Valenti,
University of Verona, Italy

REVIEWED BY
Jeffrey A. Knauf,
Cleveland Clinic, United States
Ximena Volpini,
Medical Research Institute Mercedes and Martín Ferreyra (INIMEC), Argentina

*CORRESPONDENCE
Tao Huang
huangtaowh@163.com
Fang Dong
dongf0323@163.com

†These authors have contributed equally to this work and share the first authorship

SPECIALTY SECTION
This article was submitted to Molecular and Cellular Oncology, a section of the journal Frontiers in Oncology

RECEIVED 29 August 2022
ACCEPTED 26 October 2022
PUBLISHED 21 November 2022

CITATION
Zhou J, Xu M, Tan J, Zhou L, Dong F and Huang T (2022) MMP1 acts as a potential regulator of tumor progression and dedifferentiation in papillary thyroid cancer. *Front. Oncol.* 12:1030590. doi: 10.3389/fonc.2022.1030590

MMP1 acts as a potential regulator of tumor progression and dedifferentiation in papillary thyroid cancer

Jun Zhou†, Ming Xu†, Jie Tan, Lin Zhou, Fang Dong* and Tao Huang*

Department of Breast and Thyroid Surgery, Union Hospital, Tongji Medical College, Huazhong University of Science and Technology, Wuhan, China

Papillary thyroid cancer (PTC) is one of the malignancies with an excellent prognosis. However, in PTC, progression or dedifferentiation into poorly differentiated thyroid cancer (PDTC) or anaplastic thyroid cancer (ATC) extremely jeopardizes patients' prognosis. MMP1 is a zinc-dependent endopeptidase, and its role in PTC progression and dedifferentiation is unclear. In this study, transcriptome data of PDTC/ATC and PTC from the Gene Expression Omnibus and The Cancer Genome Atlas databases were utilized to perform an integrated analysis of MMP1 as a potential regulator of tumor progression and dedifferentiation in PTC. Both bulk and single-cell RNA-sequencing data confirmed the high expression of MMP1 in ATC tissues and cells, and further study verified that MMP1 possessed good diagnostic and prognostic value in PTC and PDTC/ATC. Up-regulated MMP1 was found to be positively related to more aggressive clinical characteristics, worse survival, extracellular matrix-related pathways, oncogenic immune microenvironment, more mutations, higher stemness, and more dedifferentiation of PTC. Meanwhile, *in vitro* experiments verified the high level of MMP1 in PDTC/ATC cell lines, and MMP1 knockdown and its inhibitor triolein could both inhibit the cell viability of PTC and PDTC/ATC. In conclusion, our findings suggest that MMP1 is a potential regulator of tumor progression and dedifferentiation in PTC, and might become a novel therapeutic target for PTC, especially for more aggressive PDTC and ATC.

KEYWORDS

papillary thyroid cancer, poorly differentiated thyroid cancer, anaplastic thyroid carcinoma, dedifferentiation, MMP1

Introduction

Papillary thyroid cancer (PTC) accounts for more than 80-85% of all thyroid cancers (TCs) (1), and PTC patients usually have a 10-year survival rate greater than 90% (2). Most PTC responds well to the current treatments, including surgery, thyroid-stimulating hormone suppression, and radioactive iodine therapies (2). However, 10-15% PTCs eventually experience recurrence or metastasis, dedifferentiate into more aggressive poorly differentiated TCs (PDTCs), and develop treatment resistance, consequently leading to cancer-related mortality (3–5). It was reported that the 5-year survival rate of PDTC patients was only 50-64% (6, 7), leaving large gaps with other PTC patients. Anaplastic thyroid cancer (ATC) is an undifferentiated TC that accounts for only 1-2% of all TCs. As one of the most lethal malignancies in humans, ATC has cancer-specific mortality at one year of nearly 100%, and it often originates from a pre-existing presence of differentiated thyroid cancer (DTC) including PTC or occurs *de novo* (2, 8, 9). Therefore, it is clinically important to precisely stratify the aggressive PTC for active intervention to avoid its progression and dedifferentiation into PDTC/ATC.

Clinical variables of PTC, including the tumor node metastasis (TNM) stage, are routinely applied to clarify the mortality or recurrence risks of PTC (2). Nevertheless, despite their role in treatment selections, these factors remain insufficient to predict tumor progression after surgical treatment, especially the potential for dedifferentiation. Recent genomic studies on PDTC and ATC provided deep insights into the molecular pathogenesis and facilitating tumoral progression from PTC to PDTC/ATC through the accumulation of crucial genetic alterations, such as *BRAF* and *TERT* mutations (10–13). Although these findings help assess subtyping, prognostication, and therapy, while some targeted therapies are effective in a small fraction of PDTC/ATC patients (14), the deeper molecular mechanisms of PTC progression and dedifferentiation are only partially explained. It remains challenging to identify novel biomarkers, as well as potential therapeutic targets for further research.

MMP1, a zinc-dependent endopeptidase, is a member of matrix metalloproteinases (MMPs) and has been reported to be involved in multiple biochemical mechanisms in cardiovascular renal disorders, inflammation, and malignancy (15). Currently, very few studies have comprehensively explored the role of MMP1 in PTC and PDTC/ATC. Recent three studies indicated that MMP1 expression levels positively correlated with higher clinical stages of PTC (16–18), but its association with differentiation level and prognosis remains unclear. Paul Weinberger et al. also reported up-regulated MMP1 in ATC (19), but no further studies have been carried out.

In the present study, we screened the Gene Expression Omnibus (GEO) datasets to discover differentially expressed genes (DEGs) between PDTC/ATC and PTC, and then the role of MMP1 in PTC progression, immune infiltration, mutation, stemness, and differentiation was further discovered and validated using The Cancer Genome Atlas (TCGA) cohort *via* integrated bioinformatics analysis. Our results demonstrate the clinical utility of MMP1 and the implicational potential as a biomarker for PTC and PDTC/ATC, and the *in vitro* functional experiments confirmed its role as a potential therapeutic target.

Methods and materials

Study design and data source

The process of this study is shown in the flow chart (Figure 1). The gene expression data and clinicopathological data were obtained from TCGA (https://www.cancer.gov/tcga) and GEO (https://www.ncbi.nlm.nih.gov/geo/) databases. Multiple analyses were performed using R (http://www.r-project.org, version 4.1) in this study. Sequencing data from different GEO datasets were batch-normalized using the "sva" package (20) and subsequently analyzed. The GEO accession codes of microarray data were all base on an identical platform (Affymetrix Human Genome U133 Plus 2.0 Array) and utilized in this study (GSE76039, GSE66030, GSE29265, GSE53157, and GSE65144). PDTC and ATC samples from GEO were pooled together in cross-comparison with PTC samples. Clinical information of 37 PDTC/ATC patients from GSE76039 was downloaded from cBioPortal (http://www.cbioportal.org/) (21). The median RNA sequencing value was chosen as the cut-off value of the cohorts included in this study.

Identification of DEGs and MMP1

The R package "limma" (22) was used to screen DEGs with the adjusted P-value <0.05. The "umap" package (23) was used to perform the sample heterogeneity analysis between PTC and PDTC/ATC. The "ComplexHeatmap" package (24) was used for customizing the heatmap and the "ggplot2" package (25) was used for visualization.

Single-cell RNA sequencing analysis

We downloaded the original single-cell RNA sequencing data from five ATC patients and six PTC patients on the GEO database (GSE148673 and GSE191288). After standard data quality control, batch effect adjustment, and normalization using the "Seurat" package (26), we clustered all cells using the Uniform Manifold Approximation and Projection (UMAP) method (27) as four basic types: tumor/epithelial cells,

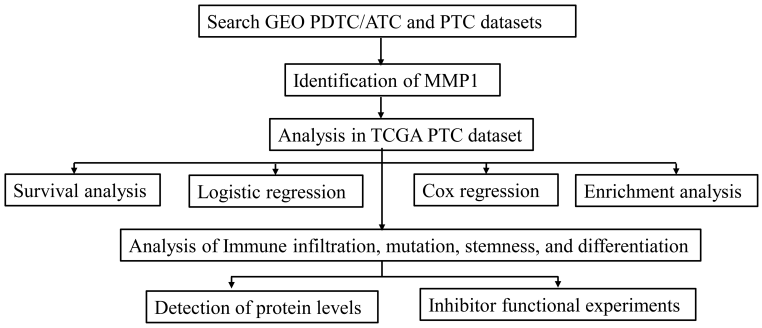

FIGURE 1
Flow diagram of this study. The details of data collection and analysis were exhibited in a flow diagram. GEO, the Gene Expression Omnibus; PDTC, poorly differentiated thyroid cancer; ATC, anaplastic thyroid cancer; PTC, papillary thyroid cancer; TCGA, The Cancer Genome Atlas.

immune cells, endothelial cells, and fibroblasts *via* cell markers (Supplementary Figure 1A). MMP1 expression was analyzed in PTC/ATC and all kinds of cells.

Correlation analysis

The "DESeq2" and "corrplot" packages (28, 29) were used to perform a spearman correlation analysis between the expression levels of MMP1 and other different indicators, and a P-value <0.05 was selected as a cutoff criterion. The receiver operator characteristic (ROC) curve analysis was performed using the "pROC" package (30) to evaluate the diagnostic value of MMP1. Logistics regression and Cox regression with 95% confidence intervals (CIs) were performed in R to calculate the odds ratios (ORs) and hazard ratios (HRs) to assess the value of MMP1 in predicting some pathological characteristics and outcomes of PTC patients from TCGA, respectively,

Survival analysis

The survival data were obtained from the TCGA-THCA dataset. Considering the favorable prognosis of most PTC patients, the correlation between the number of death events and overall survival (OS) was pretty low, and we focused on the progression-free survival (PFS) and disease-free interval (DFI) of the patients. The median of MMP1 expression was defined as the cutoff point for dividing the samples into high and low-expression groups. The survival probability was estimated *via* Statistical Product and Service Solutions (SPSS, version 26.0) using the Kaplan-Meier method, and a log-rank P-value <0.05 was considered statistically significant. Data from Gene Set Cancer Analysis (GSCA) database (31) (http://bioinfo.life.hust.edu.cn/GSCA/#/) were also adopted into survival analysis. Although there is a difference in the prognosis between ATC and PDTC that we cannot ignore, their outcomes are still very poor compared with PTC. Referring to the study (32) of Wen et al., we pooled ATC and PDTC from GSE76039 together to analyze the relationship between their prognosis and MMP1 level. Cox proportional hazard regression model was used to assess the survival difference and hazard ratio (HR) of MMP1 in PTC patients.

Enrichment analysis

Enrichment analysis has been widely used in recent years to identify gene properties, based on the hypothesis that genes with similar expression profiles may be regulated by common pathways and involved in related functions (33). In this study, Gene Ontology (GO), Kyoto Encyclopedia of Genes and Genomes (KEGG) enrichment analysis, and Gene set enrichment analysis (GSEA) were performed in different sample groupings to find potential molecular mechanisms. The "clusterProfiler" package (34) was used, and nominal P <0.05 and false discovery rate (FDR) <0.25 were selected as cutoff criteria.

Immune infiltration analysis

Multiple gene set signature-based methods for comprehensively estimating the abundance of different immune cell types were utilized in this study. To estimate the variation of involved immune cells over PTC samples, a gene set enrichment analysis called Gene Set Variation Analysis (GSVA) was performed (35). The "ESTIMATE" package (36) was applied to calculate the immune scores of each PTC sample, and the correlation between immune cell infiltrate and the GSVA enrichment score of PTC was further verified. The immune

infiltration landscape of PTC was also conducted *via* the "ssGSEA" algorithm in the "GSVA" package (37), "TIMER" and "xCELL" algorithms in the "IOBR" package (38, 39) to identify immune cells that might be significantly associated with MMP1.

Analysis of the mutation, stemness, and differentiation

The stemness level of a tumor could be quantified based on the RNA expression and DNA methylation signature (40), and the Epigenetically regulated RNA expression-based Stemness Score (EREG.EXPss, 103 probes) and DNA methylation-based Stemness Score (DNAss, 219 probes) were utilized in this study to assess the stemness of PTC from TCGA. $BRAF^{V600E}$-*RAS* score (BRS) was developed by the TCGA group to quantify the extent to which the gene expression profile of PTC resembles either the $BRAF^{V600E}$- or *RAS*-mutant profiles (41). Thyroid differentiation Score (TDS) was also developed by the TCGA group to quantify the PTC differentiation level (41) and it was calculated based on the expression levels of 16 thyroid metabolism and function genes (DIO1, DIO2, DUOX1, DUOX2, FOXE1, GLIS3, NKX2-1, PAX8, SLC26A4, SLC5A5, SLC5A8, TG, THRA, THRB, TPO, TSHR). Data of stemness scores, BRS, and TDS were obtained from TCGA and their relationships with MMP1 in PTC were also further explored.

Cell culture

The PTC cell lines TPC-1 and K1, PDTC cell line KTC-1, and ATC cell line CAL-62 used in this study were purchased from the American Type Culture Collection (ATCC). All cells were cultured in the 37°C and 5% CO_2 culture environment, and in specific mediums (Gibco, USA) suggested by ATCC with 10% fetal bovine serum (FBS).

Western blotting analysis

The total protein of cells was extracted with protein extraction reagent Radio-immunoprecipitation Assay buffer (Beyotime, China) containing 1mM Phenylmethylsulfonyl fluoride (Beyotime, China), and quantified by the BCA Protein Assay Kit (Beyotime, China). Equal amounts of protein were subjected to 10% SDS-PAGE and then transferred to a PVDF membrane (Millipore, USA). The immunoblots were incubated with primary antibodies against MMP1 (1: 800 dilution, Proteintech, China), and GAPDH (1: 3000 dilution, Cell Signaling Technology, USA) as the internal control. The protein signals were visualized with the ChemiDoc XRS+ System (Bio-Rad, USA) using the ECL detection kit (Beyotime, China).

Cell transfection

Short interference RNA (siRNA) for MMP1 and corresponding siRNA negative control were purchased from RiboBo (China). Transient transfection was performed using Lipofectamine 3000 (Thermo Fisher, USA) according to the manufacturer′s protocol. The transfection efficiency was evaluated using western blot and the siRNA target sequence for MMP1 was as follows: 5′- ACACAAGAGCAAGATGTGG-3′; The cells were harvested at 48 hours after transfection and then used for further experiments.

Cell viability assays

The cell viability assays were analyzed by the Cell Counting Kit-8 (CCK8) and colony formation assay to evaluate the cell proliferation of different cells according to the manufacturer's protocol.

CCK8 assay: A total of 1000 cells were seeded into 96-well plates with different concentrations of MMP1 inhibitor Triolein (42). After 48 hours, the medium was removed and a 100 μL serum-free medium with 10% CCK8 solution (Dojindo, Japan) inside was added to each well of the plate. After incubation for 2 hours at 37°C, the spectrometric absorbance of each well at 450 nm was measured on a microplate reader (Thermo Fisher, USA).

Colony formation assay: A total of 1000 cells were seeded into 6-well plates with 50 μM Triolein. All cells were cultured in their corresponding medium, and the medium was renewed every three days over the next 15 days. Cell clones were stained with 0.2% crystal violet (Beyotime, China) and then photographed.

Statistical analysis

SPSS 26.0 (IBM, USA), R 4.1 (Lucent Technologies, USA), and Graphpad Prism 8.0 (GraphPad Software, USA) were used for statistical analysis. ImageJ 1.53k (NIH, USA) was used for colony formation counting. Unless stated otherwise, the Student's t-test, two-way analysis of variance, or Chi-square test was performed to compare the differences between different groups, respectively. Results of $P < 0.05$ were considered significant: NS means not significant, *P <0.05, **P <0.01, ***P <0.001, and ****P <0.0001.

Results

Identification of MMP1 between PTC and PDTC/ATC

Bulk gene expression data were extracted from 5 GEO datasets and samples were listed in Figure 2A. 73 advanced

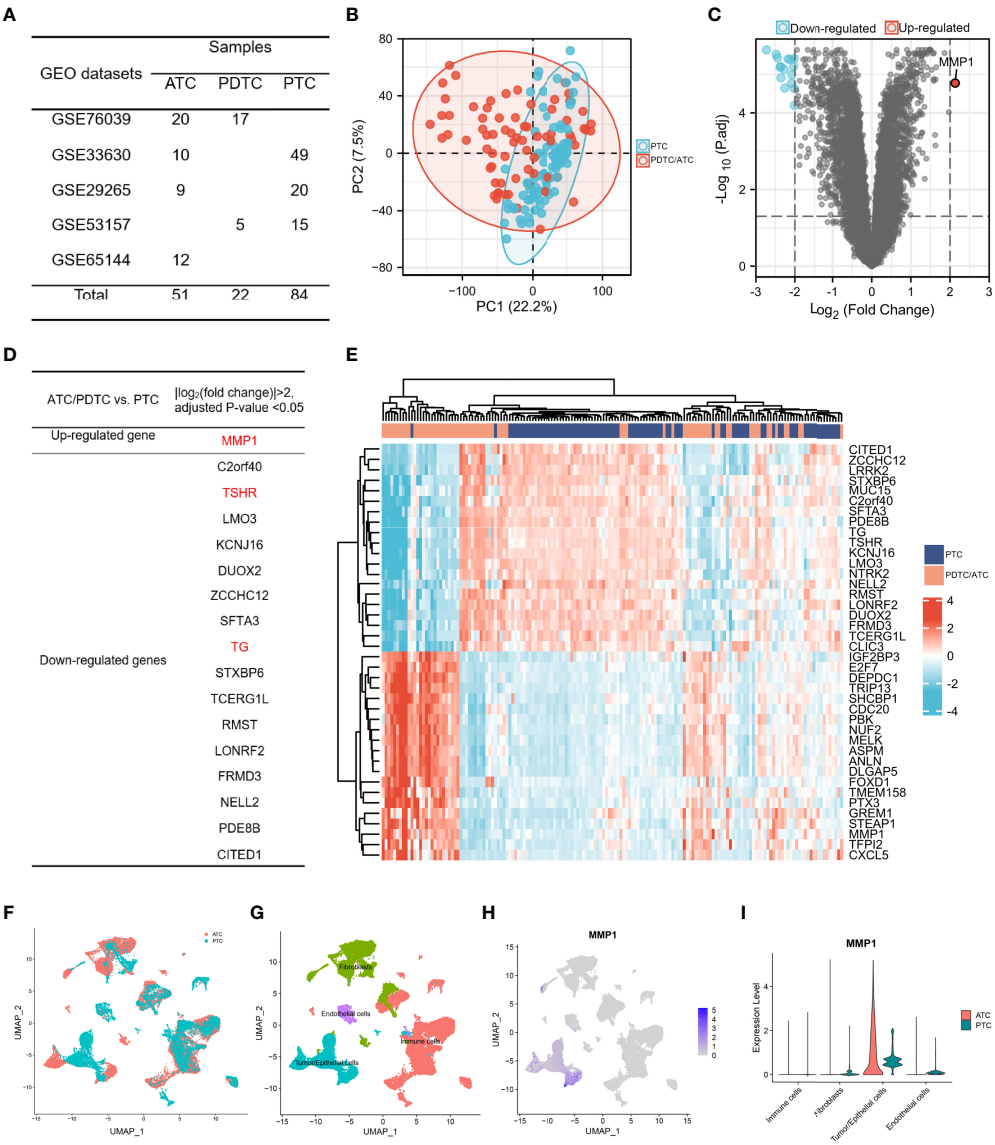

FIGURE 2
The identification of MMP1. **(A)** TC samples from the GEO database included in this study; **(B)** PCA map between PDTC/ATC and PTC. The difference between PTC and PDTC/ATC samples was not very large. **(C)** Volcano plots exhibited the DEGs between PDTC/ATC and PTC. **(D)** List of DEGs between PDTC/ATC and PTC. **(E)**. Heat map of MMP1 and another top 40 DEGs between PDTC/ATC and PTC. **(F)** Single-cell sequencing data in five ATC and six PTC patients. **(G)** Four basic types of cells in single cell sequencing data: tumor/epithelial cells, immune cells, endothelial cells and fibroblasts. **(H)** MMP1 expression in different cells. **(I)** Relative quantification of MMP1 expression level. GEO, the Gene Expression Omnibus; PDTC, poorly differentiated thyroid cancer; ATC, anaplastic thyroid cancer; PTC, papillary thyroid cancer; DEG, differentially expressed gene.

thyroid tumors (22 PDTCs and 51 ATCs) and 84 PTCs met the sequencing quality standards and are included in this study. The sample-to-sample heterogeneity between PDTC/ATC and PTC was detected by principal component analysis (PCA) (43) (Figure 2B). 351 DEGs between these two groups were screened (Details in Supplementary Table 1) while the cutoff criteria were $|\log_2$ (fold change)| >1. As shown in Figure 2C, MMP1 was the only highly expressed gene in PDTC/ATC relative to PTC when we chose $|\log_2$ (fold change)| >2 as the cutoff criteria. Another 16 down-regulated genes were listed in Figure 2D, among which TG and TSHR are characteristic genes for PTC. In addition, MMP1 and other top 40 DEGs were exhibited in a heat map (Figure 2E).

Even if the above bulk RNA data from GEO showed MMP1 as a significantly upregulated gene in PDTC/ATC, MMP1 can be secreted by many cells including immune cells and stromal cells. To

10.3389/fonc.2022.1030590

illustrate the expression of MMP1 in different cells, we used single-cell sequencing data in five ATC and six PTC patients (Figure 2F). After analyzing a total of 32168 cells, we found 29 clusters of different cells (Supplementary Figure 1B) and defined all cells as four basic types (Figure 2G). MMP1 was expressed mostly in tumor cells but rarely in other cells as shown in Figure 2H. Comparing its expression in PTC and ATC tumor cells, we found that MMP1 showed major expression in ATC tumor cells but lower expression in PTC tumor cells (Figure 2I). This reminds us that MMP1 expression in tumor cells might be related to the heterogeneity of different TC cells, and MMP1 was upregulated in ATC cells.

Clinical significance of MMP1 in PTC and PDTC/ATC

Data of MMP1 mRNA expression levels in PTC tissues and normal thyroid tissues were obtained from TCGA to demonstrate the role of MMP1 expression in PTC tumorigenesis. As shown in Figures 3A, B, MMP1 expression in PTC tumor tissues was significantly higher than that in normal thyroid tissues, whether they were paired samples or not. ROC curves were plotted to investigate the diagnostic value of MMP1, and the area under the curve (AUC) was 0.840 (Figure 3C) and 0.705 (Figure 3D)

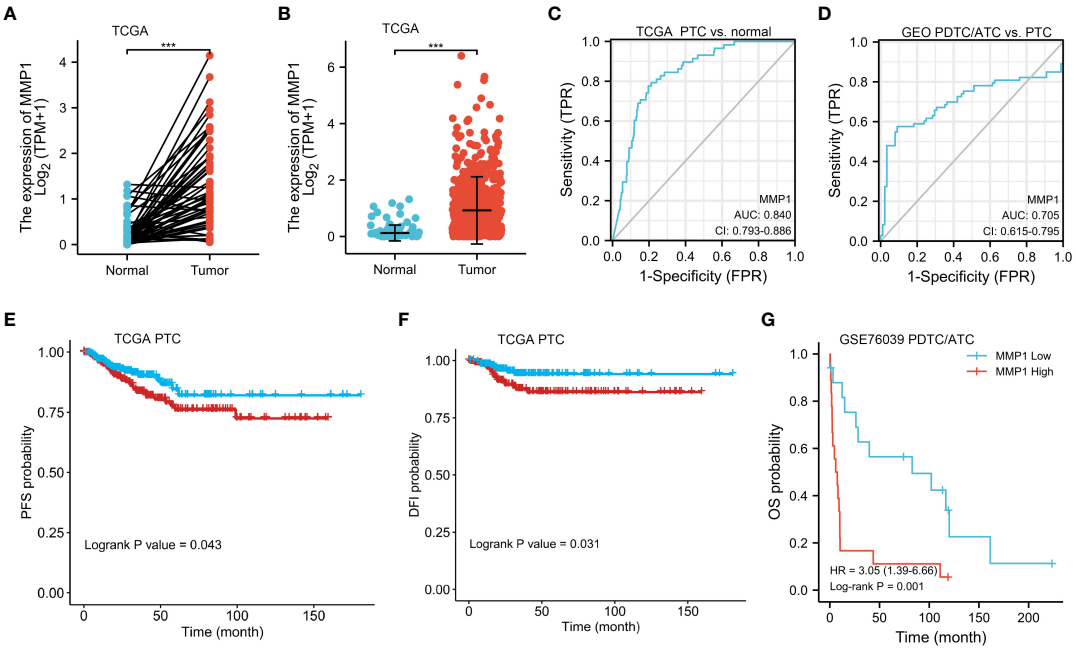

H

Characteristics	Total (N)	Odds Ratio in MMP1 expression (95% CI)	P value
T stage (T3&T4 vs. T1&T2)	508	1.366 (0.955-1.955)	0.088
N stage (N1 vs. N0)	460	1.720 (1.191-2.492)	0.004
M stage (M1 vs. M0)	295	3.000 (0.711-20.368)	0.175
Gender (Male vs. Female)	510	1.581 (1.068-2.352)	0.023
Extrathyroidal extension (Yes vs. No)	492	1.583 (1.079-2.333)	0.019
Primary neoplasm focus type (Multifocal vs. Unifocal)	500	0.923 (0.649-1.311)	0.654
Pathologic stage (Stage III&IV vs. Stage I&II)	508	1.180 (0.816-1.708)	0.38
Histological type (Follicular vs. Classical)	465	0.244 (0.145-0.399)	<0.001

FIGURE 3
Clinical significance of MMP1 in PTC and PDTC/ATC. **(A)** The mRNA levels of MMP1 were up-regulated in PTC samples, which were downloaded from the TCGA database containing 58 paired PTC and normal tissue samples. **(B)** MMP1 was up-regulated in PTC samples, which were downloaded from the TCGA database containing 510 PTC samples and 58 normal tissue samples. **(C)** MMP1 effectively discriminated between PTC and normal tissues from the TCGA database. **(D)** MMP1 effectively discriminated between PDTC/ATC and PTC tissues from the GEO database. PTC patients with higher MMP1 levels harbor worse **(E)** PFS and **(F)** DFI. PDTC/ATC patients with higher MMP1 levels harbor worse **(G)** OS. **(H)** Forest plot of MMP1 in univariate logistic regression analyses of clinicopathological characteristics of the PTC patients from TCGA database. GEO, the Gene Expression Omnibus; PDTC, poorly differentiated thyroid cancer; ATC, anaplastic thyroid cancer; PTC, papillary thyroid cancer; TCGA, The Cancer Genome Atlas; AUC, the area under the curve; CI, confidence interval; vs., versus; HR, hazard ratio; PFS, progression-free survival; DFI, disease-free interval; OS, overall survival. ***P <0.001.

respectively, which can be used to distinguish the normal tissues from PTC, as well as PTC from PDTC/ATC, respectively. The clinicopathological characteristics of PTC patients from TCGA were summarized in Table 1. MMP1 expression was significantly associated with gender (P=0.029), T stage (P =0.004), N stage (P =0.005), extrathyroidal extension (P =0.025), histological type (P <0.001) and the thyroid gland disorder history (P <0.001).

Kaplan-Meier survival analysis with a log-rank test was applied to determine the association between patients' survival and MMP1 expression. As shown in Figures 3E, F, the MMP1 low-expressing group had significantly longer PFS and DFI in PTC patients from TCGA (P =0.043 and 0.031, respectively). Additionally, we collected OS data of 17 PDTC patients and 20 ATC patients from the GSE76039 dataset, and the prognosis of the MMP1 low-expressing group was still significantly better (Figure 3G, P =0.001), while the level of MMP1 in ATC is significantly higher than that in PDTC (8.24 versus 3.90, P <0.01). Next, univariate logistic regression analyses were performed to explore the relationship between MMP1 and some clinicopathological characteristics of the PTC patients from TCGA (Figure 3H), and MMP1 was positively related with N stage (OR =1.720, 95% CI = 1.191-2.492, P =0.004), and

TABLE 1 Clinical characteristics of PTC patients from TCGA database according to MMP1 low or high expression.

Characteristics	Low expression of MMP1 (n=255)	High expression of MMP1 (n=255)	P-value
Age, median (IQR)	48 (36, 58)	46 (34, 58)	0.597
Gender, n (%)			**0.029**
Female	197 (38.6%)	174 (34.1%)	
Male	58 (11.4%)	81 (15.9%)	
T stage, n (%)			**0.004**
T1	83 (16.3%)	60 (11.8%)	
T2	82 (16.1%)	85 (16.7%)	
T3	86 (16.9%)	89 (17.5%)	
T4	4 (0.8%)	19 (3.7%)	
N stage, n (%)			**0.005**
N0	127 (27.6%)	102 (22.2%)	
N1	97 (21.1%)	134 (29.1%)	
M stage, n (%)			0.190
M0	132 (44.7%)	154 (52.2%)	
M1	2 (0.7%)	7 (2.4%)	
Pathologic stage, n (%)			0.291
Stage I	144 (28.3%)	142 (28%)	
Stage II	29 (5.7%)	23 (4.5%)	
Stage III	58 (11.4%)	55 (10.8%)	
Stage IV	22 (4.3%)	35 (6.9%)	
Extrathyroidal extension, n (%)			**0.025**
No	179 (36.4%)	159 (32.3%)	
Yes	64 (13%)	90 (18.3%)	
Primary neoplasm focus type, n (%)			0.720
Multifocal	119 (23.8%)	114 (22.8%)	
Unifocal	131 (26.2%)	136 (27.2%)	
Histological type, n (%)			**< 0.001**
Classical	160 (31.4%)	204 (40%)	
Follicular	77 (15.1%)	24 (4.7%)	
Other	4 (0.8%)	5 (1%)	
Tall Cell	14 (2.7%)	22 (4.3%)	
Thyroid gland disorder history, n (%)			**< 0.001**
Lymphocytic Thyroiditis	47 (10.4%)	27 (6%)	
Nodular Hyperplasia	47 (10.4%)	21 (4.6%)	
Normal	119 (26.3%)	166 (36.7%)	
Other, specify	12 (2.7%)	13 (2.9%)	

Bold values show P < 0.05.
PTC, papillary thyroid cancer; TCGA, The Cancer Genome Atlas; IQR, interquartile range.

extrathyroidal extension (OR =1.583, 95% CI =1.079-2.033, P =0.023), respectively. The HRs for DFI of PTC patients from TCGA were explored to investigate the survival significance of MMP1. Only features with P <0.1 in univariate Cox regression were included in multivariate regression analysis. M1 stage, Pathologic stage III/IV, and high MMP1 were all confirmed to be independent risk factors for DFI in PTC patients (Table 2).

Function enrichment analysis

Multiple functional enrichment analyses were performed using the GEO cohort and TCGA cohort to explore the different pathogenesis involved in this study. GO enrichment analysis (Figure 4A) indicated that the DEGs between PDTC/ATC and PTC samples from the GEO cohort were mostly enriched in extracellular matrix-related pathways (Details in Supplementary Table 2), which were reported to be significantly associated with the MMPs family (44), including MMP1. GSEA of the DEGs was also performed (Figure 4B), and the top 5 pathways between PDTC/ATC and PTC were cell cycle checkpoints (normalized enrichment score (NES) =2.73, P <0.01), GTPases active formins (NES= 2.73, P <0.01), resolution of sister chromatid cohesion (NES= 2.92, P <0.01), separation of sister chromatids (NES= 2.92, P <0.01), and mitotic metaphase and anaphase (NES= 2.84, P <0.01) (45) (Details in Supplementary Table 3). To more precisely explore the pathway associated with MMP1, we analyzed genes associated with MMP1 expression from the TCGA PTC samples, and the top 10 positively associated genes and top 10 negatively associated genes with MMP1 were shown in the co-expression heatmap (Figure 4C). Genes with |spearman correlation coefficient| >2 and p <0.05 were included in the subsequent GO and KEGG analysis, and the representative pathways are shown in Figure 4D (Details in Supplementary Table 4).

TABLE 2 Risk factors for DFI of PTC patients from the TCGA database.

Characteristics	Total (n)	Univariate analysis		Multivariate analysis	
		Hazard ratio (95% CI)	P-value	Hazard ratio (95% CI)	P-value
Gender	510				
Female	371	Reference			
Male	139	1.694 (0.975-2.945)	0.062	1.228 (0.553-2.730)	0.614
T stage	508				
T1&T2	310	Reference			
T3&T4	198	2.450 (1.417-4.236)	**0.001**	1.113 (0.306-4.042)	0.871
N stage	460				
N0	229	Reference			
N1	231	1.658 (0.936-2.934)	0.083	0.848 (0.380-1.892)	0.687
M stage	295				
M0	286	Reference			
M1	9	7.305 (2.780-19.197)	**<0.001**	4.366 (1.057-18.034)	**0.022**
Pathologic stage	508				
Stage I&II	338	Reference			
Stage III&IV	170	2.597 (1.520-4.437)	**<0.001**	2.850 (1.097-7.405)	**0.032**
Histological type	465				
Classical	364	Reference			
Follicular	101	0.574 (0.243-1.355)	0.206		
Primary neoplasm focus type	500				
Unifocal	267	Reference			
Multifocal	233	1.025 (0.595-1.764)	0.929		
Extrathyroidal extension	492				
No	338	Reference			
Yes	154	1.874 (1.092-3.216)	**0.023**	1.019 (0.323-3.216)	0.974
MMP1	510				
Low	255	Reference			
High	255	1.650 (1.249-2.870)	**0.036**	1.196 (1.046-2.224)	**0.042**

Patients with unknown key data were excluded from this analysis, and the number of patients included in this analysis was shown in the table. Bold values show P < 0.05.
DFI, disease-free interval; PTC, papillary thyroid cancer; TCGA, The Cancer Genome Atlas; CI, confidence interval; IQR, interquartile range.

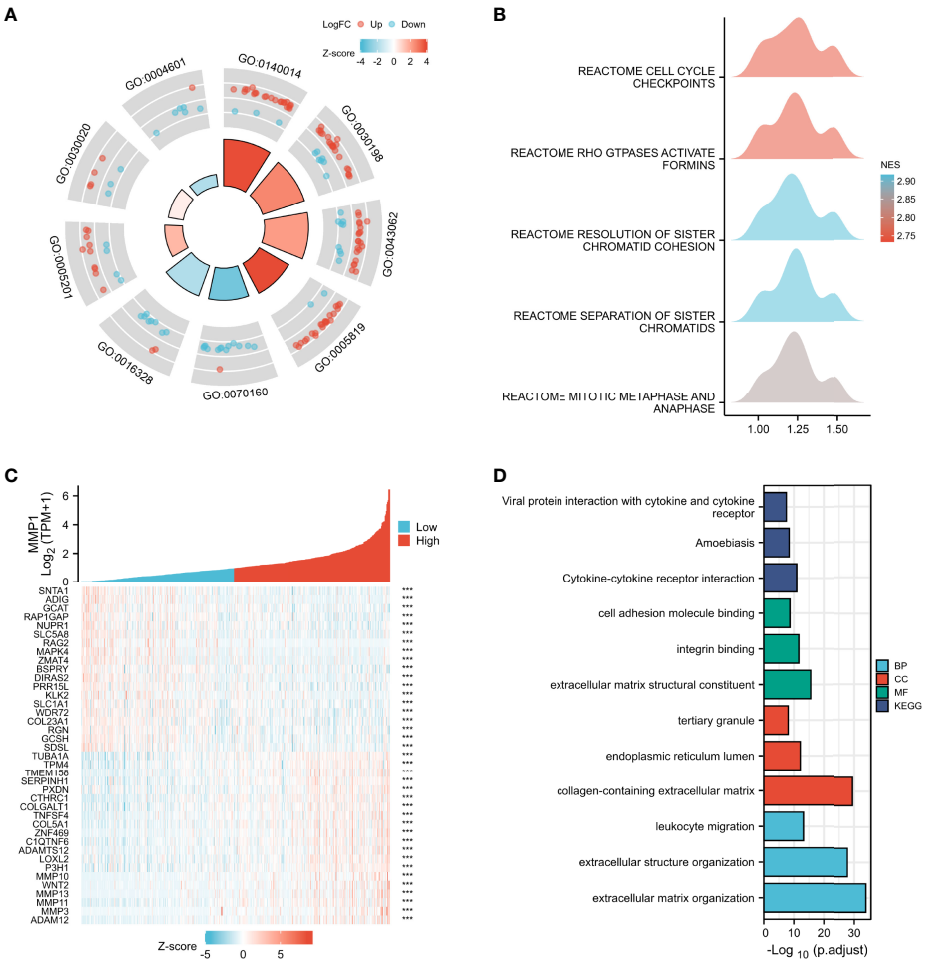

FIGURE 4
Enrichment analysis. GO **(A)** and GSEA **(B)** enrichment analyses of DEGs between PDTC/ATC and PTC samples. **(C)** Co-expression heatmap of top 10 positively associated genes and top 10 negatively associated genes with MMP1 form TGGA PTC samples. **(D)** GO and KEGG enrichment analyses of main associated genes of MMP1. GEO, the Gene Expression Omnibus; PDTC, poorly differentiated thyroid cancer; ATC, anaplastic thyroid cancer; PTC, papillary thyroid cancer; TCGA, The Cancer Genome Atlas; GO, Gene Ontology; GSEA, Gene set enrichment analysis; KEGG, Kyoto Encyclopedia of Genes and Genomes; NES, normalized enrichment score; BP, Biological Process; CC, Cellular Component; MF, Molecular Function; ***P <0.001.

Immune infiltration analysis

Immune infiltration in the tumor is a complex microenvironment that interacts with tumorigenesis, progression, and metastasis (46). We further explored the infiltration of immune cells in PTC, and the correlation between the GSVA scores and immune cell infiltrates over the PTC samples from TCGA is shown in Figure 5A. In addition, we explored the relationship between infiltrating immune cells and MMP1 expression levels. ImmuneScore is an indicator to characterize the immune landscape, and it was reported to be significantly correlated with PTC progression and dedifferentiation (47). MMP1 was identified to be positively correlated with ImmuneScore in this study (Figure 5B), which suggested that MMP1 might be involved in immune infiltration. ssGSEA (Figure 5C), TIMER (Figure 5D), and xCELL (Figure 5E) were then used to explore specific immune cells associated with MMP1, and dendritic cells (DCs), macrophages, and neutrophils were immune cells confirmed to be significantly associated with MMP1 in PTC *via* the 3 algorithms in this study. As shown in Figures 5A, C, D, Treg cells were also found to be significantly positively correlated with MMP1. Taken together, the above results demonstrated that MMP1 might influence the infiltration of immune cells in the PTC microenvironment.

10.3389/fonc.2022.1030590

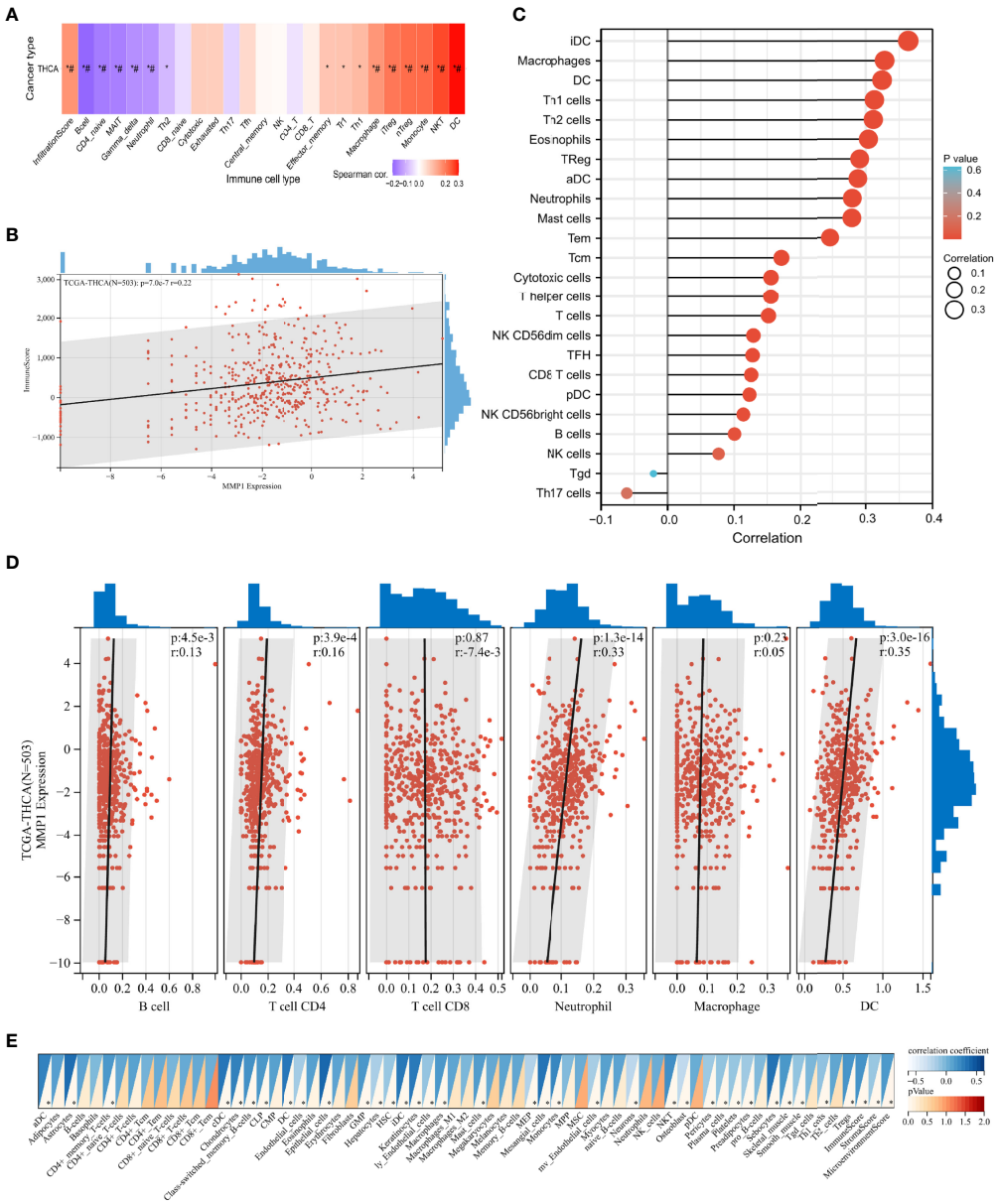

FIGURE 5
Correlation analysis of the expression of MMP1 with complex immune infiltration level in PTC samples from TCGA. **(A)** The correlation-heatmap between the GSVA scores and immune cell infiltrates over the PTC samples; **(B)** Correlation scatters plot of MMP1 levels and ImmuneScore of PTC samples. Different analyses of the correlation between MMP1 levels and immune infiltration: ssGSEA **(C)**, TIMER **(D)**, and xCELL **(E)**. PTC, papillary thyroid cancer; THCA, thyroid cancer. TCGA, The Cancer Genome Atlas; *P <0.05. # false discovery rate <0.05.

Analysis of the mutation, stemness, and differentiation

The mutation indicators BRS of PTC samples from TCGA was displayed in Figures 6A, B, and the higher MMP1, the lower BRS, which means the high MMP1 group had a higher propensity for *BRAF*-like mutations. In other words, MMP1 may be involved in the $BRAF^{V600E}$- or *RAS*-mutant profiles in PTC. The stemness (self-renewal, differentiation, and fate determination) of a tumor could participate in multi-step tumorigenesis, recurrence, and metastasis (48). We quantified the stemness level of PTC samples from TCGA and explored its relationship with MMP1. The expression level of MMP1 was significantly positively correlated with the PTC stemness *via* both EREG.EXPss method (Figure 6D) and DNAss method (Figure 6E). As for the differentiation indicator, we used TDS to assess the differentiation level of PTC samples from TCGA.

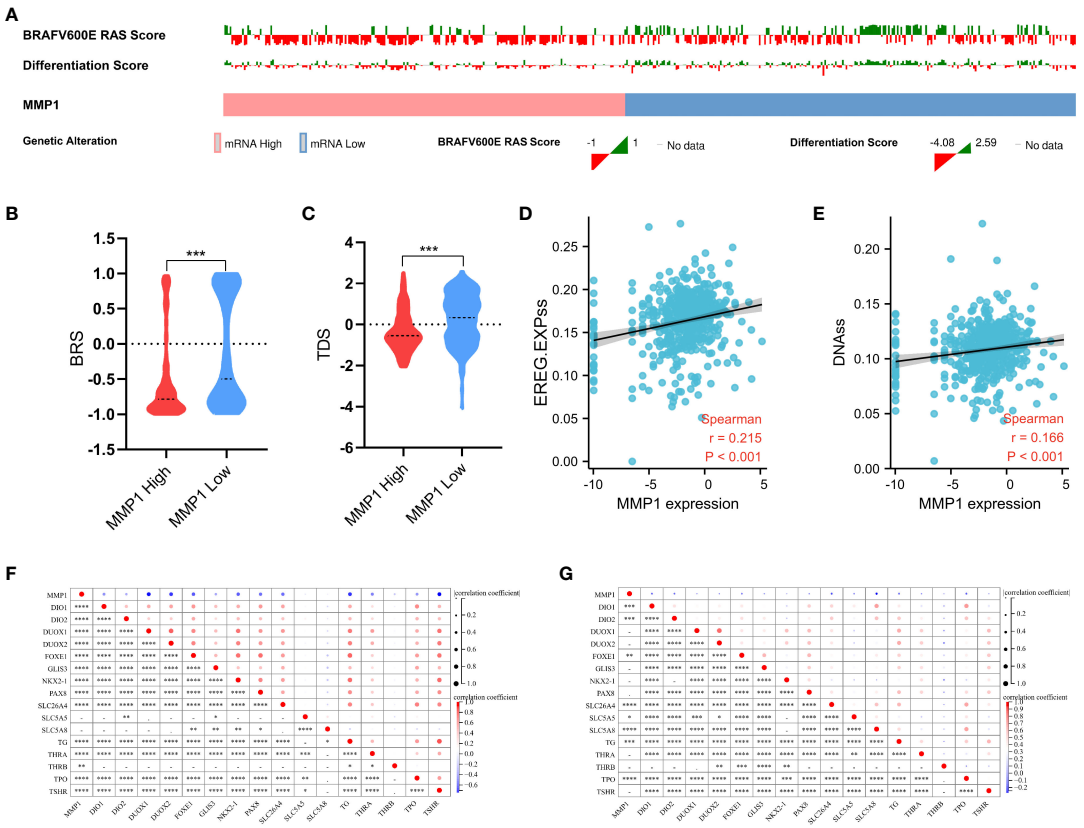

FIGURE 6
Analysis of the mutation, stemness, and differentiation. **(A)** Landscape of *BRAF*^{V600E}*-RAS* score and thyroid differentiation score based on MMP1 levels in PTC samples from TCGA. MMP1 high group had higher BRS **(B)** and lower TDS **(C)**. MMP1 was significantly positively correlated with the PTC stemness *via* both EREG.EXPss method **(D)** and DNAss method **(E)**. MMP1 was significantly negatively correlated with most TDS genes in both the GEO cohort of PDTC/ATC and PTC **(F)** and TCGA cohort of PTC **(G)**. GEO, the Gene Expression Omnibus; PDTC, poorly differentiated thyroid cancer; ATC, anaplastic thyroid cancer; PTC, papillary thyroid cancer; TCGA, The Cancer Genome Atlas; BRS, *BRAF*^{V600E}*-RAS* score; TDS, thyroid differentiation score. *P <0.05, **P <0.01, ***p <0.001, and ****p <0.0001.

The results revealed that the higher MMP1 expression group had the lower TDS (Figure 6C). Specific associations between MMP1 and the 16 TDS-related genes were also explored, and the expression levels of MMP1 and most TDS genes were negatively correlated in both the GEO cohort of PDTC/ATC and PTC (Figure 6F) and TCGA cohort of PTC (Figure 6G). Given the above, MMP1 was considered to be involved in the dedifferentiation of PTC and could serve as a potential indicator for the differentiation level.

Exploration of MMP1 in cell lines

Since our findings above were based on RNA sequencing data obtained from public databases, we further explored and verified the expression and function of MMP1 in cell lines. PTC cell lines TPC-1 and K1, PDTC cell line KTC-1, and ATC cell line CAL-62 were used to perform western blotting assays. As shown in Figure 7A, high levels of MMP1 protein were detected in KTC-1 and CAL-62, especially in the ATC cell line CAL-62. Exogenous introduction of MMP1 siRNA was used to knock down the expressing levels of MMP1 in TPC-1, K1, KTC-1, and CAL-62 (Figure 7B). To further explore the potential of MMP1 as a therapeutic target in PDTC/ATC or PTC, a specific inhibitor triolein for MMP1 was used in this study. CCK8 assays were performed to determine cell viability in cell lines treated with different concentrations of triolein, and the half-maximal inhibitory concentrations (IC_{50}) of triolein in different cell lines were also detected. The IC_{50} of triolein was 72.52 μM for TPC-1, 79.97 μM for K1, 51.80 μM for KTC-1, and 64.52 μM for CAL-62 (Figure 7C), respectively. Colony formation assays were also performed to analyze the cell viability of tumor cells under triolein treatment and MMP1 knockdown, where we observed that triolein and MMP1 knockdown both inhibited cell proliferation of all the TC cell lines (Figures 7D, E). Collectively, these results provide us with robust evidence

10.3389/fonc.2022.1030590

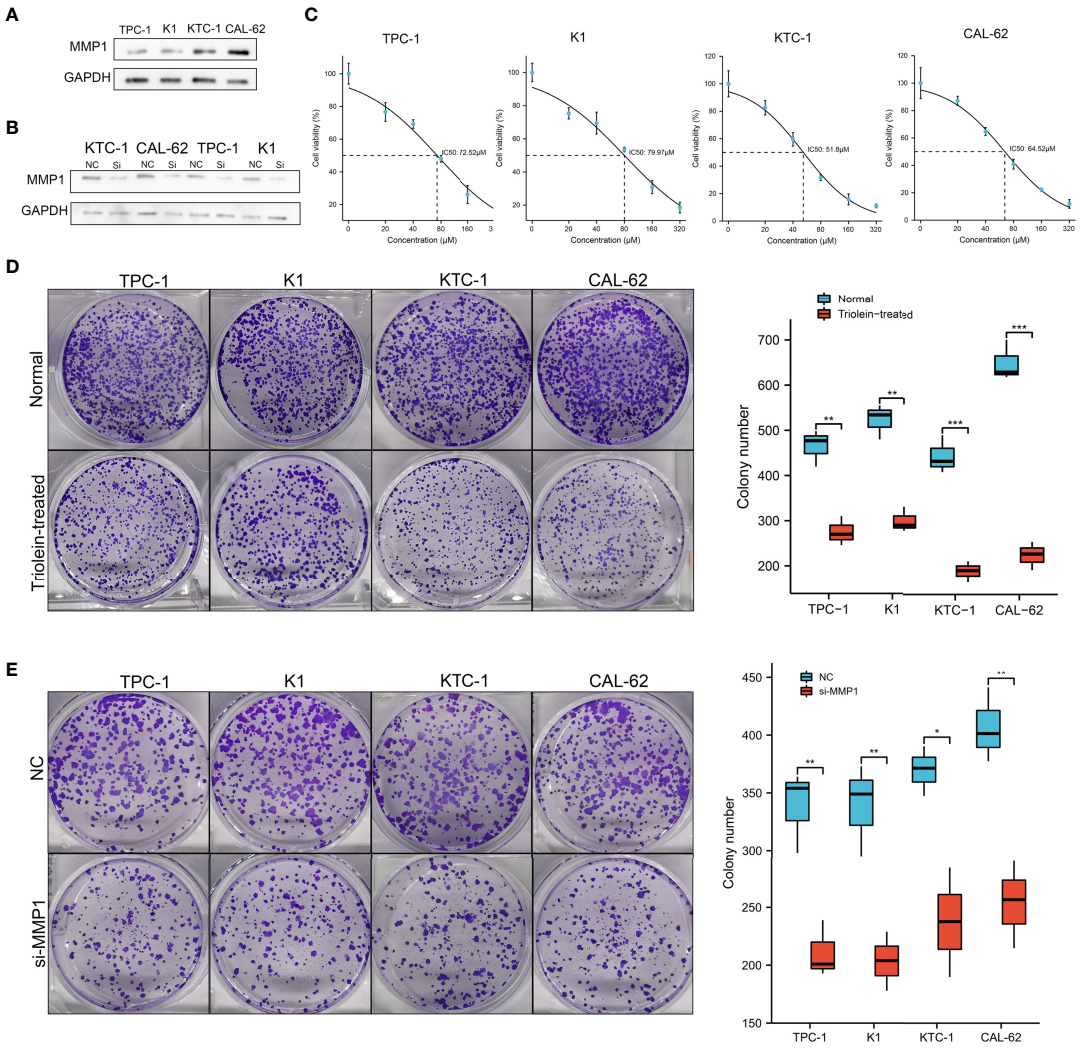

FIGURE 7
Exploration of MMP1 *via in vitro* experiments. **(A)** MMP1 was up-regulated in PDTC cell line KTC-1 and ATC cell line CAL-62. **(B)** MMP1 was significantly down-regulated in cells after transfection with MMP1 siRNA detected by western blot. **(C)** IC_{50} of triolein in different cell lines. Triolein **(D)** and MMP1 knockdown **(E)** inhibited colony formation in different cell lines. PDTC, poorly differentiated thyroid cancer; ATC, anaplastic thyroid cancer; PTC, papillary thyroid cancer; IC_{50}, half-maximal inhibitory concentration. *P <0.05, **P <0.01, and ***p <0.001.

indicating that MMP1 may serve as a novel biomarker and therapeutic target for PDTC/ATC and probably as a potential therapeutic target for PTC with the risk of progression or dedifferentiation.

Discussion

The progression and dedifferentiation of PTC greatly affect the prognosis of patients (7), thus early detection and timely intervention for aggressive PTC are very necessary. In this study, we used transcriptome data of two cohorts, the GEO cohort of PDTC/ATC and PTC, and the TCGA cohort of PTC to perform differential analysis and functional annotation to evaluate the role of MMP1 as a potential regulator of tumor progression and dedifferentiation in PTC. Comprehensive and detailed assessments for the association between MMP1 and PTC clinicopathologic characteristics, survival, function, immune microenvironment, mutation, stemness, and dedifferentiation were conducted. In addition, our *in vitro* functional experiments preliminarily explored the effect of MMP1 inhibitor triolein on PTC and provided a potential therapeutic target for the treatment of aggressive TC, especially PDTC and ATC.

MMP1 along with other members of MMPs is a proteolytic enzyme that degrades multiple components of the extracellular matrix (49). The catalysis activity of MMP1 on fibrils depends on

the random motion and substrate properties as well as on active site catalysis and conformational dynamics applicable to both fibrils and monomers (50). In this study, we only focused on the total forms of MMP1. In addition to playing a role in extracellular matrix transformation, MMPs participate in tumor progression by regulating signaling pathways that control cell growth, inflammation, or angiogenesis, and may even act in a non-proteolytic role (51, 52). A previous study (53) tried to determine the usefulness of MMP1 for differential diagnosis of follicular thyroid lesions, particularly between minimally invasive carcinoma and adenoma. However, no discriminative effect of MMP1 was found. The tumor-promoting roles of MMP1 have been reported in multiple cancers, including ovarian cancer (54), pancreatic cancer (55), and liver cancer (56), et al. In previous reports, MMP1 was identified to be associated with higher clinical stages of PTC (16–18), and MMP1 was overexpressed in ATC upon microarray analysis (19).

In our study, further analysis indicated that MMP1 might play an important role in the progression and dedifferentiation in PTC and PDTC/ATC, and as far as we knew, it was the first study to explore the role of MMP1 in these two groups. Both bulk and single-cell sequencing data indicated that MMP1 was high-expressed in PDTC/ATC. The ROC analysis proved the excellent diagnostic efficacy of MMP1 in predicting PTC and PDTC/ATC, and survival analysis also demonstrated its role in predicting the PFS/DFI in PTC patients and OS in ATC/PDTC patients. Due to the limited sample size and data sources, we pooled ATC and PDTC from GSE76039 together to analyze the correlation between their prognosis and MMP1 level instead of analyzing them separately. However, it is worth noting that since MMP1 levels are significantly higher in ATC than in PDTC, there is a possibility that the difference in survival is more related to tumor type than MMP1 expression, which should be explored by further studies. Both Logistic and Cox regressions confirmed the correlations between MMP1 and worse outcomes for PTC patients. Enrichment analysis of our study demonstrated that extracellular matrix-related pathways were significantly elevated in PDTC/ATC compared with PTC, while MMP1 played important roles in these pathways.

The associations between immune infiltration and PTC progression and dedifferentiation have long been demonstrated (47, 57). DCs, macrophages, neutrophils, and Treg cells are important components in the immune microenvironment of PTC and have been proven to promote tumor progression and poor prognosis (58–60). In our study, MMP1 was found to be positively associated with the above immune cells in PTC, which demonstrated that MMP1 might promote PTC progression by interacting with the tumor-associated immune infiltration. Our study also found other immune cells, such as NK cells and monocytes, significantly associated with MMP1 in PTC *via* different immune cell function analyses in different ways, detailed mechanisms should be confirmed by further studies.

Gene mutations, including $BRAF^{V600E}$, *RAS*, and *TERT* promoter mutations, exert extensive effects on oncogenic signaling pathways in PTC and PDTC/ATC (61). The expression level of MMP1 was also significantly correlated with the mutation indicator BRS in our study. As for stemness and differentiation, they are usually analyzed together. There is homeostasis between stemness and differentiation, and the stronger the stemness, the higher potential of the differentiation, or in the other words, the more poorly differentiated (62). In this study, a positive correlation was found between MMP1 and stemness, and a negative correlation was found between MMP1 and the differentiation level of PTC, which strongly suggested that MMP1 might promote the dedifferentiation. Since MMP1 was also correlated with many differentiation and dedifferentiation markers of thyroid, such as TDS-related genes, MAPK4, SERPINE1, LOXL2, COL5A1, et al., the potential interactions between them require further investigations to verify the above findings. MMPs are thought to be ideal therapeutic targets for cancer as more and more novel, highly selective, and potent MMP inhibitors are now available (63). SD-7300, an oral inhibitor of MMP-2, -9, and -13, has shown promising preclinical therapeutic effects for breast cancer (64). Triolein and its analogs have been shown to have some antitumor effects in other tumors (65, 66). In this study, we preliminarily verified the inhibitory effect of the MMP1 inhibitor triolein on TC cells, especially on PDTC and ATC.

To the best of our knowledge, the current study is the first to comprehensively disclose that MMP1 may be a potential regulator of tumor progression and dedifferentiation in PTC. Furthermore, we also explored the role of MMP1 in PTC clinicopathologic characteristics, survival, function, immune microenvironment, mutation, stemness, and dedifferentiation. The *in vitro* functional experiments in this study further proved that MMP1 could be used as a potential therapeutic target for aggressive TC. However, there are still some limitations to the present study. First of all, a large number of findings and results were based on data from public databases, and some detailed data were not available, which might cause some bias. Second, we have not thoroughly explored the underlying mechanisms by which MMP1 exerts its tumor-promoting effects in PTC. Finally, we only validated the function of MMP1 and its inhibitor triolein *via in vitro* experiments, while *in vivo* experiments may give us more insight into this topic.

Conclusion

In conclusion, the integrated bioinformatic analysis revealed that MMP1 might act as a regulator for tumor progression and

dedifferentiation in PTC, which was confirmed *via* the *in vitro* experiments. Our findings suggested that MMP1 could be a potential biomarker and therapeutic target for PTC, especially for the aggressive PTC that might dedifferentiate into PDTC or ATC.

Data availability statement

The original contributions presented in the study are included in the article/Supplementary Material. Further inquiries can be directed to the corresponding authors.

Author contributions

TH conceived, designed, and supervised the study with FD, JZ, and MX. JZ and MX collected and analyzed data, and wrote the draft of the manuscript. JT, LZ, and FD analyzed the data and reviewed the manuscript. TH and FD oversaw the bioinformatics data analyses and modified and improved the manuscript. All authors contributed to the article and approved the submitted version.

Funding

This study is supported by the National Natural Science Foundation of China (Grant 82002834) and Key Program of Natural Science Foundation of Hubei Province (Grant No. 2021BCA142).

Acknowledgments

Thanks to all the members who assisted in this study. Thanks for the guidance of the Sangerbox group on bioinformatics.

Conflict of interest

The authors declare that the research was conducted in the absence of any commercial or financial relationships that could be construed as a potential conflict of interest.

Publisher's note

Supplementary material

The Supplementary Material for this article can be found online at: https://www.frontiersin.org/articles/10.3389/fonc.2022.1030590/full#supplementary-material

SUPPLEMENTARY FIGURE 1
(A) Cell markers. **(B)** 29 clusters of different cells form ATC and PTC.

References

1. Aschebrook-Kilfoy B, Ward MH, Sabra MM, Devesa SS. Thyroid cancer incidence patterns in the united states by histologic type, 1992-2006. *Thyroid.* (2011) 21(2):125–34. doi: 10.1089/thy.2010.0021

2. Haugen. 2015 American thyroid association management guidelines for adult patients with thyroid nodules and differentiated thyroid cancer: The American thyroid association guidelines task force on thyroid nodules and differentiated thyroid cancer. *Thyroid* (2016) 26(1):1–133. doi: 10.1089/thy.2015.0020

3. Schlumberger MJ. Papillary and follicular thyroid carcinoma. *N Engl J Med* (1998) 338(5):297–306. doi: 10.1056/NEJM199801293380506

4. Kitahara CM, Sosa JA. The changing incidence of thyroid cancer. *Nat Rev Endocrinol* (2016) 12(11):646–53. doi: 10.1038/nrendo.2016.110

5. Cabanillas ME, McFadden DG, Durante C. Thyroid cancer. *Lancet.* (2016) 388(10061):2783–95. doi: 10.1016/S0140-6736(16)30172-6

6. Sherman SI. Thyroid carcinoma. *Lancet.* (2003) 361(9356):501–11. doi: 10.1016/s0140-6736(03)12488-9

7. Ma B. Clinicopathological and survival outcomes of well-differentiated thyroid carcinoma undergoing dedifferentiation: A retrospective study from FUSCC. *Int J Endocrinol* (2018) 2018:2383715. doi: 10.1155/2018/2383715

8. Molinaro E, Romei C, Biagini A, Sabini E, Agate L, Mazzeo S, et al. Anaplastic thyroid carcinoma: from clinicopathology to genetics and advanced therapies. *Nat Rev Endocrinol* (2017) 13(11):644–60. doi: 10.1038/nrendo.2017.76

9. Simoes-Pereira J, Capitao R, Limbert E, Leite V. Anaplastic thyroid cancer: Clinical picture of the last two decades at a single oncology referral centre and novel therapeutic options. *Cancers (Basel)* (2019) 11(8):1188. doi: 10.3390/cancers11081188

10. Yuan X, Larsson C, Xu D. Mechanisms underlying the activation of TERT transcription and telomerase activity in human cancer: old actors and new players. *Oncogene.* (2019) 38(34):6172–83. doi: 10.1038/s41388-019-0872-9

11. Pozdeyev N, Gay LM, Sokol ES, Hartmaier R, Deaver KE, Davis S, et al. Genetic analysis of 779 advanced differentiated and anaplastic thyroid cancers. *Clin Cancer Res* (2018) 24(13):3059–68. doi: 10.1158/1078-0432.CCR-18-0373

12. Melo M, da Rocha AG, Vinagre J, Batista R, Peixoto J, Tavares C, et al. TERT promoter mutations are a major indicator of poor outcome in differentiated thyroid carcinomas. *J Clin Endocrinol Metab* (2014) 99(5):E754–65. doi: 10.1210/jc.2013-3734

13. Xing M, Liu R, Liu X, Murugan AK, Zhu G, Zeiger MA, et al. BRAF V600E and TERT promoter mutations cooperatively identify the most aggressive papillary thyroid cancer with highest recurrence. *J Clin Oncol* (2014) 32(25):2718–26. doi: 10.1200/JCO.2014.55.5094

14. Porter A, Wong DJ. Perspectives on the treatment of advanced thyroid cancer: Approved therapies, resistance mechanisms, and future directions. *Front Oncol* (2020) 10:592202. doi: 10.3389/fonc.2020.592202

15. Bassiouni W, Ali MAM, Schulz R. Multifunctional intracellular matrix metalloproteinases: implications in disease. *FEBS J* (2021) 288(24):7162–82. doi: 10.1111/febs.15701

16. Bumber. Role of matrix metalloproteinases and their inhibitors in the development of cervical metastases in papillary thyroid cancer. *Clin Otolaryngol* (2020) 45(1):55–62. doi: 10.1111/coa.13466

17. Buergy D. Urokinase receptor, MMP-1 and MMP-9 are markers to differentiate prognosis, adenoma and carcinoma in thyroid malignancies. *Int J Cancer* (2009) 125(4):894–901. doi: 10.1002/ijc.24462

18. Mizrachi A, Koren R, Hadar T, Yaniv E, Morgenstern S, Shvero J. Expression of MMP-1 in invasive well-differentiated thyroid carcinoma. *Eur Arch Otorhinolaryngol* (2011) 268(1):131–5. doi: 10.1007/s00405-010-1343-7

19. Weinberger P. Cell cycle m-phase genes are highly upregulated in anaplastic thyroid carcinoma. *Thyroid* (2017) 27(2):236–52. doi: 10.1089/thy.2016.0285

20. Leek JT, Johnson WE, Parker HS, Jaffe AE, Storey JD. The sva package for removing batch effects and other unwanted variation in high-throughput experiments. *Bioinformatics.* (2012) 28(6):882–3. doi: 10.1093/bioinformatics/bts034

21. Gao J, Aksoy BA, Dogrusoz U, Dresdner G, Gross B, Sumer SO, et al. Integrative analysis of complex cancer genomics and clinical profiles using the cBioPortal. *Sci Signal* (2013) 6(269):l1. doi: 10.1126/scisignal.2004088

22. Ritchie ME, Phipson B, Wu D, Hu Y, Law CW, Shi W, et al. Limma powers differential expression analyses for RNA-sequencing and microarray studies. *Nucleic Acids Res* (2015) 43(7):e47. doi: 10.1093/nar/gkv007

23. Yang Y, Sun H, Zhang Y, Zhang T, Gong J, Wei Y, et al. Dimensionality reduction by UMAP reinforces sample heterogeneity analysis in bulk transcriptomic data. *Cell Rep* (2021) 36(4):109442. doi: 10.1016/j.celrep.2021.109442

24. Gu Z, Eils R, Schlesner M. Complex heatmaps reveal patterns and correlations in multidimensional genomic data. *Bioinformatics.* (2016) 32 (18):2847–9. doi: 10.1093/bioinformatics/btw313

25. Ito K, Murphy D. Application of ggplot2 to pharmacometric graphics. *CPT Pharmacometrics Syst Pharmacol* (2013) 2:e79. doi: 10.1038/psp.2013.56

26. Hao Y, Hao S, Andersen-Nissen E, Mauck WM, Zheng S, Butler A, et al. Integrated analysis of multimodal single-cell data. *Cell* (2021) 184(13):3573–3587.e29. doi: 10.1016/j.cell.2021.04.048

27. Milosevic D, Medeiros AS, Stojkovic Piperac M, Cvijanovic D, Soininen J, Milosavljevic A, et al. The application of uniform manifold approximation and projection (UMAP) for unconstrained ordination and classification of biological indicators in aquatic ecology. *Sci Total Environ* (2022) 815:152365. doi: 10.1016/j.scitotenv.2021.152365

28. Love MI, Huber W, Anders S. Moderated estimation of fold change and dispersion for RNA-seq data with DESeq2. *Genome Biol* (2014) 15(12):550. doi: 10.1186/s13059-014-0550-8

29. Salome PA, Merchant SS. Co-Expression networks in chlamydomonas reveal significant rhythmicity in batch cultures and empower gene function discovery. *Plant Cell* (2021) 33(4):1058–82. doi: 10.1093/plcell/koab042

30. Robin X, Turck N, Hainard A, Tiberti N, Lisacek F, Sanchez JC, et al. pROC: an open-source package for r and s+ to analyze and compare ROC curves. *BMC Bioinf* (2011) 12:77. doi: 10.1186/1471-2105-12-77

31. Liu CJ, Hu FF, Xia MX, Han L, Zhang Q, Guo AY. GSCALite: a web server for gene set cancer analysis. *Bioinformatics.* (2018) 34(21):3771–2. doi: 10.1093/bioinformatics/bty411

32. Wen S, Qu N, Ma B, Wang X, Luo Y, Xu W, et al. Cancer-associated fibroblasts positively correlate with dedifferentiation and aggressiveness of thyroid cancer. *OncoTargets Ther* (2021) 22:14:1205–1217. doi: 10.2147/OTT.S294725

33. Fabris F, Palmer D, de Magalhaes JP, Freitas AA. Comparing enrichment analysis and machine learning for identifying gene properties that discriminate between gene classes. *Brief Bioinform* (2020) 21(3):803–14. doi: 10.1093/bib/bbz028

34. Yu G, Wang LG, Han Y, He QY. clusterProfiler: an r package for comparing biological themes among gene clusters. *OMICS.* (2012) 16(5):284–7. doi: 10.1089/omi.2011.0118

35. Hanzelmann S, Castelo R, Guinney J. GSVA: gene set variation analysis for microarray and RNA-seq data. *BMC Bioinf* (2013) 14:7. doi: 10.1186/1471-2105-14-7

36. Yoshihara K, Shahmoradgoli M, Martinez E, Vegesna R, Kim H, Torres-Garcia W, et al. Inferring tumour purity and stromal and immune cell admixture from expression data. *Nat Commun* (2013) 4:2612. doi: 10.1038/ncomms3612

37. Lei J, Zhang D, Yao C, Ding S, Lu Z. Development of a predictive immune-related gene signature associated with hepatocellular carcinoma patient prognosis. *Cancer Control* (2020) 27(1):1073274820977114. doi: 10.1177/1073274820977114

38. Li T, Fan J, Wang B, Traugh N, Chen Q, Liu JS, et al. TIMER: A web server for comprehensive analysis of tumor-infiltrating immune cells. *Cancer Res* (2017) 77(21):e108–10. doi: 10.1158/0008-5472.CAN-17-0307

39. Aran D, Hu Z, Butte AJ. xCell: digitally portraying the tissue cellular heterogeneity landscape. *Genome Biol* (2017) 18(1):220. doi: 10.1186/s13059-017-1349-1

40. Malta TM, Sokolov A, Gentles AJ, Burzykowski T, Poisson L, Weinstein JN, et al. Machine learning identifies stemness features associated with oncogenic dedifferentiation. *Cell* (2018) 173(2):338–354.e15. doi: 10.1016/j.cell.2018.03.034

41. Cancer Genome Atlas Research N. Integrated genomic characterization of papillary thyroid carcinoma. *Cell* (2014) 159(3):676–90. doi: 10.1016/j.cell.2014.09.050

42. Leiros GJ, Kusinsky AG, Balana ME, Hagelin K. Triolein reduces MMP-1 upregulation in dermal fibroblasts generated by ROS production in UVB-irradiated keratinocytes. *J Dermatol Sci* (2017) 85(2):124–30. doi: 10.1016/j.jdermsci.2016.11.010

43. Song Y, Westerhuis JA, Aben N, Michaut M, Wessels LFA, Smilde AK. Principal component analysis of binary genomics data. *Brief Bioinform* (2019) 20 (1):317–29. doi: 10.1093/bib/bbx119

44. Najafi M, Farhood B, Mortezaee K. Extracellular matrix (ECM) stiffness and degradation as cancer drivers. *J Cell Biochem* (2019) 120(3):2782–90. doi: 10.1002/jcb.27681

45. Jassal B, Matthews L, Viteri G, Gong C, Lorente P, Fabregat A, et al. The reactome pathway knowledgebase. *Nucleic Acids Res* (2020) 48(D1):D498–503. doi: 10.1093/nar/gkz1031

46. Domingues P, Gonzalez-Tablas M, Otero A, Pascual D, Miranda D, Ruiz L, et al. Tumor infiltrating immune cells in gliomas and meningiomas. *Brain Behav Immun* (2016) 53:1–15. doi: 10.1016/j.bbi.2015.07.019

47. Na KJ, Choi H. Immune landscape of papillary thyroid cancer and immunotherapeutic implications. *Endocr Relat Canc* (2018) 25(5):523–31. doi: 10.1530/ERC-17-0532

48. Plaks V, Kong N, Werb Z. The cancer stem cell niche: how essential is the niche in regulating stemness of tumor cells? *Cell Stem Cell* (2015) 16(3):225–38. doi: 10.1016/j.stem.2015.02.015

49. Coussens LM, Fingleton B, Matrisian LM. Matrix metalloproteinase inhibitors and cancer: trials and tribulations. *Science.* (2002) 295(5564):2387–92. doi: 10.1126/science.1067100

50. Kumar L, Nash A, Harms C, Planas-Iglesias J, Wright D, Klein-Seetharaman J, et al. Allosteric communications between domains modulate the activity of matrix metalloprotease-1. *Biophys J* (2020) 119(2):360–74. doi: 10.1016/j.bpj.2020.06.010

51. Kessenbrock K, Plaks V, Werb Z. Matrix metalloproteinases: regulators of the tumor microenvironment. *Cell.* (2010) 141(1):52–67. doi: 10.1016/j.cell.2010.03.015

52. Gobin E, Bagwell K, Wagner J, Mysona D, Sandirasegarane S, Smith N, et al. A pan-cancer perspective of matrix metalloproteases (MMP) gene expression profile and their diagnostic/prognostic potential. *BMC Canc* (2019) 19(1):581. doi: 10.1186/s12885-019-5768-0

53. Cho Mar K, Eimoto T, Tateyama H, Arai Y, Fujiyoshi Y, Hamaguchi M. Expression of matrix metalloproteinases in benign and malignant follicular thyroid lesions. *Histopathology.* (2006) 48(3):286–94. doi: 10.1111/j.1365-2559.2005.02325.x

54. Yokoi A, Yoshioka Y, Yamamoto Y, Ishikawa M, Ikeda SI, Kato T, et al. Malignant extracellular vesicles carrying MMP1 mRNA facilitate peritoneal dissemination in ovarian cancer. *Nat Commun* (2017) 8:14470. doi: 10.1038/ncomms14470

55. Chen Y, Peng S, Cen H, Lin Y, Huang C, Chen Y, et al. MicroRNA hsa-miR-623 directly suppresses MMP1 and attenuates IL-8-induced metastasis in pancreatic cancer. *Int J Oncol* (2019) 55(1):142–56. doi: 10.3892/ijo.2019.4803

56. Liu H, Lan T, Li H, Xu L, Chen X, Liao H, et al. Circular RNA circDLC1 inhibits MMP1-mediated liver cancer progression *via* interaction with HuR. *Theranostics.* (2021) 11(3):1396–411. doi: 10.7150/thno.53227

57. Liotti F, Visciano C, Melillo RM. Inflammation in thyroid oncogenesis. *Am J Cancer Res* (2012) 2(3):286–97.

58. Bergdorf K, Ferguson DC, Mehrad M, Ely K, Stricker T, Weiss VL. Papillary thyroid carcinoma behavior: clues in the tumor microenvironment. *Endocr Relat Canc* (2019) 26(6):601–14. doi: 10.1530/ERC-19-0074

59. Ryder M, Ghossein RA, Ricarte-Filho JC, Knauf JA, Fagin JA. Increased density of tumor-associated macrophages is associated with decreased survival in advanced thyroid cancer. *Endocr Relat Canc* (2008) 15(4):1069–74. doi: 10.1677/ERC-08-0036

60. French JD, Kotnis GR, Said S, Raeburn CD, McIntyre RCJr., Klopper JP, et al. Programmed death-1+ T cells and regulatory T cells are enriched in tumor-involved lymph nodes and associated with aggressive features in papillary thyroid cancer. *J Clin Endocrinol Metab* (2012) 97(6):E934–43. doi: 10.1210/jc.2011-3428

61. Prete A, Borges de Souza P, Censi S, Muzza M, Nucci N, Sponziello M. Update on fundamental mechanisms of thyroid cancer. *Front Endocrinol (Lausanne)* (2020) 11:102. doi: 10.3389/fendo.2020.00102

62. Prasad S, Ramachandran S, Gupta N, Kaushik I, Srivastava SK. Cancer cells stemness: A doorstep to targeted therapy. *Biochim Biophys Acta Mol Basis Dis* (2020) 1866(4):165424. doi: 10.1016/j.bbadis.2019.02.019

63. Winer A, Adams S, Mignatti P. Matrix metalloproteinase inhibitors in cancer therapy: Turning past failures into future successes. *Mol Cancer Ther* (2018) 17(6):1147–55. doi: 10.1158/1535-7163.MCT-17-0646

64. Winer A, Janosky M, Harrison B, Zhong J, Moussai D, Siyah P, et al. Inhibition of breast cancer metastasis by presurgical treatment with an oral matrix metalloproteinase inhibitor: A preclinical proof-of-Principle study. *Mol Cancer Ther* (2016) 15(10):2370–7. doi: 10.1158/1535-7163.MCT-16-0194

65. Guardiola-Serrano F, Beteta-Gobel R, Rodriguez-Lorca R, Ibarguren M, Lopez DJ, Teres S, et al. The novel anticancer drug hydroxytriolein inhibits lung cancer cell proliferation *via* a protein kinase calpha- and extracellular signal-regulated kinase 1/2-dependent mechanism. *J Pharmacol Exp Ther* (2015) 354 (2):213–24. doi: 10.1124/jpet.114.222281

66. Perez RL, Mitchell JR, Lozzio BB. Relevance of lipids to heterotransplantation of human malignancies. *Oncology*. (1982) 39(3):179–84. doi: 10.1159/000225632

frontiers | Frontiers in Oncology

TYPE Original Research
PUBLISHED 21 December 2022
DOI 10.3389/fonc.2022.1057198

OPEN ACCESS

EDITED BY
João Pessoa,
University of Coimbra, Portugal

REVIEWED BY
Li Zhang,
Nanjing General Hospital of Nanjing Military Command, China
Narendra Thapa,
University of Wisconsin-Madison, United States
Luca Falzone,
G. Pascale National Cancer Institute Foundation (IRCCS), Italy
Xiushan Feng,
Fujian Medical University, China

*CORRESPONDENCE
Ruobing Leng
ruobingleng2005@163.com

SPECIALTY SECTION
This article was submitted to Molecular and Cellular Oncology, a section of the journal Frontiers in Oncology

RECEIVED 29 September 2022
ACCEPTED 06 December 2022
PUBLISHED 21 December 2022

CITATION
Leng R, Meng Y, Sun X and Zhao Y (2022) NUF2 overexpression contributes to epithelial ovarian cancer progression *via* ERBB3-mediated PI3K-AKT and MAPK signaling axes. *Front. Oncol.* 12:1057198. doi: 10.3389/fonc.2022.1057198

NUF2 overexpression contributes to epithelial ovarian cancer progression *via* ERBB3-mediated PI3K-AKT and MAPK signaling axes

Ruobing Leng[1]*, Yunfang Meng[2], Xiaomei Sun[3] and Yingzi Zhao[1]

[1]Department of Gynecology, Shandong Provincial Hospital Affiliated to Shandong First Medical University, Jinan, Shandong, China, [2]Department of Dermatology, Shandong Provincial Hospital Affiliated to Shandong First Medical University, Jinan, Shandong, China, [3]Department of Obstetrics, Shandong Provincial Hospital Affiliated to Shandong First Medical University, Jinan, Shandong, China

Introduction: NDC80 kinetochore complex component (NUF2) is upregulated and plays an important role in various human cancers. However, the function and mechanism of NUF2 in epithelial ovarian cancer (EOC) remain unclear.

Methods: NUF2 expression was detected in EOC tissues and cell lines. The effects of NUF2 downregulation on cell proliferation, migration and invasion in EOC were analyzed by CCK-8 and Transwell assays. Meanwhile, the effect of NUF2 downregulation on tumor growth in vivo was determined by xenograft tumor models. The mechanisms by which NUF2 regulates EOC progression were detected by RNA sequencing and a series of in vitro assays.

Results: We showed that NUF2 was significantly upregulated in EOC tissues and cell lines, and high NUF2 expression was associated with FIGO stage, pathological grade and poor EOC prognosis. NUF2 downregulation decreased cell proliferation, migration, invasion and tumor growth in nude mice. RNA sequencing studies showed that NUF2 knockdown inhibited several genes enriched in the phosphatidylinositol-4,5-bisphosphate 3-kinase (PI3K)-AKT serine/threonine kinase (AKT) and mitogen-activated protein kinase (MAPK) signaling pathways. Erb-B2 receptor tyrosine kinase 3 (ERBB3) was the key factor involved in both of the above pathways. We found that ERBB3 silencing could inhibit EOC progression and repress activation of the PI3K-AKT and MAPK signaling pathways. Furthermore, the exogenous overexpression of ERBB3 partially reversed the inhibitory effects on EOC progression induced by NUF2 downregulation, while LY294002 and PD98059 partially reversed the effects of ERBB3 upregulation.

10.3389/fonc.2022.1057198

Conclusion: These results showed that NUF2 promotes EOC progression through ERBB3-induced activation of the PI3K-AKT and MAPK signaling axes. These findings suggest that NUF2 might be a potential therapeutic target for EOC.

KEYWORDS

NUF2, ERBB3, epithelial ovarian cancer, AKT, MAPK

1 Introduction

Ovarian cancer is the fifth most lethal malignancy in women, and epithelial ovarian cancer (EOC) is the most common histological type (1). Due to the absence of specific symptoms and diagnostic biomarkers, greater than 70% of EOC patients are diagnosed with clinical stage Federation International of Gynecology and Obstetrics (FIGO) III or IV, which has a five-year survival rate of only 20% to 30% (1). Several studies showed that a multidisciplinary approach for the treatment of ovarian cancer has significantly improved the quality of life and prognosis of patients and is now a well-established part of clinical care (2–5). A multidisciplinary team is able to face clinical, molecular, pathological and psychological issues of patients with ovarian cancer, ensuring a high standard of care supporting the process of personalized medicine. Although the multidisciplinary approach has improved the quality of life of patients, it is still urgent to continuously improve the molecular, biological and therapeutic knowledge in the field of ovarian cancer care. Thus, it is crucial to identify novel molecular biomarkers and therapeutic targets for diagnosis and the in-depth understanding of the molecular pathogenesis of EOC.

NDC80 kinetochore complex component (NUF2), also named cell division associated 1 (CDCA1), was first reported as a centromere protein and is a key element of the Ndc80 kinetochore complex (6). Further studies revealed that NUF2 binds to centromere protein E (CENPE) and is required for stable spindle kinetochore-microtubule attachment (7). Evidence has shown that NUF2 is overexpressed in a series of human cancers and is significantly associated with poor prognosis (8–12). For example, NUF2 mRNA is significantly upregulated in breast cancer, and upregulated NUF2 is significantly associated with malignant features and poor prognosis (10). In kidney renal clear cell carcinoma (KIRC), NUF2 mRNA and protein are also significantly upregulated, and NUF2 mRNA is an independent prognostic risk factor for KIRC patients (11). Moreover, NUF2 contributes to the malignant progression of tumor, including colorectal cancer, gastric cancer, pancreatic cancer, breast cancer, and renal clear cell carcinoma (9, 13–16). For instance, NUF2 knockdown inhibited cell proliferation and colony formation and induced apoptosis in breast cancer (9). Likewise, NUF2 knockdown by siRNA significantly inhibited cell proliferation and induced apoptosis in colorectal cancer and gastric cancer cells (15). These results suggest that NUF2 may be a good candidate for molecular targeted therapy as well as diagnosis in some cancers. Interestingly, NUF2 has been reported to be upregulated in ovarian cancer, and NUF2 knockdown by small interfering RNA (siRNA) inhibited cell viability and induced apoptosis (17). However, the role and precise mechanism of NUF2 in ovarian cancer progression remain unclear.

In the present study, we found that NUF2 is highly expressed in human EOC specimens compared with normal ovarian epithelial tissues. The high expression of NUF2 was associated with poor EOC prognosis. NUF2 knockdown inhibited cell proliferation, migration and invasion through the Erb-B2 receptor tyrosine kinase 3 (ERBB3)-mediated phosphatidylinositol-4,5-bisphosphate 3-kinase (PI3K)-AKT serine/threonine kinase (AKT) and mitogen-activated protein kinase (MAPK) signaling axes.

2 Material and methods

2.1 Patients and specimens

In our study, a total of 109 paraffin-embedded tissue samples, including 89 EOC tissues and 20 normal ovarian epithelial tissues, were retrieved from the archives of the Department of Pathology, Shandong Provincial Hospital Affiliated to Shandong First Medical University, China, between May 2010 and August 2015. None of the patients were treated with chemotherapy or radiotherapy before they underwent surgery. The specimens were used with the written informed consent from the patients and the approval of the Ethics Committee of Shandong Provincial Hospital Affiliated to Shandong First Medical University (Approval No. 2021-774). The study was performed in accordance with the ethical standards as laid down in the 1964 Declaration of Helsinki and its later amendments or comparable ethical standards. Follow-up was performed monthly for the first year, then quarterly until 2 years, every 6 months until 3 years, and once 3 year thereafter. Medical examination and telephonic interviews were performed for follow-up and those who survived beyond March 20, 2018 were recorded as censored data. Patients were considered lost to follow-up if no further medical records and no record of death existed. In these cases,

patients were censored at the time of their last medical encounter. Patients were excluded if they were lost to follow-up within six months.

2.2 Immunohistochemical staining

The paraffin-embedded blocks were sectioned at a thickness of 4 μm. After deparaffinization, rehydration, antigen retrieval and blocking of endogenous peroxidases, the sections were washed with PBS and incubated in normal goat serum at 37°C for 30 min. The tissues were subsequently incubated with anti-NUF2 antibody (1:100; ab230313, Abcam, Waltham, MA, USA) overnight at 4 °C. After washing with PBS, tissues were incubated with peroxidase-labeled secondary antibody at 37°C for 1 hour. The sections were visualized after DAB staining and counterstaining with hematoxylin.

The NUF2 staining score was determined as previously described (18). The staining intensity was scored as follows: 0, no staining or only weak staining; 1, moderate staining; and 2, strong staining. The positive proportion of stained tumor cells was scored as follows: 0, ≤ 5% positive cells; 1, 6–50% positive cells; 2, ≥ 51% positive cells. The NUF2 staining score was the sum of the staining intensity score and the positive staining cell rate score: 0–2, low expression; 3–4, high expression.

2.3 Cell culture

The CAOV3, OVCAR3 and SKOV3 cell lines were purchased from the Cell Bank of the Type Culture Collection of the Chinese Academy of Science (Shanghai, China), the A2780 cell line was obtained from Huiying Biotechnology Co., Ltd. (Shanghai, China), and the KGN cell line was obtained from Procell Life Science & Technology Co., Ltd. (Wuhan, China). The CAOV3, A2780 and KGN cell lines were cultured in DMEM (Thermo Fisher Scientific Inc., Waltham, MA, USA) supplemented with 10% (v/v) fetal bovine serum (FBS) (Thermo Fisher Scientific Inc., Waltham, MA, USA), OVCAR3 cells were maintained in RPMI-1640 medium (Thermo Fisher Scientific Inc., Waltham, MA, USA) supplemented with 10% (v/v) FBS, and SKOV3 cells were cultured in McCoy's 5A medium (Thermo Fisher Scientific Inc., Waltham, MA, USA) supplemented with 10% (v/v) FBS, all in a humidified atmosphere of 5% CO_2 at 37°C.

2.4 Plasmid construction and transfection

NUF2 and ERBB3 small hairpin RNAs (shRNAs) were synthesized and cloned into the phU6-shRNA-CMV-puromycin vector by Sesh-Biotech (Shanghai, China). The sequences of NUF2 shRNA (shNUF2) and ERBB3 shRNA (shERBB3) were shown in Supplemental Table S1. To overexpress ERBB3, ERBB3 cDNA was amplified and subcloned into pcDNA3.1 with hygromycin (Sino Biological, Inc., Shanghai, China).

The shNUF2, shERBB3 and ERBB3 overexpression (ERBB3-ov) plasmids were transfected into A2780 and OVCAR3 cells ($3x10^5$ cells per well in 6-well plates) using Lipofectamine 2000 (Thermo Fisher Scientific Inc., Waltham, MA, USA) according to the manufacturer's protocols.

2.5 RNA sequencing

Total RNA of OVCAR3 cells after transfection with shNC and shNUF2 was extracted in accordance with the manual of TRIzol™ reagent (Thermo Fisher Scientific Inc., Waltham, MA, USA). RNA integrity was analyzed *via* agarose gel electrophoresis. Library preparation and transcriptome sequencing on the Illumina NovaSeq 6000 (Illumina, San Diego, CA, USA) were carried out at Personalbio Technology Co., Ltd. (Shanghai, China). Fold change (FC) was used to describe the differentially expressed genes (DEGs). DEGs with FC values greater than 1 or less than -1 and a *P* value less than 0.05 were considered significant. Gene ontology (GO) term and kyoto encyclopedia of genes and genomes (KEGG) pathway enrichment analyses were carried out Personalbio Technology Co., Ltd. (Shanghai, China). The KEGG pathway maps were obtained from the KEGG database (http://www.kegg.jp/).

2.6 Real-time quantitative PCR

The total RNA of A2780 and OVCAR3 cells after transfection with shNC and shNUF2 was extracted with the TRIzol™ reagent (Thermo Fisher Scientific Inc., Waltham, MA, USA) according to the manufacturer's instructions, and M-MLV reverse transcriptase (Promega Corporation, Madison, WI, USA) was used to synthesize cDNA. ERBB3 mRNA expression was analyzed using SYBR Master Mix (Takara, Dalian, China). The thermocycling conditions were as follows: Pre-denaturation at 95˚C for 15 sec, followed by 40 cycles of denaturation at 95˚C for 5 sec, annealing at 60˚C for 30 sec and extension at 60˚C for 30 sec. Relative quantification of ERBB3 mRNA was determined using the $2^{-\Delta\Delta Ct}$ method after normalization to the GAPDH. The PCR primers used in this study were shown in Supplemental Table S2.

2.7 Western blot

Cells were lysed using RIPA lysis buffer (Beyotime, Shanghai, China) supplemented with 1 mM phenylmethanesulfonyl fluoride (PMSF). After centrifugation at 14,000 rpm for 10 min at 4°C, a BCA protein assay kit (Beyotime, Shanghai, China) was used to

determine the protein concentrations. Equal amounts of total proteins from each sample were loaded onto a 12.5% SDS-PAGE gel and transferred to PVDF membranes. The membranes were blocked and then incubated with primary antibodies at 4°C overnight. The primary antibodies used in this study were as follows: anti-NUF2 (1:800; 15731-1-AP, Proteintech Group, Inc, Wuhan, China), anti-ERBB3 (1:500; 10369-1-AP, Proteintech Group, Inc, Wuhan, China), anti-AKT (1:2,000; 10176-2-AP, Proteintech Group, Inc, Wuhan, China), anti-p-AKT (Ser473) (1:3,000; 28731-1-AP, Proteintech Group, Inc, Wuhan, China), anti-ERK1/2 (1:10,000; Abcam, Waltham, MA, USA), anti-p-ERK1/2 (Thr202/Tyr204) (1:1,000; #4695, Cell Signaling Technology, Boston, MA, USA) and anti-GAPDH (1:10,000; 10494-1-AP, Proteintech Group, Inc, Wuhan, China). The membranes were washed and incubated with the appropriate secondary antibodies. The target proteins bands on the membranes were detected using an ECL Western blotting Detection Kit (Beyotime, Shanghai, China). The gray values of the protein bands were analyzed using Quantity One software and normalized to GAPDH.

2.8 Cell viability assay

Cell viability was determined by a CCK-8 kit (Beyotime, Shanghai, China). After treatment, cells were seeded in 96-well plates (1×10^4 cells per well) and maintained for 0, 24, 48, 72 and 96 h. 10 µl of CCK-8 solution were added to each well of the plate. After incubation for 2 h, the absorbance at 450 nm was determined using a microplate reader (Bio-Rad, Hercules, CA, USA).

2.9 Transwell assay

The cell migration ability was determined using Transwell chambers (BD Biosciences, San Jose, CA, USA) with a pore size of 8 µm, and the cell invasion ability was analyzed using Matrigel-coated Transwell chambers (BD Biosciences, San Jose, CA, USA) with a pore size of 8 µm. After treatment, A2780 and OVCAR3 cells were seeded onto the upper chambers at a final concentration of 4×10^4 cells/well and cultured in 100 µl of serum-free medium. Complete medium was added to the lower chamber. After incubation for 48 h, the cells in the upper chamber were removed with a cotton swab. Cells on the lower surface of the membrane were stained with crystal violet, and the number of cells was counted in five random fields under a light microscope.

2.10 Nude mouse model

Four-week-old BALB/c male nude mice were obtained from the Animal Center of the Chinese Academy of Science (Shanghai, China). Stable NUF2-silenced OVCAR3 cells (shNUF2, 4×10^6 cells in 100 µl of sterilized PBS) and stable negative control OVCAR3 cells (shNC, 4×10^6 cells in 100 µl of sterilized PBS) were injected into the right and left dorsal flanks (n = 5), respectively. The tumor volumes were measured every week with a micrometer caliper. Tumor volumes were calculated using the Formula V=length × width^2/2. After injection for 5 weeks, the mice were euthanized and the tumor samples were removed. All of the procedures were approved by the Institution Animal Care Committee of Shandong Provincial Hospital Affiliated to Shandong First Medical University (Approval No. 2021-774).

2.11 Statistical analysis

The SPSS 18.0 statistical analysis software (IBM Corp., Armonk, NY, USA) was used to analyze the experimental data. All data are presented as the mean ± standard deviation (SD). The Student's t test or one-way ANOVA was used to evaluate the significant differences between groups. Associations between the expression levels of NUF2 and ERBB3 were analyzed by the Pearson's correlation. P values < 0.05 were considered statistically significant.

3 Results

3.1 NUF2 is upregulated in EOC and predicts poor prognosis

The Gene Expression database of Normal and Tumor tissue 2 (GENT2) (https://gent2.appex.kr/gent2/) (19) and the Gene Expression Profiling Interactive Analysis (GEPIA) database (http://gepia.cancer-pku.cn/) (20) were used to determine the expression of NUF2 in EOC. We found that NUF2 gene expression was significantly upregulated in EOC (Figure 1A). To further verify the effect of NUF2 expression on the prognosis of EOC, we performed survival analysis using an online database. Data from the Kaplan–Meier Plotter database (http://www.kmplot.com) (21) showed that patients with higher NUF2 mRNA expression had worse overall survival than patients with lower NUF2 expression (Figure 1B). We subsequently analyzed the expression of NUF2 protein in 89 EOC tissues and 20 normal ovarian epithelial tissues. As shown in Figures 1C, D, NUF2 was found to be increased in EOC tissues compared to normal ovarian epithelial tissues. High NUF2 expression was associated with poor EOC prognosis (Figure 1E). In addition, we analyzed the association between the NUF2 expression and clinicopathological features in 89 EOC samples (Table S3). We found that high NUF2 expression was associated with FIGO stage (P = 0.007) and pathological grade (P = 0.015) (Table 1). Univariate analysis indicated that the FIGO stage and upregulated NUF2 expression were associated with overall survival (P = 0.026 and P = 0.043, respectively) (Table 2).

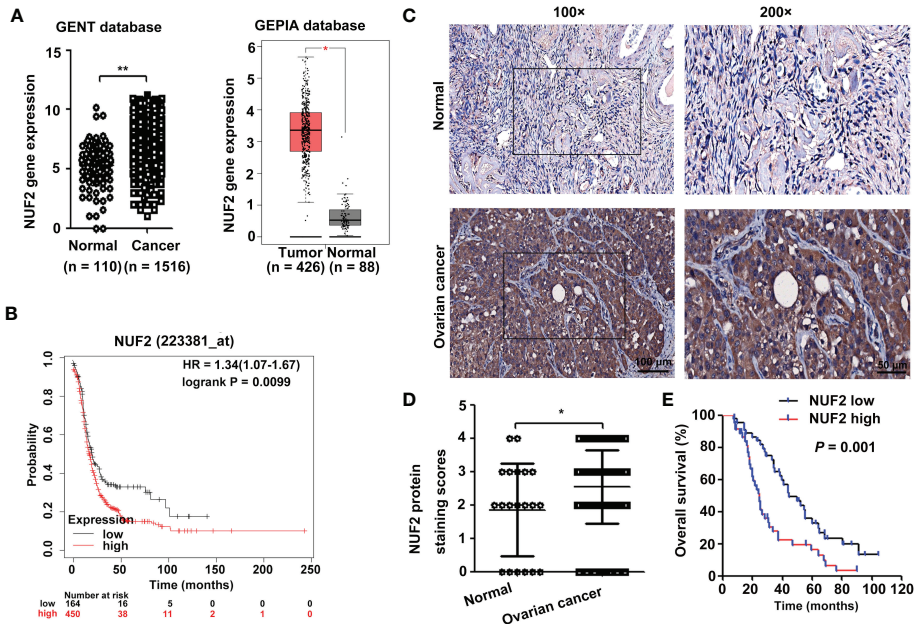

FIGURE 1
NUF2 expression is upregulated in EOC tissues. **(A)** NUF2 gene expression was determined in two databases (GENT2 and GEPIA). *$P < 0.05$, **$P < 0.01$. **(B)** Kaplan-Meier analysis based on Kaplan–Meier Plotter databases showed that patients with low NUF2 levels exhibited significantly better overall survival than patients with high NUF2 levels. **(C)** Representative images of IHC staining of NUF2 expression in EOC tissues and normal ovarian epithelial tissues are shown in the upper panel (original magnification, left × 100, right × 200). **(D)** NUF2 protein expression was significantly higher in 89 EOC tissues than in 20 normal ovarian epithelial tissues. *$P < 0.05$. **(E)** The High NUF2 expression was associated with poor EOC prognosis ($P = 0.001$).

Multivariate analysis showed that the FIGO stage and upregulated NUF2 expression were independent prognostic factors for overall survival ($P = 0.008$ and $P = 0.003$, respectively) (Table 2).

3.2 NUF2 downregulation inhibits EOC cell proliferation, migration and invasion *in vitro*

To determine the role of NUF2 in EOC, we first analyzed the expression of NUF2 in four human EOC cell lines (A2780, OVCAR3, CAOV3 and SKOV3) and one human immortalized EOC cell line (KGN). We found that NUF2 expression in KGN was the lowest among the cell lines, and NUF2 expression was higher in the A2780 and OVCAR3 cell lines than in the CAOV3 and SKOV3 cell lines (Figure 2A). The A2780 and OVCAR3 cell lines were selected for the subsequent experiments. Then, we established stable A2780 and OVCAR3 cells with NUF2 silencing. As shown in Figure 2B, NUF2 shRNA significantly inhibited NUF2 protein levels in A2780 and OVCAR3 cells. To determine the effect of NUF2 on EOC cell proliferation, a CCK-8 assay was performed. Our results showed that NUF2 knockdown significantly repressed the proliferation capacity of A2780 and OVCAR3 cells when compared with those transfected with shNC (Figure 2C). Moreover, we observed that the migratory and invasive capacities of A2780 and OVCAR3 cells transfected with shNUF2 were significantly inhibited compared with those transfected with shNC (Figures 2D, E).

3.3 Global gene expression changes in OVCAR3 cells transfected with shNUF2 and shNC

To investigate the underlying mechanism of NUF2 in regulating EOC progression, RNA-seq was performed to identify the signaling pathways influenced by NUF2. Gene expression heatmaps and volcano plots showed that a total of 548 genes were downregulated (FC, <-1-fold) and 1536 genes were upregulated (FC, >1-fold) (Figures 3A, B). RNA-seq data have been submitted to the GEO repository (series entry GSE213611) (https://www.ncbi.nlm.nih.gov/geo/query/acc.cgi?acc=GSE213611). To identify genes and pathways affected by NUF2, we performed GO and KEGG pathway enrichment. The top 10 GO terms, covering cellular component, molecular function, and biological process, are shown in Figure 3C and Datasheet_1. DEGs were obviously enriched in relevant terms, such as cell migration, cell motility, regulation of cell motility and regulation of cell

TABLE 1 Relationship between NUF2 expression and clinicopathological characteristics in 89 patients with EOC.

Characteristics	All cases	NUF2		*P* value
		Low expression	High expression	
Age (years)				0.169
< 50	47	20	27	
≥ 50	42	24	18	
Tumor diameter (cm)				0.597
< 10	44	23	21	
≥10	45	21	24	
FIGO stage				0.007**
I+II	52	32	20	
III+IV	37	12	25	
Pathological grade				0.015*
G1	39	25	14	
G2+G3	50	19	31	
Lymph node metastasis				0.069
Negative	77	41	36	
Positive	12	3	9	
Histological type				0.603
Serous	51	24	27	
Other types	38	20	18	

*Statistically significant (P < 0.05), **Statistically significant (P < 0.01).

TABLE 2 Cox proportional hazard models for prognostic factors.

	Univariate analysis		Multivariate analysis	
	HR(95% CI)	*P* value	HR(95% CI)	*P* value
Age (≥ 50 *vs.* < 50)	0.869 (0.530-1.425)	0.578		
Tumor diameter (≥10 *vs.* ≥10)	1.152 (0.691-1.922)	0.587		
FIGO stage (III+IV *vs.* I+II)	1.833 (1.074-3.130)	0.026*	1.948 (1.191-3.186)	0.008**
Pathological grade (G2+G3 *vs.* G1)	1.320 (0.773-2.255)	0.310		
Lymph node metastasis (positive *vs.* negative)	1.702 (0.818-3.541)	0.155		
Histological type (Other types *vs.* Serous)	0.972 (0.592-1.597)	0.911		
NUF2 expression (high vs. low)	1.778 (1.019-3.100)	0.043*	2.135 (1.305-3.494)	0.003**

*Statistically significant (P < 0.05), **Statistically significant (P < 0.01).

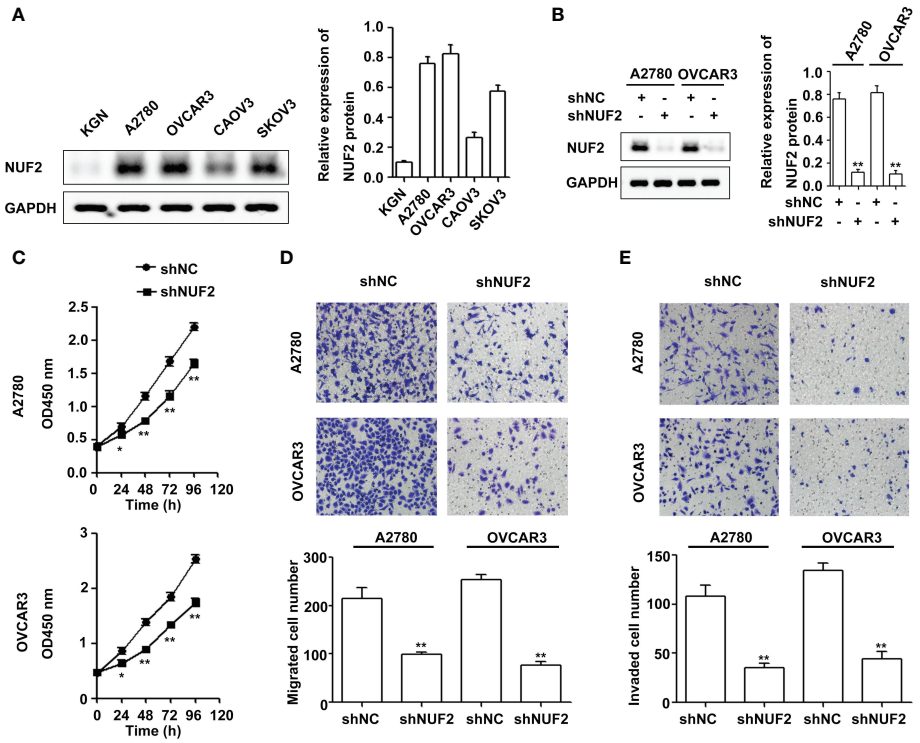

FIGURE 2
NUF2 downregulation inhibits EOC progression *in vitro*. **(A)** The protein levels of NUF2 were determined in four human EOC cell lines (A2780, OVCAR3, CAOV3 and SKOV3) and one human immortalized EOC cell line (KGN). **(B)** NUF2 expression in A2780 and OVCAR3 cells after transfection with shNC and shNUF2 was detected by Western blot. $^{**}P < 0.01$ vs. the shNC group. **(C)** A CCK-8 assay was used to determine the viability of A2780 and OVCAR3 cells after transfection with shNC and shNUF2. $^{*}P < 0.05$, $^{**}P < 0.01$ vs. the shNC group. **(D, E)** Transwell assays were used to determine the migration and invasion of A2780 and OVCAR3 cells after transfection with shNC and shNUF2 (original magnification, × 200). $^{**}P < 0.01$ vs. the shNC group.

migration (Figure 3C). As shown in Figure 3D and Datasheet_2, the KEGG results showed that the differentially expressed gene sets were significantly related to focal adhesion, the PI3K-AKT signaling pathway and the MAPK signaling pathway. These results verified the role of NUF2 in EOC cell migration and invasion, which were consistent with our observations.

3.4 NUF2 downregulation inhibits ERBB3 expression in EOC cells

Studies have shown that the PI3K/AKT and MAPK signaling pathways are essential for EOC progression (22, 23). We retrieved the downregulated gene sets from the PI3K/AKT and MAPK signaling pathways, and the results of the two gene sets were integrated by drawing a Venn diagram. As shown in Figure 4A and Table S4, ERBB3 was the overlapping gene in the PI3K/AKT and MAPK signaling pathways. Interestingly, ERBB3 is involved in the progression and metastasis of ovarian cancer (24). The GENT2 database showed that ERBB3 gene expression was significantly upregulated in EOC and was positively correlated with the expression of NUF2 (Figures 4B, C). Furthermore, the mRNA and protein levels of ERBB3 were significantly reduced in the A2780 and OVCAR3 cells transfected with shNUF2 compared with the shNC cells (Figures 4D, E). Based on literature reports and informatics analysis, we chose ERBB3 for further research.

3.5 ERBB3 downregulation inhibits EOC progression *via* the PI3K-AKT and MAPK signaling pathways

To confirm the effect of ERBB3 on EOC progression, ERBB3 shRNA was transfected into A2780 and OVCAR3 cells. As shown in Figure 5A, ERBB3 protein levels were significantly reduced in the shERBB3-transfected cells compared with shNC-transfected cells. The CCK-8 assay showed that ERBB3 knockdown significantly suppressed the viability of A2780 and OVCAR3 cells (Figure 5B). In addition, the Transwell assay showed that ERBB3 knockdown significantly inhibited the migration and invasion of A2780 and OVCAR3 cells (Figure 5C). Western blot assays indicated that the levels of p-

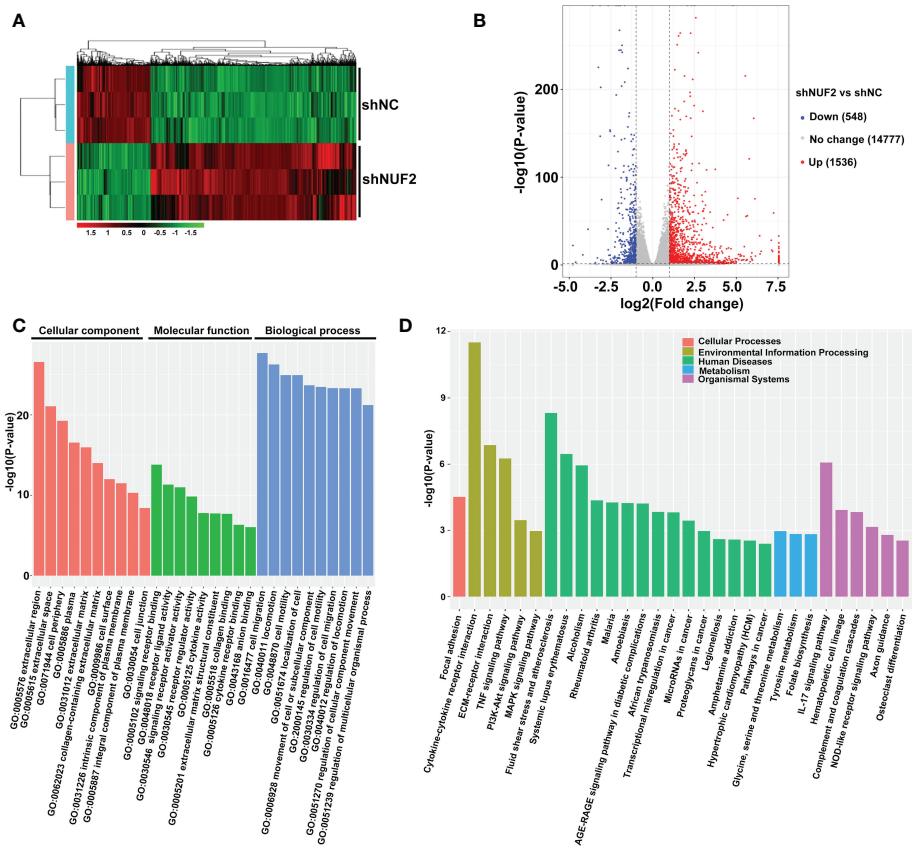

FIGURE 3
Global gene expression changes in OVCAR3 cells transfected with shNUF2 and shNC. **(A, B)** Heatmaps and volcano plots of the DEGs (FC, <-1-fold or >1-fold) in OVCAR3 cells infected with shNUF2 and shNC. **(C, D)** GO analysis and KEGG pathway enrichment of the DEGs in OVCAR3 cells infected with shNUF2 and shNC.

AKT and p-ERK1/2 were significantly downregulated by ERBB3 inhibition in the A2780 and OVCAR3 cells (Figure 5D).

3.6 NUF2 promotes EOC progression by the ERBB3-mediated PI3K-AKT and MAPK signaling axes

Since ERBB3 expression was regulated by NUF2 in EOC cells, we further determined whether NUF2 promoted EOC progression by mediating ERBB3. ERBB3 expression plasmids together with shNUF2 plasmids were transfected into A2780 and OVCAR3 cells. As shown in Figure 6A, ERBB3 expression plasmids significantly reversed the inhibition of ERBB3 expression induced by shNUF2 in A2780 and OVCAR3 cells. CCK-8 and Transwell assays showed that the restoration of ERBB3 expression partially reversed the proliferative, migratory and invasive capacities of A2780 and OVCAR3 cells inhibited by NUF2 repression (Figures 6B, C). Western blot assays showed that the restoration of ERBB3 expression partially reversed the downregulation of p-AKT and p-ERK1/2 expression induced by NUF2 knockdown (Figure 7A). To determine whether ERBB3 regulates EOC progression by PI3K-AKT and MAPK signaling axes, two independent inhibitors of the PI3K (LY294002, inhibits AKT activity) and MAPK (PD98059, inhibits ERK activity) signaling pathways were used in A2780 and OVCAR3 cells transfected with ERBB3 expression plasmids together with shNUF2 plasmids. The levels of p-AKT and p-ERK1/2 induced by ERBB3 expression plasmids were decreased by LY294002 and PD98059 in A2780 and OVCAR3 cells transfected shNUF2, respectively (Figure 6A). In addition, cell proliferation, migration and invasion induced by ERBB3 expression plasmids were partially reversed by LY294002 and PD98059 in A2780 and OVCAR3 cells transfected with shNUF2 (Figures 6B, C).Thus, these results suggest that NUF2 activates the PI3K-AKT and MAPK signaling axes mediated by ERBB3, which regulates the malignant behaviors in EOC cells.

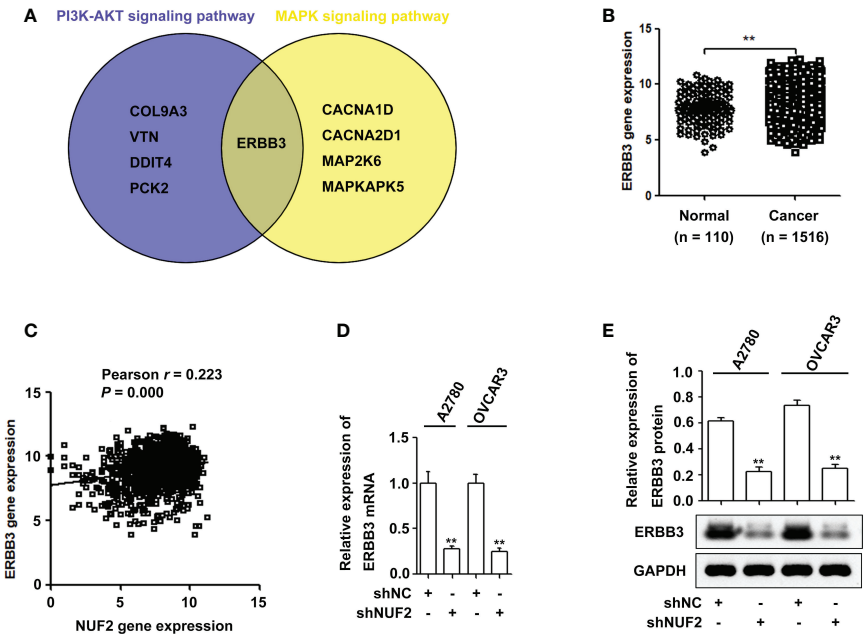

FIGURE 4
NUF2 downregulation inhibits ERBB3 expression in EOC cells. **(A)** A Venn diagram was used to represent common genes between the PI3K-AKT and MAPK signaling axes. **(B)** ERBB3 gene expression was significantly higher in EOC tissues than in the normal ovarian epithelial tissues. $^{**}P < 0.01$. **(C)** The Pearson correlation analysis was used to explore the association between NUF2 and ERBB3 expression ($r = 0.223$, $P = 0.000$). **(D)** and **(E)** The mRNA and protein levels of ERBB3 were significantly reduced in NUF2 silenced cells when compared with A2780 and OVCAR3 cells transfected with shNC. $^{**}P < 0.01$ vs. the shNC group.

3.7 NUF2 downregulation inhibited EOC tumorigenesis and induced the suppression of the ERBB3 expression and the PI3K-AKT and MAPK signaling axes *in vivo*

To further confirm the biological functions of NUF2, we established a xenograft tumor model by inoculating OVCAR3 cells transfected with shNUF2 or shNC and monitored tumor size. The results showed that the tumor size of OVCAR3 cells transfected with shNUF2 was smaller than that of OVCAR3 cells transfected with shNC (Figure 7A). Western blot assays showed that ERBB3, p-AKT and p-ERK1/2 expression levels were significantly inhibited in the shNUF2 group when compared to the shNC group (Figure 7B). Thus, these results suggest that NUF2 activates the PI3K-AKT and MAPK signaling axes mediated by ERBB3, which regulates the malignant behaviors in EOC cells (Figure 7C).

4 Discussion

NUF2 is an essential component of the kinetochore-associated NDC80 complex that plays a regulatory role in chromosome segregation and spindle checkpoint activity in mitosis (6). Several studies have shown that NUF2 is upregulated in multiple cancers and is associated with poor prognosis (8–12). In the present study, we found that NUF2 mRNA and protein expression levels were higher in EOC tissues than in normal tissues (Figures 1A, D). Consistent with our results, one report also showed that NUF2 mRNA expression levels were significantly elevated in ovarian carcinoma tissues when compared with those in normal ovarian tissues (17). Moreover, our results showed that patients with low NUF2 expression levels exhibited a longer overall survival rate than patients with high NUF2 expression levels (Figures 1B, E). Univariate and Multivariate analyses indicated that upregulated NUF2 expression was associated with overall survival and was an independent prognostic factor for overall survival (Table 2). NUF2 was also aberrantly overexpressed in ovarian carcinoma cell lines (Figure 2A). Thus, NUF2 may be a novel prognostic biomarker for EOC.

Previous studies have indicated that NUF2 functions as an oncogene in different types of malignant tumors (9, 13–16). For instance, NUF2 depletion induces apoptosis and causes alterations in cell cycle distribution by inducing cell cycle arrest at the G0/G1 phase (9). Moreover, one report showed that NUF2 inhibition repressed cell viability and induced apoptosis in EOC cells (17). Consistent with these results, we also found that silencing NUF2 significantly inhibited cell

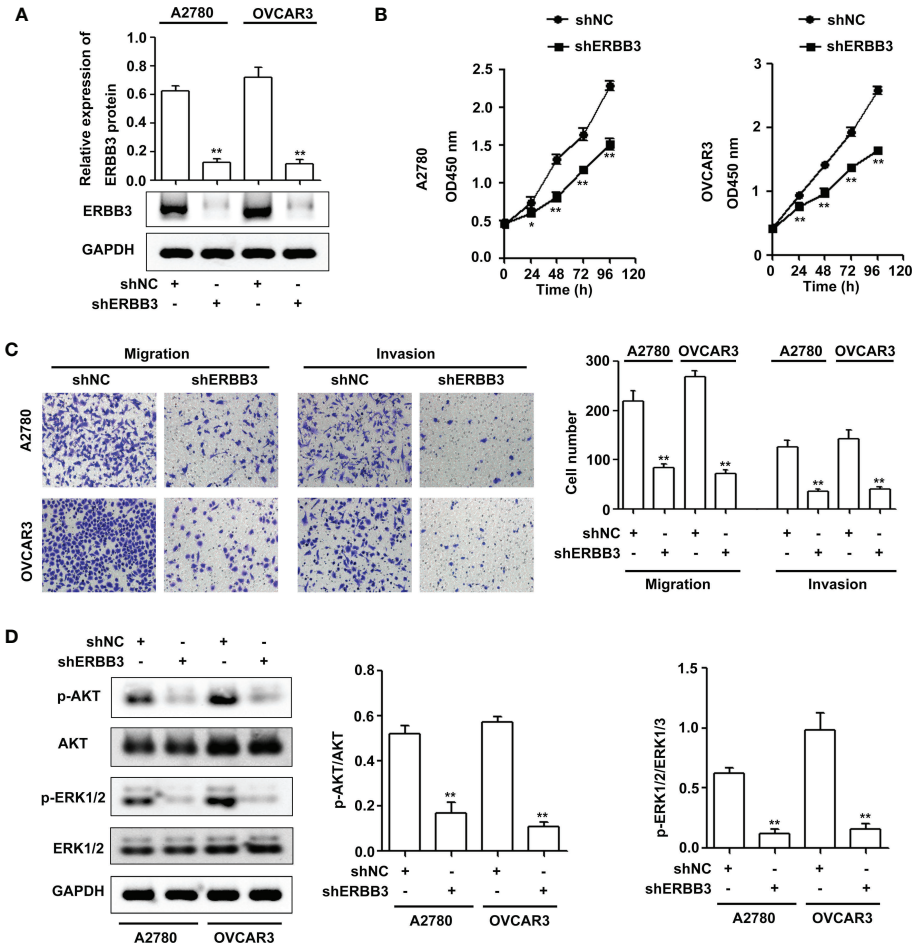

FIGURE 5
ERBB3 downregulation inhibits EOC progression *via* the PI3K-AKT and MAPK signaling axes. **(A)** NUF2 expression in A2780 and OVCAR3 cells after transfection with shNC and shERBB3 was detected by western blot. $^{**}P < 0.01$ vs. the shNC group. **(B)** A CCK-8 assay was used to determine the viability of A2780 and OVCAR3 cells after transfection with shNC and shERBB3. $^{*}P < 0.05$, $^{**}P < 0.01$ vs. the shNC group. **(C)** Transwell assays were used to determine the migration and invasion of A2780 and OVCAR3 cells after transfection with shNC and shERBB3 (original magnification, × 200). $^{**}P < 0.01$ vs. the shNC group. **(D)** Effects of ERBB3 silencing on the phosphorylation of AKT and ERK1/2. GAPDH was used as an internal control. $^{**}P < 0.01$ vs. the shNC group.

proliferation *in vitro* (Figure 2C) and tumor growth *in vivo* (Figure 7A). Thus, NUF2 acts as an oncogene in EOC cells. Peritoneal dissemination is the main metastatic process of EOC, which generally leads to a sharp rise in the clinical stage and poor clinical prognosis (25). Thus, there is an urgent need to discover the mechanism of peritoneal dissemination to increase survival rates in ovarian cancer patients. Interestingly, NUF2 knockdown significantly inhibited pancreatic ductal adenocarcinoma cell migration and invasion (26). In this study, we demonstrate for the first time that NUF2 knockdown significantly reduced the migration and invasion in EOC cells (Figures 2D, E). Thus, NUF2 may be an ideal therapeutic target for EOC.

To elucidate the underlying mechanisms of EOC progression elicited by NUF2, we performed RNA-seq analysis to evaluate the DEGs in OVCAR3 cells after treatment with shNUF2 and shNC. As shown in Figure 3C, DEGs were obviously enriched in relevant terms, such as cell migration, cell motility, regulation of cell motility and regulation of cell migration. The KEGG results showed that the differentially expressed gene sets were significantly related to focal adhesion, the PI3K-AKT signaling pathway and the MAPK signaling pathway (Figure 3D). It has been reported that both the PI3K/AKT and MAPK signaling pathways are involved in EOC progression (27, 28). This may further explain the function of NUF2 in EOC cell migration and invasion. In addition, NUF2 is a key element of the Ndc80 kinetochore complex, which contributes to kinetochore–microtubule attachment and spindle assembly in mitosis (29). Interestingly, MAPK physically interacts with and regulates microtubule dynamics under certain unique circumstances such as meiosis (30). The

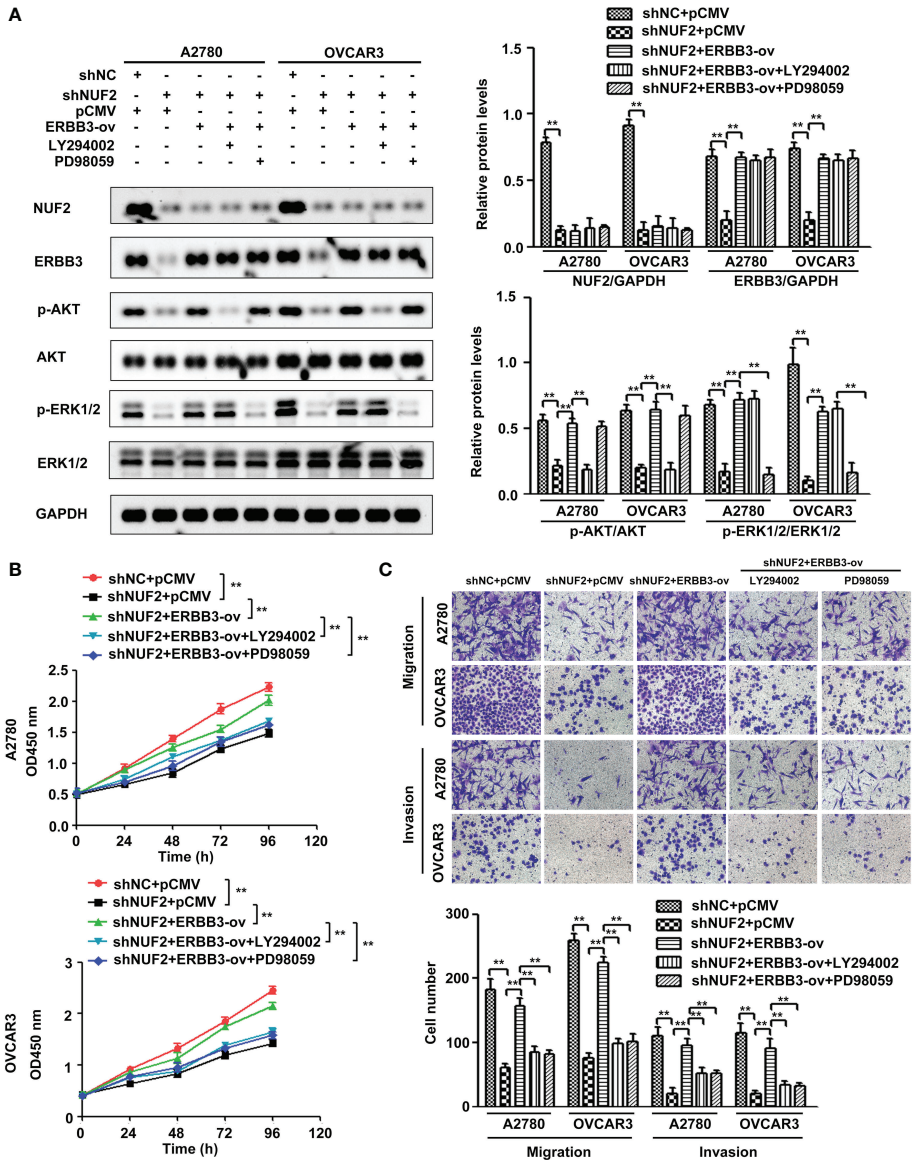

FIGURE 6
NUF2 promotes EOC progression by the ERBB3-mediated PI3K-AKT and MAPK signaling axes. **(A)** A2780 and OVCAR3 cells were treated with shNC+pCMV, shNUF2+pCMV, shNUF2+ERBB3-ov, shNUF2+ERBB3-ov+LY294002 (15 μM), and shNUF2+ERBB3-ov+PD98059 (10 μM). Western blotting was used to determine the protein expression of NUF2, ERBB3, p-AKT, AKT and p-ERK1/2, ERK1/2. **(B, C)** CCK-8 and transwell assays were used to determine the effects of ERBB3 restoration on the proliferative, migratory and invasive capacities of NUF2-downregulated cell lines. $^{**}P < 0.01$. original magnification, × 200.

microtubule-binding domain (MTBD) of the microtubule-associated protein 4 (MAP4) binds directly to the C2 domain of the p110α catalytic subunit and controls the interaction of PI3Kα with activated receptors at endosomal compartments along microtubules (31). Thus, increased NUF2 in EOC and other cancers may directly or indirectly regulate the PI3K-Akt and MAPK signaling because of NUF2 link with microtubules. Among the DEGs, ERBB3 overlapped in the PI3K/AKT and MAPK signaling pathways (Figure 4A), which is involved in the progression and metastasis of ovarian cancer and many other cancers (32–37). It is reported that ERBB3, the only member of the ErbB family incorporating multiple PI3k binding sites, is a major recruiter of PI3K (38). When ERBB3 binds to the regulatory p85 subunit of PI3K, the p110α catalytic subunit of PI3K is recruited, and AKT is then activated by PDK1 and mTORC2 (39). In the ERBB3 C terminus, there is a specific residue (Tyr1325), which contributes to the binding of SHC. And the mutagenesis of Tyr1325 abolished the interaction of

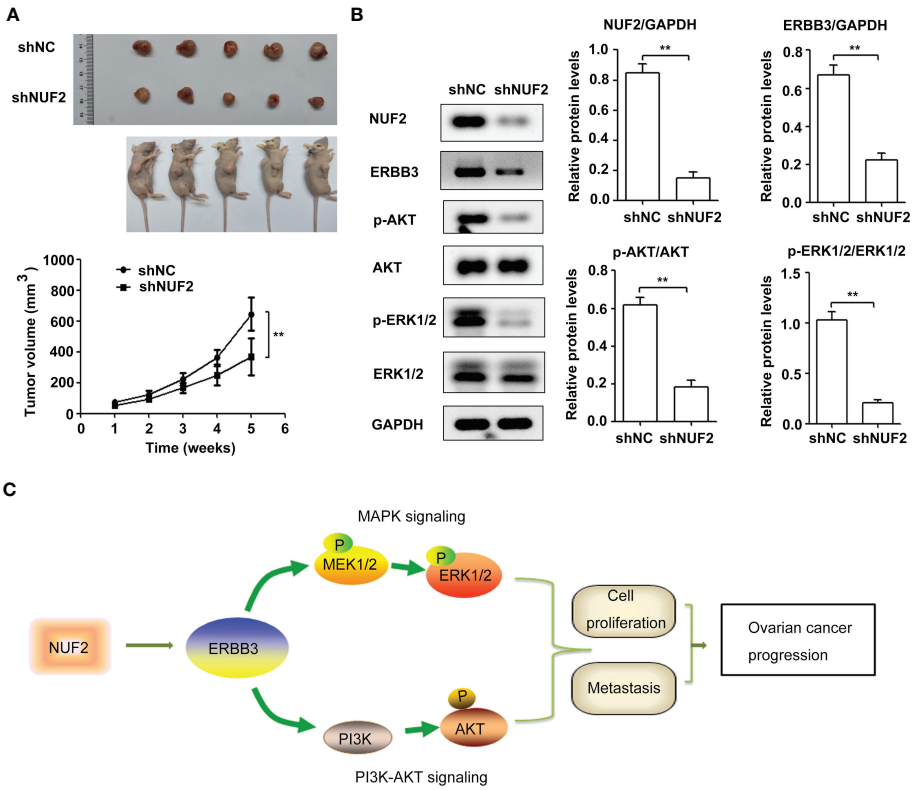

FIGURE 7
NUF2 knockdown repressed EOC tumorigenesis and inhibited ERBB3, p-AKT and p-ERK1/2 expression *in vivo*. **(A)** Representative photographs of mice and OVCAR3-shNUF2 and OVCAR3-shNC tumor samples 5 weeks after injection. Tumor volumes were measured at the indicated time points in all mice. $^{**}P < 0.01$ vs. the shNC group. **(B)** Western blot assay was used to determine the expression levels of ERBB3, p-AKT and p-ERK1/2 proteins in tumors. $^{**}P < 0.01$. **(C)** Schematic diagram summarizing the role and mechanism of NUF2 in promoting EOC progression. NUF2 promotes the PI3K-AKT and MAPK signaling axes mediated by ERBB3, thereby inducing the malignant behaviors in ovarian cancer cells.

ERBB3 with SHC, which could not effectively activate the Ras/MAPK signaling pathway (40). Moreover, we showed ERBB3 gene expression was significantly upregulated in EOC and was positively correlated with NUF2 expression (Figures 4B, C). Similar to the function of NUF2, ERBB3 knockdown significantly inhibited EOC cell proliferation, migration and invasion (Figures 5B, C). In addition, the levels of p-AKT and p-ERK1/2 were significantly downregulated by ERBB3 inhibition in EOC cells (Figure 5D). Thus, it is reasonable to speculate that NUF2 promotes EOC progression by ERBB3-mediated activation of the PI3K/AKT and MAPK signaling pathways. As expected, we found that ERBB3 restoration reversed the inhibition of proliferation, migration and invasion of EOC cells caused by NUF2 knockdown (Figure 6). ERBB3 restoration partially reversed the downregulation of p-AKT and p-ERK1/2 expression induced by NUF2 knockdown (Figure 6A). In addition, two independent inhibitors of the PI3K (LY294002, inhibits AKT activity) and MAPK (PD98059, inhibits ERK activity) signaling pathways were used in A2780 and OVCAR3 cells transfected with ERBB3 expression plasmids together with shNUF2 plasmids. We found that cell proliferation, migration and invasion induced by ERBB3 expression plasmids were partially reversed by LY294002 and PD98059 in A2780 and OVCAR3 cells transfected with shNUF2 (Figure 6B, C). These results indicated that NUF2 promoted EOC progression by inducing activation of the PI3K/AKT and MAPK signaling pathways *via* regulating ERBB3.

In summary, our study is the first to elucidate the role and mechanism of NUF2 in EOC cell migration and invasion *via* ERBB3-mediated activation of the PI3K/AKT and MAPK signaling pathways. However, the mechanism of how NUF2 affects ERBB3 expression deserves further exploration. A recent report showed that NUF2 promotes clear cell renal cell carcinoma progression through epigenetic activation of high-mobility group AT-hook 2 (HMGA2) transcription by suppressing lysine demethylase 2A (KDM2A) expression and affecting its occupancy on the HMGA2 promoter region to regulate histone H3 lysine 36 di-methylation (H3K36me2) modification (41). Thus, does NUF2

affect the promoter activity of ERBB3 gene? These mechanisms will be our future research direction.

Data availability statement

The datasets presented in this study can be found in online repositories. The names of the repository/repositories and accession number(s) can be found in the article/Supplementary Material.

Ethics statement

The studies involving human participants were reviewed and approved by Shandong Provincial Hospital Affiliated to Shandong First Medical University. The patients/participants provided their written informed consent to participate in this study. The animal study was reviewed and approved by Shandong Provincial Hospital Affiliated to Shandong First Medical University.

Author contributions

RL and YM conceived and designed the study. RL, XS, and YZ performed experiments. RL and YM analyzed the data. RL wrote the manuscript. All authors contributed to the article and approved the submitted version.

Funding

This research was funded by Natural Science Foundation of Shandong Province, China (ZR2016HQ22 and ZR2020MH170).

Conflict of interest

The authors declare that the research was conducted in the absence of any commercial or financial relationships that could be construed as a potential conflict of interest.

Publisher's note

Supplementary material

The Supplementary Material for this article can be found online at: https://www.frontiersin.org/articles/10.3389/fonc.2022.1057198/full#supplementary-material

References

1. Webb PM, Jordan SJ. Epidemiology of epithelial ovarian cancer. *Best Pract Research: Clin Obstetrics Gynaecology* (2017) 41:3–14. doi: 10.1016/j.bpobgyn.2016.08.006

2. Falzone L, Scandurra G, Lombardo V, Gattuso G, Lavoro A, Distefano AB, et al. A multidisciplinary approach remains the best strategy to improve and strengthen the management of ovarian cancer (Review). *Int J Oncol* (2021) 59:1–14. doi: 10.3892/IJO.2021.5233

3. Scott R, Hawarden A, Russell B, Edmondson RJ. Decision-making in gynaecological oncology multidisciplinary team meetings: A cross-sectional, observational study of ovarian cancer cases. *Oncol Res Treat* (2020) 43:70–6. doi: 10.1159/000504260

4. Lavoro A, Scalisi A, Candido S, Zanghì GN, Rizzo R, Gattuso G, et al. Identification of the most common BRCA alterations through analysis of germline mutation databases: Is droplet digital PCR an additional strategy for the assessment of such alterations in breast and ovarian cancer families? *Int J Oncol* (2022) 60:1–13. doi: 10.3892/ijo.2022.5349

5. Ugwumadu L, Chakrabarti R, Williams-Brown E, Rendle J, Swift I, John B, et al. The role of the multidisciplinary team in the management of deep infiltrating endometriosis. *Gynecological Surg* (2017) 14:15. doi: 10.1186/s10397-017-1018-0

6. Nabetani A, Koujin T, Tsutsumi C, Haraguchi T, Hiraoka Y. A conserved protein, Nuf2, is implicated in connecting the centromere to the spindle during chromosome segregation: A link between the kinetochore function and the spindle checkpoint. *Chromosoma* (2001) 110:322–34. doi: 10.1007/s004120100153

7. Liu D, Ding X, Du J, Cai X, Huang Y, Ward T, et al. Human NUF2 interacts with centromere-associated protein e and is essential for a stable spindle microtubule-kinetochore attachment. *J Biol Chem* (2007) 282:21415–24. doi: 10.1074/jbc.M609026200

8. Jiang X, Jiang Y, Luo S, Sekar K, Koh CKT, Deivasigamani A, et al. Correlation of NUF2 overexpression with poorer patient survival in multiple cancers. *Cancer Res Treat* (2021) 53:944–61. doi: 10.4143/crt.2020.466

9. Lv S, Xu W, Zhang Y, Zhang J, Dong X. NUF2 as an anticancer therapeutic target and prognostic factor in breast cancer. *Int J Oncol* (2020) 57:1358–67. doi: 10.3892/ijo.2020.5141

10. Xu W, Wang Y, Wang Y, Lv S, Xu X, Dong X. Screening of differentially expressed genes and identification of NUF2 as a prognostic marker in breast cancer. *Int J Mol Med* (2019) 44:390–404. doi: 10.3892/ijmm.2019.4239

11. Shan L, Zhu XL, Zhang Y, Gu GJ, Cheng X. Expression and clinical significance of NUF2 in kidney renal clear cell carcinoma. *Trans Andrology Urol* (2021) 10:3628–37. doi: 10.21037/tau-21-620

12. Xie X, Jiang S, Li X. Nuf2 is a prognostic-related biomarker and correlated with immune infiltrates in hepatocellular carcinoma. *Front Oncol* (2021) 11:621373. doi: 10.3389/fonc.2021.621373

13. Xie X, Lin J, Fan X, Zhong Y, Chen Y, Liu K, et al. LncRNA CDKN2B-AS1 stabilized by IGF2BP3 drives the malignancy of renal clear cell carcinoma through epigenetically activating NUF2 transcription. *Cell Death Dis* (2021) 12:201. doi: 10.1038/s41419-021-03489-y

14. Hu P, Shangguan J, Zhang L. Downregulation of NUF2 inhibits tumor growth and induces apoptosis by regulating lncRNA AF339813. *Int J Clin Exp Pathol* (2015) 8:2638–48.

15. Kaneko N, Miura K, Gu Z, Karasawa H, Ohnuma S, Sasaki H, et al. siRNA-mediated knockdown against CDCA1 and KNTC2, both frequently overexpressed in colorectal and gastric cancers, suppresses cell proliferation and induces apoptosis. *Biochem Biophys Res Commun* (2009) 390:1235–40. doi: 10.1016/j.bbrc.2009.10.127

16. Hu P, Chen X, Sun J, Bie P, Zhang LD. SiRNA-mediated knockdown against NUF2 suppresses pancreatic cancer proliferation *in vitro* and *in vivo*. *Bioscience Rep* (2015) 35:1–11. doi: 10.1042/BSR20140124

17. Sethi G, Pathak HB, Zhang H, Zhou Y, Einarson MB, Vathipadiekal V, et al. An RNA interference lethality screen of the human druggable genome to identify molecular vulnerabilities in epithelial ovarian cancer. *PLoS One* (2012) 7:e47086. doi: 10.1371/journal.pone.0047086

18. Wang L, Meng Y, Xu JJ, Zhang QY. The transcription factor AP4 promotes oncogenic phenotypes and cisplatin resistance by regulating LAPTM4B expression. *Mol Cancer Res* (2018) 16:857–68. doi: 10.1158/1541-7786.MCR-17-0519

19. Park SJ, Yoon BH, Kim SK, Kim SY. GENT2: An updated gene expression database for normal and tumor tissues. *BMC Med Genomics* (2019) 12:1–8. doi: 10.1186/s12920-019-0514-7

20. Tang Z, Li C, Kang B, Gao G, Li C, Zhang Z. GEPIA: A web server for cancer and normal gene expression profiling and interactive analyses. *Nucleic Acids Res* (2017) 45:W98–W102. doi: 10.1093/nar/gkx247

21. Lánczky A, Győrffy B. Web-based survival analysis tool tailored for medical research (KMplot): Development and implementation. *J Med Internet Res* (2021) 23:1–7. doi: 10.2196/27633

22. Li X, Wang C, Wang S, Hu Y, Jin S, Liu O, et al. YWHAE as an HE4 interacting protein can influence the malignant behaviour of ovarian cancer by regulating the PI3K/AKT and MAPK pathways. *Cancer Cell Int* (2021) 21:1–18. doi: 10.1186/s12935-021-01989-7

23. Weng H, Feng X, Lan Y, Zheng Z. TCP1 regulates PI3K/AKT/mTOR signaling pathway to promote proliferation of ovarian cancer cells. *J Ovarian Res* (2021) 14:1–11. doi: 10.1186/s13048-021-00832-x

24. Chen C, Gupta P, Parashar D, Nair GG, George J, Geethadevi A, et al. ERBB3-induced furin promotes the progression and metastasis of ovarian cancer *via* the IGF1R/STAT3 signaling axis. *Oncogene* (2020) 39:2921–33. doi: 10.1038/s41388-020-1194-7

25. Kipps E, Tan DSP, Kaye SB. Meeting the challenge of ascites in ovarian cancer : new avenues for therapy and research Europe PMC funders author manuscripts. *Nat Rev Cancer* (2013) 13:273–82. doi: 10.1038/nrc3432.Meeting

26. Wong CH, Lou UK, Li Y, Chan SL, Tong JHM, KF To, et al. CircFOXK2 promotes growth and metastasis of pancreatic ductal adenocarcinoma by complexing with RNA-binding proteins and sponging MiR-942. *Cancer Res* (2020) 80:2138–49. doi: 10.1158/0008-5472.CAN-19-3268

27. Liang F, Ren C, Wang J, Wang S, Yang L, Han X, et al. The crosstalk between STAT3 and p53/RAS signaling controls cancer cell metastasis and cisplatin resistance *via* the Slug/MAPK/PI3K/AKT-mediated regulation of EMT and autophagy. *Oncogenesis* (2019) 8:59. doi: 10.1038/s41389-019-0165-8

28. Chen Y, Cao W, Wang L, Zhong T. AMPH1 functions as a tumour suppressor in ovarian cancer *via* the inactivation of PI3K/AKT pathway. *J Cell Mol Med* (2020) 24:7652–9. doi: 10.1111/jcmm.15400

29. Sundin LJR, Guimaraes GJ, DeLuca JG. The NDC80 complex proteins Nuf2 and Hec1 make distinct contributions to kinetochore-microtubule attachment in mitosis. *Mol Biol Cell* (2011) 22:759–68. doi: 10.1091/mbc.E10-08-0671

30. Reszka AA, Seger R, Diltz CD, Krebs EG, Fischer EH. Association of mitogen-activated protein kinase with the microtubule cytoskeleton. *Proc Natl Acad Sci United States America* (1995) 92:8881–5. doi: 10.1073/pnas.92.19.8881

31. Thapa N, Chen M, Horn HT, Choi S, Wen T, Anderson RA. Phosphatidylinositol-3-OH kinase signalling is spatially organized at endosomal compartments by microtubule-associated protein 4. *Nat Cell Biol* (2020) 22:1357–70. doi: 10.1038/s41556-020-00596-4

32. Li LW, Xiao HQ, Ma R, Yang M, Li W, Lou G. MiR-152 is involved in the proliferation and metastasis of ovarian cancer through repression of ERBB3. *Int J Mol Med* (2018) 41:1529–35. doi: 10.3892/ijmm.2017.3324

33. Hao Y, Li J, Zhang H, Guan G, Guo Y. MicroRNA-205 targets HER3 and suppresses the growth, chemosensitivity and metastasis of human nasopharyngeal carcinoma cells. *J BUON* (2020) 25:350–6.

34. Peng LX, Wang MD, Xie P, Yang JP, Sun R, Zheng LS, et al. LACTB promotes metastasis of nasopharyngeal carcinoma *via* activation of ERBB3/EGFR-ERK signaling resulting in unfavorable patient survival. *Cancer Lett* (2021) 498:165–77. doi: 10.1016/j.canlet.2020.10.051

35. Gaborit N, Lindzen M, Yarden Y. Emerging anti-cancer antibodies and combination therapies targeting HER3/ERBB3. *Hum Vaccines Immunotherapeutics* (2016) 12:576–92. doi: 10.1080/21645515.2015.1102809

36. Tiwary S, Preziosi M, Rothberg PG, Zeitouni N, Corson N, Xu L. ERBB3 is required for metastasis formation of melanoma cells. *Oncogenesis* (2014) 3:e110. doi: 10.1038/oncsis.2014.23

37. Chen N, Ye XC, Chu K, Navone NM, Sage EH, Yu-Lee LY, et al. A secreted isoform of ErbB3 promotes osteonectin expression in bone and enhances the invasiveness of prostate cancer cells. *Cancer Res* (2007) 67:6544–8. doi: 10.1158/0008-5472.CAN-07-1330

38. Vijapurkar U, Kim MS, Koland JG. Roles of mitogen-activated protein kinase and phosphoinositide 3′-kinase in ErbB2/ErbB3 coreceptor-mediated heregulin signaling. *Exp Cell Res* (2003) 284:289–300. doi: 10.1016/S0014-4827(02)00040-X

39. Hellyer NJ, Cheng K, Koland JG. ErbB3 (HER3) interaction with the p85 regulatory subunit of phosphoinositide 3-kinase. *Biochem J* (1998) 333:757–63. doi: 10.1042/bj3330757

40. Vijapurkar U, Cheng K, Koland JG. Mutation of a shc binding site tyrosine residue in ErbB3/HER3 blocks heregulin-dependent activation of mitogen-activated protein kinase. *J Biol Chem* (1998) 273:20996–1002. doi: 10.1074/jbc.273.33.20996

41. Lin J, Chen X, Yu H, Min S, Chen Y, Li Z, et al. NUF2 drives clear cell renal cell carcinoma by activating HMGA2 transcription through KDM2A-mediated H3K36me2 demethylation. *Int J Biol Sci* (2022) 18:3621–35. doi: 10.7150/ijbs.70972

frontiers | Frontiers in Oncology

TYPE Review
PUBLISHED 22 December 2022
DOI 10.3389/fonc.2022.1047177

OPEN ACCESS

EDITED BY
João Pessoa,
University of Coimbra, Portugal

REVIEWED BY
Ahmet Acar,
Middle East Technical University, Turkey
Deguan Lv,
University of Pittsburgh Medical Center, United States

*CORRESPONDENCE
Ping Lin
linping@scu.edu.cn
Yimin Hua
nathan_hua@126.com
Chuan Wang
805101396@qq.com

SPECIALTY SECTION
This article was submitted to Molecular and Cellular Oncology, a section of the journal Frontiers in Oncology

RECEIVED 17 September 2022
ACCEPTED 23 November 2022
PUBLISHED 22 December 2022

CITATION
Guo Y, Lin P, Hua Y and Wang C (2022) TRIM31: A molecule with a dual role in cancer.
Front. Oncol. 12:1047177.
doi: 10.3389/fonc.2022.1047177

TRIM31: A molecule with a dual role in cancer

Yafei Guo[1,2], Ping Lin[3]*, Yimin Hua[1,2]* and Chuan Wang[1,2]*

[1]Key Laboratory of Birth Defects and Related Diseases of Women and Children of MOE, Department of Pediatrics, West China Second University Hospital, Sichuan University, Chengdu, China, [2]The Cardiac Development and Early Intervention Unit, West China Institute of Women and Children's Health, West China Second University Hospital, Sichuan University, Chengdu, Sichuan, China, [3]Lab of Experimental Oncology, State Key Laboratory of Biotherapy and Cancer Center, West China Hospital, Sichuan University, Chengdu, China

Tripartite motif (TRIM) 31 is a new member of the TRIM family and functions as an E3 ubiquitin ligase. Abnormal TRIM31 expression leads to a variety of pathological conditions, such as cancer, innate immunity diseases, sepsis-induced myocardial dysfunction, cerebral ischemic injury, nonalcoholic fatty liver disease and hypertensive nephropathy. In this review, we comprehensively overview the structure, expression and regulation of TRIM31 in cancer. Moreover, we discuss the dual role of TRIM31 in human cancer, and this dual role may be linked to its involvement in the selective regulation of several pivotal cellular signaling pathways: the p53 tumor suppressor, mTORC1, PI3K-AKT, NF-κB and Wnt/β-catenin pathways. In addition, we also discuss the emerging role of TRIM31 in innate immunity, autophagy and its growing sphere of influence across multiple human pathologies. Finally, a better understanding of the dual role of TRIM31 in cancer may provide new therapeutic strategies aimed at inhibiting the cancer-promoting effects of TRIM31 without affecting its tumor suppressor effects.

KEYWORDS

TRIM31, cancer, oncogene, tumor suppressor, innate immunity

1 Introduction

Ubiquitination is a common posttranslational modification of proteins. It participates in various cellular processes and physiological responses in cancer, inflammatory disorders, infection and other diseases by regulating the degradation and activation of intracellular proteins (1). The ubiquitination process is catalyzed by E1, E2 and E3, among which E3 ubiquitin ligase is mainly involved in the recognition and binding of target proteins (2). E3 ubiquitin ligases can be divided into two major classes: homologous to E6-AP COOH terminal (HECT) E3 ubiquitin ligases and RING finger-containing E3 ubiquitin ligases. Although TRIMs are considered to be RING finger-containing E3 ubiquitin ligases, not all TRIM E3 ubiquitin ligases have a RING domain.

To date, there are 9 ring-domain-free TRIM proteins in humans (3). Apart from the RING finger domain, TRIM proteins also contain one or two zinc-binding motifs, named B-boxes, and a coiled-coil domain. According to their domains, TRIM proteins are divided into I to XI subfamilies (4–6). TRIM proteins regulate important cellular processes, such as intracellular signal transduction, innate immunity, transcriptional regulation, autophagy, and carcinogenesis (7, 8). In cancer research, TRIM members act as oncogenes or tumor suppressor genes in ovarian cancer, renal cell carcinoma, gastric cancer, and breast cancer by controlling multiple processes such as transcriptional regulation, DNA repair, cell proliferation, apoptosis, and metastasis (9–13).

TRIM31 is a member of the TRIM family, and structural analysis found that it contains a RING domain, which makes it an E3 ubiquitin-protein ligase (14). The RING domain is a zinc-binding motif located in amino acids 10-20 of the first methionine in nearly all TRIM protein N-terminal portions (15). General insights into RING domain function are derived from the report that the RING domain contains the CBL protein, which has shown that the RING domain regulates ubiquitination events (16–18). It has been reported that C16, C36, C53, C56, and C58 are the key amino acids of the RING domain, and mutation of these amino acid sites can inhibit the E3 ubiquitin ligase activity of TRIM31 (19–21). Apart from the RING domain, TRIM31 also contains one zinc-finger domain named the B box (type 2 box). B-box domains exist in more than 1500 proteins from a variety of organisms, and they can be divided into two groups, in which the intervals of 7-8 zinc binding residues of type 1 and type 2 B-box domains are different. Type 2 B-box proteins play a role in the ubiquitination process. After the B boxes are the coiled-coil region at the N-terminus, this domain regulates homomeric and heteromeric interactions between TRIM proteins and other proteins, especially self-association. In our research, the coiled-coil region was important for the binding of TRIM31 and p53 (22). TRIM31 has no domain at the C-terminus (Figure 1).

Recent studies on TRIM31 strongly advocate for the critical role of TRIM31 in cancer, immunity and inflammation. In this review, in addition to accumulating recent corroborations that endorse this dual role of TRIM31 in cancer, we also discuss the emerging role of TRIM31 in innate immunity, inflammation and autophagy and its growing sphere of influence across multiple other human pathologies.

2 Expression of TRIM31 in cancer and its clinical value

To date, the clinical correlation of TRIM31 in cancer is still elusive. Several reports have revealed that there is a positive correlation between the expression of TRIM31 and cancer prognosis in specific cancer types. TRIM31 is upregulated in gastric adenocarcinoma and may be a potential biomarker of gastric cancer because it is overexpressed in the precancerous stage (23). TRIM31 was markedly upregulated in hepatocellular carcinoma, gallbladder cancer, colorectal cancer, high-grade glioma, pancreatic cancer and acute myeloid leukemia, and the high expression of TRIM31 was also associated with an aggressive phenotype, advanced disease status and poor prognosis (24–29). Multivariate survival analysis demonstrated that TRIM31 was an independent prognostic factor for glioma patients (27). From the Human Protein Atlas data, immunohistochemical analysis found that TRIM31 was more highly expressed in liver, gastric, pancreatic, gallbladder, colorectal tumors and glioma (Figure 2, more information please see www.proteinatlas.org). It is suggested that upregulation of TRIM31 is a common feature of many epithelial cancers and predicts a poor prognosis. However, several reports have indicated that TRIM31 is downregulated in cancer; for example, TRIM31 expression is downregulated in lung cancer tissues and cell lines and correlates with clinic-pathological factors (30). Our research showed that TRIM31 expression was decreased in breast cancer tissues and that lower TRIM31 levels

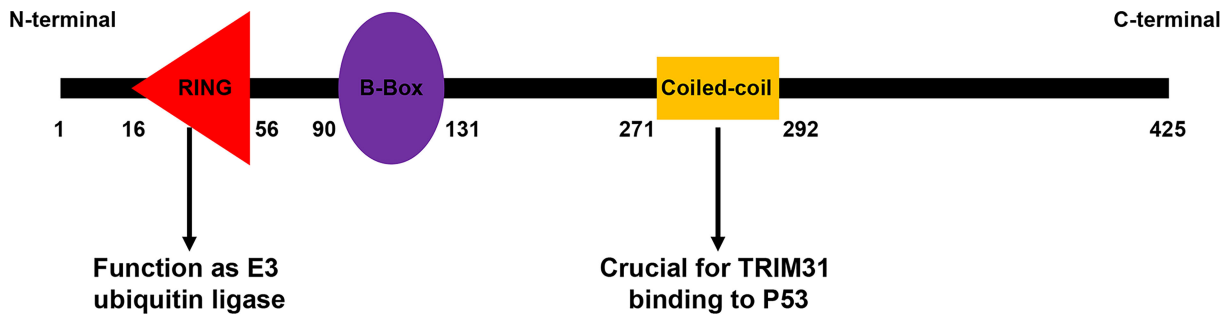

FIGURE 1
Domain organization of the TRIM31 protein. The different TRIM31 domains are reported with numbers and indicate the first and last amino acids of each domain.

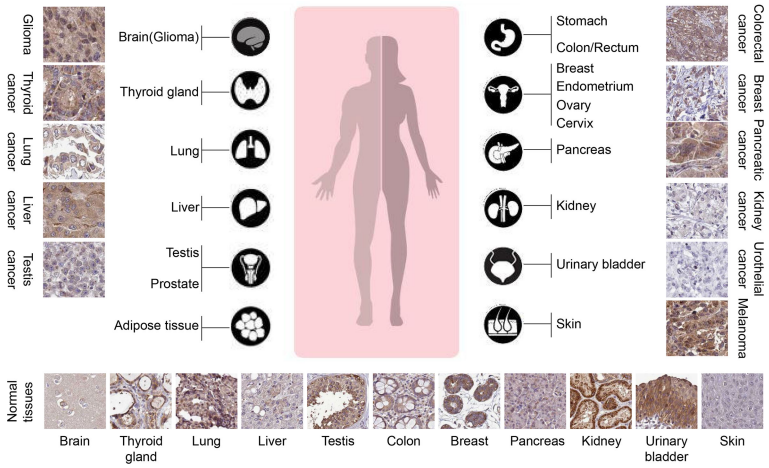

FIGURE 2
TRIM31 is highly expressed in several types of tumors (The Human Protein Atlas data). The rabbit polyclonal antibody HPA046400 (Sigma Aldrich) was used for the immunohistochemistry assay. The cancer tissues of glioma, melanoma, thyroid gland, pancreatic cancer and liver cancer were strongly cytoplasmic stained. Occasional membranous positivity was observed in colorectal cancer. Urothelial cancer and most kidney cancers were negatively stained. Normal tissues showed weak to strong cytoplasmic positivity with HPA046400 antibody, as presented at the bottom. In glioma, thyroid cancer, liver cancer, colorectal cancer, and pancreatic cancer, the expression of TRIM31 in cancer cell cytoplasm is higher than that in adjacent normal tissues. However, in lung cancer, testis cancer, kidney cancer, and urothelial cancer, the expression of TRIM31 was lower than that in adjacent normal tissues.

were associated with worse survival of breast cancer patients (22). Altogether, the aforementioned studies showed that TRIM31 was upregulated in liver, gastric, pancreatic, gallbladder, colorectal tumors and glioma, and higher levels of TRIM31 are related to the poor prognosis of cancer patients. However, there are also opposite conclusions. TRIM31 was downregulated in lung and breast cancer, and higher expression of the TRIM31 gene is linked to better overall survival of patients.

3 Regulation of TRIM31 expression

The expression of TRIM31 in diverse cancer cells is different, and its expression is tightly controlled by various factors. Recent reports have shown that TRIM31 expression is regulated by retinoid, microRNA and posttranslational modifications. Retinoids, natural or synthetic derivatives of vitamin A, are effective in the treatment of acute promyelocytic leukemia (APL) and are used in the chemoprophylaxis of cancers such as breast, skin, head and neck and liver cancers. Retinoid bound to the promoter of TRIM31 to induce TRIM31 expression and then suppressed the proliferation of breast cancer (31). MicroRNA is a small single-stranded noncoding RNA with a length of 21-23 nt that regulates the transcriptional inhibition, cleavage and degradation of mRNA (32). According to related studies, abnormal miRNA function is closely related to tumor invasion and metastasis (33, 34). In ovarian cancer, microRNA-551b downregulates TRIM31 expression by targeting its 3' UTR to promote cancer progression (35). In addition, microRNA-29c-3p is abnormally expressed in many cancers, including gastric cancer, colon cancer, pancreatic cancer and hepatocellular carcinoma (36–38). Overexpression of microRNA-29c-3p significantly inhibited the proliferation and migration of hepatocellular carcinoma (HCC) cells *in vitro* and the growth of HCC tumors *in vivo*. Mechanistically, microRNA-29c-3p directly bound to the TRIM31 promoter and suppressed TRIM31 expression (39).

Posttranslational modifications including phosphorylation, ubiquitination and acetylation have been shown to modulate various biological functions, such as cell signal conduction, protein–protein interactions, protein transport, cell differentiation and proliferation through regulating the protein conformation, localization, stability and activity (40, 41). The TRIM31 protein is polyubiquitinated in gastric cancer, which leads to its proteasomal degradation. Furthermore, the ubiquitin proteasome-regulated degradation of TRIM31 was confirmed in AsPC-1 pancreatic cancer cells (23). These discoveries suggest that posttranslational modification can control the abundance of endogenous TRIM31.

4 The dual role of TRIM31 in cancer: Oncogene or Tumor Suppressor?

4.1 The tumor suppressor role of TRIM31

Recently, increasing evidence has shown that TRIM31 plays an important tumor suppressor role in the occurrence and

development of various cancers. TRIM31 was first reported in breast cancer in 2002. Retinoid induced proliferation inhibition of breast carcinoma cells by targeting the TRIM31 promoter (31). In our study, we found that TRIM31 directly interacted with p53 and subsequently stabilized and activated p53 by inducing K63-linked ubiquitination as well as inhibiting MDM2-mediated K48-linked ubiquitination of p53 and then suppressing breast cancer progression (22). In addition, TRIM31 plays a potential tumor suppressor role in non-small cell lung cancer. The expression of TRIM31 in lung cancer cell lines was lower than that in the normal bronchial cell line HBE. TRIM31 inhibited the cell proliferation rate and colony formation by reducing the expression of the cell cycle regulators cyclin D1 and cyclin E (30). Moreover, TRIM31 can be recognized as a growth suppressor at the early stage of gastric adenocarcinoma (23). Therefore, TRIM31 may act as a tumor suppressor in the early stage of the tumor. Altogether, these studies have shown that TRIM31 might play a tumor suppressor role in breast cancer, non-small cell lung cancer and the early stage of gastric adenocarcinoma (Figure 3).

4.2 The oncogene role of TRIM31

Recently, studies have shown that TRIM31 is an oncogene in various cancers. A number of carcinogenic mechanisms have been proposed for TRIM31, such as regulating the P53, mTORC1, PI3K-Akt, NF-kB and Wnt/β-catenin pathways to promote tumor onset and progression (24–30). P53 is one of the most important tumor suppressor proteins. In differentiated cells, the abundance and activity of p53 are strictly regulated. With an increased risk of acquiring mutations, the accumulation and activation of p53 protein are regulated by posttranslational modifications (42). TRIM31 was significantly upregulated in the anchorage-deprived HCC cells compared with their attached counterparts and promoted anoikis resistance. TRIM31 can directly interact with p53, which is an inhibitor of the AMPK pathway, and regulate the K48-linked ubiquitous degradation of p53. It was further confirmed that excessive activation of the AMPK pathway is the cause of TRIM31-mediated HCC cell resistance to anoikis. That is, TRIM31 facilitates anoikis resistance by targeting the degradation of p53 and subsequently overactivating the AMPK pathway (24). AMPK phosphorylates tuberous sclerosis complex 2 (TSC2) and enhances its activity (43). TSC2 is an upstream inhibitor of the mTORC1 pathway. MTOR forms two unique catalytic subunits of the complex, called mTORC1 and mTORC2, and it plays critical roles in a variety of biological processes, such as cell growth, survival, autophagy, metabolism, and immunity (44, 45). TRIM31 facilitates the malignant behaviors of HCC cells by overactivating the target of the mTORC1 pathway. Further studies have shown that TRIM31 plays a carcinogenic role by directly interacting with the TSC1 and TSC2 complexes and facilitating the ubiquitination of K48 and the degradation of the complex (19).

The phosphoinositide 3-kinase (PI3K)–AKT pathway is an important node in controlling cell growth, migration,

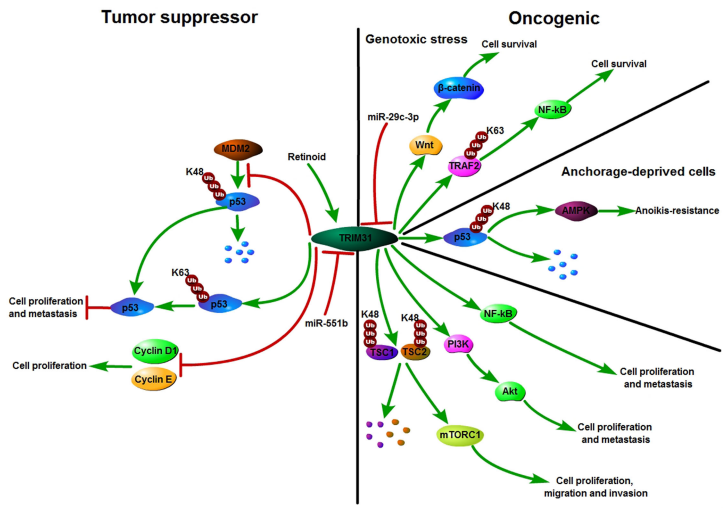

FIGURE 3
Schematic diagram of TRIM31 function in cancer. TRIM31 can act as either a tumor suppressor or an oncogene. TRIM31 inhibits cell growth by reducing the expression of Cyclin D1 and Cyclin E. TRIM31 stabilizes P53 expression to suppress tumor cell proliferation and metastasis. TRIM31 promotes tumor onset and progression by regulating the P53, mTORC1, PI3K-Akt, NF-kB and Wnt/β-catenin pathways. Retinoid induced cell growth arrest by targeting the promoter of TRIM31. miR-551b suppresses the expression of TRIM31 by targeting its 3′-UTR and further promotes cell invasion and drug resistance. miR-29c-3p can inhibit TRIM31 expression by targeting its 3′-UTR. TRIM31 activated Wnt/β-catenin signaling to promote cell survival.

proliferation, and metabolism in mammalian cells and is the most commonly activated pathway in human cancers (46). In glioma, by silencing or overexpressing TRIM31 expression, the proliferation, invasion and migration of glioma cells could be downregulated or upregulated through the PI3K/Akt signaling pathway (27). Moreover, TRIM31 can activate the PI3K/Akt signaling pathway to enhance chemoresistance in glioblastoma (47). In gallbladder cancer, TRIM31 promotes proliferation and invasion *via* the PI3K/Akt signaling pathway (25). The PI3K/AKT/IKK alpha pathway regulates the activation of NF kappa B and β-catenin in CRC cell lines (48). Nuclear factor kappa B (NF-κB) is activated in various cancers and not only coordinates with immunity and inflammation but also plays a vital role in the development of cancer (49, 50).. Past research has shown that ubiquitin modification plays an important role in the regulation of NF-κB signaling (51–53). As an E3 ubiquitin ligase, TRIM31 promotes K63-linked polyubiquitination of tumor necrosis factor receptor-associated factor 2 (TRAF2) to upregulate the levels of nuclear p65 and then maintains the activation of NF-κB in pancreatic cancer cells. Furthermore, TRIM31 promotes gemcitabine resistance in pancreatic cancer cells by activating the NF-κB signaling pathway (28). In addition, TRIM31 activates the NF-κB pathway to promote migration and invasion in glioma and colorectal cancer (26, 54). TRIM31 regulates Wnt/β-catenin signaling to promote acute myeloid leukemia progression and sensitivity to daunorubicin (29). Collectively, TRIM31 plays an oncogene role in cancer by regulating the p53, mTORC1, NF-κB, and PI3K-Akt pathways (Figure 3).

4.3 The possible mechanism of TRIM31 in promoting or suppressing cancer

TRIM31 is a critical factor that is able to perform multiple functions in cancer, and the complex function of TRIM31 makes it difficult to identify TRIM31 as an oncogene or tumor suppressor. Here, we will discuss why TRIM31 can promote or inhibit cancer from the following aspects. First, TRIM genes are usually expressed in a variety of splicing forms (55). There are three isoforms of TRIM31 (TRIM31α, TRIM31β and TRIM31γ). TRIM31α was the most common splicing form and has been registered in the public database. TRIM31 β is a truncated form of TRIM31 at the C-terminus. TRIM31 γ is a mutant protein of TRIM31 truncated at the C-terminus. Studies have shown that the TRIM31 isoforms have different biological roles in cancer. Therefore, the differential expression of TRIM31 isoforms may lead to the different roles of TRIM31 in cancer. Second, proteins containing a RING finger domain can serve as E3 ubiquitin ligases (17), and Sugiura proved that TRIM31 has autoubiquitylating activity *in vitro*. It has been demonstrated that the autoubiquitination activity of TRIM31 regulates the intracellular abundance of TRIM31 (23). The strict regulation of the TRIM31 protein level may be linked to its seemingly contradictory behaviors in the cancer process. Third, several cancer-associated proteins that can be posttranslationally regulated by TRIM31 have been reported, such as TRAF2, TSC1/TSC2 and P53. The different target proteins of TRIM31 may decide the tumor promoter or tumor suppressor of TRIM31 in cancer. Therefore, discovering new target proteins of TRIM31 is necessary to further understand the role of TRIM31 in cancer.

5 TRIM31: Growing influence in innate immunity and autophagy

5.1 The emerging role of TRIM31 in innate immunity

Innate immunity provides the first line of defense against invading pathogens. Activation of innate immunity requires the recognition of pathogen-associated molecular patterns through pattern-recognition receptors (56, 57). As a regulator of Mitochondrial antiviral signaling protein (MAVS) aggregation, TRIM31 can be recruited to mitochondria after viral infection and specifically regulate antiviral signaling mediated by RIG-I-like receptor (RLR) pattern-recognition receptors. Further study showed that TRIM31 interacted with MAVS and catalyzed the Lys63 (K63)-linked polyubiquitination of MAVS by Lys10, Lys311 and Lys461. This modification promoted the formation of prion-like aggregates of MAVS after viral infection (20). Moreover, USP18 interacts with TRIM31 to promote the K63-linked polyubiquitination of MAVS and then positively regulates innate antiviral immunity (58). PB1-F2, Rac1, PRMT7 and FAF1 disrupt TRIM31 interaction with MAVS to inhibit MAVS activation and negatively regulate innate antiviral immune responses (59–62). HBV (hepatitis B virus) infection was reported to induce type III IFNs, and TRIM31 was found to be a type III IFN-stimulated gene. IFN-induced TRIM5γ recruits TRIM31 to degrade HBx, resulting in suppression of hepatitis B virus replication (63, 64). In addition to its crucial role in antiviral processes, TRIM31 also has an important role in promoting viral infection. COVID-19 caused by the novel severe acute respiratory syndrome (SARS) coronavirus 2 (SARS-CoV-2) is rapidly emerging and spreading worldwide. Wang et al. reported that the dimeric domain protein (SARS2-NP) of the SARS-CoV-2 nucleocapsid is required for liquid-liquid phase separation of SARS2-NP and RNA, which suppresses Lys63-linked polyubiquitination and aggregation of MAVS by reducing TRIM31 binding to MAVS, thus inhibiting the innate antiviral immune response (65). Moreover, Temena et al. also found that TRIM31 is positively correlated with SARS

–CoV–2 associated genes TMPRSS2–TMPRSS4 and knockdown of TRIM31 significantly altered viral replication and viral processes in gastrointestinal cancer samples. This result suggests that TRIM31 may play a role in increasing the susceptibility to SARS-CoV-2 viral infection in patients with gastrointestinal cancers (66).

The NLRP3 inflammasome is a multiprotein platform that comprises NLRP3, ASC, and caspase-1 and plays crucial roles in host defense against pathogens. The NLRP3 inflammasome is involved in many kinds of diseases, such as cancer, gout, autoimmune disorders, atherosclerosis, type 2 diabetes and obesity (67–70). TRIM31 has been reported to be a feedback suppressor of the NLRP3 inflammasome. TRIM31 directly binds to NLRP3 and promotes K48-linked polyubiquitination and proteasomal degradation of NLRP3. Furthermore, TRIM31 deficiency attenuates the severity of dextran sodium sulfate (DSS)-induced colitis, an inflammatory bowel disease model in which NLRP3 exerts a protective effect (21). Moreover, AKT bound to NLRP3 and phosphorylated it on S5. This phosphorylation event also stabilized NLRP3 by reducing its ubiquitination on lysine 496, which inhibits its proteasome-mediated degradation by TRIM31 (71). In addition, TRIM31 promoted the ubiquitination of NLRP3 to alleviate IL–1ß secretion and diminished the development of apical periodontitis (72). TRIM31 also inhibited the NLRP3 inflammasome and pyroptosis through ubiquitination of NLRP3 in retinal pigment epithelial cells (73). CRNDE interacted with NLRP3 and decreased TRIM31-mediated NLRP3 ubiquitination to activate the NLRP3 inflammasome and exacerbate IgA nephropathy progression (74). In addition to the NLRP3 inflammasome, TRIM31 also plays a crucial role in fungal infections. TRIM31 regulates antifungal immunity by facilitating K27-linked polyubiquitination of SYK (75).

5.2 TRIM31 and autophagy

Autophagy is one of the major intracellular degradation systems in addition to the ubiquitin–proteasome system. A primary role of autophagy is to maintain cellular homoeostasis by degrading intracytoplasmic proteins and organelles through starvation and by recycling multiple sources (76–78). Recent studies have shown that several TRIM proteins regulate cancer progression *via* autophagy. TRIM59 inhibits p62 selective autophagy degradation of PDCD10 to promote the motility of breast cancer (79). In A549/DDP cells, knockdown of TRIM65 can inhibit autophagy and cisplatin resistance by regulating miR-138-5P/ATG7 (80). TRIM31, an intestine-specific protein localized in mitochondria, is essential for promoting lipopolysaccharide-induced Atg5/Atg7-independent autophagy. TRIM31 directly interacts with phosphatidylethanolamine in a palmitoylation-dependent manner, leading to the induction of autolysosome formation (81). Altogether, TRIM31 plays an important role in innate immunity, autophagy and other human pathologies (Figure 4).

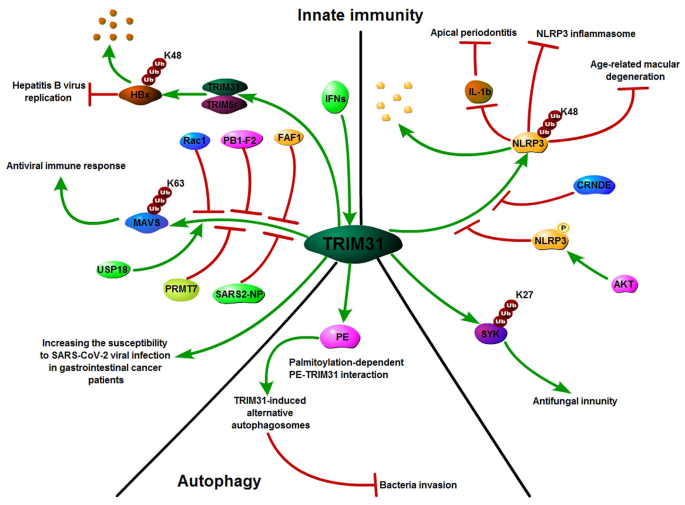

FIGURE 4
TRIM31: Growing influence in innate immunity and autophagy. TRIM31 plays an important role in innate immunity; TRIM31 interacts with MAVS and catalyzes the Lys63 (K63)-linked polyubiquitination of MAVS to promote the formation of prion-like MAVS aggregates after viral infection. USP18 promotes TRIM31-mediated K63-linked MAVS polyubiquitination, while PB1-F2, Rac1, PRMT7, SARS2-NP and FAF1 inhibit TRIM31-mediated K63-linked MAVS polyubiquitination. TRIM31 directly binds to NLRP3 and promotes K48-linked polyubiquitination and proteasomal degradation of NLRP3. AKT and CRNDE decreased TRIM31-mediated NLRP3 ubiquitination. Alongside its emerging role in innate immunity, TRIM31 is also known to be involved in autophagy.

TABLE 1 The TRIM31 targets or interacting proteins.

Target or interacting proteins	Modification	Effect	Outcome	Reference
P53	K48-linked poly-ubiquitination	Degradation of p53	Promoting the anoikis-resistance	(24)
TSC1/TSC2	K48-linked poly-ubiquitination	Degradation of TSC1/TSC2	Promoting HCC progression	(19)
TRAF2	K63-linked poly-ubiquitination	Activation of NF-κB	Promoting the gemcitabine resistance	(28)
P53	K63-linked poly-ubiquitination	Activation of p53	Suppressing the proliferation and migration of breast cancer cell	(22)
MAVS	K63-linked poly-ubiquitination	Promoting the formation of prion-like aggregates	Activation of antiviral immunity	(20)
USP18	No	Promoting the K63-linked polyubiquitination of MAVS	Activation of antiviral immunity	(58)
HBx	K48-linked poly-ubiquitination	Degradation of HBx	Inhibiting HBV Replication	(62)
NLRP3	K48-linked poly-ubiquitination	Degradation of NLRP3	Attenuating NLRP3 inflammasome activation	(70)
SYK	K27-linked poly-ubiquitination	Activation of SYK	Promoting antifungal immunity	(74)

6 Conclusion and future perspectives

In conclusion, although the function of TRIM31 has been studied for many years, there is still much to be clarified regarding the role of TRIM31 in cancer. A number of studies suggest that TRIM31 may serve as an oncogene when it is highly expressed and may facilitate cancer progression, metastasis and drug resistance by inducing the mTORC1 pathway (19), activating the NF-κB and AKT signaling pathways (25–28), and downregulating the activity of p53 (24). However, some studies have shown that TRIM31 can act as a tumor suppressor, and its high expression inhibits the proliferation and metastasis of cancer by stabilizing p53 or decreasing the expression of cyclin D1 and cyclin E. Although TRIM31 has been extensively studied, some questions should also be considered. First, the regulation of TRIM31 in cancer should be further researched. Recent research has shown only that TRIM31 can be regulated by posttranslational modification, and whether there are other regulatory mechanisms is still unclear. Second, the mechanism by which TRIM31 promotes and suppresses cancer needs further study. For example, whether TRIM31 regulates cancer progression *via* autophagy or innate immunity is unknown. Third, as an E3 ubiquitin ligase, TRIM31 can target many proteins (Table 1). Therefore, it is very important to find new target proteins for studying the function of TRIM31 in cancer. Although there are still many questions to be addressed, we believe that in-depth understanding of the TRIM31 in carcinogenesis may help to answer whether TRIM31 possesses the potential to become a new anticancer target.

Currently, pharmaceutical companies have entered the era of E3 ubiquitin ligase-targeted therapy, and targeting the E3 ligase is gradually becoming a considerable cancer treatment option (82). Proteolysis-targeting chimera (PROTAC) has been developed as a useful protein-targeted degradation technique. A bifunctional PROTAC molecule is composed of a ligand of the protein of interest (POI) and a covalently linked ligand of an E3 ubiquitin ligase (E3). Upon binding to POI, PROTAC can recruit E3 for POI ubiquitination, which is subject to proteasome-mediated degradation (83). However, the PROTAC technique has not been applied to the TRIM31 protein, and future studies may focus on the application of PROTAC to TRIM31 protein.

Author contributions

Conception and design: YG and PL. Initial manuscript writing: YG. Confirmation of Manuscript: PL, YH and CW. All authors contributed to the article and approved the submitted version.

Funding

This study was funded by the National Natural Science Foundation of China (No. 81971457) and the Science-technology Support Plan Projects in Sichuan province (No. 2022YFS0240).

Conflict of interest

The authors declare that the research was conducted in the absence of any commercial or financial relationships that could be construed as a potential conflict of interest.

Publisher's note

References

1. Popovic D, Vucic D, Dikic I. Ubiquitination in disease pathogenesis and treatment. *Nat Med* (2014) 20(11):1242–53. doi: 10.1038/nm.3739

2. Hershko A, Heller H, Elias S, Ciechanover A. Components of ubiquitin-protein ligase system. resolution, affinity purification, and role in protein breakdown. *J Biol Chem* (1983) 258:8206–14. doi: 10.1016/S0021-9258(20)82050-X

3. Hatakeyama S. TRIM family proteins: Roles in autophagy, immunity, and carcinogenesis. *Trends Biochem Sci* (2017) 42(4):297–311. doi: 10.1016/j.tibs.2017.01.002

4. Short KM, Cox TC. Subclassification of the RBCC/TRIM superfamily reveals a novel motif necessary for microtubule binding. *J Biol Chem* (2006) 281(13):8970–80. doi: 10.1074/jbc.M512755200

5. Ozato K, Shin DM, Chang TH, Morse HC. TRIM family proteins and their emerging roles in innate immunity. *Nat Rev Immunol* (2008) 8(11):849–60. doi: 10.1038/nri2413

6. McNab FW, Rajsbaum R, Stoye JP, O'Garra A. Tripartite-motif proteins and innate immune regulation. *Curr Opin Immunol* (2011) 23(1):46–56. doi: 10.1016/j.coi.2010.10.021

7. Hatakeyama S. TRIM proteins and cancer. *Nat Rev Cancer* (2011) 11 (11):792–804. doi: 10.1038/nrc3139

8. Napolitano LM, Meroni G. TRIM family: Pleiotropy and diversification through homomultimer and heteromultimer formation. *IUBMB Life* (2012) 64 (1):64–71. doi: 10.1002/iub.580

9. Cambiaghi V, Giuliani V, Lombardi S, Marinelli C, Toffalorio F, Pelicci PG. TRIM proteins in cancer. *Adv Exp Med Biol* (2012) 770:77–91. doi: 10.1007/978-1-4614-5398-7_6

10. Qiao HY, Zhang Q, Wang JM, Jiang JY, Huyan LY, Yan J, et al. TRIM29 regulates the SETBP1/SET/PP2A axis *via* transcription factor VEZF1 to promote progression of ovarian cancer. *Cancer Lett* (2022) 529:85–99. doi: 10.1016/j.canlet.2021.12.029

11. Miao CK, Liang C, Li P, Liu BJ, Qin C, Yuan H, et al. TRIM37 orchestrates renal cell carcinoma progression via histone H2A ubiquitination-dependent manner. *J Exp Clin Cancer Res* (2021) 40(1):195. doi: 10.1186/s13046-021-01980-0

12. Li RZ, Xu P, Jin XS, Shi ZC, Zhang QQ, Ye FP, et al. TRIM50 inhibits proliferation and metastasis of gastric cancer *via* promoting β-catenin degradation. *J Oncol* (2022) 2022:5936753. doi: 10.1155/2022/5936753

13. Wang R, Huang KL, Xing LX. TRIM35 functions as a novel tumor suppressor in breast cancer by inducing cell apoptosis through ubiquitination of PDK1. *Neoplasma* (2022) 69(2):370–82. doi: 10.4149/neo_2021_210823N1205

14. Reymond A, Meroni G, Fantozzi A, Merla G, Cairo S, Luzi L, et al. The tripartite motif family identifies cell compartments. *EMBO J* (2001) 20(9):2140–51. doi: 10.1093/emboj/20.9.2140

15. Torok M, Etkin LD. Two b or not two b? overview of the rapidly expanding b-box family of proteins. *Differentiation* (2001) 67(3):63–71. doi: 10.1046/j.1432-0436.2001.067003063.x

16. Joazeiro CA, Wing SS, Huang H, Leverson JD, Hunter T, Liu YC. The tyrosine kinase negative regulator c-cbl as a RING-type, E2-dependent ubiquitin-protein ligase. *Science* (1999) 286(5438):309–12. doi: 10.1126/science.286.5438.309

17. Lorick KL, Jensen JP, Fang S, Ong AM, Hatakeyama S, Weissman AM. RING fingers mediate ubiquitin-conjugating enzyme (E2)-dependent ubiquitination. *Proc Natl Acad Sci U S A* (1999) 96(20):11364–9. doi: 10.1073/pnas.96.20.11364

18. Waterman H, Levkowitz G, Alroy I, Yarden Y. The RING finger of c-cbl mediates desensitization of the epidermal growth factor receptor. *J Biol Chem* (1999) 274(32):22151–4. doi: 10.1074/jbc.274.32.22151

19. Guo P, Ma X, Zhao W, Huai W, Li T, Qiu Y, et al. TRIM31 is upregulated in hepatocellular carcinoma and promotes disease progression by inducing ubiquitination of TSC1-TSC2 complex. *Oncogene* (2018) 37(4):478–88. doi: 10.1038/onc.2017.349

20. Liu B, Zhang M, Chu H, Zhang H, Wu H, Song G, et al. The ubiquitin E3 ligase TRIM31 promotes aggregation and activation of the signaling adaptor MAVS through Lys63-linked polyubiquitination. *Nat Immunol* (2017) 18 (2):214–24. doi: 10.1038/ni.3641

21. Song H, Liu B, Huai W, Yu Z, Wang W, Zhao J, et al. The E3 ubiquitin ligase TRIM31 attenuates NLRP3 inflammasome activation by promoting proteasomal degradation of NLRP3. *Nat Commun* (2016) 7:13727. doi: 10.1038/ncomms13727

22. Guo YF, Li Q, Zhao G, Zhang J, Yuan H, Feng TY, et al. Loss of TRIM31 promotes breast cancer progression through regulating K48- and K63-linked ubiquitination of p53. *Cell Death Dis* (2021) 12(10):945. doi: 10.1038/s41419-021-04208-3

23. Sugiura T, Miyamoto K. Characterization of TRIM31, upregulated in gastric adenocarcinoma, as a novel RBCC protein. *J Cell Biochem* (2008) 105(4):1081–91. doi: 10.1002/jcb.21908

24. Guo PB, Qiu YM, Ma XM, Li T, Ma XX, Zhu LH, et al. Tripartite motif 31 promotes resistance to anoikis of hepatocarcinoma cells through regulation of p53-AMPK axis. *Exp Cell Res* (2018) 368(1):59–66. doi: 10.1016/j.yexcr.2018.04.013

25. Li H, Zhang Y, Hai J, Wang JX, Zhao B, Du LX, et al. Knockdown of TRIM31 suppresses proliferation and invasion of gallbladdercancer cells by down-regulating MMP2/9 through the PI3K/Akt signaling pathway. *BioMed Pharmacother* (2018) 103:1272–8. doi: 10.1016/j.biopha.2018.04.120

26. Wang HY, Yao L, Gong YD, Zhang B. TRIM31 regulates chronic inflammation *via* NF-κB signal pathway to promote invasion and metastasis in colorectal cancer. *Am J Transl Res* (2018) 10(4):1247–59.

27. Shi G, Lv C, Yang Z, Qin T, Sun L, Pan P, et al. TRIM31 promotes proliferation, invasion and migration of glioma cells through akt signaling pathway. *Neoplasma* (2019) 66(5):727–35. doi: 10.4149/neo_2019_190106N21

28. Yu C, Chen SY, Guo YT, Sun CY. Oncogenic TRIM31 confers gemcitabine resistance in pancreatic cancer *via* activating the NF-κB signaling pathway. *Theranostics* (2018) 8(12):3224–36. doi: 10.7150/thno.23259

29. Xiao Y, Deng TR, Ming X, Xu JH. TRIM31 promotes acute myeloid leukemia progression and sensitivity to daunorubicin through the wnt/β-catenin signaling. *Biosci Rep* (2020) 40(4):BSR20194334. doi: 10.1042/BSR20194334

30. Li H, Zhang Y, Zhang Y, Bai X, Peng Y, He P. TRIM31 is downregulated in non-small cell lung cancer and serves as a potential tumor suppressor. *Tumour Biol* (2014) 35(6):5747–52. doi: 10.1007/s13277-014-1763-x

31. Dokmanovic M, Chang BD, Fang J, Roninson IB. Retinoid-induced growth arrest of breast carcinoma cells involves co-activation of multiple growth-inhibitory genes. *Cancer Biol Ther* (2002) 1(1):24–7. doi: 10.4161/cbt.1.1.35

32. Li Z, Rana TM. Therapeutic targeting of microRNAs: current status and future challenges. *Nat Rev Drug Discov* (2014) 13(8):622–38. doi: 10.1038/nrd4359

33. Calin GA, Croce CM. MicroRNA-cancer connection: the beginning of a new tale. *Cancer Res* (2006) 66(15):7390–4. doi: 10.1158/0008-5472.CAN-06-0800

34. Hayes CN, Chayama K. MicroRNAs as biomarkers for liver disease and hepatocellular carcinoma. *Int J Mol Sci* (2016) 17(3):280. doi: 10.3390/ijms17030280

35. Wei Z, Liu Y, Wang Y, Zhang Y, Luo Q, Man X, et al. Downregulation of Foxo3 and TRIM31 by miR-551b in side population promotes cell proliferation, invasion, and drug resistance of ovarian cancer. *Med Oncol* (2016) 33(11):126. doi: 10.1007/s12032-016-0842-9

36. Dong XZ, Song Y, Lu YP, Hu Y, Liu P, Zhang L. Sanguinarine inhibits the proliferation of BGC-823 gastric cancer cells *via* regulating miR-96-5p/miR-29c-3p and the MAPK/JNK signaling pathway. *J Nat Med* (2019) 73(4):777–88. doi: 10.1007/s11418-019-01330-7

37. Chen G, Zhou T, Li Y, Yu Z, Sun L. p53 target miR-29c-3p suppresses colon cancer cell invasion and migration through inhibition of PHLDB2. *Biochem Biophys Res Commun* (2017) 487(1):90–5. doi: 10.1016/j.bbrc.2017.04.023

38. Lu Y, Tang L, Zhang Z, Li S, Liang S, Ji L, et al. Long noncoding RNA TUG1/miR-29c axis affects cell proliferation, invasion, and migration in human pancreatic cancer. *Dis Markers* (2018) 2018:6857042. doi: 10.1155/2018/6857042

39. Lv T, Jiang L, Kong L, Yang J. MicroRNA−29c−3p acts as a tumor suppressor gene and inhibits tumor progression in hepatocellular carcinoma by targeting TRIM31. *Oncol Rep* (2020) 43(3):953–64.

40. Marcelli S, Corbo M, Iannuzzi F, Negri L, Blandini F, Nistico R, et al. The involvement of post-translational modifications in alzheimer's disease. *Curr Alzheimer Res* (2018) 15(4):313–35. doi: 10.2174/1567205014666170505095109

41. Wu Z, Huang R, Yuan L. Crosstalk of intracellular post-translational modifications in cancer. *Arch Biochem Biophys* (2019) 676:108138. doi: 10.1016/j.abb.2019.108138

42. Boehme KA, Blattner C. Regulation of p53–insights into a complex process. *Crit Rev Biochem Mol Biol* (2009) 44(6):367–92. doi: 10.3109/10409230903401507

43. Inoki K, Zhu TQ, Guan KL. TSC2 mediates cellular energy response to control cell growth and survival. *Cell* (2003) 115(5):577–90. doi: 10.1016/S0092-8674(03)00929-2

44. Saxton RA, Sabatini DM. mTOR signaling in growth, metabolism, and disease. *Cell* (2017) 168(6):960–76. doi: 10.1016/j.cell.2017.02.004

45. Harwood FC, Klein Geltink RI, O'Hara BP, Cardone M, Janke L, Finkelstein D, et al. ETV7 is an essential component of a rapamycin-insensitive mTOR complex in cancer. *Sci Adv* (2018) 4(9):eaar3938. doi: 10.1126/sciadv.aar3938

46. Lawrence MS, Stojanov P, Mermel CH, Robinson JT, Garraway LA, Golub TR, et al. Discovery and saturation analysis of cancer genes across 21 tumour types. *Nature* (2014) 505(7484):495–501. doi: 10.1038/nature12912

47. Fan MD, Zhao XY, Qi JN, Jiang Y, Liu BY, Dun ZP, et al. TRIM31 enhances chemoresistance in glioblastoma through activation of the PI3K/Akt signaling pathway. *Exp Ther Med* (2020) 20(2):802–9. doi: 10.3892/etm.2020.8782

48. Agarwal A, Das KH, Lerner NL, Sathe S, Cicek M, Casey G, et al. The AKT/I kappa b kinase pathway promotes angiogenic/metastatic gene expression in colorectal cancer by activating nuclear factor-kappa b and β-catenin. *Oncogene* (2005) 24(6):1021–31. doi: 10.1038/sj.onc.1208296

49. DiDonato JA, Mercurio F, Karin M. NF-κB and the link between inflammation and cancer. *Immunol Rev* (2012) 246(1):379–400. doi: 10.1111/j.1600-065X.2012.01099.x

50. Karin M. NF-kappaB as a critical link between inflammation and cancer. *Cold Spring Harb Perspect Biol* (2009) 1(5):a000141. doi: 10.1101/cshperspect.a000141

51. Chen ZJ, Fuchs SY. Ubiquitin-dependent activation of NF-kappaB: K63-linked ubiquitin chains: a link to cancer? *Cancer Biol Ther* (2004) 3(3):286–8. doi: 10.4161/cbt.3.3.798

52. Lang V, Rodríguez MS. Innate link between NF-kappaB activity and ubiquitin-like modifiers. *Biochem Soc Trans* (2008) 36(Pt 5):853–7. doi: 10.1042/BST0360853

53. Haas AL. Linear polyubiquitylation: the missing link in NF-kappaB signalling. *Nat Cell Biol* (2009) 11(2):116–8. doi: 10.1038/ncb0209-116

54. Zhou L, Deng ZZ, Li HY, Jiang N, Wei ZS, Hong MF, et al. TRIM31 promotes glioma proliferation and invasion through activating NF-κB pathway. *Onco Targets Ther* (2019) 12:2289–97. doi: 10.2147/OTT.S183625

55. Meroni G, Diez-Roux G. TRIM/RBCC, a novel class of 'single protein RING finger' E3 ubiquitin ligases. BioEssays: news and reviews in molecular, cellular and developmental biology. *Bioessays* (2005) 27(11):1147–57. doi: 10.1002/bies.20304

56. Kawai T, Akira S. The role of pattern-recognition receptors in innate immunity: update on toll-like receptors. *Nat Immunol* (2010) 11(5):373–84. doi: 10.1038/ni.1863

57. Cao X. Self-regulation and cross-regulation of pattern-recognition receptor signalling in health and disease. *Nat Rev Immunol* (2016) 16(1):35–50. doi: 10.1038/nri.2015.8

58. Hou JX, Han LL, Zhao Z, Liu HQ, Zhang L, Ma CH, et al. USP18 positively regulates innate antiviral immunity by promoting K63-linked polyubiquitination of MAVS. *Nat Commun* (2021) 12(1):2970. doi: 10.1038/s41467-021-23219-4

59. Cheung PH, Lee TT, Kew C, Chen HL, Yuen KY, Chan CP, et al. Virus subtype-specific suppression of MAVS aggregation and activation by PB1-F2 protein of influenza a (H7N9) virus. *PloS Pathog* (2020) 16(6):e1008611. doi: 10.1371/journal.ppat.1008611

60. Yang SG, Harding AT, Sweeney C, Miao D, Swan G, Zhou C, et al. Control of antiviral innate immune response by protein geranylgeranylation. *Sci Adv* (2019) 5(5):eaav7999. doi: 10.1126/sciadv.aav7999

61. Zhu JJ, Li X, Cai XL, Zha HY, Zhou ZW, Sun XY, et al. Arginine monomethylation by PRMT7 controls MAVS-mediated antiviral innate immunity. *Mol Cell* (2021) 81(15):3171–86.e8. doi: 10.1016/j.molcel.2021.06.004

62. Dai T, Wu LM, Wang SA, Wang J, Xie F, Zhang ZK, et al. FAF1 regulates antiviral immunity by inhibiting MAVS but is antagonized by phosphorylation upon viral infection. *Cell Host Microbe* (2018) 24(6):776–90.e5. doi: 10.1016/j.chom.2018.10.006

63. Tan GG, Yi ZH, Song HX, Xu FC, Li F, Aliyari R, et al. Type-I-IFN-Stimulated gene TRIM5γ inhibits HBV replication by promoting HBx degradation. *Cell Rep* (2019) 29(11):3551–63.e3. doi: 10.1016/j.celrep.2019.11.041

64. Xu FC, Song HX, Xiao QF, Wei Q, Pang XL, Gao YL, et al. Type-III interferon stimulated gene TRIM31 mutation in an HBV patient blocks its ability in promoting HBx degradation. *Virus Res* (2022) 308:198650. doi: 10.1016/j.virusres.2021.198650

65. Wang S, Dai T, Qin ZR, Pan T, Chu F, Lou LF, et al. Targeting liquid-liquid phase separation of SARS-CoV-2 nucleocapsid protein promotes innate antiviral immunity by elevating MAVS activity. *Nat Cell Biol* (2021) 23(7):718–32. doi: 10.1038/s41556-021-00710-0

66. Temena MA, Acar A. Increased TRIM31 gene expression is positively correlated with SARS-CoV-2 associated genes TMPRSS2 and TMPRSS4 in gastrointestinal cancers. *Sci Rep* (2022) 12(1):11763. doi: 10.1038/s41598-022-15911-2

67. Strowig T, Henao-Mejia J, Elinav E, Flavell R. Inflammasomes in health and disease. *Nature* (2012) 481(7381):278–86. doi: 10.1038/nature10759

68. Wen HT, Ting JPY, O'Neill LAJ. A role for the NLRP3 inflammasome in metabolic diseases–did warburg miss inflammation? *Nat Immunol* (2012) 13(4):352–7. doi: 10.1038/ni.2228

69. Choi AJ, Ryter SW. Inflammasomes: molecular regulation and implications for metabolic and cognitive diseases. *Mol Cells* (2014) 37(6):441–8. doi: 10.14348/molcells.2014.0104

70. Broderick L, Nardo DD, Franklin BS, Hoffman HM, Latz E. The inflammasomes and autoinflammatory syndromes. *Annu Rev Pathol* (2015) 10:395–424. doi: 10.1146/annurev-pathol-012414-040431

71. Zhao W, Shi CS, Harrison K, Hwang IY, Nabar NR, Wang M. AKT regulates NLRP3 inflammasome activation by phosphorylating NLRP3 serine 5. *J Immunol* (2020) 205(8):2255–64. doi: 10.4049/jimmunol.2000649

72. Wu XY, Lu MM, Ding S, Zhong Q. Tripartite motif 31 alleviates IL-1ß secretion *via* promoting the ubiquitination of pyrin domain domains-containing protein 3 in human periodontal ligament fibroblasts. *Odontology* (2020) 108(3):424–32. doi: 10.1007/s10266-020-00519-7

73. Huang PR, Liu WJ, Chen JQ, Hu YF, Wang YW, Sun JR. TRIM31 inhibits NLRP3 inflammasome and pyroptosis of retinal pigment epithelial cells through ubiquitination of NLRP3. *Cell Biol Int* (2020) 44(11):2213–9. doi: 10.1002/cbin.11429

74. Shen M, Pan XY, Gao YJ, Ye HY, Zhang J, Chen Y. LncRNA CRNDE exacerbates IgA nephropathy progression by promoting NLRP3 inflammasome activation in macrophages. *Immunol Invest* (2022) 51(5)1515–27. doi: 10.1080/08820139.2021.1989461

75. Wang XE, Zhang HH, Shao ZG, Zhuang WX, Sui C, Liu F, et al. TRIM31 facilitates K27-linked polyubiquitination of SYK to regulate antifungal immunity. *Signal Transduct Target Ther* (2021) 6(1):298. doi: 10.1038/s41392-021-00711-3

76. Levine B, Mizushima N, Virgin HW. Autophagy in immunity and inflammation. *Nature* (2011) 469(7330):323–35. doi: 10.1038/nature09782

77. Mizushima N, Yoshimori T, Ohsumi Y. The role of atg proteins in autophagosome formation. *Annu Rev Cell Dev Biol* (2011) 27:107–32. doi: 10.1146/annurev-cellbio-092910-154005

78. Mizushima N, Levine B, Cuervo AM, Klionsky DJ. Autophagy fights disease through cellular self-digestion. *Nature* (2008) 451(7182):1069–75. doi: 10.1038/nature06639

79. Tan P, Ye YQ, He L, Xie JS, Jing J, Ma GL. TRIM59 promotes breast cancer motility by suppressing p62-selective autophagic degradation of PDCD10. *PloS Biol* (2018) 16(11):e3000051. doi: 10.1371/journal.pbio.3000051

80. Pan X, Chen Y, Shen Y, Tantai J. Knockdown of TRIM65 inhibits autophagy and cisplatin resistance in A549/DDP cells by regulating miR-138-5p/ATG7. *Cell Death Dis* (2019) 10(6):429. doi: 10.1038/s41419-019-1660-8

81. Ra EA, Lee TA, Won Kim S, Park A, Choi HJ, Jang I, et al. TRIM31 promotes Atg5/Atg7-independent autophagy in intestinal cells. *Nat Commun* (2016) 7:11726. doi: 10.1038/ncomms11726

82. Bhaduri U, Merla G. Rise of TRIM8: A molecule of duality. *Mol Ther Nucleic Acids* (2020) 22:434–44. doi: 10.1016/j.omtn.2020.08.034

83. Li X, Song YC. Proteolysis-targeting chimera (PROTAC) for targeted protein degradation and cancer therapy. *J Hematol Oncol* (2020) 13(1):50. doi: 10.1186/s13045-020-00885-3

frontiers | Frontiers in Oncology

TYPE Original Research
PUBLISHED 06 January 2023
DOI 10.3389/fonc.2022.1046974

OPEN ACCESS

EDITED BY
Julia Kzhyshkowska,
Heidelberg University, Germany

REVIEWED BY
Saima Wajid,
Jamia Hamdard University, India
Swaroop Kumar Pandey,
Ben-Gurion University of the Negev, Israel
João Pessoa,
University of Coimbra, Portugal

*CORRESPONDENCE
Poonam Gautam
gautam.poonam@gmail.com;
poonamgautam.nip@gov.in
Puja Sakhuja
pujasak@gmail.com

SPECIALTY SECTION
This article was submitted to Molecular and Cellular Oncology, a section of the journal Frontiers in Oncology

RECEIVED 17 September 2022
ACCEPTED 13 December 2022
PUBLISHED 06 January 2023

CITATION
Akhtar J, Jain V, Kansal R, Priya R, Sakhuja P, Goyal S, Agarwal AK, Ghose V, Polisetty RV, Sirdeshmukh R, Kar S and Gautam P (2023) Quantitative tissue proteome profile reveals neutrophil degranulation and remodeling of extracellular matrix proteins in early stage gallbladder cancer. *Front. Oncol.* 12:1046974. doi: 10.3389/fonc.2022.1046974

Quantitative tissue proteome profile reveals neutrophil degranulation and remodeling of extracellular matrix proteins in early stage gallbladder cancer

Javed Akhtar[1,2], Vaishali Jain[1,3], Radhika Kansal[1], Ratna Priya[1,2], Puja Sakhuja[4]*, Surbhi Goyal[4], Anil Kumar Agarwal[4], Vivek Ghose[3,5], Ravindra Varma Polisetty[6], Ravi Sirdeshmukh[3,5], Sudeshna Kar[2] and Poonam Gautam[1]*

[1]Laboratory of Molecular Oncology, Indian Council of Medical Research (ICMR) - National Institute of Pathology, New Delhi, India, [2]Jamia Hamdard- Institute of Molecular Medicine, Jamia Hamdard, New Delhi, India, [3]Department (Nil), Manipal Academy of Higher Education (MAHE), Manipal, India, [4]Department of Pathology, Govind Ballabh Pant Institute of Postgraduate Medical Education and Research (GIPMER), New Delhi, India, [5]Institute of Bioinformatics, International Tech Park, Bangalore, India, [6]Department of Biochemistry, Sri Venkateswara College, University of Delhi, New Delhi, India

Gallbladder cancer (GBC) is an aggressive malignancy of the gastrointestinal tract with a poor prognosis. It is important to understand the molecular processes associated with the pathogenesis of early stage GBC and identify proteins useful for diagnostic and therapeutic strategies. Here, we have carried out an iTRAQ-based quantitative proteomic analysis of tumor tissues from early stage GBC cases (stage I, n=7 and stage II, n=5) and non-tumor controls (n=6) from gallstone disease (GSD). We identified 357 differentially expressed proteins (DEPs) based on ≥ 2 unique peptides and ≥ 2 fold change with p value < 0.05. Pathway analysis using the STRING database showed, 'neutrophil degranulation' to be the major upregulated pathway that includes proteins such as MPO, PRTN3, S100A8, MMP9, DEFA1, AZU, and 'ECM organization' to be the major downregulated pathway that includes proteins such as COL14A1, COL1A2, COL6A1, COL6A2, COL6A3, BGN, DCN. Western blot and/or IHC analysis confirmed the elevated expression of MPO, PRTN3 and S100A8 in early stage of the disease. Based on the above results, we hypothesize that there is an increased neutrophil infiltration in tumor tissue and neutrophil degranulation leading to degradation of extracellular matrix (ECM) proteins promoting cancer cell invasion in the early stage GBC. Some of the proteins (MPO, MMP9, DEFA1) associated with 'neutrophil degranulation' showed the presence of 'signal sequence' suggesting their potential as circulatory markers for early detection of GBC. Overall, the study presents a protein dataset associated with early stage GBC.

KEYWORDS

gallbladder cancer, early stage, neutrophil degranulation, tissue proteomics, iTRAQ

1 Introduction

Gallbladder cancer (GBC) is the fifth most common and aggressive malignancy of the gastrointestinal tract, with a marked geographical variation in its incidence. There are two major groups of high-risk populations for GBC, in Latin America (Chile, US Native Americans, Mexicans) and in Asia (Northern India, Pakistan, Korea, Japan and China) (1, 2). Among the Asian countries, GBC has the highest prevalence and incidence rate in northern and northeast India (1, 3, 4). Gallstone disease (GSD) cases and female population are at high risk for GBC (5). GBC is generally diagnosed at an advanced stage due to its anatomic position and non-specific symptoms. Imaging techniques and the available blood tests (CEA, CA19-9) are generally employed for the diagnosis of GBC, however, the detection of the disease at early stage remains a challenge. The treatment includes extended resection in combination with chemotherapy, radio-therapy and targeted therapy (6).

In early stage GBC (Stage I and II), the tumor is restricted to the gallbladder while in advanced stages (Stages III and IV), the tumor invades beyond the gallbladder serosa to the liver or other nearby structures *via* direct invasion or lymphatic, peritoneal and hematogenous dissemination (7). Application of high throughput approaches to understand the molecular profile of 'early stage GBC' is important to identify 'tumor-associated proteins' and associated molecular pathways which may be useful as new diagnostic markers and therapeutic targets.

There are several studies on genetic, epigenetic and transcript analysis of tumor tissues and cell lines to understand the molecular changes associated with GBC (8–10). p53 mutation, mitochondrial DNA mutation, cyclooxygenase-2 (COX2) overexpression, methylation of tumor suppressor gene (TSG) promoters and/or KRAS mutations have been reported to be associated with the development of GBC (2, 11). Various groups have applied high-throughput proteomic approaches to study altered expression levels of proteins in tumor tissue from GBC patients. Tan et al. studied protein expression profiles of benign and GBC tissue using two-dimensional gel electrophoresis (2-DE) and identified 17 differentially expressed proteins (DEPs) (12, 13). The proteomic patterns of primary gallbladder cancer (PGC) in comparison to cholecystitis and normal gallbladder tissues using 2-DE revealed six DEPs (14). Another group applied iTRAQ-based quantitative proteomics using pooled GBC tissue lysate and identified 512 DEPs (15). However, the proteomic analysis using tumor tissue from early stage GBC is not yet performed.

In the present study, we have applied iTRAQ-based quantitative proteomic analysis to identify DEPs in early stage GBC in comparison to GSD (non-tumor controls) followed by verification of functionally relevant proteins by Western blot and IHC analysis.

2 Materials and methods

2.1 Clinical samples

Adult patients with age ≥ 20 years diagnosed with GBC or GSD cases (non-tumor control) visiting Govind Ballabh Pant Institute of Postgraduate Medical Education and Research (GIPMER), New Delhi, were recruited for the study. Clinical samples and data were also obtained from National Liver Disease Biobank- Institute of Liver and Biliary Sciences (NLDB-ILBS), New Delhi, India, after approval from the Maulana Azad Medical College- Institutional Ethics Committee, New Delhi (F.1/IEC/MAMC/80/08/2020/No. 314) and ICMR-National Institute of Pathology- Institutional Ethics Committee, New Delhi (NIP-IEC/10-12-19/06). All the participants provided written informed consent to participate in the study. Tumor Staging was done on the basis of clinical data of patients, histopathological evaluation and imaging tools, as per AJCC, 8th edition staging system (7). Tissue samples from GBC cases (n=12) and GSD cases with no dysplasia (n=6) were used in this study. Tissue samples were collected immediately after surgical resection from patients with GBC or GSD and stored at -80° C until used for further analysis. Formalin fixed paraffin embedded (FFPE) tissue samples were used for 'immunohistochemistry' (IHC) analysis. Clinico-pathological data of these subjects are detailed in Table 1. Clinical parameters for the patients, wherever available (~50%), such as white cell count, liver enzymes (SGOT/SGPT/ALP) and cholestasis, and details of the sample used for quantitative proteomics and/or Western blot and/or IHC analysis are shown in Supplementary data Table S1.

2.2 Protein extraction

Tissue from individual cases (tumor tissue from GBC patients) or controls (GB tissue from GSD cases) was ground in liquid nitrogen followed by the addition of modified RIPA buffer with a 2% protease inhibitor cocktail. The tissue homogenate was then sonicated and centrifuged at 13,000 g for 20 min at 4°C. The supernatant was collected and protein estimation was done using the Bradford assay. SDS-PAGE was performed to analyze the protein profile of the tissue lysate from different groups and normalized the protein concentration based on total density.

2.3 iTRAQ labeling

For iTRAQ experiments, a pool of GSD tissue lysate (n=6) was used as a control while individual tissue lysate from GBC cases (n=7 for stage I and n=5 for stage II) was used for the analysis. For this, two iTRAQ experiments were performed. Experiment I included

TABLE 1 Clinico-pathological parameters of the patients used for the study.

Subjects	Total number	Number of males	Number of females	Mean age (Years)	Age range (years)
Total GBC Cases	24	5	19	51.5	27-65
Stages					
GBC, Stage I	8	3	5	51.5	38-65
GBC, Stage II	6	0	6	56.8	36-65
GBC, Stage III	6	2	4	42.7	27-65
GBC, Stage IV	4	0	4	56.8	47-61
Histological grade					
Well-differentiated (G1)	5	2	3	—	—
Moderately-differentiated (G2)	10	2	8	—	—
Poorly-differentiated (G3)	8	1	7	—	—
LN status					
LN negative	20	3	17	—	—
LN positive	4	2	2	—	—
Controls- GSD	16	2	14	46.6	24-68

pooled GSD vs individual GBC cases (stage I) while Experiment II included pooled GSD vs individual GBC cases (stage II). The experimental design is shown in Supplementary Figures S1, S2.

For Experiment I, proteins (100 µg) from control (n=6, pooled sample) and GBC stage-I (n=7, individual samples) were reduced, alkylated and digested with trypsin followed by labeling of peptides with 8-plex iTRAQ reagents separately with specific iTRAQ labels (Reagent 113, 114, 115, 116, 117, 118, 119 and 121) as per the manufacturer's instructions (iTRAQ Reagents Multiplex kit; Applied Biosystems). The labeled samples were pooled vacuum-dried and subjected to strong cation exchange (SCX) clean up (Cation exchange cartridge, Sciex, US), and desalted using a C18 column (Zorbax 300SB-C18, Agilent Technologies, US) as per the manufacturer's instructions. The samples were then vacuum-dried and used for mass spectrometric analysis (nano-LC MS/MS analysis).

Similarly, for Experiment II, proteins (100 µg) from control (n=6, pooled samples) and GBC stage-II (n=5, individual samples) were reduced, alkylated and subjected to trypsin digestion and the peptides were labeled with 6-plex iTRAQ reagents separately with specific iTRAQ labels (Reagent 113, 114, 115, 116, 117 and 118) as mentioned above. The same pool of GSD samples was used as a control in both the iTRAQ experiments. The labeled samples were pooled vacuum-dried and subjected to SCX clean up and desalted using a C18 column followed by nano-LC MS/MS analysis.

2.4 LC-MS/MS analysis

Nanoflow electrospray ionization tandem mass spectrometric analysis was carried out using Orbitrap Fusion (Thermo Scientific, Bremen, Germany) interfaced with Easy-nLC 1000 nanoflow LC system. Peptides from each sample were enriched using a C18 trap column (75 µm × 2 cm) at a flow rate of 3 µl/min and fractionated on an analytical column (75 µm × 50 cm) at a flow rate of 280 nl/min using a linear gradient of 8-60% acetonitrile (ACN) over 46 min. Mass spectrometric analysis was performed in a data dependent manner with a cycle time of 3 seconds using the Orbitrap mass analyzer at a mass resolution of 120,000 at m/z 200. For each MS cycle, top most intense precursor ions were selected and subjected to MS/MS fragmentation and detected at a mass resolution of 50,000 at m/z 200. The fragmentation was carried out using higher-energy collision dissociation (HCD) mode. Normalized collision energy (CE) of 30% was used to obtain the release of reporter ions from all peptides detected in the full scan. The ions selected for fragmentation were excluded for the next 30 sec. The automatic gain control for full FT MS and FT MS/MS was set to $3e^6$ ions and $1e^5$ ions respectively with a maximum time of accumulation of 50 msec for MS and 75 msec for MS/MS. The lock mass with a 10 ppm error window option was enabled for accurate mass measurements (16). The LC-MS/MS analysis was performed three times for both experiments (I and II).

2.5 Identification and quantification of proteins

Protein identification, quantification and annotations of DEPs were carried out as described earlier by Priya et al. (16). The MS/MS data was analyzed using Proteome Discoverer

(Thermo Fisher Scientific, version 2.2) with Mascot and Sequest HT search engine nodes using NCBI RefSeq database (release 89). Search parameters included trypsin as the enzyme with 2 missed cleavage allowed; precursor and fragment mass tolerance were set to 10 ppm and 0.1 Da, respectively; Methionine oxidation and deamidation of asparagines and glutamine amino acids was set as a dynamic modification while methylthio modification at cysteine and iTRAQ modification at N-terminus of the peptide and lysines were set as static modifications. The peptide and protein information was extracted using high peptide confidence and top one peptide rank filters. The FDR was calculated using percolator node in proteome discoverer 2.2. High confidence peptide identifications were obtained by setting a target FDR threshold of 1% at the peptide level. The labeling efficiency was > 95% for both the iTRAQ experiments (Stage I and II).

The iTRAQ intensity of proteins from each of the three replicates was used for the PCA plot analysis (17) to determine the correlation among the triplicate dataset as well as the correlation of GSD vs individual GBC stage I or stage II proteome dataset.

Relative quantitation of proteins was carried out based on the intensities of reporter ions released during MS/MS fragmentation of peptides. The proteins identified in all three replicates were used for the analysis. The average relative intensities of the two reporter ions for each of the unique peptide identifiers for a protein were used to determine the relative quantity of a protein and percentage variability. Proteins identified with ≥ 2 unique peptides, with 2-fold-change or above and FDR adjusted p value < 0.05 were considered significant and used for further analysis (16). The volcano maps were prepared by using log2 fold change and -log10 (p-value) as the co-ordinates and significant fold change ≥ 2.0 and p-value < 0.05 were considered to screen the proteins.

The data was analyzed for DEPs in individual patient with stage I or stage II and represented as Venn diagram. Further, the non-redundant list of DEPs in early stage GBC was derived and used for bioinformatics analysis.

2.6 Transcriptomics data comparison

We have compared the non-redundant list of DEPs from our study with the published transcriptome data in GBC (18–21). The proteins showing a positive correlation in their expression levels with transcriptome data are represented as scatter plot.

2.7 Bioinformatic analysis

Mapping of DEPs in early stage GBC (non-redundant list of DEPs from stage I and II) for localization, associated molecular functions, pathways and protein-protein interaction analysis was performed using the STRING (Search Tool for the Retrieval of Interacting Genes/Proteins) database (22). Signal sequence was predicted using SignalP software version 6.0 (https://services.healthtech.dtu.dk/service.php?SignalP) (23). From the non-redundant list of DEPs, the proteins with quantitation values for all 12 GBC patients were used for hierarchical clustering using Perseus software (17).

2.8 Western blot analysis

Western blot analysis was performed to further confirm the expression of myeloperoxidase precursor (MPO), myeloblastin precursor (PRTN3) and protein S100-A8 isoform d (S100A8) in the tissue lysates from individual GBC and GSD specimens (GBC stage I, n=7; GBC stage II, n=5; GSD, n=6). Briefly, tissue lysates were resolved on 12% SDS gel and transferred onto the PVDF membrane. Non-specific sites were blocked using 5% skimmed milk followed by incubation with primary antibody overnight (MPO, catalogue no. ab208670, dilution 1:4000; PRTN3, catalogue no. ab133613, dilution 1:10,000; S100A8, catalogue no. ab92331, dilution 1:2000). The blots were then incubated with secondary antibody (anti Rabbit-HRP, catalogue no. G-21234, 1/20,000) for 1 hr at RT and developed using the enhanced chemiluminescent (ECL) Kit (Millipore, USA) followed by image acquisition (24). The total density of the proteins in each lane was analyzed using densitometric analysis after SDS-PAGE analysis and was used for normalization (24). For quantitative analysis, the maximum density among GSD cases was considered to define the fold change in expression in individual GBC cases. The relative expression of target proteins in the individual GBC cases in Western blot analysis and quantitative proteomics data was represented as a bar diagram using Log2 fold change values.

2.9 Immunohistochemistry analysis

IHC was performed on FFPE tissues using individual tissue sections from controls (GSD cases), early stage GBC and advanced GBC cases (n=10 in each group) (Supplementary Table S1) to analyze the expression of MPO and S100A8 protein. IHC analysis was performed as described earlier by Akhtar et al. (25). In brief, after deparaffinization and rehydration of FFPE tissue sections, antigen retrieval was performed by immersing the slide in antigen retrieval buffer (20 mM Tris buffer, pH 9.0) at 90°C for 20 min. Endogenous peroxidases were blocked with 0.03% hydrogen peroxide, and nonspecific binding was blocked with protein blocking reagent. Sections were then incubated for 1 h at RT with primary antibody against MPO (dilution 1:8000, catalogue no. ab208670, Abcam, USA) and S100A8 (dilution 1:2000, catalogue no. ab92331) followed by incubation with PolyExcel

PolyHRP for 40 minutes at RT. Tissue sections were then incubated with Stunn DAB working solution for 5 min at RT (PathnSitu Biotechnologies, USA). Sections were counter stained with Mayer's hematoxylin, dehydrated and images were taken under the microscope. The distribution of staining and staining intensity across the section was observed under the microscope. For MPO, the number of neutrophils was counted and ≥20 was considered as 'Positive', while <20 was considered as 'Negative'. For S100A8, scoring criteria were based on both staining intensity and distribution. The 2+ or higher intensity, with ≥10% distribution was considered as 'Positive', while 1+ positivity or < 10% distribution was considered as 'Negative'. IHC data analysis was done by two independent pathologists.

The statistical analysis (Fisher's exact test) was performed using GraphPad Prism 5 (26) to study the correlation of MPO and S100A8 expression among cases and controls (early stage GBC vs controls; advanced stage vs controls; all GBC vs controls). The *p*-value less than 0.05 indicated statistical significance.

3 Results

In the present study, we performed the differential protein profiling of tumor tissue from early stage GBC cases to identify the proteins and associated molecular pathways. The overall work plan of the study is shown in Figure 1.

3.1 Identification of differentially expressed proteins in early stage GBC

We performed iTRAQ based LC-MS/MS analysis of 12 early stage GBC patients (stage I-n=7, stage II- n=5) using two independent experimental setups. The experimental setup-1 consists of 7 GBC - stage I samples vs pooled GSD samples while the experimental setup-2 consists of 5 GBC -stage II samples vs pooled GSD samples (Figure 1, Supplementary Figure S1, S2). The analysis led to the identification of a total of 1450 proteins from stage I and 2662 proteins in stage II. PCA plot analysis of the proteome profile of 12 GBC patients along with GSD control showed a significant correlation among the three replicate datasets of each stage (Figure 2). We found 184 DEPs with ≥ 2 fold change and adjusted p-value ≤0.05 in GBC stage I (Supplementary Table S2) while a total of 256 DEPs with ≥ 2 fold change and adjusted p-value ≤0.05 were identified in GBC stage II (Supplementary Table S3).

We analyzed the DEPs across individual patients and the data is represented as Volcano plots in Supplementary Figure S3. The analysis showed a total of 357 DEPs (non-redundant) in early stage GBC (stage I and II). We further compared our proteomics data with the published transcriptome data in GBC and found 97 proteins mapping with the transcriptome data. Of these, 71 proteins (73%) showed a positive correlation with transcript data. The proteins showing positive correlation are represented in Supplementary Figure S4.

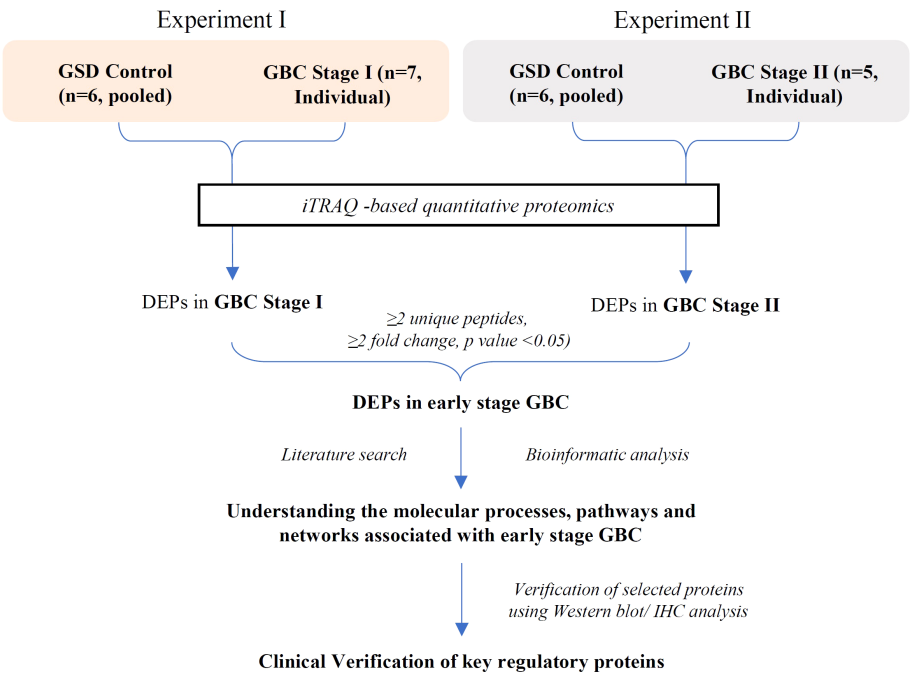

FIGURE 1
Overall workflow of the study. GSD, Gallstone disease; GBC, Gallbladder cancer; DEPs, Differentially expressed proteins.

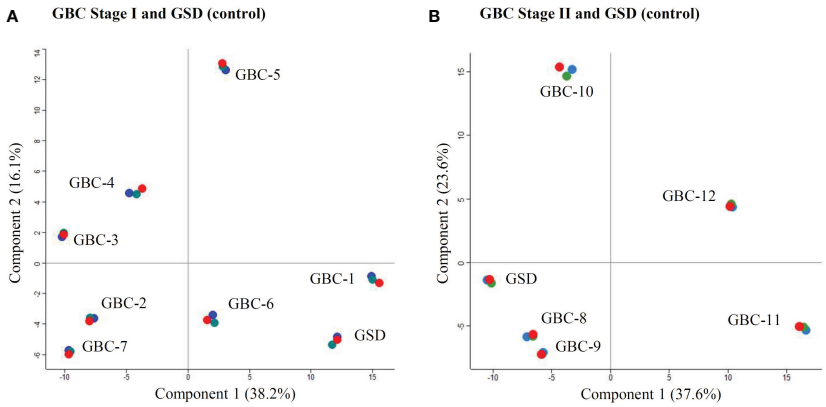

FIGURE 2
PCA Plot showing the correlation of the individual patients with GBC stage I and II. **(A)** includes seven individual samples from GBC stage I and one pooled GSD control while **(B)** includes five individual samples from GBC stage II along with one pooled GSD control. Four patients, two from stage I (GBC-1 and 6) **(A)** and two from stage II (GBC-8 and 9) **(B)** showed similar profile as GSD (non-tumor control). The technical replicates showed a significant correlation. Replicates R1, R2 and R3 are shown in red, green and blue color. The PCA plot is derived using the iTRAQ reporter intensity from the quantitative proteomics data.

Out of 357 DEPs, a total of 83 proteins are common to both stage I and II, while 101 proteins are specific to stage I and 173 proteins are specific to stage II (Figure 3, Supplementary Table S4). Out of 83 DEPs, the majority of the proteins (~95%) showed a similar trend (up or down) of expression in both stages. A total of 29 proteins were found to be differentially expressed in ≥ 50% GBC cases (i.e. 6 patients) and are shown in Table 2. Some of the functionally relevant proteins include Myeloperoxidase precursor (MPO), Myeloblastin precursor (PRTN3), Neutrophil defensin 1 isoform X1 (DEFA1), Protein S100-A8 isoform d (S100A8), Desmin (DES), creatine kinase B-type isoform 2 (CKB), Transgelin (TAGLN), Annexin A3 (ANXA3).

3.2 Signal sequence analysis and literature survey

The Signal sequence analysis of 357 proteins showed 109 proteins with a signal sequence. Literature survey showed a total of 106 proteins that are reported to be differentially abundant in plasma or serum in cancer. Overall, we found 51 proteins to have signal sequence as well as reported to be differentially abundant in plasma or serum in cancer (Supplementary Figure S5, Supplementary Table S5). These proteins are potential circulatory markers for the detection of GBC

3.3 Bioinformatic analysis

A gene ontology analysis for the localization of 357 DEPs showed that 54.3% of them belong to the cytoplasm, 18.8% are from the extracellular region, 13.7% are associated to the nucleus, 12.6% are from the plasma membrane and less than 1% are associated with other localization (Figure 4A). The top molecular functions include Opsonin binding, MHC class II protein complex binding, Lipase inhibitor activity, Lipoprotein particle receptor binding and MHC class I protein binding (Figure 4B, Supplementary Table S6). Pathway analysis using 191 upregulated

FIGURE 3
Venn diagram showing DEPs in early stage GBC. A total of 83 proteins are common to both stage I and II, while 101 proteins are specific to stage I and 173 proteins are specific to stage II. The details of all the proteins are shown in Supplementary Table S4.

TABLE 2 A list of 29 DEPs in ≥ 6 early stage GBC patients.

	GBC Stage I							GBC Stage II							
Gene Symbol	GBC-1	GBC-2	GBC-3	GBC-4	GBC-5	GBC-6	GBC-7	GBC-8	GBC-9	GBC-10	GBC-11	GBC-12	No. of GBC stage I patients with DE	No. of GBC stage II patients with DE	No. of early stage GBC patients with DE
ALB	1.25	**0.41**	**0.21**	**0.29**	0.87	**0.44**	**0.40**	**0.46**	**0.40**	0.65	**0.18**	0.53	5	3	8
ANXA3	1.44	**2.60**	**3.76**	**3.91**	2.43	1.23	**2.45**	1.19	1.04	**2.71**	**2.30**	**2.51**	4	3	7
AOC3	0.69	**0.24**	**0.29**	**0.21**	**0.26**	**0.42**	**0.18**	0.72	1.56	0.35	**0.29**	**0.28**	5	2	7
BGN	1.21	**0.40**	**0.39**	**0.47**	**0.29**	0.72	**0.38**	1.06	0.93	0.42	**0.44**	**0.34**	5	2	7
CKB	**0.41**	**0.46**	**0.35**	**0.42**	**0.26**	**0.29**	**0.39**	**0.47**	0.88	0.51	**0.42**	**0.29**	7	3	10
COL6A1	1.29	0.41	0.37	**0.38**	**0.27**	**0.43**	**0.38**	**2.64**	1.12	0.54	0.72	**0.41**	4	2	6
DCN	**2.06**	**0.29**	**0.26**	**0.29**	**0.27**	0.73	**0.29**	0.62	1.42	0.48	**0.30**	**0.30**	6	2	8
DEFA1	2.61	**3.61**	**10.42**	**2.59**	4.62	2.16	4.01	**3.62**	0.94	**4.95**	**4.54**	**3.12**	3	4	7
DES	0.40	**0.09**	**0.09**	**0.08**	**0.07**	**0.09**	**0.08**	**0.48**	**0.27**	0.12	**0.10**	**0.09**	6	4	10
FLNA	0.66	**0.47**	**0.40**	**0.39**	**0.35**	0.71	**0.47**	0.93	0.56	0.33	**0.34**	**0.37**	5	2	7
HBB	0.70	**0.31**	**0.26**	1.30	0.79	**0.42**	**0.48**	0.57	**0.50**	**7.28**	**0.50**	0.52	4	3	7
HSP90B1	0.64	**2.60**	2.22	1.86	1.09	**3.24**	**2.40**	1.68	**2.15**	1.07	**2.06**	**2.11**	3	3	6
HSPA5	0.97	**2.52**	**2.26**	**2.13**	1.16	**2.46**	**2.19**	1.49	1.71	1.11	**2.03**	1.73	5	1	6
HSPE1	0.80	**3.02**	**3.50**	**3.35**	1.42	1.51	**2.54**	0.98	1.26	1.04	**4.45**	**3.37**	4	2	6
KRT18	**0.48**	1.18	**3.18**	**2.65**	1.41	0.48	**2.43**	**0.45**	**0.43**	0.33	0.69	1.58	4	2	6
KRT8	0.61	**2.24**	**3.61**	**2.09**	1.30	**0.42**	1.93	**0.44**	**0.41**	0.40	0.96	1.87	4	2	6
LUM	1.89	**0.17**	**0.15**	**0.31**	**0.20**	0.84	**0.17**	0.55	1.52	0.42	**0.20**	**0.23**	5	2	7
MPO	2.53	**2.57**	**6.15**	**2.60**	**10.27**	1.60	**2.97**	**2.78**	1.28	2.82	**3.09**	1.16	5	2	7
MYL6	0.80	**0.30**	**0.27**	**0.49**	**0.37**	0.58	**0.28**	0.67	1.03	0.25	**0.46**	**0.38**	5	2	7
MYL9	0.61	**0.18**	**0.14**	**0.23**	**0.12**	**0.39**	**0.14**	0.57	0.98	0.16	**0.18**	**0.15**	6	2	8
P4HB	0.99	**2.53**	**3.83**	**2.43**	1.53	**2.94**	**3.53**	1.23	1.23	0.95	1.31	**2.93**	5	1	6
PRELP	1.45	**0.21**	**0.19**	**0.22**	0.27	**0.45**	0.20	1.16	1.56	0.47	**0.25**	**0.31**	5	2	7
PRTN3	3.59	**11.49**	**30.01**	**13.09**	16.06	2.94	**7.52**	**2.82**	1.45	**16.93**	**2.40**	**2.23**	4	4	8
S100A8	3.43	**3.51**	**4.97**	2.12	**6.96**	**2.49**	**4.66**	**2.80**	0.81	1.99	**2.25**	1.42	5	2	7

(Continued)

10.3389/fonc.2022.1046974

TABLE 2 Continued

Gene Symbol	GBC Stage I							GBC Stage II							No. of GBC stage I patients with DE	No. of GBC stage II patients with DE	No. of early stage GBC patients with DE
	GBC-1	GBC-2	GBC-3	GBC-4	GBC-5	GBC-6	GBC-7	GBC-8	GBC-9	GBC-10	GBC-11	GBC-12					
SERPINA1	0.37	**0.25**	**0.28**	**0.41**	0.89	1.12	**0.43**	**0.29**	0.62	0.75	**0.26**	0.66			4	2	6
SOD2	1.03	**2.75**	**2.91**	**11.37**	1.53	**5.06**	**2.31**	1.60	**2.05**	1.07	1.25	**2.99**			5	2	7
TAGLN	0.75	**0.17**	**0.14**	**0.15**	**0.13**	0.54	**0.20**	0.80	0.74	**0.29**	**0.15**	**0.19**			5	3	8
TPM2	**0.41**	**0.12**	**0.08**	**0.11**	**0.09**	**0.27**	**0.12**	0.56	1.13	0.22	**0.19**	**0.20**			7	2	9
TPSAB1	0.82	**0.28**	**0.20**	**0.21**	**0.17**	**0.47**	**0.22**	0.77	0.98	**0.30**	**0.19**	**0.23**			6	3	9

The proteins marked in bold are DE with 2 fold change, adjusted p value < 0.05 and identified with ≥ 2 unique peptides. ND- Not detected, DEPs- Differentially expressed proteins.

proteins showed 'Neutrophil degranulation' among the top upregulated pathway (Figure 4C, Supplementary Table 7A) while the analysis using 62 downregulated proteins showed 'ECM organization' to be the top downregulated pathway (Figure 4D, Supplementary Table 7B).

Protein-protein interaction analysis of 29 proteins (DE in ≥ 6 patients) revealed three clusters which include the proteins associated with neutrophil degranulation (MPO, DEFA1, S100A8, PRTN3, AOC3), ECM proteins (COL6A1, BGN, DCN, LUM, PRELP) and cytoskeletal or intermediate filament (DES, MYL6, MYL9, TPM2) (Figure 5).

We also performed the pathway analysis using the DEPs across individual patients and obtained the data for 10 out of 12 patients. 'Neutrophil degranulation' was among the top pathways in 9 patients (Supplementary Table S8). The data for two patients was not obtained as the number of DEPs was low.

A hierarchical clustering analysis done using a non-redundant list of 308 proteins with quantitation value for all the 12 patients showed two distinct clusters or groups on the basis of their molecular profile (Figure 6A). The majority of Stage I and II samples were clustered and represented as Cluster A and B respectively. Among 308 proteins, we observed keratin family proteins (KRT7, KRT8, KRT18 and KRT19) to be upregulated in cluster A and downregulated in cluster B (Figure 6B).

3.4 Validation of target protein expression by western blot and immunohistochemistry analysis

We selected three proteins (MPO3, PRTN3 and S100A8) based on their association with 'neutrophil degranulation pathway' and 'overexpression in ≥6 patients in quantitative proteomics data' for validation by Western blot analysis. Their relative expression (log2 fold change) in individual patients from the quantitative proteomics dataset is shown in Figure 7. Western blot analysis was performed using individual tissue lysates and showed overexpression of MPO, PRTN3 and S100A8 in early stage GBC cases and GSD controls. Both MPO and PRTN3 showed significant overexpression in 66.7% (n=8/12) of the GBC cases whereas there was a weak or no signal observed in GSD. The protein S100A8 showed significant overexpression in 83.3% (n=10/12) of the GBC cases in comparison to GSD. Western blot image is shown in Figure 8 and full-length blot image is shown in Supplementary Figure S6. The relative expression of selected proteins in the individual GBC cases using Western blot analysis and quantitative proteomics data is shown in Supplementary Figure S7.

We performed IHC analysis to study the expression of two of the proteins, MPO and S100A8 in controls, early stage GBC and advanced stage GBC (n=10 in each group). Figure 9A shows the representative IHC images of controls, early stage GBC and advanced stage GBC. The number of MPO positive neutrophils was found to be 'positive' in 50% of early stage GBC and 30% of

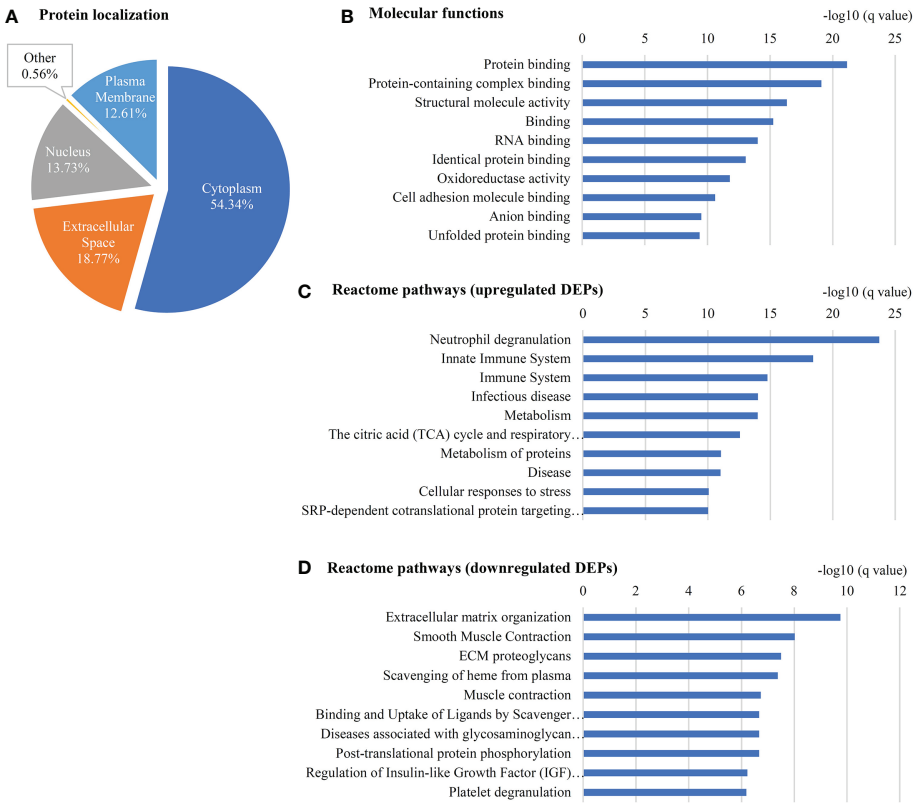

FIGURE 4
Gene ontology of 357 DEPs in early stage GBC. **(A)** Localization of **(B)** Molecular functions **(C)** Reactome pathways using upregulated proteins and **(D)** downregulated proteins as observed using STRING database.

advanced stage GBC cases. All GSD cases showed 'negative' expression. The expression of S100A8 was found to be 'positive' in 10% GSD cases, 60% early and 50% advanced stage GBC. The statistical analysis between cases and controls showed a significant difference (p value ≤0.05) of MPO positive neutrophils in early stage GBC vs controls and all GBC vs controls while a significant difference of S100A8 was observed in all GBC vs controls (Figure 9B). The controls (≥ 90%) showed 'Negative' expression levels. We performed IHC analysis for PRTN3, however, the results were not clear due to technical reasons.

4 Discussion

GBC is generally diagnosed at advanced stages and has a poor prognosis. The detection of the disease at the early stage may significantly improve the treatment strategy and survival outcome of the patients. There are few studies applying high throughput proteomics approach to understand the molecular processes in GBC (12–15), however, none of these focused on early stage GBC. The present study applied iTRAQ-based quantitative proteomics approach and analyzed the differential proteome in early stage GBC (stage I and II). The data from both the stages were combined to obtain a non-redundant list of DEPs. The correlation of expression between these DE proteins (our study) and DE transcript dataset in GBC available in the public domain was analyzed. Further, gene ontology analysis was carried out to identify the significantly altered pathways. Based on the pathway analysis, we propose a hypothesis on the dysregulated molecular processes/events in early stage GBC. We then analyzed the proteins for the presence of 'signal sequence' to identify those having the potential for early detection of GBC.

The present study identified a non-redundant list of 357 DEPs in early stage GBC, of these, 68 proteins are reported earlier in GBC including KRTs (KRT7, KRT8, KRT18 KRT19, KRT20), VIM, DES, CEACAM5 or CEA, S100A8, TAGLN, HMGB1, ANXA3, while others are novel to GBC. A total of 272 proteins are reported to be differentially expressed in other cancers and 17 are novel. Comparison with the already published transcriptome dataset showed 97 proteins mapping with the transcriptome data, of which 71 proteins (73%) showed a positive correlation in expression. Pathway analysis showed 'neutrophil degranulation' to be the top upregulated pathway and 'ECM organization' to be the top downregulated pathway in early stage GBC. The individual patient data analysis showed 29 DEPs in ≥ 50% of GBC cases (≥ 6 patients) (Table 2). Some of the proteins associated with neutrophil degranulation such as

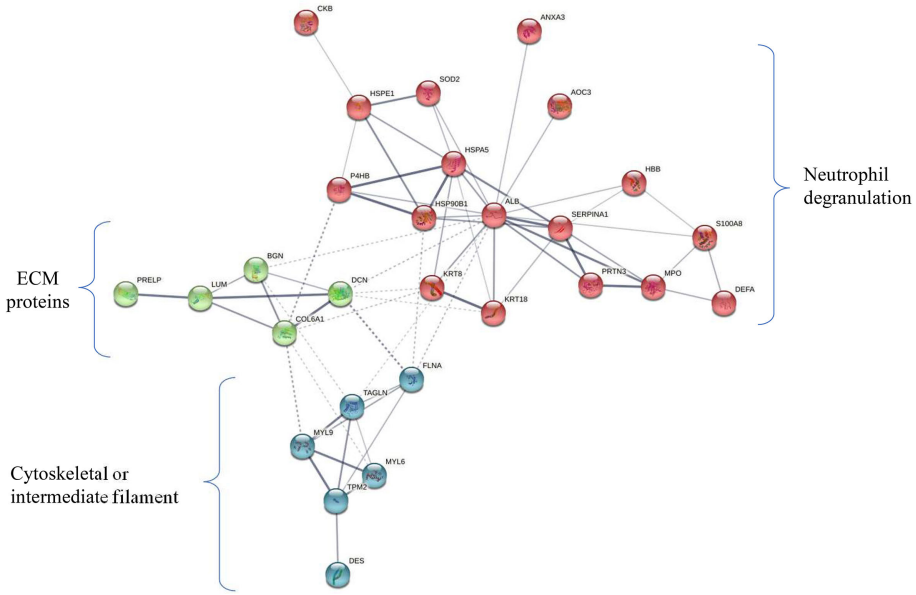

FIGURE 5
Protein-protein-interaction (PPI) network of 29 deregulated proteins. PPI analysis showed four clusters including majorly the proteins associated with neutrophil degranulation (MPO, DEFA1, S100A8, PRTN3, AOC3) (marked in red), ECM proteins (COL6A1, BGN, DCN, LUM, PRELP) (green), cytoskeletal or intermediate filament (DES, MYL6, MYL9, TPM2) (blue). The subset of 29 proteins showed differential expression in ≥ 50% of early stage GBC (i.e. ≥ 6 patients).

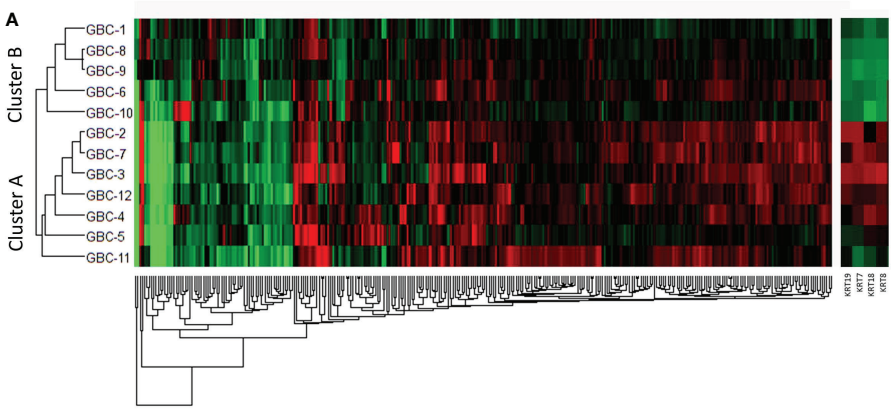

B

	Cluster A							Cluster B				
	GBC-2	GBC-3	GBC-4	GBC-5	GBC-7	GBC-11	GBC-12	GBC-1	GBC-6	GBC-8	GBC-9	GBC-10
KRT7	**3.10**	**2.72**	1.74	0.81	**2.86**	0.51	1.53	0.64	0.53	**0.48**	**0.39**	0.52
KRT8	**2.24**	**3.61**	**2.09**	1.30	1.93	0.96	1.87	0.61	**0.42**	**0.44**	**0.41**	0.40
KRT18	1.18	**3.18**	**2.65**	1.41	**2.43**	0.69	1.58	**0.48**	0.48	**0.45**	**0.43**	0.33
KRT19	**2.96**	**2.93**	1.14	0.79	1.41	0.98	**2.02**	0.72	**0.47**	0.54	**0.48**	0.54

FIGURE 6
Hierarchical clustering using non-redundant list of 308 DE proteins in 12 early stage GBC patients. **(A)** Hierarchical clustering showed two clusters with cluster A majorly including stage I samples and cluster B majorly including stage II samples. **(B)** We observed cytokeratins KRT7, KRT8, KRT18 and KRT19 showing upregulation in Cluster A and downregulation in Cluster B. Log2 (fold change) values for 308 proteins were used for the analysis. Red- Upregulated, Green- Downregulated.

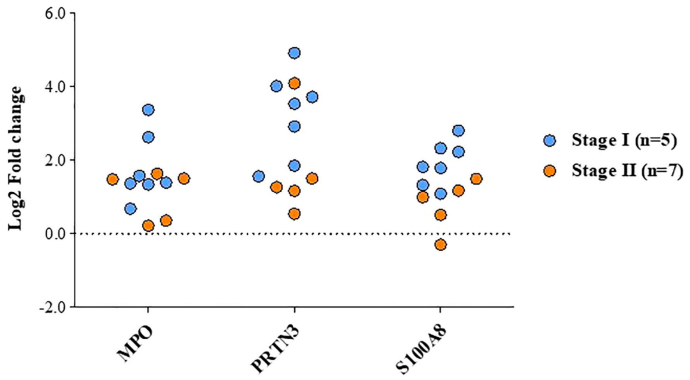

FIGURE 7
Altered levels of functionally relevant proteins in early stage GBC as observed in quantitative proteomics data. The plot showing the levels of MPO, PRTN3 and S100A8 in individual patients, GBC stage-I (n=7) and stage-II (n=5).

MPO, MMP9, DEFA1 showed the presence of 'signal sequence' and could be the potential circulatory markers for early detection of GBC.

Immune cell infiltration (neutrophils, macrophages) is well reported in several cancers. Neutrophils are associated with cancer-related inflammation with a dual role in pro and anti-tumor effects (27). In different types of cancer, neutrophils have been reported to have pro-tumorigenic properties *via* DNA damage, immunosuppression and angiogenesis, which contribute to the progression of the disease in the tumor microenvironment (TME) (28). We found overexpression of PRTN3 (proteomics data) which is reported to be associated with neutrophil trans-endothelial migration to the tissue (29). We observed an overexpression of neutrophil intracellular marker protein (MPO) and cell surface marker proteins (CEACAM8, ITGAM and ITGB2) in early stage GBC in comparison to GSD (non-tumor controls) suggesting neutrophil infiltration in tumor tissue. Increased expression of CEACAM8, ITGAM and ITGB2 is reported to be associated with exocytosis or degranulation of primary, secondary and tertiary neutrophil granules respectively. We also found overexpression of various neutrophil granule proteins including primary granule (Azurophil) proteins such as AZU1, DEFA1, PRTN3, CD63, CTSG, ELANE, MPO, secondary granule proteins such as LCN2, LTF, tertiary granules (Gelatinase) such as MMP9 and other granule proteins such as S100A8 and S100A9, in the early stage GBC (our proteomics data). As per the HPA data, AZU1, DEFA1, PRTN3, CTSG, ELANE, MPO, LTF, MMP9, S100A8 and S100A9 are bone marrow and lymphoid tissue specific or enriched proteins suggesting that the expression of these proteins detected in our data is from immune cells.

MPO is a member of the heme peroxidase superfamily and is the most abundant protein expressed by neutrophils. It is reported to generate reactive oxygen species (ROS) leading to DNA damage and mutation inducing carcinogenesis and thus resulting in tissue damage (30). PRTN3 is a serine protease secreted by cells of myeloid lineage and allocated to the cell surface of neutrophils and endothelial cells. It has an elastase-like specificity for small aliphatic residues such as Ala, Val, Ser, Met and degrades various ECM proteins and known to activate MMP and is associated with tumor invasion and metastasis (31). S100A8 is a calcium-binding S100 protein secreted by granulocytes and monocytes. S100A8 has emerged as an inflammatory factor and is associated with cancer. S100A8 overexpression is associated with tumorigenesis and poor

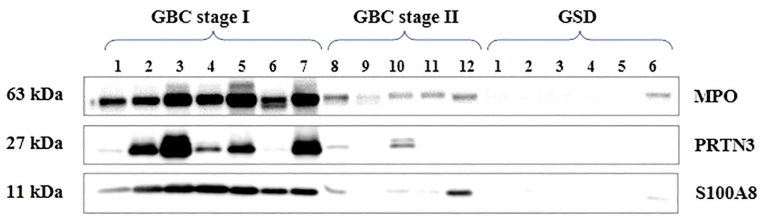

FIGURE 8
Western blot images showing expression of MPO, PRTN3, S100A8 in the individual tissue samples from early stage GBC and GSD cases. A significant overexpression of MPO, PRTN3, S100A8 was found in 66.7% (n=8/12), 66.7% (n=8/12) and 83.3% (10/12) early stage GBC cases respectively.

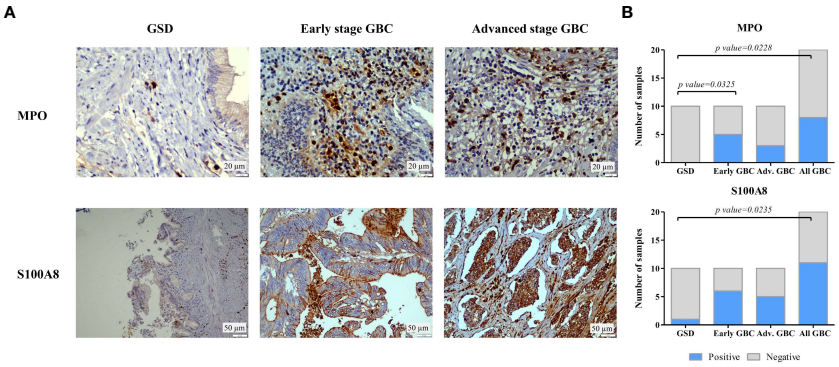

FIGURE 9
IHC analysis to study the expression of MPO and S100A8 in controls and GBC cases. **(A)** Representative IHC images showing the expression of MPO and S100A8 in controls and GBC cases. IHC was performed on formalin-fixed paraffin-embedded (FFPE) individual tissue sections of 10 controls (GSD cases with no dysplasia), 10 early stage GBC (stage I and II) cases and 10 advanced stage GBC cases (stage III and IV). The IHC results showed that the number of MPO positive neutrophils was found to be 'positive' in 50% of early stage GBC and 30% of advanced stage GBC cases. All GSD cases showed 'negative' expression. The expression of S100A8 was found to be 'positive' in 10% GSD cases, 60% early and 50% advanced stage GBC. **(B)** The statistical analysis between cases and controls showed a significant difference of MPO positive neutrophils in early stage GBC vs controls and all GBC vs controls while a significant difference of S100A8 was observed in all GBC vs controls. The controls (≥ 90%) showed 'Negative' expression levels.

differentiation in melanoma and prostate cancers, although the biological function of S100A8 in cancer is not clear (32). Western blot analysis confirmed the overexpression of tissue MPO, PRTN3 and S100A8 in early stage GBC cases (Figure 8) and IHC analysis confirmed the overexpression of MPO in early stage GBC.

PRTN3, ELANE, CTSG and MMP9 are the serine proteases released by the activated neutrophils and have been reported to degrade ECM proteins and promote cancer cell invasion (33–36). We also observed downregulation of ECM proteins (COL14A1, COL1A2, COL6A1, COL6A2, COL6A3, BGN, DCN, LUM, PRELP). Majority of these proteins are already reported to be involved in cell invasion. Based on the above results, we hypothesize that there is an increased neutrophil infiltration and degranulation in the tumor tissue leading to degradation of ECM proteins and promoting cancer cell invasion in early stage GBC

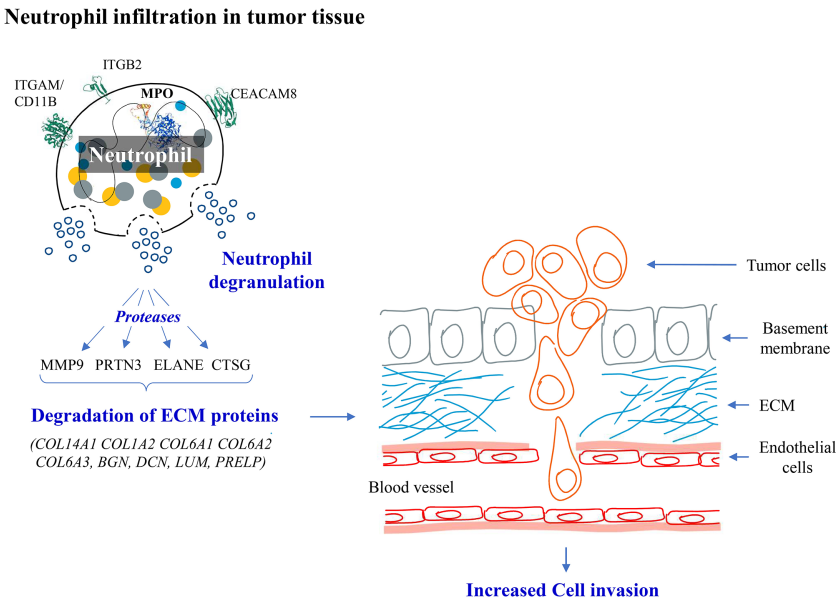

FIGURE 10
Hypothesis showing molecular events in early stage GBC. We observed overexpression of neutrophil degranulation pathway proteins and downregulation of ECM proteins. We hypothesize that there is neutrophil infiltration and degranulation in GBC tissue resulting in release of proteases which possibly degrades ECM proteins promoting cancer cell invasion.

(Figure 10). Protein-protein interaction analysis of the proteins associated with 'neutrophil degranulation' showed MPO, ELANE, ITGAM, MMP9, LTF to be the hub molecules (Supplementary Figure S8). Based on the bioinformatic analysis and literature search, some of the proteins associated with neutrophil degranulation such as MPO, ELANE, DEFA1, MMP9 were found to have 'signal sequence' and could be further explored as circulatory markers for early detection of GBC.

The limitations of the study include the low sample size. We used GSD cases as non-tumor controls in the present study, however, inclusion of other controls such as GB polyp, xanthogranulomatous cholecystitis would be important.

5 Conclusions

In the present study, we analyzed the differential proteome profile of early stage GBC patients and identified 357 differentially expressed proteins. 'Neutrophil degranulation' pathway was found to be enriched with upregulated proteins and 'ECM organization' with downregulated proteins. We hypothesize that there is neutrophil infiltration and degranulation in tumor tissue which leads to degradation of ECM proteins and promote tumor progression from early stage GBC. The overexpression of 'neutrophil degranulation' pathway proteins was further confirmed by Western blot and IHC analysis. The neutrophil degranulation proteins having signal sequences identified in the present study could be explored as circulatory markers for early detection of GBC.

Data availability statement

The original contributions presented in the study are included in the article/Supplementary Material. Further inquiries can be directed to the corresponding authors.

Ethics statement

The studies involving human participants were reviewed and approved by Maulana Azad Medical College- Institutional Ethics Committee, New Delhi and ICMR-National Institute of Pathology- Institutional Ethics Committee, New Delhi. The patients/participants provided their written informed consent to participate in this study.

Author contributions

PG, PS designed the experiment. PS, AA, SG, JA, VJ and RP contributed to clinical sample collection and clinical data management. JA and VJ did experimental work and data compilation. Mass spectrometric data acquisition and analysis: VG, JA, VJ. Literature search and interpretation of overall data was done by PG, RS, RP, PS, AA, SG, SK, JA, VJ, RP, RK. Drafting and editing of the manuscript was done by PG, JA, PS, AA, RS, RP, SK, VG. All authors read and approved the final manuscript. All authors contributed to the article and approved the submitted version.

Funding

The work reported here was financially supported by Science and Engineering Research Board (SERB) (Project ID- CRG/2020/002100) and Indian Council of Medical Research (ICMR), Govt. of India, New Delhi. JA is a Ph.D. student registered at Jamia Hamdard, New Delhi and a recipient of Senior Research Fellowship (SRF) from the Council of Scientific and Industrial Research (CSIR) and ICMR- National Institute of Pathology, Govt. of India. VJ is a Ph.D. student registered at recipient of Senior Research Fellowship (SRF) from the CSIR, Govt. of India. RP is a Ph.D. student registered at Jamia Hamdard, New Delhi and DST- Innovation in Science Pursuit for Inspired Research (INSPIRE)- Senior Research Fellow (SRF). RK was Junior Research Fellow (JRF) under the SERB project. VG is SRF from Department of Biotechnology (DBT), Govt. of India.

Conflict of interest

The authors declare that the research was conducted in the absence of any commercial or financial relationships that could be construed as a potential conflict of interest.

The reviewer SW declared a shared affiliation with the authors JA, RP, SK to the handling editor at the time of review.

Publisher's note

Supplementary material

The Supplementary Material for this article can be found online at: https://www.frontiersin.org/articles/10.3389/fonc.2022.1046974/full#supplementary-material

References

1. Randi G, Franceschi S, La Vecchia C. Gallbladder cancer worldwide: geographical distribution and risk factors. *Int J Cancer.* (2006) 118(7):1591–602. doi: 10.1002/ijc.21683

2. Wistuba II, Gazdar AF. Gallbladder cancer: lessons from a rare tumour. *Nat Rev Cancer.* (2004) 4(9):695–706. doi: 10.1038/nrc1429

3. Murthy NS, Rajaram D, Gautham M, Shivraj N, Pruthvish S, George PS, et al. Trends in incidence of gallbladder cancer – Indian scenario. *Gastrointestinal Cancer: Targets Ther* (2011) 1:1–9. doi: 10.2147/GICTT.S16578

4. Shukla HS, Sirohi B, Behari A, Sharma A, Majumdar J, Ganguly M, et al. Indian Council of medical research consensus document for the management of gall bladder cancer. *Indian J Med Paediatr Oncol* (2015) 36(2):79–84. doi: 10.4103/0971-5851.158829

5. Hsing AW, Gao YT, Han TQ, Rashid A, Sakoda LC, Wang BS, et al. Gallstones and the risk of biliary tract cancer: a population-based study in China. *Br J Cancer.* (2007) 97(11):1577–82. doi: 10.1038/sj.bjc.6604047

6. Benson AB, D'Angelica MI, Abbott DE, Anaya DA, Anders R, Are C, et al. Hepatobiliary cancers, version 2.2021, NCCN clinical practice guidelines in oncology. *J Natl Compr Canc Netw* (2021) 19(5):541–65. doi: 10.6004/jnccn.2021.0022

7. Giannis D, Cerullo M, Moris D, Shah KN, Herbert G, Zani S, et al. Validation of the 8th edition American joint commission on cancer (AJCC) gallbladder cancer staging system: Prognostic discrimination and identification of key predictive factors. *Cancers (Basel).* (2021) 13(3):547. doi: 10.3390/cancers13030547

8. Pandey A, Stawiski EW, Durinck S, Gowda H, Goldstein LD, Barbhuiya MA, et al. Integrated genomic analysis reveals mutated ELF3 as a potential gallbladder cancer vaccine candidate. *Nat Commun* (2020) 11(1):4225. doi: 10.1038/s41467-020-17880-4

9. Kim JH, Kim HN, Lee KT, Lee JK, Choi SH, Paik SW, et al. Gene expression profiles in gallbladder cancer: the close genetic similarity seen for early and advanced gallbladder cancers may explain the poor prognosis. *Tumour Biol* (2008) 29(1):41–9. doi: 10.1159/000132570

10. Washiro M, Ohtsuka M, Kimura F, Shimizu H, Yoshidome H, Sugimoto T, et al. Upregulation of topoisomerase IIalpha expression in advanced gallbladder carcinoma: a potential chemotherapeutic target. *J Cancer Res Clin Oncol* (2008) 134(7):793–801. doi: 10.1007/s00432-007-0348-0

11. Barreto SG, Dutt A, Chaudhary A. A genetic model for gallbladder carcinogenesis and its dissemination. *Ann Oncol* (2014) 25(6):1086–97. doi: 10.1093/annonc/mdu006

12. Tan Y, Meng HP, Wang FQ, Cheng ZN, Wu Q, Wu HR. Comparative proteomic analysis of human gallbladder cancer. *Zhonghua Zhong Liu Za Zhi.* (2010) 32(1):29–32.

13. Tan Y, Meng HP, Wu Q, Wang FQ, Wu HR. Proteomic study of gallbladder cancer, with special reference on the expression and significance of annexin A3. *Zhonghua Bing Li Xue Za Zhi.* (2010) 39(6):382–6.

14. Huang HL, Yao HS, Wang Y, Wang WJ, Hu ZQ, Jin KZ. Proteomic identification of tumor biomarkers associated with primary gallbladder cancer. *World J Gastroenterol* (2014) 20(18):5511–8. doi: 10.3748/wjg.v20.i18.5511

15. Sahasrabuddhe NA, Barbhuiya MA, Bhunia S, Subbannayya T, Gowda H, Advani J, et al. Identification of prosaposin and transgelin as potential biomarkers for gallbladder cancer using quantitative proteomics. *Biochem Biophys Res Commun* (2014) 446(4):863–9. doi: 10.1016/j.bbrc.2014.03.017

16. Priya R, Jain V, Akhtar J, Chauhan G, Sakhuja P, Goyal S, et al. Plasma-derived candidate biomarkers for detection of gallbladder carcinoma. *Sci Rep* (2021) 11(1):23554. doi: 10.1038/s41598-021-02923-7

17. Tyanova S, Temu T, Sinitcyn P, Carlson A, Hein MY, Geiger T, et al. The Perseus computational platform for comprehensive analysis of (prote)omics data. *Nat Methods* (2016) 13(9):731–40. doi: 10.1038/nmeth.3901

18. Miller G, Socci ND, Dhall D, D'Angelica M, DeMatteo RP, Allen PJ, et al. Genome wide analysis and clinical correlation of chromosomal and transcriptional mutations in cancers of the biliary tract. *J Exp Clin Cancer Res* (2009) 28(1):62. doi: 10.1186/1756-9966-28-62

19. Wang J, Xu C, Cheng Q, Zhao J, Wu S, Li W, et al. RNA Sequencing revealed signals of evolution from gallbladder stone to gallbladder carcinoma. *Front Oncol* (2020) 10:823. doi: 10.3389/fonc.2020.00823

20. Zuo M, Rashid A, Wang Y, Jain A, Li D, Behari A, et al. RNA Sequencing-based analysis of gallbladder cancer reveals the importance of the liver X receptor and lipid metabolism in gallbladder cancer. *Oncotarget* (2016) 7(23):35302–12. doi: 10.18632/oncotarget.9181

21. Ge C, Zhu X, Niu X, Zhang B, Chen L. A transcriptome profile in gallbladder cancer based on annotation analysis of microarray studies. *Mol Med Rep* (2021) 23(1):25. doi: 10.3892/mmr.2020.11663

22. Szklarczyk D, Gable AL, Lyon D, Junge A, Wyder S, Huerta-Cepas J, et al. STRING v11: protein-protein association networks with increased coverage, supporting functional discovery in genome-wide experimental datasets. *Nucleic Acids Res* (2019) 47(D1):D607–13. doi: 10.1093/nar/gky1131

23. Teufel F, Almagro Armenteros JJ, Johansen AR, Gíslason MH, Pihl SI, Tsirigos KD, et al. SignalP 6.0 predicts all five types of signal peptides using protein language models. *Nat Biotechnol* (2022) 40(7):1023–5. doi: 10.1038/s41587-021-01156-3

24. Tripathi PH, Akhtar J, Arora J, Saran RK, Mishra N, Polisetty RV, et al. Quantitative proteomic analysis of GnRH agonist treated GBM cell line LN229 revealed regulatory proteins inhibiting cancer cell proliferation. *BMC Cancer.* (2022) 22(1):133. doi: 10.1186/s12885-022-09218-8

25. Akhtar J, Priya R, Jain V, Sakhuja P, Agarwal AK, Goyal S, et al. Immunoproteomics approach revealed elevated autoantibody levels against ANXA1 in early stage gallbladder carcinoma. *BMC Cancer.* (2020) 20(1):1175. doi: 10.1186/s12885-020-07676-6

26. *Fisher's exact test was performed using GraphPad prism version 5.0 for windows*. San Diego, California USA: GraphPad Software (accessed on July 2022).

27. Powell DR, Huttenlocher A. Neutrophils in the tumor microenvironment. *Trends Immunol* (2016) 37(1):41–52. doi: 10.1016/j.it.2015.11.008

28. Xiong S, Dong L, Cheng L. Neutrophils in cancer carcinogenesis and metastasis. *J Hematol Oncol* (2021) 14(1):173. doi: 10.1186/s13045-021-01187-y

29. Kuckleburg CJ, Tilkens SB, Santoso S, Newman PJ. Proteinase 3 contributes to transendothelial migration of NB1-positive neutrophils. *J Immunol* (2012) 188(5):2419–26. doi: 10.4049/jimmunol.1102540

30. Weng M, Yue Y, Wu D, Zhou C, Guo M, Sun C, et al. Increased MPO in colorectal cancer is associated with high peripheral neutrophil counts and a poor prognosis: A TCGA with propensity score-matched analysis. *Front Oncol* (2022) 12:940706. doi: 10.3389/fonc.2022.940706

31. Hu D, Ansari D, Zhou Q, Sasor A, Said Hilmersson K, Andersson R. Low P4HA2 and high PRTN3 expression predicts poor survival in patients with pancreatic cancer. *Scand J Gastroenterol* (2019) 54(2):246–51. doi: 10.1080/00365521.2019.1574360

32. Wu Z, Jiang D, Huang X, Cai M, Yuan K, Huang P. S100A8 as a promising biomarker and oncogenic immune protein in the tumor microenvironment: An integrative pancancer analysis. *J Oncol* (2022) 2022:6947652. doi: 10.1155/2022/6947652

33. Fatalska A, Rusetska N, Bakuła-Zalewska E, Kowalik A, Zięba S, Wroblewska A, et al. Inflammatory proteins HMGA2 and PRTN3 as drivers of vulvar squamous cell carcinoma progression. *Cancers (Basel).* (2020) 13(1):27. doi: 10.3390/cancers13010027

34. Winkler J, Abisoye-Ogunniyan A, Metcalf KJ, Werb Z. Concepts of extracellular matrix remodelling in tumour progression and metastasis. *Nat Commun* (2020) 11(1):5120. doi: 10.1038/s41467-020-18794-x

35. Morimoto-Kamata R, Yui S. Insulin-like growth factor-1 signaling is responsible for cathepsin G-induced aggregation of breast cancer MCF-7 cells. *Cancer Sci* (2017) 108(8):1574–83. doi: 10.1111/cas.13286

36. Christoffersson G, Vågesjö E, Vandooren J, Lidén M, Massena S, Reinert RB, et al. VEGF-a recruits a proangiogenic MMP-9-delivering neutrophil subset that induces angiogenesis in transplanted hypoxic tissue. *Blood* (2012) 120(23):4653–62. doi: 10.1182/blood-2012-04-421040

frontiers | Frontiers in Oncology

TYPE Review
PUBLISHED 31 January 2023
DOI 10.3389/fonc.2023.1078768

OPEN ACCESS

EDITED BY
João Pessoa,
University of Coimbra, Portugal

REVIEWED BY
Binghan Zhou,
Huazhong University of Science and Technology, China
Olivier Meurette,
Université Claude Bernard Lyon 1, France
Xiawa Mao,
Zhejiang University, China

*CORRESPONDENCE
Xiaochen Li
lixiaochen3n2b@163.com

SPECIALTY SECTION
This article was submitted to Molecular and Cellular Oncology, a section of the journal Frontiers in Oncology

RECEIVED 24 October 2022
ACCEPTED 19 January 2023
PUBLISHED 31 January 2023

CITATION
Guo M, Niu Y, Xie M, Liu X and Li X (2023) Notch signaling, hypoxia, and cancer. *Front. Oncol.* 13:1078768. doi: 10.3389/fonc.2023.1078768

Notch signaling, hypoxia, and cancer

Mingzhou Guo[1,2], Yang Niu[1,2], Min Xie[1,2], Xiansheng Liu[1,2] and Xiaochen Li[1,2]*

[1]Department of Pulmonary and Critical Care Medicine, Tongji Hospital, Tongji Medical College, Huazhong University of Science and Technology, Wuhan, China, [2]Key Laboratory of Pulmonary Diseases of National Health Commission, Tongji Hospital, Tongji Medical College, Huazhong University of Sciences and Technology, Wuhan, China

Notch signaling is involved in cell fate determination and deregulated in human solid tumors. Hypoxia is an important feature in many solid tumors, which activates hypoxia-induced factors (HIFs) and their downstream targets to promote tumorigenesis and cancer development. Recently, HIFs have been shown to trigger the Notch signaling pathway in a variety of organisms and tissues. In this review, we focus on the pro- and anti-tumorigenic functions of Notch signaling and discuss the crosstalk between Notch signaling and cellular hypoxic response in cancer pathogenesis, including epithelia-mesenchymal transition, angiogenesis, and the maintenance of cancer stem cells. The pharmacological strategies targeting Notch signaling and hypoxia in cancer are also discussed in this review.

KEYWORDS

Notch signaling, hypoxia, hypoxia-induced factors pathway, cancer, therapeutics

1 Introduction

The discovery of Notch signaling dates back to the early 1900s when a specific *Drosophila* wing phenotype showed notches on the wings which resulted from the mutations in the Notch receptor. Meanwhile, several other mutations have also been identified, such as Delta and Serrate, which similarly turned out to reside in genes encoding ligands related to the Notch pathway (1). Studies of the Notch signaling have flourished since then and the principal components and process of the signaling transduction cascade were identified. As a juxtacrine signaling, Notch signaling relies on the interaction between receptors and ligands expressed on juxtaposed cells to initiate signaling. The Notch signaling has been extensively characterized as a highly conserved pathway involved in cell proliferation, fate, differentiation, and stem cell maintenance (2). It is universally acknowledged that the normal Notch signaling is vital to most developmental decision-making in animals, and that pathway dysfunction is involved in many conditions, including cancer (3).

The Notch signaling pathway plays a critical role in tumor initiation and progression. Notch can function as an oncogene or a tumor suppressor in different cancers. Hypoxia is a common feature in a majority of malignant tumors. Hypoxia triggers a complex signaling

network in tumor cells to alter cell metabolism and regulate angiogenesis, epithelia-mesenchymal transition (EMT), and the maintenance and functions of cancer stem cells (CSCs). Hypoxia-induced factors (HIFs), as global regulators of cellular hypoxia responses, can interact with Notch and directly regulate the Notch signaling pathway. This review systematically summarizes the intersection between Notch signaling and the cellular hypoxic response and highlights the underlying molecular mechanisms involved in the cancer pathogenesis, which contributes to the discovery and development of a combinational strategy targeting Notch and hypoxia in cancer treatment.

2 Notch signaling pathway

Notch signaling exerts its effect in a canonical or noncanonical fashion. The specific mechanisms of canonical and non-canonical Notch signaling are described as follows.

2.1 Canonical Notch signaling

Canonical Notch signaling is initiated by γ-secretase-mediated cleavage of the Notch receptor, resulting in the release of the active intracellular domain of Notch, which migrates to the nucleus and interacts with CSL (for CBF1, Suppressor of Hairless, Lag1; also known as RBPJ), leading to the activation of downstream target genes (Figure 1). In mammals, there are four Notch receptors (Notch 1/2/3/4) and five ligands (Delta-like 1/3/4 or Jagged 1/2). The Notch receptors and ligands are structurally related in some ways. They both contain a large number of epidermal growth factor (EGF)-like repeats in their extracellular domains. Briefly, Notch receptors are produced in the endoplasmic reticulum and synthesized as single precursor proteins, which are then trafficked to the Golgi compartment. In the Golgi compartment, Notch receptor precursors undergo S1 cleavage by a furin-like protease, creating the heterodimeric Notch receptor consisting of a Notch extracellular domain (NECD) and a Notch transmembrane and intracellular domain (TMIC). The part of the extracellular domain of Notch receptor consists of 36 EGF-like repeats and a negative regulatory region. EGF-like repeats 11 and 12 function as specific protein binding domains mediating interaction with ligands (4). The ligand-receptor interaction triggers proteolytic cleavages by an ADAM metalloprotease (S2-cleavage). In this process, ligand will be endocytosed after it binds to Notch receptor. Epsin-dependent ligand endocytosis exerts force on the negative regulatory region exposing the S2 site for cleavage (5). Then, the remainder of the receptor subjected to S3 cleavage by the γ-secretase complex releases the Notch intracellular domain (NICD), which translocates into the nucleus. In the nucleus, NICD interacts with a DNA-binding protein CSL, converting CSL from a transcriptional repressor to an activator. The NICD-CSL interaction is stabilized by Mastermind like transcriptional coactivator (MAML), forming a ternary NICD/MAML/CSL complex to activate the transcription of downstream genes including Hes (hairy-enhancer of split), Hey (Hes related to YRPW), and so on (6, 7). Different ligands could generate diverse Notch activity dynamics in signaling receiving cells, inducing different cell fates *via* activating distinct target gene programs (8).

2.2 Non-canonical Notch signaling

Non-canonical Notch signaling is an important arm of Notch signaling. Notch is proved active in cells where the canonical ligands and downstream effectors were defective, indicating that Notch acts in a second way independently (9). Non-canonical Notch signaling can be initiated by a non-canonical ligand *via* CSL-independent manner (10–12).

Notch signaling can be elicited by diverse non-canonical ligands, including ligands structurally similar to canonical ligands, structurally unrelated ligands, and secreted proteins (13, 14). Delta like non-canonical Notch ligand 1 is an integral membrane protein containing tandem EGF-like repeats in its extracellular domain but lacking the DSL domain. It can directly interact with Notch1 and act as an antagonist (14). Another structurally similar non-canonical ligand Delta/Notch-like EGF-related receptor functioned as a trans-ligand to affect glial morphological changes (15). A diverse group of structurally unrelated non-canonical ligands have also been identified as Notch activators. F3/contactin1 and NB3/contactin6 interacted with Notch EGF-like repeat distal to the DSL domain binding site to induce oligodendrocyte differentiation (11, 16). In addition, a number of secreted proteins act as non-canonical ligands of Notch. In vertebrates, CCN3 and MAGP-2 can bind to the extracellular domains of Notch receptor, resulting in its cleavage and activation (17, 18). In *Drosophila*, Scabrous activated transcription of the Notch target gene E(spl)C m3 to regulate eye ommatidia and sensory bristles (19, 20).

In CSL-independent non-canonical Notch signaling, the cleaved NICD interacts with multiple pathways and regulates cell survival. The CSL knockout mice developed breast tumors similar to CSL heterozygous and control mice, indicating that Notch-induced breast tumor development was CSL-independent (21). Interleukin-6 has been identified as a novel Notch target in breast tumor cells. The Notch-mediated interleukin-6 up-regulation required two NF-κB signaling-related proteins and P53 (22). The membrane-tethered NICD inhibited cell apoptosis through interacting with mTOR and Rictor (companion of mTOR) to trigger Akt phosphorylation in activated T cells (23). Notch activated the PI3K-Akt pathway *via* Deltex1 and played oncogenic functions in cervical cancer (24). In addition, Notch1 was demonstrated to directly regulate vascular barrier function through a flow-mediated, non-canonical, transcription-independent signaling mechanism (25, 26).

Abbreviations: HIFs, Hypoxia-induced factors; EMT, Epithelial-mesenchymal transition; CSCs, Cancer stem cells; EGF, Epidermal growth factor; NICD, Notch intracellular domain; MAML, Mastermind like transcriptional coactivator; ALL, Acute lymphoblastic leukemia; TME, Tumor microenvironment; FIH-1, Factor inhibiting HIF-1; VEGF, Vascular endothelial growth factor; Dll4, Delta-like 4; GSIs, γ-secretase inhibitors; NcRNAs, Non-coding RNAs; MiRNAs, MicroRNAs; LncRNAs, Long non-coding RNAs; HAPs, Hypoxia activated prodrugs; Hsp90, Heat shock protein 90; HDACs, Histone deacetylases.

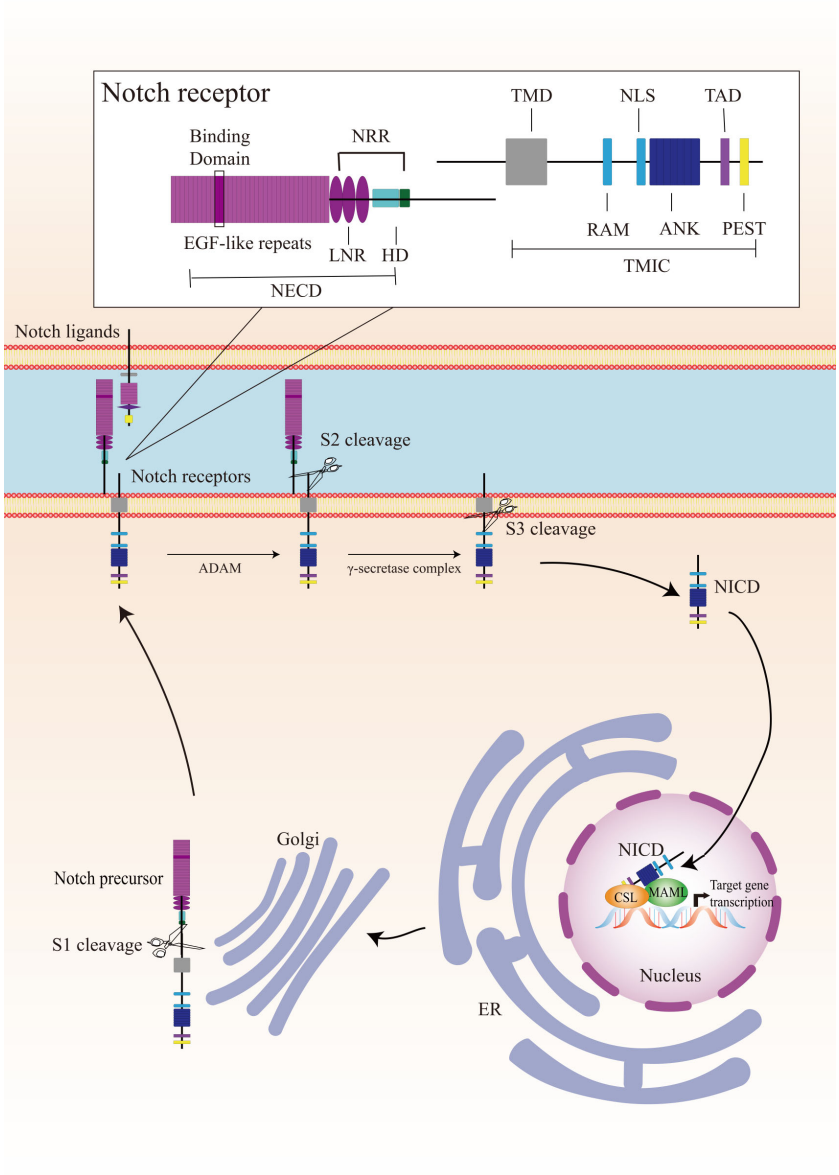

FIGURE 1
Overview of the Notch signaling pathway. The Notch receptor is produced in the endoplasmic reticulum (ER) and undergoes S1-cleavage in the Golgi compartment. The cleavage results in the formation of a heterodimer receptor, consisting of a Notch extracellular domain (NECD) and a Notch transmembrane and intracellular domain (TMIC), which is then transported to the plasma membrane. Upon interacting with a transmembrane ligand, the Notch receptor undergoes two sequentially cleavage, releases the Notch intracellular domain (NICD), which translocates into the nucleus. In the cell nucleus, NICD forms a ternary complex with the DNA-binding protein CSL and MAML to regulate transcription of downstream genes. A detailed description of the various domains in Notch receptor is presented in the box on the top. Notch receptor consists of a NECD, a transmembrane domain (TMD), and a NICD. NECD consists of epidermal growth factor (EGF) - like repeats domain, and a negative regulatory region (NRR), which including three Lin Notch repeats (LNR) and a heterodimerization (HD) domain. EGF-like repeats 11 and 12 function as specific protein binding domains mediating interaction with ligands. NICD consists of a RBPJ associated molecule (RAM), ankyrin repeats (ANK), a translational active domain (TAD), and a PEST domain.

3 Notch signaling pathway in cancer

The mutations in the Notch signaling pathway genes and dysregulated Notch signaling pathways exhibit dual biological functions in tumorigenesis and cancer progression (Table 1). Notch1 mutation was first identified in patients with acute T-cell acute lymphoblastic leukemia (T-ALL) and occurs in approximately 50% of T-ALL (27). Oncogenic and gain-of-function mutations of Notch genes have been implicated in chronic lymphocytic leukemia (30), splenic marginal zone B-cell lymphoma (31), squamous cell lung carcinoma (44) and salivary adenoid cystic carcinomas (58). Moreover, aberrant activation of Notch signaling has been found in many solid tumors including prostate (59), breast (60), cervical (61), melanoma (62), and lung cancer (63, 64).

In addition, Notch signaling can interact with other signaling pathways to promote tumorigenesis and cancer progression (Table 2). The Notch signaling contributed to the development of leukemia and breast cancer through interacting with the NF-κB pathway (22, 65, 82). Notch inhibited cervical cancer cell apoptosis *via* the mTOR–Rictor pathway (23).

TABLE 1 The Oncogenic and tumor suppressive roles of Notch signaling in human cancers.

Tumor Type	Oncogenic or Tumor Suppressive	Mutations
Acute lymphoblastic T-cell leukemia	Oncogenic	Notch1 (27), Notch3 (28), FBXW7 (29)
Chronic lymphocytic leukemia	Oncogenic	Notch1 (30)
Splenic marginal zone lymphoma	Oncogenic	Notch2 (31)
Diffuse large cell B lymphoma	Oncogenic	Notch1 (32), Notch2 (33)
Adenoid cystic carcinoma	Oncogenic	Notch1, Notch2 (34, 35)
Breast cancer	Oncogenic	Notch1, Notch2 (36)
Infantile myofibromatosis	Oncogenic	Notch3 (37)
Glomus tumors	Oncogenic	Notch1, Notch2, Notch3 (38)
Head and neck squamous cell carcinomas	Tumor Suppressive	Notch1 (39, 40)
Small cell lung cancers	Tumor Suppressive	Notch1, Notch2, Notch3, Notch4 (41)
Bladder cancer	Tumor Suppressive	Notch1, Notch2, Notch3, MAML (42, 43)
Cutaneous and lung squamous cell carcinoma	Tumor Suppressive	Notch1, Notch2 (44)
Cholangiocellular carcinoma	Oncogenic	No mutations (45)
Hepatocellular carcinoma	Oncogenic and Tumor Suppressive	No mutations (46–48)
Pancreatic ductal adenocarcinoma	Oncogenic and Tumor Suppressive	No mutations (49, 50)
Melanoma	Oncogenic	No mutations (51, 52)
Prostate cancer	Oncogenic	No mutations (53, 54)
Glioblastoma	Oncogenic	No mutations (55–57)

MAML, Mastermind like transcriptional coactivator.

In addition to its oncogenic role in human malignancies, Notch also functions as a tumor suppressor (83). Nicolas et al. has demonstrated that Notch1 deficiency in skin resulted in the sustained expression of Gli2 and derepressed β-catenin signaling, causing the development of tumor (84). In addition, Notch was reported to play a suppressive role in B cell ALL (85), human hepatocellular carcinoma (86), small cell lung cancer (41), and neuroendocrine tumors (87). In a word, Notch acts as an oncogene or tumor suppressor in cancer depending on different contexts. To comprehend the full spectrum of Notch effects, efforts were required to identify the specific ligand-receptor interactions, the downstream targets of Notch signaling, and the functions of Notch modifiers (88).

Tumor microenvironment is comprised of a complex network, including stromal cells, immune cells, fibroblasts, blood vessels, and secreted factors (89). The interaction between tumor cells and tumor microenvironment (TME) is interdependent. A normal TME has a potential to suppress tumors. Lim et al. has suggested that tumor-stroma interactions can drive disease progression in squamous cell carcinoma arising in different tissues, indicating that the tumor context defines metastatic progression (90).

Accumulating evidence suggested that Notch signaling plays a role in regulating the immune responses in tumors, which may be associated with the critical role of Notch signaling in hematopoiesis and immune development (88, 91). A single-cell RNA-sequencing

TABLE 2 The cross-talk between Notch signaling and other pathways in cancers.

Interaction with other pathways	Tumor Type
NF-κB pathway	Leukemic T cells (65), prostate cancer (66), breast cancer (22)
PI3K/Akt pathway	Cervical cancer (24), melanoma (67), breast cancer (68), lung adenocarcinoma (69)
Wnt/β-catenin pathway	Colorectal cancer (70)
HIF pathway	Pancreatic cancer (71), breast cancer (72), glioblastoma (73)
MAPK pathway	Melanoma (67), thyroid papillary cancer (74), breast cancer (75), head and neck squamous cell carcinoma (76)
TGF-β/smad pathway	Breast cancer (77), clear cell renal cell carcinoma (78)
mTOR pathway	Cervical cancer (23)
P53 pathway	Lung adenocarcinoma (79), keratinocyte cancer (80), T-cell lymphoma (81)

analysis has revealed that Jagged1-Notch pathway regulated immune cell homeostasis during minimal residual disease in hematologic neoplasm, which was a potential target to delay tumor recurrence (92). In breast cancer, the Jagged1-Notch pathway regulated tumor-associated macrophage differentiation towards M2 phenotype to induce aromatase inhibitor resistance (93). Activation of the Notch signaling in triple-negative breast cancer resulted in the secretion of pro-inflammatory cytokines and the recruitment of pro-tumoral macrophages to the TME (94). Delta-like 1 (Dll1)-mediated Notch signaling was implicated in the crosstalk between tumor cells and cancer-associated fibroblasts to promote radio-resistance in breast cancer (95). In general, Notch signaling plays a critical role in regulating tumor cells and TME, which may provide new strategies for Notch-targeted cancer therapy.

4 Hypoxia in cancer

Oxygen is indispensable for mammals that maintain intracellular ATP levels and serves as an electron acceptor in a large number of biochemical reactions (96). Hypoxia is a major feature of solid tumor and associated with poor prognosis and resistance to therapy (97–99). Under hypoxic condition, tumor cells undergo various biological processes including cell proliferation, migration, apoptosis, and EMT (100). Hypoxia also triggers multiple signaling pathways to regulate advanced but dysfunctional vascularization in TME (101).

The transcriptional factor HIFs are principal regulators and orchestrate cellular adaptive mechanisms in responses to hypoxia. HIFs contain two different subunits: α and β. The α-subunit protein is regulated by cellular oxygen levels, whereas the β subunit is constitutively expressed (102, 103). HIF-α proteins are oxygen-sensitive that contain an oxygen-dependent degradation domain with target prolyl residues, and a C-terminal transactivation domain which contains the target asparaginyl residue. Under normoxic condition, HIF-α subunits are hydroxylated by prolyl hydroxylases. After hydroxylation, the von-Hippel Lindau tumor suppressor gene interacts with HIF-α and tags it for 26s proteasomal degradation (104, 105). Under hypoxic condition, HIF-α hydroxylation is prevented due to the inactivation of prolyl hydroxylases, resulting in the inhibition of ubiquitin-mediated proteasome degradation of HIF-α. HIF-α is stabilized and form the HIF heterodimer, which then enters the nucleus and combines with hypoxia-response elements to activate the downstream genes (106). Moreover, HIF transcriptional activity is modulated by factor inhibiting HIF-1 (FIH-1), which hydroxylates an asparagine residue in the transactivation domain of HIF-α subunits, thereby blocking its transactivation function (107, 108).

There are three known α subunits (HIF-1α, HIF-2α, and HIF-3α) and three β subunits (HIF-1β, HIF-2β, and HIF-3β). HIF-1α is widely expressed in most human tissues, while HIF-2α and HIF-3α are detected in more restricted tissues, such as lung, kidney, and so on (109, 110). In canonical HIF signaling, hypoxia leads to the stabilization of the labile protein HIF-1α or HIF-2α which complexes with HIF-β, forming heterodimers that bind to hypoxia-response elements in target genes (111). HIF-1α and HIF-2α are structurally closely related and share both common and distinct target genes (112). The role of HIF-3α in the regulation of the HIF pathway is not completely understood and mainly regarded as a negative regulator of HIF-1α and HIF-2α (113).

HIFs are overexpressed and significantly associated with poor prognosis in a variety of cancers (114–117). HIFs-regulated genes encode proteins involved in critical aspects of cancer biology, including energy metabolism, cell survival and invasion, angiogenesis, EMT, and so on. Tumor cells tend to turn metabolism from an oxygen-dependent tricarboxylic acid cycle to glycolysis (118). HIF-1 regulates glycolytic enzymes, including hexokinase 2 and phosphofructokinase 1, which involved in tumor initiation and growth (119, 120). A number of growth factors regulated by HIFs played a role in cell survival, such as transforming growth factor-β, insulin-like growth factor 2, endothelin-1, erythropoietin, and epidermal growth factor receptor (100, 121–123). HIFs mediated angiogenesis *via* activating the transcription of multiple angiogenic growth factors, including vascular endothelial growth factor (VEGF), placenta-like growth factor, angiopoietin (124, 125). HIF-1 can directly induces the transcription of ZEB1, TWIST, and TCF3, which promote EMT in cancers (126–128). In a word, HIFs play a key role in cancer initiation and progression.

5 Crosstalk between Notch signaling and hypoxia pathway

HIF signaling pathway is the primary regulator in the physiological and pathological response to hypoxia. The Notch signaling pathway plays a critical role in cell fate control, including tumorigenesis and progression. The link between Notch signaling and hypoxia was first described in a transcriptomic analysis, in which the Notch target gene Hes1 was upregulated in hypoxic neuroblastoma cell lines (129). Thereafter, a study of Notch and hypoxia-activated genes in glioblastoma tumor confirmed a combined gene signature of these two pathways and their role in tumor prognosis (130). Gustaffson et al. provided important evidence that hypoxia directly regulated Notch signaling (131). In this study, HIF-1α was recruited to Notch-responsive promoters and interacted with NICD, leading to stabilization of NICD and activation of Notch downstream genes (Hes and Hey). HIF-1α can also be recruited to the Hey-2 promoter in myogenic cell (131). The up-regulation of the Notch ligands (Jagged 2 and Delta-like 4) induced by hypoxia leaded to activation of Notch signaling (132–134). HIF-2α promoted stem phenotype conversion and resistance to Paclitaxel by activating Notch and Wnt pathways in breast cancer cells (72). Besides, HIF-1α was revealed to interact with γ-secretase and upregulate γ-secretase activity to promote cell invasion and metastasis through a novel function independent of transcription factor (135). HIF-1α and HIF-2α synergized with the Notch co-activator MAML1 to potentiate Notch activity in breast cancer cells (136). The indirect regulation of Notch signaling by HIF was reported in lung cancer cells that HIF-mediated miR-1275 up-regulation exerted its tumorigenic effect

through co-activating Notch and Wnt/β-catenin signaling pathways (137).

On the other hand, Notch signaling can also regulate hypoxic response. Notch was demonstrated to transcriptionally upregulate the expression of HIF-2α in certain tumor cells *via* a HIF1α-to-HIF2α switch (138). The γ-secretase inhibitor of Notch decreased the mRNA expression of the HIF-1 target PGK-1 (131).

FIH-1 is involved in the crosstalk between hypoxia and Notch signaling pathways. Both HIF-1α and Notch are substrates for the asparagine hydroxylase FIH-1. Two asparagine residues in the NICD ankyrin repeat domain are hydroxylated by FIH-1, leading to inactivation of Notch signaling. FIH-1 binds to NICD more efficiently than HIF-1α, indicating that NICD sequesters FIH-1 away from HIF-1α, which results in an under-hydroxylation on HIF1α (139, 140). This may shed light on another oxygen-dependent interface that modulates HIF signaling.

To summarize, the crosstalk between Notch signaling and the cellular hypoxic response is extensive and the underlying molecular mechanism is complex (Figure 2). A Notch-hypoxia crosstalk has been involved in a variety of physiological situations and pathological conditions, including vascular diseases and cancers (64, 141).

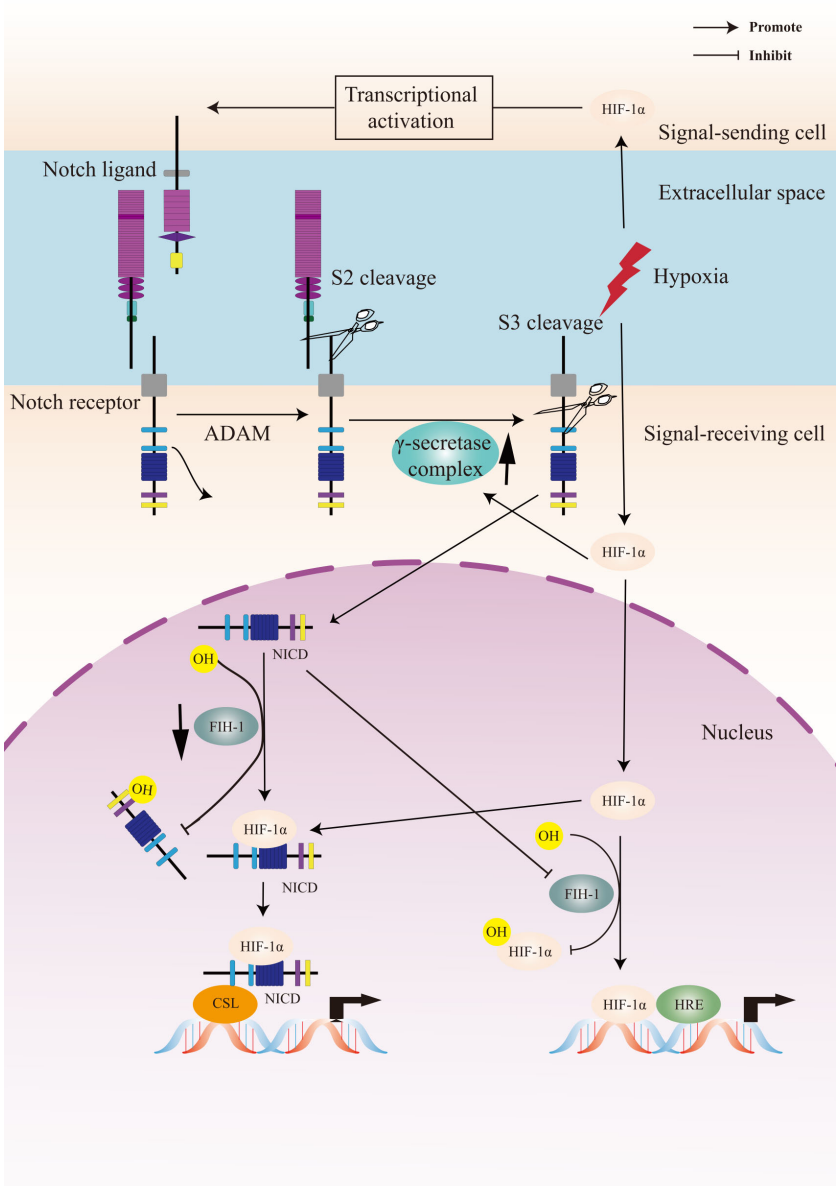

FIGURE 2
A Crosstalk between Notch signaling and hypoxia pathway. Upon activation of the Notch receptor, the Notch intracellular domain (NICD) accumulates in the cell nucleus and activates target genes. Hypoxia induces the canonical hypoxia response pathway, which involves the activation of hypoxia response element (HRE)-driven target genes. Under hypoxic conditions, hypoxia-induced factors-1α (HIF-1α) potentiates Notch-dependent activation of target genes through interaction with the NICD. Besides, HIF-1α interacts with γ-secretase and upregulated γ-secretase activity. Factor-inhibiting HIF-1 (FIH-1) hydroxylates the asparagine residues of HIF-α and NICD, leading to inactivation of Notch and hypoxia signaling pathways. Hypoxia decreases the activity of FIH-1. In addition, FIH-1 binds NICD more efficiently than HIF-1α. NICD sequesters FIH-1 away from HIF-1α, indirectly resulting in an activation of HRE-driven target genes.

6 Biological processes in cancer regulated by a Notch-hypoxia crosstalk

A functional relationship between hypoxia and Notch signaling pathways has been observed in many types of tumors. Accumulating evidences have revealed that the crosstalk between Notch and the cellular hypoxic response has diverse roles in cancer pathogenesis by regulating several important biological processes, including EMT, angiogenesis, the maintenance of CSCs, and so on.

6.1 A Notch-hypoxia crosstalk in cancer EMT

EMT is one of the critical mechanisms of cancer metastasis (142, 143). The hallmark of EMT is the loss of E-cadherin expression through the up-regulation of its repressors (144, 145). E-cadherin repressors are classified into two groups depending on their effects on the E-cadherin promoter. Snail, Zeb, E47, and KLF8 bind to and repress the activity of the E-cadherin promoter (146, 147), whereas several factors such as Twist, Goosecoid, E2.2, and FoxC2 indirectly repress E-cadherin transcription (148).

HIF-1 was reported to upregulate the expression of Twist to promote EMT (149). A number of studies suggested that hypoxia induced EMT *via* activating Notch signaling in tumor cells (136, 150–152). Notch can regulate the expression of Snail-1 *via* two distinct mechanisms in hypoxia. One relied on the transcriptional up-regulation of Snail-1. The other concerned the protein stabilization of Snail-1 *via* the increase of lysyl oxidase which was transcriptionally regulated by HIF-1α and potentiated by Notch (150). Hypoxia-mediated increase in Snail and Slug required Notch pathway in the initiation of EMT in breast cancer cells (136). HIF-1α can also exert a non-transcriptional function in regulating the expression of NICD and E-cadherin in lung cancer cells (153).

6.2 A Notch-hypoxia crosstalk in angiogenesis

Tumor growth is fed by nearby blood vessels. Hypoxia occurs as the tumor grows. New blood vessels are essential for continued primary tumor growth. The ability of forming vasculature has been termed angiogenesis. Activation of endothelial cells was a key step of angiogenesis and a number of growth factors upregulated by HIF were involved in the process, such as VEGF (154).

Notch signaling was activated and played an important role in the process of angiogenesis (155). The expression of Notch ligand Dll4 was much higher in the endothelium of tumor blood vessels compared to nearby normal blood vessels, indicating that Notch signaling were implicated in tumor angiogenesis (132, 156, 157). Dll4 was upregulated by VEGF as a negative feedback modulator, which prevented VEGF-induced overexuberant angiogenic sprouting and branching *via* Notch signaling, guaranteeing the formation of a well-differentiated vascular network (158, 159). HIF1α-induced basic fibroblast growth factor and VEGF were reported to play a synergistic role in the regulation of Dll4 in tumor cells (156). Hypoxia-induced up-regulation of Dll4 and Hey repressed COUP-TFII (known as a regulator of vein identity) in endothelial progenitor cells, which may contribute to tumor angiogenesis (160). Another Notch ligand Jagged 2 was transcriptionally activated by HIF-1α, which triggered Notch signaling and activated Hey1 to promote vascular development and angiogenesis (133).

6.3 A Notch-hypoxia crosstalk in the maintenance of CSCs

CSCs represent a discrete subpopulation of cancer cells with stem cell properties, which is responsible for tumor growth. CSCs are self-renewal and can produce more committed progenitor or "transit-amplifying" cells whose progeny differentiate aberrantly to promote the tumorigenesis (161, 162). Stem cell "niches" are considered as particular microenvironments that maintain the combined properties of CSCs self-renewal and multipotency. The Notch signaling is highly conserved and is critical for cell fate decisions and the maintenance of stem cells (163). HIF stabilization in hypoxic tumor cells can promote stem cell properties, including self-renewal and multipotency partly *via* inducing the expression and activity of the Notch signaling pathway (164–167). Hypoxia-induced the 66-kDa isoform of the SHC gene controlled the expression of Notch3 to regulate the stem cell properties (168). In glioblastomas, HIF-1α played an important role in the hypoxia-mediated maintenance of glioma stem cells *via* the interaction with NICD (73). A further study suggested that hypoxia can promote glioma stem cells proliferation and maintain the characteristics of stem cells through activating Notch1 and Oct3/4 (169). In addition, HIF-1α was reported to promote pancreatic cancer cell dedifferentiation into stem-like cell phenotypes by activating Notch signaling, revealing a novel regulatory mechanism (71).

7 Strategies for cancer therapy

7.1 Therapeutic targets in the Notch signaling pathway

In view of the critical role of Notch signaling in tumor pathogenesis, Notch is regarded as a promising therapeutic target. Numerous approaches have been developed to inhibit different steps of Notch signaling pathway for therapy: γ-secretase inhibitors (GSIs), antibodies targeting ligands or receptors, compounds targeting transcription activation, and so on (Figure 3). The drugs are listed by therapeutic category in Table 3.

GSIs were the first and most extensively studied small-molecule Notch inhibitors. Initially, GSIs were developed for treating Alzheimer's disease because γ-secretase catalyzed the production of the β-amyloid peptide from amyloid precursor protein (196). The use of GSIs for cancer treatment is based on inhibiting the cleavage of γ-secretase which mediates S3 cleavage to generate NICD, resulting in blocking Notch signaling. However, studies have shown that systemic inhibition of Notch signaling by GSIs results in "on-target" gastrointestinal toxicity because of the accumulation of secretory goblet cells in the intestine. The above observation can be explained by alterations in the differentiation of intestinal stem cells following

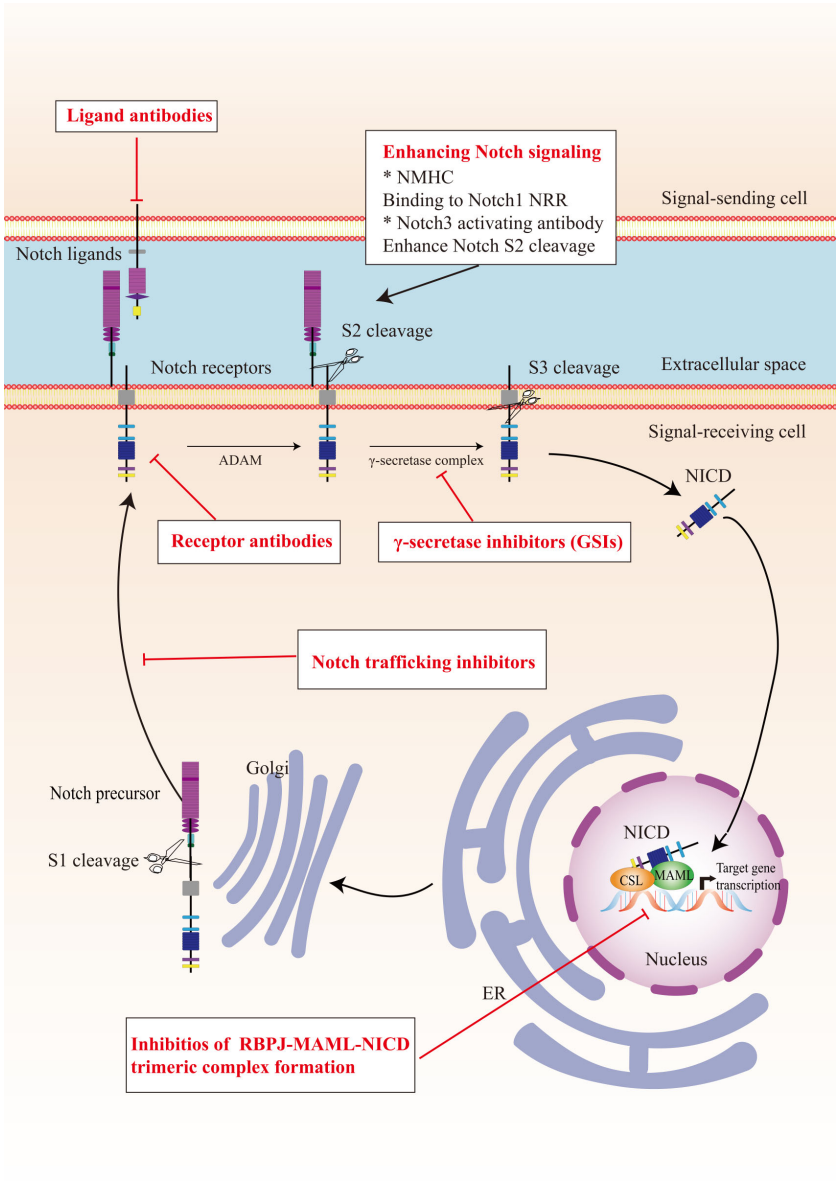

FIGURE 3
The potential therapeutics targeting Notch signaling pathway. Here are several strategies to modulate Notch signaling pathway: (I) inhibitors of Notch pre-processing, (II) receptor and ligand antibodies blocking ligand-receptor interaction, (III) inhibitors of the trimeric transcriptional complex assembly, (IV) molecules activating Notch signaling. ER, endoplasmic reticulum; NICD, Notch intracellular domain; NRR, negative regulatory region; NMHC, N-methylhemeanthidine chloride; MAML, Mastermind like transcriptional coactivator; GSIs, γ-secretase inhibitors.

the dual inhibition of Notch1 and Notch2 (197). Co-administration of glucocorticoid may alleviate the toxicity through inducing transcriptional up-regulation of cyclin D2 and protecting mice from developing the GSIs-induced intestinal goblet cell metaplasia in a preclinical mouse model of T-ALL (198).

Considering the inherent mechanism-based toxicity caused by pan-Notch inhibitor GSIs, novel inhibitors that selectively target individual Notch ligands and receptors have been developed. Selective blocking of Notch1 signaling inhibited cancer cell growth and deregulation of angiogenesis (199). The antibodies against Notch receptors are divided into two classes, one directed against the EGF-like repeat region and the other directed against the Notch negative regulatory region (200). Several potent and selective inhibitors against Notch1, Notch2, and Notch3 have been developed (199, 201, 202). However, there is a lack of inhibitor against Notch 4. The antibodies that selectively target the canonical ligands have also been investigated, such as Jagged antagonism (203).

In the past decades, several molecules targeting Notch trafficking and processing have been developed. The dihydropyridine FLI-06 as the first small molecular chemical compound functioned at an early stage in secretory traffic through disrupting the Golgi apparatus and inhibiting general secretion before exiting from the endoplasmic reticulum (204). FLI-06 was also demonstrated to block Notch activation and decrease the self-renewal ability of tongue CSCs (205). In addition, direct inhibition of the CSL/NICD complex has been reported to treat cancers. SAHM1, as a high-affinity binding of the hydrocarbon-stapled peptide, could prevent the assembly of the active transcriptional complex, resulting in genome-wide suppression

TABLE 3 Therapeutic approaches targeting Notch signaling pathway.

Class	Target	Tumor type
GSIs	γ-secretase	T-cell acute lymphoblastic leukemia (170), breast cancer (171), lung adenocarcinoma (172), colorectal cancer (173), prostate cancer (174)
Transcription blocker	CSL/NICD complex	Hematologic cancer (175), breast cancer (176)
Antibodies against Notch receptors	Notch1	T-acute lymphoblastic leukemia (177), adenoid cystic carcinoma (178)
	Notch2/Notch3	Untreated metastatic pancreatic cancer (179), small cell lung cancer (180), and other solid tumors (181)
	Notch3	Advanced breast cancer and other solid tumors (182)
Antibodies against Notch ligands	Jagged-1	Breast cancer (183), and other malignant tumors (184)
	Delta-like ligand 3	Small cell lung cancer (185)
	Delta-like ligand 4	Ovarian cancer (186), Metastatic non-squamous non-small cell lung cancer (187), and other advanced solid tumors (188)
Enhance Notch signaling activation	Notch negative regulatory region	Acute myeloid leukemia (189)
Therapeutic non-coding RNAs	MiRNAs	Prostate cancer (190), breast cancer (191), ovarian cancer (192), pancreatic cancer (193)
	LncRNAs	Ovarian cancer (194), nasopharyngeal carcinoma (195)

GSIs=γ-secretase inhibitors; miRNAs=microRNAs; lncRNAs=long non-coding RNAs.

of Notch-activated genes for the treatment of leukemia (206). There are other small molecules inhibiting the transcriptional activation complex, which have been investigated, such as IMR-1, CB-103, and RIN1 (175, 176, 207). However, given that loss of CSL derepressed target gene promoter and promoted tumorigenesis, targeting CSL may bring potential problems (208).

As mentioned above, Notch can act as a tumor suppressor in specific contexts, thus enhancing Notch signaling activation is a potential therapeutic strategy for cancer. A study demonstrated that N-methylhemeanthidine chloride, a novel Amaryllidaceae alkaloid, activated the Notch signaling *via* docking in the hydrophobic cavity within the Notch1 negative regulatory region and promoting Notch1 proteolytic cleavage (189). A monoclonal antibody was reported to enhance Notch3 cleavage and mimic the effects of ligand-induced Notch activation *via* binding to overlapping epitopes within negative regulatory region (202).

Accumulating evidence demonstrated that the non-coding RNAs' (ncRNAs) played a critical role in cancer therapy. NcRNAs are a class of RNAs including microRNAs (miRNAs) and long ncRNAs (lncRNAs) and other short ncRNAs. miRNAs and lncRNAs regulated cell fate determination *via* various signaling pathways (209). miRNA-34 was reported to suppress Notch1 expression, inducing ovarian cancer cell death (210). In contrast, miRNA-223 as an oncogene activated Notch signaling to induce tumor cell proliferation in colorectal cancer (211). The versatility is one of the advantages of miRNA therapeutics, which can suppress or mimic the activity of a miRNA. However, the delivery of miRNA remains an important challenge. LncRNAs mostly act as oncogenes in cancers. LncRNAs can interact with Notch or act as competing endogenous RNAs for miRNAs to indirectly induce Notch signaling in various cancers (212–214). Besides, other therapeutics targeting Notch are currently under investigation, such as natural products, virotherapy, and so on.

7.2 Hypoxia targeting strategies

Considering the critical role of hypoxia in tumor initiation, progression and therapy resistance, a growing number of preclinical and clinical cancer studies targeting hypoxia have been performed. In general, the strategies can be classified into hypoxia activated prodrugs (HAPs) and pharmacological inhibitors of the HIF signaling pathway.

7.2.1 Hypoxia activated prodrugs

HAPs are bioreductive drugs which are reduced by specific reductases under hypoxic conditions and release cytotoxins to kill cells (215). Five different chemical entities have the potential to target hypoxia based on their enzymatical reductive reaction under hypoxic conditions (216), including nitro groups, quinones, aromatic N-oxides, aliphatic N-oxides and transition metals. To date, several HAPs have been developed, including EO9 (apaziquone), RH1, SR 4233 (tirapazamine), SN30000, AQ4N (banoxantrone), PR-104, and TH-302 (evofosfamide) (Table 4). The effects of HAPs are different depending on the degree of hypoxia and the activity of reductase enzymes. The selection of the appropriate agents in different patients is dependent on the clinical context and requires predictive biomarkers (225).

7.2.2 Inhibitors of HIF signaling

HIF signaling is an attractive target for cancer treatment. Several inhibitors have been developed to directly bind to HIF-1α or HIF-2α, resulting in inhibition of their heterodimerization with HIF-β, such as acriflavine (226), PT2385 (227) and PT2399 (228). Heat shock protein 90 (Hsp90) can bind to HIF-1α and block the VHL-dependent proteasomal degradation of HIF-1α. A number of

TABLE 4 Hypoxia-activated prodrugs in clinical development.

Class	Prodrug	Current status	Tumor type
Quinone	E09 (Apaziquone)	III	Bladder cancer (217)
	RH1	I	Solid tumors (218)
Aromatic N-oxide	SR 4233 (Tirapazamine)	III	Non-small-cell lung cancer (219)
	SN30000	Preclinical	Triple-negative breast cancer (220)
Aliphatic N-oxide	AQ4N (Banoxantrone)	I	Solid tumors (221, 222)
Nitro	PR-104	II	Acute myeloid leukemia/lymphoblastic leukemia (223)
	TH-302 (Evofosfamide)	III	Soft-tissue sarcomas (224)

Hsp90 inhibitors have been developed during the past two decades. Hsp90 was identified as the biological target of the ansamycin class of natural products and derivatives, which has been extensively studied in cancer treatment (229). Hsp90 inhibitors apigenin and radicicol reduced hypoxia-induced VEGF expression to decrease angiogenesis (230, 231). Hsp90 can also modulate the conformation of the HIF-1 heterodimer, increasing its interaction with hypoxia-responsive elements, inducing HIF-1 transcriptional activity (231). Hsp90 can be regulated by posttranslational modifications, including acetylation. The process of histone acetylation is regulated by opposing activities of histone acetyltransferases and histone deacetylases (HDACs). HDAC6 functions as an Hsp90 deacetylase (232). HDAC inhibitor vorinostat was developed to inhibit HIF-1 transcriptional activity *via* direct Hsp90 acetylation, decreasing Hsp90-HIF-1 affinity and the interaction between HIF and hypoxia-responsive elements (233). Chetomin, a small molecule blocking the transcriptional co-activation of HIF-1 pathway, was evaluated as a promising candidate treatment for several types of cancers (234). Paradoxically, the stabilization of HIF-1α through inhibition of prolyl hydroxylase domain-containing protein 2 has antitumor effects in certain context. The loss of EGLN1 which encodes prolyl hydroxylase domain-containing protein 2 inhibited the proliferation of clear cell ovarian cancer cells (235). In general, anti-HIF agents are classified by different molecular mechanisms, including inhibition of HIF protein synthesis, degradation, and transcriptional activity. A detailed review of experimental chemical compounds and approved drugs directly targeting HIF pathway are presented in Table 5.

Targeting HIF signaling can be performed *via* interfering with other signaling pathways. PI3K/AKT/mTOR and MAPK/ERK pathways can increase HIF-1α synthesis in a cell type-specific manner (253). PI3K inhibitors LY294002 and wortmannin have been recognized as the synthesis inhibition of HIF-1α protein in the prostate carcinoma-derived cell lines PC-3 and DU145 (254). Temsirolimus, everolimus, and sirolimus as mTOR inhibitors are currently in clinical development for the treatment of solid tumors (255). The phase III clinical trials for temsirolimus and everolimus have been completed and showed a significant gain in survival for patients of metastatic renal cell carcinoma (256).

TABLE 5 Inhibitors directly targeting the HIF pathway in cancers.

Mechanism of inhibition	Compound/drug name	Current status	Tumor type
Inhibit HIF-1α mRNA expression	EZN-2698	I	Advanced malignancies (236)
Inhibit HIF-1α protein expression	Digoxin	II	Biochemically relapsed prostate cancer (237)
	2-methoxyestradiol	II	Multiple types of cancer (238)
	PX-478	I	Advanced solid tumors and lymphomas (239)
Increased HIF-1α degradation	YC-1	Preclinical	Several solid tumors (240)
	PX-12	II	Previously treated advanced pancreatic cancer (241)
	LW6	Preclinical	Colon cancer (242)
Inhibit HIF heterodimerization	Acriflavin	Preclinical	Prostate cancer (226)
	PT-2385	I	Advanced clear cell renal cell carcinoma (243)
	PT-2399	Preclinical	pVHL-defective clear cell renal cell carcinoma (244)
Inhibit HIF-1/DNA binding	Echinomycin	II	Several advanced cancers (245–249)
Inhibit HIF-1 transcriptional activity	Chetomin	Preclinical	Multiple myeloma (250)
	Bortezomib	FDA approved	Multiple myeloma and several solid tumors (251)
	Vorinostat	II	Metastatic urothelial cancer (252)

7.3 Combination therapy

Combination therapy is an important trend in the development of anticancer agents, and targeting hypoxia is critical in the new strategy (225). The anti-hypoxia agents were combined with immune checkpoint inhibitors to enhance the effect of immune checkpoint inhibitors in cancer treatment, which was based on hypoxia-induced expression and activity of immune checkpoints and immune checkpoint ligands on immune-cells and tumor cells (257). A phase II clinical trial of pembrolizumab and HDAC inhibitor vorinostat demonstrated the combination was active for patients with recurrent/metastatic squamous cell carcinomas of the head and neck, and salivary gland cancer (258). In a neuroblastoma xenograft model, the combination of anti-angiogenic drug sunitinib with hypoxia-activated prodrug evofosfamide was demonstrated to improve survival of mice (259).

Hypoxia and cellular interaction between tumor and non-tumor cells are two important TME. There are strong links between these two themes, and hypoxia contributes to TME to adversely affect therapeutic outcomes. Notch signaling plays an important role in regulating the crosstalk between the different compartments of the TME. Therefore, a combination of targeting Notch and hypoxia implies a potential treatment strategy of cancer to alter TME. In addition, hypoxia and Notch signaling have been shown to form a complex web of interaction in cancer, providing new insights into the combination therapeutics. Notch is a key regulator of tumor angiogenesis (260). The anti-angiogenesis drugs aggravated tumor hypoxia (261), indicating that targeting Notch may induce hypoxia. While, hypoxia activated Notch signaling pathway and may reduce the effect of Notch signaling inhibitors. Therefore, the combination of anti-hypoxia and Notch-targeted agents may present a new strategy for addressing the adverse effect of hypoxia.

8 Conclusion

The Notch signaling, as an evolutionarily conserved pathway, is usually activated and extensively involved in tumor initiation and progression. Notch signaling plays a critical role in the interaction between the tumor cells and the surrounding TME, acting as an oncogene or a tumor suppressor. Hypoxia is recognized as a hallmark of TME and the HIF pathway is a master regulator of the cellular hypoxic response. The interaction of Notch and HIF pathways played a key role in multiple biological processes in hypoxic tumor, including EMT, angiogenesis, and the maintenance of CSCs. A broad spectrum of anti-hypoxia agents and Notch signaling inhibitors have been developed during the past decades. The combination therapy has been an important trend of cancer treatment. Considering the complex web of hypoxia and Notch signaling, the combination of them implies a potential treatment strategy of cancer.

Author contributions

XCL and MG conceived the study. MG drafted the manuscript. XCL revised the manuscript critically for important intellectual content. YN, MX, and XSL provided important comments on the manuscript. All authors approved the final version of the manuscript. The corresponding author attests that all listed authors meet authorship criteria and that no others meeting the criteria have been omitted. All authors contributed to the article and approved the submitted version. The reviewer BZ declared a shared affiliation with the authors to the handling editor at the time of review.

Conflict of interest

The authors declare that the research was conducted in the absence of any commercial or financial relationships that could be construed as a potential conflict of interest.

Publisher's note

References

1. Mugisha S, Di X, Disoma C, Jiang H, Zhang S. Fringe family genes and their modulation of notch signaling in cancer. *Biochim Biophys Acta Rev Cancer* (2022) 1877 (4):188746. doi: 10.1016/j.bbcan.2022.188746

2. Siebel C, Lendahl U. Notch signaling in development, tissue homeostasis, and disease. *Physiol Rev* (2017) 97(4):1235–94. doi: 10.1152/physrev.00005.2017

3. Artavanis-Tsakonas S, Muskavitch MA. Notch: the past, the present, and the future. *Curr Top Dev Biol* (2010) 92:1–29. doi: 10.1016/s0070-2153(10)92001-2

4. Rebay I, Fleming RJ, Fehon RG, Cherbas L, Cherbas P, Artavanis-Tsakonas S. Specific EGF repeats of notch mediate interactions with delta and serrate: implications for notch as a multifunctional receptor. *Cell* (1991) 67(4):687–99. doi: 10.1016/0092-8674(91)90064-6

5. Langridge PD, Struhl G. Epsin-dependent ligand endocytosis activates notch by force. *Cell* (2017) 171(6):1383–96.e12. doi: 10.1016/j.cell.2017.10.048

6. Bray SJ. Notch signalling in context. *Nat Rev Mol Cell Biol* (2016) 17(11):722–35. doi: 10.1038/nrm.2016.94

7. Sprinzak D, Blacklow SC. Biophysics of notch signaling. *Annu Rev Biophys* (2021) 50:157–89. doi: 10.1146/annurev-biophys-101920-082204

8. Nandagopal N, Santat LA, LeBon L, Sprinzak D, Bronner ME, Elowitz MB. Dynamic ligand discrimination in the notch signaling pathway. *Cell* (2018) 172(4):869–80.e19. doi: 10.1016/j.cell.2018.01.002

9. Rusconi JC, Corbin V. Evidence for a novel notch pathway required for muscle precursor selection in drosophila. *Mech Dev* (1998) 79(1-2):39–50. doi: 10.1016/s0925-4773(98)00170-1

10. Ayaz F, Osborne BA. Non-canonical notch signaling in cancer and immunity. *Front Oncol* (2014) 4:345. doi: 10.3389/fonc.2014.00345

11. Hu QD, Ang BT, Karsak M, Hu WP, Cui XY, Duka T, et al. F3/contactin acts as a functional ligand for notch during oligodendrocyte maturation. *Cell* (2003) 115(2):163–75. doi: 10.1016/s0092-8674(03)00810-9

12. Shin HM, Minter LM, Cho OH, Gottipati S, Fauq AH, Golde TE, et al. Notch1 augments NF-kappaB activity by facilitating its nuclear retention. *EMBO J* (2006) 25 (1):129–38. doi: 10.1038/sj.emboj.7600902

13. D'Souza B, Miyamoto A, Weinmaster G. The many facets of notch ligands. *Oncogene* (2008) 27(38):5148–67. doi: 10.1038/onc.2008.229

14. Traustadóttir G, Jensen CH, Thomassen M, Beck HC, Mortensen SB, Laborda J, et al. Evidence of non-canonical NOTCH signaling: Delta-like 1 homolog (DLK1) directly interacts with the NOTCH1 receptor in mammals. *Cell Signal* (2016) 28(4):246–54. doi: 10.1016/j.cellsig.2016.01.003

15. Eiraku M, Tohgo A, Ono K, Kaneko M, Fujishima K, Hirano T, et al. DNER acts as a neuron-specific notch ligand during bergmann glial development. *Nat Neurosci* (2005) 8 (7):873–80. doi: 10.1038/nn1492

16. Cui XY, Hu QD, Tekaya M, Shimoda Y, Ang BT, Nie DY, et al. NB-3/Notch1 pathway *via* Deltex1 promotes neural progenitor cell differentiation into oligodendrocytes. *J Biol Chem* (2004) 279(24):25858–65. doi: 10.1074/jbc.M313505200

17. Heath E, Tahri D, Andermarcher E, Schofield P, Fleming S, Boulter CA. Abnormal skeletal and cardiac development, cardiomyopathy, muscle atrophy and cataracts in mice with a targeted disruption of the Nov (Ccn3) gene. *BMC Dev Biol* (2008) 8:18. doi: 10.1186/1471-213x-8-18

18. Miyamoto A, Lau R, Hein PW, Shipley JM, Weinmaster G. Microfibrillar proteins MAGP-1 and MAGP-2 induce Notch1 extracellular domain dissociation and receptor activation. *J Biol Chem* (2006) 281(15):10089–97. doi: 10.1074/jbc.M600298200

19. Baker NE, Mlodzik M, Rubin GM. Spacing differentiation in the developing drosophila eye: a fibrinogen-related lateral inhibitor encoded by scabrous. *Science* (1990) 250(4986):1370–7. doi: 10.1126/science.2175046

20. Powell PA, Wesley C, Spencer S, Cagan RL. Scabrous complexes with notch to mediate boundary formation. *Nature* (2001) 409(6820):626–30. doi: 10.1038/35054566

21. Raafat A, Lawson S, Bargo S, Klauzinska M, Strizzi L, Goldhar AS, et al. Rbpj conditional knockout reveals distinct functions of Notch4/Int3 in mammary gland development and tumorigenesis. *Oncogene* (2009) 28(2):219–30. doi: 10.1038/onc.2008.379

22. Jin S, Mutvei AP, Chivukula IV, Andersson ER, Ramsköld D, Sandberg R, et al. Non-canonical notch signaling activates IL-6/JAK/STAT signaling in breast tumor cells and is controlled by p53 and IKKα/IKKβ. *Oncogene* (2013) 32(41):4892–902. doi: 10.1038/onc.2012.517

23. Perumalsamy LR, Nagala M, Banerjee P, Sarin A. A hierarchical cascade activated by non-canonical notch signaling and the mTOR-rictor complex regulates neglect-induced death in mammalian cells. *Cell Death Differ* (2009) 16(6):879–89. doi: 10.1038/cdd.2009.20

24. Veeraraghavalu K, Subbaiah VK, Srivastava S, Chakrabarti O, Syal R, Krishna S. Complementation of human papillomavirus type 16 E6 and E7 by Jagged1-specific Notch1-phosphatidylinositol 3-kinase signaling involves pleiotropic oncogenic functions independent of CBF1;Su(H);Lag-1 activation. *J Virol* (2005) 79(12):7889–98. doi: 10.1128/jvi.79.12.7889-7898.2005

25. Polacheck WJ, Kutys ML, Yang J, Eyckmans J, Wu Y, Vasavada H, et al. A non-canonical notch complex regulates adherens junctions and vascular barrier function. *Nature* (2017) 552(7684):258–62. doi: 10.1038/nature24998

26. Fischer A, Braga VMM. Vascular permeability: Flow-mediated, non-canonical notch signalling promotes barrier integrity. *Curr Biol* (2018) 28(3):R119–r121. doi: 10.1016/j.cub.2017.11.065

27. Weng AP, Ferrando AA, Lee W, JPt M, LB S, Sanchez-Irizarry C, et al. Activating mutations of NOTCH1 in human T cell acute lymphoblastic leukemia. *Science* (2004) 306 (5694):269–71. doi: 10.1126/science.1102160

28. Bernasconi-Elias P, Hu T, Jenkins D, Firestone B, Gans S, Kurth E, et al. Characterization of activating mutations of NOTCH3 in T-cell acute lymphoblastic leukemia and anti-leukemic activity of NOTCH3 inhibitory antibodies. *Oncogene* (2016) 35(47):6077–86. doi: 10.1038/onc.2016.133

29. King B, Trimarchi T, Reavie L, Xu L, Mullenders J, Ntziachristos P, et al. The ubiquitin ligase FBXW7 modulates leukemia-initiating cell activity by regulating MYC stability. *Cell* (2013) 153(7):1552–66. doi: 10.1016/j.cell.2013.05.041

30. Fabbri G, Rasi S, Rossi D, Trifonov V, Khiabanian H, Ma J, et al. Analysis of the chronic lymphocytic leukemia coding genome: role of NOTCH1 mutational activation. *J Exp Med* (2011) 208(7):1389–401. doi: 10.1084/jem.20110921

31. Kiel MJ, Velusamy T, Betz BL, Zhao L, Weigelin HG, Chiang MY, et al. Whole-genome sequencing identifies recurrent somatic NOTCH2 mutations in splenic marginal zone lymphoma. *J Exp Med* (2012) 209(9):1553–65. doi: 10.1084/jem.20120910

32. Lohr JG, Stojanov P, Lawrence MS, Auclair D, Chapuy B, Sougnez C, et al. Discovery and prioritization of somatic mutations in diffuse large b-cell lymphoma (DLBCL) by whole-exome sequencing. *Proc Natl Acad Sci U.S.A.* (2012) 109(10):3879–84. doi: 10.1073/pnas.1121343109

33. Lee SY, Kumano K, Nakazaki K, Sanada M, Matsumoto A, Yamamoto G, et al. Gain-of-function mutations and copy number increases of Notch2 in diffuse large b-cell lymphoma. *Cancer Sci* (2009) 100(5):920–6. doi: 10.1111/j.1349-7006.2009.01130.x

34. Xie M, Wei S, Wu X, Li X, You Y, He C. Alterations of notch pathway in patients with adenoid cystic carcinoma of the trachea and its impact on survival. *Lung Cancer* (2018) 121:41–7. doi: 10.1016/j.lungcan.2018.04.020

35. Stephens PJ, Davies HR, Mitani Y, Van Loo P, Shlien A, Tarpey PS, et al. Whole exome sequencing of adenoid cystic carcinoma. *J Clin Invest* (2013) 123(7):2965–8. doi: 10.1172/jci67201

36. Pappas K, Martin TC, Wolfe AL, Nguyen CB, Su T, Jin J, et al. NOTCH and EZH2 collaborate to repress PTEN expression in breast cancer. *Commun Biol* (2021) 4(1):312. doi: 10.1038/s42003-021-01825-8

37. Wu D, Wang S, Oliveira DV, Del Gaudio F, Vanlandewijck M, Lebouvier T, et al. The infantile myofibromatosis NOTCH3 L1519P mutation leads to hyperactivated ligand-independent notch signaling and increased PDGFRB expression. *Dis Model Mech* (2021) 14(2):dmm046300. doi: 10.1242/dmm.046300

38. Mosquera JM, Sboner A, Zhang L, Chen CL, Sung YS, Chen HW, et al. Novel MIR143-NOTCH fusions in benign and malignant glomus tumors. *Genes Chromosomes Cancer* (2013) 52(11):1075–87. doi: 10.1002/gcc.22102

39. Agrawal N, Frederick MJ, Pickering CR, Bettegowda C, Chang K, Li RJ, et al. Exome sequencing of head and neck squamous cell carcinoma reveals inactivating mutations in NOTCH1. *Science* (2011) 333(6046):1154–7. doi: 10.1126/science.1206923

40. Stransky N, Egloff AM, Tward AD, Kostic AD, Cibulskis K, Sivachenko A, et al. The mutational landscape of head and neck squamous cell carcinoma. *Science* (2011) 333 (6046):1157–60. doi: 10.1126/science.1208130

41. George J, Lim JS, Jang SJ, Cun Y, Ozretić L, Kong G, et al. Comprehensive genomic profiles of small cell lung cancer. *Nature* (2015) 524(7563):47–53. doi: 10.1038/nature14664

42. Maraver A, Fernandez-Marcos PJ, Cash TP, Mendez-Pertuz M, Dueñas M, Maietta P, et al. NOTCH pathway inactivation promotes bladder cancer progression. *J Clin Invest* (2015) 125(2):824–30. doi: 10.1172/jci78185

43. Rampias T, Vgenopoulou P, Avgeris M, Polyzos A, Stravodimos K, Valavanis C, et al. A new tumor suppressor role for the notch pathway in bladder cancer. *Nat Med* (2014) 20(10):1199–205. doi: 10.1038/nm.3678

44. Wang NJ, Sanborn Z, Arnett KL, Bayston LJ, Liao W, Proby CM, et al. Loss-of-function mutations in notch receptors in cutaneous and lung squamous cell carcinoma. *Proc Natl Acad Sci U.S.A.* (2011) 108(43):17761–6. doi: 10.1073/pnas.1114669108

45. Zender S, Nickeleit I, Wuestefeld T, Sörensen I, Dauch D, Bozko P, et al. A critical role for notch signaling in the formation of cholangiocellular carcinomas. *Cancer Cell* (2013) 23(6):784–95. doi: 10.1016/j.ccr.2013.04.019

46. Gramantieri L, Giovannini C, Lanzi A, Chieco P, Ravaioli M, Venturi A, et al. Aberrant Notch3 and Notch4 expression in human hepatocellular carcinoma. *Liver Int* (2007) 27(7):997–1007. doi: 10.1111/j.1478-3231.2007.01544.x

47. Ning L, Wentworth L, Chen H, Weber SM. Down-regulation of Notch1 signaling inhibits tumor growth in human hepatocellular carcinoma. *Am J Transl Res* (2009) 1 (4):358–66.

48. Qi R, An H, Yu Y, Zhang M, Liu S, Xu H, et al. Notch1 signaling inhibits growth of human hepatocellular carcinoma through induction of cell cycle arrest and apoptosis. *Cancer Res* (2003) 63(23):8323–9.

49. Ye J, Wen J, Ning Y, Li Y. Higher notch expression implies poor survival in pancreatic ductal adenocarcinoma: A systematic review and meta-analysis. *Pancreatology* (2018) 18(8):954–61. doi: 10.1016/j.pan.2018.09.014

50. Hanlon L, Avila JL, Demarest RM, Troutman S, Allen M, Ratti F, et al. Notch1 functions as a tumor suppressor in a model of K-ras-induced pancreatic ductal adenocarcinoma. *Cancer Res* (2010) 70(11):4280–6. doi: 10.1158/0008-5472.Can-09-4645

51. Balint K, Xiao M, Pinnix CC, Soma A, Veres I, Juhasz I, et al. Activation of Notch1 signaling is required for beta-catenin-mediated human primary melanoma progression. *J Clin Invest* (2005) 115(11):3166–76. doi: 10.1172/JCI25001

52. Müller CS. Notch signaling and malignant melanoma. *Adv Exp Med Biol* (2012) 727:258–64. doi: 10.1007/978-1-4614-0899-4_19

53. Zhang L, Sha J, Yang G, Huang X, Bo J, Huang Y. Activation of notch pathway is linked with epithelial-mesenchymal transition in prostate cancer cells. *Cell Cycle* (2017) 16(10):999–1007. doi: 10.1080/15384101.2017.1312237

54. Zhu H, Zhou X, Redfield S, Lewin J, Miele L. Elevated jagged-1 and notch-1 expression in high grade and metastatic prostate cancers. *Am J Transl Res* (2013) 5 (3):368–78.

55. Bazzoni R, Bentivegna A. Role of notch signaling pathway in glioblastoma pathogenesis. *Cancers (Basel)* (2019) 11(3):292. doi: 10.3390/cancers11030292

56. El Hindy N, Keyvani K, Pagenstecher A, Dammann P, Sandalcioglu IE, Sure U, et al. Implications of Dll4-notch signaling activation in primary glioblastoma multiforme. *Neuro Oncol* (2013) 15(10):1366–78. doi: 10.1093/neuonc/not071

57. Purow BW, Haque RM, Noel MW, Su Q, Burdick MJ, Lee J, et al. Expression of notch-1 and its ligands, delta-like-1 and jagged-1, is critical for glioma cell survival and proliferation. *Cancer Res* (2005) 65(6):2353–63. doi: 10.1158/0008-5472.Can-04-1890

58. Ho AS, Ochoa A, Jayakumaran G, Zehir A, Valero Mayor C, Tepe J, et al. Genetic hallmarks of recurrent/metastatic adenoid cystic carcinoma. *J Clin Invest* (2019) 129 (10):4276–89. doi: 10.1172/jci128227

59. Santagata S, Demichelis F, Riva A, Varambally S, Hofer MD, Kutok JL, et al. JAGGED1 expression is associated with prostate cancer metastasis and recurrence. *Cancer Res* (2004) 64(19):6854–7. doi: 10.1158/0008-5472.Can-04-2500

60. Reedijk M, Odorcic S, Chang L, Zhang H, Miller N, McCready DR, et al. High-level coexpression of JAG1 and NOTCH1 is observed in human breast cancer and is associated with poor overall survival. *Cancer Res* (2005) 65(18):8530–7. doi: 10.1158/0008-5472.CAN-05-1069

61. Zagouras P, Stifani S, Blaumueller CM, Carcangiu ML, Artavanis-Tsakonas S. Alterations in notch signaling in neoplastic lesions of the human cervix. *Proc Natl Acad Sci U.S.A.* (1995) 92(14):6414–8. doi: 10.1073/pnas.92.14.6414

62. Hendrix MJ, Seftor RE, Seftor EA, Gruman LM, Lee LM, Nickoloff BJ, et al. Transendothelial function of human metastatic melanoma cells: role of the microenvironment in cell-fate determination. *Cancer Res* (2002) 62(3):665–8.

63. Chen Y, De Marco MA, Graziani I, Gazdar AF, Strack PR, Miele L, et al. Oxygen concentration determines the biological effects of NOTCH-1 signaling in adenocarcinoma of the lung. *Cancer Res* (2007) 67(17):7954–9. doi: 10.1158/0008-5472.Can-07-1229

64. Li X, Cao X, Zhao H, Guo M, Fang X, Li K, et al. Hypoxia activates Notch4 *via* ERK/JNK/P38 MAPK signaling pathways to promote lung adenocarcinoma progression and metastasis. *Front Cell Dev Biol* (2021) 9:780121. doi: 10.3389/fcell.2021.780121

65. Vacca A, Felli MP, Palermo R, Di Mario G, Calce A, Di Giovine M, et al. Notch3 and pre-TCR interaction unveils distinct NF-kappaB pathways in T-cell development and leukemia. *EMBO J* (2006) 25(5):1000–8. doi: 10.1038/sj.emboj.7600996

66. Zhang J, Kuang Y, Wang Y, Xu Q, Ren Q. Notch-4 silencing inhibits prostate cancer growth and EMT *via* the NF-κB pathway. *Apoptosis* (2017) 22(6):877–84. doi: 10.1007/s10495-017-1368-0

67. Liu ZJ, Xiao M, Balint K, Smalley KS, Brafford P, Qiu R, et al. Notch1 signaling promotes primary melanoma progression by activating mitogen-activated protein kinase/phosphatidylinositol 3-kinase-Akt pathways and up-regulating n-cadherin expression. *Cancer Res* (2006) 66(8):4182–90. doi: 10.1158/0008-5472.Can-05-3589

68. Li X, Wang S, Deng N, Guo X, Fu M, Ma Y, et al. N-((1-(4-Fluorophenyl)-1H-1,2,3-triazol-4-yl)methyl)-2-methylene-3-oxo-olean-12-en-28-amide induces apoptosis in human breast cancer cells by stimulating oxidative stress and inhibiting the notch-akt signaling pathway. *Oxid Med Cell Longev* (2022) 2022:8123120. doi: 10.1155/2022/8123120

69. Wang W, Sun R, Zeng L, Chen Y, Zhang N, Cao S, et al. GALNT2 promotes cell proliferation, migration, and invasion by activating the Notch/Hes1-PTEN-PI3K/Akt signaling pathway in lung adenocarcinoma. *Life Sci* (2021) 276:119439. doi: 10.1016/j.lfs.2021.119439

70. Camps J, Pitt JJ, Emons G, Hummon AB, Case CM, Grade M, et al. Genetic amplification of the NOTCH modulator LNX2 upregulates the WNT/β-catenin pathway in colorectal cancer. *Cancer Res* (2013) 73(6):2003–13. doi: 10.1158/0008-5472.Can-12-3159

71. Mu R, Zou YK, Tu K, Wang DB, Tang D, Yu Z, et al. Hypoxia promotes pancreatic cancer cell dedifferentiation to stem-like cell phenotypes with high tumorigenic potential by the HIF-1α/Notch signaling pathway. *Pancreas* (2021) 50(5):756–65. doi: 10.1097/mpa.0000000000001828

72. Yan Y, Liu F, Han L, Zhao L, Chen J, Olopade OI, et al. HIF-2α promotes conversion to a stem cell phenotype and induces chemoresistance in breast cancer cells by activating wnt and notch pathways. *J Exp Clin Cancer Res* (2018) 37(1):256. doi: 10.1186/s13046-018-0925-x

73. Qiang L, Wu T, Zhang HW, Lu N, Hu R, Wang YJ, et al. HIF-1α is critical for hypoxia-mediated maintenance of glioblastoma stem cells by activating notch signaling pathway. *Cell Death Differ* (2012) 19(2):284–94. doi: 10.1038/cdd.2011.95

74. Yamashita AS, Geraldo MV, Fuziwara CS, Kulcsar MA, Friguglietti CU, da Costa RB, et al. Notch pathway is activated by MAPK signaling and influences papillary thyroid cancer proliferation. *Transl Oncol* (2013) 6(2):197–205. doi: 10.1593/tlo.12442

75. Izrailit J, Berman HK, Datti A, Wrana JL, Reedijk M. High throughput kinase inhibitor screens reveal TRB3 and MAPK-ERK/TGFβ pathways as fundamental notch regulators in breast cancer. *Proc Natl Acad Sci U.S.A.* (2013) 110(5):1714–9. doi: 10.1073/pnas.1214014110

76. Zeng Q, Li S, Chepeha DB, Giordano TJ, Li J, Zhang H, et al. Crosstalk between tumor and endothelial cells promotes tumor angiogenesis by MAPK activation of notch signaling. *Cancer Cell* (2005) 8(1):13–23. doi: 10.1016/j.ccr.2005.06.004

77. Sun Y, Lowther W, Kato K, Bianco C, Kenney N, Strizzi L, et al. Notch4 intracellular domain binding to Smad3 and inhibition of the TGF-beta signaling. *Oncogene* (2005) 24(34):5365–74. doi: 10.1038/sj.onc.1208528

78. Sjölund J, Boström AK, Lindgren D, Manna S, Moustakas A, Ljungberg B, et al. The notch and TGF-β signaling pathways contribute to the aggressiveness of clear cell renal cell carcinoma. *PLoS One* (2011) 6(8):e23057. doi: 10.1371/journal.pone.0023057

79. Licciulli S, Avila JL, Hanlon L, Troutman S, Cesaroni M, Kota S, et al. Notch1 is required for kras-induced lung adenocarcinoma and controls tumor cell survival *via* p53. *Cancer Res* (2013) 73(19):5974–84. doi: 10.1158/0008-5472.Can-13-1384

80. Lefort K, Mandinova A, Ostano P, Kolev V, Calpini V, Kolfschoten I, et al. Notch1 is a p53 target gene involved in human keratinocyte tumor suppression through negative regulation of ROCK1/2 and MRCKalpha kinases. *Genes Dev* (2007) 21(5):562–77. doi: 10.1101/gad.1484707

81. Beverly LJ, Felsher DW, Capobianco AJ. Suppression of p53 by notch in lymphomagenesis: implications for initiation and regression. *Cancer Res* (2005) 65(16):7159–68. doi: 10.1158/0008-5472.Can-05-1664

82. Shin HM, Tilahun ME, Cho OH, Chandiran K, Kuksin CA, Keerthivasan S, et al. NOTCH1 can initiate NF-κB activation *via* cytosolic interactions with components of the T cell signalosome. *Front Immunol* (2014) 5:249. doi: 10.3389/fimmu.2014.00249

83. Maillard I, Pear WS. Notch and cancer: best to avoid the ups and downs. *Cancer Cell* (2003) 3(3):203–5. doi: 10.1016/s1535-6108(03)00052-7

84. Nicolas M, Wolfer A, Raj K, Kummer JA, Mill P, van Noort M, et al. Notch1 functions as a tumor suppressor in mouse skin. *Nat Genet* (2003) 33(3):416–21. doi: 10.1038/ng1099

85. Zweidler-McKay PA, He Y, Xu L, Rodriguez CG, Karnell FG, Carpenter AC, et al. Notch signaling is a potent inducer of growth arrest and apoptosis in a wide range of b-cell malignancies. *Blood* (2005) 106(12):3898–906. doi: 10.1182/blood-2005-01-0355

86. Viatour P, Ehmer U, Saddic LA, Dorrell C, Andersen JB, Lin C, et al. Notch signaling inhibits hepatocellular carcinoma following inactivation of the RB pathway. *J Exp Med* (2011) 208(10):1963–76. doi: 10.1084/jem.20110198

87. Crabtree JS, Singleton CS, Miele L. Notch signaling in neuroendocrine tumors. *Front Oncol* (2016) 6:94. doi: 10.3389/fonc.2016.00094

88. Maillard I, Adler SH, Pear WS. Notch and the immune system. *Immunity* (2003) 19(6):781–91. doi: 10.1016/s1074-7613(03)00325-x

89. Casey SC, Amedei A, Aquilano K, Azmi AS, Benencia F, Bhakta D, et al. Cancer prevention and therapy through the modulation of the tumor microenvironment. *Semin Cancer Biol* (2015) 35 Suppl(Suppl):S199–s223. doi: 10.1016/j.semcancer.2015.02.007

90. Lim YZ, South AP. Tumour-stroma crosstalk in the development of squamous cell carcinoma. *Int J Biochem Cell Biol* (2014) 53:450–8. doi: 10.1016/j.biocel.2014.06.012

91. Maillard I, He Y, Pear WS. From the yolk sac to the spleen: New roles for notch in regulating hematopoiesis. *Immunity* (2003) 18(5):587–9. doi: 10.1016/s1074-7613(03)00119-5

92. Janghorban M, Yang Y, Zhao N, Hamor C, Nguyen TM, Zhang XH, et al. Single-cell analysis unveils the role of the tumor immune microenvironment and notch signaling in dormant minimal residual disease. *Cancer Res* (2022) 82(5):885–99. doi: 10.1158/0008-5472.Can-21-1230

93. Liu H, Wang J, Zhang M, Xuan Q, Wang Z, Lian X, et al. Jagged1 promotes aromatase inhibitor resistance by modulating tumor-associated macrophage differentiation in breast cancer patients. *Breast Cancer Res Treat* (2017) 166(1):95–107. doi: 10.1007/s10549-017-4394-2

94. Jaiswal A, Murakami K, Elia A, Shibahara Y, Done SJ, Wood SA, et al. Therapeutic inhibition of USP9x-mediated notch signaling in triple-negative breast cancer. *Proc Natl Acad Sci U.S.A.* (2021) 118(38):e2101592118. doi: 10.1073/pnas.2101592118

95. Nandi A, Debnath R, Nayak A, To TKJ, Thacker G, Reilly M, et al. Dll1-mediated notch signaling drives tumor cell cross-talk with cancer-associated fibroblasts to promote radioresistance in breast cancer. *Cancer Res* (2022) 82(20):3718–33. doi: 10.1158/0008-5472.Can-21-1225

96. Lee P, Chandel NS, Simon MC. Cellular adaptation to hypoxia through hypoxia inducible factors and beyond. *Nat Rev Mol Cell Biol* (2020) 21(5):268–83. doi: 10.1038/s41580-020-0227-y

97. Vaupel P, Mayer A. Hypoxia in cancer: significance and impact on clinical outcome. *Cancer Metastasis Rev* (2007) 26(2):225–39. doi: 10.1007/s10555-007-9055-1

98. Brahimi-Horn MC, Chiche J, Pouysségur J. Hypoxia and cancer. *J Mol Med (Berl)* (2007) 85(12):1301–7. doi: 10.1007/s00109-007-0281-3

99. Qiu GZ, Jin MZ, Dai JX, Sun W, Feng JH, Jin WL. Reprogramming of the tumor in the hypoxic niche: The emerging concept and associated therapeutic strategies. *Trends Pharmacol Sci* (2017) 38(8):669–86. doi: 10.1016/j.tips.2017.05.002

100. Harris AL. Hypoxia–a key regulatory factor in tumour growth. *Nat Rev Cancer* (2002) 2(1):38–47. doi: 10.1038/nrc704

101. Muz B, de la Puente P, Azab F, Azab AK. The role of hypoxia in cancer progression, angiogenesis, metastasis, and resistance to therapy. *Hypoxia (Auckl)* (2015) 3:83–92. doi: 10.2147/hp.S93413

102. Semenza GL. Hypoxia-inducible factors in physiology and medicine. *Cell* (2012) 148(3):399–408. doi: 10.1016/j.cell.2012.01.021

103. Kaelin WGJr., Ratcliffe PJ. Oxygen sensing by metazoans: the central role of the HIF hydroxylase pathway. *Mol Cell* (2008) 30(4):393–402. doi: 10.1016/j.molcel.2008.04.009

104. Jaakkola P, Mole DR, Tian YM, Wilson MI, Gielbert J, Gaskell SJ, et al. Targeting of HIF-alpha to the von hippel-lindau ubiquitylation complex by O2-regulated prolyl hydroxylation. *Science* (2001) 292(5516):468–72. doi: 10.1126/science.1059796

105. Cockman ME, Masson N, Mole DR, Jaakkola P, Chang GW, Clifford SC, et al. Hypoxia inducible factor-alpha binding and ubiquitylation by the von hippel-lindau tumor suppressor protein. *J Biol Chem* (2000) 275(33):25733–41. doi: 10.1074/jbc.M002740200

106. Wu D, Potluri N, Lu J, Kim Y, Rastinejad F. Structural integration in hypoxia-inducible factors. *Nature* (2015) 524(7565):303–8. doi: 10.1038/nature14883

107. Mahon PC, Hirota K, Semenza GL. FIH-1: a novel protein that interacts with HIF-1alpha and VHL to mediate repression of HIF-1 transcriptional activity. *Genes Dev* (2001) 15(20):2675–86. doi: 10.1101/gad.924501

108. Lando D, Peet DJ, Gorman JJ, Whelan DA, Whitelaw ML, Bruick RK. FIH-1 is an asparaginyl hydroxylase enzyme that regulates the transcriptional activity of hypoxia-inducible factor. *Genes Dev* (2002) 16(12):1466–71. doi: 10.1101/gad.991402

109. Yang SL, Wu C, Xiong ZF, Fang X. Progress on hypoxia-inducible factor-3: Its structure, gene regulation and biological function (Review). *Mol Med Rep* (2015) 12(2):2411–6. doi: 10.3892/mmr.2015.3689

110. Talks KL, Turley H, Gatter KC, Maxwell PH, Pugh CW, Ratcliffe PJ, et al. The expression and distribution of the hypoxia-inducible factors HIF-1alpha and HIF-2alpha in normal human tissues, cancers, and tumor-associated macrophages. *Am J Pathol* (2000) 157(2):411–21. doi: 10.1016/s0002-9440(10)64554-3

111. Suzuki N, Gradin K, Poellinger L, Yamamoto M. Regulation of hypoxia-inducible gene expression after HIF activation. *Exp Cell Res* (2017) 356(2):182–6. doi: 10.1016/j.yexcr.2017.03.013

112. Kenneth NS, Rocha S. Regulation of gene expression by hypoxia. *Biochem J* (2008) 414(1):19–29. doi: 10.1042/bj20081055

113. Heikkilä M, Pasanen A, Kivirikko KI, Myllyharju J. Roles of the human hypoxia-inducible factor (HIF)-3α variants in the hypoxia response. *Cell Mol Life Sci* (2011) 68(23):3885–901. doi: 10.1007/s00018-011-0679-5

114. Frolova O, Samudio I, Benito JM, Jacamo R, Kornblau SM, Markovic A, et al. Regulation of HIF-1α signaling and chemoresistance in acute lymphocytic leukemia under hypoxic conditions of the bone marrow microenvironment. *Cancer Biol Ther* (2012) 13(10):858–70. doi: 10.4161/cbt.20838

115. Dales JP, Garcia S, Meunier-Carpentier S, Andrac-Meyer L, Haddad O, Lavaut MN, et al. Overexpression of hypoxia-inducible factor HIF-1alpha predicts early relapse in breast cancer: retrospective study in a series of 745 patients. *Int J Cancer* (2005) 116 (5):734–9. doi: 10.1002/ijc.20984

116. Rasheed S, Harris AL, Tekkis PP, Turley H, Silver A, McDonald PJ, et al. Hypoxia-inducible factor-1alpha and -2alpha are expressed in most rectal cancers but only hypoxia-inducible factor-1alpha is associated with prognosis. *Br J Cancer* (2009) 100 (10):1666–73. doi: 10.1038/sj.bjc.6605026

117. Schmitz KJ, Müller CI, Reis H, Alakus H, Winde G, Baba HA, et al. Combined analysis of hypoxia-inducible factor 1 alpha and metallothionein indicates an aggressive subtype of colorectal carcinoma. *Int J Colorectal Dis* (2009) 24(11):1287–96. doi: 10.1007/s00384-009-0753-8

118. Vander Heiden MG, Cantley LC, Thompson CB. Understanding the warburg effect: the metabolic requirements of cell proliferation. *Science* (2009) 324(5930):1029–33. doi: 10.1126/science.1160809

119. Wolf A, Agnihotri S, Micallef J, Mukherjee J, Sabha N, Cairns R, et al. Hexokinase 2 is a key mediator of aerobic glycolysis and promotes tumor growth in human glioblastoma multiforme. *J Exp Med* (2011) 208(2):313–26. doi: 10.1084/jem.20101470

120. Yi W, Clark PM, Mason DE, Keenan MC, Hill C, Goddard WA3rd. Phosphofructokinase 1 glycosylation regulates cell growth and metabolism. *Science* (2012) 337(6097):975–80. doi: 10.1126/science.1222278

121. Maxwell PH, Pugh CW, Ratcliffe PJ. Activation of the HIF pathway in cancer. *Curr Opin Genet Dev* (2001) 11(3):293–9. doi: 10.1016/s0959-437x(00)00193-3

122. Grimshaw MJ. Endothelins and hypoxia-inducible factor in cancer. *Endocr Relat Cancer* (2007) 14(2):233–44. doi: 10.1677/erc-07-0057

123. Smith K, Gunaratnam L, Morley M, Franovic A, Mekhail K, Lee S. Silencing of epidermal growth factor receptor suppresses hypoxia-inducible factor-2-driven VHL-/- renal cancer. *Cancer Res* (2005) 65(12):5221–30. doi: 10.1158/0008-5472.Can-05-0169

124. Rey S, Semenza GL. Hypoxia-inducible factor-1-dependent mechanisms of vascularization and vascular remodelling. *Cardiovasc Res* (2010) 86(2):236–42. doi: 10.1093/cvr/cvq045

125. Kelly BD, Hackett SF, Hirota K, Oshima Y, Cai Z, Berg-Dixon S, et al. Cell type-specific regulation of angiogenic growth factor gene expression and induction of angiogenesis in nonischemic tissue by a constitutively active form of hypoxia-inducible factor 1. *Circ Res* (2003) 93(11):1074–81. doi: 10.1161/01.Res.0000102937.50486.1b

126. Zhang W, Shi X, Peng Y, Wu M, Zhang P, Xie R, et al. HIF-1α promotes epithelial-mesenchymal transition and metastasis through direct regulation of ZEB1 in colorectal cancer. *PLoS One* (2015) 10(6):e0129603. doi: 10.1371/journal.pone.0129603

127. Yang MH, Wu MZ, Chiou SH, Chen PM, Chang SY, Liu CJ, et al. Direct regulation of TWIST by HIF-1alpha promotes metastasis. *Nat Cell Biol* (2008) 10(3):295–305. doi: 10.1038/ncb1691

128. Krishnamachary B, Zagzag D, Nagasawa H, Rainey K, Okuyama H, Baek JH, et al. Hypoxia-inducible factor-1-dependent repression of e-cadherin in von hippel-lindau tumor suppressor-null renal cell carcinoma mediated by TCF3, ZFHX1A, and ZFHX1B. *Cancer Res* (2006) 66(5):2725–31. doi: 10.1158/0008-5472.Can-05-3719

129. Jögi A, Øra I, Nilsson H, Lindeheim A, Makino Y, Poellinger L, et al. Hypoxia alters gene expression in human neuroblastoma cells toward an immature and neural crest-like phenotype. *Proc Natl Acad Sci U.S.A.* (2002) 99(10):7021–6. doi: 10.1073/pnas.102660199

130. Irshad K, Mohapatra SK, Srivastava C, Garg H, Mishra S, Dikshit B, et al. A combined gene signature of hypoxia and notch pathway in human glioblastoma and its prognostic relevance. *PLoS One* (2015) 10(3):e0118201. doi: 10.1371/journal.pone.0118201

131. Gustafsson MV, Zheng X, Pereira T, Gradin K, Jin S, Lundkvist J, et al. Hypoxia requires notch signaling to maintain the undifferentiated cell state. *Dev Cell* (2005) 9 (5):617–28. doi: 10.1016/j.devcel.2005.09.010

132. Mailhos C, Modlich U, Lewis J, Harris A, Bicknell R, Ish-Horowicz D. Delta4, an endothelial specific notch ligand expressed at sites of physiological and tumor angiogenesis. *Differentiation* (2001) 69(2-3):135–44. doi: 10.1046/j.1432-0436.2001.690207.x

133. Pietras A, von Stedingk K, Lindgren D, Påhlman S, Axelson H. JAG2 induction in hypoxic tumor cells alters notch signaling and enhances endothelial cell tube formation. *Mol Cancer Res* (2011) 9(5):626–36. doi: 10.1158/1541-7786.Mcr-10-0508

134. Lanner F, Lee KL, Ortega GC, Sohl M, Li X, Jin S, et al. Hypoxia-induced arterial differentiation requires adrenomedullin and notch signaling. *Stem Cells Dev* (2013) 22 (9):1360–9. doi: 10.1089/scd.2012.0259

135. Villa JC, Chiu D, Brandes AH, Escorcia FE, Villa CH, Maguire WF, et al. Nontranscriptional role of hif-1α in activation of γ-secretase and notch signaling in breast cancer. *Cell Rep* (2014) 8(4):1077–92. doi: 10.1016/j.celrep.2014.07.028

136. Chen J, Imanaka N, Chen J, Griffin JD. Hypoxia potentiates notch signaling in breast cancer leading to decreased e-cadherin expression and increased cell migration and invasion. *Br J Cancer* (2010) 102(2):351–60. doi: 10.1038/sj.bjc.6605486

137. Jiang N, Zou C, Zhu Y, Luo Y, Chen L, Lei Y, et al. HIF-1α-regulated miR-1275 maintains stem cell-like phenotypes and promotes the progression of LUAD by simultaneously activating wnt/β-catenin and notch signaling. *Theranostics* (2020) 10 (6):2553–70. doi: 10.7150/thno.41120

138. Mutvei AP, Landor SK, Fox R, Braune EB, Tsoi YL, Phoon YP, et al. Notch signaling promotes a HIF2α-driven hypoxic response in multiple tumor cell types. *Oncogene* (2018) 37(46):6083–95. doi: 10.1038/s41388-018-0400-3

139. Coleman ML, McDonough MA, Hewitson KS, Coles C, Mecinovic J, Edelmann M, et al. Asparaginyl hydroxylation of the notch ankyrin repeat domain by factor inhibiting hypoxia-inducible factor. *J Biol Chem* (2007) 282(33):24027–38. doi: 10.1074/jbc.M704102200

140. Zheng X, Linke S, Dias JM, Zheng X, Gradin K, Wallis TP, et al. Interaction with factor inhibiting HIF-1 defines an additional mode of cross-coupling between the notch and hypoxia signaling pathways. *Proc Natl Acad Sci U.S.A.* (2008) 105(9):3368–73. doi: 10.1073/pnas.0711591105

141. Guo M, Zhang M, Cao X, Fang X, Li K, Qin L, et al. Notch4 mediates vascular remodeling *via* ERK/JNK/P38 MAPK signaling pathways in hypoxic pulmonary hypertension. *Respir Res* (2022) 23(1):6. doi: 10.1186/s12931-022-01927-9

142. Dongre A, Weinberg RA. New insights into the mechanisms of epithelial-mesenchymal transition and implications for cancer. *Nat Rev Mol Cell Biol* (2019) 20 (2):69–84. doi: 10.1038/s41580-018-0080-4

143. Lin YT, Wu KJ. Epigenetic regulation of epithelial-mesenchymal transition: focusing on hypoxia and TGF-β signaling. *J BioMed Sci* (2020) 27(1):39. doi: 10.1186/s12929-020-00632-3

144. Wells A, Yates C, Shepard CR. E-cadherin as an indicator of mesenchymal to epithelial reverting transitions during the metastatic seeding of disseminated carcinomas. *Clin Exp Metastasis* (2008) 25(6):621–8. doi: 10.1007/s10585-008-9167-1

145. Schmalhofer O, Brabletz S, Brabletz T. E-cadherin, beta-catenin, and ZEB1 in malignant progression of cancer. *Cancer Metastasis Rev* (2009) 28(1-2):151–66. doi: 10.1007/s10555-008-9179-y

146. Peinado H, Olmeda D, Cano A. Snail, zeb and bHLH factors in tumour progression: an alliance against the epithelial phenotype? *Nat Rev Cancer* (2007) 7 (6):415–28. doi: 10.1038/nrc2131

147. Wang X, Zheng M, Liu G, Xia W, McKeown-Longo PJ, Hung MC, et al. Krüppel-like factor 8 induces epithelial to mesenchymal transition and epithelial cell invasion. *Cancer Res* (2007) 67(15):7184–93. doi: 10.1158/0008-5472.Can-06-4729

148. Sobrado VR, Moreno-Bueno G, Cubillo E, Holt LJ, Nieto MA, Portillo F, et al. The class I bHLH factors E2-2A and E2-2B regulate EMT. *J Cell Sci* (2009) 122(Pt 7):1014–24. doi: 10.1242/jcs.028241

149. Yang MH, Wu KJ. TWIST activation by hypoxia inducible factor-1 (HIF-1): implications in metastasis and development. *Cell Cycle* (2008) 7(14):2090–6. doi: 10.4161/cc.7.14.6324

150. Sahlgren C, Gustafsson MV, Jin S, Poellinger L, Lendahl U. Notch signaling mediates hypoxia-induced tumor cell migration and invasion. *Proc Natl Acad Sci U.S.A.* (2008) 105(17):6392–7. doi: 10.1073/pnas.0802047105

151. Ishida T, Hijioka H, Kume K, Miyawaki A, Nakamura N. Notch signaling induces EMT in OSCC cell lines in a hypoxic environment. *Oncol Lett* (2013) 6(5):1201–6. doi: 10.3892/ol.2013.1549

152. Tian Q, Xue Y, Zheng W, Sun R, Ji W, Wang X, et al. Overexpression of hypoxia-inducible factor 1α induces migration and invasion through notch signaling. *Int J Oncol* (2015) 47(2):728–38. doi: 10.3892/ijo.2015.3056

153. Fujiki K, Inamura H, Miyayama T, Matsuoka M. Involvement of Notch1 signaling in malignant progression of A549 cells subjected to prolonged cadmium exposure. *J Biol Chem* (2017) 292(19):7942–53. doi: 10.1074/jbc.M116.759134

154. Cook KM, Figg WD. Angiogenesis inhibitors: current strategies and future prospects. *CA Cancer J Clin* (2010) 60(4):222–43. doi: 10.3322/caac.20075

155. Li JL, Harris AL. Notch signaling from tumor cells: a new mechanism of angiogenesis. *Cancer Cell* (2005) 8(1):1–3. doi: 10.1016/j.ccr.2005.06.013

156. Patel NS, Li JL, Generali D, Poulsom R, Cranston DW, Harris AL. Up-regulation of delta-like 4 ligand in human tumor vasculature and the role of basal expression in endothelial cell function. *Cancer Res* (2005) 65(19):8690–7. doi: 10.1158/0008-5472.Can-05-1208

157. Gale NW, Dominguez MG, Noguera I, Pan L, Hughes V, Valenzuela DM, et al. Haploinsufficiency of delta-like 4 ligand results in embryonic lethality due to major defects in arterial and vascular development. *Proc Natl Acad Sci U.S.A.* (2004) 101 (45):15949–54. doi: 10.1073/pnas.0407290101

158. Hainaud P, Contrerès JO, Villemain A, Liu LX, Plouët J, Tobelem G, et al. The role of the vascular endothelial growth factor-delta-like 4 ligand/Notch4-ephrin B2 cascade in tumor vessel remodeling and endothelial cell functions. *Cancer Res* (2006) 66(17):8501–10. doi: 10.1158/0008-5472.Can-05-4226

159. Hellström M, Phng LK, Hofmann JJ, Wallgard E, Coultas L, Lindblom P, et al. Dll4 signalling through Notch1 regulates formation of tip cells during angiogenesis. *Nature* (2007) 445(7129):776–80. doi: 10.1038/nature05571

160. Diez H, Fischer A, Winkler A, Hu CJ, Hatzopoulos AK, Breier G, et al. Hypoxia-mediated activation of Dll4-Notch-Hey2 signaling in endothelial progenitor cells and adoption of arterial cell fate. *Exp Cell Res* (2007) 313(1):1–9. doi: 10.1016/j.yexcr.2006.09.009

161. Huntly BJ, Gilliland DG. Leukaemia stem cells and the evolution of cancer-stem-cell research. *Nat Rev Cancer* (2005) 5(4):311–21. doi: 10.1038/nrc1592

162. Keith B, Simon MC. Hypoxia-inducible factors, stem cells, and cancer. *Cell* (2007) 129(3):465–72. doi: 10.1016/j.cell.2007.04.019

163. Liu J, Sato C, Cerletti M, Wagers A. Notch signaling in the regulation of stem cell self-renewal and differentiation. *Curr Top Dev Biol* (2010) 92:367–409. doi: 10.1016/s0070-2153(10)92012-7

164. Wang K, Ding R, Ha Y, Jia Y, Liao X, Wang S, et al. Hypoxia-stressed cardiomyocytes promote early cardiac differentiation of cardiac stem cells through HIF-1α/Jagged1/Notch1 signaling. *Acta Pharm Sin B* (2018) 8(5):795–804. doi: 10.1016/j.apsb.2018.06.003

165. Main H, Lee KL, Yang H, Haapa-Paananen S, Edgren H, Jin S, et al. Interactions between notch- and hypoxia-induced transcriptomes in embryonic stem cells. *Exp Cell Res* (2010) 316(9):1610–24. doi: 10.1016/j.yexcr.2009.12.012

166. Moriyama H, Moriyama M, Isshi H, Ishihara S, Okura H, Ichinose A, et al. Role of notch signaling in the maintenance of human mesenchymal stem cells under hypoxic conditions. *Stem Cells Dev* (2014) 23(18):2211–24. doi: 10.1089/scd.2013.0642

167. Zhang S, Chan RWS, Ng EHY, Yeung WSB. Hypoxia regulates the self-renewal of endometrial mesenchymal Stromal/Stem-like cells *via* notch signaling. *Int J Mol Sci* (2022) 23(9):4613. doi: 10.3390/ijms23094613

168. Sansone P, Storci G, Giovannini C, Pandolfi S, Pianetti S, Taffurelli M, et al. p66Shc/Notch-3 interplay controls self-renewal and hypoxia survival in human stem/progenitor cells of the mammary gland expanded *in vitro* as mammospheres. *Stem Cells* (2007) 25(3):807–15. doi: 10.1634/stemcells.2006-0442

169. Zeng F, Chen H, Zhang Z, Yao T, Wang G, Zeng Q, et al. Regulating glioma stem cells by hypoxia through the Notch1 and Oct3/4 signaling pathway. *Oncol Lett* (2018) 16(5):6315–22. doi: 10.3892/ol.2018.9442

170. Papayannidis C, DeAngelo DJ, Stock W, Huang B, Shaik MN, Cesari R, et al. A phase 1 study of the novel gamma-secretase inhibitor PF-03084014 in patients with T-cell acute lymphoblastic leukemia and T-cell lymphoblastic lymphoma. *Blood Cancer J* (2015) 5(9):e350. doi: 10.1038/bcj.2015.80

171. Sardesai S, Badawi M, Mrozek E, Morgan E, Phelps M, Stephens J, et al. A phase I study of an oral selective gamma secretase (GS) inhibitor RO4929097 in combination with neoadjuvant paclitaxel and carboplatin in triple negative breast cancer. *Invest New Drugs* (2020) 38(5):1400–10. doi: 10.1007/s10637-020-00895-5

172. Morgan KM, Fischer BS, Lee FY, Shah JJ, Bertino JR, Rosenfeld J, et al. Gamma secretase inhibition by BMS-906024 enhances efficacy of paclitaxel in lung adenocarcinoma. *Mol Cancer Ther* (2017) 16(12):2759–69. doi: 10.1158/1535-7163.Mct-17-0439

173. Akiyoshi T, Nakamura M, Yanai K, Nagai S, Wada J, Koga K, et al. Gamma-secretase inhibitors enhance taxane-induced mitotic arrest and apoptosis in colon cancer cells. *Gastroenterology* (2008) 134(1):131–44. doi: 10.1053/j.gastro.2007.10.008

174. Cui D, Dai J, Keller JM, Mizokami A, Xia S, Keller ET. Notch pathway inhibition using PF-03084014, a γ-secretase inhibitor (GSI), enhances the antitumor effect of docetaxel in prostate cancer. *Clin Cancer Res* (2015) 21(20):4619–29. doi: 10.1158/1078-0432.Ccr-15-0242

175. Hurtado C, Safarova A, Smith M, Chung R, Bruyneel AAN, Gomez-Galeno J, et al. Disruption of NOTCH signaling by a small molecule inhibitor of the transcription factor RBPJ. *Sci Rep* (2019) 9(1):10811. doi: 10.1038/s41598-019-46948-5

176. Lehal R, Zaric J, Vigolo M, Urech C, Frismantas V, Zangger N, et al. Pharmacological disruption of the notch transcription factor complex. *Proc Natl Acad Sci U.S.A.* (2020) 117(28):16292–301. doi: 10.1073/pnas.1922606117

177. Agnusdei V, Minuzzo S, Frasson C, Grassi A, Axelrod F, Satyal S, et al. Therapeutic antibody targeting of Notch1 in T-acute lymphoblastic leukemia xenografts. *Leukemia* (2014) 28(2):278–88. doi: 10.1038/leu.2013.183

178. Ferrarotto R, Eckhardt G, Patnaik A, LoRusso P, Faoro L, Heymach JV, et al. A phase I dose-escalation and dose-expansion study of brontictuzumab in subjects with selected solid tumors. *Ann Oncol* (2018) 29(7):1561–8. doi: 10.1093/annonc/mdy171

179. Hu ZI, Bendell JC, Bullock A, LoConte NK, Hatoum H, Ritch P, et al. A randomized phase II trial of nab-paclitaxel and gemcitabine with tarextumab or placebo in patients with untreated metastatic pancreatic cancer. *Cancer Med* (2019) 8(11):5148–57. doi: 10.1002/cam4.2425

180. Lu H, Jiang Z. Advances in antibody therapeutics targeting small-cell lung cancer. *Adv Clin Exp Med* (2018) 27(9):1317–23. doi: 10.17219/acem/70159

181. Smith DC, Chugh R, Patnaik A, Papadopoulos KP, Wang M, Kapoun AM, et al. A phase 1 dose escalation and expansion study of tarextumab (OMP-59R5) in patients with solid tumors. *Invest New Drugs* (2019) 37(4):722–30. doi: 10.1007/s10637-018-0714-6

182. Rosen LS, Wesolowski R, Baffa R, Liao KH, Hua SY, Gibson BL, et al. A phase I, dose-escalation study of PF-06650808, an anti-Notch3 antibody-drug conjugate, in patients with breast cancer and other advanced solid tumors. *Invest New Drugs* (2020) 38(1):120–30. doi: 10.1007/s10637-019-00754-y

183. Pandya K, Wyatt D, Gallagher B, Shah D, Baker A, Bloodworth J, et al. PKCα attenuates jagged-1-Mediated notch signaling in ErbB-2-Positive breast cancer to reverse trastuzumab resistance. *Clin Cancer Res* (2016) 22(1):175–86. doi: 10.1158/1078-0432.Ccr-15-0179

184. Masiero M, Li D, Whiteman P, Bentley C, Greig J, Hassanali T, et al. Development of therapeutic anti-JAGGED1 antibodies for cancer therapy. *Mol Cancer Ther* (2019) 18(11):2030–42. doi: 10.1158/1535-7163.Mct-18-1176

185. Saunders LR, Bankovich AJ, Anderson WC, Aujay MA, Bheddah S, Black K, et al. A DLL3-targeted antibody-drug conjugate eradicates high-grade pulmonary neuroendocrine tumor-initiating cells in vivo. *Sci Transl Med* (2015) 7(302):302ra136. doi: 10.1126/scitranslmed.aac9459

186. Perez-Fidalgo JA, Ortega B, Simon S, Samartzis EP, Boussios S. NOTCH signalling in ovarian cancer angiogenesis. *Ann Transl Med* (2020) 8(24):1705. doi: 10.21037/atm-20-4497

187. McKeage MJ, Kotasek D, Markman B, Hidalgo M, Millward MJ, Jameson MB, et al. Phase IB trial of the anti-cancer stem cell DLL4-binding agent demcizumab with pemetrexed and carboplatin as first-line treatment of metastatic non-squamous NSCLC. *Target Oncol* (2018) 13(1):89–98. doi: 10.1007/s11523-017-0543-0

188. Chiorean EG, LoRusso P, Strother RM, Diamond JR, Younger A, Messersmith WA, et al. A phase I first-in-Human study of enoticumab (REGN421), a fully human delta-like ligand 4 (Dll4) monoclonal antibody in patients with advanced solid tumors. *Clin Cancer Res* (2015) 21(12):2695–703. doi: 10.1158/1078-0432.Ccr-14-2797

189. Ye Q, Jiang J, Zhan G, Yan W, Huang L, Hu Y, et al. Small molecule activation of NOTCH signaling inhibits acute myeloid leukemia. *Sci Rep* (2016) 6:26510. doi: 10.1038/srep26510

190. Rios-Colon L, Chijioke J, Niture S, Afzal Z, Qi Q, Srivastava A, et al. Leptin modulated microRNA-628-5p targets jagged-1 and inhibits prostate cancer hallmarks. *Sci Rep* (2022) 12(1):10073. doi: 10.1038/s41598-022-13279-x

191. Park EY, Chang E, Lee EJ, Lee HW, Kang HG, Chun KH, et al. Targeting of miR34a-NOTCH1 axis reduced breast cancer stemness and chemoresistance. *Cancer Res* (2014) 74(24):7573–82. doi: 10.1158/0008-5472.Can-14-1140

192. Jeong JY, Kang H, Kim TH, Kim G, Heo JH, Kwon AY, et al. MicroRNA-136 inhibits cancer stem cell activity and enhances the anti-tumor effect of paclitaxel against chemoresistant ovarian cancer cells by targeting Notch3. *Cancer Lett* (2017) 386:168–78. doi: 10.1016/j.canlet.2016.11.017

193. Zhao Z, Shen X, Zhang D, Xiao H, Kong H, Yang B, et al. miR-153 enhances the therapeutic effect of radiotherapy by targeting JAG1 in pancreatic cancer cells. *Oncol Lett* (2021) 21(4):300. doi: 10.3892/ol.2021.12561

194. Bai L, Wang A, Zhang Y, Xu X, Zhang X. Knockdown of MALAT1 enhances chemosensitivity of ovarian cancer cells to cisplatin through inhibiting the Notch1 signaling pathway. *Exp Cell Res* (2018) 366(2):161–71. doi: 10.1016/j.yexcr.2018.03.014

195. Shen Z, Wu Y, He G. Long non-coding RNA PTPRG-AS1/microRNA-124-3p regulates radiosensitivity of nasopharyngeal carcinoma *via* the LIM homeobox 2-dependent notch pathway through competitive endogenous RNA mechanism. *Bioengineered* (2022) 13(4):8208–25. doi: 10.1080/21655979.2022.2037364

196. Imbimbo BP, Panza F, Frisardi V, Solfrizzi V, D'Onofrio G, Logroscino G, et al. Therapeutic intervention for alzheimer's disease with γ-secretase inhibitors: still a viable option? *Expert Opin Investig Drugs* (2011) 20(3):325–41. doi: 10.1517/13543784.2011.550572

197. Riccio O, van Gijn ME, Bezdek AC, Pellegrinet L, van Es JH, Zimber-Strobl U, et al. Loss of intestinal crypt progenitor cells owing to inactivation of both Notch1 and Notch2 is accompanied by derepression of CDK inhibitors p27Kip1 and p57Kip2. *EMBO Rep* (2008) 9(4):377–83. doi: 10.1038/embor.2008.7

198. Real PJ, Tosello V, Palomero T, Castillo M, Hernando E, de Stanchina E, et al. Gamma-secretase inhibitors reverse glucocorticoid resistance in T cell acute lymphoblastic leukemia. *Nat Med* (2009) 15(1):50–8. doi: 10.1038/nm.1900

199. Wu Y, Cain-Hom C, Choy L, Hagenbeek TJ, de Leon GP, Chen Y, et al. Therapeutic antibody targeting of individual notch receptors. *Nature* (2010) 464(7291):1052–7. doi: 10.1038/nature08878

200. Aste-Amézaga M, Zhang N, Lineberger JE, Arnold BA, Toner TJ, Gu M, et al. Characterization of Notch1 antibodies that inhibit signaling of both normal and mutated Notch1 receptors. *PLoS One* (2010) 5(2):e9094. doi: 10.1371/journal.pone.0009094

201. Sharma A, Gadkari RA, Ramakanth SV, Padmanabhan K, Madhumathi DS, Devi L, et al. A novel monoclonal antibody against Notch1 targets leukemia-associated mutant Notch1 and depletes therapy resistant cancer stem cells in solid tumors. *Sci Rep* (2015) 5:11012. doi: 10.1038/srep11012

202. Li K, Li Y, Wu W, Gordon WR, Chang DW, Lu M, et al. Modulation of notch signaling by antibodies specific for the extracellular negative regulatory region of NOTCH3. *J Biol Chem* (2008) 283(12):8046–54. doi: 10.1074/jbc.M800170200

203. Lafkas D, Shelton A, Chiu C, de Leon Boenig G, Chen Y, Stawicki SS, et al. Therapeutic antibodies reveal notch control of transdifferentiation in the adult lung. *Nature* (2015) 528(7580):127–31. doi: 10.1038/nature15715

204. Krämer A, Mentrup T, Kleizen B, Rivera-Milla E, Reichenbach D, Enzensperger C, et al. Small molecules intercept notch signaling and the early secretory pathway. *Nat Chem Biol* (2013) 9(11):731–8. doi: 10.1038/nchembio.1356

205. Gan RH, Lin LS, Xie J, Huang L, Ding LC, Su BH, et al. FLI-06 intercepts notch signaling and suppresses the proliferation and self-renewal of tongue cancer cells. *Onco Targets Ther* (2019) 12:7663–74. doi: 10.2147/ott.S221231

206. Moellering RE, Cornejo M, Davis TN, Del Bianco C, Aster JC, Blacklow SC, et al. Direct inhibition of the NOTCH transcription factor complex. *Nature* (2009) 462(7270):182–8. doi: 10.1038/nature08543

207. Astudillo L, Da Silva TG, Wang Z, Han X, Jin K, VanWye J, et al. The small molecule IMR-1 inhibits the notch transcriptional activation complex to suppress tumorigenesis. *Cancer Res* (2016) 76(12):3593–603. doi: 10.1158/0008-5472.Can-16-0061

208. Kulic I, Robertson G, Chang L, Baker JH, Lockwood WW, Mok W, et al. Loss of the notch effector RBPJ promotes tumorigenesis. *J Exp Med* (2015) 212(1):37–52. doi: 10.1084/jem.20121192

209. Slack FJ, Chinnaiyan AM. The role of non-coding RNAs in oncology. *Cell* (2019) 179(5):1033–55. doi: 10.1016/j.cell.2019.10.017

210. Jia Y, Lin R, Jin H, Si L, Jian W, Yu Q, et al. MicroRNA-34 suppresses proliferation of human ovarian cancer cells by triggering autophagy and apoptosis and inhibits cell invasion by targeting notch 1. *Biochimie* (2019) 160:193–9. doi: 10.1016/j.biochi.2019.03.011

211. Liu Z, Ma T, Duan J, Liu X, Liu L. MicroRNA–223–induced inhibition of the FBXW7 gene affects the proliferation and apoptosis of colorectal cancer cells *via* the notch and Akt/mTOR pathways. *Mol Med Rep* (2021) 23(2):154. doi: 10.3892/mmr.2020.11793

212. Pan T, Ding H, Jin L, Zhang S, Wu D, Pan W, et al. DNMT1-mediated demethylation of lncRNA MEG3 promoter suppressed breast cancer progression by repressing Notch1 signaling pathway. *Cell Cycle* (2022) 21(21):2323–37. doi: 10.1080/15384101.2022.2094662

213. Deng Y, Zhang L. LncRNA SNHG11 accelerates the progression of lung adenocarcinoma *via* activating notch pathways. *Pathol Res Pract* (2022) 234:153849. doi: 10.1016/j.prp.2022.153849

214. Jiang H, Li X, Wang W, Dong H. Long non-coding RNA SNHG3 promotes breast cancer cell proliferation and metastasis by binding to microRNA-154-3p and activating the notch signaling pathway. *BMC Cancer* (2020) 20(1):838. doi: 10.1186/s12885-020-07275-5

215. Phillips RM. Targeting the hypoxic fraction of tumours using hypoxia-activated prodrugs. *Cancer Chemother Pharmacol* (2016) 77(3):441–57. doi: 10.1007/s00280-015-2920-7

216. Wilson WR, Hay MP. Targeting hypoxia in cancer therapy. *Nat Rev Cancer* (2011) 11(6):393–410. doi: 10.1038/nrc3064

217. Phillips RM, Loadman PM, Reddy G. Inactivation of apaziquone by haematuria: implications for the design of phase III clinical trials against non-muscle invasive bladder cancer. *Cancer Chemother Pharmacol* (2019) 83(6):1183–9. doi: 10.1007/s00280-019-03812-7

218. Danson SJ, Johnson P, Ward TH, Dawson M, Denneny O, Dickinson G, et al. Phase I pharmacokinetic and pharmacodynamic study of the bioreductive drug RH1. *Ann Oncol* (2011) 22(7):1653–60. doi: 10.1093/annonc/mdq638

219. Williamson SK, Crowley JJ, Lara PNJr., McCoy J, Lau DH, Tucker RW, et al. Phase III trial of paclitaxel plus carboplatin with or without tirapazamine in advanced non-small-cell lung cancer: Southwest oncology group trial S0003. *J Clin Oncol* (2005) 23 (36):9097–104. doi: 10.1200/jco.2005.01.3771

220. Hunter FW, Hsu HL, Su J, Pullen SM, Wilson WR, Wang J. Dual targeting of hypoxia and homologous recombination repair dysfunction in triple-negative breast cancer. *Mol Cancer Ther* (2014) 13(11):2501–14. doi: 10.1158/1535-7163.Mct-14-0476

221. Albertella MR, Loadman PM, Jones PH, Phillips RM, Rampling R, Burnet N, et al. Hypoxia-selective targeting by the bioreductive prodrug AQ4N in patients with solid tumors: results of a phase I study. *Clin Cancer Res* (2008) 14(4):1096–104. doi: 10.1158/1078-0432.Ccr-07-4020

222. Papadopoulos KP, Goel S, Beeram M, Wong A, Desai K, Haigentz M, et al. A phase 1 open-label, accelerated dose-escalation study of the hypoxia-activated prodrug AQ4N in patients with advanced malignancies. *Clin Cancer Res* (2008) 14(21):7110–5. doi: 10.1158/1078-0432.Ccr-08-0483

223. Konopleva M, Thall PF, Yi CA, Borthakur G, Coveler A, Bueso-Ramos C, et al. Phase I/II study of the hypoxia-activated prodrug PR104 in refractory/relapsed acute myeloid leukemia and acute lymphoblastic leukemia. *Haematologica* (2015) 100(7):927–34. doi: 10.3324/haematol.2014.118455

224. Tap WD, Papai Z, Van Tine BA, Attia S, Ganjoo KN, Jones RL, et al. Doxorubicin plus evofosfamide versus doxorubicin alone in locally advanced, unresectable or metastatic soft-tissue sarcoma (TH CR-406/SARC021): an international, multicentre, open-label, randomised phase 3 trial. *Lancet Oncol* (2017) 18(8):1089–103. doi: 10.1016/s1470-2045(17)30381-9

225. Singleton DC, Macann A, Wilson WR. Therapeutic targeting of the hypoxic tumour microenvironment. *Nat Rev Clin Oncol* (2021) 18(12):751–72. doi: 10.1038/s41571-021-00539-4

226. Lee K, Zhang H, Qian DZ, Rey S, Liu JO, Semenza GL. Acriflavine inhibits HIF-1 dimerization, tumor growth, and vascularization. *Proc Natl Acad Sci U.S.A.* (2009) 106 (42):17910–5. doi: 10.1073/pnas.0909353106

227. Xie C, Gao X, Sun D, Zhang Y, Krausz KW, Qin X, et al. Metabolic profiling of the novel hypoxia-inducible factor 2α inhibitor PT2385 *In vivo* and in vitro. *Drug Metab Dispos* (2018) 46(4):336–45. doi: 10.1124/dmd.117.079723

228. Chen W, Hill H, Christie A, Kim MS, Holloman E, Pavia-Jimenez A, et al. Targeting renal cell carcinoma with a HIF-2 antagonist. *Nature* (2016) 539(7627):112–7. doi: 10.1038/nature19796

229. Porter JR, Ge J, Lee J, Normant E, West K. Ansamycin inhibitors of Hsp90: nature's prototype for anti-chaperone therapy. *Curr Top Med Chem* (2009) 9(15):1386–418. doi: 10.2174/156802609789895719

230. Osada M, Imaoka S, Funae Y. Apigenin suppresses the expression of VEGF, an important factor for angiogenesis, in endothelial cells *via* degradation of HIF-1alpha protein. *FEBS Lett* (2004) 575(1-3):59–63. doi: 10.1016/j.febslet.2004.08.036

231. Hur E, Kim HH, Choi SM, Kim JH, Yim S, Kwon HJ, et al. Reduction of hypoxia-induced transcription through the repression of hypoxia-inducible factor-1alpha/aryl hydrocarbon receptor nuclear translocator DNA binding by the 90-kDa heat-shock protein inhibitor radicicol. *Mol Pharmacol* (2002) 62(5):975–82. doi: 10.1124/mol.62.5.975

232. Kovacs JJ, Murphy PJ, Gaillard S, Zhao X, Wu JT, Nicchitta CV, et al. HDAC6 regulates Hsp90 acetylation and chaperone-dependent activation of glucocorticoid receptor. *Mol Cell* (2005) 18(5):601–7. doi: 10.1016/j.molcel.2005.04.021

233. Zhang C, Yang C, Feldman MJ, Wang H, Pang Y, Maggio DM, et al. Vorinostat suppresses hypoxia signaling by modulating nuclear translocation of hypoxia inducible factor 1 alpha. *Oncotarget* (2017) 8(34):56110–25. doi: 10.18632/oncotarget.18125

234. Kung AL, Zabludoff SD, France DS, Freedman SJ, Tanner EA, Vieira A, et al. Small molecule blockade of transcriptional coactivation of the hypoxia-inducible factor pathway. *Cancer Cell* (2004) 6(1):33–43. doi: 10.1016/j.ccr.2004.06.009

235. Price C, Gill S, Ho ZV, Davidson SM, Merkel E, McFarland JM, et al. Genome-wide interrogation of human cancers identifies EGLN1 dependency in clear cell ovarian cancers. *Cancer Res* (2019) 79(10):2564–79. doi: 10.1158/0008-5472.Can-18-2674

236. Greenberger LM, Horak ID, Filpula D, Sapra P, Westergaard M, Frydenlund HF, et al. A RNA antagonist of hypoxia-inducible factor-1alpha, EZN-2968, inhibits tumor cell growth. *Mol Cancer Ther* (2008) 7(11):3598–608. doi: 10.1158/1535-7163.Mct-08-0510

237. Lin J, Zhan T, Duffy D, Hoffman-Censits J, Kilpatrick D, Trabulsi EJ, et al. A pilot phase II study of digoxin in patients with recurrent prostate cancer as evident by a rising PSA. *Am J Cancer Ther Pharmacol* (2014) 2(1):21–32.

238. Tinley TL, Leal RM, Randall-Hlubek DA, Cessac JW, Wilkens LR, Rao PN, et al. Novel 2-methoxyestradiol analogues with antitumor activity. *Cancer Res* (2003) 63 (7):1538–49.

239. Lee K, Kim HM. A novel approach to cancer therapy using PX-478 as a HIF-1α inhibitor. *Arch Pharm Res* (2011) 34(10):1583–5. doi: 10.1007/s12272-011-1021-3

240. Yeo EJ, Chun YS, Cho YS, Kim J, Lee JC, Kim MS, et al. YC-1: a potential anticancer drug targeting hypoxia-inducible factor 1. *J Natl Cancer Inst* (2003) 95(7):516–25. doi: 10.1093/jnci/95.7.516

241. Ramanathan RK, Abbruzzese J, Dragovich T, Kirkpatrick L, Guillen JM, Baker AF, et al. A randomized phase II study of PX-12, an inhibitor of thioredoxin in patients with advanced cancer of the pancreas following progression after a gemcitabine-containing combination. *Cancer Chemother Pharmacol* (2011) 67(3):503–9. doi: 10.1007/s00280-010-1343-8

242. Lee K, Kang JE, Park SK, Jin Y, Chung KS, Kim HM, et al. LW6, a novel HIF-1 inhibitor, promotes proteasomal degradation of HIF-1alpha *via* upregulation of VHL in a colon cancer cell line. *Biochem Pharmacol* (2010) 80(7):982–9. doi: 10.1016/j.bcp.2010.06.018

243. Courtney KD, Infante JR, Lam ET, Figlin RA, Rini BI, Brugarolas J, et al. Phase I dose-escalation trial of PT2385, a first-in-Class hypoxia-inducible factor-2α antagonist in patients with previously treated advanced clear cell renal cell carcinoma. *J Clin Oncol* (2018) 36(9):867–74. doi: 10.1200/jco.2017.74.2627

244. Cho H, Du X, Rizzi JP, Liberzon E, Chakraborty AA, Gao W, et al. On-target efficacy of a HIF-2α antagonist in preclinical kidney cancer models. *Nature* (2016) 539 (7627):107–11. doi: 10.1038/nature19795

245. Taylor SA, Metch B, Balcerzak SP, Hanson KH. Phase II trial of echinomycin in advanced soft tissue sarcomas. a southwest oncology group study. *Invest New Drugs* (1990) 8(4):381–3. doi: 10.1007/bf00198595

246. Brown TD, Goodman PJ, Fleming TR, Taylor SA, Macdonald JS. Phase II trial of echinomycin in advanced colorectal cancer. a southwest oncology group study. *Invest New Drugs* (1991) 9(1):113–4. doi: 10.1007/bf00194561

247. Schilsky RL, Faraggi D, Korzun A, Vogelzang N, Ellerton J, Wood W, et al. Phase II study of echinomycin in patients with advanced breast cancer: a report of cancer and leukemia group b protocol 8641. *Invest New Drugs* (1991) 9(3):269–72. doi: 10.1007/bf00176982

248. Marshall ME, Wolf MK, Crawford ED, Taylor S, Blumenstein B, Flanigan R, et al. Phase II trial of echinomycin for the treatment of advanced renal cell carcinoma. a southwest oncology group study. *Invest New Drugs* (1993) 11(2-3):207–9. doi: 10.1007/bf00874157

249. Shevrin DH, Lad TE, Guinan P, Kilton LJ, Greenburg A, Johnson P, et al. Phase II trial of echinomycin in advanced hormone-resistant prostate cancer. an Illinois cancer council study. *Invest New Drugs* (1994) 12(1):65–6. doi: 10.1007/bf00873239

250. Viziteu E, Grandmougin C, Goldschmidt H, Seckinger A, Hose D, Klein B, et al. Chetomin, targeting HIF-1α/p300 complex, exhibits antitumour activity in multiple myeloma. *Br J Cancer* (2016) 114(5):519–23. doi: 10.1038/bjc.2016.20

251. Richardson PG, Mitsiades C, Hideshima T, Anderson KC. Bortezomib: proteasome inhibition as an effective anticancer therapy. *Annu Rev Med* (2006) 57:33–47. doi: 10.1146/annurev.med.57.042905.122625

252. Quinn DI, Tsao-Wei DD, Twardowski P, Aparicio AM, Frankel P, Chatta G, et al. Phase II study of the histone deacetylase inhibitor vorinostat (Suberoylanilide hydroxamic acid; SAHA) in recurrent or metastatic transitional cell carcinoma of the urothelium - an NCI-CTEP sponsored: California cancer consortium trial, NCI 6879. *Invest New Drugs* (2021) 39(3):812–20. doi: 10.1007/s10637-020-01038-6

253. Albadari N, Deng S, Li W. The transcriptional factors HIF-1 and HIF-2 and their novel inhibitors in cancer therapy. *Expert Opin Drug Discovery* (2019) 14(7):667–82. doi: 10.1080/17460441.2019.1613370

254. Jiang BH, Jiang G, Zheng JZ, Lu Z, Hunter T, Vogt PK. Phosphatidylinositol 3-kinase signaling controls levels of hypoxia-inducible factor 1. *Cell Growth Differ* (2001) 12(7):363–9.

255. Wang D, Eisen HJ. Mechanistic target of rapamycin (mTOR) inhibitors. *Handb Exp Pharmacol* (2022) 272:53–72. doi: 10.1007/164_2021_553

256. Ravaud A, Bernhard JC, Gross-Goupil M, Digue L, Ferriere JM. [mTOR inhibitors: temsirolimus and everolimus in the treatment of renal cell carcinoma]. *Bull Cancer* (2010) 97:45–51. doi: 10.1684/bdc.2010.1069

257. Kopecka J, Salaroglio IC, Perez-Ruiz E, Sarmento-Ribeiro AB, Saponara S, De Las Rivas J, et al. Hypoxia as a driver of resistance to immunotherapy. *Drug Resist Update* (2021) 59:100787. doi: 10.1016/j.drup.2021.100787

258. Rodriguez CP, Wu QV, Voutsinas J, Fromm JR, Jiang X, Pillarisetty VG, et al. A phase II trial of pembrolizumab and vorinostat in recurrent metastatic head and neck squamous cell carcinomas and salivary gland cancer. *Clin Cancer Res* (2020) 26(4):837–45. doi: 10.1158/1078-0432.Ccr-19-2214

259. Kumar S, Sun JD, Zhang L, Mokhtari RB, Wu B, Meng F, et al. Hypoxia-targeting drug evofosfamide (TH-302) enhances sunitinib activity in neuroblastoma xenograft models. *Transl Oncol* (2018) 11(4):911–9. doi: 10.1016/j.tranon.2018.05.004

260. Akil A, Gutiérrez-García AK, Guenter R, Rose JB, Beck AW, Chen H, et al. Notch signaling in vascular endothelial cells, angiogenesis, and tumor progression: An update and prospective. *Front Cell Dev Biol* (2021) 9:642352. doi: 10.3389/fcell.2021.642352

261. Hu H, Chen Y, Tan S, Wu S, Huang Y, Fu S, et al. The research progress of antiangiogenic therapy, immune therapy and tumor microenvironment. *Front Immunol* (2022) 13:802846. doi: 10.3389/fimmu.2022.802846

frontiers | Frontiers in Oncology

TYPE Original Research
PUBLISHED 09 February 2023
DOI 10.3389/fonc.2023.1095046

OPEN ACCESS

EDITED BY
João Pessoa,
University of Coimbra, Portugal

REVIEWED BY
Swaroop Kumar Pandey,
GLA University, India
Xiao-Bin Lv,
Third Affiliated Hospital of Nanchang University, China
Jianjun Li,
Army Medical University, China

*CORRESPONDENCE
Ram Kumar Mishra
rkmishra@iiserb.ac.in

SPECIALTY SECTION
This article was submitted to Molecular and Cellular Oncology, a section of the journal Frontiers in Oncology

RECEIVED 10 November 2022
ACCEPTED 16 January 2023
PUBLISHED 09 February 2023

CITATION
Singh U, Bindra D, Samaiya A and Mishra RK (2023) Overexpressed Nup88 stabilized through interaction with Nup62 promotes NF-κB dependent pathways in cancer. *Front. Oncol.* 13:1095046. doi: 10.3389/fonc.2023.1095046

Overexpressed Nup88 stabilized through interaction with Nup62 promotes NF-κB dependent pathways in cancer

Usha Singh[1], Divya Bindra[1], Atul Samaiya[2] and Ram Kumar Mishra[1]*

[1]Nups and Sumo Biology Group, Department of Biological Sciences, Indian Institute of Science Education and Research (IISER), Bhopal, Madhya Pradesh, India, [2]Department of Surgical Oncology, Bansal Hospital, Bhopal, Madhya Pradesh, India

Bidirectional nucleo-cytoplasmic transport, regulating several vital cellular processes, is mediated by the Nuclear Pore Complex (NPC) comprising the nucleoporin (Nup) proteins. Nup88, a constituent nucleoporin, is overexpressed in many cancers, and a positive correlation exists between progressive stages of cancer and Nup88 levels. While a significant link of Nup88 overexpression in head and neck cancer exists but mechanistic details of Nup88 roles in tumorigenesis are sparse. Here, we report that Nup88 and Nup62 levels are significantly elevated in head and neck cancer patient samples and cell lines. We demonstrate that the elevated levels of Nup88 or Nup62 impart proliferation and migration advantages to cells. Interestingly, Nup88-Nup62 engage in a strong interaction independent of Nup-glycosylation status and cell-cycle stages. We report that the interaction with Nup62 stabilizes Nup88 by inhibiting the proteasome-mediated degradation of overexpressed Nup88. Overexpressed Nup88 stabilized by interaction with Nup62 can interact with NF-κB (p65) and sequesters p65 partly into nucleus of unstimulated cells. NF-κB targets like Akt, c-myc, IL-6 and BIRC3 promoting proliferation and growth are induced under Nup88 overexpression conditions. In conclusion, our data indicates that simultaneous overexpression of Nup62 and Nup88 in head and neck cancer stabilizes Nup88. Stabilized Nup88 interacts and activates p65 pathway, which perhaps is the underlying mechanism in Nup88 overexpressing tumors.

KEYWORDS

nucleoporins (NUPs), head and neck cancer, NFkB, Nup88, Nup62

Abbreviations: NUP, Nucleoporin; NF-κB, Nuclear Factor Kappa-light-chain-enhancer of activated B cells; IκB, Inhibitor of nuclear factor kappa B; Crm1, Chromosomal Maintenance 1; APC/C, Anaphase promoting complex/cyclosome; PLK1, Polo-like kinase 1; ROCK1, Rho-associated coiled-coil containing protein kinase 1; GAPDH, Glyceraldehyde 3-phosphate dehydrogenase; CRN, Cancer RNA-Seq Nexus; MTT, 3-(4,5-dimethylthiazol-2-yl)-2,5-diphenyl tetrazolium bromide; GBP, GFP Binding protein; PPL, Periplakin; ELYS, Embryonic large molecule derived from yolk sac; IL-6, Interleukin-6.

Introduction

Nucleoporins (Nups) are the constituent proteins of the megadalton assemblies called nuclear pores. Nups form biochemically distinct and stable sub-complexes and localize to the nuclear pores and mediate nucleo-cytoplasmic transport during interphase. Interestingly, these subcomplexes disassemble, and some of them localize to chromatin and regulate mitotic spindle assembly, microtubule dynamics, and chromosome segregation in mitosis (1–3).

Nup88 forms a stable subcomplex with Nup214 and constitutes the cytoplasmic face of the nuclear pores (4). Point mutations and expression level changes in nucleoporins have links with occurrences and progression of cancer (5). Particularly, Nup88 mRNA and protein levels were reported to be enhanced in human ovarian tumors (6). Further, elevated Nup88 levels were found in several cancers irrespective of their type, degree of differentiation, or site of occurrence (7). Moreover, Nup88 levels exhibit a positive correlation with progressive stages of cancer (8). CAN (Nup214), a proto-oncogene linked with myeloid leukemogenesis (9), forms a complex with Nup88 and regulates CRM1 mediated nuclear export of macromolecules (10). Nonetheless, Nup214 is not co-overexpressed in Nup88 overexpressing cancers (11). Overexpression of Nup88 induced multinucleated phenotypes, and a multipolar spindle phenotype when depleted. Interestingly, Nup214 co-expression in Nup88 overexpressing cells ameliorated above phenotypes, highlighting the balance between free levels of Nup88 and its complexation with Nup214 in cellular homeostasis (12). Moreover, overexpression of Nup88 sequestered Nup98-Rae1 away from APC/C complex triggering early degradation of PLK1 that induced aneuploidy and tumorigenesis (13). Also, the interaction of Nup88 with Vimentin affects Vimentin organization resulting in multinucleated cells and aneuploidy (14).

Nup159, the yeast ortholog of Nup214, is mono-ubiquitinated and affects the cell-cycle progression and aneuploidy (15). In yeast, Nup88 interacted with Nup62 through the helical domain (16), and mutations in Nup62 affected the mRNA export (17). Nup62 glycosylation is an important determinant of Nup88 stability (18), and the ubiquitination of Nup88 and Nup62 affects their stability (15). Nup62 overexpression is reported from the prostate, and ovarian cancers (19, 20), and ROCK1 dependent Nup62 phosphorylation induces p63 nuclear localization and cell proliferation (21). The idea that perturbation of multiple cellular processes when Nup88 is overexpressed (22) is very general and does not provide any specific insight. Moreover, limited information about the Nup88 and Nup62 expression level changes in various cancers including head and neck cancer (11, 21) impedes our understanding of the process. Since Nup88 and Nup62 form stable complexes and their expression levels show alterations in different cancers, we have probed how the expression and interactions of Nup88 and Nup62 correlate with head and neck cancers.

Here, we report that Nup88 and Nup62 mRNA and protein levels are elevated in head and neck cancer tissues. Nup88 and Nup62 engage in a conserved interaction through their respective carboxy-terminal regions and this interaction is independent of cell cycle dynamics and glycosylation status of Nup62. Nup62 co-overexpression primarily stabilizes Nup88 and prevents its ubiquitination mediated degradation. Stabilized Nup88 interacts efficiently with NF-κB and affects proliferation, inflammation, and anti-apoptosis responses downstream of NF-κB signaling to promote tumorigenic growth.

Results

Nup88 and Nup62 are overexpressed in head and neck cancer

We performed a comprehensive analysis and investigated the levels of different nucleoporins in the tissue datasets available at MiPanda. The analysis revealed that Nup62 as well as Nup88 levels are upregulated in all different types of cancers analyzed, like the cancers of head and neck, breast, and stomach (Figures S1A, B). We analyzed this co-upregulation of Nup88, and Nup62 in head and neck cancer tissue lysates, and observed that both Nup88 and Nup62 levels were higher in tumor tissues (Figure 1A, n=4). Control gene (GAPDH) levels varied among patient samples, but the ratiometric analysis of Nup62 or Nup88 with GAPDH indicates that both Nups are significantly overexpressed in oral cancer tissues (Figures 1B, C, n=4). Although the Nup88 and Nup62 are abundant proteins, both were poorly detected in control samples, possibly due to the limited control tissue volume. Antibodies for Nup62 and Nup88 recognize respective antigens with variable affinities. The Nup62 antibody detected antigen with much higher affinity. Accordingly, invariably higher Nup62 protein levels were detected (~2 folds) upon analysis of additional oral cancer tissues (Figure 1D, and S1c n=10). Using Rps16 as a loading control, we observed that Nup62 and Nup88 mRNA levels were enhanced by 1.2 and 1.6 fold, respectively (Figures 1E, F, n=7). Next, we analyzed the expression of Nup62 and Nup88 using the Oncomine database (23) in the Ginos Head and neck cancer statistics (24). The analysis revealed a 2.1 and 1.15 fold increase in the transcript levels of Nup62 and Nup88, respectively (Figure S1D). Analysis of head and neck carcinoma MiPanda database revealed that Nup88 is particularly elevated in metastatic tumors when compared to benign tumors and cell lines (Figure 1G). We also analyzed the co-expression of Nup62 and Nup88 in oral cancers in a collection of available datasets at MiPanda (25), and found that Nup62 and Nup88 transcript levels were significantly higher in primary tumors when compared to normal samples (Figure S1E). Cancer RNA-Seq Nexus (CRN) (26) analysis showed that Nup62 transcript levels are higher in progressive stages of oral cancer (Figure S1F). However, the Kaplan-Meier survival curve generated using Onco-Lnc (27) indicated no significant difference in survival (log rank p-value = 0.4) between low and high Nup88 expression conditions (Figure 1H) indicating Nup88 expression levels increasing in high grade tumors is affecting growth but no direct impact on survival.

Overexpression of Nup88 and Nup62 can induce tumorigenic transformations

Next, we asked in a cell culture setup if Nup62 and Nup88 overexpression can contribute to vital characteristics like

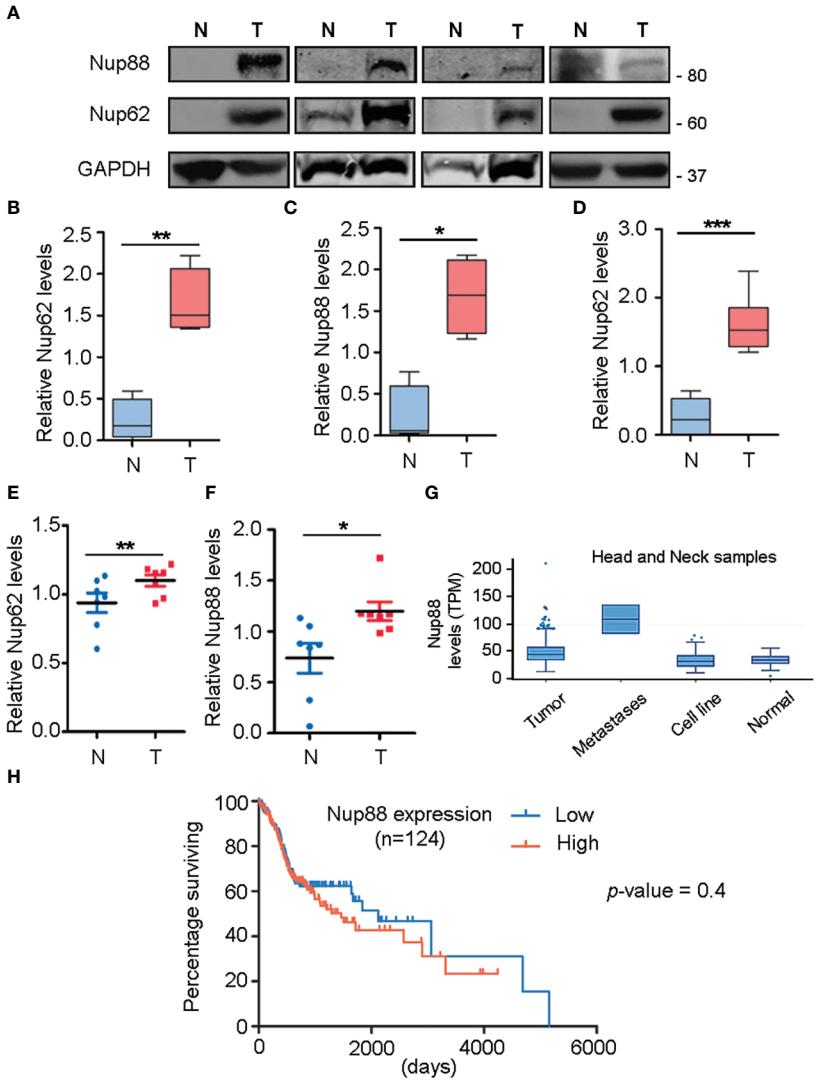

FIGURE 1
Nup88 and Nup62 are overexpressed in oral cancer. **(A)** Western blot analysis of lysates prepared from oral cancer patient tissues using antibodies against Nup88, Nup62, and GAPDH. **(B, C)** Quantification of Nup62 and Nup88 band intensities relative to GAPDH protein levels from normal and tumor tissues, shown in **(A)**. **(D)** Nup62 protein levels relative to GAPDH in oral cancer tissues (n=10) (N= Adjacent normal tissues, and T= Tumor). The asterisk represents the significance value. Values on the y-axis represent data obtained by normalizing with the GAPDH band intensity. The asterisk indicates statistical significance p<0.05. **(E, F)** Graphs indicate fold changes in Nup62 and Nup88 mRNA levels, respectively, in oral cancer tissue samples (n=7). Y-axis values indicate Nups level relative to Rps16 control levels. **(G)** Nup88 expression in TCGA head and neck statistics analyzed in Mi-Panda. **(H)** Kaplan-Meier survival curve for Nup88 using OncoLnc on oral cancer TCGA data. (Student's t-test - paired t-test) *p < 0.05, **p < 0.01 and ***p < 0.001.

enhanced proliferation, migration, and loss of contact inhibition exhibited by cells in cancerous tissues. We have used SCC9 and H413 cells representing head and neck cancer for these studies. MTT assay based assessments in SCC9 cells confirmed that GFP-Nup62 and/or GFP-Nup88 expressing cells exhibit significantly increased viability (~1.5 – 2.0 folds) as compared to GFP expressing cells, suggesting an increase in metabolic activity (Figure 2A). The wound healing experiment was employed to assess growth and migration of cells, where a wound was created in a monolayer of SCC-9 cells and assessed for healing over different time points. Wound healing observations and its quantitation suggests that more than 95% of wound is closed by 36 hours post wounding (hpw) in GFP-Nup62 or GFP-Nup88 overexpressing cells. However, in the GFP control expressing cells, only ~60-65% wound closure was observed (Figures 2B, C). We assessed the loss of contact inhibition property in H413 cells expressing GFP alone or GFP-Nup62 or GFP-Nup88 using the colony-forming assay (CFA). As compared to GFP control, approximately two fold change in colony number was observed in GFP-Nup62, and GFP-Nup88 expressing cells (Figures 2D, E). Further, immunofluorescence analysis performed with custom generated rabbit polyclonal antibodies in H413 and SCC9 cells identified signals overlapping with Nup62 at the nuclear periphery (Figure 2F and Figure S2). Our *in cellulae* observations made with altering Nup62 and Nup88 expression levels indicated that both Nup62 and Nup88 can induce tumorigenic transformation and suggest a strong localization and interaction between Nup88 and Nup62.

10.3389/fonc.2023.1095046

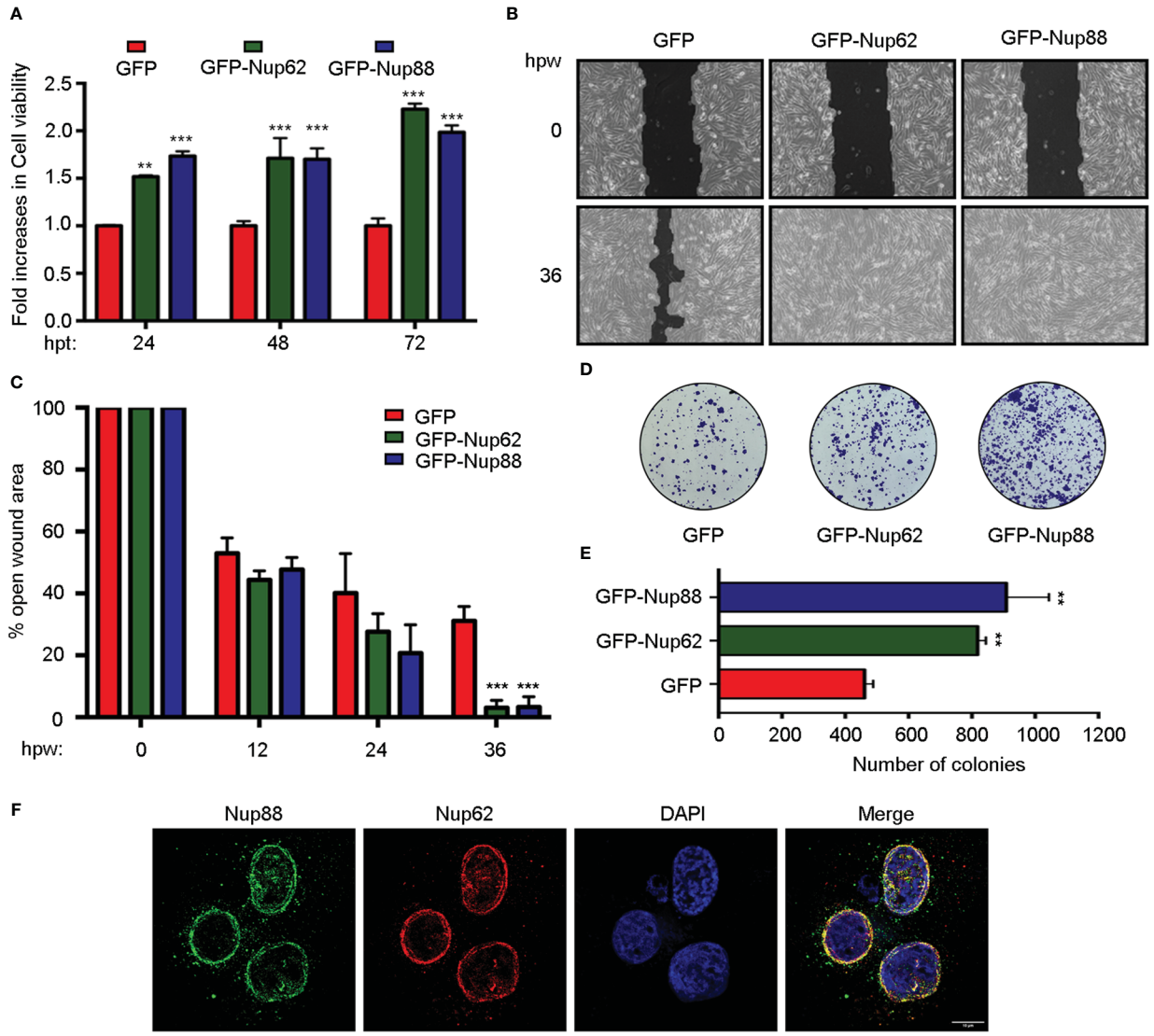

FIGURE 2
Overexpression of Nup88 and Nup62 induces tumorigenic transformations. **(A)** MTT assay based cell viability assessment in GFP, GFP-Nup62, and GFP-Nup88 transfected SCC9 cells. **(B)** Representative images of 0 h and 36 h wound healing assay in SCC9 cells expressing GFP, GFP-Nup62, and GFP-Nup88. The images were acquired at 10X magnification under an inverted microscope. **(C)** Quantification of the closure of the wound area at 0, 12, 24, and 36 h as seen in **(B)** using TScratch software. **(D)** Colony formation assay in H413 cells overexpressing GFP, GFP-Nup62, and GFP-Nup88. **(E)** Quantification of the number of colonies using Image-J/Fiji software. **(F)** Immunolocalization analysis of Nup88 and Nup62 in oral cancer cell line H413, anti-Nup88 (green), anti-Nup62 (red) and chromatin/DAPI (blue). Scale bar = 10 μm. Images are a representative from at least n=3 repeat experiments. Error bars show mean values ± SEM. Asterisks indicate statistical significance (Student's t-test) *p < 0.05, **p < 0.01 and ***p < 0.001.

Conserved interaction between Nup88 and Nup62 occurs through their carboxy termini

We asked if Nup88 and Nup62 can interact as reported in yeast (16) to mediate the Nup88 overexpression dependent cancer phenotypes. We have used HEK-293T cells to perform all relevant protein-protein interaction and other biochemical and molecular biology studies of the work reported here as HEK-293T cells are great model cell lines for expressing proteins. Similarly, the HeLa cells were used in protein localization studies by immunofluorescence due to their robust cellular components and versatile use. Accordingly, anti-Nup62 interaction antibodies mediated immunoprecipitation (IP) from HEK-293T and MCF7 cell lysates, co-immunoprecipitated endogenous Nup88 and established the robustness of this Nup88-Nup62 interaction (Figure 3A). For reasons beyond explanation Nup88 antibodies invariably failed to pick the Nup88 signal in input samples. Secondary structure prediction analysis on the Nup88 sequence (Uniprot ID: Q99567) suggests a much smaller coiled-coil domain mentioned in previous studies (12). To map the domains involved in Nup88-Nup62 interaction, we generated Nup88 constructs containing only the coiled-coil domain (Nup88-C) and the one lacking the coiled-coil domain (Nup88-delC) (Figure 3B). Using recombinant GST-Nup88-C proteins on beads, endogenous Nup62 from cell lysates was pulled down efficiently (Figure 3C). Similarly, GFP-Nup88 and GFP-Nup88-C immobilized on GFP-binding protein (GBP) pulled down endogenous Nup62 from HEK293T cell lysates. In a complementary observation, GFP-Nup88-delC failed to pull down Nup62 from HEK293T cell lysates (Figure 3D). To understand if the C-terminal

10.3389/fonc.2023.1095046

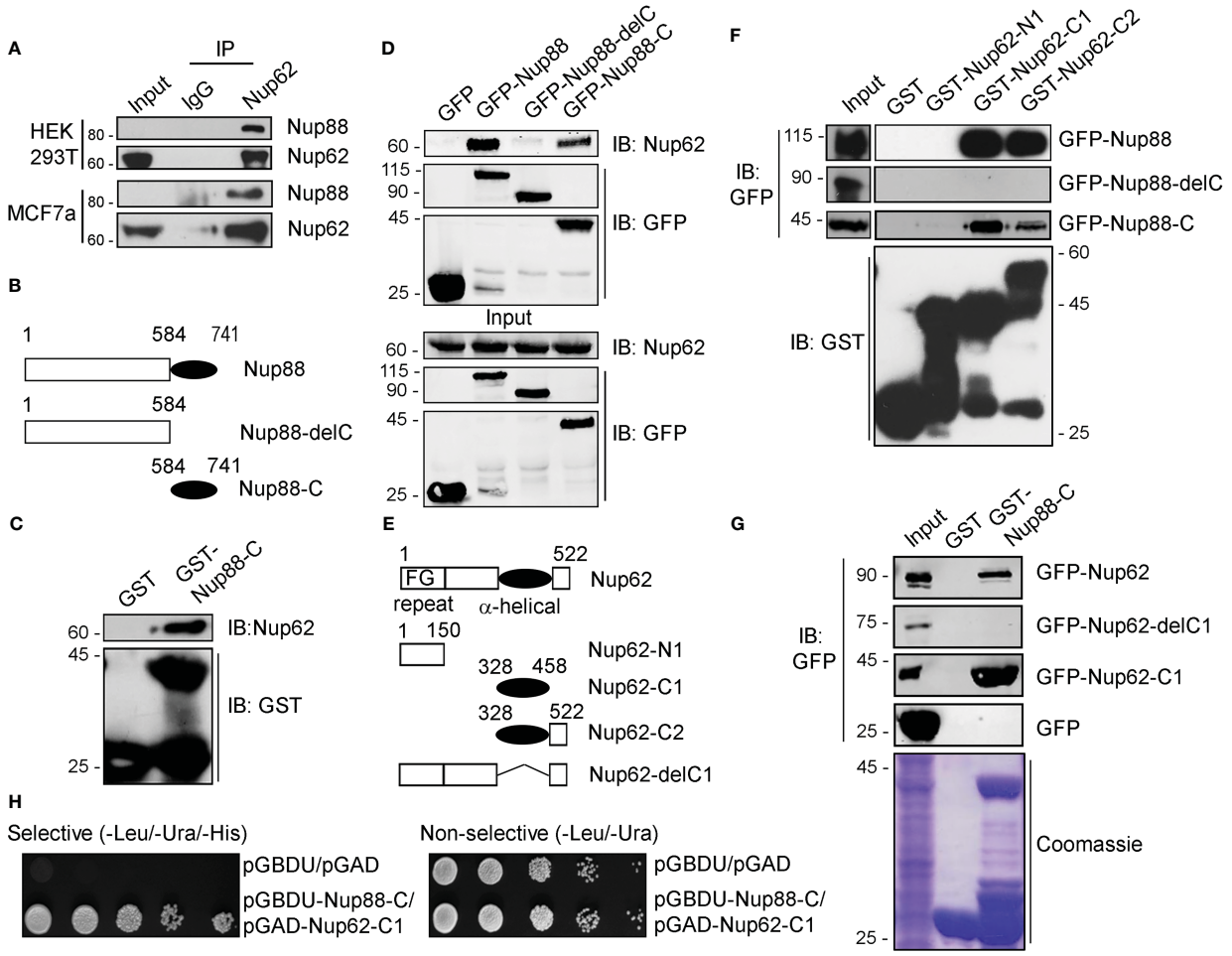

FIGURE 3
Nup88 and Nup62 interact through their carboxy-termini. **(A)** Anti-Nup62 antibody-mediated immunoprecipitation (IP) from HEK293T and MCF7 cell lysates and immunoblotting (IB) for indicated proteins. **(B)** Schematic representation of Nup88 domain constructs used in cellular transfection and GST and GFP binding protein (GBP) pulldown experiments. **(C)** Pull down of endogenous Nup62 on GST and GST-Nup88-C coated beads from HEK293T lysates and detection by indicated antibodies. **(D)** GBP pulldown from HEK293T lysates expressing either GFP-Nup88 or GFP-Nup88-delC or GFP-Nup88-C. Pulldown and input samples were probed with indicated antibodies. **(E)** Schematic representation of Nup62 constructs used in this study. **(F)** Beads coated with recombinant proteins indicated on top of the lanes used in pulldown experiments from HEK293T cell lysates expressing GFP-Nup88, or Nup88-delC or Nup88-C proteins. Pulldown samples and input fractions were immunoblotted with the indicated antibodies. **(G)** Pulldown from HEK293T cell lysate expressing GFP-Nup62, or Nup62-delC1 or Nup62-C1 or GFP on GST or GST-Nup88-C. Pulldown samples and input fractions were immunoblotted with the anti-GFP antibody. **(H)** Yeast two-hybrid interaction analysis using the DNA binding domain (pGBDU) construct of Nup88-C and activation domain (pGAD) construct of Nup62-C1. Doubly transformed yeast colonies were grown on selective and non-selective media to score for the interaction. Images are a representative from at least n=3 repeat experiments.

alpha-helical region of Nup62 is involved in conserved interaction with Nup88, we generated Nup62 truncations (Figure 3E) as described elsewhere (28). GST-Nup62 truncations (N1, C1, and C2) coated GSH-beads were incubated with cell lysates expressing GFP-Nup88, GFP-Nup88-C or GFP-Nup88-delC. Both the C-terminal alpha-helical region bearing truncations, Nup62-C1 and Nup62-C2, pulled down Nup88 and Nup88-C, but the Nup88-delC could not be pulled down (Figure 3F). In a reciprocal pulldown, GST-Nup88-C coated beads efficiently pulled down Nup62 and Nup62-C1 but not the Nup62-delC1 (Figure 3G). Using the yeast two-hybrid system, we further established that the minimal coiled-coil region of Nup88 and alpha-helical region of Nup62 are sufficient to mediate the Nup88-Nup62 interaction (Figure 3H). Importantly, Nup62-C1 exhibited a strong and specific interaction with the Nup88 coiled-coil domain as it did not bind with a random coiled-coil domain of an intermediate filament binding protein Periplakin (PPL-C). Additionally, the Nup88-C efficiently pulled down the endogenous Nup62 and exogenously expressed GFP-Nup62-C1, but the PPL-C could not (Figure S3). Thus the carboxy-terminal alpha-helical region of Nup62 and the coiled-coil region of Nup88 engage in a strong Nup88-Nup62 interaction.

Nup88 and Nup62 interaction is cell-cycle independent

Nucleoporins exhibit cell-cycle dependent differences in their subcellular localization (29) and stability (30). The alpha-helical domain of Nup62 (Nup62-C1) assists in its centrosome localization (28). We asked if the localization and interaction between Nup88 and Nup62 changes during different cell-cycle phases. We checked

the localization of Nup88 (full length, Nup88-delC, Nup88-C), and Nup62 (full length, Nup62-delC1, Nup62-C1) in cells either normally fixed (Figure S4A) or first extracted with Triton X-100 before fixation (pre-extraction) which allowed clear nuclear rim visualization of expressed proteins (Figure S4B). Full-length Nup88 and Nup62 primarily localized in the cytoplasm and at nuclear envelope, but, in a contrasting observation, Nup88-C did not localize to the nuclear envelope (NE), whereas Nup62-C1 was found at the NE (Figure S4B). We then asked if the NE localization of endogenous Nup88 changes under Nup62-delC1 overexpression conditions. The Nup62-fl and Nup62-C1 reactivity were strong at the nuclear rim, but the Nup62-delC1 remained diffused inside the nucleoplasm. Importantly, in all these cases, endogenous Nup88 was found in the NE (Figures 4A–C). We asked if the Nup88-Nup62 interaction and their protein levels exhibit any cell cycle-dependent variations. Lysates obtained from asynchronous, G1/S, and mitotic phase synchronized HeLa cells (Figure S5) were used in immunoprecipitation (IP) with control (IgG) and anti-Nup62 antibodies. We detected an efficient IP of Nup88 under all cell synchronization conditions (Figure 4D). Similarly, the GST-Nup62-C1 pulled out endogenous Nup88 (Figure 4E), and GST-Nup88-C pulled out endogenous Nup62 (Figure 4F) from asynchronous and synchronized HeLa cell lysates establishing strong and stable cell-cycle independent interaction between Nup88 and Nup62.

We next probed if the cell-cycle stages exert any effect on overexpressed Nup88. HeLa cells synchronized at G1/S boundary were released from the arrest for indicated time intervals, and GFP-Nup88 was pulled down on GBP coated beads to assess interaction with Nup62. Importantly, the interaction between Nup88 and Nup62 remained unperturbed (Figure 4G, first panel), indicating a strong cell-cycle stage independent interaction. Interestingly, the levels of GFP-Nup88 decreased ~18 h post G1/S release, a time-point indicative of the early G1 phase (Figure 4G, first and third panel). In contrast, the endogenous Nup62 levels did not change significantly (Figure 4G, second and fourth panels). Our data highlights the fact that Nup88-Nup62 interaction is cell-cycle independent but surprisingly overexpressed Nup88 is unstable.

Nup62 interaction with Nup88 protects Nup88 from ubiquitination mediated degradation

Reduced glycosylation of Nup62 induces Nup88 degradation (18) and we observed that overexpressed Nup88 is unstable at the onset of G1/S phase (Figure 4G). These observations suggest strong effects of Nup62 interaction on Nup88 stability. We, thus, probed the role of Nup62 interaction on Nup88 stability. GFP-Nup62 transfected cells (+) were treated with cycloheximide, and endogenous Nup88 levels were detected in total lysates. Although the anti-Nup88 antibody used in the study poorly detected endogenous protein, we could observe

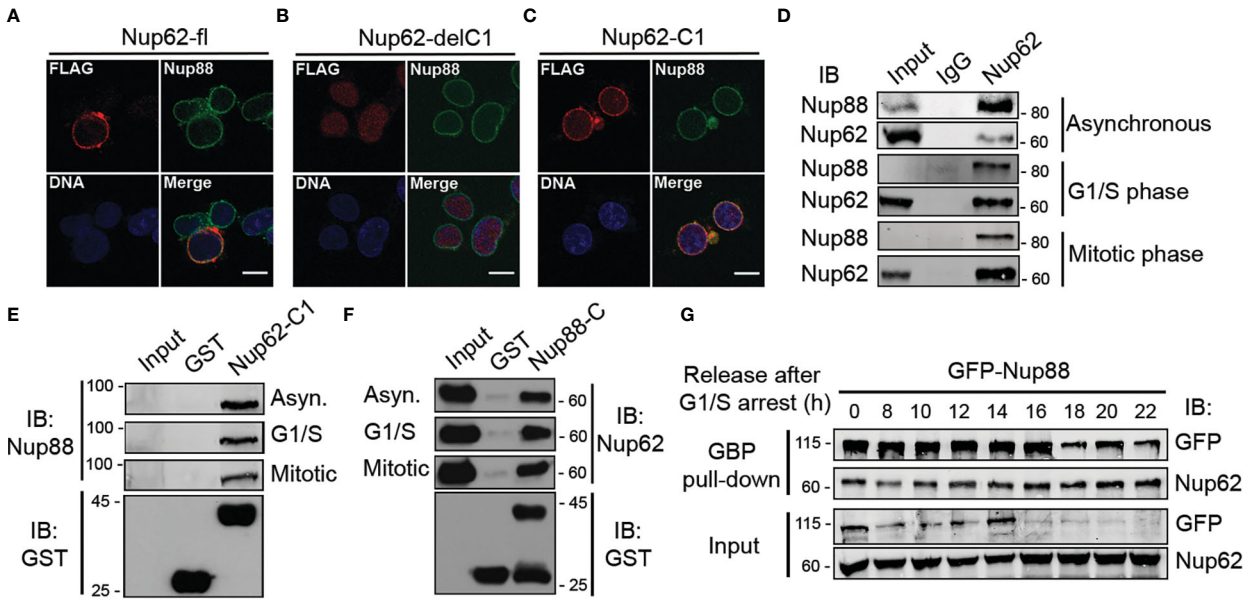

FIGURE 4
Nup88 interacts with Nup62 independent of the cell cycle phases. **(A–C)** Localization of FLAG-Nup62 constructs Nup62-fl, Nup62-delC1, and Nup62-C1 respectively in cells and detection by anti-FLAG (red) and anti-Nup88 (green) antibodies. Chromatin is stained with Hoechst 33342. Scale bar = 10 μm. **(D)** Immunoprecipitation using control and anti-Nup62 IgG from HeLa cell lysates synchronized in different phases (as indicated) of the cell-cycle. IP samples were immunoblotted with anti-Nup88 and anti-Nup62 antibodies. **(E)** Pull down on GST or GST-Nup62-C1 coated beads from HeLa lysates synchronized as indicated. Pull down material is immunoblotted with the anti-Nup88 antibody. The GST-tagged proteins were detected by anti-GST antibodies (bottom panel). **(F)** Same as in **(E)**, but the beads are coated with GST or GST-Nup88-C, and anti-Nup62 antibody used for immunoblotting. **(G)** GBP pull down from GFP-Nup88 expressing HeLa cell lysates prepared from cells released for indicated time intervals after synchronization at G1/S phase. Pull down, and input fractions were immunoblotted (IB) with anti-GFP and anti-Nup62 antibodies. Images are a representative from at least n=3 repeat experiments.

relative enrichment of Nup88 protein in GFP-Nup62 expressing cells (Figure S6). In GFP-Nup88 overexpressing cells, GFP-Nup88 levels decreased by ~50% (from 1.00 to 0.46) within 2 h of cycloheximide treatment, while the endogenous Nup62 levels remained unchanged (Figure 5A). Moreover, a distinct stabilization of GFP-Nup88 was observed (~2 folds at t= 0 h to ~8 folds at t= 4 h) when cells treated with cycloheximide also expressed FLAG-Nup62 (Figure 5B). These observations indicate that overexpressed Nup88 is stabilized when Nup62 is co-expressed, probably by sequestering and forming a stable complex.

We asked if Nup88 degradation is ubiquitination dependent and if the presence of Nup62 imparts stability to Nup88 against ubiquitination. Cellular levels of GFP-Nup88 and GFP-Nup88-C, capable of interacting with Nup62, increased ~ 2 folds and ~1.25 folds, respectively, when FLAG-Nup62 was coexpressed. However, the levels of Nup88-delC, unable to interact with Nup62, decreased by ~1.35 fold even when the Nup62 was co-expressed (Figure 5C). Subsequently, we treated HA-Ubiquitin and Nup88 and Nup62 construct expressing cells with MG132. While GFP-Nup88 expressing cells display significant ubiquitination, the GFP-Nup62 lacked any sign of ubiquitination. The Nup88 ubiquitination reversed and was undetectable when Nup62 was co-expressed (Figure 5D). Further, we explored the importance of Nup62 interaction on Nup88 ubiquitination. Cells co-expressing HA-Ubiquitin and GFP-Nup88 were transfected with various Nup62 constructs, and treated with MG132. GFP-Nup88 was pulled down from cell lysate on GBP beads and quantitated to assess the stability. Observations reveal that Nup62 and Nup62-C1, capable of interacting with Nup88, when expressed stabilized Nup88 (~2 fold, Figure 5E upper panel). In contrast, GFP-Nup88 levels were comparable to the vector and Nup62-delC1 co-expression conditions (Figure 5E). From a similar experimental setup (MG132 treatment of Ubiquitin and Nup88 co-expressing cells), Nup88 showed enhanced ubiquitination under Nup62-delC1 expressing conditions. However, the co-expression of Nup62 or Nup62-C1 drastically reduced Nup88 ubiquitination (Figure 5F). From these experiments, it is evident that Nup88 is ubiquitinated, while interaction with Nup62 reduces possibility of Nup88 ubiquitination and thus stabilizes Nup88.

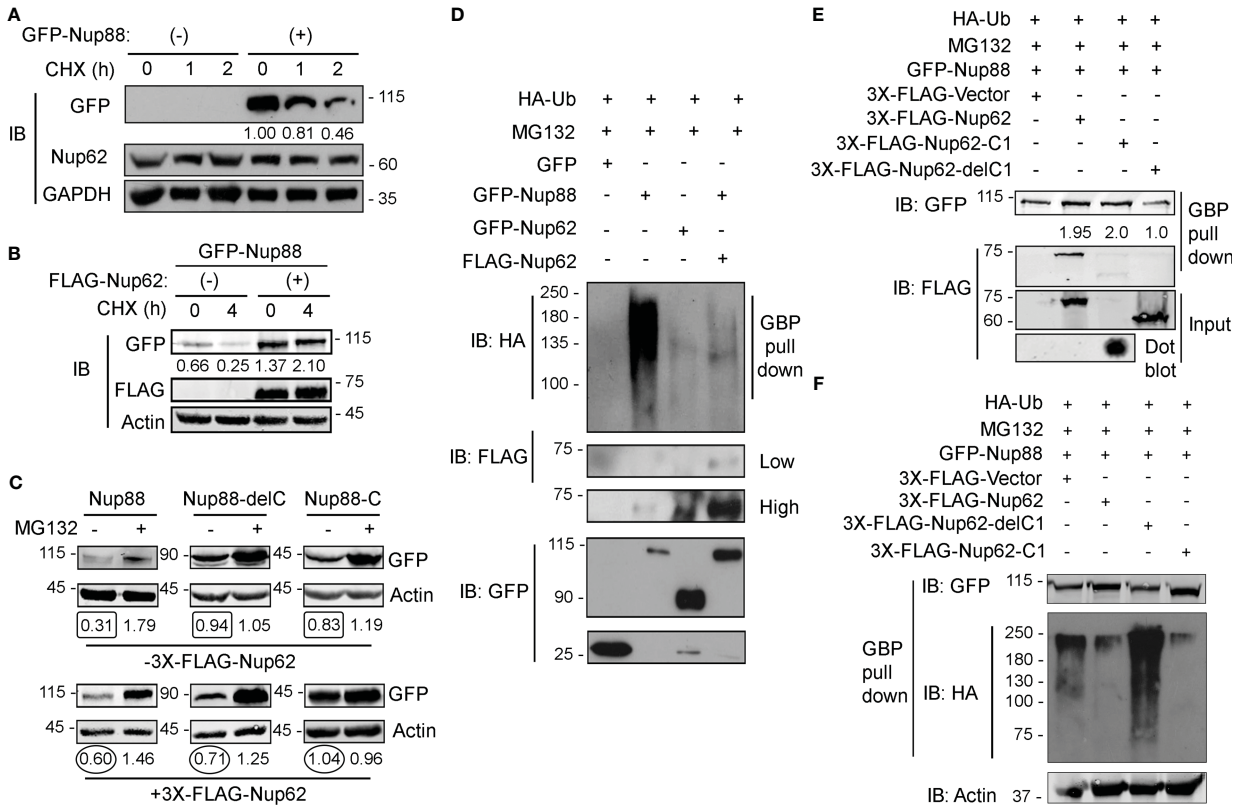

FIGURE 5
Nup62 stabilizes Nup88 protein by protecting it from degradation. **(A)** Detection of GFP-Nup88 in lysates of GFP-transfected and GFP-Nup88 transfected cells treated with cycloheximide for the indicated time points (h). Nup62 and GAPDH were used as internal loading controls and GAPDH for relative level quantification. **(B)** GFP-Nup88 transfected cells, cotransfected with 3x-FLAG-Nup62 (+), were treated with cycloheximide for the indicated time points (h). Total cell lysates were probed with anti-GFP, anti-FLAG, and anti-Actin antibodies. **(C)** HEK293T cells transfected with Nup88 constructs indicated on top of each panel was cotransfected with vector control (- 3X-FLAG-Nup62) or FLAG-Nup62 (+ 3X-FLAG-Nup62) and treated [(+) lanes], or not-treated [(-) lanes] with MG132 and lysates from these cells were immunoblotted with anti-GFP and anti-Actin antibodies. Values below each lane represent relative Nup88 levels quantified by normalizing the densitometry values of Nup88 with the respective loading control (Actin) using ImageJ. **(D)** HEK293T cells were transfected with HA-Ubiquitin and treated with MG132. These cells were cotransfected as indicated above the lanes. GBP pulldown material was immunoblotted with anti-GFP, anti-HA, and anti-FLAG antibodies. Images are a representative from at least n=3 repeat experiments. **(E)** HA-Ubiquitin transfected, and MG132 treated HEK293T cells were simultaneously cotransfected as indicated above the lanes. GBP pulldown material was probed with anti-GFP and anti-FLAG antibodies. **(F)** same as in **(E)**, and the GBP pull down material was probed with anti-HA, anti-GFP, and anti-Actin antibodies.

Nup88 interacts with NF-kB and affects its downstream proliferative and inflammatory pathways

Nup88-214 sub-complex and Crm1 together regulate the nuclear export of cargo proteins like NF-κB/Dorsal (p65) (31). In addition to genetic interaction, weak biochemical interaction between *Dorsal* and *mbo* (Nup88) is reported only from *Drosophila*. In HEK293T cell culture setup, we asked if Nup88 and p65 interact and whether Nup88 and Nup62 interaction has any role to play in p65 dependent functions. In this direction, first, we demonstrated that p65 redistributes inside the nucleus when GFP-Nup88 overexpressing cells are treated with tumor necrosis factor-α (TNF-α) (Figure 6A). Importantly, p65 was pulled down strongly on GFP-Nup88, but only when full length Nup62 was co-expressed. p65 interacted with Nup88 even when Nup62-C1 was co-expressed, but the strength of interaction was feeble. However, p65 did not interact with Nup88 under Nup62-delC1 co-expression conditions (Figure 6B). We further tested the involvement of interacting domains, Nup88C and Nup62-C1, in p65 pulldown. Nup88C and Nup62-C1 pulled down endogenous Nup62 and Nup88, respectively, but both failed to individually pulldown p65 (Figure 6C). Thus, the presence of stable Nup88-Nup62 seems imperative for interaction with p65. While analyzing the Nup88 expressing cells, we found a small fraction of overexpressed Nup88 inside the nucleus (Figure S7A). It is not uncommon for nucleoporins to be present in the nucleoplasm (32). Thus, we asked if nuclear Nup88 can interact and sequester p65 inside the nucleus of unstimulated cells. Indeed, the p65 was seen inside the nucleus of unstimulated GFP-Nup88 expressing cells (Figure S7B). We further probed if nuclear p65 is active and can induce the transcription of its target genes directly involved in the tumorigenic transformation. Comparative qRT-PCR analysis of p65 target genes in unstimulated GFP and GFP-Nup88 expressing cells suggested a significant increase in inflammatory cytokine, IL-6, levels (Figure 6D), and of Ki-67 (a proliferation antigen) levels (Figure 6E). Besides, enhancement in the expression of Akt and c-myc (growth and survival marker) and Bcl-2 and BIRC3 (apoptotic regulators) were seen (Figure 6F). We strengthened the observation made in cell line overexpression studies by analyzing p65 target genes in GEO & Oncomine oral cancer datasets already reported for Nup88 and Nup62 upregulation. We found the upregulation of IL6, Ki67, c-myc, Akt, and BIRC3 genes in the oral cancer dataset-GSE30784 (Figure 6G) as well as in the analyzed head and neck statistics available at Oncomine (Figure S8). Together, these observations indicate a direct interaction between Nup88 and p65, leading to the activation of the NF-κB pathway during Nup88 overexpression.

Discussion

Nup88 overexpression is becoming synonymous with cancer progression (6). Further, it is becoming evident that levels of many nucleoporins change when in association with a disease (33). The Nup88-Nup214 complex in coordination with CRM1 regulates the transport of NF-κB and pre-ribosomal assemblies (31, 34–37). We find elevated Nup88 and Nup62 mRNA and protein levels in oral cancer tissues and a positive correlation between elevated Nup88 levels vis-a-vis poor survival rates (Figure 1). Possibly the co-overexpression of Nup62 and Nup88 allows the formation of a stoichiometric complex stabilizing Nup88 manifesting cancerous

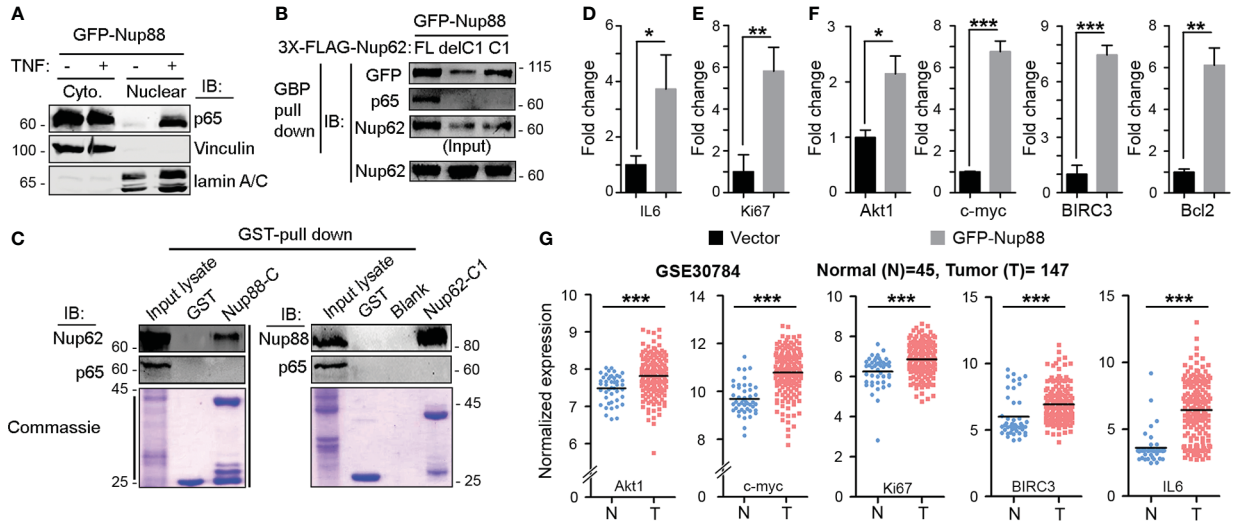

FIGURE 6
Stable Nup88 interacts with NF-κB and activates downstream pathways. **(A)** Cytosolic and nuclear fractions from GFP-Nup88 expressing cells treated (+) or not-treated (-) with TNF-α immunoblotted with anti-p65, anti-vinculin, and anti-lamin A/C antibodies. **(B)** GBP pulldown from GFP-Nup88 expressing cells cotransfected with FLAG-Nup62 constructs indicated above the lanes. The pulldown material was probed with anti-GFP, anti-p65, and anti-Nup62 antibodies. **(C)** Beads coated with GST-tagged proteins indicated on top of the wells were used in pulldown from cell lysates. Pulldown material was immunoblotted with anti-Nup62, anti-Nup88, and anti-p65 antibodies. Lower panels show Coomassie of input lysates and bead-bound samples. **(D, E)** Rps16 normalized qRT-PCR data for IL-6 and Ki67 from GFP-Nup88 transfected cells. **(F)** Actin normalized qRT-PCR data of indicated target genes from GFP-Nup88 expressing cells. All experiments were carried out in HEK293T cells. **(G)** IL-6, Ki67, Akt, c-myc, and BIRC3 expression analyzed through microarray data analysis of publically available oral cancer dataset (GSE30784) on GEO database. Error bars indicate mean values ± SEM. Asterisks indicate statistical significance (Student's t-test) *p < 0.05, **p < 0.01 and ***p < 0.001.

outcomes. While Nup88 protein levels were reported to be increasing with progressive stages of cancer (38), overexpression of no other nucleoporin could parallel these phenotypes (11). We report significantly enhanced levels of Nup88 and Nup62 protein in oral cancers. Cells overexpressing Nup88 were reported to induce multi-nuclear structures (12), and Nup62 glycosylation levels affect Nup88 stability (18). Correspondingly, elevated expression of these proteins in oral cancer cells resulted in increased cell proliferation, colony forming abilities and migration properties. These observations are in sync with reports from HeLa cells (39). While it is evident that altered expression of these nucleoporins imparts carcinogenic properties, we further need to investigate how NF-kB levels, nucleo-cytoplasmic distribution and its transcriptional factor roles are integrated when Nup88 is overexpressed.

Nucleoporins do exhibit a cell-cycle dependent difference in their stability and localization and thus are involved in cell-cycle specific interactions (34). Although Nup62 is not reported to be a stable member of the Nup88-214 subcomplex, however, *in vitro* studies with Nup62, Nup88 and Nup214 fragments (40) and the cell-cycle stage independent interaction of Nup62 with Nup88 and not perturbing the Nup88 nuclear envelope localization suggests otherwise (Figure 4). Similarly, the Nup107 complex exhibits cell-cycle independent interactions and mediates several functions (41). We believe that more detailed analysis needs to be performed in tissues samples but our observation from biochemical, cell biological studies suggests that overexpressed and endogenous Nup62 can form a stable subcomplex with Nup88. Interestingly, the overexpressed Nup88 when not in complex with Nup62 or Nup214 degrades over time, providing a rationale for Nup88 ubiquitination. Such stabilizing interaction is known for other proteins, including that of interaction between NF-κB and its inhibitor IκB. Thus co-overexpression of Nup62 in cancers may probably work through the stabilization of Nup88, and stable Nup88 can engage in proliferative activities inducing tumorigenic transformation.

ELYS, a dual nucleoporin, is known to affect the intranuclear dynamics of p65 (42), and *Drosophila* Nup88 (*mbo*) can perturb p65 nuclear export when the immune pathway is activated (34). While an indirect and feeble Nup88 and p65 interaction is reported in flies (34, 43), we describe a direct and strong Nup88-p65 interaction (Figure 6). We also suggest that Nup62 co-expression can stabilize overexpressed Nup88 and strengthens the Nup88-p65 interaction.

NF-κB signaling plays an important role in regulating cell proliferation, apoptosis, and inflammation (44), moreover, the inflammatory milieu is known to support tumor growth and progression (45). Nup88-p65 interaction induces the expression of the right combination of pro-growth and anti-apoptotic molecules supporting tumorigenesis. The unique presence of NF-κB in the nucleus of unstimulated Nup88 overexpressing cells favored production of inflammatory cytokines like IL-6 and other survival signals capable of inducing neoplastic transformations (Figure 6). Coincidently, this observation aligns well with the IL-6 expression and inflammatory milieu in cancer (46). Our observation is in coherence with nucleoporins affecting the EGFR signaling pathway (47) and multiple roles attributed to overexpressed Nup88 inducing cancerous growth. Together, our data indicate that when cancers overexpress Nup88, often Nup62 is co-expressed. It allows Nup88 stabilization and perhaps deregulation of the NF-κB transcriptional paradigm. The dysregulated Nup88-NF-κB axis is inclined towards p65 dependent inflammatory and pro-growth axis. In agreement with this, a recent report suggests multiple roles for overexpressed Nup88 (22). We propose that NF-κB pathway activation seems to be one of the mechanisms operating in Nup88 overexpressing cancer (Figure 7).

Material and methods

Cancer tissue collection

Head and neck cancer tissue samples (T) and adjacent normal tissues (N) were collected from Bansal Hospital, Bhopal, India. The study was approved by the Institute Ethics Committee of Indian Institute of Science Education and Research (IISER) Bhopal (IEC approval document # IISERB/IEC/2016/meetings/05/04) and samples were collected with the consent of the patients. The tissues were snap-frozen immediately after surgery and stored at -80° C until use. The tissues for RNA isolation were collected in RNA Later (Thermo Fisher Scientific, # AM7024). The clinical characteristics of patients used in the study are listed in Supplementary Table 1.

Bioinformatics analysis

The co-expression plot for Nup88 and Nup62 in normal, primary cancer, metastasis and cell lines for oral cancer was extracted from MiPanda (http://mipanda.org). The cancer stage-specific expression was analyzed using Cancer RNA-Seq Nexus (CRN) (http://syslab4.nchu.edu.tw/). The differential expression graph for both the genes was plotted using GraphPad Prism. The survival curves specific to Nup88 and Nup62 were obtained from OncoLnc (http://www.oncolnc.org). The differential expression pattern of Nup88 and Nup62 in oral cancer was analyzed with the help of Oncomine database. The graph of analyzed expression data of Nup88 and Nup62 in oral cancer was saved for the representation.

Plasmids

The full-length construct of Ubiquitin (HA-Ubiquitin Plasmid # 18712) and Nup88 (pEGFP-Nup88 Plasmid # 64283) were obtained from Addgene. The C-terminal coiled-coil domain (Nup88-C, amino acids 585-741) of Nup88 was PCR amplified from human testis cDNA and cloned into pGEX6P1 with EcoRI and SalI enzyme sites. This domain was further subcloned into the pEGFP vector. The Nup88 construct lacking the coiled coil domain (Nup88-delC) was created by inserting a stop codon after 584th amino acid through site directed mutagenesis (Q5 Site Directed Mutagenesis Kit, NEB-E0554S) using pEGFP-Nup88 as template. pEGFP-Nup62 was a kind gift from Dr Radha Chauhan (NCCS, Pune). The N-terminal and C-terminal truncations of Nup62 were PCR amplified and cloned

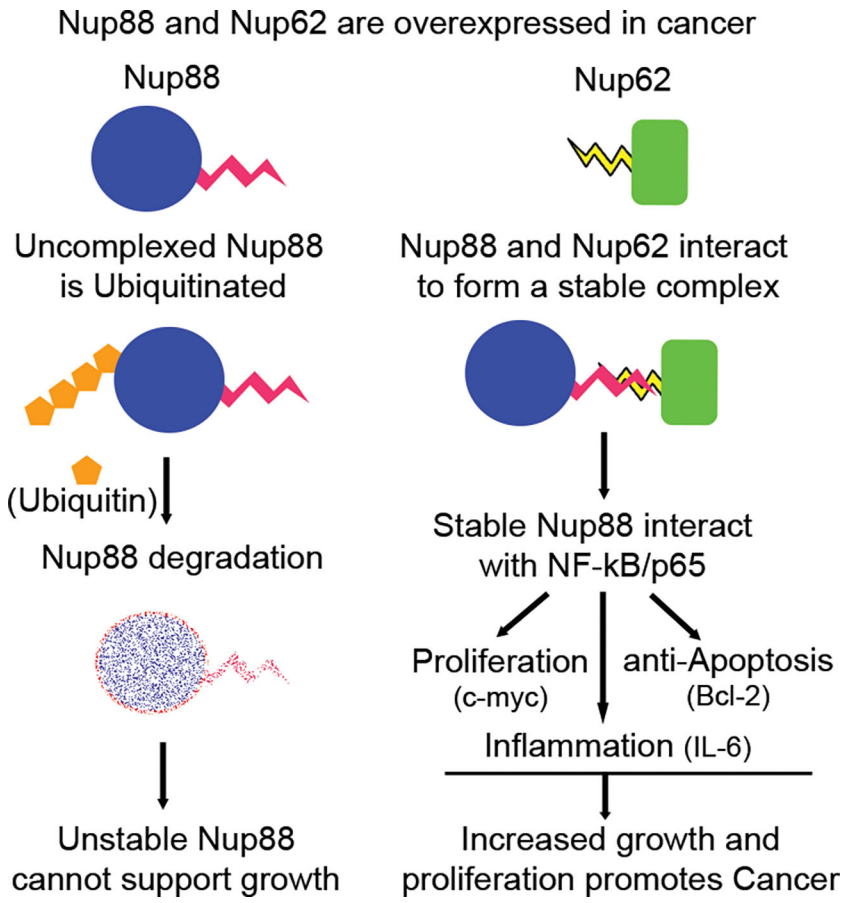

FIGURE 7
Nup88 in complex with Nup62 is stable and affects growth, proliferation and survival arm of NF-κB pathway in cancer. Nup88 and Nup62 are overexpressed in cancer, including head and neck cancer. Excess Nup88 in these cancer tissues can be targeted for degradation by ubiquitin-mediated proteasomal pathway, whereas Nup88 when complexed with co-expressed Nup62 in these tissues is stable. Stabilized Nup88 interacts with p65 and sequesters active p65 inside the nucleus. The extended presence of p65 inside the nucleus under Nup88 overexpressing conditions promotes the expression of target genes like c-myc, Bcl2, and IL-6 to simultaneously regulate growth, proliferation, apoptosis, and inflammation driving tumorigenesis.

into pGEX6P1, pCMV3Tag1a and pEGFP vectors. The yeast-two hybrid constructs for Nup88 and Nup62 truncations were made by subcloning them into pGADC1 and pBDUC1 vectors. Nup88-C (aa 585-741) and Nup62-C1 (aa 328-458) coding sequence were inserted into pGADC1 vector harboring GAL4 activation domain (AD) and pBDUC1 vector harboring GAL4 DNA binding domain (BD).

Reagents and antibodies

Reagents and antibodies used in this study were purchased from miscellaneous sources. Cycloheximide (MP Biomed, # 100183) was used at 1 μg/ml for different time points. MG132 (HiMedia, 474787-10MG) was used at 10 μM concentration for 8 h. The antibodies used for western blotting are anti-Nup88 (BD Biosciences, # 611896, 1:2000 dilutions), anti-Nup62 (BD Biosciences, # 610497, 1:6000 dilutions), anti-GAPDH (Abgenex, # 10-10011, 1:6000 dilutions), anti-GFP (Santa Cruz, # 9996 1:5000 dilutions), anti-GST (1:500 dilutions), anti-HA (Sigma, # H6908, 1:2000 dilutions), anti-FLAG (Sigma, # F7425, 1:2000), anti-Actin (BD Biosciences, # 612656, 1:5000 dilutions), anti-Lamin A/C (BD Biosciences, # 612162, 1:2000 dilutions), anti-NFκB p65 (BD Biosciences, # 610868, 1:2000 dilutions), goat anti-rabbit IgG-HRP (GeNei, # 114038001A, 1:10000 dilutions), goat anti-mouse IgG-HRP (GeNei, # 114068001A, 1:10000 dilutions). A polyclonal antibody was generated against Nup88 by immunizing rabbits with Nup88 fragment (aa 1 - 584) lacking the C-terminal coiled coil-domain as an antigen. Antibodies were purified from immunized serum over NHS-Sepharose beads immobilized with appropriate antigen.

Cell culture

HEK293T, HeLa, SCC9, and MCF7 cells were obtained from American Type Culture Collection (ATCC). The H413 cells were obtained from Sigma Aldrich. HEK293T, HeLa, and MCF7 cells were grown and maintained in Dulbecco's Modified Eagle's Medium (DMEM, Gibco, # 11995-065), while SCC9 and H413 cells were grown and maintained in DMEM nutrient mixture F12 (Thermo, # 11320082), supplemented with 10% fetal bovine serum (FBS, Invitrogen, # 16000044) and antibiotics (100 units/ml Penicillin and Streptomycin, Invitrogen, # 15140122) in a humidified incubator with 5% CO_2 at 37° C.

Cell synchronization and FACS analysis

HeLa cells were synchronized in G1/S phase by double thymidine block and into M-phase by a thymidine block followed by nocodazole treatment. Cells were cultured at 30% confluency, and two cycles of 2 mM thymidine was added for 18 h with 9 h post-release between the two treatments to synchronize cells at G1/S boundary. For the M-phase block, cells were cultured at 40% confluency and treated with 2 mM thymidine for 24 h. Cells were then released for 5 h and treated with 100 ng/ml nocodazole for 12 h. Shake-off method was used to collect the mitotic cells. For FACS analysis, HeLa cells blocked in G1/S were trypsinized, and the cells blocked in M-phase were collected by mitotic shake-off, washed twice with PBS, and fixed in 70% ethanol at -20° C for 12 h. Fixed cells were resuspended in PBS containing 50 µg/ml each of RNase A and propidium iodide. The cell cycle distribution was acquired by BD Calibur flow cytometry and analyzed by Modfit LT software.

Lentivirus production

HEK293T cells were transfected with pLKO.1 shRNA plasmid (Sigma, Mission human genome shRNA library) and packaging plasmids- delta 8.9, VSV-G in a ratio of 10:5:1 with polyethylene-imine (PEI) following the standard protocol. After 12 h the media was replaced with fresh DMEM media containing 10% FBS and antibiotics. After 24 h and 48 h the supernatant was collected and spun to remove the cellular debris. The supernatant was filtered through a 0.45 µm filter and stored at -80° C until further use.

RNA interference and quantitative RT-PCR

Total RNA from cultured cells or tumor tissue was extracted by TRIzol (MP Biomed, #15596018) method. The genomic DNA contamination was removed by RNAse free DNAse. 1 µg of RNA was reverse transcribed to cDNA by iScript cDNA synthesis kit (Bio-Rad, #17088) as per the manufacturer's instructions. RT-PCR was performed using SYBR Green PCR master mix on a (BIO-RAD CFX Connect™ Real-Time System) Rps16 and Actin gene was used as the control gene, and the relative transcript level was calculated by CT value ($2^{-\Delta\Delta CT}$). Student's t-test was used to compare the differences in the gene expression, and p-value < 0.05 was considered significant. The primers used are listed in Supplementary Table 2.

Cell fractionation

Cells were harvested after the respective treatment and washed twice with 1X PBS and resuspended in Extraction Buffer A (10 mM HEPES, 1 mM EDTA, 1 mM EGTA, 10 mM KCl, 1 mM DTT, 5 mM NaF, 1 mM Sodium vanadate, 10 mM Sodium molybdate, 0.5 mM PMSF and 1X Protease inhibitor cocktail) and was incubated on ice for 15 min. 0.3 µl of 10% NP-40 was added to it and vortexed for 30 sec at 4° C. The lysate was centrifuged at 10000xg for 1 min at 4° C. The supernatant was collected as the cytosolic fraction. The pellet was resuspended in Extraction Buffer B (20 mM HEPES, 1 mM EDTA, 1 mM EGTA, 400 mM NaCl, 1 mM DTT, 5 mM NaF, 1 mM Sodium vanadate, 10 mM Sodium molybdate, 0.5 mM PMSF and 1X Protease inhibitor cocktail). It was incubated for 30 min on a shaker at 4° C and then centrifuged at 20,000xg for 5 min. The supernatant was collected as nuclear fractions.

Western blot

HEK293T, MCF7, SCC9 and HeLa cells were lysed in RIPA buffer (50 mM Tris pH 7.5, 10 mM EDTA, 1 mM EGTA, 150 mM NaCl, 1% Triton X 100, 0.2% Sodium deoxycholate and 1X Protease Inhibitor (Amresco, # M250). Cell lysates were sonicated and centrifuged at maximum speed (14,800 rpm) to collect the supernatant. The homogenized head and neck tissues were lysed in GLyse AT buffer (GCC BIOTECH, # GPA-004). The total protein is quantified using Bradford assay, and samples were prepared by adding 6X SDS sample buffer and boiled for 10 min at 100° C. The electrophoresed protein samples were transferred to polyvinylidene difluoride membrane (PVDF) and blocked with 5% (w/v) non-fat milk and probed with suitable primary and secondary antibodies. The bands were detected with enhanced chemiluminescence substrate (BIO-RAD Clarity™ Western ECL Substrate, # 170-5060) method or by using the Odyssey infrared imaging system (LICOR Odyssey).

Immunoprecipitation

The confluent HEK293T, MCF7, SCC9 and HeLa cell monolayer was lysed in 500 µl of RIPA buffer, sonicated and centrifuged at maximum speed. The collected supernatant was incubated with 5 µg of anti-Nup62 and anti-mouse IgG and incubated at 4° C on rocker 12 h. 20 µl of Protein-G sepharose beads were added to it and further incubated at 4° C on a rocker for 4 h. Bead bound samples were centrifuged, and unbound fractions were collected separately, and beads were washed four times with chilled PBS. The eluted protein samples were processed with 6X SDS sample buffer, and samples were analyzed by western blotting as described earlier.

GST pulldown assay

The GST and GST-fused proteins were purified from bacterial strains- *E. coli* BL21DE3 Star and Codon plus cells. 20 µg of each protein was allowed to bind glutathione beads for 1h at 4° C on a rocker. The unbound protein was removed, and the beads were washed 4 times with a wash buffer (20 mM Tris, 150 mM NaCl and 1 mM EDTA). The pulldown was performed by adding 500 µg of HEK293T or HeLa cell lysate (asynchronous or synchronous, depending on the experiment) and allowed to bind for another 1 h at 4° C on a rocker. The unbound fraction was removed, and washes were given as above. The eluted protein was analyzed by western blotting.

GBP pulldown assay

The experiment was performed as described previously (48). In brief, HEK293T cells were transfected with pEGFP-Nup88, pEGFP-Nup62, and their truncations. 48 h post-transfection cells were harvested, lysed, sonicated, and centrifuged. The supernatant fraction was incubated with GST-GBP protein at 4° C on the rocker for 12 h. 20 µl of glutathione beads were added and incubated at 4° C on a rocker for 4 h. Further washing and elution steps are similar to the GST pulldown experiment.

Yeast two-hybrid assay

The pGADC1 and pGBDUC1 constructs of Nup88 and Nup62 truncations were co-transformed into yeast two-hybrid strain PJ69-4A. Double transformants were obtained on a non-selective (lacking Leu and Ura, double drop out) media. The ten-fold serial dilutions of equivalent numbers of transformants were spotted on non-selective (lacking Leu and Ura, double drop out) and selective media (lacking Leu, Ura, and His, triple drop out) and incubated at 30° C for three days for transformants to appear.

Cell viability assay

SCC9 cells were transfected with pEGFP, pEGFP-Nup88, and pEGFP-Nup62 in a six-well culture plate. 24 h post-transfection cells were harvested, and $5x10^3$ cells were seeded in each well of a 96 well culture plate in triplicates and allowed to grow for another 24 h, 48 h, and 72 h. The cell growth was measured by the conversion of MTT-tetrazolium salt to formazan crystal. 20 µl of MTT (2 mg/ml) was added to each well, incubated for 4h, and the reaction was terminated by adding 100 µl of DMSO. Viability and cell proliferation were assessed by measuring the optical density at 570 nm in a plate reader (BioTek Eon, 11-120-611).

Wound healing assay

Oral cancer cells (SCC9) were transfected with pEGFP, pEGFP-Nup88, and pEGFP-Nup62 in a six-well culture plate setup. At 90% confluence, a scratch was created with a 10 µl pipette tip. The cellular debris (dislodged cells) was removed by thorough PBS washing. The cells were imaged at 12, 24 and 36 h intervals on an inverted microscope (Leica Microsystems Model- DMIL LED Fluo). The wound closure rate in each case was measured from images using TScratch software (49).

Colony-forming assay

H413 cells were transfected with pEGFP, pEGFP-Nup88, and pEGFP-Nup62 in a six-well culture plate. After 24 h of transfection, cells were harvested and seeded (2000 cells/well) in a six-well culture plate and were allowed to grow for 15 days. The cells were washed with PBS and imaged on an inverted microscope (Leica Microsystems Model- DMIL LED Fluo) to determine the colony size and area. Number of the colonies obtained in each case was determined with ImageJ software, and the graph was plotted using GraphPad. Further, cells were fixed in 3:1 ratio of methanol: acetic acid for 5 min. After fixation, cells were stained with 0.05% crystal violet in methanol for 15 min and washed with water to remove excess stain. The crystal-violet stained images were captured with a camera and used for the representation.

Immunofluorescence

HeLa, H413 and SCC9 cells were grown in a six-well culture plate with coverslips. Adhered HeLa cells were washed with PBS and pre-extracted using PHEM buffer (60 mM PIPES, 20 mM HEPES, 10 mM EGTA, 0.2% Triton X-100 and 4 mM $MgSO_4$) for 5 min at room temperature (RT). The H413 and SCC9 cells were washed with PBS and pre-extracted with 0.05% Digitonin for 2-5 minutes at RT. Pre-extracted cells were fixed with 4% paraformaldehyde for 15 min and permeabilized with rehydration buffer (10 mM Tris pH 7.4, 150 mM NaCl, 0.1% Triton X-100) for another 15 min at RT. The cells were blocked using 5% normal goat serum for 30 min and incubated with corresponding primary antibody (anti-Nup88, 1:200 and anti-Nup62, 1:1000) at 4° C for 12 h. After three PBS washes, 1:800 dilutions of Alexa-fluor conjugated secondary antibody (Alexa Fluor 488, Invitrogen, # A11034, Alexa Fluor 568, Invitrogen, # A11031) was added to the cells and allowed to incubate for an hour at RT. Again, three washes of PBS were given, and nuclei were stained with Hoechst 33342 (Invitrogen, # H1399, 1 mg/ml, 1:5000 dilutions). The coverslips were mounted on slides with VECTASHIELD mounting medium (# H1000), and images were captured on a Zeiss LSM 780 Confocal Microscope and Olympus Confocal Laser Scanning Microscope-FY3000. All images were analyzed using ZEN (Zeiss) or Image J/Fiji software.

Statistical analysis

The statistical analysis was performed with GraphPad Prism5. Student's t-test and two-way ANOVA were used to calculate the significance value. In the bar graphs, differences between two groups were compared using an unpaired two-tailed Student's t-test or Dunnett's multiple comparisons test. In case of cancer tissue analysis, paired two-tailed Student's t-test was used to study the significance. The differences were considered statistically significant with $*p<0.05$, $**$ $p<0.01$, and $***$ $p<0.001$.

Data availability statement

The original contributions presented in the study are included in the article/Supplementary Material. Further inquiries can be directed to the corresponding author.

Ethics statement

The studies involving human participants were reviewed and approved by Institute Ethics Committee of IISER Bhopal and Ethics Committee of Bansal Hospital. Written informed consent to participate in this study was provided by the participants' legal guardian/next of kin.

Author contributions

US and DB designed and performed all experiments, analyzed and interpreted data. RM helped in experiment designing and data interpretation. US, DB, and RM wrote the manuscript. AS provided cancer patient's tissue and patient data for all relevant analyses.

Funding

This work has been supported by SERB grant # EMR/2016/001819, CRG/2020/000496 and intramural funding from the Department of Biological Sciences Indian Institute of Science Education and Research Bhopal and institute fellowship to US. DB is a fellow of and is supported by the Prime Minister's Research Fellow (PMRF) scheme.

Acknowledgments

Authors thank Dr. Radha Chauhan (NCCS, Pune) generously for providing the pEGFP-Nup62 construct. We also thank Dr. Chandan Sahi, Dr. Sourav Datta, Dr. Himanshu Kumar, Dr. Sunando Datta and Dr. Sanjeev Shukla (IISER, Bhopal) for providing reagents helpful in this study. We thank the members of Nup and Sumo Biology Group for discussions and comments on the manuscript. We thank FIST project SR/FST/LSI-643/2015 for the Olympus Confocal Laser Scanning Microscope-FY3000.

Conflict of interest

The authors declare that the research was conducted in the absence of any commercial or financial relationships that could be construed as a potential conflict of interest.

Publisher's note

Supplementary material

The Supplementary Material for this article can be found online at: https://www.frontiersin.org/articles/10.3389/fonc.2023.1095046/full#supplementary-material

References

1. Chow KH, Factor RE, Ullman KS. The nuclear envelope environment and its cancer connections. *Nat Rev Cancer* (2012) 12:196–209. doi: 10.1038/nrc3219

2. Capelson M, Liang Y, Schulte R, Mair W, Wagner U, Hetzer MW. Chromatin-bound nuclear pore components regulate gene expression in higher eukaryotes. *Cell* (2010) 140(3):372–83. doi: 10.1016/j.cell.2009.12.054

3. Mor A, White MA, Fontoura BMA. Nuclear trafficking in health and disease. *Curr Opin Cell Biol* (2014) 28:28–35. doi: 10.1016/j.ceb.2014.01.007

4. Bastos R, De Pouplana LR, Enarson M, Bodoor K, Burke B. Nup84, a novel nucleoporin that is associated with CAN/Nup214 on the cytoplasmic face of the nuclear pore complex. *J Cell Biol* (1997) 137:989–1000. doi: 10.1083/jcb.137.5.989

5. Xu S, Powers MA. Nuclear pore proteins and cancer. *Semin Cell Dev Biol* (2009) 20:620–30. doi: 10.1016/j.semcdb.2009.03.003

6. Martínez N, Alonso A, Moragues MD, Pontón J, Schneider J. The nuclear pore complex protein Nup88 is overexpressed in tumor cells. *Cancer Res* (1999) 59:5408–11.

7. Gould VE, Orucevic A, Zentgraf H, Gattuso P, Martinez N, Alonso A. Nup88 (karyoporin) in human malignant neoplasms and dysplasias: Correlations of immunostaining of tissue sections, cytologic smears, and immunoblot analysis. *Hum Pathol* (2002) 33:536–44. doi: 10.1053/hupa.2002.124785

8. Zhang H, Schneider J, Rosdahl I. Expression of p16, p27, p53, p73 and Nup88 proteins in matched primary and metastatic melanoma cells. *Int J Oncol* (2002) 21(1):43–8. doi: 10.3892/ijo.21.1.43

9. Kraemer D, Wozniak RW, Blobel G, Radu A. The human CAN protein, a putative oncogene product associated with myeloid leukemogenesis, is a nuclear pore complex protein that faces the cytoplasm. *Proc Natl Acad Sci USA* (1994) 91:1519–23. doi: 10.1073/pnas.91.4.1519

10. Fornerod M, Deursen JV, Baal SV, Reynolds A, Davis D, Murti KG, et al. The human homologue of yeast CRM1 is in a dynamic subcomplex with CAN/Nup214 and a novel nuclear pore component Nup88. *EMBO J* (1997) 16:807–16. doi: 10.1093/emboj/16.4.807

11. Gould VE, Martinez N, Orucevic A, Schneider J. & alonso, a. a novel, nuclear pore-associated, widely distributed molecule overexpressed in oncogenesis and development. *Am J Pathol* (2000) 157:1605–13. doi: 10.1016/S0002-9440(10)64798-0

12. Hashizume C, Nakano H, Yoshida K, Wong RW. Characterization of the role of the tumor marker Nup88 in mitosis. *Mol Cancer* (2010) 9:1–7. doi: 10.1186/1476-4598-9-119

13. Naylor RM, Jeganathan KB, Cao X, Van Deursen JM. Nuclear pore protein NUP88 activates anaphase promoting complex to promote aneuploidy. *J Clin Invest.* (2016) 126:543–59. doi: 10.1172/JCI82277

14. Makise M, Nakamura H, Kuniyasu A. The role of vimentin in the tumor marker Nup88-dependent multinucleated phenotype. *BMC Cancer* (2018) 18:1–12. doi: 10.1186/s12885-018-4454-y

15. Hayakawa A, Babour A, Sengmanivong L, Dargemont C. Ubiquitylation of the nuclear pore complex controls nuclear migration during mitosis in s. cerevisiae. *J Cell Biol* (2012) 196:19–27. doi: 10.1083/jcb.201108124

16. Grandi P, Emig S, Weise C, Hucho F, Pohl T, Hurt EC. A novel nuclear pore protein Nup82p which specifically binds to a fraction of Nsp1p. *J Cell Biol* (1995) 130:1263–73. doi: 10.1083/jcb.130.6.1263

17. Bailer SM, Balduf C, Hurt E. The Nsp1p carboxy-terminal domain is organized into functionally distinct coiled-coil regions required for assembly of nucleoporin subcomplexes and nucleocytoplasmic transport. *Mol Cell Biol* (2001) 21:7944–55. doi: 10.1128/MCB.21.23.7944-7955.2001

18. Mizuguchi-Hata C, Ogawa Y, Oka M, Yoneda Y. Quantitative regulation of nuclear pore complex proteins by O-GlcNAcylation. *Biochim Biophys Acta - Mol Cell Res* (2013) 1833:2682–9. doi: 10.1016/j.bbamcr.2013.06.008

19. Kinoshita Y, Kalir T, Dottino P, Kohtz DS. Nuclear distributions of NUP62 and NUP214 suggest architectural diversity and spatial patterning among nuclear pore complexes. *PloS One* (2012) 7(4):e36137. doi: 10.1371/journal.pone.0036137

20. Karacosta LG, Kuroski LA, Hofmann WA, Azabdaftari G, Mastri M, Gocher AM. Nucleoporin 62 and Ca2+/calmodulin dependent kinase kinase 2 regulate androgen receptor activity in castrate resistant prostate cancer cells. *Prostate* (2016) 76:294–306. doi: 10.1002/pros.23121

21. Hazawa M, Lin DC, Kobayashi A, Jiang YY, Xu L, Dewi FRP, et al. ROCK-dependent phosphorylation of NUP 62 regulates p63 nuclear transport and squamous cell carcinoma proliferation. *EMBO Rep* (2018) 19:73–88. doi: 10.15252/embr.201744523

22. Li J, Zhao J, Li Y. Multiple biological processes may be associated with tumorigenesis under NUP88-overexpressed condition. *Genes Chromosom. Cancer* (2017) 56:117–27. doi: 10.1002/gcc.22417

23. Rhodes DR, Yu J, Shanker K, Deshpande N, Varambally R, Ghosh D, et al. ONCOMINE: A cancer microarray database and integrated data-mining platform. *Neoplasia* (2004) 6:1–6. doi: 10.1016/S1476-5586(04)80047-2

24. Ginos MA, Page GP, Michalowicz BS, Patel KJ, Volker SE, Pambuccian SE, et al. Identification of a gene expression signature associated with recurrent disease in squamous cell carcinoma of the head and neck. *Cancer Res* (2004) 64:55–63. doi: 10.1158/0008-5472.CAN-03-2144

25. Niknafs YS, Pandian B, Gajjar T, Gaudette Z, Wheelock K, Maz MP, et al. MiPanda: A resource for analyzing and visualizing next-generation sequencing transcriptomics data. *Neoplasia* (2018) 20:1144–9. doi: 10.1016/j.neo.2018.09.001

26. Li JR, Sun CH, Li W, Chao RF, Huang CC, Zhou XJ, et al. Cancer RNA-seq nexus: A database of phenotype-specific transcriptome profiling in cancer cells. *Nucleic Acids Res* (2016) 44:D944–51. doi: 10.1093/nar/gkv1282

27. Anaya J. OncoLnc: Linking TCGA survival data to mRNAs, miRNAs, and lncRNAs. *PeerJ Comput Sci* (2016) 2:e67. doi: 10.7717/peerj-cs.67

28. Hashizume C, Moyori A, Kobayashi A, Yamakoshi N, Endo A, Wong RW. Nucleoporin Nup62 maintains centrosome homeostasis. *Cell Cycle* (2013) 12:3804–16. doi: 10.4161/cc.26671

29. Mishra RK, Chakraborty P, Arnaoutov A, Fontoura BMA, Dasso M. The Nup107-160 complex and gamma-TuRC regulate microtubule polymerization at kinetochores. *Nat Cell Biol* (2010) 12:164–9. doi: 10.1038/ncb2016

30. Chakraborty P, Wang Y, Wei JH, Deursen JV, Yu H, Malureanu L, et al. Nucleoporin levels regulate cell cycle progression and phase-specific gene expression. *Dev Cell* (2008) 15(5):657–67. doi: 10.1016/j.devcel.2008.08.020

31. Xylourgidis N, Roth P, Sabri N, Tsarouhas V, Samakovlis C. The nucleoporin Nup214 sequesters CRM1 at the nuclear rim and modulates NF-κB activation in drosophila. *J Cell Sci* (2006) 119:4409–19. doi: 10.1242/jcs.03201

32. Morchoisne-Bolhy S, Geoffroy MC, Bouhlel IB, Alves A, Audugé N, Baudin X, et al. Intranuclear dynamics of the Nup107-160 complex. *Mol Biol Cell* (2015) 26:2343–56. doi: 10.1091/mbc.E15-02-0060

33. Bindra D, Mishra RK. In pursuit of distinctiveness: Transmembrane nucleoporins and their disease associations. *Front Oncol* (2021) 11:784319. doi: 10.3389/fonc.2021.784319

34. Uv AE, Roth P, Xylourgidis N, Wickberg A, Cantera R, Samakovlis C. Members only encodes a drosophila nucleoporin required for rel protein import and immune response activation. *Genes Dev* (2000) 14:1945–57. doi: 10.1101/gad.14.15.1945

35. Roth P, Xylourgidis N, Sabri N, Uv A, Fornerod M, Samakovlis C. The drosophila nucleoporin DNup88 localizes DNup214 and CRM1 on the nuclear envelope and attenuates NES-mediated nuclear export. *J Cell Biol* (2003) 163:701–6. doi: 10.1083/jcb.200304046

36. Bernad R, Engelsma D, Sanderson H, Pickersgill H, Fornerod M. Nup214-Nup88 nucleoporin subcomplex is required for CRM1-mediated 60 s preribosomal nuclear export. *J Biol Chem* (2006) 281:19378–86. doi: 10.1074/jbc.M512585200

37. Takahashi N, van Kilsdonk JW, Ostendorf B, Smeets R, Bruggeman SW, Alonso A, et al. Tumor marker nucleoporin 88 kDa regulates nucleocytoplasmic transport of NF-κB. *Biochem Biophys Res Commun* (2008) 374:424–30. doi: 10.1016/j.bbrc.2008.06.128

38. Brustmann H, Hager M. Nucleoporin 88 expression in normal and neoplastic squamous epithelia of the uterine cervix. *Ann Diagn Pathol* (2009) 13:303–7. doi: 10.1016/j.anndiagpath.2009.05.005

39. Makise M, Uchimura R, Higashi K, Mashiki Y, Shiraishi R, Shutoku Y, et al. Overexpression of the nucleoporin Nup88 stimulates migration and invasion of HeLa cells. *Histochem Cell Biol* (2021) 156(5):409–21. doi: 10.1007/s00418-021-02020-w

40. Madheshiya PK, Shukla E, Singh J, Bawaria S, Ansari MY, Chauhan R. Insights into the role of Nup62 and Nup93 in assembling cytoplasmic ring and central transport channel of the nuclear pore complex. *Mol Biol Cell* (2022) 33(14):ar139. doi: 10.1091/mbc.E22-01-0027

41. Walther TC, Alves A, Pickersgill H, Loïodice I, Hetzer M, Galy V, et al. The conserved Nup107-160 complex is critical for nuclear pore complex assembly. *Cell* (2003) 113:195–206. doi: 10.1016/S0092-8674(03)00235-6

42. Mehta SJK, Kumar V, Mishra RK. Drosophila ELYS regulates dorsal dynamics during development. *J Biol Chem* (2020) 295:2421–37. doi: 10.1074/jbc.RA119.009451

43. Bhattacharya A, Steward R. The drosophila homolog of NTF-2, the nuclear transport factor-2, is essential for immune response. *EMBO Rep* (2002) 3:378–83. doi: 10.1093/embo-reports/kvf072

44. Lu H, Ouyang W, Huang C. Inflammation, a key event in cancer development. *Mol Cancer Res* (2006) 4:221–33. doi: 10.1158/1541-7786.MCR-05-0261

45. Candido J, Hagemann T. Cancer-related inflammation. *J Clin Immunol* (2013) 33 (Suppl 1):S79–84. doi: 10.1007/s10875-012-9847-0

46. Hodge DR, Hurt EM, Farrar WL. The role of IL-6 and STAT3 in inflammation and cancer. *Eur J Cancer* (2005) 41:2502–12. doi: 10.1016/j.ejca.2005.08.016

47. Giri DK, Ali-Seyed M, Li LY, Lee DF, Ling P, Bartholomeusz G, et al. Endosomal transport of ErbB-2 : Mechanism for nuclear entry of the cell surface receptor. *Mol Cell Biol* (2005) 25:11005–18. doi: 10.1128/MCB.25.24.11005-11018.2005

48. Gujrati M, Mittal R, Ekal L, Mishra RK. SUMOylation of periplakin is critical for efficient reorganization of keratin filament network. *Mol Biol Cell* (2019) 30:357–69. doi: 10.1091/mbc.E18-04-0244

49. Gebäck T, Schulz MMP, Koumoutsakos P, Detmar M. TScratch: A novel and simple software tool for automated analysis of monolayer wound healing assays. *Biotechniques* (2009) 46:265–74. doi: 10.2144/000113083

frontiers | Frontiers in Oncology

TYPE Original Research
PUBLISHED 16 February 2023
DOI 10.3389/fonc.2023.1023292

OPEN ACCESS

EDITED BY
Julia Kzhyshkowska,
Heidelberg University, Germany

REVIEWED BY
Ejaz Ahmad,
Michigan Medicine, University of Michigan, United States
Jagadeesh Uppala,
University of Wisconsin–Milwaukee, United States
Valentyn Oksenych,
University of Oslo, Norway

*CORRESPONDENCE
YouXiang Chen
chenyx102@126.com
ChunYan Zeng
zcy896@163.com

†These authors have contributed equally to this work and share first authorship

SPECIALTY SECTION
This article was submitted to Molecular and Cellular Oncology, a section of the journal Frontiers in Oncology

RECEIVED 19 August 2022
ACCEPTED 17 January 2023
PUBLISHED 16 February 2023

CITATION
Jin R, Luo Z, Jun-Li, Tao Q, Wang P, Cai X, Jiang L, Zeng C and Chen Y (2023) USP20 is a predictor of poor prognosis in colorectal cancer and associated with lymph node metastasis, immune infiltration and chemotherapy resistance. *Front. Oncol.* 13:1023292. doi: 10.3389/fonc.2023.1023292

USP20 is a predictor of poor prognosis in colorectal cancer and associated with lymph node metastasis, immune infiltration and chemotherapy resistance

RuiRi Jin[1†], ZhiPeng Luo[2†], Jun-Li[1], Qing Tao[1], Peng Wang[1], XueSheng Cai[1], LongZhou Jiang[1], ChunYan Zeng[1,3*†] and YouXiang Chen[1*†]

[1]Department of Gastroenterology, Digestive Disease Hospital, The First Affiliated Hospital of Nanchang University, Nanchang, China, [2]Department of Abdominal Tumor Surgery, Jiangxi Cancer Hospital, Nanchang, China, [3]Jiangxi Provincial Key Laboratory of Interdisciplinary Science, Nanchang University, Nanchang, China

Background: Colorectal cancer (CRC) is a highly prevalent malignancy with a poor prognosis. USP20 can support progression of variety of tumors. USP20 was shown to promote breast tumor metastasis, and proliferation of oral squamous carcinoma cells. However, the role of USP20 in CRC remains unclear.

Methods: We used bioinformatics to analyze the expression and prognosis of USP20 in pan-cancer and explore the relationship between USP20 expression and immune infiltration, immune checkpoints, and chemotherapy resistance in CRC. The differential expression and prognostic role of USP20 in CRC was validated by qRT-PCR and immunohistochemistry. Cox univariate and multivariate analyses were performed to assess risk factors for poor prognosis of CRC, and new prognostic prediction models were constructed and evaluated by decision curve analysis (ROC) and receiver operating characteristic (DCA). USP20 was overexpressed in CRC cell lines to explore the effect of USP20 on the functionalities of CRC cells. Enrichment analyses were used to explore the possible mechanism of USP20 in CRC.

Results: The expression of USP20 was lower in CRC tissues than adjacent normal tissues. Compared with low USP20 expression patients, CRC patients with high USP20 expression level had shorter OS. Correlation analysis showed that USP20 expression was associated with lymph node metastasis. Cox regression analysis revealed USP20 as an independent risk factor for poor prognosis in CRC patients. ROC and DCA analyses showed that the performance of the newly constructed prediction model was better than the traditional TNM model. Immune infiltration analysis shown that USP20 expression is closely associated with T cell infiltration in CRC. A co-expression analysis showed that USP20 expression was positively correlated with several immune checkpoint genes including ADORA2A, CD160, CD27 and TNFRSF25 genes and positively associated with multiple multi-drug resistance genes such as MRP1, MRP3, and MRP5 genes. USP20 expression positively correlated with the sensitivity of cells to multiple anticancer drugs. Overexpression of USP20 enhanced the migration and invasive ability of CRC

cells. Enrichment pathway analyses showed the USP20 may play a role *via* the Notch pathway, Hedgehog pathway and beta-catenin pathway.

Conclusion: USP20 is downregulated in CRC and associated with prognosis in CRC. USP20 enhances CRC cells metastasis and is associated with immune infiltration, immune checkpoints, and chemotherapy resistance.

KEYWORDS

colorectal cancer (CRC), ubiquitin specific peptidase 20 (USP20), lymph node metastasis, infiltrating immune, bioinformatics analysis, predictive models

Introduction

Colorectal cancer (CRC) is the third most common cancer and the third most common cause of cancer-related death in the United States. The American Cancer Society estimates that there will be over 151,030 new cases of CRC in the United States in 2022, with an estimated 54,250 deaths (1). Currently, surgery is the most effective treatment for CRC, however it is a curative treatment for only early-stage CRC patients. In recent years, neoadjuvant chemotherapy has substantially improved CRC outcomes by reducing tumor burden, increasing the rates of rectal preservation, improving the 5-year survival rate, and providing an opportunity for advanced-stage cancer patients to undergo surgery to improve prognosis (2–4). However, postoperative tumor recurrence is still an issue for CRC patients, leading to cancer progression and even death. Therefore, further clarifying the pathophysiological mechanism of CRC, exploring new therapeutic targets, and reducing the postoperative recurrence of CRC are of great significance to improve patient prognosis.

Ubiquitination is one of the main pathways that regulates the stability of intracellular proteins and involves the modification of target proteins by ubiquitin. Ubiquitination is a dynamic and reversible process that plays a role in numerous biological processes including the cell cycle, proliferation, apoptosis, differentiation, metastasis and other biological processes. Multiple studies have demonstrated an important function of ubiquitination in cancer. Previous reports showed that ROR-γt ubiquitination inhibits IL-17 mediated colon inflammation and tumorigenesis (5). In non-small cell lung cancer, circIGF2BP3 inhibits CD8+ T-cell responses to facilitate tumor immune evasion by promoting the deubiquitination of PD-L1 (6). SPOP-mediated ubiquitination and degradation of PDK1 suppresses AKT kinase activity and oncogenic functions (7). Deubiquitinating enzymes are vital to maintain the ubiquitination balance. Compared with the research on ubiquitinase enzymes, the research on deubiquitinases is scarce.

Ubiquitin specific peptidase 20 (USP20) is a member of the peptidase C19 family and the encoding gene is located on chromosome 9. USP20 was first identified as a deubiquitinating enzyme in 2002 (8). Studies have shown that USP20 is involved in the regulation of autophagy, inflammatory response, viral immune response, and cholesterol biosynthesis (9–12). Several reports have examined the role of USP20 in cancer, and the results have been controversial. Some researchers found that USP20 promotes the metastasis of breast cancer (13). However, another study showed that USP20 suppresses the malignant characteristics of gastric cancer cells (14). These results suggest an important role of USP20 in cancer. However, its potential function in CRC has not been investigated.

In this study, we explored the expression and possible mechanism of USP20 in CRC using bioinformatics analysis and we preliminarily verified our results through cytological experiments. We analyzed clinical samples to explore the prognostic value and clinical relevance of USP20 in CRC. Our results may help provide new insights into the mechanisms of CRC mechanisms and the development of new therapeutic approaches for CRC.

Abbreviations: ACC, Adrenocortical Carcinom; AJCC, American Joint Committee on Cancer; BLCA, Bladder Urothelial Carcinoma; BRCA, Breast invasive carcinoma; CESC, Cervical squamous cell carcinoma and endocervical adenocarcinoma; CHOL, Cholangiocarcinoma; COAD, Colon adenocarcinoma; CRC, Colorectal cancer; DLBC, Lymphoid Neoplasm Diffuse Large B-cell Lymphoma; DEGs, Differentially expressed genes; DCA, decision curve analysis; ESCA, Esophageal carcinoma; GBM, Glioblastoma multiforme; GO, Gene ontology; GTEx, The Genotype-Tissue Expression; HNSC, Head and Neck squamous cell carcinoma; HE, hematoxylin and eosin staining; IHC, Immunohistochemistry; KEGG, Kyto encyclopedia of genes and genomes; KICH, Kidney Chromophobe; KIRC, Kidney renal clear cell carcinoma; KIRP, Kidney renal papillary cell carcinoma; LAML, Acute Myeloid Leukemia; LGG, Brain Lower Grade Glioma; LIHC, Liver hepatocellular carcinoma; LUAD, Lung adenocarcinoma; LUSC, Lung squamous cell carcinoma; MESO, Mesothelioma; OS, overall survival; OV, Ovarian serous cystadenocarcinoma; PAAD, Pancreatic adenocarcinoma; PCPG, Pheochromocytoma and Paraganglioma; PRAD, Prostate adenocarcinoma; READ, Rectum adenocarcinoma; ROC, receiver operating characteristic; SARC, Sarcoma; SKCM, Skin Cutaneous Melanoma; STAD, Stomach adenocarcinoma; TCGA, The cancer genome atlas; TGCT, Testicular Germ Cell Tumors; THCA, Thyroid carcinoma; THYM, Thymoma; UCEC, Uterine Corpus Endometrial Carcinoma; UCS, Uterine Carcinosarcoma; UVM, Uveal Melanoma; USP20, Ubiquitin Specific Peptidase 20; PTC, Papillary thyroid carcinoma.

Materials and methods

Patients and samples

A total of 92 formalin-fixed paraffin-embedded pairs of tumor and adjacent normal tissue samples were collected from CRC patients

undergoing surgery at Jiangxi Cancer Hospital (Nanchang, China) from 2017 to 2019. The specimens were stained by hematoxylin and eosin (HE) and observed by multiple pathologists to confirm the diagnosis of CRC. Regular telephone interviews were conducted after surgery. The clinicopathological characteristics of patients are shown in Table 1. An additional independent set of samples was obtained from 23 CRC patients who underwent surgery at Jiangxi Cancer Hospital between 2021 and 2022. These samples were stored in liquid nitrogen for quantitative real-time PCR(qRT-PCR) analysis. The clinicopathological characteristics of this patient cohort are shown in Table 2. All patients provided written informed consent. This study conformed to the Declaration of Helsinki and was approved by the

TABLE 1 Association between USP20 protein expression and clinicopathologic characteristics of patients with CRC in the first study cohort (n=92).

			USP20 protein level		
Characterstic	Level	Overall	Low	High	P-value
n		92	41	51	
Status (%)	Alive	72 (78.3)	39 (95.1)	33 (64.7)	0.001
	Dead	20 (21.7)	2 (4.9)	18 (35.3)	
Sex (%)	M ale	66 (71.7)	27 (65.9)	39 (76.5)	0.373
	Fem ale	26 (28.3)	14 (34.1)	12 (23.5)	
Age (year) (%)	<60	46 (50.0)	16 (39.0)	30 (58.8)	0.093
	60	46 (50.0)	25 (61.0)	21 (41.2)	
Primary tumor location (%)	Rightcobn	40 (43.5)	19 (46.3)	21 (41.2)	0.119
	Rectum	5 (5.4)	0 (0.0)	5 9.8)	
	Leftcoln	47 (51.1)	22 (53.7)	25 (49.0)	
T (%)	T1/T2	9 (9.8)	6 (14.6)	3 (5.9)	0.293
	T3/T4	83 (90.2)	35 (85.4)	48 (94.1)	
N %)	NO	46 (50.0)	31 (75.6)	15 (29.4)	<0.001
	N 1/N2	46 (50.0)	10 (24.4)	36 (70.6)	
M (%)	MO	88 (95.7)	40 (97.6)	48 (94.1)	0.771
	M 1	4 (4.3)	1 (2.4)	3 (5.9)	
Degree of differentiation (%)	Poor	25 (27.2)	7 (17.1)	18 (35.3)	0,09
	Well	1 (1.1)	1 (2.4)	0 (0.0)	
	Moderate	66 (71.7)	33 (80.5)	33 (64.7)	
Pathological type (%)	High-grade intraepithelial neoplasia	1 (1.1)	1 (2.4)	0 (0.0)	0.037
	adenocarcinoma	79 (85.9)	39 (95.1)	40 (78.4)	
	Signet ring cell carcinomas	3 (3.3)	0 (0.0)	3 (5.9)	
	Mucinous Adenocarcinoma.	9 (9.8)	1 (2.4)	8 (15.7)	
Tumor size (%)	≥5cm	69 (75.0)	30 (73.2)	39 (76.5)	0.904
	<5cm	23 (25.0)	11 (26.8)	12 (23.5)	
Perineural invasion (%)	Postive	25 (27.2)	10 (24.4)	15 (29.4)	0.762
	Negative	67 (72.8)	31 (75.6)	36 (70.6)	
Lymphovascular invasion (%)	Postive	38 (41.3)	14 (34.1)	24 (47.1)	0.3
	Negative	(58.7)	27 (65.9)	27 (52.9)	
AJCC stage (%)	I + II	(50.0)	30 (73.2)	16 (31.4)	<0.001
	III + IV	(50.0)	11 (26.8)	35 (68.6)	
Adjuvant chemotherapy (%)	No	(23.9)	8 (19.5)	14 (27.5)	0.521
	Yes	70 (76.1)	33 (80.5)	37 (72.5)	

Institutional Ethics Committee of Jiangxi Cancer Hospital (Nanchang, Jiangxi, China, ethics approval no. 2022ky061).

Data and software availability

All bioinformatics data were downloaded from The Cancer Genome Atlas (TCGA) (https://ca-ncergenome.nih.gov/), GTEx database (https://gtexportal.org/), Gene Expression Omnibus (GEO) (https://www.ncbi.nlm.nih.gov/geo), and Therapeutically Applicable Research To Generate Effective Treatments (TARGET) (https://ocg.cancer.gov/programs/target) databases. The differential expression of USP20 levels between tumor and normal tissues across TCGA database was analyzed by the TIMER online system (https://cistrome.shinyapps.io/timer/) (15). R 4.1.0 was used to integrate the original data and verify the results analyzed by the website database. Data from TCGA, GTEx, and TARGET were downloaded using the online tool xiantao-love (https://www.xiantao.love/).

TABLE 2 Clinicopathological characteristics of the second study cohort (n=23) for assessing USP20 mRNA level.

Characteristic	N
Sex	
Female	10
Male	13
Age (years)	
<60	11
≥60	12
Tumor location	
Rectum	9
Colon	14
Degree of differentiation	
Well + moderate	13
Poor	10
Tumor size (cm)	
<5	14
≥5	9
Local invasion	
pT1-T2	3
pT3-T4	20
Lymph node metastasis	
N0	14
N1+N2	9
TNM stage	
I + II	14
III+IV	9
Perineural invasion	
Postive	8
Negative	15
Lymphovascular invasion	
Postive	12
Negative	11

Analysis of differentially expressed genes (DEGs)

CRC samples from TCGA were divided into high USP20 expression and low USP20 expression groups using the median expression value of USP20. Differential gene expression between different groups of samples were analyzed by the DESeq2 package (16). We used adjusted P-values to avoid false-positive results. The screening criteria for DEGs genes in this study were set as $|\log2(FC)| > 1$, $P.adj < 0.05$. The results of the differential gene expression analysis were presented by volcano plots using the ggplot2 package.

Enrichment analysis

To explore the target and possible mechanism of USP20 in CRC, ClusterProfiler package was used for DEG enrichment analysis, including GO Enrichment and KEGG Enrichment (17). The results of USP20 single gene differential analysis showed that the USP20 was mainly accompanied by the low expression of DEGs. We selected the top 100 significantly downregulated DEGs for GO and KEGG analysis. To further observe the effect of USP20 on CRC, the enrichment of Hallmark pathways related to USP20 expression were analyzed by GSEA (18).

Survival analysis

Univariate and multivariable Cox analyses were used to analyze the relationship between USP20 expression and CRC patient overall survival (OS). Kaplan–Meier (KM) curves were used to demonstrate the difference in OS between patients with different USP20 expression levels. Clinical prediction models were constructed on the basis of Cox regression results. Clinical usefulness as well as net benefit of model was estimated by decision curve analysis (DCA). The prognostic performance of the different models was assessed by receiver operating characteristic (ROC) curve analysis.

Immunological correlation analysis

Using the immune cell scores of CRC in the TIMER database, we analyzed the correlation between gene expression and immune cell scores. Furthermore, the correlation between USP20 and CD4+ T cell subsets was calculated using ssGSEA method implemented by R package GSVA (19). We collected more than 40 common immune checkpoint genes and performed molecular correlation analysis with USP20 in TCGA.

Immunohistochemistry

CRC tissues and adjacent normal tissues were warmed at 70°C for 1.5 h, dewaxed sequentially with xylene and anhydrous ethanol, heated at high temperature in a microwave oven for 15 min, and incubated in citrate buffer for antigen retrieval. After natural cooling, the tissues were incubated with primary antibody overnight at 4°C. The next day, after washing with PBS, the tissues were incubated with secondary antibody for 30 min at room temperature. The tissues were stained with DAB reagent (TransGen Biotech, Beijing, China) and the nuclei were stained with hematoxylin. Staining was scored following the methods described in a previous article (20). Two histopathologists were blindly assigned to review the slides and score the staining. The staining was considered as positive when the score was ≥6.

Immunofluorescence

Tissue was dewaxed and antigen-repaired following the same steps described above. After antigen repair, the tissue was permeabilized with 0.2% Triton X-100, following by blocking in 5% BSA and incubation overnight with the primary antibody. The next day, the tissues were washed with PBS and incubated with secondary antibody under light-proof conditions. After sealing with nail polish, the tissue was observed under a confocal microscope.

Cell culture and transfection

Human CRC cell lines (HCT116, DLD-1 and SW480) and a normal colon mucosal epithelial cell line (NCM460) were purchased from the Cell Bank of the Chinese Academy of Sciences. Cells were cultured in RPMI-1640 medium (Gibco, Grand Island, NY, USA) supplemented with 10% FBS (Gibco, USA), 100 U/ml penicillin, and 50 mg/ml streptomycin at 37 °C in a humidified atmosphere containing 5% CO_2. SW480 cells were transfected with the USP20 overexpression plasmid or control plasmid using Lipo3000 Transfection Reagent (Invitrogen, USA). The USP20 plasmid and control plasmid were constructed by Public Protein/Plasmid Library (Nanjing, China). For knockdown of USP20, three siRNAs targeting USP20 were constructed by Public Protein/Plasmid Library (Nanjing, China). The above 3 siRNAs are named siRNA-1-208, siRNA-2-1310 and siRNA-3-1816 respectively. Sequences of the siRNAs were as follows: siRNA-1-208(CCAUAGGAGAGGUGACCAATT), siRNA-2-1310(GGACAAUGAUGCUCACCUATT), siRNA-3-1816 (CUGAUGAGUUAAAGGGUGATT), negative control siRNA (UUCUCCGAACGUGUCACGUTT). SW480 cells were transfected with control siRNA or with siRNAs against USP20, by using Lipo3000 Transfection Reagent (Invitrogen, USA).

Quantitative real-time PCR

Total RNA was extracted with TRIzol reagent (ET111-01, TransGen Biotech, Beijing), phase-separated with chloroform, and precipitated using isopropanol. RNA concentration was measured with a NanoDrop 2000 spectrophotometer (Thermo Scientific, Wilmington, DE, USA). Reverse transcription of total RNA was performed using PrimeScript RT Master Mix (RR036A, Takara, Kusatsu, Japan) following the manufacturer's instructions. qRT-PCR was performed with kit reagents (RR420A, Takara, Kusatsu, Japan) to detect USP20 mRNA levels. The sequences of primers for qRT-PCR were as follows: USP20 forward: 5′- CCTCACCTTGACT CCATAGGA -3′ and reverse: 5′-CCCATAGGTTTGGTCCGGT -3′; CD4 forward: 5′-TGCCTCAGTATGCTGGCTCT-3′ and reverse: 5′-GAGACCTTTGCCTCCTTGTTC-3′;ADORA2A forward: 5′-CGCT CCGGTACAATGGCTT -3′ and reverse: 5′-TTGTTCCAACCT AGCATGGGA -3′;CD160 forward: 5′-GCTGAGGGGTTTGTAGT GTTT-3′ and reverse: 5′-GTGTGACTTGGCTTATGGTGA-3′;CD27 forward: 5′-CAGAGAGGCACTACTGGGCT-3′ and reverse: 5′-CG GTATGCAAGGATCACACTG-3′;CD200 forward: 5′-AAGTGGT GACCCAGGATGAAA and reverse: 5′-AGGTGATGGTTGA GTTTTGGAG; GAPDH forward: 5′- CCATGTTCGTCATGG TGTG -3′ and reverse: 5′- GGTGCTAAGCAGTTGTGGTG -3′.

Western blot

Total protein was extracted from CRC cells using radioimmunoprecipitation assay (RIPA) buffer (Solarbio Life Science, Beijing, China), which was mixed with protease inhibitor on precooled plates. The details of the experimental conditions are described in the Methods section and in our previous paper (21). Throughout this study, primary antibodies targeting the proteins are listed as follows: GAPDH (1:1000, TransGen Biotech, Beijing,China), β-actin (1:1000, TransGen Biotech, Beijing,China), and USP20 (17491-1-AP, 1:1000, Proteintech, China).

Cell proliferation assay

The Cell Counting Kit-8 (40203E; Yeasen, Shanghai, China) was used for cell proliferation assays. Cells were seeded in 96-well plates at a density of 1×10^3 cells per well, incubated at 37°C for 24 h, and transfected with the USP20 overexpression plasmid or control plasmid. After cultivation for 24 h, 48 h, or 72 h, 10 μl CCK-8 reagent was added to each well and cells were incubated for 2 h. The optical density (OD) values were read at 450 nm.

Cell migration and invasion assays

Transwell assays were used to determine the invasion and migration of CRC cells. SW480 cells were transfected with the USP20 overexpression plasmid or control plasmid. After transfection, 10×10^5 SW480 cells were seeded into the upper chamber of a Transwell system (8 μm pore size, Corning, USA) with or without Matrigel (BD Biosciences, USA). Then, 800 μl medium with 20% FBS was added to the lower chamber. The Transwell chambers were incubated for 48 h. Transwell chambers were then placed in 4% paraformaldehyde and stained with 0.5% crystal violet for 30 min. Stained cells were quantified using a microscope at 200× magnification. We randomly selected five visual

fields, recorded the number of cells in each field, and calculated the mean value.

Anti-tumor drug sensitivity analysis

We accessed the NCI-60 database at the CellMiner website and downloaded gene expression data for 60 different cancer lines of cells and data for 263 antitumor drugs for Pearson correlation analysis (https://discover.nci.nih.gov/cellminer) (22). The gene expression and anti-tumor drug data are shown in Table S1-S2.

Statistical analysis

R (4.10) software was used for statistical analysis. Data are presented as means ± SD of the mean. The data for two group comparisons were first subjected to normality tests. If the data sets fit a normal distribution, unpaired, two-tailed t-test was used; if not, nonparametric Mann–Whitney and Wilcoxon signed-rank tests were used. Differences among more than two groups were evaluated by one-way ANOVA. All statistical tests were 2-sided; $P < 0.05$ indicated statistical significance.

Results

Bioinformatics analysis for pan-cancer analysis of USP20

We investigated the expression of USP20 in pan-cancer by applying the TIMER online tool to obtain RNA-seq data in TCGA. We discovered that USP20 expression levels were increased in cholangiocarcinoma (CHOL), colon adenocarcinoma (COAD), esophageal carcinoma (ESCA), head and neck squamous cell carcinoma (HNSC), liver hepatocellular carcinoma (LIHC), lung adenocarcinoma (LUAD), pheochromocytoma and paraganglioma (PCPG), rectum adenocarcinoma (READ), and stomach adenocarcinoma (STAD), but decreased in bladder urothelial carcinoma (BLCA), glioblastoma multiforme (GBM), kidney renal clear cell carcinoma (KIRC), thyroid carcinoma (THCA) and uterine corpus endometrial carcinoma (UCEC) compared with normal tissue (Figure 1A). We further performed survival analysis in pan cancer. Kaplan–Meier survival plots showed that high USP20 expression in CRC was associated with markedly shorter OS (Figures 1B, C). In contrast, high USP20 expression may be associated with longer OS in GBM, pancreatic adenocarcinoma (PAAD), and thymoma (THYM) (Figures 1B, C).

Bioinformatics analysis of the relationship between USP20 expression and CRC patient clinicopathological characteristics

We downloaded clinical data and gene expression data of CRC in TCGA and analyzed the relationship between USP20 expression and clinicopathological parameters in CRC patients. The parameters examined included sample type (normal/primary tumor), gender (female/male), age (≤65/ >65), T stage (T1&T2/T3&T4), N stage (N0/N1&N2), M stage (M0/M1), pathologic stage (stage I & stage II/ stage III& stage IV), lymphatic invasion (no/yes), perineural invasion (no/yes), and CEA level (≤5/ >5). USP20 expression was higher in CRC tissues than in normal samples (Figure 2A). No correlations between USP20 expression and age, gender, T stage were found (Figures 2B–D). USP20 expression was significantly higher in CRC in N1&N2 stages than N0 stage (Figure 2E) and no correlations between USP20 expression and M stage was found (Figure 2F). Furthermore, USP20 expression was significantly higher in CRC with lymphatic invasion than CRC without lymphatic invasion (Figure 2G). These results suggest a potential function for USP20 in lymph node metastasis of CRC. USP20 expression was markedly higher in advanced pathologic stage (III& IV) CRC samples than in early pathologic stage (I& II) CRC samples (Figure 2H) USP20 expression is not significantly correlated with perineural invasion and CEA level, indicating that USP20 expression correlates with CRC progression.

Validation of USP20 expression in CRC

TCGA data showed that USP20 was highly expressed in CRC compared with normal tissue; however, the opposite result was seen in the GEO data analysis (Supplement Figure 1). We therefore examined the expression of USP20 in CRC and normal samples in cell lines and tissues. We performed qRT-PCR of USP20 mRNA in CRC cell lines and NCM460 cells. The results showed that USP20 mRNA levels were lower in CRC cell lines compared with NCM460 cells (Figure 3A). We further examined USP20 mRNA in 23 pairs of CRC and adjacent normal tissue specimens and found that USP20 was expressed at low levels in CRC tissues compared with normal adjacent tissues (Figure 3B). We then examined USP20 protein expression in 10 pairs of CRC and adjacent normal tissues by immunohistochemistry. HE staining was performed to distinguish CRC tissue and normal tissue (Figure 3C). Scoring revealed that the protein expression of USP20 was down-regulated in CRC tissues compared with the cancer adjacent tissues (Figure 3D). We additionally analyzed the expression and subcellular distribution of USP20 by immunofluorescence. The results showed that USP20 expression was lower in CRC tissue than that in normal adjacent tissues; furthermore, USP20 was mainly located in the cell cytoplasm (Figure 3E).

Association between USP20 levels and clinicopathological characteristics

Next, the relationship between USP20 expression levels and clinicopathological characteristics in CRC patients was examined. The tumor specimens from 92 patients examined by immunohistochemistry were scored according to the intensity and extent of staining (Figure 4A). The 92 patients were divided into USP20-high (n=51) and USP20-low (n=41) groups using the median USP20 expression levels in this cohort. High USP20 expression was shown to be associated with lymph node metastasis ($P<0.001$) and

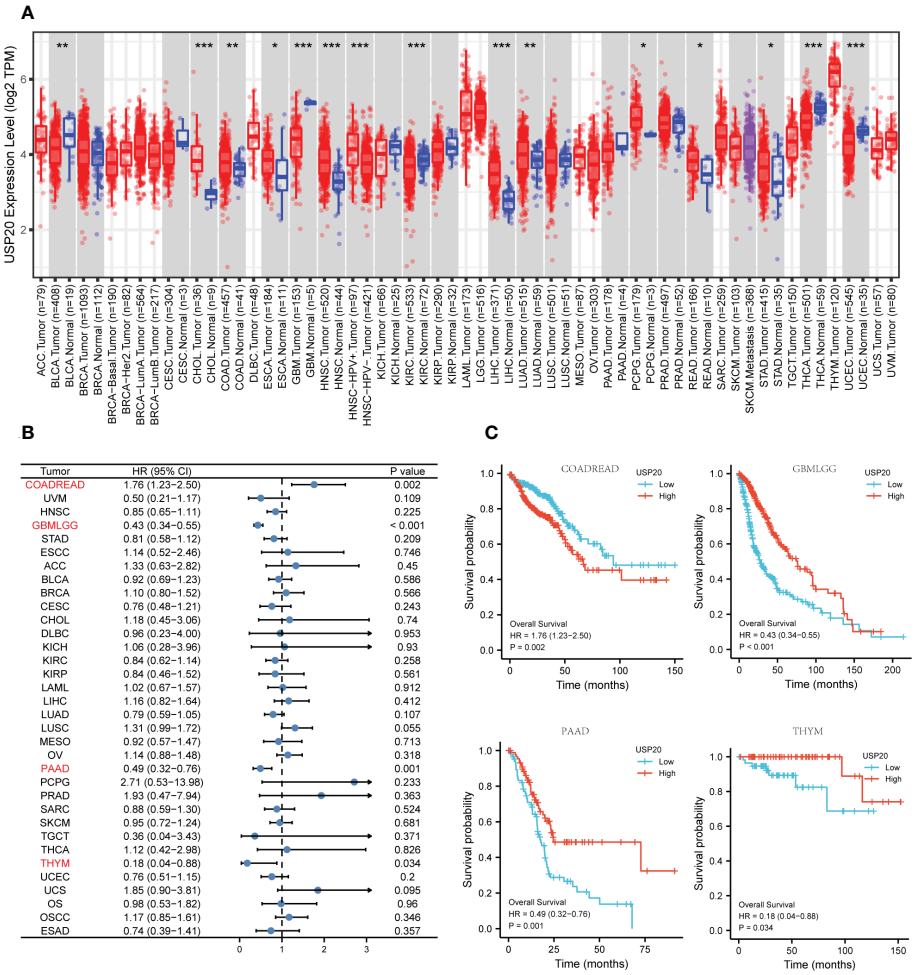

FIGURE 1
Pan-cancer analysis of USP20; **(A)** USP20 expression of different tumor types and normal tissue in TCGA were analyzed by the TIMER online database; **(B, C)** Univariate survival analysis was used to analyze the relationship between USP20 expression and survival time in Pan cancer; **(B)** forest plot showing the relationship between USP20 expression and OS; **(C)** KM curves of high and low USP20 expression in Pan cancer significantly associated with OS survival; (*P < 0.05; **P < 0.01; ***P < 0.001; ****P < 0.0001; NS, not significant).

American Joint Committee on Cancer (AJCC) stage (P<0.001, Table 1). There was no significant relationship between USP20 expression levels and other clinical characteristics including gender, age, tumor location, tumor differentiation grade, and adjuvant chemotherapy status. Our results suggest that high USP20 expression is closely associated with lymph node metastasis in CRC patients.

Association between USP20 expression and postoperative survival

The relationship between USP20 protein expression and OS was analyzed in 92 CRC patients in the immunohistochemical cohort. KM curves showed that the OS of the USP20 high expression group was significantly shorter than the OS of the USP20 low expression group (Figure 4B). Univariable and multivariable Cox regression analyses were performed to determine predictive factors for OS. The results revealed that USP20 expression was an independent risk factor for CRC prognosis (Table 3). We then constructed a base risk prediction multivariable Cox regression model with USP20 expression, perineural invasion, adjuvant chemotherapy and AJCC stage. We assessed the performance of the model by ROC curve analysis. The results indicated that the USP20 joint model performed better than the AJCC stage model in predicting 5-year survival (Figure 4C). We subsequently compared the clinical performance of the USP20 joint model to the AJCC stage model using decision curve analysis. The result showed that the USP20 joint model was associated with a higher net benefit than the AJCC stage model (Figure 4D). These results suggest that the USP20 joint model outperforms the AJCC stage model.

Correlation between immune infiltration and USP20 expression in CRC

Immune infiltration plays a crucial role in promoting tumor progression. TIMER was used to investigate the relationships

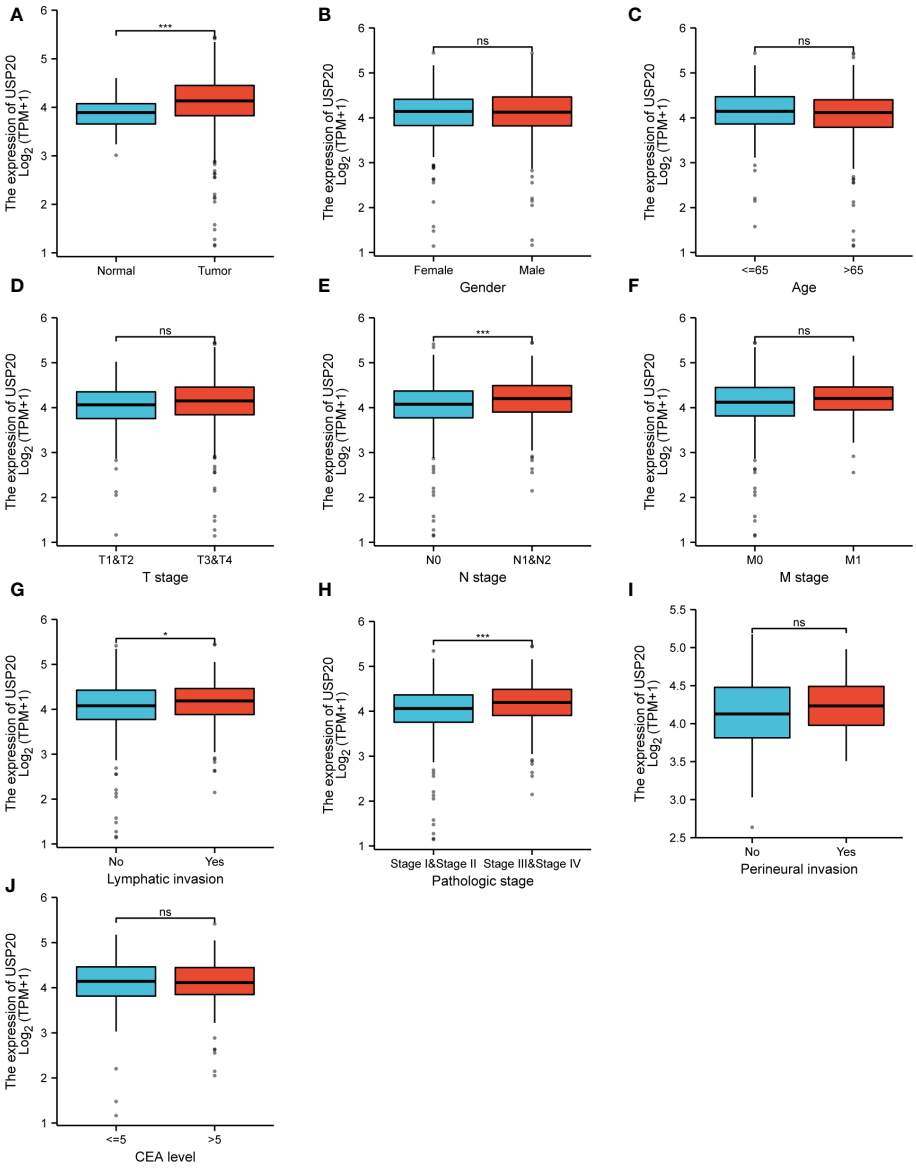

FIGURE 2
Relationship between USP20 expression and CRC patient clinicopathological characteristics in TCGA; **(A)** analysis of USP20 expression between normal and cancer tissues; **(B)** analysis of USP20 expression between female CRC patients and male CRC patients; **(C)** analysis of USP20 expression between CRC patients who were younger than or older than 65 years of age; **(D)** analysis of USP20 expression between T1&T2 CRC patients and T3&T4 CRC patients; **(E)** analysis of USP20 expression between N0 CRC patients and N1&N2 CRC patients;**(F)** analysis of USP20 expression between M0 CRC patients and M1 CRC patients; **(G)** analysis of USP20 expression between CRC patients who with lymphatic invasion or not; **(H)** analysis of USP20 expression between pathologic stage I& stage II CRC patients and stage III& stage IV CRC patients; **(I)** analysis of USP20 expression between CRC patients who with perineural invasion or not; **(J)** analysis of USP20 expression between CRC patients who CEA levels more than or less than 5; (*P < 0.05; **P < 0.01; ***P < 0.001; ****P < 0.0001; NS, not significant). (*P <0.05; ***P < 0.001; NS, not significant).

between USP20 expression and immune cell infiltration in CRC. The results showed that the expression of USP20 was significantly positively correlated with CD4+ T cells and negatively correlated with CD8+ T cells in COAD. In READ, the expression of USP20 was significantly positively correlated with CD4+ T cells and dendritic cells and negatively correlated with neutrophils (Figure 5A). Considering that USP20 is closely related to CD4+ T cells in both COAD and READ, we further analyzed the subsets of CD4+ T cells in TCGA COAD&READ database through GSVA. The results showed that the expression of USP20 positively correlated with Treg cells and negatively correlated with Th2 cells (Figure 5B). Tumors can elude immune cytotoxicity through immune checkpoints. Therefore, we explored the relationship between USP20 expression and immune checkpoints. More than 40 common immune checkpoint genes were collected for molecular correlation analysis in pan cancer. In a variety of tumors, USP20 expression positively correlated with the expression levels of several immune checkpoint genes, including ADORA2A, CD160, CD27 and TNFRSF25 genes (Figure 5C). This suggests that USP20 may regulate tumor immunity by regulating the expression level of specific immune checkpoint genes. Then, we validated the gene expression correlation with 20 fresh colon cancer tissues collected in our center. The correlation between USP20 expression

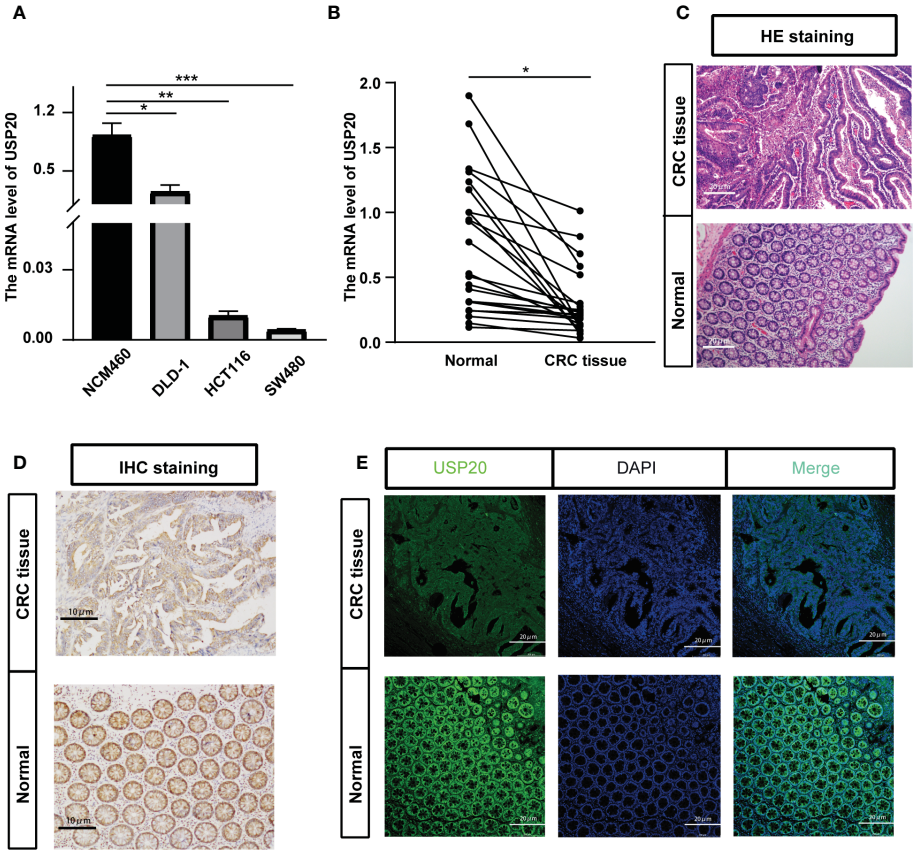

FIGURE 3
Verification the USP20 expression in CRC samples; **(A)** Quantitative real-time PCR (qRT-PCR) was performed to detect the mRNA level of USP20 in CRC cell lines and normal human colonic epithelial (NCM460) cells; **(B)** Quantitative real-time PCR (qRT-PCR) was performed to detect the mRNA level of USP20 in 23 CRC tissues and correspond adjacent normal tissues; **(C)** HE staining clarified the CRC tissue and normal tissue in the pathological tissue (100x); **(D)** Immunohistochemical (IHC) staining was used to detect the difference in expression of USP20 between CRC tissues and adjacent normal tissues(200x); **(E)** immunofluorescence assays was used to determine the subcellular localization of the USP20 protein in CRC tissues(200x); (*P < 0.05; **P < 0.01; ***P < 0.001; ****P < 0.0001; NS, not significant). (*P <0.05; **P < 0.01; ***P < 0.001).

and immune cell marker CD4, immune checkpoint gene ADORA2A, CD160, CD200 and CD27 were analyzed by qRT-PCR. The results showed that USP20 was positively correlated with the expression of all the above genes and the correlation of USP20 with CD4 and CD200 expression was statistically significant. (Supplement Figure 2)

Analysis of the correlation between USP20 expression and multidrug resistance–related genes and chemotherapeutics

To assess the role of USP20 in predicting resistance to CRC chemotherapy, we analyzed the expression levels of multidrug resistance–associated genes in different USP20 expression groups and the correlation between USP20 expression and drug resistance–associated gene expression. The results showed that drug resistance genes, such as MRP1, MRP3 and MRP5 genes, were more highly expressed in the USP20 high expression group (Figure 6A). Correlation analysis showed that USP20 expression positively correlated with the expression of MRP1, MRP3 and MRP5 genes (Figure 6B), suggesting that USP20 expression may be associated with drug resistance in CRC. To further explore the relationship between USP20 and chemoresistance, we analyzed USP20 expression and the IC50 of chemotherapeutic drugs in tumor cells. The results showed that USP20 negatively correlated with the sensitivity of many chemotherapeutic drugs (Figure 7). Among these drugs, lomustine and raltitrexed are used in the clinical treatment of CRC, and raltitrexed is the main drug used in the treatment of advanced rectal cancer. Together these findings indicate that USP20 expression has the potential to predict chemotherapy resistance in CRC and may also be an intervention target for chemotherapy resistance in CRC.

USP20 promotes the metastasis of CRC cells

To examined whether USP20 promotes CRC progression, the cells were transiently transfected with USP20 plasmid or negative plasmid. We established SW480 cells that overexpressed USP20 or negative control by plasmid transfection. qRT-PCR and Western Blot analysis confirmed that USP20 level was markedly upregulated in the cells transfected with USP20-expressing plasmid (Figures 8A, B). We next examined the effect of USP20 on CRC cell proliferation using

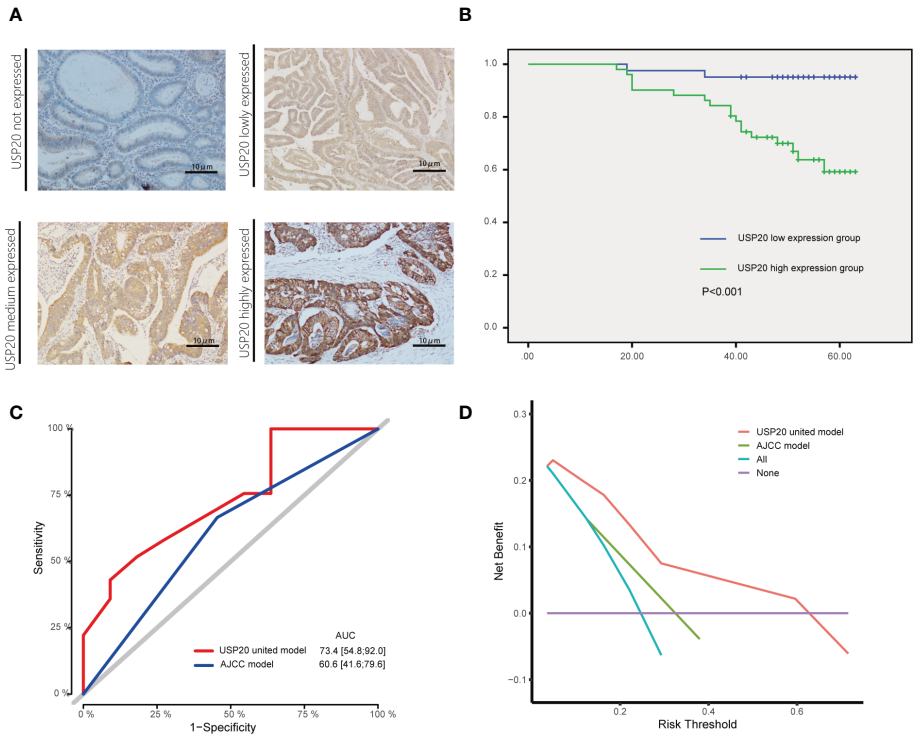

FIGURE 4
Association between USP20 expression and postoperative survival in IHC cohort CRC patients; **(A)** The USP20 IHC samples were classified into not expressed, lowly expressed, medium expressed and highly expressed categories; **(B)** The Kaplan-Meier(KM) method was used to compare the relationship between different USP20 expression levels and the overall survival of patients; **(C)** The receiver operating characteristic (ROC) curve analysis was used to evaluate the prognostic validity of the USP20 joint model and AJCC model; **(D)** The decision curve analysis(DCA) was used to estimate the clinical usefulness and net benefit of USP20 joint model and AJCC model.

CCK-8 assay. The results showed that overexpression of USP20 had no effects on the cell proliferation of SW480 cells (Figure 8C). We next used a Transwell chamber to assess the effects of USP20 on migration and invasiveness. The results showed that overexpression of USP20 significantly enhanced SW480 cell migration and invasion (Figures 8D–G). Then, we knocked down USP20 in SW480 cells using siRNAs. qRT-PCR and Western blots confirmed that USP20 level was markedly downregulated in the cells transfected with the siRNAs (Figures 8H, I). The effect of siRNA-1-208 was most obvious and was used for subsequent experiments. The CCK-8 results showed that the knockdown of USP20 displayed no obvious effects on the cell proliferation of SW480 cells (Figure 8J). Transwell results showed

TABLE 3 Univariate and multivariate analyses of factors influencing patient overall survival in the first study cohort.

		Univariate analysis				Multivariate analysis			
Variable	Comparison	HR	95% CI		P-value	HR	95% CI		P-value
Sex	Female/male	0.56	0.19	1.68	0.303	–	–	–	–
Age (years)	≥60/<60	1.22	0.5	2.94	0.663	–	–	–	–
Tumor location	Rectum+left colon/right colon	1.06	0.43	2.6	0.895	–	–	–	–
Tumor size (cm)	≥5/<5	3.38	0.78	14.57	0.102	–	–	–	–
Degree of differentiation	Poor/well + moderate	2.01	0.82	4.91	0.128	–	–	–	–
perineural invasion	Postive/negative	4.28	1.75	10.45	0.001	3.78	1.23	11.65	0.02
vascular invasion	Postive/negative	2.51	1.02	6.15	0.045	0.96	0.31	2.99	0.944
AJCC stage	III+IV/I + II	3.61	1.31	9.96	0.013	1.47	0.47	4.57	0.506
adjuvant chemotherapy	Yes/no	0.44	0.18	1.07	0.071	0.41	0.16	1.02	0.055
USP20 protein level	High/low	8.49	1.97	36.64	0.004	6.64	1.43	30.78	0.016

HR, hazard ratio; 95% CI, 95% confidence interval; USP20, Ubiquitin Specific Peptidase 20.

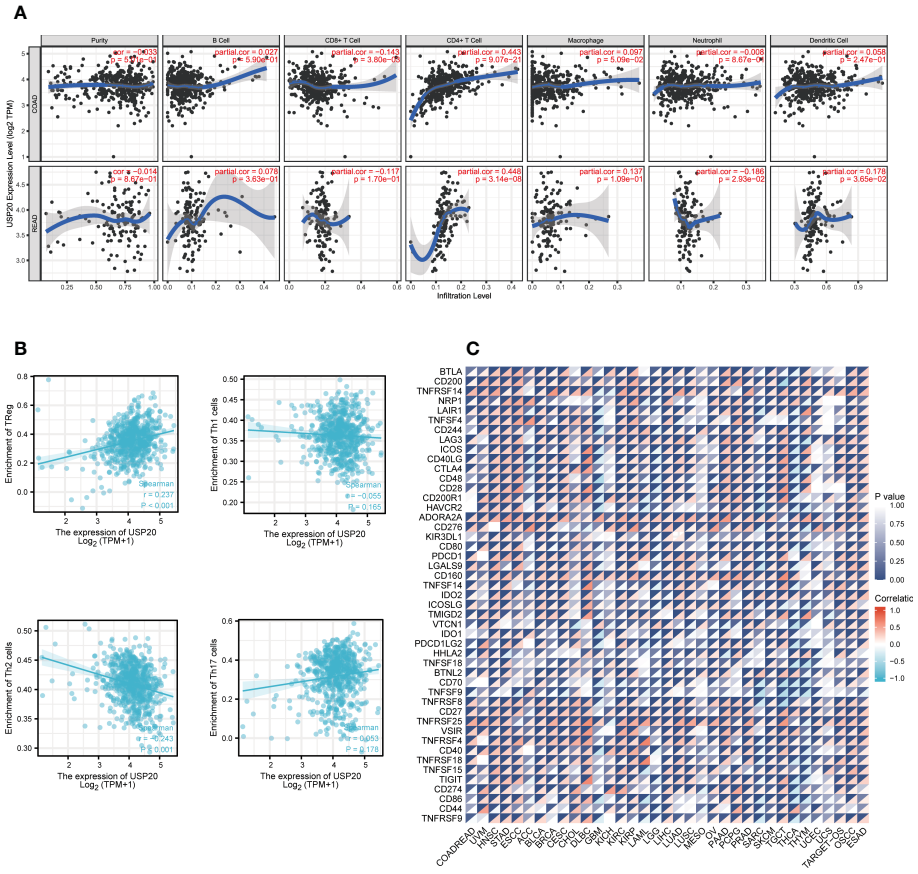

FIGURE 5
Correlation between immune and USP20 expression in CRC; **(A)** Using TIMER database to analyze the correlation between gene expression and immune cell scores **(B)** Using ssGSEA method to calculate the correlation between USP20 and CD4 + T cell subsets; **(C)** Correlation analysis of USP20 expression in pan-cancer with immune checkpoint gene expression.

that knockdown of USP20 significantly decreased SW480 cell migration and invasion (Figures 8K–N). Overall, these results suggest that USP20 overexpression may promote CRC metastasis to promote cancer progression in CRC.

Differential gene expression analysis and enrichment analysis

To explore the possible mechanism of action of USP20 in CRC, differential gene analysis and enrichment analysis were performed in TCGA CRC samples. First, differential expression analysis was performed to identify DEGs between high and low USP20 CRC sample groups in TCGA. We obtained a total of 5,413 DEGs (|log2 (FC)| > 1, Padj< 0.05), including 117 upregulated genes and 5296 downregulated genes (Figure 9A; Table S3). Among the DEGs, we selected the top 100 downregulated genes for GO and KEGG enrichment analyses. GO enrichment analysis showed that the DEGs were mainly concentrated in spliceosome snRNP complex, small nuclear ribonucleoprotein complex, spliceosome tri-snRNP complex, and U4/U6 x U5 tri–snRNP complex (Figure 9B). KEGG analysis showed that the DEGs were enriched in spliceosome and RNA transport pathways (Figure 9C). We then performed GSEA for hallmark gene sets and found that the Notch pathway, Hedgehog pathway and beta-catenin pathway were enriched (Figure 9D).

Discussion

CRC is one of the most common and deadliest cancers worldwide, in part as the frequency of colonoscopy in the average-risk population is low. Patients with CRC usually have no obvious symptoms in the early stage, which leads to many CRC patients presenting with advanced stage at initial diagnosis. Therefore, it is very helpful to find new non-invasive markers and new therapeutic targets to improve the diagnosis and treatment of CRC.

The identification of prognostic markers of CRC is not only helpful to evaluate the prognostic status of patients, but also help screen treatment-related target molecules. For example, RAS gene mutation is not only related to the prognosis of CRC patients (23), but it also predicts the efficacy of anti-EGFR treatment in CRC patients (24). In the study of immunotherapy, researchers found that targeting NKG2A enhances the anti-tumor CD8 T cell response in human CRC (25). Therefore, the use of bioinformatics may help identify potential

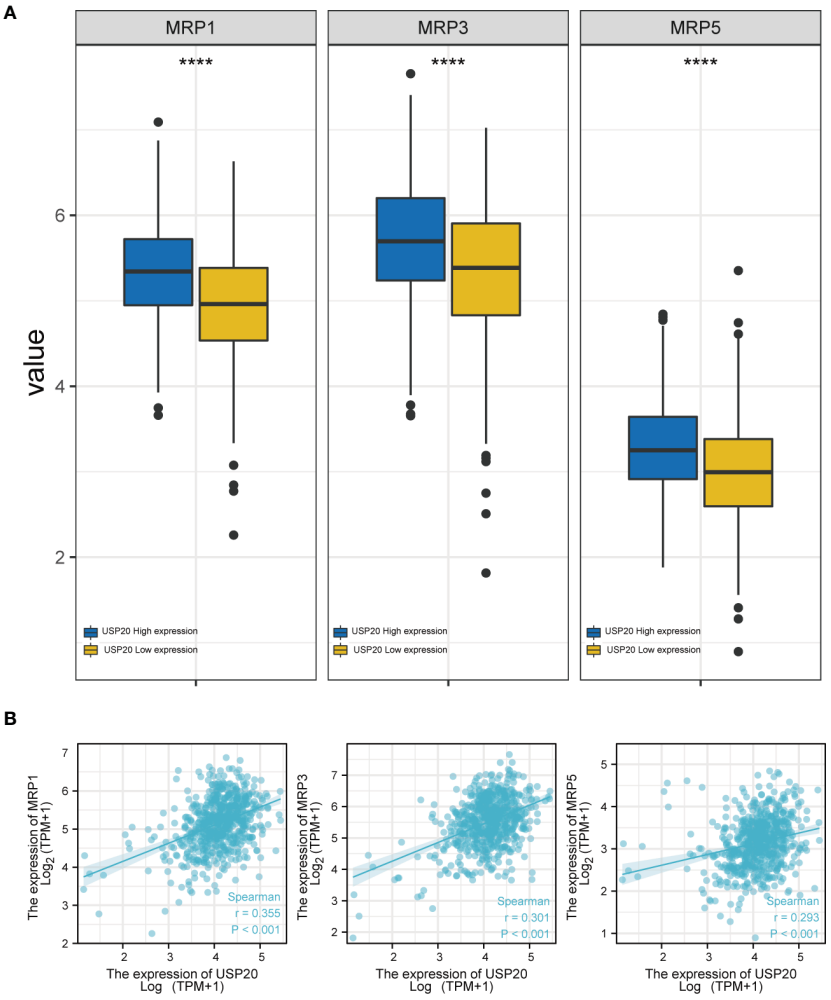

FIGURE 6
The relationship between anti-tumor drug genes and USP20 expression group; **(A)** Expression of anti-tumor drug genes (MRP1, MRP3, MRP5) in different USP20 expression CRC group; **(B)** The co-expression analysis between USP20 and anti-tumor drug genes (MRP1, MRP3, MRP5) in CRC; (*P < 0.05; **P < 0.01; ***P < 0.001; ****P < 0.0001; NS, not significant).

prognostic markers for CRC and it is an efficient way to improve the level of diagnosis and treatment of CRC.

Deubiquitination is a reversal of the ubiquitination process and is mediated by deubiquitinating enzymes. Similar to ubiquitination, deubiquitination is also involved in many tumor-related biological processes. Researchers have confirmed that deubiquitination plays a key role in regulating T cell immune response (26). It also participates in fat metabolism and exacerbates colorectal carcinogenesis by stabilizing ME1 (27). NLRP7 deubiquitination by USP10 promotes tumor progression and tumor-associated macrophage polarization in CRC (28). These studies suggest that deubiquitination has great potential in the development of treatments for CRC. In recent years, USP20 has been found to play a crucial role in a variety of biological processes (9, 11, 29). Only one study thus far reported the role of USP20 in CRC (30). The authors confirmed that USP20 enhances invasive ability in a small number of CRC cell lines. However, the specific mechanisms and prognostic significance of USP20 expression in CRC have been unknown.

Through analysis of TCGA database, we found that USP20 was differentially expressed in a variety of cancers compared with normal tissues, suggesting that it is a tumor-associated molecule. In TCGA database, USP20 was shown to be highly expressed in CRC compared with normal tissues. However, the GEO database showed low expression of USP20 in CRC compared with normal tissues. In this study, we found that USP20 expression in CRC was lower than that in normal tissues through analysis of 22 pairs of CRC specimens, 10 pairs of immunohistochemical specimens, and cell lines, suggesting that USP20 is a CRC-related differentially expressed gene and is expressed at low levels in CRC.

We further explored the relationship between USP20 expression and the survival prognosis of CRC patients. CRC patients with high expression of USP20 were shown to have a shorter survival compared with those with low expression in both TCGA database and our cohort patients. These results suggest USP20 may predict the survival prognosis of patients with CRC. Additional analyses in TCGA samples and our cohort showed that USP20 was associated with

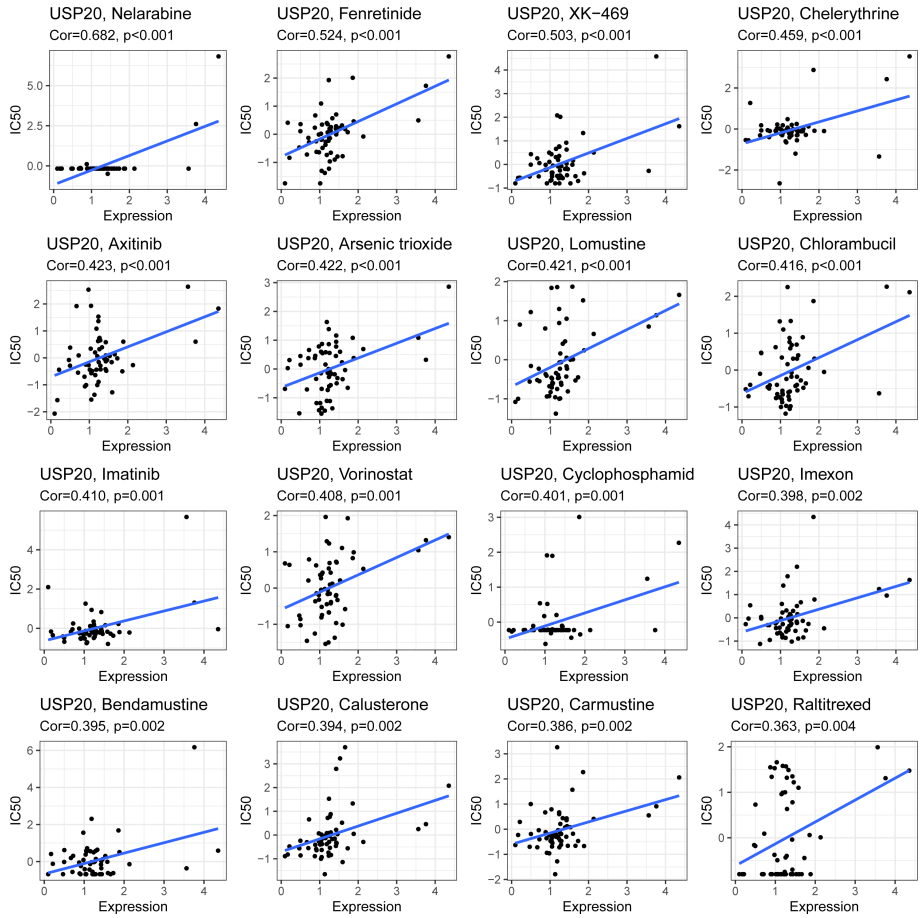

FIGURE 7
Scatter plots of the association between the USP20 expression and anti-tumor drugs IC50.

lymph node metastasis in patients with CRC. We speculate that USP20 may promote tumor progression by promoting lymph node metastasis. In cell line experiments, we found that USP20 overexpression enhanced the migration and invasive ability of CRC cells, which is consistent with the findings of the clinical correlation analysis.

Furthermore, we identified USP20 high expression as an independent risk factor for poor prognosis in CRC patients by univariate and multivariate Cox regression analysis. Using the Cox multivariate regression results, we constructed a predictive model for the prognosis of CRC. Through ROC and DCA analysis, we found that the predictive efficiency and net benefit of the newly constructed model was higher than that of the conventional TNM model. Our work provides a new model for further improving the prognosis of patients with CRC.

Tumors and the immune system are closely related. The immune system functions to exert killing effects on tumors and can inhibit the progression of tumors. However, a strong anti-tumor immune response will trigger a physiological response, which aims at inhibiting effector T cells, preventing tissue damage and maintaining tissue stability. These physiological reactions protect and even promote tumors. A variety of inhibitory pathways are known to play a role in the tumor microenvironment, including cells such as Th2 macrophages and immature T regulatory cells (Tregs), and molecules such as checkpoints that control T cell differentiation (such as CTLA-4 and IDO) and effector function (such as PD-1). We found that USP20 expression was significantly positively correlated with Treg cells in CRC tissue. Tregs are immune inhibitory lymphocytes that often accumulate within the tumor microenvironment and are regulated by tumor cells through cytokines/chemokines (31, 32). Tregs promote CRC progression by inhibiting the antitumor activity promoted by natural killer cells and CD8 T cells (33). Our results suggest that USP20 may be involved in regulating the immune infiltration of Treg cells in CRC tissues, so as to promote the progression of CRC. Immune checkpoint inhibitors are a hot spot in tumor therapy. Molecular correlation analysis showed that USP20 significantly and positively correlated with the expression of multiple immune checkpoints such as ADORA2A and CD160 in a variety of cancers. This suggests that USP20 may affect the tumor immune response by regulating the expression of immune checkpoints. Studies on immune checkpoints have shown that ADORA2A is a main pathway for Treg cells to inhibit CD8+ T cell viability (34), which is consistent with our results in the above immune infiltration studies.

Chemotherapy resistance is one of the major challenges in current oncology treatment. In the treatment of CRC, pharmacological chemotherapy is the main treatment for advanced CRC.

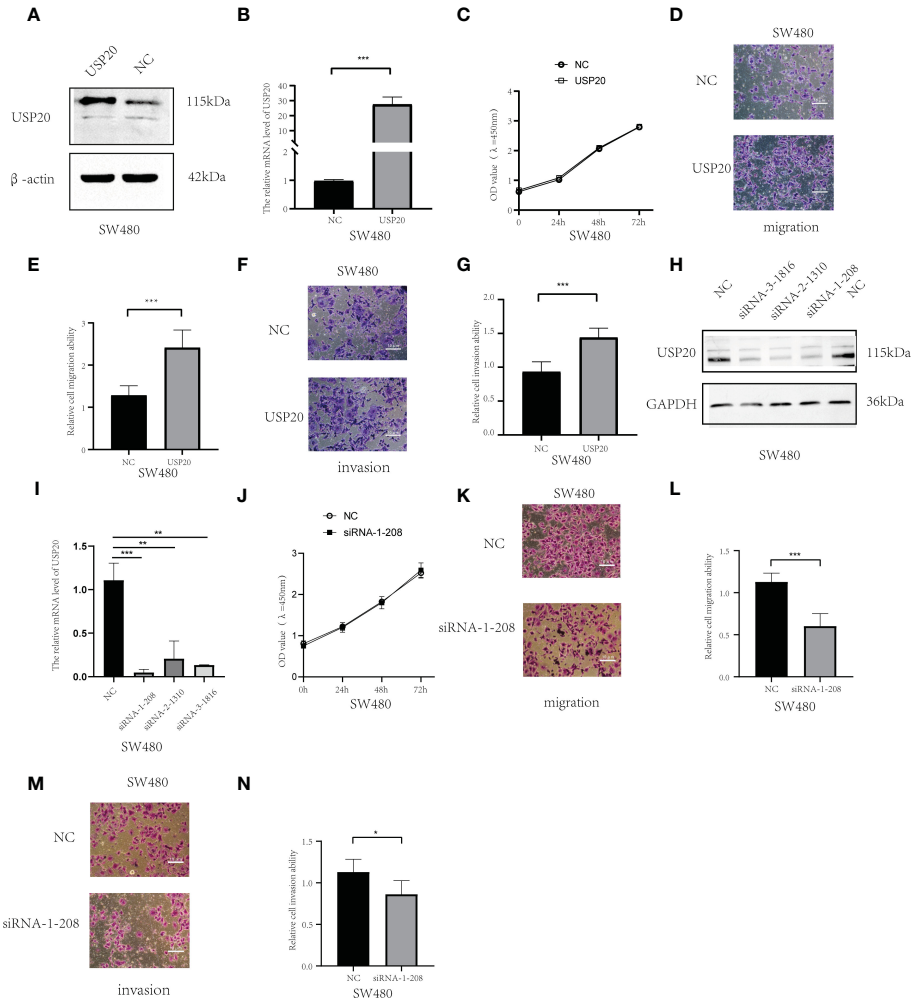

FIGURE 8
USP20 promotes the metastasis of CRC cells; **(A)** USP20 Plasmid transfection efficiency was determined by Western blots. **(B)**; USP20 Plasmid transfection efficiency was determined by qRT-PCR. **(C)** The CCK-8 results showed that the overexpression of USP20 displayed no obvious effects in cell proliferation of SW480. **(D–G)** Overexpression of USP20 enhanced CRC cell migration and invasion abilities were demonstrated *via* Transwell migration assays and Transwell invasion assays. **(H)** Western blots showing knockdown efficiency of the siRNAs. **(I)** The efficiency of siRNAs was verified by qRT-PCR. **(J)** The CCK-8 results showed that the knockdown of USP20 displayed no obvious effects in cell proliferation of SW480. **(K–N)** Knowdown of USP20 decreased CRC cell migration and invasion abilities were demonstrated *via* Transwell migration assays and Transwell invasion assays. (*P < 0.05; **P < 0.01; ***P < 0.001; NS, not significant).

Chemotherapy can reduce the recurrence of CRC after surgery. This study showed that USP20 expression in CRC positively correlated with multi-drug resistant gene expression. USP20 expression also correlated with drug resistance to various anticancer drugs, suggesting that USP20 expression may have a role in predicting drug resistance in CRC patients. This finding also suggests that USP20 may be involved in the mechanism of drug resistance in CRC.

Through differential and enrichment analysis, we explore the possible mechanisms of USP20 in CRC. We conducted single-gene level differential expression analysis and identified 5413 DEGs, including 117 upregulated and 5296 downregulated genes. This result suggests that USP20 may play a role in CRC by reducing the expression of related genes. Enrichment analysis of the top 100 significantly downregulated genes showed that the DEGs were mainly enriched in nucleic acid modifications and transport. GSEA hallmark analysis of DEGs showed the DEGs were mainly enriched in the Notch pathway, Hedgehog pathway and beta-catenin pathway. Previous studies have shown that the above pathways are closely related to tumor cell migration, invasion, and chemoresistance (35–39). We therefore hypothesize that USP20 regulates the NOTCH pathway, HEDGEHOG pathway, BETA CATENIN pathway through affecting mRNA modification and transport, thereby promoting metastasis and chemoresistance in colorectal cancer.

In summary, USP20 is downregulated in CRC and associated with the prognosis of CRC. USP20 may promote tumor metastasis and is associated with immune infiltration and drug resistance in CRC. USP20 may act through pathways such as the Notch pathway, Hedgehog pathway and beta-catenin pathways. We constructed a new prognostic model related to USP20, which provides a new option to further improve the prognosis prediction of patients with CRC.

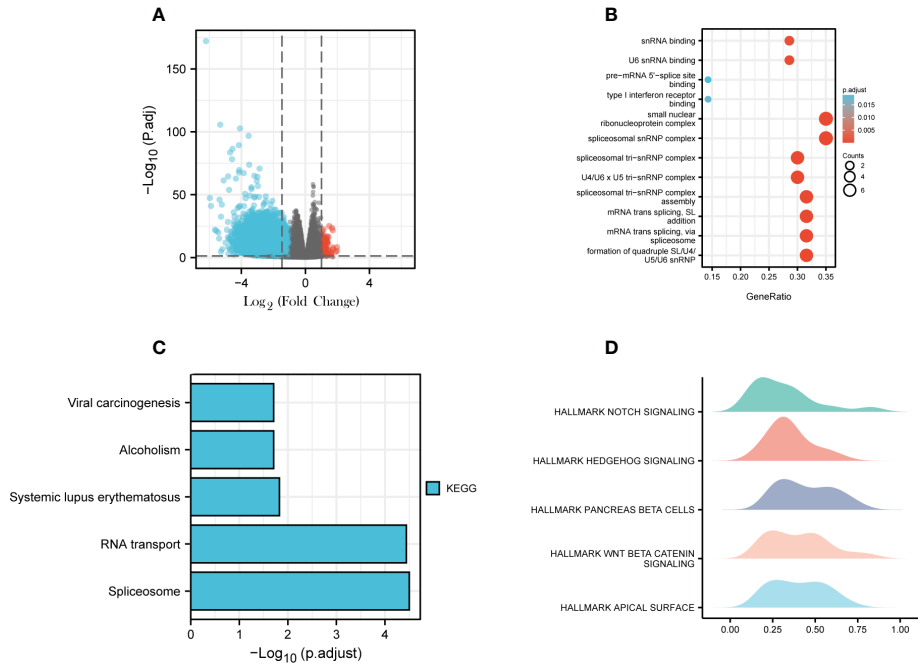

FIGURE 9
Differential Gene Expression Analysis and Enrichment Analysis; **(A)** USP20 CRC high group/ USP20 CRC low group differential expression genes analysis; volcano plot: red dots indicate significantly differentially up-regulated genes and blue dots indicate significantly differentially down-regulated genes;**(B)** GO enrichment analysis of top 100 downregulated expression genes related to USP20;**(C)** KEGG enrichment analysis of top 100 downregulated expression genes related to USP20;**(D)** GSEA analysis of USP20 in TCGA.

Data availability statement

The datasets presented in this study can be found in online repositories. The names of the repository/repositories and accession number(s) can be found in the article/Supplementary Material.

Ethics statement

The studies involving human participants were reviewed and approved by Institutional Ethics Committee of Jiangxi Cancer Hospital. The patients/participants provided their written informed consent to participate in this study.

Author contributions

YC designed the study. CZ performed graphing and writing. RJ and ZL performed immunohistochemistry experiments. JL and PW performed cytology experiments. QT and RJ were responsible for language revisions. YC and CZ helped modify articles and supervise the study. authors contributed to the article, reviewed the manuscript, and approved the submitted version. XC and LJ help completed the experiments required for article revision. All authors contributed to the article and approved the submitted version.

Funding

This study was funded by the National Natural Science Foundation of China (grant No. 82060448, PI: YC), the Project of Health Commission of Jiangxi Province (grant No.202210475, PI: CZ and grant No. 202210414,PI: YC) and Special Fund for Postgraduate Innovation in Jiangxi Province (YC2021-B046). The project of Interdisciplinary Innovation Fund of Natural Science, NanChang University(Grant No.9167-27060003-YB2109,PI:CZ).

Acknowledgments

We thank Gabrielle White Wolf, PhD, from Liwen Bianji (Edanz) (www.liwenbianji.cn) for editing the English text of a draft of this manuscript.

Conflict of interest

The authors declare that the research was conducted in the absence of any commercial or financial relationships that could be construed as a potential conflict of interest.

Publisher's note

All claims expressed in this article are solely those of the authors and do not necessarily represent those of their affiliated organizations,

or those of the publisher, the editors and the reviewers. Any product that may be evaluated in this article, or claim that may be made by its manufacturer, is not guaranteed or endorsed by the publisher.

Supplementary material

The Supplementary Material for this article can be found online at: https://www.frontiersin.org/articles/10.3389/fonc.2023.1023292/full#supplementary-material

SUPPLEMENTARY FIGURE 1
The USP20 expression in CRC from GEO database (GSE32323);

SUPPLEMENTARY FIGURE 2
Gene co-expression correlation analysis of USP20 in colorectal cancer. Twenty cases of fresh colorectal cancer tissues were collected for gene co-expression analysis. **(A)**. Correlation analysis of USP20 with CD4 T-cell markers. **(B)**. Correlation analysis of USP20 with the immune checkpoint gene ADORA2A. **(C)**. Correlation analysis of USP20 with the immune checkpoint gene CD160. **(D)**. Correlation analysis of USP20 with the immune checkpoint gene CD200. **(E)**. Correlation analysis of USP20 with the immune checkpoint gene CD27. Correlation was examined by Pearson's correlation analysis. (*P < 0.05; **P < 0.01; ***P < 0.001; ****P < 0.0001; NS, not significant)

References

1. Siegel RL, Miller KD, Fuchs HE, Jemal A. Cancer statistics 2022. *CA Cancer J Clin* (2022) 72:7–33. doi: 10.3322/caac.21708

2. Polanco PM, Mokdad AA, Zhu H, Choti MA, Huerta S. Association of adjuvant chemotherapy with overall survival in patients with rectal cancer and pathologic complete response following neoadjuvant chemotherapy and resection. *JAMA Oncol* (2018) 4:938–43. doi: 10.1001/jamaoncol.2018.0231

3. Smith JJ, Strombom P, Chow OS, Roxburgh CS, Lynn P, Eaton A, et al. Assessment of a watch-and-Wait strategy for rectal cancer in patients with a complete response after neoadjuvant therapy. *JAMA Oncol* (2019) 5:e185896. doi: 10.1001/jamaoncol.2018.5896

4. Karoui M, Rullier A, Piessen G, Legoux JL, Barbier E, De Chaisemartin C, et al. Perioperative FOLFOX 4 versus FOLFOX 4 plus cetuximab versus immediate surgery for high-risk stage II and III colon cancers: A phase II multicenter randomized controlled trial (PRODIGE 22). *Ann Surg* (2020) 271:637–45. doi: 10.1097/SLA.0000000000003454

5. Kathania M, Khare P, Zeng M, Cantarel B, Zhang H, Ueno H, et al. Itch inhibits IL-17-mediated colon inflammation and tumorigenesis by ROR-gammat ubiquitination. *Nat Immunol* (2016) 17:997–1004. doi: 10.1038/ni.3488

6. Liu Z, Wang T, She Y, Wu K, Gu S, Li L, et al. N(6)-methyladenosine-modified circIGF2BP3 inhibits CD8(+) T-cell responses to facilitate tumor immune evasion by promoting the deubiquitination of PD-L1 in non-small cell lung cancer. *Mol Cancer* (2021) 20:105. doi: 10.1186/s12943-021-01398-4

7. Jiang Q, Zheng N, Bu L, Zhang X, Zhang X, Wu Y, et al. SPOP-mediated ubiquitination and degradation of Pdk1 suppresses akt kinase activity and oncogenic functions. *Mol Cancer* (2021) 20:100. doi: 10.1186/s12943-021-01397-5

8. Li Z, Wang D, Na X, Schoen SR, Messing EM, Wu G. Identification of a deubiquitinating enzyme subfamily as substrates of the von hippel-lindau tumor suppressor. *Biochem Biophys Res Commun* (2002) 294:700–9. doi: 10.1016/S0006-291X(02)00534-X

9. Jean-Charles PY, Wu JH, Zhang L, Kaur S, Nepliouev I, Stiber JA, et al. USP20 (Ubiquitin-specific protease 20) inhibits TNF (Tumor necrosis factor)-triggered smooth muscle cell inflammation and attenuates atherosclerosis. *Arterioscler Thromb Vasc Biol* (2018) 38:2295–305. doi: 10.1161/ATVBAHA.118.311071

10. Ha J, Kim M, Seo D, Park JS, Lee J, Lee J, et al. The deubiquitinating enzyme USP20 regulates the TNFalpha-induced NF-kappaB signaling pathway through stabilization of p62. *Int J Mol Sci* (2020) 21. doi: 10.3390/ijms21093116

11. Lu XY, Shi XJ, Hu A, Wang JQ, Ding Y, Jiang W, et al. Feeding induces cholesterol biosynthesis *via* the mTORC1-USP20-HMGCR axis. *Nature* (2020) 588:479–84. doi: 10.1038/s41586-020-2928-y

12. Zhang HY, Liao BW, Xu ZS, Ran Y, Wang DP, Yang Y, et al. USP44 positively regulates innate immune response to DNA viruses through deubiquitinating MITA. *PloS Pathog* (2020) 16:e1008178. doi: 10.1371/journal.ppat.1008178

13. Li W, Shen M, Jiang YZ, Zhang R, Zheng H, Wei Y, et al. Deubiquitinase USP20 promotes breast cancer metastasis by stabilizing SNAI2. *Genes Dev* (2020) 34:1310–5. doi: 10.1101/gad.339804.120

14. Wang C, Yang C, Ji J, Jiang J, Shi M, Cai Q, et al. Deubiquitinating enzyme USP20 is a positive regulator of claspin and suppresses the malignant characteristics of gastric cancer cells. *Int J Oncol* (2017) 50:1136–46. doi: 10.3892/ijo.2017.3904

15. Li T, Fan J, Wang B, Traugh N, Chen Q, Liu JS, et al. TIMER: A web server for comprehensive analysis of tumor-infiltrating immune cells. *Cancer Res* (2017) 77:e108–10. doi: 10.1158/1538-7445.AM2017-108

16. Love MI, Huber W, Anders S. Moderated estimation of fold change and dispersion for RNA-seq data with DESeq2. *Genome Biol* (2014) 15:550. doi: 10.1186/s13059-014-0550-8

17. Yu G, Wang LG, Han Y, He QY. clusterProfiler: an r package for comparing biological themes among gene clusters. *OMICS* (2012) 16:284–7. doi: 10.1089/omi.2011.0118

18. Subramanian A, Tamayo P, Mootha VK, Mukherjee S, Ebert BL, Gillette MA, et al. Gene set enrichment analysis: a knowledge-based approach for interpreting genome-wide expression profiles. *Proc Natl Acad Sci U.S.A.* (2005) 102:15545–50. doi: 10.1073/pnas.0506580102

19. Hanzelmann S, Castelo R, Guinney J. GSVA: Gene set variation analysis for microarray and RNA-seq data. *BMC Bioinf* (2013) 14:7. doi: 10.1186/1471-2105-14-7

20. Cui X, Cui Y, Du T, Jiang X, Song C, Zhang S, et al. SHMT2 drives the progression of colorectal cancer by regulating UHRF1 expression. *Can J Gastroenterol Hepatol* (2022) 2022:3758697. doi: 10.1155/2022/3758697

21. Jin RR, Zeng C, Chen Y. MiR-22-3p regulates the proliferation, migration and invasion of colorectal cancer cells by directly targeting KDM3A through the hippo pathway. *Histol Histopathol* (2022) 37:1241–52. doi: 10.14670/HH-18-526

22. Reinhold WC, Sunshine M, Liu H, Varma S, Kohn KW, Morris J, et al. CellMiner: a web-based suite of genomic and pharmacologic tools to explore transcript and drug patterns in the NCI-60 cell line set. *Cancer Res* (2012) 72:3499–511. doi: 10.1158/0008-5472.CAN-12-1370

23. Brudvik KW, Jones RP, Giuliante F, shinDOH J, Passot G, Chung MH, et al. RAS MUTATION CLINICAL risk score to predict survival after resection of colorectal liver metastases. *Ann Surg* (2019) 269:120–6. doi: 10.1097/SLA.0000000000002319

24. Schrock AB, Lee JK, Sandhu J, Madison R, Cho-Phan C, Snider JW, et al. RAS amplification as a negative predictor of benefit from anti-EGFR-Containing therapy regimens in metastatic colorectal cancer. *Oncologist* (2021) 26:469–75. doi: 10.1002/onco.13679

25. Ducoin K, Oger R, Bilonda Mutala L, Deleine C, Jouand N, Desfrancois J, et al. Targeting NKG2A to boost anti-tumor CD8 T-cell responses in human colorectal cancer. *Oncoimmunology* (2022) 11:2046931. doi: 10.1080/2162402X.2022.2046931

26. Malynn BA, Ma A. Ubiquitin makes its mark on immune regulation. *Immunity* (2010) 33:843–52. doi: 10.1016/j.immuni.2010.12.007

27. Zhu Y, Gu L, Lin X, Zhou X, Lu B, Liu C, et al. USP19 exacerbates lipogenesis and colorectal carcinogenesis by stabilizing ME1. *Cell Rep* (2021) 37:110174. doi: 10.1016/j.celrep.2021.110174

28. Li B, QI ZP, He DL, Chen ZH, Liu JY, Wong MW, et al. NLRP7 deubiquitination by USP10 promotes tumor progression and tumor-associated macrophage polarization in colorectal cancer. *J Exp Clin Cancer Res* (2021) 40:126. doi: 10.1186/s13046-021-01920-y

29. Pan R, Xie Y, Fang W, Liu Y, Zhang Y. USP20 mitigates ischemic stroke in mice by suppressing neuroinflammation and neuron death *via* regulating PTEN signal. *Int Immunopharmacol* (2022) 103:107840. doi: 10.1016/j.intimp.2021.107840

30. Wu C, Luo K, Zhao F, Yin P, Song Y, Deng M, et al. USP20 positively regulates tumorigenesis and chemoresistance through beta-catenin stabilization. *Cell Death Differ* (2018) 25:1855–69. doi: 10.1038/s41418-018-0138-z

31. Fantini MC, Favale A, Onali S, Facciotti F. Tumor infiltrating regulatory T cells in sporadic and colitis-associated colorectal cancer: The red little riding hood and the wolf. *Int J Mol Sci* (2020) 21. doi: 10.3390/ijms21186744

32. Shin JH, Jeong J, Maher SE, Lee HW, Lim J, Bothwell ALM. Colon cancer cells acquire immune regulatory molecules from tumor-infiltrating lymphocytes by trogocytosis. *Proc Natl Acad Sci U.S.A.* (2021) 118. doi: 10.1073/pnas.2110241118

33. Olguin JE, Medina-Andrade I, Rodriguez T, Rodriguez-Sosa M, Terrazas LI. Relevance of regulatory T cells during colorectal cancer development. *Cancers (Basel)* (2020) 12. doi: 10.3390/cancers12071888

34. Hausler SF, Del Barrio IM, Strohschein J, Chandran PA, Engel JB, Honig A, et al. Ectonucleotidases CD39 and CD73 on OvCA cells are potent adenosine-generating enzymes responsible for adenosine receptor 2A-dependent suppression of T cell function and NK cell cytotoxicity. *Cancer Immunol Immunother* (2011) 60:1405–18. doi: 10.1007/s00262-011-1040-4

35. Lei J, Ma J, Ma Q, Li X, Liu H, Xu Q, et al. Hedgehog signaling regulates hypoxia induced epithelial to mesenchymal transition and invasion in pancreatic cancer cells *via* a ligand-independent manner. *Mol Cancer* (2013) 12:66. doi: 10.1186/1476-4598-12-66

36. Eberl M, Mangelberger D, Swanson JB, Verhaegen ME, Harms PW, Frohm ML, et al. Tumor architecture and notch signaling modulate drug response in basal cell carcinoma. *Cancer Cell* (2018) 33:229–243 e4. doi: 10.1016/j.ccell.2017.12.015

37. Whitson RJ, Lee A, Urman NM, Mirza A, Yao CY, Brown AS, et al. Noncanonical hedgehog pathway activation through SRF-MKL1 promotes drug resistance in basal cell carcinomas. *Nat Med* (2018) 24:271–81. doi: 10.1038/nm.4476

38. Hu G, Ma J, Zhang J, Chen Y, Liu H, Huang Y, et al. Hypoxia-induced lncHILAR promotes renal cancer metastasis *via* ceRNA for the miR-613/206/ 1-1-3p/Jagged-1/ Notch/CXCR4 signaling pathway. *Mol Ther* (2021) 29:2979–94. doi: 10.1016/ j.ymthe.2021.05.020

39. Zhao H, Ming T, Tang S, Ren S, Yang H, Liu M, et al. Wnt signaling in colorectal cancer: Pathogenic role and therapeutic target. *Mol Cancer* (2022) 21:144. doi: 10.1186/ s12943-022-01616-7

frontiers | Frontiers in Oncology

TYPE Original Research
PUBLISHED 21 February 2023
DOI 10.3389/fonc.2023.1058337

OPEN ACCESS

EDITED BY
Alexandre Corthay,
Oslo University Hospital, Norway

REVIEWED BY
Elena Gershtein,
Russian Cancer Research Center NN Blokhin, Russia
Sergei Kusmartsev,
University of Florida, United States
Hirendra Banerjee,
University of North Carolina, United States

*CORRESPONDENCE
Irina Larionova
larionovaiv@onco.tnimc.ru

†These authors share senior authorship

SPECIALTY SECTION
This article was submitted to Molecular and Cellular Oncology, a section of the journal Frontiers in Oncology

RECEIVED 30 September 2022
ACCEPTED 11 January 2023
PUBLISHED 21 February 2023

CITATION
Kazakova E, Rakina M, Sudarskikh T, Iamshchikov P, Tarasova A, Tashireva L, Afanasiev S, Dobrodeev A, Zhuikova L, Cherdyntseva N, Kzhyshkowska J and Larionova I (2023) Angiogenesis regulators S100A4, SPARC and SPP1 correlate with macrophage infiltration and are prognostic biomarkers in colon and rectal cancers. *Front. Oncol.* 13:1058337. doi: 10.3389/fonc.2023.1058337

Angiogenesis regulators S100A4, SPARC and SPP1 correlate with macrophage infiltration and are prognostic biomarkers in colon and rectal cancers

Elena Kazakova[1,2], Militsa Rakina[1,2], Tatiana Sudarskikh[1], Pavel Iamshchikov[1,2], Anna Tarasova[2], Liubov Tashireva[2], Sergei Afanasiev[2], Alexei Dobrodeev[2], Lilia Zhuikova[2], Nadezhda Cherdyntseva[1,2,3], Julia Kzhyshkowska[1,3,4,5†] and Irina Larionova[1,2,3*†]

[1]Laboratory of Translational Cellular and Molecular Biomedicine, Tomsk State University, Tomsk, Russia, [2]Cancer Research Institute, Tomsk National Research Medical Center, Russian Academy of Sciences, Tomsk, Russia, [3]Laboratory of Genetic Technologies, Siberian State Medical University, Tomsk, Russia, [4]Institute of Transfusion Medicine and Immunology, Institute for Innate Immunoscience (MI3), Medical Faculty Mannheim, University of Heidelberg, Mannheim, Germany, [5]German Red Cross Blood Service Baden-Württemberg – Hessen, Mannheim, Germany

Introduction: Increasing evidence suggests that it is necessary to find effective and robust clinically validated prognostic biomarkers that can identify "high-risk" colorectal cancer (CRC) patients. Currently, available prognostic factors largely include clinical-pathological parameters and focus on the cancer stage at the time of diagnosis. Among cells of tumor microenvironment (TME) only Immunoscore classifier based on T lymphocytes showed high predictive value.

Methods: In the present study, we performed the complex analysis of mRNA and protein expression of crucial regulators of tumor angiogenesis and tumor progression, expressed by tumor-associated macrophages (TAMs): S100A4, SPP1 and SPARC. Colon and rectal cancer patients were investigated independently and in a combined cohort (CRC). For mRNA expression, we analyzed RNA sequencing data obtained from TCGA (N=417) and GEO (N=92) cohorts of colorectal cancer patients. For protein expression, we performed IHC digital quantification of tumor tissues obtained from 197 patients with CRC treated in the Department of abdominal oncology in Clinics of Tomsk NRMC.

Results: High S100A4 mRNA expression accurately predicted poor survival for patients with CRC independently of cancer type. SPARC mRNA level was independent prognostic factors for survival in colon but not in rectal cancer. SPP1 mRNA level had significant predictive value for survival in both rectal and colon cancers. Analysis of human CRC tissues revealed that S100A4, SPP1 and SPARC are expressed by stromal compartments, in particular by TAMs, and have a strong correlation with macrophage infiltration. Finally, our results indicate that chemotherapy-based treatment can change the predictive direction of S100A4 for rectal cancer patients. We found that S100A4 stromal levels were higher in patients

with better response to neoadjuvant chemotherapy/chemoradiotherapy, and S100A4 mRNA levels predicted better DFS among non-responders.

Discussion: These findings can help improve the prognosis of patients with CRC based on S100A4, SPP1 and SPARC expression levels.

KEYWORDS

colorectal cancer, tumor-associated macrophage, SPP1, S100A4, SPARC, angiogenesis, chemotherapy, prognosis

1 Introduction

Colorectal cancer (CRC) is the third most common malignancy and the second-leading cause of cancer death in the world due to the unmet screening programs, therapeutic strategies, and increasing incidence rates (1). Colorectal cancer is characterized by high inter- and intra-tumoral heterogeneity (2, 3). Although colorectal cancer is a more general and widely used term, there is still a differentiation into two distinct localizations: colon cancer (CC) and rectal cancer (RC). There are evidences accumulated towards considering CC and RC as self-standing tumor entities due to their topography, surgical challenge, therapy, complications, and relapse patterns (4, 5). CRC heterogeneity determines difficulties in choosing anticancer treatment, and also poses an obstacle in reaching therapeutic complete response (6). Although the response rate to systemic chemotherapies goes up to 50%, nearly all patients with CRC develop drug resistance, which limits the therapeutic efficacy of anticancer drugs and ultimately leads to chemotherapy failure (7, 8). These difficulties pose a demand for biomarker discovery that will help in improving treatment efficiency, early detection, and could be of value as diagnostic or prognostic markers.

Tumor microenvironment (TME), which consists of stromal and immune cells, has an essential role in tumor development (9). The key component of innate immunity in the TME is tumor-associated macrophages (TAMs) (10). TAMs regulate tumor growth by supporting cancer cell survival and proliferation, angiogenesis, and metastasis, as well as the response of cancer cells to therapeutic intervention (11). Angiogenesis is a basic process that provides the tumor with crucial nutrients and oxygen (12). The main pro-angiogenic regulator in tumors is VEGF (12). Despite the growing list of FDA-approved anti-VEGF drugs, the success of anti-angiogenic therapy is limited. Failure in VEGF-targeted therapy can be explained by the switching on the alternative pro-angiogenic activators (13). Recently collected data demonstrated that TAMs can be essential sources for plenty of novel angiogenesis-related proteins that belong to S100A class, SEMA family, chitinase-like proteins, growth factors, and proteins regulating cell-matrix interactions, etc (13). Among them, pro-angiogenic factors S100A4 and osteopontin (OPN, or SPP1) as well as anti-angiogenic factor SPARC, which have drawn our attention, since we have recently identified the deregulation of their expression in TAMs under chemotherapy exposure *in vitro* (unpublished data).

In the present study, for the first time we performed the complex analysis of mRNA and protein expression of S100A4, SPP1 and SPARC. We establish their prognostic significance in terms of survival rates and clinical and pathological parameters of tumor state in patients with colon and rectal cancer. Also, we identified that neoadjuvant chemotherapy/chemoradiotherapy can reverse their predictive value in more favorable way.

Abbreviations: AUC, area under curve; CC, colon cancer; CI, confidence interval; CRC, colorectal cancer; DFS, disease-free survival; DSS, disease-specific survival; GEO, gene expression omnibus; HR, hazard ratio; IHC,; immunohistochemistry; NAC, neoadjuvant chemotherapy; NCRT, neoadjuvant chemoradiotherapy; OS, overall survival; PFS, progression-free survival; RC, rectal cancer; RFS, recurrence-free survival; TCGA, the cancer genome atlas; TAM, tumor-associated macrophage; TME, tumor microenvironment.

2 Materials and methods

2.1 Dataset analysis

The Cancer Genome Atlas (TCGA) data (TCGA-COAD and TCGA-READ datasets) and NCBI GEO (GSE190826 dataset) were used to examine the expression of SPP1, S100A4 and SPARC and to perform survival analysis in colorectal cancer patients. TCGA data included information about SPP1, S100A4 and SPARC expression, that was evaluated in the following groups of patients: a) with colorectal cancer (common group) (N=417), b) with colon cancer, including transverse colon, ascending colon, descending colon, sigmoid colon, cecum, hepatic flexure, splenic flexure (n=305), c) with rectal cancer, including rectosigmoid junction and rectum (N=112), with available clinical information and records on recurrence and survival rates (in details in Supplementary Table S1). Patients with advanced stage IV were excluded. GSE190826 dataset included 92 patients with rectal cancer treated with neoadjuvant chemoradiotherapy (NCRT); information about pre-treatment levels of SPP1, S100A4 and SPARC mRNA expression was obtained. The TCGA biolinks was used for retrieving RNA-seq data from the GDC database. The raw sequencing reads were processed *via* the DESeq2 R package. The raw counts were depth normalized and variance stabilized *via* the variance stabilizing transformation (VST) for downstream survival analysis.

2.2 CIBERSORT analysis

Cell type deconvolution of colorectal cancer TCGA RNA-seq data was performed *via* the TIMER2.0 (14) web platform, which provides a facility for robust estimation of immune infiltration levels of user-provided tumor profiles. TIMER2.0 utilizes the immunedeconv (15), an R package which integrates six distinct cell-type deconvolution algorithms, including CIBERSORT (16). CIBERSORT uses highly robust-to-noise linear support vector regression (SVR) to deconvolve the mixture of cell types of interest. Inferred immune cell-types were used to assess cell-type association of SPP1, S100A4, and SPARC genes by the Spearman correlation.

2.3 Clinical material

The IHC study included patients with colorectal adenocarcinoma with morphologically verified diagnosis, treated in the Department of abdominal oncology, Cancer Research Institute of Tomsk National Research Medical Center (Tomsk, Russia). The study was carried out according to Declaration of Helsinki (from 1964, revised in 1975 and 1983) and was approved by the local committee of Medical Ethics of Tomsk Cancer Research Institute; all patients signed informed consent for the study. Patients were divided as we did for TCGA cohort with the exception that the number of patients in SPARC/SPP1 group differed from S100A4 group: a) with colorectal cancer (common group for SPARC/SPP1) (N=118), b) with colon cancer (N=54), c) with rectal cancer (N=64) (Supplementary Table S2). For S100A4 group: a) with colorectal cancer (common group) (N=197), b) with colon cancer (N=89), c) with rectal cancer (N=107) (Supplementary Table S3). Patients with rectal cancer and cancer of the rectosigmoid junction received neoadjuvant chemotherapy (NAC) or chemoradiotherapy (NCRT). Five-grade Mandard Tumor Regression Grading (TRG) system was used for assessment of response in patients, where TRG1 – no residual cancer, TRG2 – residual isolated cancer cells, TRG3 – fibrosis outgrowing residual cancer, TRG4 – residual cancer outgrowing fibrosis, TRG5 – absence of regressive changes (14). All patients underwent surgical treatment. In adjuvant regime, according to indications, patients received chemotherapy under the same schemes for up to 6 months. Cases of stage IV disease were excluded.

2.4 Immunohistochemical analysis

FFPE tissue sections were obtained from all CRC patients after tumor resection. Immunohistochemical analysis (IHC) was carried out by standard method. Following antibodies were used: polyclonal rabbit anti-S100A4 (1:1000, PA5-82322, Thermo Fisher Scientific, USA), polyclonal goat anti-SPARC (1:80, AF941, R&D Systems, USA), polyclonal goat anti-SPP1 (1:80, AF1433, R&D Systems, USA). To visualize the antigen-antibody reaction, rabbit anti-goat IgG (1:250, VB2932894, Invitrogen, USA) or poly-HRP anti-mouse/rabbit system (Bond oracle IHC system, TA9145, Leica Biosystems, Germany) were used. The nuclei were counterstained with hematoxylin.

2.5 Digital quantification

Tumor tissue slides were scanned by using the Leica Aperio AT2 histoscanning station (Leica, Germany) and ScanScope software (Aperio ScanScope XT Leica). QuPath software (free from https://qupath.github.io) was used to analyze and quantify marker expression. Individual tumor regions were selected and analyzed using cell detection and cell intensity classification. "Cell: DAB OD mean" was used for the analysis of both membranous and cytoplasmic staining of SPP1, S100A4 and SPARC. Intensity thresholds were set to further subclassify cells as being negative, weak (1+), moderate (2+) or strongly positive (3+) for marker staining based upon mean nuclear DAB optical density. The results were obtained in two scales: percentage of positive cells among all counted cells per section (%) and H-score – a parameter that takes into account both the percentage of positive cells and the intensity of staining. These parameters were counted automatically by the program.

2.6 Immunofluorescence and confocal microscopy

For IF double staining mouse anti-CD68 monoclonal antibody (1:100, #NBP2-44539, clone KP1, Novus Biologicals); polyclonal rabbit anti-S100A4 (1:1000, PA5-82322, Thermo Fisher Scientific, USA), polyclonal goat anti-SPARC (1:80, AF941, R&D Systems, USA) and polyclonal goat anti-SPP1 (1:80, AF1433, R&D Systems, USA) were used. Combination of secondary antibodies were applied: donkey Cy3-conjugated anti-rabbit antibody (#711-165-152, Dianova, Germany, dilution 1:400), donkey AlexaFluor488-conjugated anti-mouse antibody (#715-545-150, Dianova, Germany, dilution 1:400) and donkey Cy3-conjugated anti-goat antibody (#706-167-003, Dianova, Germany, dilution 1:400). Samples were mounted with Fluoroshield Mounting Medium with DAPI (#ab104135, Abcam, USA) and analyzed by confocal microscopy. Confocal laser scanning microscopy was performed with Carl Zeiss LSM 780 NLO laser scanning spectral confocal microscope (Carl Zeiss, Germany), equipped with 40x objective. Data were acquired and analyzed with Black Zen software (RRID : SCR_018163). All three-color images were acquired using a sequential scan mode.

2.7 NGS-GeoMx Digital Spatial Profiler (DSP) analysis

NanoString GeoMx digital spatial profiling (DSP) was applied to perform spatially resolved RNA profiling analysis in colorectal cancer tissue. The Cancer Transcriptome Atlas (CTA) panel was used. The 97 areas of illumination (AOIs) across all slides in mixed stroma/tumor regions was selected. The resulted libraries were sequenced by the Illumina NextSeq 500 platform using 2 x 27 base paired reads. The raw counts were processed in the NanoString's GeoMx NGS pipeline v.2.1 where they were converted to the digital count conversion (DCC) files. The GeomxTools was used for quality control (QC) and downstream analysis of the DCC files in R (17). The adjusted p-values were calculated using the Benjamini-Hochberg correction. Differential gene expression analysis between CK+ and CD45+ regions was performed

using a linear mixed model (LMM) with random slope and random intercept as recommended in the GeomxTools manual.

2.8 Statistical analysis

Statistical analysis was performed using STATISTICA 12.0 for Windows (STATISTICA, RRID : SCR_014213) and GraphPad Prism 8.4.2 (GraphPad Prism, RRID : SCR_002798). The Mann-Whitney U-test and t-test for independent groups were implemented. The prognostic values of SPP1, S100A4 and SPARC (area under curve (AUC), confidence interval (CI), sensitivity, specificity, and cut-off value) were determined using receiver operating characteristic (ROC) analysis. The survival rates were determined by the Kaplan–Meier method, and the log-rank test was used. Cox's proportional-hazard model was applied for survival analysis and the hazard ratio (HR [95%CI]) evaluation. Results were presented using GraphPad Prism 8.4.2 software. Results were considered to be significant with p<0,05. Data with marginal significance (p-value >0,05 and <0,1) were also discussed.

3 Results

3.1 High S100A4 mRNA expression is a robust predictor for shorter survival rates independent of cancer type

S100A4 is a pro-angiogenic factor belonging to the family of calcium-binding proteins (13). In the pathogenesis of cancer, increased S100A4 expression correlates with a high incidence of metastasis and poor prognosis in cancer (18).

To reveal the prognostic value of S100A4 mRNA expression, we performed survival analysis using TCGA data. The mRNA expression was defined further as log-normalized counts. We analyzed a combined group of CRC patients and two separate cohorts of patients with colon cancer and rectal cancer.

We applied Cox regression analysis, ROC analysis, and Kaplan–Meier curves to evaluate significance of S100A4 on disease prognosis in the combined CRC group, as well as CC and RC patients. In each group, all patients were categorized into high- and low-risk groups based on S100A4 expression according to the cut-off meanings determined by ROC analysis that allowed to predict overall death, death from the disease, recurrence and progression (Supplementary Table S4). Kaplan–Meier survival curve indicated that CRC patients in S100A4 high-risk group (>cut-off) had shorter overall survival (OS) (p=0,0159), disease-specific survival (DSS) (p<0,0001), disease-free survival (DFS) (p<0,0001), and progression-free survival (PFS) (p<0,0001) than those in low-risk group (<cut-off) (Figure 1A). The similar results were found for OS, DSS, DFS, and PFS in both patients with colon and rectal cancer (Figures 1B, C), indicating that prognostic significance of S100A4 mRNA expression does not depend on cancer type.

To investigate further, whether S100A4 mRNA expression could serve as an independent prognostic criterion of death or recurrence/progression, uni- and multivariate Cox regression analyses were applied. Univariate Cox regression analysis showed that S100A4 mRNA expression more than cut-off has prognostic value for poorer OS (HR=2,19; 95% CI [1,277-3,753], p=0,004), poorer DFS (HR=2,74; 95% CI [1,604-4,689], p=0,0002)

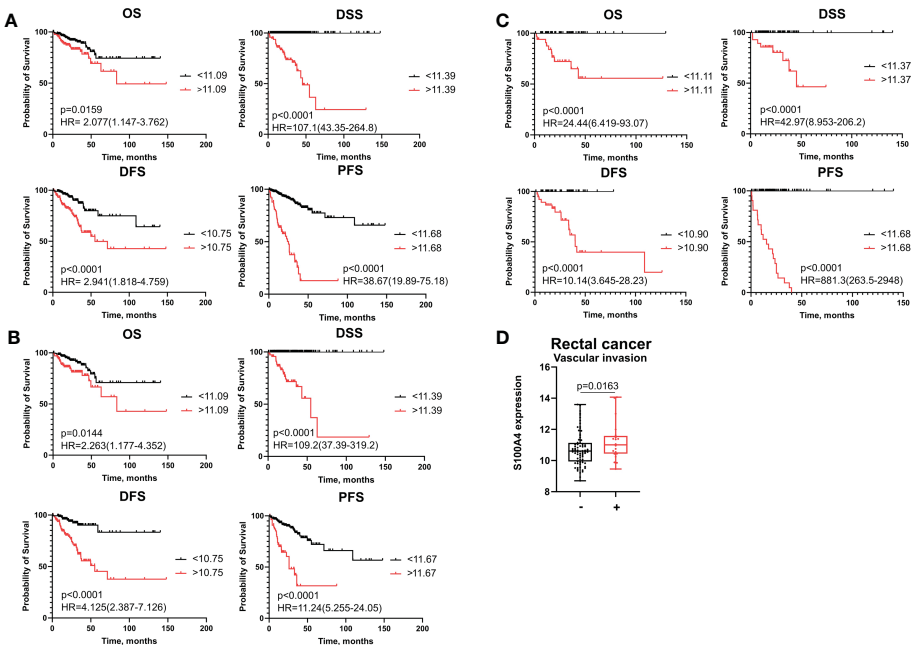

FIGURE 1
S100A4 mRNA expression is an unfavorable prognostic factor for colon and rectal cancer patients. **(A)** Kaplan–Meier curve of TCGA survival data (OS, DSS, DFS, and PFS) for high-risk and low-risk patients in combined CRC group. **(B)** Kaplan–Meier curve of TCGA survival data for high-risk and low-risk groups in colon cancer patients. **(C)** Kaplan–Meier curve of TCGA survival data for high-risk and low-risk groups of rectal cancer patients. Log-rank test p-values are shown in Kaplan–Meier curves. **(D)** S100A4 mRNA expression is associated with vascular invasion in rectal cancer patients (TCGA-READ data). Mann-Whitney U test was applied. Box plot depicts gene expression (min, Q1, median, Q3, max).

and poorer PFS (HR=8,01; 95% CI [5,066-12,680], p<0,0001) in common CRC group (Table 1 and Supplementary Table S5). In univariate COX regression high S100A4 gene expression was prognostic for worse OS (HR=2,43; 95% CI [1,331-4,438], p=0,003), worse DFS (HR=4,73; 95% CI [2,332-9,626], p<0,0001), and worse PFS (HR=4,35; 95% CI [2,521-7,524], p<0,0001) in colon cancer patients (Table 2 and Supplementary Table S6). After adjusting for the clinical and pathological parameters such as age, tumor stage, tumor size, lymphovascular invasion, vascular invasion and lymph node metastasis the S100A4 mRNA expression remained an independent prognostic factor for DFS in the CRC group (HR=3,73; 95% CI [1,917-7,274], p<0,0001) and the CC group (HR=10,52; 95% CI [3,655-30,310], p<0,0001) (Tables 1, 2). Multivariate Cox analysis displayed that S100A4 mRNA expression more than 11,68 (HR=9,97; 95% CI [5,800-17,150], p<0,0001), large tumor size (HR=2,41; 95% CI [1,216-4,790], p=0,011) and positive vascular invasion (HR=2,36; 95% CI [1,357-4,097], p=0,002) were associated with worse PFS in CRC patients (Supplementary Table S5). The same factors were indicative for the prognosis of poor PFS in colon cancer group: S100A4 mRNA expression more than 11,68 (HR=5,85; 95% CI [3,071-11,150], p<0,0001), large tumor size (HR=2,25; 95% CI [1,024-4,970], p=0,043) and positive vascular invasion (HR=2,36; 95% CI [1,252-4,460], p=0,007) (Supplementary Table S6). In rectal cancer patients, COX analysis did not show the prognostic significance of S100A4 mRNA expression.

In colon cancer patients, ROC analysis determined the most optimal cut-off meanings for S100A4 mRNA expression to predict OS, DFS and PFS with higher sensitivity and specificity (indicated in Supplementary Table S4). Thus, S100A4 mRNA expression more than cut-off predicted poor OS (AUC=0,956, p<0,0001), poor DSS (AUC=0,988, p<0,0001) DFS (AUC=0,997, p<0,0001), and poor PFS (AUC=0,983, p<0,0001) (Supplementary Table S4). In the RC group, increased gene expression of S100A4 (>11,68) was the most robust criteria for the prognosis of short PFS with the corresponding sensitivity 100% and specificity 100% (AUC=1,0, p<0,0001) (Figure 1C and Supplementary Table S4).

Statistical analysis showed that high S100A4 expression was associated with positive vascular invasion in RC patients (11,23 ± 1,26 vs. 10,75 ± 1,07; p=0,0163) (Figure 1D). No significant associations were found with other clinical-pathological parameters. In CRC patients and colon cancer patients, no significant differences in S100A4 gene expression that was related to clinical-pathological parameters were found.

TABLE 1 The prognostic significance of S100A4 mRNA levels for disease-free survival in patients with CRC revealed by univariate and multivariate COX analysis.

Parameter	Univariate			Multivariate		
	HR	95% CI	p-value	HR	95% CI	p-value
Disease-free survival						
Age *<70 years>70 years*	1,100	0,682-1,796	0,678	1,140	0,598-2,197	0,680
Stage *Early (1-2) Advanced (3)*	2,100	1,293-3,416	0,002	3,760	0,409-34,586	0,240
Tumor size *T1-2 T3-4*	2,220	1,102-4,502	0,020	1,360	0,588-3,162	0,469
Vascular invasion *Negative Positive*	1,470	0,825-2,622	0,190	1,040	0,508-2,168	0,895
Lymphovascular invasion *Negative Positive*	1,650	0,997-2,732	0,050	1,630	0,802-3,336	0,175
Lymphatic metastasis *Negative Positive*	2,220	1,382-3,595	0,001	6,440	0,747-55,591	0,090
S100A4 expression *<10,75>10,75*	2,740	1,604-4,689	0,0002	3,730	1,917-7,274	0,0001

TABLE 2 The prognostic significance of S100A4 mRNA levels for disease-free survival with colon cancer revealed by univariate and multivariate COX analysis.

Parameter	Univariate			Multivariate		
	HR	95% CI	p-value	HR	95% CI	p-value
Disease-free survival						
Age *<70 years>70 years*	1,300	0,754-2,241	0,344	1,267	0,607-1,439	0,527
Stage *Early (1-2) Advanced (3)*	1,820	1,040-3,185	0,035	0,393	0,038-4,047	0,433
Tumor size *T1-2 T3-4*	2,190	0,895-4,867	0,054	1,762	0,654-4,749	0,262
Vascular invasion *Negative Positive*	1,680	0,896-3,151	0,105	1,195	0,506-2,821	0,684
Lymphovascular invasion *Negative Positive*	1,790	1,000-3,206	0,049	1,609	0,673-3,843	0,284
Lymphatic metastasis *Negative Positive*	1,990	1,154-3,441	0,013	3,850	0,424-34,939	0,230
S100A4 expression *<10,75 >10,75*	4,730	2,332-9,626	<0,0001	10,526	3,655-30,310	<0,0001

3.2 Elevated SPARC mRNA expression is an accurate independent prognostic factor for poor DFS and PFS in colon but not rectal cancer

SPARC (secreted protein acidic and rich in cysteine, also known as osteonectin or BM-40) is a calcium-binding matricellular protein. In the TME, SPARC is anti-angiogenic and affects tumor growth, extracellular matrix deposition (19). Similar to S100A4, ROC analysis allowed to divide all patients into high- and low-risk groups for prognosis of overall death, death from the disease, recurrence and progression based on SPARC mRNA level (Supplementary Table S7). SPARC mRNA expression more than cut-off in the high-risk group was significantly associated with worse DSS (p=0,0017) and worse PFS (p=0,0039), but with better OS (p=0,0401) in patients with CRC (Figure 2A). Similar tendency was shown for colon cancer patients (Figure 2B). In rectal cancer, SPARC mRNA expression more than cut-off was associated with poor OS (p=0,0061), poor DFS (p=0,0371) and poor PFS (p=0,0120) (Figure 2C). In univariate COX analysis SPARC gene expression more than cut-off predicted worse DSS (HR=2,88; 95% CI [1,377-6,006], p=0,004) and worse PFS (HR=2,06; 95% CI [1,308-3,258], p=0,002) in CRC group, as well as worse DSS (HR=2,64; 95% CI [1,141-6,110], p=0,023) and worse PFS (HR=1,98; 95% CI [1,172-3,360], p=0,010) in colon cancer patients (Table 3 and Supplementary Tables S8, S9). After adjusting for age, tumor stage, tumor size, lymphovascular invasion, vascular invasion and lymph node metastasis, multivariate Cox regression analysis revealed that increased SPARC mRNA expression remained an independent prognostic factor for poor DSS (HR=6,65; 95% CI [2,208-20,100], p=0,0007) and poor PFS (HR=1,88; 95% CI [1,144-3,120], p=0,001) in CRC patients (Table 3). In colon cancer patients, SPARC mRNA expression in high-risk group also independently predicted short DSS (H=7,44; 95% CI [2,082-26,600], p=0,002) and short PFS (HR=1,83; 95% CI [1,021-3,302], p=0,042) (Supplementary Table S9). In RC patients, SPARC mRNA level more than cut-off was prognostic in terms of short OS (HR=5,84; 95% CI [1,404-21,421], p=0,014), short DFS (HR=2,83; 95% CI [1,019-7,907], p=0,045), and short PFS (HR=4,50; 95% CI [1,332-15,225], p=0,015) in univariate COX analysis. But it was not an independent criterion in multivariate analysis (Supplementary Table S10). Thus, we concluded that SPARC mRNA expression could serve as an independent prognostic factor for DFS and PFS in colon but not rectal cancer.

High SPARC gene expression indicated advanced tumor stage (14,58 ± 1,06 vs. 14,3 ± 1,10; p=0,014) and positive lymph node metastasis (14,59 ± 1,05 vs. 14,29 ± 1,09; p=0,00073) in CRC (Figure 2D). In colon cancer patients, high SPARC mRNA expression was associated with advanced tumor stage (14,62 ± 1,13 vs. 14,24 ± 1,15; p=0,007), positive lymph node metastasis (14,64 ± 1,12 vs. 14,23 ± 1,13; p=0,003) and positive vascular invasion (14,28 ± 1,2 vs 14,51 ± 0,93, p=0,043) (Figure 2D). No significant differences in SPARC expression were found for clinical-pathological parameters in rectal cancer patients.

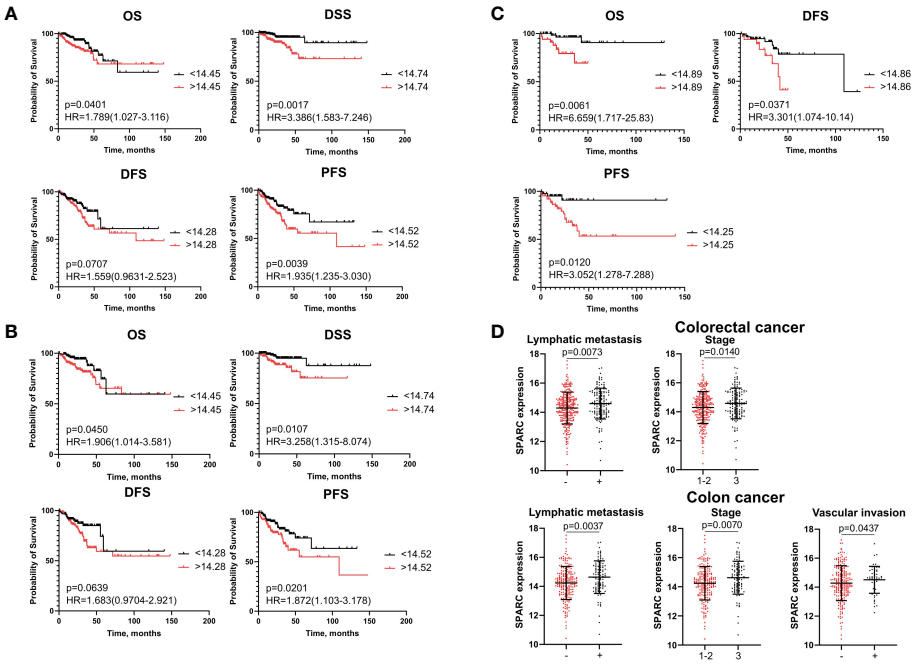

FIGURE 2
SPARC mRNA expression is associated with survival and clinical-pathological parameters. **(A)** Kaplan–Meier curve of TCGA survival data (OS, DSS, DFS, and PFS) for high-risk and low-risk patients in combined CRC group. **(B)** Kaplan–Meier curve of TCGA survival data for high-risk and low-risk groups in colon cancer patients. **(C)** Kaplan–Meier curve of TCGA survival data for high-risk and low-risk groups in rectal cancer patients. Log-rank test p-values are shown in Kaplan–Meier curves. **(D)** SPARC mRNA expression is associated with lymph node metastasis and tumor stage in CRC patients, and with lymph node metastasis, stage and vascular invasion in colon cancer patients. Student's t-test was applied. Scatter plots depict gene expression as mean with SD.

3.3 Increased SPP1 mRNA expression is an independent unfavorable criterion for PFS in both rectal and colon cancers

Secreted phosphoprotein 1 (SPP1, OPN, osteopontin) is an integrin-binding matricellular protein that has been found to be involved in many cellular processes such as cell signaling pathways, cell adhesion and migration, cell-mediated immunity, angiogenesis, and metastasis (20).

Kaplan–Meier analysis demonstrated that high-risk group based on SPP1 mRNA level more than cut-off had worse OS (p=0,0312), worse DFS (p=0,0308) and worse PFS (p=0,0018) compared to the low-risk group (<cut-off) in the combined CRC group (Figure 3A). In patients with colon cancer, OS (p=0,0108) and PFS (p=0,0139) rates were lower in cases with higher expression of SPP1 (>cut-off) (Figure 3B). For RC patients, the high-risk group had decreased rates of DFS (p=0,0375) and PFS (p=0,0417) (Figure 3C).

Univariate Cox regression analysis showed that mRNA levels of SPP1 more than cut-off were associated with decreased rates of DFS (HR=2,22; 95% CI [1,382-3,595], p=0,001) and PFS (HR=2,20; 95% CI [1,382-3,526], p=0,0009) in the CRC group (Supplementary Table S11). In univariate analysis, high SPP1 gene expression was prognostic for worse OS (HR=2,12; 95% CI [1,092-4,149], p=0,026) and worse PFS (HR=2,08; 95% CI [1,212-3,585], p=0,007) in colon cancer, and for worse DFS (HR=2,81; 95% CI [1,016-7,741], p=0,046) and PFS (HR=2,78; 95% CI [1,089-7,125], p=0,032) in rectal cancer (Supplementary Tables S12, S13). After including the clinical and pathological parameters in multivariate Cox analysis, the SPP1 expression more than cut-off remained independent prognostic factor for short PFS in both colon (HR=2,35; 95% CI [1,294-4,283], p=0,005) and rectal cancers (HR=3,32; 95% CI [1,124-9,809], p=0,029) patients (Supplementary Tables S12, S13).

Statistical data showed that elevated SPP1 mRNA expression correlated with positive vascular invasion (11,08 ± 2,00 vs. 10,23 ± 2,11; p=0,0017), positive lymphatic metastasis (10,82 ± 2,10 vs. 10,31 ± 2,12; p=0,0205) and advanced tumor stage (10,33 ± 2,11 vs. 10,18 ± 2,13; p=0,048) in combined CRC group. The same correlations were found in patients with colon cancer (Figure 3D). In the RC group, an increased SPP1 expression was related to positive vascular invasion (11,33 ± 1,58 vs. 10,44 ± 2,11; p=0,010) (Figure 3D).

3.4 S100A4, SPP1 and SPARC are expressed by tumor-associated macrophages in human colorectal cancer tissue

Using digital quantification, we performed IHC analysis of S100A4, SPP1 and SPARC in human colon and rectal cancer tissue. To increase the reproducibility and accuracy of quantification analysis, we used two methods to quantify protein expression. One of them was based on H-score, and the second included a percentage of positive cells. Correlation analysis showed that expression based on % and h-score had strong correlations (R=0,99 for S100A4; R=0,97 for SPARC, and R=0,99 for SPP1). Further, we used protein level in %, as it was more statistically significant.

We demonstrated that in protein level S100A4 and SPARC are more abundantly expressed by the cells of stroma compartments compared to tumor nest [17,69 (10,03–28,65) S100A4 stroma vs. 4,18 (1,31-13,93) S100A4 tumor, p<0,0001 and 16,04 (7,29-29,62) stroma SPARC vs. 2,08 (0,78-7,72) tumor SPARC, p<0,0001)] (Figure 4A).

TABLE 3 The prognostic significance of SPARC mRNA levels in patients with CRC revealed by univariate and multivariate COX analysis.

Parameter	Univariate			Multivariate		
	HR	95% CI	p-value	HR	95% CI	p-value
Disease-specific survival						
Age *<70 years>70 years*	1,570	0,775-3,199	0,208	1,180	0,475-3,000	0,716
Stage *Early (1-2)Advanced (3)*	2,620	1,001-6,894	0,0049	5,710	0,00005-591217	0,767
Tumor size *T1-2 T3-4*	1,670	0,642-4,364	0,291	3,760	0,853-16,700	0,080
Vascular invasion *Negative Positive*	2,420	1,067-5,496	0,034	2,050	0,772-5,500	0,148
Lymphovascular invasion *Negative Positive*	1,170	0,549-2,507	0,679	1,130	0,398-3,200	0,821
Lymphatic metastasis *Negative Positive*	2,240	0,917-5,502	0,228	0,040	0-5131	0,609
SPARC expression *<14,74>14,74*	2,870	1,377-6,006	0,004	6,650	2,208-20,100	0,0007
Progression-free survival						
Age *<70 years>70 years*	1,370	0,889-2,139	0,150	1,420	0,882-2,290	0,148
Stage *Early (1-2) Advanced (3)*	0,840	0,527-1,340	0,467	6,920	0,003-1773	0,493
Tumor size *T1-2 T3-4*	1,310	0,758-2,276	0,330	1,840	0,954-3,569	0,068
Vascular invasion *Negative Positive*	1,610	0,962-2,697	0,069	1,640	0,556-2,816	0,072
Lymphovascular invasion *Negative Positive*	1,250	0,793-1978	0,333	1,480	0,844-2,600	0,170
Lymphatic metastasis *Negative Positive*	0,820	0,517-1,315	0,118	0,090	0,003-23,335	0,396
SPARC expression *<14,52>14,52*	2,060	1,308-3,258	0,002	1,880	1,144-3,120	0,001

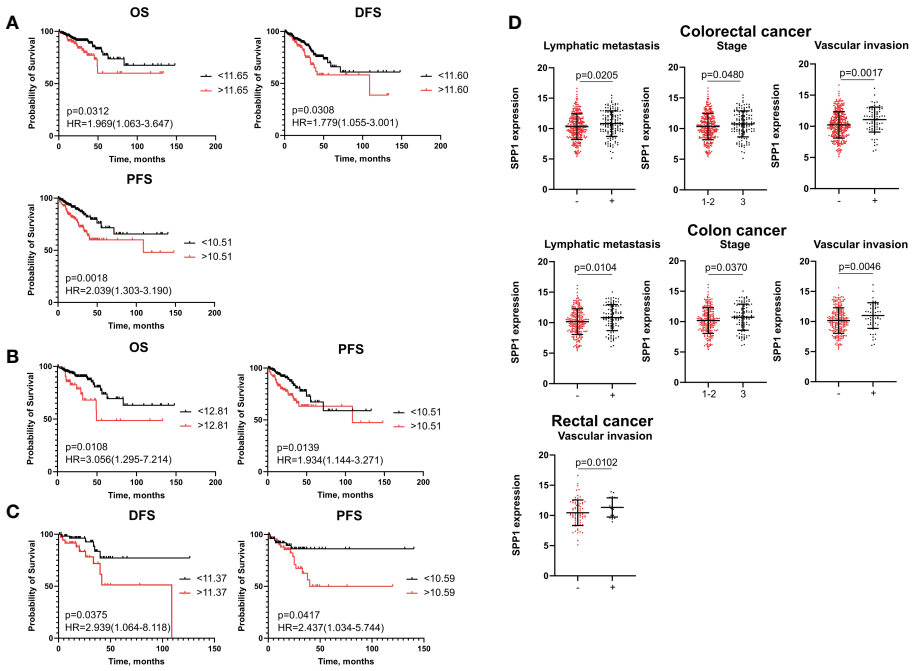

FIGURE 3
SPP1 mRNA expression is associated with poor survival and clinical-pathological parameters. **(A)** Kaplan–Meier curve of TCGA survival data (OS, DFS, and PFS) for high-risk and low-risk patients in combined CRC group. **(B)** Kaplan–Meier curve of TCGA survival data (OS and PFS) for high-risk and low-risk groups in colon cancer patients. **(C)** Kaplan–Meier curve of TCGA survival data (DFS and PFS) for high-risk and low-risk groups in rectal cancer patients. Log-rank test p-values are shown in Kaplan–Meier curves. **(D)** SPP1 mRNA expression is associated with lymph node, tumor stage and vascular invasion in CRC patients and colon cancer patients, and with vascular invasion in rectal cancer patients. Student's t-test was applied. Scatter plots depict gene expression as mean with SD.

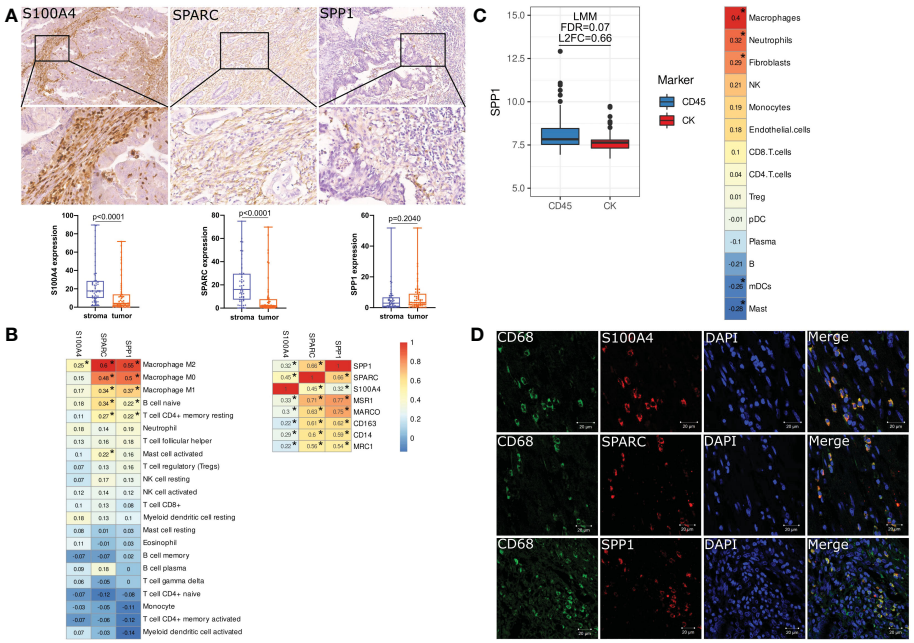

FIGURE 4
S100A4, SPARC and SPP1 are expressed by tumor-associated macrophages in colorectal cancer. **(A)** IHC representative images (x400) of stromal S100A4, SPARC and SPP1 in tumor tissue. Zoom images is given in the lower panel (x800). Stromal expression of S100A4 and SPARC is higher than tumor expression. The protein level of SPP1 does not have differences between tumor and stroma. Student's t-test was applied. **(B)** Immune cell-type deconvolution analysis that was performed *via* the TIMER2.0 web platform using the CIBERSORT method. S100A4, SPP1 and SPARC gene expression correlates with macrophages. *: |rho|>0.2 and FDR<0.05. **(C)** Nanostring GeoMX DSP revealed increased expression of SPP1 in the immune compartment and its correlation with macrophages. *: |rho|>0.2 and FDR<0.05. **(D)** Confocal microscopy confirmed the co-localization of S100A4, SPARC and SPP1 in CD68+ TAMs. Scale bars equal 20 μm.

SPP1 was less expressed in CRC tissue, and its expression was equal in the stromal compartment and in the tumor nest [2,93(0,63-6,67) stroma SPP1 vs. 3,31 (1,52-9,04) tumor SPP1, p=0,204) (Figure 4A).

Using CIBERSORT method, we demonstrated that mRNA expression of SPP1 and SPARC is significantly associated with M0, M1 and M2 macrophage phenotypes, naive B cells and CD4 T cells, while S100A4 gene expression correlates with M2 macrophage phenotype (Figure 4B). SPP1 and SPARC mRNA expression strongly correlated with the expression of MSR1, CD163, MRC1 and MARCO – markers associated with M2 TAM phenotype (Figure 4B).

Additional Nanostring analysis allowed us to reveal that SPP1 is differentially expressed in immune CD45+ and tumor cytokeratin (CK)+ regions. The gene expression of SPP1 was higher in CD45+ compartments compared to CK+ regions (FDR=0.07, L2FC=0.66). SPP1 expression in the distinct regions of CRC was mostly associated with macrophages (Figure 4C).

To confirm the expression of S100A4, SPP1, and SPARC in TAMs, we performed three-color IF analysis of human CRC tissue using confocal microscopy. IF analysis demonstrated that S100A4, SPP1 and SPARC were all expressed in CD68+ TAMs (Figure 4D).

Thus, we demonstrated that levels of S100A4, SPP1 and SPARC are mostly inherent to the stromal component, in particular macrophages. Taken into account the observations made above, we used stromal-derived protein expression of S100A4, SPP1, and SPARC for further survival and correlation analysis.

3.5 Stromal levels of S100A4, SPARC and SPP1 retained an unfavorable prognostic value for patient outcome but became favorable for the pathological tumor parameters

Protein levels of S100A4, SPARC and SPP1 remained unfavorable parameters for survival. In univariate COX analysis and Kaplan–Meier survival analysis, the protein level of S100A4 in high-risk group (expression more than cut-off meaning) remained prognostic only for OS in both combined CRC group of patients (HR=2,141; 95% CI [1,152-3,978], p=0,016) and patients with colon cancer (HR=2,679; 95% CI [1,136-6,320], p=0,024) (Figures 5A, B). In multivariate Cox analysis, S100A4 mRNA expression was not an independent parameter. High protein expression of SPARC and SPP1 was associated with shorter recurrence-free survival (RFS) and PFS, respectively, in patients with rectal cancer (Figures 5C, D, respectively). However, these parameters were not prognostic according to univariate and multivariate Cox analysis.

Interesting that in contrast to mRNA expression, increased protein expression of S100A4, SPARC and SPP1 was a favorable criterion for clinical and pathological parameters. Thus, S100A4 expression was higher in rectal cancer patients having tumor stages I-II compared to patients with stage III (28,20 ± 22,29 vs 21,47 ± 19,29, p=0,046) (Figure 5A). SPARC expression was lower in patients with positive lymphovascular invasion (8,76 (5,62;39,13) vs. 26,19 (14,74;40,15), p=0,0091) and positive vascular invasion (7,68 (5,62;15,19) vs. 23,26 (12,84;40,15), p=0,0047) in CRC group; similar trend was observed in the same groups of RC patients (8,76 (5,62;47,06) vs. 27,53 (19,84;41,00), p=0,014; 8,04 (5,78;14,22) vs. 25,06 (15,30;41,00), p=0,0072) (Figure 5C). Low protein expression of SPP1 was associated with positive vascular invasion in CRC (1,98 (0,60;3,62) vs. 4,14 (1,23;10,80), p=0,0463) and RC (1,01 (0,41;3,43) vs. 3,75 (1,08;12,23), p=0,0341) and with positive lymphovascular invasion in RC patients (2,47 (0,42;3,53) vs. 3,92 (1,08;12,23), p=0,0210) (Figure 5D). No significant associations were found for S100A4, SPARC, and SPP1 with other clinical and pathological parameters.

3.6 Neoadjuvant chemotherapy/ chemoradiotherapy reverse the prognostic value of S100A4

Finally, we found that neoadjuvant chemotherapy (NACT)/ chemoradiotherapy (NCRT) can reverse the activity of S100A4 from the pro-tumor to favorable one. In general, it can be hypothesized, that pro-angiogenic factors can induce formation of blood vessels with different functionality – with different permeability for soluble factors or infiltration of immune cells from one side, and different permeability for cancer cells enhancing metastasis from another side (21, 22). It can be assumed that specific type of vasculature can be beneficial for tumor growth before the treatment onset, while the same type of vasculature can be converted to the favorable for patients once chemotherapy is applied (23, 24). The possible explanation of such effect can be enhanced permeability for the chemotherapy agent or for the selective anti-tumor immune cells. The idea of this study was based on our recent observation that chemotherapy can induce reprogramming of TAMs and launch the dysregulation in the expression of angiogenesis-associated factors (data not shown). Here, we found that stromal levels of S100A4 after treatment were lower in patients treated with NACT/NCRT compared to untreated patients (29,24 ± 22,49 vs. 19,04 ± 17,97, p=0,002), indicating that chemotherapy-based treatment can suppress its expression (Figure 6A). Surprisingly, post-treatment stromal expression of S100A4 was higher in patients who have better response to NACT/NCRT (20,17 (12,87,35,00) for TRG1-2 vs. 12,78 (6,31;26,52) for TRG3-5, p=0,0438) (Figure 6A). Response to NACT/NCRT was estimated by Mandard Tumor Regression Grading (TRG) system.

Using GSE190826 cohort we showed that pre-treatment S100A4 mRNA expression in rectal cancer patients who had not achieve pathological complete response (pCR) after CRT and suffered from the recurrence, was lower than in patients without progression (7,25 ± 0,81 vs. 6,64 ± 0,82, p=0,049) (Figure 6B). The same association was found for SPARC (11,52 ± 1,06 vs. 10,85 ± 0,98, p=0,013) (Figure 6B). Moreover, among non-pCR patients, DFS survival was better in cases with higher expression of S100A4 compared to lower expression (HR=3,068; 95% CI [1,361-6,913], p=0,0068) (Figure 6B).

Our previous observations indicated that S100A4 can be expressed by both M1 and M2 macrophages in tumor tissues (unpublished data). We suppose that chemotherapy can induce re-population of S100A4-expressed M1 and M2 macrophages in tumors.

4 Discussion

Currently, CRC prognosis is largely based on clinical and pathological parameters and focuses on the cancer stage at the time

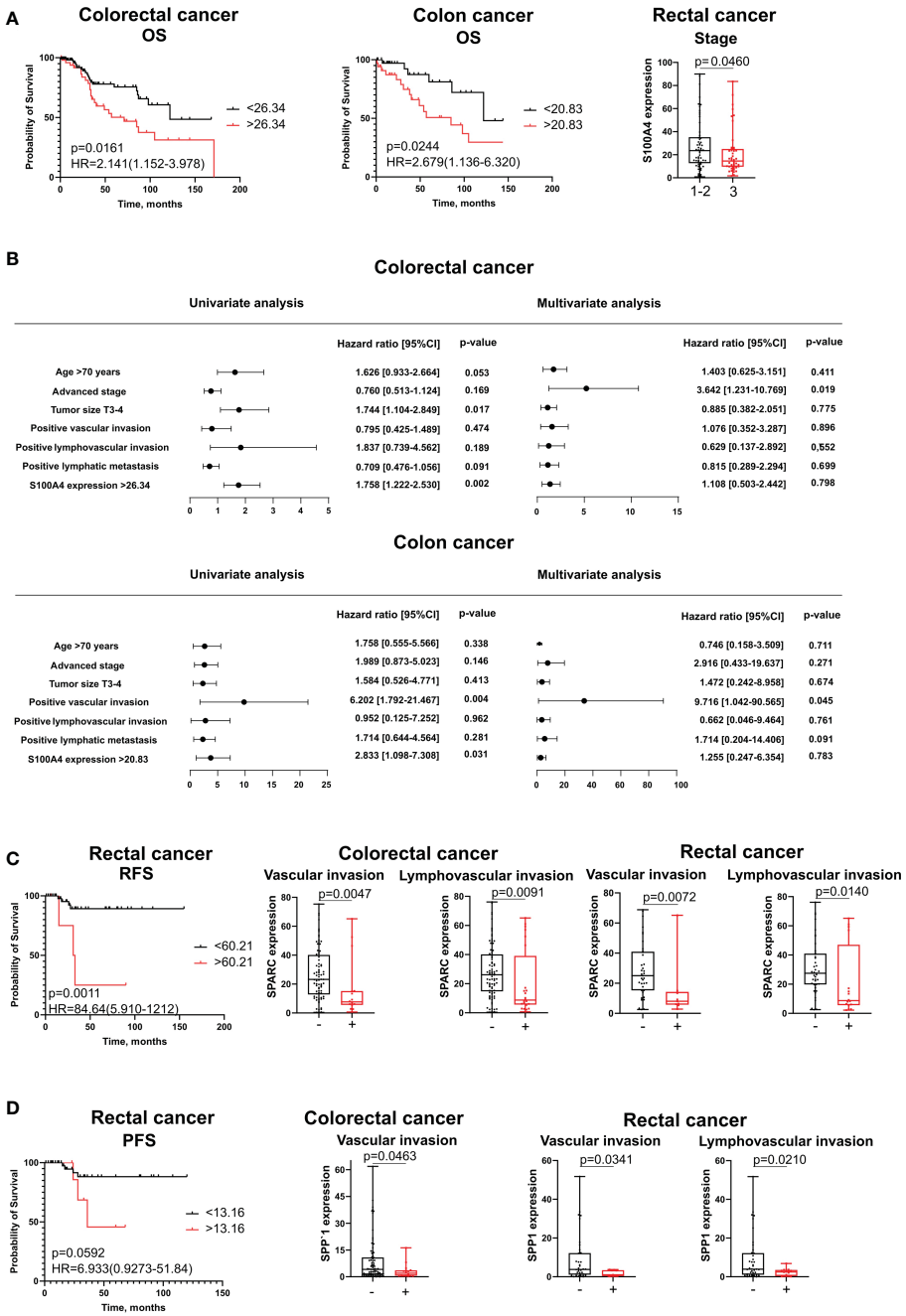

FIGURE 5
The association of stromal expression of S100A4, SPARC and SPP1 with survival and clinical-pathological parameters. **(A)** S100A4 stromal expression predicts poor OS for CRC patients and colon cancer patients, but is negatively correlated with tumor stage in rectal cancer. **(B)** The prognostic significance of S100A4 protein levels for overall survival in patients with CRC and CC revealed by univariate and multivariate COX analysis. **(C)** SPARC stromal expression is an unfavorable parameter for RFS in rectal cancer patients. SPARC protein expression is negatively associated with clinical-pathological parameters in combined CRC group and in rectal cancer patients. **(D)** SPP1 stromal expression is unfavorable for PFS in patients with rectal cancer. SPP1 protein expression is negatively associated with clinical-pathological parameters in combined CRC group and in rectal cancer patients. Log-rank test p-values are shown in Kaplan-Meier plots. Mann-Whitney U test was applied for the comparison of two groups. Box plots depict protein expression (min, Q1, median, Q3, max).

of diagnosis (25). Clinically validated prognostic biomarkers that can identify "high-risk" CRC patients are currently missing (25). Among cells of immune infiltrate, only T lymphocytes were included in Immunoscore classifier that was proposed for survival prediction: patients with "hot" tumors (where CD3+ and CD8+ T cells were detected) exhibit better RFS than patients with "cold" tumors (26, 27).

Here, for the first time, we performed the complex analysis of mRNA expression using TCGA and GEO datasets, and protein expression using quantitative IHC of clinical samples for crucial regulators of tumor angiogenesis and tumor progression, expressed by tumor-associated macrophages: S100A4, SPP1 and SPARC (13). We considered colon and rectal cancer as two tumor entities as

10.3389/fonc.2023.1058337

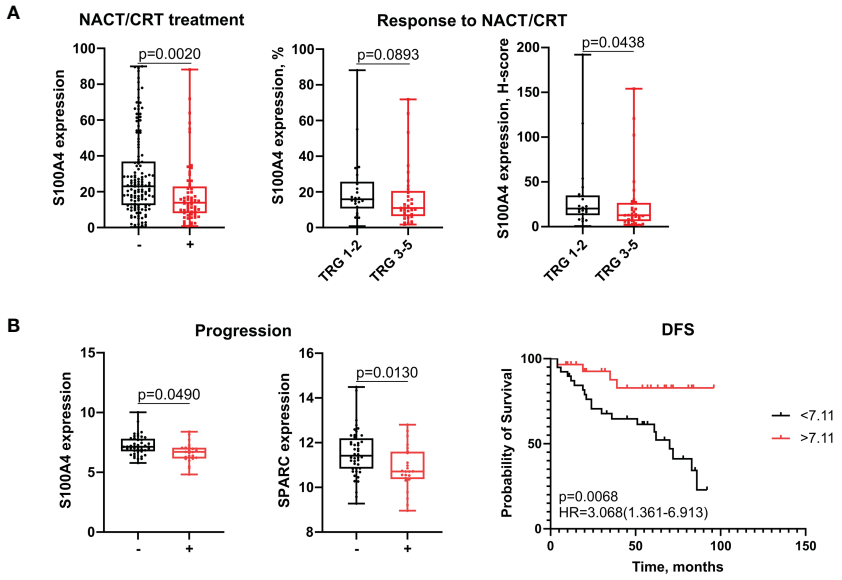

FIGURE 6
S100A4 is associated with improved outcomes in patients undergone neoadjuvant chemotherapy-based treatment. **(A)** Stromal expression of S100A4 decreased in treated patients and correlated with favorable response to NACT/CRT. **(B)** S100A4 and SPARC mRNA expression decreased in non-responders with progression. S100A4 high-risk score predicts better DFS. Mann-Whitney U test was applied. Box plots depict protein **(A)** and gene **(B)** expression (min, Q1, median, Q3, max). Log-rank test p-value is shown in Kaplan-Meier plot.

accumulating clinical data showed their differences in the prognosis and treatment strategies (28).

Using TCGA, survival analysis demonstrated that S100A4, SPP1 and SPARC could be promising predictors for the unfavorable outcome. In particular, S100A4 accurately predicted poor survival with high sensitivity and specificity for patients with CRC independently on cancer type, so S100A4 can be a universal unfavorable predictor in colon and rectal cancers. SPARC mRNA expression was a more specific marker for colon cancer patients. SPP1 mRNA expression was found to have a more significant predictive value for PFS in both rectal and colon cancers. Multivariate COX analysis also revealed that prognostic model consisting of S100A4 (HR=8,43; 95% CI [5,296-13,426], p<0,0001), SPARC (HR=1,86; 95% CI [1,141-3,041], p=0,012) and SPP1 (HR=1,86; 95% CI [1,124-308], p=0,058) can be established for the PFS in CRC cohort. Literature data indicate that in several cohorts of CRC, high SPP1 gene mRNA expression was associated with shorter OS, higher S100A4 expression – with shorter DFS and OS, and high SPARC expression – with worse DFS (29–33). These cohorts include patients with I-IV stages of CRC or only colon cancer, or only rectal cancer. We for the first time performed complex analysis of S100A4, SPP1 and SPARC mRNA levels in terms of survival rates in common CRC groups and in patients with colon and rectal cancer separately.

Next, we found significant correlation of S100A4, SPP1 and SPARC with the amount and M2 phenotype of TAMs. Confocal analysis confirmed the co-expression of these proteins in CD68+ TAMs in human CRC tissue. The co-expression of S100A4 and SPARC in CD68+ TAMs in human CRC tissue was demonstrated by us for the first time. We were able to find only one study describing the co-localization of CD68 and SPP1 in tumor stromal components in human CRC (34). Additionally, Nanostring technology allowed to find elevated expression of SPP1 in CD45+ immune compartment compared to CK+ tumor cell compartment as well as strong correlation of SPP1 with macrophage count in CRC tissues.

We found that, in contrast to mRNA expression level, S100A4, SPP1 and SPARC, stromal level negatively correlated with clinical-pathological parameters. These data correspond to the results found for other cohorts analyzed by IHC using tissue microarrays. In a cohort of 134 patients with CRC, negative correlations were found between SPP1 expression and distant metastasis, tumor invasion, tumor grade, and recurrence (35). In a cohort of 114 patients with colon cancer, a significant negative association was observed for SPARC expression in mesenchymal and stromal cells with the differentiation of tumors (36). For S100A4, several studies did not show any association of its protein expression with pathological parameters other than survival rates (32, 37, 38).

Interestingly, that stromal expression of SPARC and SPP1 was prognostic for the reduced RFS and PFS, respectively, only in rectal cancer patients, while S100A4 correlated with poor OS rates in CRC and colon cancer patients. Such controversial data can be explained by the dual role of TAMs in CRC progression. A few reports indicate that high amounts of TAMs that are the most abundant innate immune cell population in CRC are beneficial to CRC patients (39, 40).

Finally, we found that neoadjuvant chemotherapy (NACT)/chemoradiotherapy (NCRT) can reverse the association of S100A4 with prognosis from the tumor progression-associated to favorable one. Accumulating evidence showed that chemotherapy can induce re-polarization of macrophages in the TME (8). Chemotherapy-based treatment suppressed stromal expression of S100A4. Notably, S100A4 stromal levels were higher in patients with better response to NACT/CRT, and S100A4 mRNA levels predicted better DFS among non-responders. It can be explained by the mechanism of re-population of TAMs after chemotherapeutic intervention. It can be also assumed that

specific type of vasculature can be beneficial for tumor growth before the treatment onset, while the same type of vasculature can be converted to the favorable for patients once chemotherapy is applied (23, 24).

Thus, we demonstrated high prognostic significance of angiogenesis-associated factors S100A4, SPP1 and SPARC that are produced by TAMs in colorectal cancer. Our findings can help improve the prognosis of patients with CRC based on S100A4, SPP1 and SPARC expression levels. S100A4, SPP1 and SPARC can be helpful targets for developing novel immunotherapy and anti-angiogenic therapy approaches.

Data availability statement

All data needed to evaluate the conclusions in the paper are presented in the paper and the Supplementary Material. Additional data related to this paper may be requested from authors. GEO data set was accessed *via* NCBI GEO Repositorium: https://www.ncbi.nlm.nih.gov/geo/query/acc.cgi?acc=GSE190826. TCGA-COAD and TCGA-READ data sets were obtained from NIH GDC data portal: https://portal.gdc.cancer.gov/. Results of NGS-GeoMx DSP analysis are presented in NCBI data portal (GSE221924): https://www.ncbi.nlm.nih.gov/geo/query/acc.cgi?acc=GSE221924.

Ethics statement

This study was performed in line with the principles of the Declaration of Helsinki. Approval was granted by the local committee of Medical Ethics of Tomsk Cancer Research Institute. Informed consent was obtained from all individual participants included in the study.

Author contributions

The study was conceptualized by IL and JK; EK, MR, TS, LT performed experiments and analyzed data; PI prepared the bioinformatics data analysis; AT, SA, AD, LZ and NC provided clinical data and enrolled the patients; IL, EK and MR wrote the manuscript with input from all authors. IL and JK interpreted data and contributed to the discussion.

Funding

This work was supported by Russian Foundation for Basic Research (RFBR), project number 20-015-00384A (to I. Larionova), Russian Science Foundation (RSF), project number 19-15-00151 (to J. Kzhyshkowska), and by Tomsk State University Development Programme (Priority-2030). Work was carried out on equipment of Tomsk regional common use center and The Core Facility «Medical genomics», Tomsk NRMC. Nanostring technology was performed at the NanoString Center (Siberian State Medical University).

Conflict of interest

The authors declare that the research was conducted in the absence of any commercial or financial relationships that could be construed as a potential conflict of interest.

Publisher's note

Supplementary material

The Supplementary Material for this article can be found online at: https://www.frontiersin.org/articles/10.3389/fonc.2023.1058337/full#supplementary-material

References

1. Xi Y, Xu P. Global colorectal cancer burden in 2020 and projections to 2040. *Transl Oncol* (2021) 14:101174. doi: 10.1016/j.tranon.2021.101174

2. Molinari C, Marisi G, Passardi A, Matteucci L, De Maio G, Ulivi P. Heterogeneity in colorectal cancer: A challenge for personalized medicine? *Int J Mol Sci* (2018) 19:3733. doi: 10.3390/ijms19123733

3. Zheng Z, Yu T, Zhao X, Gao X, Zhao Y, Liu G. Intratumor heterogeneity: A new perspective on colorectal cancer research. *Cancer Med* (2020) 9:7637–45. doi: 10.1002/cam4.3323

4. Li F, Lai M. Colorectal cancer, one entity or three. *J Zhejiang Univ Sci B* (2009) 10:219–29. doi: 10.1631/jzus.B0820273

5. Jafarov S, Link KH. Colon and rectal cancer are different tumor entities according to epidemiology, carcinogenesis, molecular- and tumor biology, primary and secondary prevention: preclinical evidence. *Sib J Oncol* (2018) 17:88–98. doi: 10.21294/1814-4861-2018-17-4-88-98

6. Hossain MS, Karuniawati H, Jairoun AA, Urbi Z, Ooi J, John A, et al. Colorectal cancer: A review of carcinogenesis, global epidemiology, current challenges, risk factors, preventive and treatment strategies. *Cancers (Basel).* (2022) 14(7):1732. doi: 10.3390/cancers14071732

7. Hu T, Li Z, Gao C-Y, Cho CH. Mechanisms of drug resistance in colon cancer and its therapeutic strategies. *World J Gastroenterol* (2016) 22:6876–89. doi: 10.3748/wjg.v22.i30.6876

8. Larionova I, Cherdyntseva N, Liu T, Patysheva M, Rakina M, Kzhyshkowska J. Interaction of tumor-associated macrophages and cancer chemotherapy. *Oncoimmunology* (2019) 8:1596004. doi: 10.1080/2162402X.2019.1596004

9. Anderson NM, Simon MC. The tumor microenvironment. *Curr Biol* (2020) 30:R921–5. doi: 10.1016/j.cub.2020.06.081

10. Giraldo NA, Sanchez-Salas R, Peske JD, Vano Y, Becht E, Petitprez F, et al. The clinical role of the TME in solid cancer. *Br J Cancer* (2019) 120:45–53. doi: 10.1038/s41416-018-0327-z

11. Cassetta L, Pollard JW. Targeting macrophages: therapeutic approaches in cancer. *Nat Rev Drug Discovery* (2018) 17:887–904. doi: 10.1038/nrd.2018.169

12. Viallard C, Larrivée B. Tumor angiogenesis and vascular normalization: Alternative therapeutic targets. *Angiogenesis* (2017) 20:409–26. doi: 10.1007/s10456-017-9562-9

13. Larionova I, Kazakova E, Gerashchenko T, Kzhyshkowska J. New angiogenic regulators produced by TAMs: Perspective for targeting tumor angiogenesis. *Cancers (Basel)* (2021) 13:3253. doi: 10.3390/cancers13133253

14. Li T, Fu J, Zeng Z, Cohen D, Li J, Chen Q, et al. TIMER2.0 for analysis of tumor-infiltrating immune cells. *Nucleic Acids Res* (2020) 48:W509–14. doi: 10.1093/nar/gkaa407

15. Sturm G, Finotello F, Petitprez F, Zhang JD, Baumbach J, Fridman WH, et al. Comprehensive evaluation of transcriptome-based cell-type quantification methods for immuno-oncology. *Bioinformatics* (2019) 35(14):i436–45. doi: 10.1093/bioinformatics/btz363

16. Newman AM, Liu CL, Green MR, Gentles AJ, Feng W, Xu Y, et al. Robust enumeration of cell subsets from tissue expression profiles. *Nat Methods* (2015) 12:453–7. doi: 10.1038/nmeth.3337

17. Ortogero N, Yang Z, Vitancol R, Griswold M HD. GeomxTools: NanoString GeoMx tools. *R Package version* (2022) 3:. doi: 10.18129/B9.bioc.GeomxTools

18. Ambartsumian N, Klingelhöfer J, Grigorian M. The multifaceted S100A4 protein in cancer and inflammation BT - calcium-binding proteins of the EF-hand superfamily: From basics to medical applications. *Springer New York* (2019) 1929:339–65. doi: 10.1007/978-1-4939-9030-6_22

19. Said N, Frierson HF, Sanchez-Carbayo M, Brekken RA, Theodorescu D. Loss of SPARC in bladder cancer enhances carcinogenesis and progression. *J Clin Invest.* (2013) 123(2):751–66. doi: 10.1172/JCI64782

20. Butti R, Kumar TVS, Nimma R, Banerjee P, Kundu IG, Kundu GC. Osteopontin signaling in shaping tumor microenvironment conducive to malignant progression. *Adv Exp Med Biol* (2021) 1329:419–41. doi: 10.1007/978-3-030-73119-9_20

21. Nagy JA, Benjamin L, Zeng H, Dvorak AM, Dvorak HF. Vascular permeability, vascular hyperpermeability and angiogenesis. *Angiogenesis* (2008) 11:109–19. doi: 10.1007/s10456-008-9099-z

22. Tomita T, Kato M, Hiratsuka S. Regulation of vascular permeability in cancer metastasis. *Cancer Sci* (2021) 112:2966–74. doi: 10.1111/cas.14942

23. Ma J, Waxman DJ. Combination of antiangiogenesis with chemotherapy for more effective cancer treatment. *Mol Cancer Ther* (2008) 7:3670–84. doi: 10.1158/1535-7163.MCT-08-0715

24. Mpekris F, Baish JW, Stylianopoulos T, Jain RK. Role of vascular normalization in benefit from metronomic chemotherapy. *Proc Natl Acad Sci USA* (2017) 114:1994–9. doi: 10.1073/pnas.1700340114

25. Koncina E, Haan S, Rauh S, Letellier E. Prognostic and predictive molecular biomarkers for colorectal cancer: Updates and challenges. *Cancers (Basel)* (2020) 12. doi: 10.3390/cancers12020319

26. Pagès F, Mlecnik B, Marliot F, Bindea G, Ou F-S, Bifulco C, et al. International validation of the consensus immunoscore for the classification of colon cancer: a prognostic and accuracy study. *Lancet* (2018) 391:2128–39. doi: 10.1016/S0140-6736(18)30789-X

27. Galon J, Pagès F, Marincola FM, Angell HK, Thurin M, Lugli A, et al. Cancer classification using the immunoscore: a worldwide task force. *J Transl Med* (2012) 10:205. doi: 10.1186/1479-5876-10-205

28. van der Sijp MPL, Bastiaannet E, Mesker WE, van der Geest LGM, Breugom AJ, Steup WH, et al. Differences between colon and rectal cancer in complications, short-term survival and recurrences. *Int J Colorectal Dis* (2016) 31:1683–91. doi: 10.1007/s00384-016-2633-3

29. Wei T, Bi G, Bian Y, Ruan S, Yuan G, Xie H, et al. The significance of secreted phosphoprotein 1 in multiple human cancers. *Front Mol Biosci* (2020) 7:565383. doi: 10.3389/fmolb.2020.565383

30. Choe EK, Yi JW, Chai YJ, Park KJ. Upregulation of the adipokine genes ADIPOR1 and SPP1 is related to poor survival outcomes in colorectal cancer. *J Surg Oncol* (2018) 117:1833–40. doi: 10.1002/jso.25078

31. Liu Y, Tang W, Wang J, Xie L, Li T, He Y, et al. Clinicopathological and prognostic significance of S100A4 overexpression in colorectal cancer: A meta-analysis. *Diagn Pathol* (2013) 8:181. doi: 10.1186/1746-1596-8-181

32. Boye K, Jacob H, Frikstad K-AM, Nesland JM, Mælandsmo GM, Dahl O, et al. Prognostic significance of S100A4 expression in stage II and III colorectal cancer: Results from a population-based series and a randomized phase III study on adjuvant chemotherapy. *Cancer Med* (2016) 5:1840–9. doi: 10.1002/cam4.766

33. Drev D, Harpain F, Beer A, Stift A, Gruber ES, Klimpfinger M, et al. Impact of fibroblast-derived SPARC on invasiveness of colorectal cancer cells. *Cancers (Basel)* (2019) 11. doi: 10.3390/cancers11101421

34. Rao G, Wang H, Li B, Huang L, Xue D, Wang X, et al. Reciprocal interactions between tumor-associated macrophages and CD44-positive cancer cells *via* osteopontin/CD44 promote tumorigenicity in colorectal cancer. *Clin Cancer Res an Off J Am Assoc Cancer Res* (2013) 19:785–97. doi: 10.1158/1078-0432.CCR-12-2788

35. Assidi M, Gomaa W, Jafri M, Hanbazazh M, Al-Ahwal M, Pushparaj P, et al. Prognostic value of osteopontin (SPP1) in colorectal carcinoma requires a personalized molecular approach. *Tumor Biol* (2019) 41:1010428319863627. doi: 10.1177/1010428319863627

36. Liang J, Wang H, Xiao H, Li N, Cheng C, Zhao Y, et al. Relationship and prognostic significance of SPARC and VEGF protein expression in colon cancer. *J Exp Clin Cancer Res* (2010) 29:71. doi: 10.1186/1756-9966-29-71

37. Kwak J-M, Lee H-J, Kim S-H, Kim H-K, Mok Y-J, Park Y-T, et al. Expression of protein S100A4 is a predictor of recurrence in colorectal cancer. *World J Gastroenterol* (2010) 16:3897–904. doi: 10.3748/wjg.v16.i31.3897

38. Destek S, Gul VO. S100A4 may be a good prognostic marker and a therapeutic target for colon cancer. *J Oncol* (2018) 2018:1828791. doi: 10.1155/2018/1828791

39. Larionova I, Tuguzbaeva G, Ponomaryova A, Stakheyeva M, Cherdyntseva N, Pavlov V, et al. Tumor-associated macrophages in human breast, colorectal, lung, ovarian and prostate cancers. *Front Oncol* (2020) 10:566511. doi: 10.3389/fonc.2020.566511

40. Zhong X, Chen B, Yang Z. The role of tumor-associated macrophages in colorectal carcinoma progression. *Cell Physiol Biochem* (2018) 45:356–65. doi: 10.1159/000486816

frontiers | Frontiers in Oncology

TYPE Original Research
PUBLISHED 14 March 2023
DOI 10.3389/fonc.2023.1048521

OPEN ACCESS

EDITED BY
Carlos Pérez-Plasencia,
National Autonomous University of Mexico, Mexico

REVIEWED BY
Arsheed A. Ganaie,
University of Minnesota Twin Cities, United States
Kenichi Takayama,
Tokyo Metropolitan Institute of Gerontology, Japan
Wanting Han,
Fred Hutchinson Cancer Research Center, United States

*CORRESPONDENCE
Yongbo Zheng
zhengyongbo2019@163.com
Jiayu Liu
urologistliu2022@163.com

†These authors have contributed equally to this work

SPECIALTY SECTION
This article was submitted to Molecular and Cellular Oncology, a section of the journal Frontiers in Oncology

RECEIVED 19 September 2022
ACCEPTED 27 February 2023
PUBLISHED 14 March 2023

CITATION
Yang G, Chen X, Quan Z, Liu M, Guo Y, Tang Y, Peng L, Wang L, Wu Y, Wu X, Liu J and Zheng Y (2023) Comprehensive analysis of the FOXA1-related ceRNA network and identification of the MAGI2-AS3/DUSP2 axis as a prognostic biomarker in prostate cancer. *Front. Oncol.* 13:1048521. doi: 10.3389/fonc.2023.1048521

Comprehensive analysis of the FOXA1-related ceRNA network and identification of the MAGI2-AS3/DUSP2 axis as a prognostic biomarker in prostate cancer

Guo Yang[1†], Xiong Chen[2†], Zhen Quan[1], Miao Liu[1], Yuan Guo[1], Yangbin Tang[1], Lang Peng[1], Leilei Wang[3], Yingying Wu[3], Xiaohou Wu[1], Jiayu Liu[1*] and Yongbo Zheng[1*]

[1]Department of Urology, The First Affiliated Hospital of Chongqing Medical University, Chongqing, China, [2]Department of Urology, The Ninth People's Hospital of Chongqing, Chongqing, China, [3]Key Laboratory of Laboratory Medical Diagnostics, Ministry of Education, Chongqing Medical University, Chongqing, China

Background: Prostate cancer (PCa) is the second most common cause of cancer-related deaths in American men. Even though increasing evidence has disclosed the competitive endogenous RNA (ceRNA) regulatory networks among cancers, the complexity and behavior characteristics of the ceRNA network in PCa remain unclear. Our study aimed to investigate the forkhead box A1 (FOXA1)-related ceRNA regulatory network and ascertain potential prognostic markers associated with PCa.

Methods: RNA sequence profiles downloaded from The Cancer Genome Atlas (TCGA) were analyzed to recognize differentially expressed genes (DEGs) derived from tumor and non-tumor adjacent samples as well as FOXA1^{low} and FOXA1^{high} tumor samples. The enrichment analysis was conducted for the dysregulated mRNAs. The network for the differentially expressed long non-coding RNA (lncRNA)-associated ceRNAs was then established. Survival analysis and univariate Cox regression analysis were executed to determine independent prognostic RNAs associated with PCa. The correlation between DUSP2 and immune cell infiltration level was analyzed. Tissue and blood samples were collected to verify our network. Molecular experiments were performed to explore whether DUSP2 is involved in the development of PCa.

Results: A ceRNA network related to FOXA1 was constructed and comprised 18 lncRNAs, 5 miRNAs, and 44 mRNAs. The MAGI2-AS3~has-mir-106a/has-mir-204~DUSP2 ceRNA regulatory network relevant to the prognosis of PCa was obtained by analysis. We markedly distinguished the MAGI2-AS3/DUSP2 axis in the ceRNA. It will most likely become a clinical prognostic model and impact the changes in the tumor immune microenvironment of PCa. The abnormal MAGI2-AS3 expression level from the patients' blood manifested that it would be a novel potential diagnostic biomarker for PCa. Moreover, down-expressed DUSP2 suppressed the proliferation and migration of PCa cells.

Conclusions: Our findings provide pivotal clues to understanding the role of the FOXA1-concerned ceRNA network in PCa. Simultaneously, this MAGI2-AS3/DUSP2 axis might be a new significant prognostic factor associated with the diagnosis and prognosis of PCa.

KEYWORDS

MAGI2-AS3, DUSP2, ceRNA, prostate cancer, FOXA1

1 Introduction

Prostate cancer (PCa) is the most prevalent cancer among men and is the second leading cause of cancer-related death, with an estimated 248,530 new cases and 34,130 deaths in 2021 in the United States (1). In recent years, despite the growing numbers of PCa patients identified through prostate-specific antigen (PSA) screening, imaging technique, and histopathological scores, approximately 25% of PCa patients will experience recurrence and metastasis, and the PCa will develop into castration-resistant prostate cancer (CRPC), leading to poor progression-free survival (PFS) (2). Therefore, it is momentous to explore effective prognostic biomarkers and/or therapeutic targets for PCa to improve our cognition in the diagnosis, prevention, and treatment of this cancer.

The Forkhead box (Fox) family, an evolutionarily conserved family of transcription factors binding to condensed, inactive chromatin and initiating chromatin remodeling, plays an essential role in human health and disease (3). The forkhead box A1 (FOXA1) protein is a member of a group of special transcription factors called pioneer factors; it is a crucial transcription factor in the initiation and development of breast, prostate, and lung cancers (4–6). In PCa, FOXA1 plays an indispensable role in androgen receptor (AR)-mediated gene regulation by interacting directly with AR and co-occupying chromatin (7). In breast cancer, silencing of FOXA1 expression by Twist1 is the main cause of Twist1-induced migration, invasion, and metastasis (8). However, previous studies of the transcriptional network for FOXA1 were mostly focused on protein-coding genes and its regulatory network of long non-coding RNAs (lncRNAs), and their role in FOXA1 oncogenic activity remains unknown.

lncRNAs refer to non-protein-coding RNAs consisting of longer than 200 nucleotides. In recent years, numerous studies have expounded that lncRNA accounts for a large proportion of microRNA in the cell (mainly in the cytoplasm) and can buffer or reduce the miRNA's ability to degrade target gene mRNA and interfere with the translation process like a "sponge", which is elaborated as a ceRNA network (9). There have been studies illustrating that lncRNAs play a remarkable role in a wide range of biological processes, including autophagy, infarction, cell senescence, apoptosis, cancer cell metastasis, and resistance to chemotherapeutic agents (10, 11). Other than that, they can also accommodate gene expression by a diversity of mechanisms, such as epigenetic modification, selective splicing, nuclear import, precursors to small RNAs, and even as regulators of mRNA modifiers or decoy elements (12). A growing number of aberrantly expressed lncRNAs are found in cancer, and it has shown promise as a biomarker to improve early tumor detection, monitoring of tumor treatment and relapse, and so on (13, 14). Despite the lncRNA expression specificity opening up great opportunities for exploring new biomarkers and drug targets, it remains challenging to affirm lncRNA involved in regulatory networks.

MicroRNAs (miRNAs), a kind of small non-coding long single-stranded RNA with 19–25 nucleotides, can induce RNA silencing, are involved in post-transcriptional regulation of gene expression, and play an important role in a variety of cellular functions by binding to the 3' untranslated region (UTR) of its target mRNA (15). We have learned that miRNAs mediated approximately 30% of genes in the human genome, whereas miRNA regulates post-transcriptional regulation and requires multiple RNA-binding proteins, which are beneficial to the function of miRNA in tumorigenesis (16). In 2011, Salmena et al. first put forward the competitive endogenous RNA (ceRNA) hypothesis that lncRNA mainly regulates mRNA through a ceRNA regulation mechanism, described as a new mechanism of interaction among RNAs (17). Meanwhile, increasing studies elaborated that miRNA acts as ceRNA in lncRNA–miRNA–mRNA form and is involved in various kinds of tumorigenesis, such as stomach cancer (18), breast cancer (19), kidney cancer (20), and PCa (21).

In this study, we conducted a systemic analysis of FOXA1-regulated oncogenic lncRNAs and constructed a ceRNA network related to FOXA1, as well as related to the prognosis of PCa (Figure 1). We chose a FOXA1-inducible lncRNA MAGI2-AS3 that is expressed in PCa and selected the FOXA1/MAGI2-AS3/DUSP2 axis in the ceRNA network as a potential prognostic model. Mechanistically, our study illuminated that the downregulated MAGI2-AS3 may function as a competing endogenous RNA for has-mir-106a or has-mir-204 to regulate the expression of DUSP2. We assessed this ceRNA axis' value in the diagnosis of PCa and evaluated the potential relationship between DUSP2 and tumor-infiltrated immune cell levels. Furthermore, we verified the mRNA and protein levels of DUSP2 in clinical samples, and functional experiments showed that down-expressed DUSP2 inhibited the proliferation and migration of PCa cells.

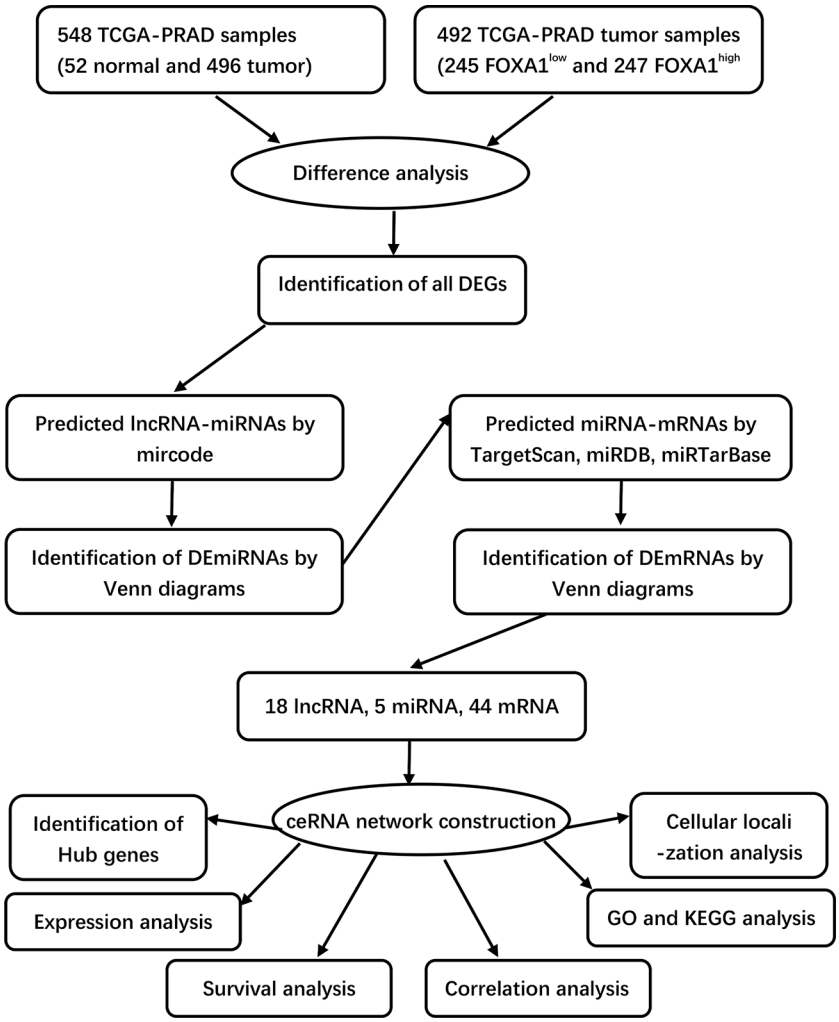

FIGURE 1
Flowchart of construction and analysis of ceRNA.

2 Materials and methods

2.1 Patient samples

A total of 20 benign prostatic hyperplasia (BPH) and 20 PCa patients' tissue specimens and corresponding anti-coagulant blood (3–4 ml) specimens were obtained from patients in the Department of Urology, the First Affiliated Hospital of Chongqing Medical University (China). Two clinicians finished the clinical diagnosis according to prostate puncture biopsy or/and PSA level. The patients provided their written informed consent to participate in this study. The studies involving human participants were reviewed and approved by the Ethics Committee of Chongqing Medical University (Ethics Approval No. 2022-K275).

2.2 Data preparation and processing

PCa datasets including RNA-seq and miRNA-seq from The Cancer Genome Atlas (TCGA)–PRAD datasets (https://portal.gdc.cancer.gov/) were downloaded; 52 normal and 496 tumor samples were included. Next, the data were constructed into a matrix. Ensemble names of genes were changed into symbol names using Microsoft R software (version 4.0.3) and then Homo sapiens. The GRCh38 database was used to distinguish gene types. All raw RNA-seq data (lncRNAs, miRNAs, and mRNAs) were normalized to fragments per kilobase of exon model per million mapped fragments (FPKM). The corresponding clinical data were also downloaded from the TCGA dataset and the needed information on tumor samples was extracted from it using R software.

Furthermore, we also downloaded two gene microarray datasets from Gene Expression Omnibus (GEO, http://www.ncbi.nlm.nih.gov/geo/), as they analyzed the gene expression profiles in tumor and normal tissues from PCa patients [GSE21036: normal, n = 28; tumor, n = 113 in which the Vcap cell line sample was deleted; GSE60329: normal, n = 28; tumor, n = 108 (22)]; the series matrix files were extracted from the GEO database, and the probe IDs were switched to gene symbols through corresponding platforms (GSE21036: GPL8227; GSE60329: GPL14550) to further validate our results. HPA (http://

www.proteinatlas.org/) search was conducted to confirm the expression of FOXA1 in PCa at the protein level. We obtained the mutation status of FOXA1 by exploring publicly available genomic data from the cBioPortal for Cancer Genomics (http://www.cbioportal.org/).

2.3 Differential expression analysis

Co-expression in PCa was evaluated using TCGA. The tumor group was compared with the non-tumor group, with $|\log_2$(fold change FC)$|$ > 1.0 and adjusted p-value < 0.05 as cutoff criteria and the "edgeR" package was used to identify differentially expressed mRNAs (DEmRNAs), differentially expressed miRNAs (DEmiRNAs), and differentially expressed lncRNAs (DElncRNAs). Because there is slightly less DEGs between the group of FOXA1^{high} and FOXA1^{low}, when performing differential expression analysis in the two groups in PCa samples, we detected DElncRNAs with a threshold of |logFC| > 0.5 and p < 0.05, DEmiRNAs with a threshold of |logFC| > 0.3 and p < 0.05, and DEmRNAs with a threshold of |logFC| >0.5 as the cutoff criteria and p < 0.05. All p-values were corrected for statistical significance using the false discovery rate (FDR) with multiple testing (Benjamini–Hochberg method). The FDR significance level was 0.05. Volcano plots of DERNAs, including DElncRNAs, DEmiRNAs, and DEmRNAs, were visualized using the "ggplot2" software package. Heatmap clusters were drawn using TBtools software (version 1.051).

2.4 LncRNA–miRNA–mRNA network construction

Based on the hypothesis that lncRNAs can indirectly regulate mRNA expression by competing with miRNAs as natural sponges in the cytoplasm, a ceRNA network was built through the following steps: (1) the Venn Diagram package in R software was developed to identify all DEGs; (2) miRcode (http://mircode.org/) was utilized to forecast the potential miRNAs targeted by DElncRNAs and the lncRNA–miRNA interaction pairs, and a Venn Diagram was used to compare the target genes with DEmiRNAs, which overlapped with DEmiRNAs selected for the next analysis; (3) miRDB (http://www.mirdb.org/), miRTarBase (http://mirtarbase.mbc.nctu.edu.tw/php/index.php), and TargetScan (http://www.targetscan.org/) were used to predict the target genes of the DEmiRNAs and construct the miRNA–mRNA interaction pairs; (4) the Venn Diagram package in R software was utilized to compare the target genes with DEmRNAs, and the target genes overlapped with DEmRNAs that were picked out for the next analysis; and (5) by integrating the lncRNA–miRNA pairs with miRNA–mRNA pairs, we constructed the lnRNA–miRNA–mRNA triple regulatory network.

The DElncRNA sequences were acquired by seeking the LNCipedia (https://lncipedia.org/) database, while the lncLocator (http://www.csbio.sjtu.edu.cn/bioinf/lncLocator/) database was utilized to predict the DElncRNA cellular localization according to the sequences. The hub triple regulatory network was identified by the Cytoscape plug-in cytoHubba tool. The generated networks were visualized by Cytoscape software (version 3.7.0, https://www.cytoscape.org/).

2.5 Functional enrichment analysis

Gene Ontology (GO) is a database constructed by the Association for Gene Ontology. GO annotations can be divided into three categories, comprising biological process (BP), cellular components (CC), and molecular function (MF). Kyoto Encyclopedia of Genes and Genomes (KEGG) is a comprehensive database integrating genomic, chemical, and systemic functional information, of which the KEGG pathway is specifically dedicated to storing genetic pathway information between different species. To explore the biological functions of the candidate gene modules, the R software package "Cluster Profiler" (version 3.14.3) was used to conduct analysis for these genes. The minimum gene set was set to 5 and the maximum gene set was set to 500. p < 0.05 and FDR < 0.25 were considered statistically significant. Moreover, the GEO dataset (GSE60329) was utilized to analyze the DUSP2 of tumor immune-related pathways *via* gene set enrichment analysis (GSEA).

2.6 Survival analysis and construction of a specific prognosis model for PCa

We used Sangerbox 3.0 (http://vip.sangerbox.com) to perform Kaplan–Meier analysis on DElncRNAs, DEmiRNAs, and DEmRNAs in the ceRNA network to determine the relationship between the expression and the PFS of PCa patients in the TCGA database. Log-rank test was used to assess statistical significance and p < 0.05 was considered statistically significant. Additionally, univariate Cox regression analysis was utilized to analyze the association between candidate genes in the ceRNA network and clinicopathological features of PCa patients.

2.7 Immune infiltrate levels and immunotherapy analysis of DUSP2

An online tool—tumor immune estimation resource (TIMER) (https://cistrome.shinyapps.io/timer/)—was applied to visualize the correlation between the expression of DUSP2 and the infiltrating level of different subsets of immune cells. Moreover, immunotherapy and drug sensitivity analysis was exerted between low DUSP2 expression and high DUSP2 expression groups *via* TICA (https://tcia.at/home) and pRRophetic R package, respectively.

2.8 Reverse transcription and quantitative real-time PCR

Total RNA was extracted from tissue and blood samples using TRIzol (Takara), and reverse transcription was performed by the Prime Script RT reagent kit according to the manufacturer's protocols (Takara). Real-time PCR was performed with the SYBR

Premix Ex Taq™ II kit (Takara). The expression of genes was calculated by the comparative $2^{-\Delta\Delta CT}$ method. The sequences of the primers were as follows: MAGI2-AS3 sense, 5′-GAGCACA TATCAATGAAGAA-3′ and antisense, 5′-ATCACCATCTC TCAAC TC-3′; and β-actin sense, 5′-TGACGT GGACATCCG CAA AG-3′ and antisense, 5′-CTGGA AGGTGGACAGCGAGG-3′. All gene expressions were normalized against β-actin and experiments were performed in triplicate at least.

2.9 Immunohistochemistry

All tissue samples were fixed in 10% neutral formalin, embedded in paraffin, and cut into 5-μm-thick sections. The tissue slides were prepared and deparaffinized by baking in an oven at 60°C for 1 h. The slices were dewaxed in xylene, rehydrated in a graded series of alcohols, and then antigen unmasking was done in a boiling container with sodium citrate buffer for 20 min, blocked with goat serum. Slides were then stained with DUSP2 antibody (1:500, Sigma, SAB4300841) overnight at 4°C. After PBS washing, the slices were incubated with goat anti-rabbit secondary antibodies for 1 h at room temperature. After adding substrate and hematoxylin staining, slides were covered and observed using a microscope. ImageJ software was used to analyze the staining intensity and positive rate score. BPH and tumor tissues were categorized as high and low expression according to whether staining cells ≥5% (23).

2.10 Cells, cell culture, and transfection

22RV1was purchased from the Cell Bank of the Chinese Academy of Sciences (Shanghai, China). Cells were cultured in RPMI 1640 (Gibco, USA) added with 10% FBS (Gibco, Thermo Fisher Scientific) under atmosphere containing 5% CO_2 at 37°C. The full-length cDNA of DUSP2 was synthesized and cloned into the lentiviral vector pcDNA3.1(+) to form overexpressing DUSP2 plasmid (oe-DUSP2). shRNA sequences characteristically targeting DUSP2 were cloned into the pLKO.1-GFP vector to generate the sh-DUSP2 plasmids, with sh-NC as the negative control. All plasmids were designed and synthesized by Tsingke Biotechnology (Beijing, China). The recombinant and empty vectors were packaged into lentiviral particles and transfected into PCa cells. Cell transfection by Lipofectamine 3000 was performed according to the manufacturer's instructions (Invitrogen, Thermo Fisher Scientific).

2.11 Cell counting kit-8 assay

22RV1 cells transfected with shRNA or vector were grown on a 96-well plate. The cell number in each well was 1×10^3 added with 100 μl of medium. After 24 h of inoculation, the CCK-8 reagent solution (10 μl; Hanbio Technology) was dropped into the plate followed by incubation for 2 h. Then, the absorbance at 450 nm of each well was detected by a microplate reader (Bio-Rad Laboratories, Inc.). The remaining plates were then sampled for these detection steps on days 2, 3, and 4 after inoculation.

2.12 Colony formation assay

The cells were digested with 0.25% trypsin and counted, and then the cell suspension was seeded on a six-well plate (1×10^3/well). The cells were then cultured for 10–14 days. The cell colonies were fixed with 4% paraformaldehyde for 20 min and stained with 1% crystal violet. The size and number of the colonies were observed and imaged.

2.13 Cell migration assay

For the transwell assay, the transfected cell suspensions (2.5×10^5 cells per well), which were starved for 6–8 h, were seeded in the upper chamber with 400 μl of serum-free medium to measure the cell migration ability. Six hundred microliters of 10% FBS was added to the bottom chamber. The plate was incubated for 1 day and stained with crystal violet. Cell counting was performed under a microscope (Nikon, Japan). Five fields were randomly selected for each treatment group.

2.14 Statistical analysis

GraphPad Prism (version 8.0, San Diego, CA, USA) and SPSS 23.0 software (SPSS, Chicago, IL, USA) were used to analyze the obtained data. Results are presented as mean ± standard deviation. The association among categorical variables was analyzed by Student's *t*-test, chi-square test, and one-way ANOVA. Kaplan–Meier method and Pearson analysis were used to assess the statistical significance. $p < 0.05$ was considered as a statistically significant difference.

3 Results

3.1 The tumorigenesis role and prognostic value of FOXA1 overexpression in PCa

To evaluate the probable role of FOXA1 in PCa, we analyzed and discovered that FOXA1 was upregulated in PCa tissues more than normal tissues (Figure 2A). Similarly, the upregulated FOXA1 was also verified by immunohistochemistry (IHC) staining from the HPA database (Figure 2B, Supplementary Table 1). Since FOXA1 is aberrantly overexpressed in PCa specimens, we then analyzed the clinical significance of FOXA1 expression in PCa patients. Our data revealed that enhanced expression of FOXA1 significantly correlated with poor overall survival (OS) and disease-free survival (DFS) in the patients of the cohort (Figures 2C, D). These results were consistent with those of previous studies (24), revealing significantly upregulated FOXA1 in PCa tissues and showing a prognostic value.

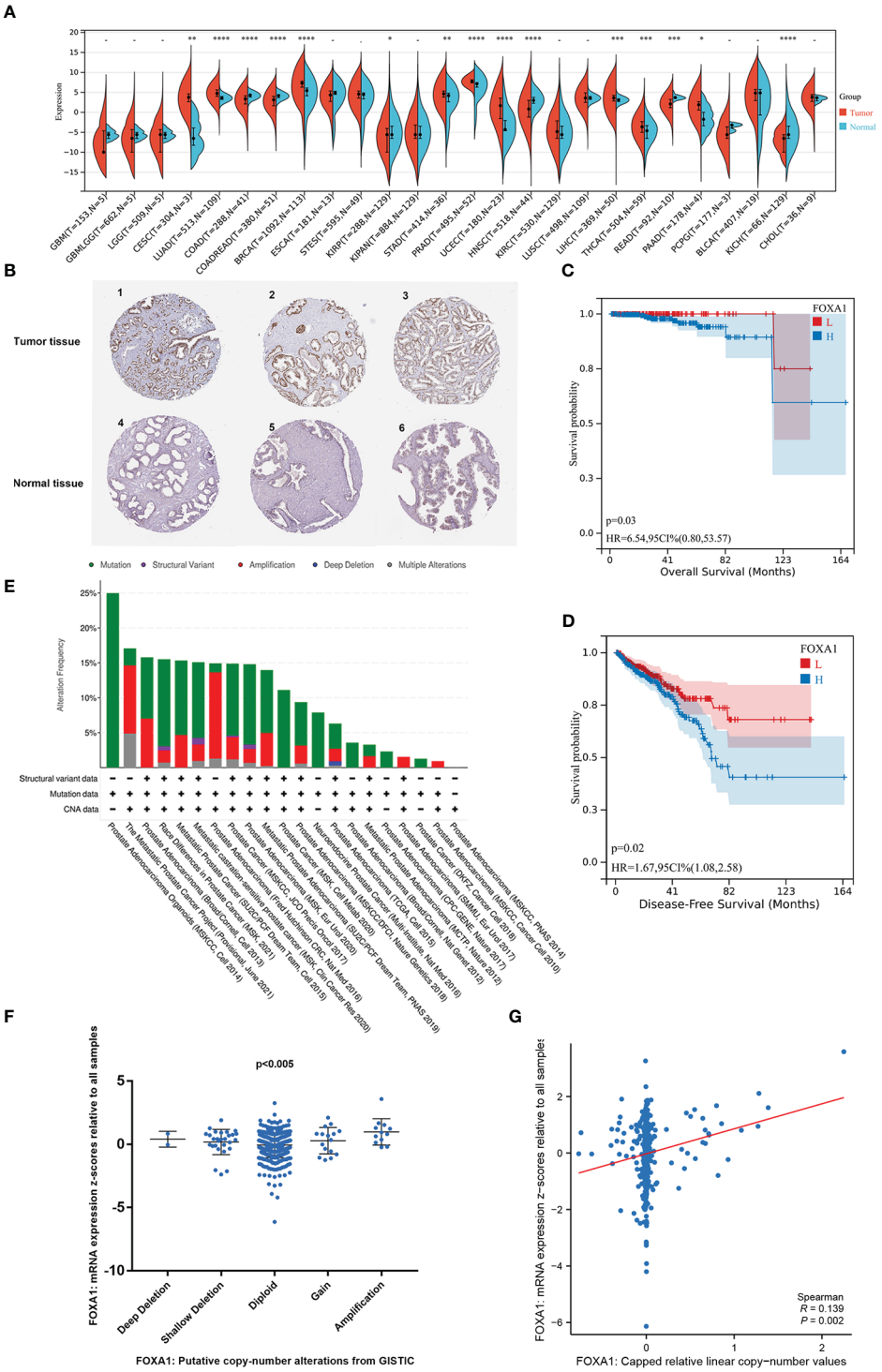

FIGURE 2
The carcinogenic role of FOXA1 in prostate cancer. **(A)** Expression distribution of FOXA1 in pan-cancer tissues. **(B)** Validation of the expression of FOXA1 on the translational level by the Human Protein Atlas database (immunohistochemistry). **(C, D)** Kaplan–Meier survival analysis of the relationship between FOXA1 expression and cancer patient prognosis in the TCGA cohort (H = FOXA1 high expression, *n* = 247; L = FOXA1 low expression, *n* = 245). **(E)** The distribution of FOXA1 genomic alterations in 21 prostate studies is shown on a cBioPortal OncoPrint plot. **(E, F)** The association between FOXA1 copy number and mRNA expression is displayed in the dot plot **(F)** and correlation plot **(G)** by cBioPortal. *P <0.05, **P < 0.01, ***P < 0.001, ****P<0.0001.

Moreover, to investigate the possible mechanism of the high FOXA1 expression in PCa, the genomic and copy numbers of FOXA1 were analyzed. As a result of our analysis on cBioPortal, we created an OncoPrint plot exhibiting the alteration frequency of the FOXA1 gene in 21 studies of prostate datasets (Figure 2E). Moreover, a higher level of mRNA expression was discovered in PCa samples with FOXA1 gain or amplification than in those with diploid or deletion (Figure 2F). Moreover, we found a positive

correlation between FOXA1 copy number value and mRNA expression in PCa samples (Figure 2G).

Taken together, the combined data testify that FOXA1 expression is elevated in PCa and that the gain and amplification of FOXA1 copy numbers are likely to be key factors that make a contribution to the upregulation of FOXA1 and play a crucial role in the progression of PCa.

3.2 Identification of differentially expressed lncRNAs, miRNAs, and mRNAs

Based on the above analysis, the ceRNAs associated with FOXA1 can potentially serve as a prognostic indicator for patients with PCa. We should be aware that the difference between the expression levels in PCa samples with FOXA1^{high} and FOXA1^{low} expression groups and those in tumor and normal groups is opposite (25). To verify this hypothesis, first, we screened DEmiRNAs, DElncRNAs, and DEmRNAs in PCa samples between the high and low FOXA1 expression group. We sorted out 81 DElncRNAs (55 upregulated and 26 downregulated), 38 DEmiRNAs (10 upregulated and 28 downregulated), and 653 DEmRNAs (248 upregulated and 405 downregulated). Simultaneously, the tumor group was compared with the non-tumor group, and we identified a total of 178 DElncRNAs (129 upregulated and 49 downregulated), 123 DEmiRNAs (69 upregulated and 54 downregulated), and 1,059 DEmRNAs (653 upregulated and 406 downregulated). We selected the mRNAs, miRNAs, and lncRNAs that were upregulated or downregulated in the first place and mapped their expression on the volcano (Figures 3A–C; Supplementary Figures 1A–C), while the heatmaps depict the expression of 20 momentous variable genes in PCa samples with FOXA1^{high} and FOXA1^{low} expression, as well as in tumor and normal samples (Figures 3D–F; Supplementary Figures 1D–F). Second, the Venn diagram for DElncRNA, DEmRNA, and DEmiRNA between the two groups was conducted individually to obtain the common DEGs, which were used for further analysis.

3.3 Construction of the triple regulatory network in lncRNA–miRNA–mRNA and identification of the hub gene

To establish a triple regulatory network in PCa, in the first place, we identified potential miRNAs targeting lncRNAs by putting the 18 DElncRNAs into the miRcode database; after taking the intersection with the common DEmiRNAs, five of the predicted miRNAs were selected. Secondly, we identified the downstream target mRNAs regarding the five DEmiRNAs by using the databases of miRDB, miRTarBase, and TargetScan together. To enhance the validity of the predictions, we also sought to ascertain candidate mRNAs that were only shared by the three databases. The results revealed that 44 of the predicted DEmRNAs conformed after taking the intersection with the common DEmRNAs. Finally, by integrating the lncRNA–miRNA pairs with miRNA–mRNA pairs, we constructed the lnRNA–miRNA–mRNA triple regulatory network; a total of 18 lncRNAs (11 upregulated and 7 downregulated), 5 miRNAs (3 upregulated and 2 downregulated), and 44 mRNAs (8 upregulated and 36 downregulated) were included (Figure 4A). In detail, 5 miRNA nodes, 18 lncRNA nodes, and 44 mRNA nodes are included in the network.

The hub genes were identified in the regulatory network using cytoHubba, and the results showed that five lncRNAs (MAGI2-AS3, MIR205HG, PCAT1, PCA3, and SNHG3), five miRNAs (has-mir-106a, has-mir-204, has-mir-206, has-mir-372, and has-mir-93) and four mRNAs (DUSP2, CLIP4, KIT, and ACSL4) were identified (Figure 4B). These genes, which were regulated by FOXA1, could form a ceRNA network to mediate PCa progression.

3.4 Functional enrichment analysis of DEmRNAs

For further insight into potential functions associated with the triple regulatory network, GO enrichment analyses for DEGs based on the mRNA–miRNA–lncRNA network were conducted first. On the BP level, the DEGs were mostly enriched in muscle organ development, gland development, and urogenital system development (Figure 4C). On the CC level, the DEGs tended to be enriched in the collagen-containing extracellular matrix and cell-substrate adherent junction (Figure 4D). Additionally, the DEGs were primarily enriched in receptor–ligand activity, heparin binding, and calcium channel activity on the MF level (Figure 4E). Afterward, we carried out KEGG enrichment analysis, and the top 10 most remarkable pathway terms were presented. The genes were largely enriched in the PI3K-Akt signaling pathway, focal adhesion, and regulation of the actin cytoskeleton (Figure 4F). Details of the top 10 markedly enriched pathways of GO and KEGG derived from DEmRNAs are shown in Supplementary Table 2.

3.5 The hub gene analysis as well as the selection of a model with PCa-specific prognostic value

As a first step to discerning a ceRNA with great prognostic value, we investigated and visualized the relationship between the hub gene expression and clinicopathological characteristics of PCa patients, including age, TMN stage, Gleason score, and survival state (Supplementary Figure 2A). As studies demonstrated that transcripts within a ceRNA network are co-regulated, we first examined the expression levels across the hub triple regulatory network in PCa samples with low- and high-expression groups of FOXA1 as well as in PCa and normal prostate tissues. Our results displayed three upregulated (PCA3, PCAT1, and SNHG3) and two downregulated (MAGI2-AS3 and MIR205HG) lncRNAs, three upregulated (has-mir-106a, has-mir-372, and has-mir-93) and two downregulated (has-mir-204, and has-mir-206) miRNAs, and four downregulated (DUSP2, CLIP4, ACSL4, and KIT) mRNAs in PCa and normal prostate tissues (Figure 5A). In the meantime, we

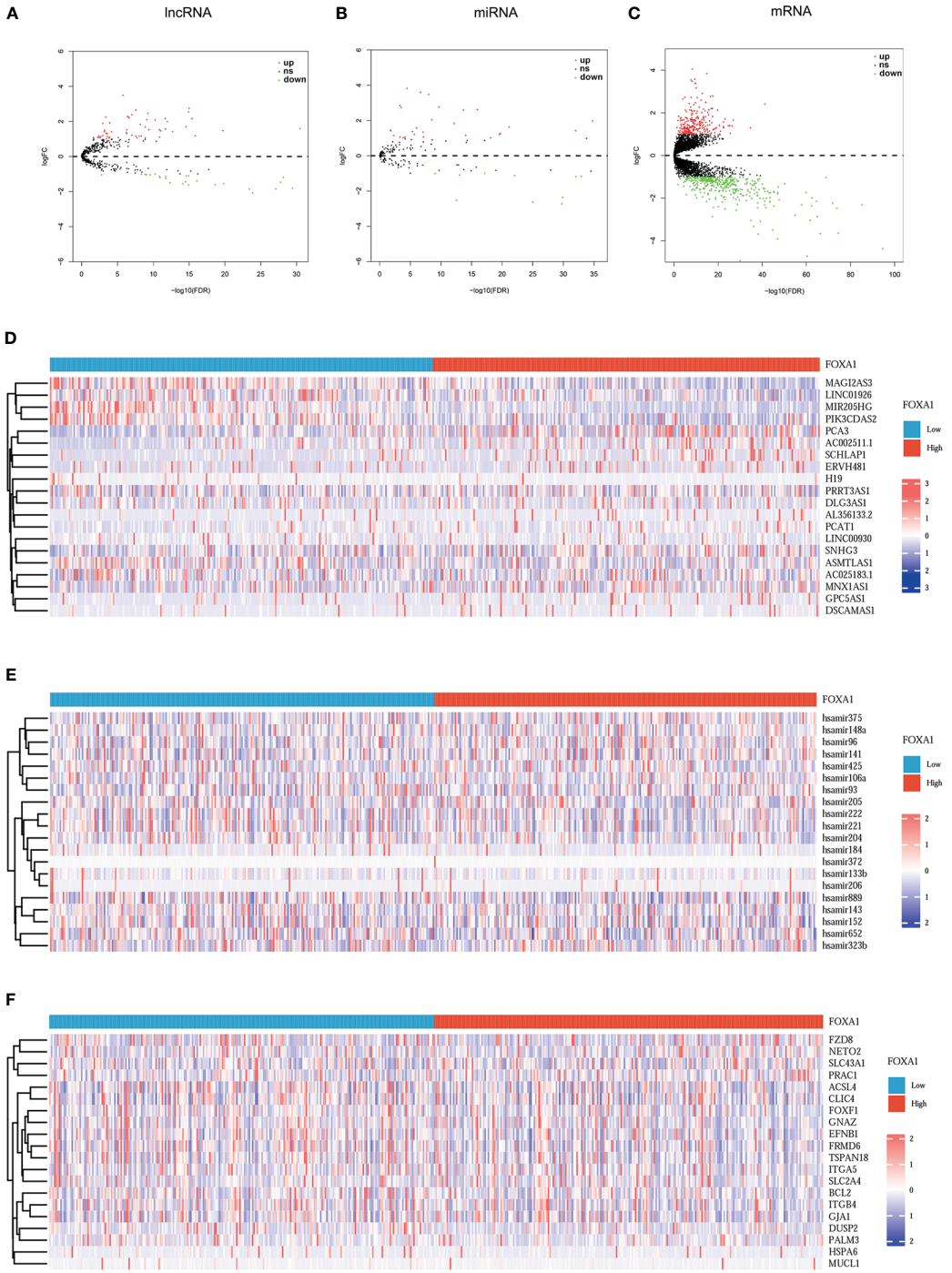

FIGURE 3
Volcano plots and heatmap plots of DElncRNAs, DEmiRNAs, and DEmRNAs between the expression of FOXA1^{high} and FOXA1^{low} in PCa samples. Red represents upregulated genes and blue indicates downregulated genes. **(A–C)** The volcano plots describe **(A)** 81 DElncRNAs (|$\log_2$fold change| > 0.5 and adjusted *p*-value < 0.05), **(B)** 38 DEmiRNAs (|$\log_2$fold change| > 0.3 and adjusted *p*-value < 0.05), and **(C)** 653 DEmRNAs (|$\log_2$fold change| > 0.5 and adjusted *p* value < 0.05). **(D–F)** The horizontal axis of the heatmap indicates the samples, and the vertical axis of the heatmap indicates 15 significant DEGs.

spotted two upregulated (MAGI2-AS3 and MIR205HG) lncRNAs, two downregulated (PCA3 and PCAT1) lncRNAs, and one undifferentiated (SNHG3) lncRNA; two downregulated (has-mir-106a and has-mir-204) and three undifferentiated (has-mir-206, has-mir-372 and has-mir-93) miRNAs; and two downregulated (DUSP2 and ACSL4) and two undifferentiated (KIT and CLIP4) mRNAs in PCa samples with FOXA1^{low} and FOXA1^{high} expression groups (Figure 5B).

On the other side, GSE21036 and GSE60329 were analyzed for the verification of these RNAs' expression levels. These findings are

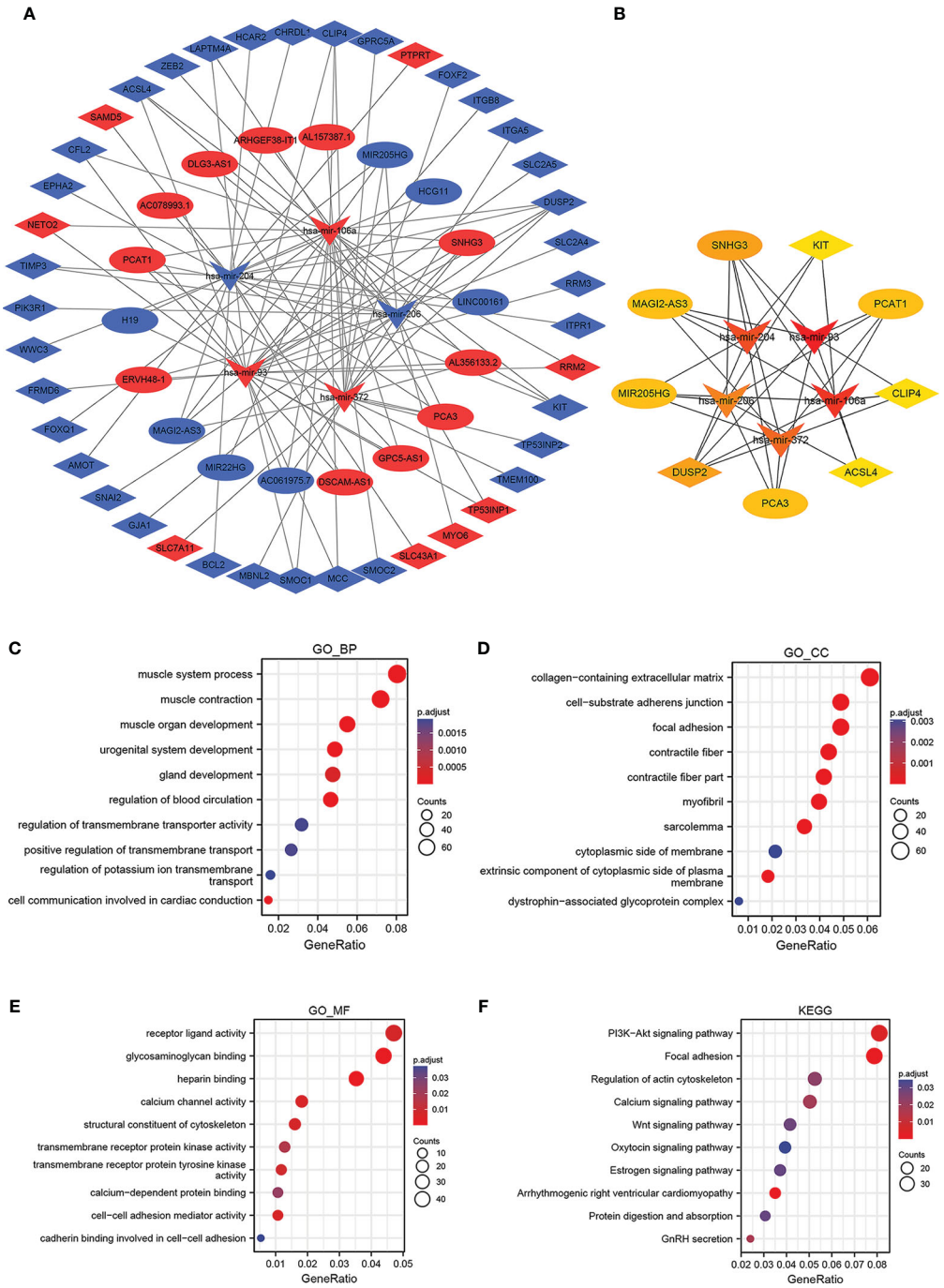

FIGURE 4
Construction and functional enrichment analysis of the lncRNA−miRNA−mRNA triple regulatory network. The ellipses denote lncRNAs, diamonds denote mRNAs, and round rectangles denote miRNAs. **(A)** The triple regulatory network in PCa. **(B)** Thirteen hub genes are in this network with a score of >2. **(C–F)** Functional enrichment analysis (GO and KEGG) of the DEmRNAs in the network.

almost consistent with the analysis that we elucidated above (Supplementary Figures 2B–D). Subsequently, we accomplish Kaplan–Meier analysis and a log-rank test for PFS in PCa patients to determine whether these RNAs were associated with PCa prognosis. In general, two DElncRNAs (MAGI2-AS3 and PCAT1), two DEmiRNAs (has-mir-106a and has-mir-204), and two DEmRNAs (DUSP2 and ACSL4) were identified to be associated with prognosis based on $p < 0.05$ (Figure 5C).

3.6 Construction and verification of the ceRNA network

Because cellular localization of lncRNAs determined the underlying mechanisms, we enforced the lncLocator analysis on the two DElncRNAs to predict the subcellular localization. The results showed that MAGI2-AS3 and PCAT1 are located predominantly in the cytoplasm (Figures 6A, B), but given the

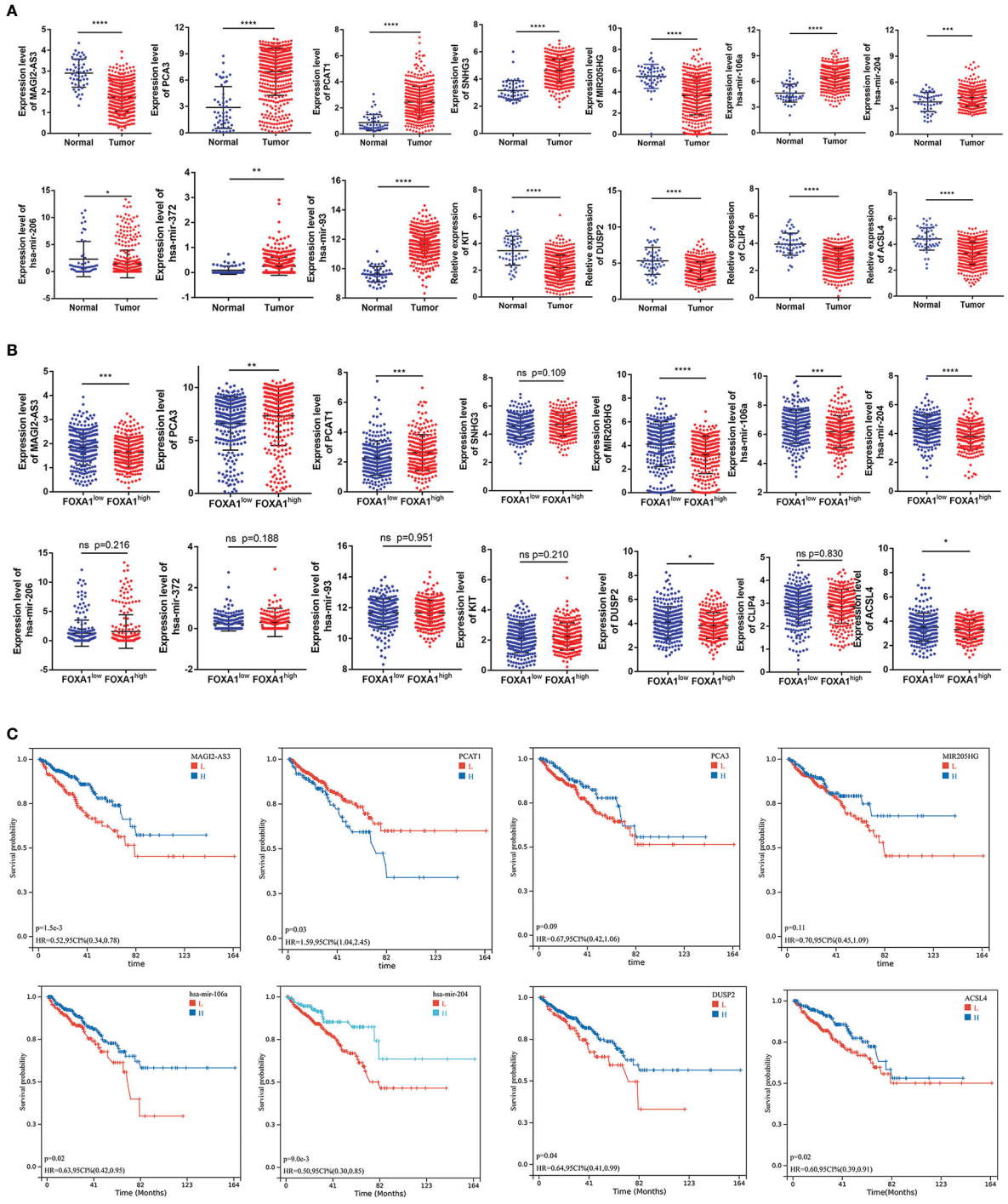

FIGURE 5
Expression and survival analysis for the hub genes. **(A)** The expression patterns of five DElncRNAs, five hub-DEmiRNAs, and four hub-DEmRNAs in PCa and adjacent normal prostate tissues and **(B)** in PCa samples with FOXA1^{high} and FOXA1^{low} expression groups. **(C)** The high- and low-expression values of hub genes were compared by a Kaplan–Meier survival curve for the TCGA prostate patient cohort. The horizontal axis indicates the overall survival time in months, and the vertical axis represents the survival rate. *P <0.05, **P < 0.01, ***P < 0.001, ****P<0.0001.

consideration that PCAT1 had been comprehensively studied in PCa, we focus on MAGI2-AS3 only. Overall, these data reminded us that MAGI2-AS3 may function as a ceRNA to enhance the expression of DUSP2 through sponging has-mir-106a/has-mir-204 (Figure 6C). The target sites in the MAGI2-AS3 and DUSP2 3' UTRs were predicted to pair with has-mir-106a and has-mir-204 by RNAInter, respectively (Figures 6D, E; Supplementary table 3). Pearson correlation analysis was carried out to verify the correlation of the independent prognostic lncRNA and mRNA factors, and the correlation of these RNAs with FOXA1 expression. We found that there is a strong positive correlation between MAGI2-AS3 and DUSP2; equally, FOXA1 had a strong negative correlation with

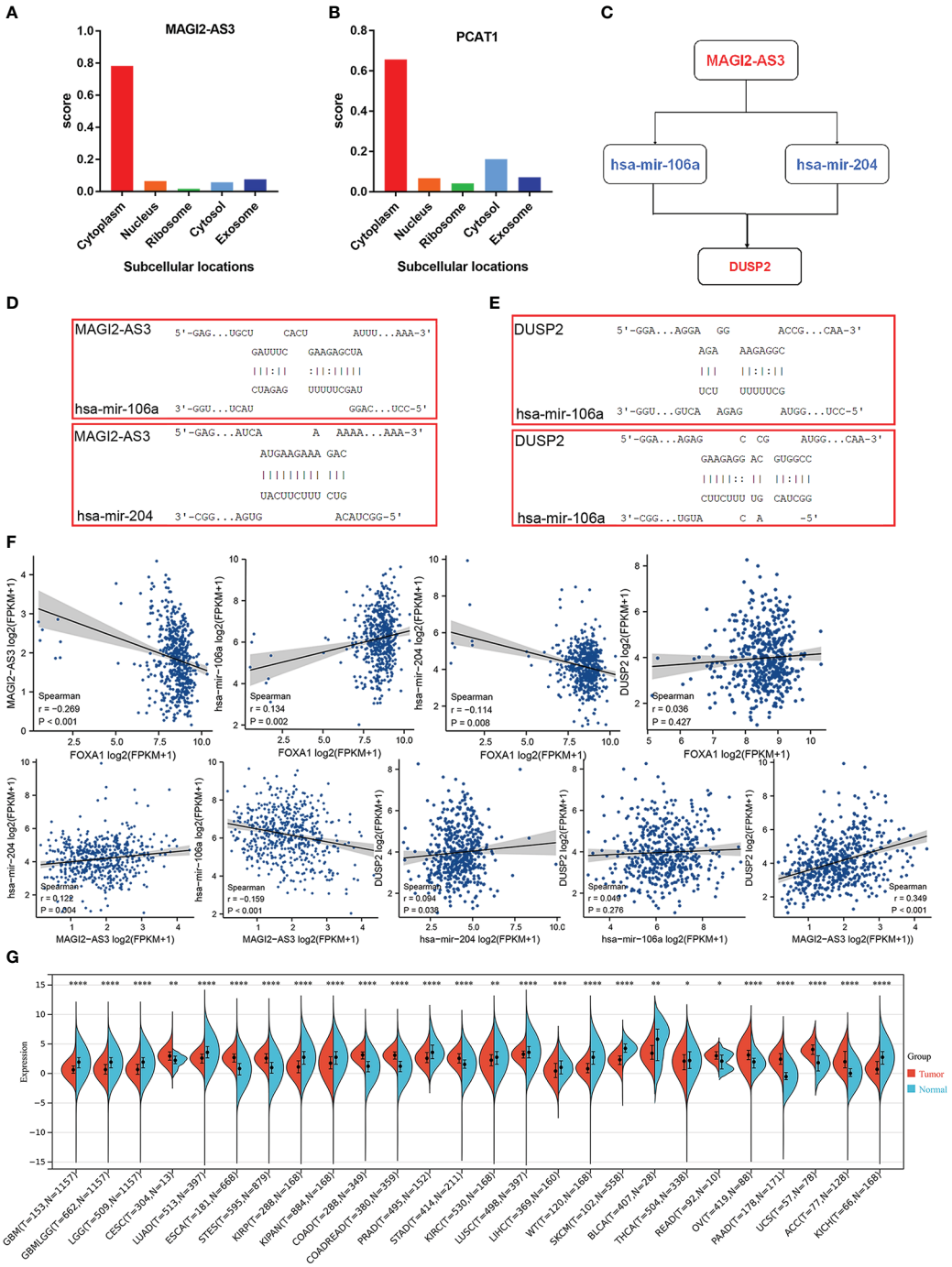

FIGURE 6
Construction and verification of the ceRNA network. **(A, B)** The cellular localization for two hub-lncRNAs (MAGI2-AS3 and PCAT1) was predicted using lncLocator. **(C)** Schematic model of ceRNA. Blue indicates upregulated; red indicates downregulated. **(D, E)** Base pairing between has-mir-106a and has-mir-204 and the target site in the MAGI2-AS3 and DUSP2 3′ UTR predicted by RNAInter, respectively. **(F)** Correlation analysis between these four predictive RNAs and FOXA1 in PCa. **(G)** Expression distribution of DUSP2 in pan-cancer tissues. *P <0.05, **P < 0.01, ***P < 0.001, ****P<0.0001.

MAGI2-AS3 (Figure 6F). These results further confirmed the regulatory network we constructed. At present, no study has yet to disclose the relationship between MAGI2-AS3 and DUSP2, or FOXA1 and MAGI2-AS3 in cancer. Consequently, the FOXA1/MAGI2-AS3/DUSP2 axis in the ceRNA network was singled out as a potential prognostic model for the next step analysis. We then performed a simple pan-cancer analysis of DUSP2 expression, which showed that DUSP2 expression was not tissue-specific and was downregulated in some cancer tissues when compared with normal tissues, including PCa (Figure 6G).

3.7 Exploring the relationship between DUSP2 expression and immune infiltration or immunotherapy in PCa

To evaluate the potential relationship between DUSP2 expression and tumor immunity in PCa, GSEA was conducted using GSE60329, and the results showed that T-cell receptor signaling pathway, adaptive immune response, immune receptor activity, and immune response regulating cell surface receptor signaling pathway were enriched in the low DUSP2 expression group (Figure 7A). The following analysis was conducted by using the TIMER tool. The "SCNA" module analysis showed that $CD4^+$ T cells' and neutrophil cells' immune infiltration levels were elevated after DUSP2 arm-level deletion (Figure 7B). These altogether suggested that DUSP2 was important for immune cell infiltration in tumor pathology.

Since immune checkpoint inhibitors (ICIs) have tremendous potential for treating cancer, we investigated whether the DUSP2 expression was related to ICI-related biomarkers and discovered that high expression of DUSP2 was positively correlated when both T-lymphocyte-associated protein 4 (CTLA-4) and programmed cell death protein 1 (PD-1) were positive, whereas there were no statistical differences when both PD-1 and CTLA-4 were negative (Figures 7C–F). Finally, we attempted to identify associations between DUSP2 and the efficacy of chemotherapeutics in the TCGA project of the PRAD dataset. Results showed that a lower DUSP2 expression was associated with a lower half-inhibitory concentration (IC_{50}) of chemotherapeutics such as BAY.61.3606, Bicalutamide, Elesclomol, IPA.3, MK.2206, and pf.4708671 (Figures 7G–L), which indicated that the model acted as a potential predictor for chemosensitivity.

3.8 Validation of the lncRNA–miRNA–mRNA network in tissue and blood sample

First, we studied the relationship between the expression of DUSP2 and the clinical characteristics of PCa. Results revealed that decreased DUSP2 expression was associated with a higher T stage, a higher Gleason score, and a higher incidence of lymph node metastases (Figures 8A–C, Supplementary Table 3). These findings inferred that the dysregulated DUSP2 participated in the progression of PCa. The expression of DUSP2 was examined by clinical samples. The statistical results presented that the proportion of DUSP2 defined as high expression in BPH tissues was observably higher than that in PCa tissues (Figures 8D, E), revealing that DUSP2 expression was lower in the tumor tissues than in the BPH tissues, and the expression was weakened by carcinoma progression, which was consistent with our bioinformatics analysis

To further verify the expression of the MAGI2-AS3/DUSP2 axis at the mRNA level, RNA was extracted from the tissue samples and detected by RT-PCR. The results showed increased expression of has-mir-106a and has-mir-204 in PCa patients in contrast to those with BPH, but decreased MAGI2-AS3 and DUSP2 (Figures 8F–I). Furthermore, we detected the relative expression of MAGI2-AS3 in blood samples to assess its role in PCa; the results showed that the MAGI2-AS3 mRNA concentrations were notably reduced in PCa patients than in BPH (Figure 8J). We also observed a positive correlation between DUSP2 expression and MAGI2-AS3 expression in tissue samples (Figure 8K). Interestingly, these results are consistent with previous analyses. The area under the curve (AUC) values were estimated based on ROC curve analysis. AUC value was 0.780 (95% CI: 0.661–0.899) (Figure 8L). Hence, the results manifested a good specificity and sensitivity and hinted that MAGI2-AS3 is of value in distinguishing PCa from BPH.

3.9 DUSP2 regulated the proliferation and migration of PCa cells

Since DUSP2 has not been reported in PCa, it is worthy to explore the biological behavior of DUSP2 in our in-depth study. Lentivirus-packed plasmids were employed to stably overexpress or knock down DUSP2 in 22RV1. Results of qRT-PCR displayed the transfection efficiency of PCa cells (Figures 9A, B). The CCK8 and colony formation assays revealed that 22RV1 cells with DUSP2 upregulation had significantly reduced growth compared to the NC group, and knockdown of MAGI2-AS3 led to the opposite results (Figures 9C–F). Additionally, cell migration assay was performed to investigate the regulatory role of DUSP2 in PCa cell migration. We demonstrated that it can inhibit cell migration in the oe-DUSP2 group compared to the control group (Figure 9G). However, downregulation of LINC01082 can improve 22RV1 cell migration (Figure 9H). These results suggested that DUSP2 is involved in the proliferation and migration of PCa cells.

4 Discussion

PCa is among the most prevalent male genitourinary malignancies and remains one of the most common causes of male cancer deaths worldwide (26). Since the utilization of PSA screening, the largest number of patients diagnosed with PCa have demonstrated locoregional disease and therefore benefited from early treatment. While only one-third of newly diagnosed advanced PCa patients in China are spread locally, the rest are diagnosed with invasive PCa with advanced or metastatic symptoms and without surgical opportunities (27). Treatment with androgen deprivation therapy for the distal metastases of hormone-sensitive PCa is the first line, but this carcinoma will eventually develop into CRPC, and the therapeutic drugs are not expected to show long-term remission, thus causing poor prognosis (28). Hence, early diagnosis and treatment are important to improve the prognosis in PCa patients; this prompts us to filter promising biomarkers to clarify the pathogenesis and molecular mechanism of PCa, to find new therapeutic targets and improve patients' outcome with this disease.

According to reports, a large number of the ceRNA regulatory network have been identified as being involved in the occurrence and development of a variety of human cancers, including lung

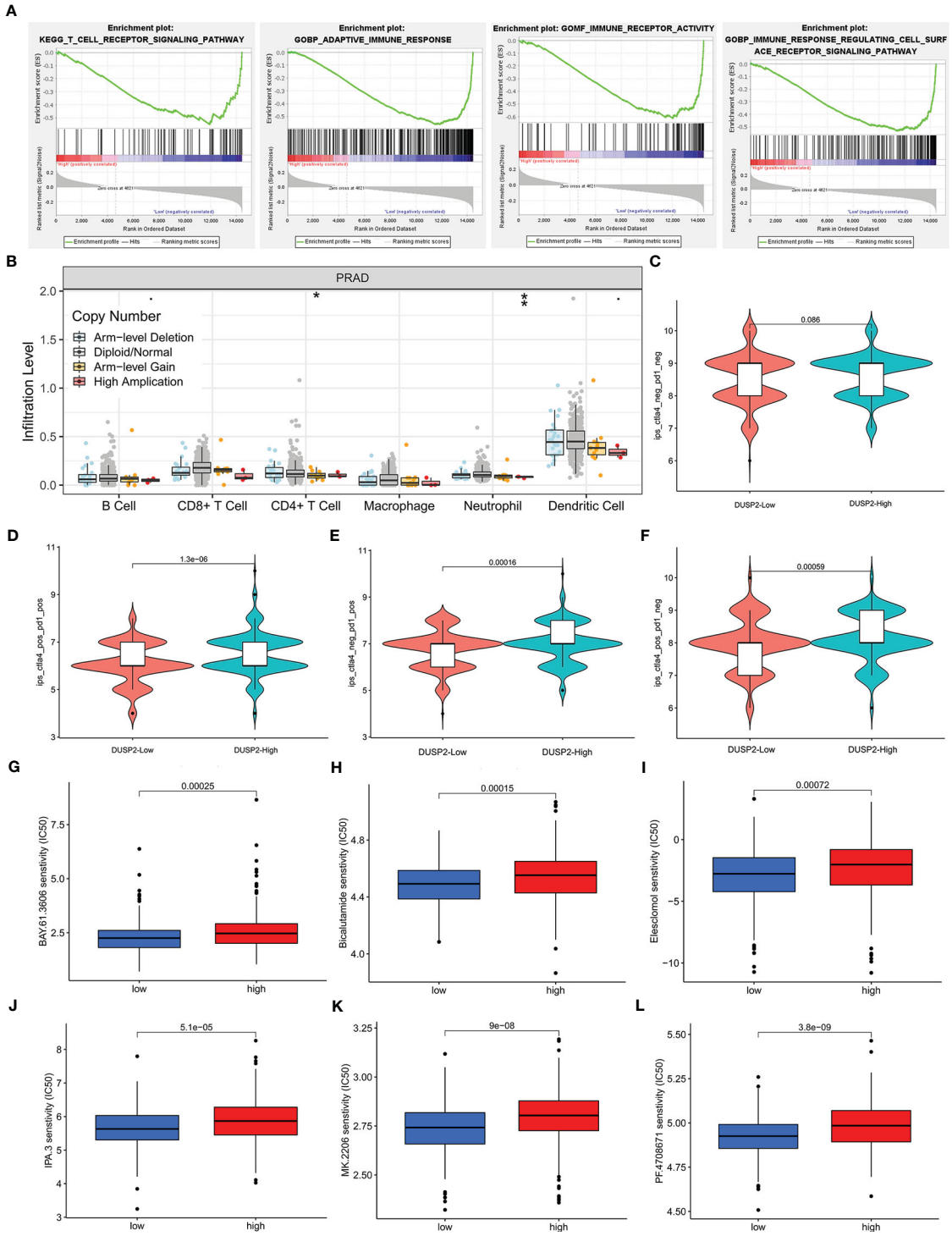

FIGURE 7
Immune infiltrate levels as well as immunotherapy or chemosensitivity analysis of DUSP2. **(A)** GSEA for DUSP2 with GSE60329. **(B)** Correlation of DUSP2 expression with immune infiltration level in PCa. **(C–F)** Low DUSP2 expression was negatively correlated with CTLA4 or/and PD1-positive levels. **(G–L)** DUSP2 acted as a potential predictor for chemosensitivity as low DUSP2 was related to a lower IC_{50} for chemotherapeutics (low = low DUSP2 expression, high = high DUSP2 expression). *P <0.05, **P < 0.01

cancer (29), gastric cancer (30), hepatocarcinoma (31), colorectal cancer (32), ovarian cancer (33), and renal cell carcinoma (34). FOXA1 is a crucial transcription factor functionally involved in the initiation and development of many types of cancers, including PCa. To our knowledge, previous studies about the FOXA1 transcriptional network were mainly focused on protein-coding genes; comprehensive analysis of its regulatory ceRNA network of lncRNAs, however, has not been attempted (35). Accordingly, in this research, we devoted to establishing a FOXA1-related ceRNA triple network in PCa, as well as associating it with prognosis.

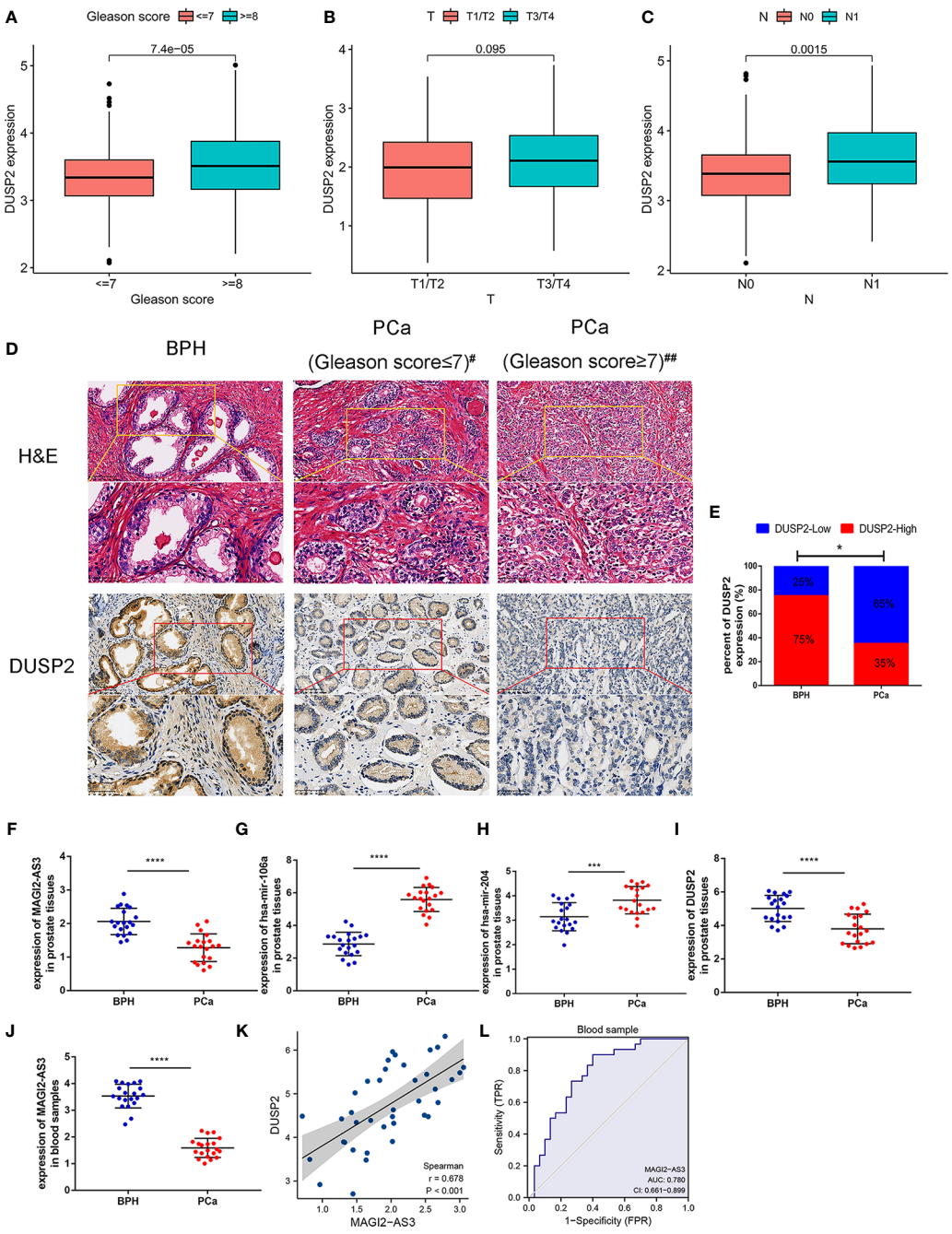

FIGURE 8
Validation of the lncRNA–miRNA–mRNA network in tissue and blood sample. **(A–E)** The correlation between DUSP2 expression and the clinical characteristics of PCa. **(F)** Representative hematoxylin and eosin (H&E) staining and immunohistochemical (IHC) staining in 20 PCa tissue samples and 20 BPH tissue samples; #Gleason score = 7(3 + 4), ##Gleason score = 7(4 + 3). **(G)** The percentage of DUSP2 staining intensity in 20 PCa patients and 20 BPH patients. **(H–K)** The network molecular expression level in fresh BPH and PCa tissues. **(L)** Positive correlation between MAGI2-AS3 and DUSP2 in prostate tissues; $r = 0.362$. **(M)** The expression of MAGI2-AS3 in the blood of patients with PCa and BPH. **(N)** ROC curves were plotted to evaluate the predictive accuracy of MAGI2-AS3 expression for PCa diagnosis; AUC = 0.780. *$p < 0.05$, ***$p < 0.001$, ****$p < 0.0001$.

Contemporaneously, adding evidence has declared that FOXA1 plays a tumorigenesis role and has a prognostic value in PCa; interestingly, we verified similar results through survival analysis, IHC, and copy number variation analysis in this survey.

In this inquiry, firstly, an lncRNA–miRNA–mRNA triple regulatory network comprising 18 lncRNAs, 5 miRNAs, and 44 mRNAs were derived from an *in silico* analysis. Enrichment analysis revealed that the DEmRNAs were primarily concentrated in the "PI3K-Akt signaling pathway", "receptor ligand activity", and "urogenital system development". Following that, a key triple regulatory network, which included five lncRNAs, five miRNAs, and four mRNAs, was identified through hub analysis based on a

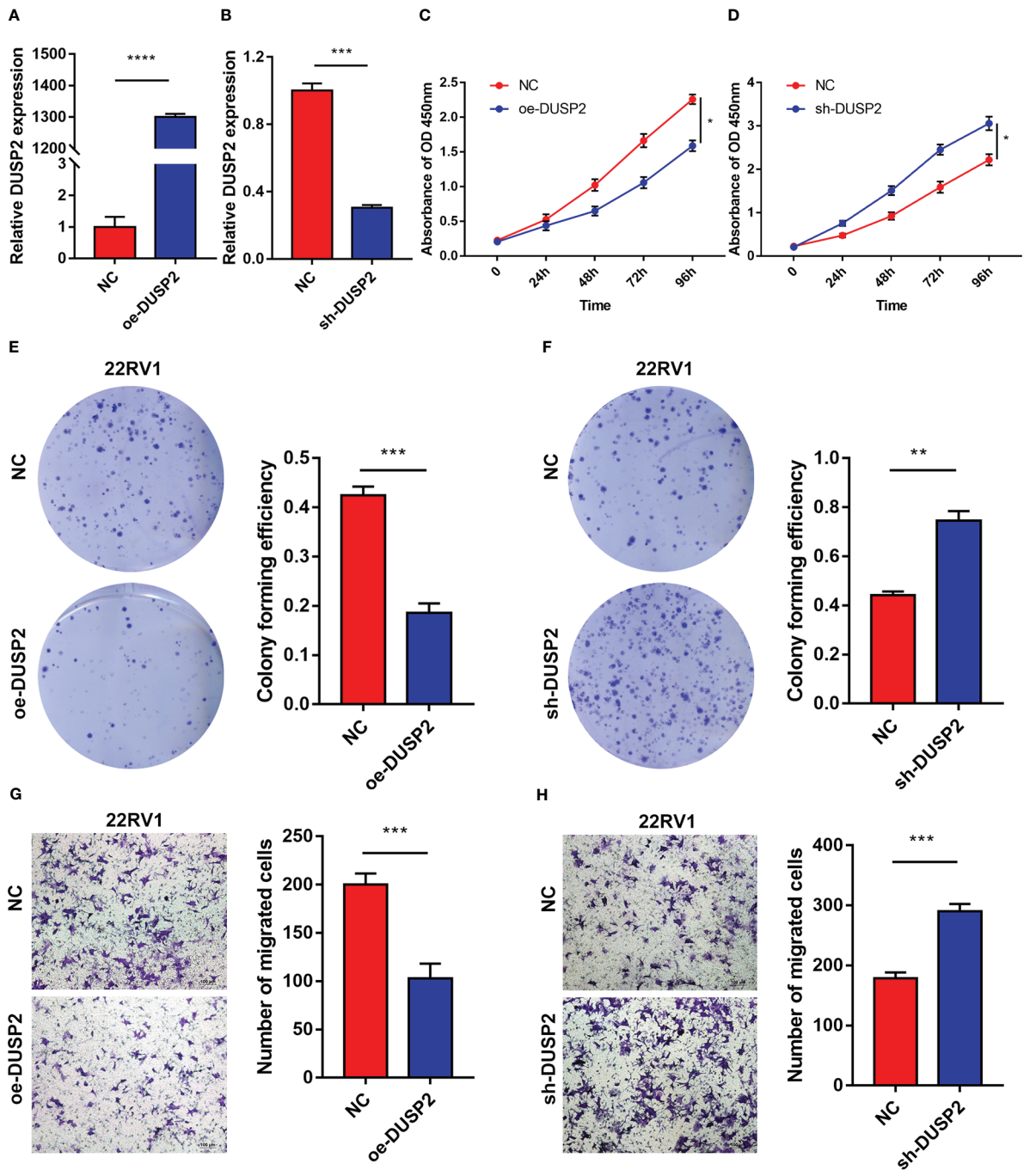

FIGURE 9
The DUSP2 regulated the proliferation and migration of PCa cells. **(A, B)** q-PCR was performed to determine the overexpression and knockdown efficiencies of DUSP2 in 22RV1 cells. **(C–F)** CCK8 assays and colony formation assays were used to determine the proliferation ability of 22RV1 cells after overexpressing or silencing DUSP2. **(G, H)** Migration capacity of cells with DUSP2 overexpression or knockdown based on transwell assays. *P <0.05, **P < 0.01, ***P < 0.001, ****P<0.0001

score >2. Whereafter, the expression analysis and survival analysis of the hub regulatory network were implemented. Furthermore, since the interactions in the ceRNA network mainly take place in the cytoplasm, we also looked at the subcellular localization of the two lncRNAs in the network. After the above bioinformatics analysis, the MAGI2-AS3~hsa-mir-106a/has-mir-204~DUSP2 ceRNA network related to the prognosis of PCa was constructed finally.

By searching for PCAT1 and MAGI2-AS3 in PubMed, we saw that PCAT1 has been explored for roles in PCa or the relationship with PCa. Shang et al. reported an essential role of lncRNA PCAT1 in regulating the PHLPP/FKBP51/IKKα complex to enhance the AKT and NF-κB signaling activity and progression of CRPC (36). Xu et al. confirmed that PCAT1 accelerated PCa cell migration, invasion, proliferation, and suppressed apoptosis by elevating FSCN1 expression mediated *via* miR-145-5p, suggesting a

possible therapeutic strategy for PCa patients (37). Consequently, we excluded lncRNA PCAT1 from our ceRNA network since it has been comprehensively studied in the above literature. Meanwhile, according to search results, no studies have been carried out to investigate the role of MAGI2-AS3 in PCa; however, reports on other types of cancer could indirectly explain its roles. For instance, Liu et al. certified that the expression level of MAGI2-AS3 was lessened in breast cancer tissues in contrast to normal adjacent tissues (38). Elevated expression of MAGI2-AS3 restrained the invasive, migratory, and proliferative capabilities, yet facilitated the apoptosis of breast cancer, bladder cancer, and hepatocellular carcinoma cells (38–40). Downregulated MAGI2-AS3 was highly correlated with tumor size, TNM stage, lymph node metastasis, and poor OS. Subsequently, the majority of the studies uncovered that MAGI2-AS3 may regulate their target genes (such as CCDC19, and SMG1) by functioning as a competing endogenous RNA for miRNAs (such as miR-15b-5p and miR-374a/b-5p) in cancers (39, 40). Nonetheless, the mechanism of MAGI2-AS3 remained unclear in PCa. Based on our bioinformatics analysis, we observed that MAGI2-AS3 was consistently downregulated in PCa and predicted that downregulated MAGI2-AS3 may be involved in PCa by functioning as a competing endogenous RNA for has-mir-106a or has-mir-204 to mediate the expression of DUSP2. This hypothesis may lead us to understand that the onco-suppressive role of MAGI2-AS3 extends to PCa.

The dysregulated miRNA has a certain impact on the initiation, development, and prognosis of tumor (41–43). Studies have elucidated that miRNA expression profiles could be used as biomarkers in the early diagnosis, classification, and prognosis of tumors (44). Aberrant expression of miRNAs has been reported in a variety of cancers, including in PCa. In this work, we constructed an lncRNA–miRNA–mRNA network, and the results manifested that the abnormal expression of lncRNAs can cause aberrant expression of five miRNAs, containing has-mir-204, has-mir-206, hsa-mir-106a, has-mir-372, and hsa-mir-93 in PCa, thus leading to mRNA degradation or posttranslational inhibition and therefore regulating the expression of the corresponding protein. After that, through bioinformatics analysis, we eventually included has-mir-106a and has-mir-204 in our network. Hsa-mir-106a was reported to have reduced expression in renal cell carcinoma cells and tissues, and it was proven that the inhibition of hsa-mir-106a expression can enhance cancer cell migration and invasion through interacting with PAK5 (45). Moreover, hsa-mir-106a has previously been certified to be upregulated in many cancer types, including gastric cancer and ovarian cancer (46, 47). Multiple studies have clarified that miR-204-5p can be used as a serum marker for various tumors (48, 49). Notably, an investigation from Daniel et al. has proved that the expression levels of a panel of seven miRNAs, comprising miR-204-5p, in the blood of PCa patients may be used as diagnostic biomarkers for the identification of PCa (50).

Previous studies have reported that immune infiltration can affect the prognosis of patients (51, 52). Therefore, how DUSP2 participates in the tumor microenvironment and influence tumor-infiltrating immune cells in PCa caught our interest. In this study, GSEA for DUSP2 was performed and we found that the tumor immune-related signaling pathways enriched in low expression of DUSP2. Moreover, the infiltration levels of CD4+ T cells and neutrophil cells were increased in the DUSP2 arm-level deletion group in PCa. These differences suggest that the MAGI2-AS3/DUSP2 axis may be closely related to PCa-infiltrated immune cells. Studies have demonstrated that the CTLA-4/B7 and PD-1/PD-L1 axes regulate physiological immune homeostasis, downregulate inflammatory responses, and presumptively facilitate immune evasion of cancer cells (53). Overexpression of PD-1 and CTLA-4 is recognized as a vital suppressor of anti-tumor immunity and is associated with better therapy response (54). In our study, the high expression of DUSP2 was positively correlated with CTLA-4 or/and PD-1 positive; it will be interesting for further studies to explore the relationship between DUSP2 and these ICIs in PCa. Moreover, the associations between DUSP2 and the efficacy of common chemotherapeutics were explored and results indicated that DUSP2 acted as a potential predictor for chemosensitivity.

DUSPs are specialized protein phosphatases that dephosphorylate both tyrosine and serine/threonine residues on the same substrate (55). DUSP2, also called activated cellular phosphatase 1, is a subfamily that acts primarily in the nucleus and predominantly inactivates ERK (56, 57). DUSP2 is mainly expressed in the hematopoietic cells, and it was largely induced by stress responses and regulates cytokine production and inflammation (58). DUSP2 is a transcription factor of the p53 gene in tumor cells, which can regulate cell apoptosis caused by oxidative damage and nutritional stress (59). In some solid tumors, the expression of DUSP2 is downregulated, and it functions as a key downstream regulator of HIF-1-mediated tumor progression and chemoresistance (60). In our exploration, the expression of DUSP2 in clinical samples of PCa was lower than that in BPH tissues, and there was a positive correlation between DUSP2 and MAGI2-AS3 expression in prostate tissues. In contrast to DUSP2 and MAGI2-AS3, has-mir-106a and has-mir-204 expression were upregulated in PCa compared to BPH tissues. On the side, we performed a molecular validation *via* functional experiments, and the results indicated that DUSP2 could regulate the proliferation and migration of PCa cells, which complement the mechanism of MAGI2-AS3 in the pathogenesis and development of PCa.

Although we have constructed a ceRNA-based molecular marker for MAGI2-AS3/DUSP2, there are still some limitations that should be noted. Firstly, the small number of PCa or BPH tissue samples would impact our findings' credibility. Secondly, further experiments are needed to determine the binding affinity between lncRNAs, miRNAs, and mRNAs obtained from databases. Last but not least, the relationship between DUSP2 and ICIs needs to be elucidated in further experiments to explore the PCa mechanism.

5 Conclusions

In this investigation, a ceRNA network (MAGI2-AS3~hsa-mir-106a/hsa-mir-204~DUSP2) related to PCa prognosis was created to

further understand the correlation of ceRNA, and the prognostic model is useful for exploring the pathogenesis of PCa. Otherwise, we identified that the lncRNA MAGI2-AS3 can be a novel vital factor in diagnosing PCa and determining the prognosis of PCa patients. In addition, DUSP2 was important for immune cell infiltration and chemosensitivity. Our study provides novel insights into immunological biomarkers and improves our understanding of FOXA1-related ceRNA in PCa.

Data availability statement

The original contributions presented in the study are included in the article/Supplementary Material. Further inquiries can be directed to the corresponding authors.

Ethics statement

The studies involving human participants were reviewed and approved by Ethics Committee of the First Affiliated Hospital of Chongqing Medical University. The patients/participants provided their written informed consent to participate in this study. Written informed consent was obtained from the individual(s) for the publication of any potentially identifiable images or data included in this article.

Author contributions

GY, XC, JL, and YZ designed the study. GY and YZ wrote the manuscript and analyzed data. GY, XC, and YZ performed the bioinformatics analysis. LP, YG, YT, LW, and YW collected the samples and verified the gene expression level. ML conducted the HE and IHC. JL and YZ wrote, reviewed, and edited the paper. ZQ and XW supervised and provided research funding for the learning. All authors contributed to the article and approved the submitted version.

Funding

This study was supported by a grant from the projects of the National Natural Science Foundation of China (NSFC) (Grant No. 81802543).

Acknowledgments

We thank the researchers and investigative groups of the GSE21036, GSE60329, and TCGA datasets who took part in the collection of specimens and shared the information openly and unselfishly.

Conflict of interest

The authors declare that the research was conducted in the absence of any commercial or financial relationships that could be construed as a potential conflict of interest.

Publisher's note

Supplementary material

The Supplementary Material for this article can be found online at: https://www.frontiersin.org/articles/10.3389/fonc.2023.1048521/full#supplementary-material

References

1. Siegel RL, Miller KD, Fuchs HE, Jemal A. Cancer statistics, 2021. *CA Cancer J Clin* (2021) 71(1):7–33. doi: 10.3322/caac.21654

2. Kodama H, Koie T, Oikawa M, Narita T, Tanaka T, Noro D, et al. Castration-resistant prostate cancer without metastasis at presentation may achieve cancer-specific survival in patients who underwent prior radical prostatectomy. *Int Urol Nephrol* (2020) 52(4):671–79. doi: 10.1007/s11255-019-02339-3

3. Herman L, Todeschini AL, Veitia RA. Forkhead transcription factors in health and disease. *Trends Genet* (2021) 37(5):460–75. doi: 10.1016/j.tig.2020.11.003

4. Bernardo GM, Lozada KL, Miedler JD, Harburg G, Hewitt SC, Mosley JD, et al. FOXA1 is an essential determinant of ERalpha expression and mammary ductal morphogenesis. *Development* (2010) 137(12):2045–54. doi: 10.1242/dev.043299

5. Hight SK, Mootz A, Kollipara RK, McMillan E, Yenerall P, Otaki Y, et al. An in vivo functional genomics screen of nuclear receptors and their co-regulators identifies FOXA1 as an essential gene in lung tumorigenesis. *Neoplasia* (2020) 22(8):294–310. doi: 10.1016/j.neo.2020.04.005

6. Teng M, Zhou S, Cai C, Lupien M, He HH. Pioneer of prostate cancer: past, present and the future of FOXA1. *Protein Cell* (2021) 12(1):29–38. doi: 10.1007/s13238-020-00786-8

7. Yang YA, Yu J. Current perspectives on FOXA1 regulation of androgen receptor signaling and prostate cancer. *Genes Dis* (2015) 2(2):144–51. doi: 10.1016/j.gendis.2015.01.003

8. Xu Y, Qin L, Sun T, Wu H, He T, Yang Z, et al. Twist1 promotes breast cancer invasion and metastasis by silencing Foxa1 expression. *Oncogene* (2017) 36(8):1157–66. doi: 10.1038/onc.2016.286

9. Zhu X, Jiang L, Yang H, Chen T, Wu X, Lv K. Analyzing the lncRNA, miRNA, and mRNA-associated ceRNA networks to reveal potential prognostic biomarkers for glioblastoma multiforme. *Cancer Cell Int* (2020) 20:3935. doi: 10.1186/s12935-020-01488-1

10. Bhan A, Soleimani M, Mandal SS. Long noncoding RNA and cancer: A new paradigm. *Cancer Res* (2017) 77(15):3965–81. doi: 10.1158/0008-5472.CAN-16-2634

11. Liu T, Han C, Fang P, Ma Z, Wang X, Chen H, et al. Cancer-associated fibroblast-specific lncRNA LINC01614 enhances glutamine uptake in lung adenocarcinoma. *J Hematol Oncol* (2022) 15(1):141. doi: 10.1186/s13045-022-01359-4

12. Lin C, Yang L. Long noncoding RNA in cancer: Wiring signaling circuitry. *Trends Cell Biol* (2018) 28(4):287–301. doi: 10.1016/j.tcb.2017.11.008

13. Gao N, Li Y, Li J, Gao Z, Yang Z, Li Y, et al. Long non-coding RNAs: The regulatory mechanisms, research strategies, and future directions in cancers. *Front Oncol* (2020) 10:5988175. doi: 10.3389/fonc.2020.598817

14. Liu S, Cao Q, An G, Yan B, Lei L. Identification of the 3-lncRNA signature as a prognostic biomarker for colorectal cancer. *Int J Mol Sci* (2020) 21(24):9359. doi: 10.3390/ijms21249359

15. Lee YS, Dutta A. MicroRNAs in cancer. *Annu Rev Pathol* (2009) 4:199–2275. doi: 10.1146/annurev.pathol.4.110807.092222

16. Lewis BP, Burge CB, Bartel DP. Conserved seed pairing, often flanked by adenosines, indicates that thousands of human genes are microRNA targets. *Cell* (2005) 120(1):15–20. doi: 10.1016/j.cell.2004.12.035

17. Salmena L, Poliseno L, Tay Y, Kats L, Pandolfi PP. A ceRNA hypothesis: the Rosetta stone of a hidden RNA language?. *Cell* (2011) 146(3):353–8. doi: 10.1016/j.cell.2011.07.014

18. Wu H, Liu B, Chen Z, Li G, Zhang Z. MSC-induced lncRNA HCP5 drove fatty acid oxidation through miR-3619-5p/AMPK/PGC1alpha/CEBPB axis to promote stemness and chemo-resistance of gastric cancer. *Cell Death Dis* (2020) 11(4):233. doi: 10.1038/s41419-020-2426-z

19. Kong X, Duan Y, Sang Y, Li Y, Zhang H, Liang Y, et al. LncRNA-CDC6 promotes breast cancer progression and function as ceRNA to target CDC6 by sponging microRNA-215. *J Cell Physiol* (2019) 234(6):9105–17. doi: 10.1002/jcp.27587

20. Cheng Q, Wang L. LncRNA XIST serves as a ceRNA to regulate the expression of ASF1A, BRWD1M, and PFKFB2 in kidney transplant acute kidney injury *via* sponging hsa-miR-212-3p and hsa-miR-122-5p. *Cell Cycle* (2020) 19(3):290–99. doi: 10.1080/15384101.2019.1707454

21. Li JH, Liu S, Zhou H, Qu LH, Yang JH. starBase v2.0: decoding miRNA-ceRNA, miRNA-ncRNA and protein-RNA interaction networks from large-scale CLIP-seq data. *Nucleic Acids Res* (2014) 42(Database issue):D92–7. doi: 10.1093/nar/gkt1248

22. Ping Y, Zhou Y, Hu J, Pang L, Xu C, Xiao Y. Dissecting the functional mechanisms of somatic copy-number alterations based on dysregulated ceRNA networks across cancers. *Mol Ther Nucleic Acids* (2020) 21:464–795. doi: 10.1016/j.omtn.2020.06.012

23. Li T, Liu N, Gao Y, Quan Z, Hao Y, Yu C, et al. Long noncoding RNA HOTAIR regulates the invasion and metastasis of prostate cancer by targeting hepaCAM. *Br J Cancer* (2021) 124(1):247–58. doi: 10.1038/s41416-020-01091-1

24. Song B, Park SH, Zhao JC, Fong KW, Li S, Lee Y, et al. Targeting FOXA1-mediated repression of TGF-beta signaling suppresses castration-resistant prostate cancer progression. *J Clin Invest* (2019) 129(2):569–82. doi: 10.1172/JCI122367

25. Shi Y, Zhang DD, Liu JB, Yang XL, Xin R, Jia CY, et al. Comprehensive analysis to identify DLEU2L/TAOK1 axis as a prognostic biomarker in hepatocellular carcinoma. *Mol Ther Nucleic Acids* (2021) 23:702–185. doi: 10.1016/j.omtn.2020.12.016

26. Cato L, de Tribolet-Hardy J, Lee I, Rottenberg JT, Coleman I, Melchers D, et al. ARv7 represses tumor-suppressor genes in castration-resistant prostate cancer. *Cancer Cell* (2019) 35(3):401–103 e6. doi: 10.1016/j.ccell.2019.01.008

27. Rajan P, Sudbery IM, Villasevil ME, Mui E, Fleming J, Davis M, et al. Next-generation sequencing of advanced prostate cancer treated with androgen-deprivation therapy. *Eur Urol* (2014) 66(1):32–9. doi: 10.1016/j.eururo.2013.08.011

28. Gillessen S, Attard G, Beer TM, Beltran H, Bjartell A, Bossi A, et al. Management of patients with advanced prostate cancer: Report of the advanced prostate cancer consensus conference 2019. *Eur Urol* (2020) 77(4):508–47. doi: 10.1016/j.eururo.2020.01.012

29. Zhou Z, Zhang S, Xiong Y. Long noncoding RNA MIAT promotes non-small cell lung cancer progression by sponging miR-149-5p and regulating FOXM1 expression. *Cancer Cell Int* (2020) 20:3485. doi: 10.1186/s12935-020-01432-3

30. Yang XZ, Cheng TT, He QJ, Lei ZY, Chi J, Tang Z, et al. LINC01133 as ceRNA inhibits gastric cancer progression by sponging miR-106a-3p to regulate APC expression and the wnt/beta-catenin pathway. *Mol Cancer* (2018) 17(1):126. doi: 10.1186/s12943-018-0874-1

31. Peng N, He J, Li J, Huang H, Huang W, Liao Y, et al. Long noncoding RNA MALAT1 inhibits the apoptosis and autophagy of hepatocellular carcinoma cell by targeting the microRNA-146a/PI3K/Akt/mTOR axis. *Cancer Cell Int* (2020) 20:1655. doi: 10.1186/s12935-020-01231-w

32. Liang H, Zhao Q, Zhu Z, Zhang C, Zhang H. Long noncoding RNA LINC00958 suppresses apoptosis and radiosensitivity of colorectal cancer through targeting miR-422a. *Cancer Cell Int* (2021) 21(1):477. doi: 10.1186/s12935-021-02188-0

33. Braga EA, Fridman MV, Moscovtsev AA, Filippova EA, Dmitriev AA, Kushlinskii NE. LncRNAs in ovarian cancer progression, metastasis, and main pathways: ceRNA and alternative mechanisms. *Int J Mol Sci* (2020) 21(22):8855. doi: 10.3390/ijms21228855

34. Wu J, Liu T, Sun L, Dong G. Long noncoding RNA SNHG4 promotes renal cell carcinoma tumorigenesis and invasion by acting as ceRNA to sponge miR-204-5p and upregulate RUNX2. *Cancer Cell Int* (2020) 20:5145. doi: 10.1186/s12935-020-01606-z

35. Goel S, Bhatia V, Kundu S, Biswas T, Carskadon S, Gupta N, et al. Transcriptional network involving ERG and AR orchestrates distal-less homeobox-1 mediated prostate cancer progression. *Nat Commun* (2021) 12(1):5325. doi: 10.1038/s41467-021-25623-2

36. Shang Z, Yu J, Sun L, Tian J, Zhu S, Zhang B, et al. LncRNA PCAT1 activates AKT and NF-kappaB signaling in castration-resistant prostate cancer by regulating the PHLPP/FKBP51/IKKalpha complex. *Nucleic Acids Res* (2019) 47(8):4211–25. doi: 10.1093/nar/gkz108

37. Xu W, Chang J, Du X, Hou J. Long non-coding RNA PCAT-1 contributes to tumorigenesis by regulating FSCN1 *via* miR-145-5p in prostate cancer. *BioMed Pharmacother* (2017) 95:1112–85. doi: 10.1016/j.biopha.2017.09.019

38. Yang Y, Yang H, Xu M, Zhang H, Sun M, Mu P, et al. Long non-coding RNA (lncRNA) MAGI2-AS3 inhibits breast cancer cell growth by targeting the Fas/FasL signalling pathway. *Hum Cell* (2018) 31(3):232–41. doi: 10.1007/s13577-018-0206-1

39. Wang F, Zu Y, Zhu S, Yang Y, Huang W, Xie H, et al. Long noncoding RNA MAGI2-AS3 regulates CCDC19 expression by sponging miR-15b-5p and suppresses bladder cancer progression. *Biochem Biophys Res Commun* (2018) 507(1–4):231–35. doi: 10.1016/j.bbrc.2018.11.013

40. Yin Z, Ma T, Yan J, Shi N, Zhang C, Lu X, et al. LncRNA MAGI2-AS3 inhibits hepatocellular carcinoma cell proliferation and migration by targeting the miR-374b-5p/SMG1 signaling pathway. *J Cell Physiol* (2019) 234(10):18825–36. doi: 10.1002/jcp.28521

41. Ferracin M, Veronese A, Negrini M. Micromarkers: miRNAs in cancer diagnosis and prognosis. *Expert Rev Mol Diagn* (2010) 10(3):297–308. doi: 10.1586/erm.10.11

42. Hayes J, Peruzzi PP, Lawler S. MicroRNAs in cancer: biomarkers, functions and therapy. *Trends Mol Med* (2014) 20(8):460–9. doi: 10.1016/j.molmed.2014.06.005

43. He B, Zhao Z, Cai Q, Zhang Y, Zhang P, Shi S, et al. miRNA-based biomarkers, therapies, and resistance in cancer. *Int J Biol Sci* (2020) 16(14):2628–47. doi: 10.7150/ijbs.47203

44. Sokilde R, Vincent M, Moller AK, Hansen A, Høiby PE, Blondal T, et al. Efficient identification of miRNAs for classification of tumor origin. *J Mol Diagn* (2014) 16(1):106–15. doi: 10.1016/j.jmoldx.2013.10.001

45. Pan YJ, Wei LL, Wu XJ, Huo FC, Mou J, Pei DS. MiR-106a-5p inhibits the cell migration and invasion of renal cell carcinoma through targeting PAK5. *Cell Death Dis* (2017) 8(8):e3155. doi: 10.1038/cddis.2017.561

46. Cui X, Wang X, Zhou X, Jia J, Chen H, Zhao W. miR-106a regulates cell proliferation and autophagy by targeting LKB1 in HPV-16-Associated cervical cancer. *Mol Cancer Res* (2020) 18(8):1129–41. doi: 10.1158/1541-7786.MCR-19-1114

47. Lin C, Xu X, Yang Q, Liang L, Qiao S. Circular RNA ITCH suppresses proliferation, invasion, and glycolysis of ovarian cancer cells by up-regulating CDH1. *via sponging miR-106a. Cancer Cell Int* (2020) 20:3365. doi: 10.1186/s12935-020-01420-7

48. Jia W, Wu Y, Zhang Q, Zhang C, Xiang Y. Identification of four serum microRNAs from a genome-wide serum microRNA expression profile as potential non-invasive biomarkers for endometrioid endometrial cancer. *Oncol Lett* (2013) 6(1):261–67. doi: 10.3892/ol.2013.1338

49. Daniel R, Wu Q, Williams V, Clark G, Guruli G, Zehner Z. A panel of MicroRNAs as diagnostic biomarkers for the identification of prostate cancer. *Int J Mol Sci* (2017) 18(6):1281. doi: 10.3390/ijms18061281

50. Chen X, Liu XS, Liu HY, Lu YY, Li Y. Reduced expression of serum miR-204 predicts poor prognosis of gastric cancer. *Genet Mol Res* (2016) 15(2):10.4238/gmr.15027702. doi: 10.4238/gmr.15027702

51. Jin Y, Chen DL, Wang F, Yang CP, Chen XX, You JQ, et al. The predicting role of circulating tumor DNA landscape in gastric cancer patients treated with immune checkpoint inhibitors. *Mol Cancer* (2020) 19(1):154. doi: 10.1186/s12943-020-01274-7

52. Yang CY, Fan MH, Miao CH, Liao YJ, Yuan RH, Liu CL, et al. Engineering chimeric antigen receptor T cells against immune checkpoint inhibitors PD-1/PD-L1 for treating pancreatic cancer. *Mol Ther Oncolytics* (2020) 17:571–855. doi: 10.1016/j.omto.2020.05.009

53. Sfanos KS, Bruno TC, Meeker AK, Marzo AM, Isaacs WB, Drake CG, et al. Human prostate-infiltrating CD8+ T lymphocytes are oligoclonal and PD-1+. *Prostate* (2009) 69(15):1694–703. doi: 10.1002/pros.21020

54. Zhang H, Dai Z, Wu W, Wang Z, Zhang N, Zhang L, et al. Regulatory mechanisms of immune checkpoints PD-L1 and CTLA-4 in cancer. *J Exp Clin Cancer Res* (2021) 40(1):184. doi: 10.1158/1557-3265.ADI21-IA-18

55. Jeffrey KL, Camps M, Rommel C, Mackay CR. Targeting dual-specificity phosphatases: manipulating MAP kinase signalling and immune responses. *Nat Rev Drug Discovery* (2007) 6(5):391–403. doi: 10.1038/nrd2289

56. Ward Y, Gupta S, Jensen P, Wartmann M, Davis RJ, Kelly K, et al. Control of MAP kinase activation by the mitogen-induced threonine/tyrosine phosphatase PAC1. *Nature* (1994) 367(6464):651–4. doi: 10.1038/367651a0

57. Rios P, Nunes-Xavier CE, Tabernero L, Kohn M, Pulido R. Dual-specificity phosphatases as molecular targets for inhibition in human disease. *Antioxid Redox Signal* (2014) 20(14):2251–73. doi: 10.1089/ars.2013.5709

58. Kim SC, Hahn JS, Min YH, Yoo NC, Ko YW, Lee WJ, et al. Constitutive activation of extracellular signal-regulated kinase in human acute leukemias: combined role of activation of MEK, hyperexpression of extracellular signal-regulated kinase, and downregulation of a phosphatase, PAC1. *Blood* (1999) 93(11):3893–9. doi: 10.1182/blood.V93.11.3893

59. Yin Y, Liu YX, Jin YJ, Hall EJ, Barrett JC. PAC1 phosphatase is a transcription target of p53 in signalling apoptosis and growth suppression. *Nature* (2003) 422(6931):527–31. doi: 10.1038/nature01519

60. Lin SC, Chien CW, Lee JC, Yeh YC, Hsu KF, Lai YY, et al. Suppression of dual-specificity phosphatase-2 by hypoxia increases chemoresistance and malignancy in human cancer cells. *J Clin Invest* (2011) 121(5):1905–16. doi: 10.1172/JCI44362

frontiers | Frontiers in Oncology

TYPE Original Research
PUBLISHED 08 May 2023
DOI 10.3389/fonc.2023.1106667

OPEN ACCESS

EDITED BY
Mohamed Hassan,
Institut National de la Santé et de la Recherche Médicale (INSERM), France

REVIEWED BY
Fahad Khan,
Noida Institute of Engineering and Technology (NIET), India
Chandra Sekhar Bhol,
National Institute of Technology Rourkela, India

*CORRESPONDENCE
Nadia Judith Jacobo-Herrera
nadia.jacobo@gmail.com
Carlos Pérez-Plasencia
carlos.pplas@gmail.com

RECEIVED 24 November 2022
ACCEPTED 28 March 2023
PUBLISHED 08 May 2023

CITATION
Delgado-Waldo I, Contreras-Romero C, Salazar-Aguilar S, Pessoa J, Mitre-Aguilar I, García-Castillo V, Pérez-Plasencia C and Jacobo-Herrera NJ (2023) A triple-drug combination induces apoptosis in cervical cancer-derived cell lines.
Front. Oncol. 13:1106667.
doi: 10.3389/fonc.2023.1106667

A triple-drug combination induces apoptosis in cervical cancer-derived cell lines

Izamary Delgado-Waldo[1,2], Carlos Contreras-Romero[2,3], Sandra Salazar-Aguilar[4], João Pessoa[5], Irma Mitre-Aguilar[1], Verónica García-Castillo[6], Carlos Pérez-Plasencia[3,6]* and Nadia Judith Jacobo-Herrera[1]*

[1]Unidad de Bioquímica Guillermo Soberón Acevedo, Instituto de Ciencias Médicas y Nutrición Salvador Zubirán, Tlalpan, Mexico, [2]Posgrado en Ciencias Biológicas, Universidad Nacional Autónoma de México. Copilco Universidad, Coyoacán, Mexico, [3]Laboratorio de Genómica, Instituto Nacional de Cancerología, Tlalpan, Mexico, [4]Laboratorio de Hematopoiesis y Leucemia, Unidad de Investigación, Diferenciación Celular y Cáncer, Facultad de Estudios Superiores Zaragoza, Universidad Nacional Autónoma de México, Iztapalapa, Mexico, [5]CNC - Center for Neuroscience and Cell Biology, CIBB - Center for Innovative Biomedicine and Biotechnology, University of Coimbra, Coimbra, Portugal, [6]Laboratorio de Genómica Funcional, Unidad de Biomedicina, FES-IZTACALA, Universidad Nacional Autónoma de México, Tlalnepantla, Mexico

Introduction: Cervical cancer is a worldwide health problem due to the number of deaths caused by this neoplasm. In particular, in 2020, 30,000 deaths of this type of tumor were reported in Latin America. Treatments used to manage patients diagnosed in the early stages have excellent results as measured by different clinical outcomes. Existing first-line treatments are not enough to avoid cancer recurrence, progression, or metastasis in locally advanced and advanced stages. Therefore, there is a need to continue with the proposal of new therapies. Drug repositioning is a strategy to explore known medicines as treatments for other diseases. In this scenario, drugs used in other pathologies that have antitumor activity, such as metformin and sodium oxamate, are analyzed.

Methods: In this research, we combined the drugs metformin and sodium oxamate with doxorubicin (named triple therapy or TT) based on their mechanism of action and previous investigation of our group against three CC cell lines.

Results: Through flow cytometry, Western blot, and protein microarray experiments, we found TT-induced apoptosis on HeLa, CaSki, and SiHa through the caspase 3 intrinsic pathway, including the critical proapoptotic proteins BAD, BAX, cytochrome-C, and p21. In addition, mTOR and S6K phosphorylated proteins were inhibited in the three cell lines. Also, we show an anti-migratory activity of the TT, suggesting other targets of the drug combination in the late CC stages.

Discussion: These results, together with our former studies, conclude that TT inhibits the mTOR pathway leading to cell death by apoptosis. Our work provides new evidence of TT against cervical cancer as a promising antineoplastic therapy.

KEYWORDS

cervical cancer, apoptosis, combinatorial therapy, repurposing drugs, mTOR pathway

1 Introduction

Despite early detection programs, cervical cancer (CC) is a public health problem that still needs to be solved. Although its incidence has decreased by approximately 40% in the last decade, it currently remains the second leading cause of cancer-related deaths in women, accounting for an estimated 270,000 women's lives annually (1). The use of cervical cancer screening has helped in an early diagnosis of this disease; however, there is still a large population in which the disease is diagnosed in locally advanced stages (2). In such a scenario, the clinical response rates to conventional treatment based on radiation therapy and/or surgery, chemotherapy (3), and immunotherapy (4) are poor. These therapies have systemic side effects on patients (5), high costs (6), and rapid development of drug resistance (7–10), which are some of the limitations that reduce their effectiveness (11).

Warburg's research in the 1920s proved that tumor cells require a high income of glucose to maintain their extremely demanded metabolism activity independently of the oxygen levels, a process known as the Warburg effect or aerobic glycolysis (12–14). In contrast to the normal cell, the tumor cell produces vast amounts of extracellular lactate *via* aerobic glycolysis (15) and consequently generates several disturbances in other cells and the tumor microenvironment (16), leading to hypoxia, promotion of angiogenesis, and distant metastasis (17, 18). The high rate of glucose consumption allows the tumor cell to obtain biosynthetic precursors necessary for the biosynthesis of nucleotides, proteins, and lipids to achieve increased proliferation, survival, and progression of tumor characteristics (19–23).

Drug repositioning is a current strategy for new anticancer treatments (24) in terms of safety, side effects, and mechanisms of action (25). In this scenario, our research group successfully proved that the combination of the known drugs metformin, doxorubicin, and sodium oxamate (named triple therapy or TT) inhibited tumor growth in cell lines derived from breast and colon cancers and in two different murine models (17, 26, 27). Metformin is widely used to treat type 2 diabetes mellitus (28). Besides it is an antitumor candidate due to its ability to inhibit respiratory-chain complex I (29), activate the protein AMPK, and inhibit the mTOR activation (30). Such events stop cell proliferation and the production of proteins, lipids, and carbohydrates (31–34). The second drug, oxamate, is a competitive inhibitor of lactate dehydrogenase A (LDH-A), an enzyme that catalyzes the pyruvate to lactate in aerobic glycolysis (35–38). Finally, doxorubicin is a well-known drug used to treat several types of cancer (39). It induces cell death in three different ways: topoisomerase II inhibition, inhibition of DNA synthesis, and induction of oxidative stress (39–41).

Previously, we have shown that the TT leads to apoptosis by the upregulation of PARP-1 and the caspase 3 cleavage, as well as mTOR and LDH-A inhibition. Additionally, in murine models, the TT was even more efficient than the doxorubicin treatment and did not present visible toxicity in organs or tissues, and the animals had a longer survival rate than those under the control drug treatment (17, 26, 27). In the present work, we aimed to establish the apoptosis pathway induced by the TT in CC cell lines as a novel proposal to treat CC patients. Hence, we showed that the TT triggered tumor cell death by apoptosis through the caspase 3 intrinsic pathway. These results indicate that the combination of drugs that inhibit different tumor pathways, in this case aerobic glycolysis, nucleic acid synthesis, and complex I of the respiratory chain, has evident antitumor effects. The use of radio- and chemotherapy affects tumor cells with high proliferative rates. Therefore, inhibition of multiple pathways, including aberrant tumor metabolism in cancer therapy, should be considered.

2 Materials and methods

2.1 Reagents and cell culture

Doxorubicin (Doxolem® RU, 10 mg/5 ml) (Dox), metformin (Met) (1-1dimethylbiguanidine hydrochloride; sc-202000A, Santa Cruz Biotech, USA), and sodium oxamate (Ox) (sc-215880, Santa Cruz Biotech, USA) were diluted with DMEM/F12 medium (GIBCO, USA) supplemented with 2% FBS (ATCC 30-2020), with the following concentrations *in vitro*: 1.5 µM/25 mM/20 mM for dox/met/ox respectively, for 12 h, and 1 µM/20 mM/15 mM for dox/met/ox, respectively, for 24 h.

The human cervical cancer cell lines Hela, SiHa, and CaSki were purchased from the American Type Culture Collection (ATCC). All cells were cultured in DMEM/F12 medium supplemented with 10% FBS and 1% penicillin–streptomycin at 37°C in a humidified atmosphere of 95% air plus 5% CO_2, as recommended by ATCC.

2.2 Cytotoxicity assay

Cell viability was determined using the sulforhodamine (SRB) cell protein stain (42). Cancer cells were seeded in 96-well plates at a density of 10,000 cells/well and allowed to adhere overnight (24 h). After 24 h of incubation, the cells were treated with different doses of metformin (15, 20, 25, 30, 40 mM), sodium oxamate (10, 15, 20, 25, 30 mM), and doxorubicin (0.5, 1, 2, 3, 4 µM) in combination for 12 and 24 h. Cells were fixed with cold trichloroacetic acid 10% (TCA) (MERCK, USA) at 4°C for 1 h and then washed four times with tap water, followed by staining with 100 µl of 0.5% SRB (S9012-5G Sigma-Aldrich) in 1% acetic acid for 30 min at room temperature (RT). Excess stain was washed four times with 1% acetic acid. The stained cells were resuspended in 200 µl of 10 mM Tris, pH 10. The optical density at 510 nm was determined using an Epoch microplate spectrophotometer (BioTek). All the experiments were done in triplicate.

2.3 Apoptosis antibody array and Western blot

The Human Apoptosis Antibody Array Kit (RayBiotech, Inc., Norcross, USA) was used to evaluate the apoptotic protein expression according to the manufacturer's instructions. The

membranes were soaked in blocking buffer at RM for 30 min. Extracted protein (1 mg/ml) from HeLa cells with treatment at 12 h was added into each well containing the membranes and was left overnight at 4°C for incubation. The membrane was added with a biotinylated antibody cocktail and subsequently with HRP-streptavidin for incubation overnight at 4°C for incubation. A total of 500 µl of the detection buffer was pipetted onto the membrane for 5 min at RM. The membranes were transferred and exposed to a chemiluminescence C-DiGit scanner employing the Image Studio (LICOR, USA) software, then they were used to quantify the intensity of each array dot and then normalized to the internal control. All incubations and washes were performed under rotation (~0.5–1 cycle/s).

In order to determine specific proteins, Western blot analysis was done; briefly, cells were collected and lysed with RIPA buffer (Santa Cruz Biotechnology sc-24948) containing protease inhibitors for 30 min on ice and then centrifuged at 13,000*g* at 4°C for 25 min. The supernatant containing total protein was harvested. The concentration was detected using Bradford assay (Bio-Rad) according to the manufacturer's instructions. Thereafter, 25 µg of proteins was separated by 12% SDS-PAGE and transferred to polyvinylidene difluoride (PVDF) membranes (GE Healthcare, USA) in a semidry Trans-Blot Turbo chamber (Bio-Rad) at 25 V, 1 mA, for 30 min. The membranes were blocked with 5% non-fat milk in TBS containing 0.1% Tween 20 for 2 h. The membrane was incubated with specific primary antibodies Caspase-3 (1:3,000, sc-7148), Caspase-8 (1:2,000, sc-56070), and p21 (1:3,000, sc-397) from Santa Cruz Biotechnology; XIAP (1:1,000, ab28151) from Abcam; and BAX (1:1,000, 12105S) and BAK (1:1000, 5023S) from Cell Signaling Technology, overnight at 4°C on a rocking platform, washed, and then incubated with the corresponding secondary antibodies anti-mouse (1:5,000, sc-23719) and anti-rabbit (1:3,000, sc-2370) for 2 h at room temperature. The control for equal protein loading was assessed using an anti-β-actin antibody (1:5,000; sc-47778). The blot was visualized using the SuperSignal West Femto chemiluminescent substrate (Pierce) in the C-DiGit scanner (LICOR)™ employing the Image Studio (LI-COR) software. All the experiments were repeated in triplicate.

2.4 Flow cytometry: Annexin V-FITC apoptosis detection

Apoptosis was detected using Annexin V-FITC Apoptosis Detection Kit I (BD 556547) by flow cytometry according to the manufacturer's instructions. There are two distinct phases in the apoptotic process, termed early and late apoptosis, which can be distinguished with an intracellular staining assay. Annexin V (AV) and propidium iodide (IP) double staining can quantitatively distinguish viable cells from dead cells. Therefore, cells were distinguished into four groups in a scatter plot: viable cells (Annexin V-/IP-) in the lower-left quadrant, early apoptotic cells (Annexin V+/IP-) in the lower-right quadrant, late apoptotic cells together with secondary necrotic cells (Annexin V+/7-AAD+) in the upper-right quadrant, and necrotic cells (Annexin V-/IP+) in the upper-left quadrant. Cancer cells were seeded in six-well plates at a density of 500,000 cells/well and allowed to adhere overnight (24 h). Then, the cells were treated with the IC_{50} of TT for 12 and 24 h. Briefly, the treated cells were harvested by trypsin, washed with PBS, collected by centrifuging at 1,500*g* for 5 min, mixed with a binding buffer, and incubated with Annexin V-FITC and propidium iodide (PI) for 15 min at RT in the dark. Afterward, labeled cells were counted by flow cytometry within 30 min. All early apoptotic cells (Annexin V–positive, PI-negative), necrotic/late apoptotic cells (double positive), and living cells (double negative) were detected using a FACSCalibur flow cytometer and subsequently analyzed using CellQuest Pro software. All the experiments were performed in triplicate.

2.5 Terminal deoxynucleotidyl transferase dUTP nick end labelling assay

DNA damage is one of the main characteristics of apoptosis. The visualization of DNA damage is achieved with terminal deoxynucleotidyl transferase dUTP nick end labeling (TUNEL) staining, which is based on the ability of the enzyme deoxynucleotidyl transferase to catalyze the addition of nucleotide dUTP to the 3′ ends free of fragmented DNA. dUTPs that are FITC-labeled fluoresce when used, and apoptotic cells can be specifically identified. For this purpose, CC cell lines were used and kept in cover slides previously treated with polylysine in six-well plates with a density of 4 × 105 cells in each well with the conditions already mentioned and with 24 h of adherence. They were exposed to the pharmacological combination for 12 and 24 h. After the drug exposure time, the cells were fixed with 4% paraformaldehyde and, through the DeadEnd Fluorometric TUNEL System Cat. G3250 kit, apoptosis was evaluated according to the manufacturer's instructions. Finally, the cells were observed under a confocal microscope and the resulting images were analyzed using Illustrator software.

2.6 Wound healing assay

A wound healing assay was performed to assess migration. An adhesive tape was placed in six-well plates. The HeLa, SiHa, and CaSki cells were seeded (4×10^5 cells per well) and maintained with 2% FBS-supplemented medium to avoid cell proliferation at 37°C, and after 24 h of adhesion, the tape was removed to form the wound. These cells were treated with triple therapy or controls for 12 and 24 h. The cells were monitored at 0, 8, 12, and 24 h.

3 Results

3.1 TT-induced cytotoxicity against HeLa, SiHa, and CaSki cell lines

The triple therapy was evaluated at 12 and 24 h against the three CC cell lines at different concentrations. The time selected for this investigation was based on our previous research on colon and

breast cancers (26, 27), where the effect exerted by the TT inducing apoptosis and autophagy starts at short times (4 h). Moreover, in the breast cancer *in vivo* model, tumor reduction with the TT was initiated at 24 h (26). These results provided the timing used in this work. The percentage of cell growth inhibition (IC_{50}) depends on the concentration of the drug and is time-dependent (Figure 1). The IC_{50} values obtained for the three cell lines were 1.5 µM/25 mM/20 mM for dox/met/ox, respectively, in 12 h, and for 24 h, the IC_{50} values were 1 µM/20 mM/15 mM for dox/met/ox, respectively, and were employed for the other tests.

3.2 The apoptosis pathway is triggered by TT in HeLa cells

We first characterized the apoptotic response with the triple therapy using a protein profile involved in apoptosis carried out on HeLa cells. For this experiment, we detected the emission of light as a result of a chemical reaction (chemiluminescence) of each point that corresponds to a specific antibody. The microarray map of Figure 2A (untreated cells) and Figure 2B (cells treated with TT) shows the location of each protein. Figures 3C, D depict the overexpression of the pro-apoptotic proteins BAD, BAX, caspase 3, cytochrome C, CD40-R, CD40L, Fas-R, Fas-L, HTRA2, p21, p27, and SMAC. Also, anti-apoptotic proteins such as XIAP, survivin, HSP27, HSP60, and HASP70 were overexpressed after TT treatment for 12 h. The experiment was performed only at 12 h, time enough to demonstrate the apoptosis induction by the triple therapy. The other proteins had no change (Figure 3D). The signal intensity of the pro-apoptotic proteins p21, HTRA2, CD40-R, caspase-3, and Bax is remarkable (Figure 3D).

The next step was to corroborate the results obtained in the microarray by WB. Proteins involved in apoptosis were evaluated in the three CC cell lines. The IC_{50} values used were those detected for each time frame, as indicated in the Materials and Methods section. Figures 2A–C shows that the activity of caspase 3 is time-dependent, increasing to 24 h in all CC cell lines treated with TT. Such results could indicate the activation of the intrinsic pathway of apoptosis due to caspase 3 detection. Caspase 8 in HeLa had no change, corresponding to the data obtained in the microarray (Figure 3A). Contrarily, in SiHa an increase in caspase-8 detection is maintained from 8 to 24 h, whereas in CaSki, an increase in caspase-8 is observed up to 12 h and decreases at 24 h. Likewise, a rise of p21 in HeLa is observed (Figure 2). The detection of XIAP in the three cell lines decreases as the exposure time with TT expires, emphasizing the absence in HeLa and SiHa at 24 h.

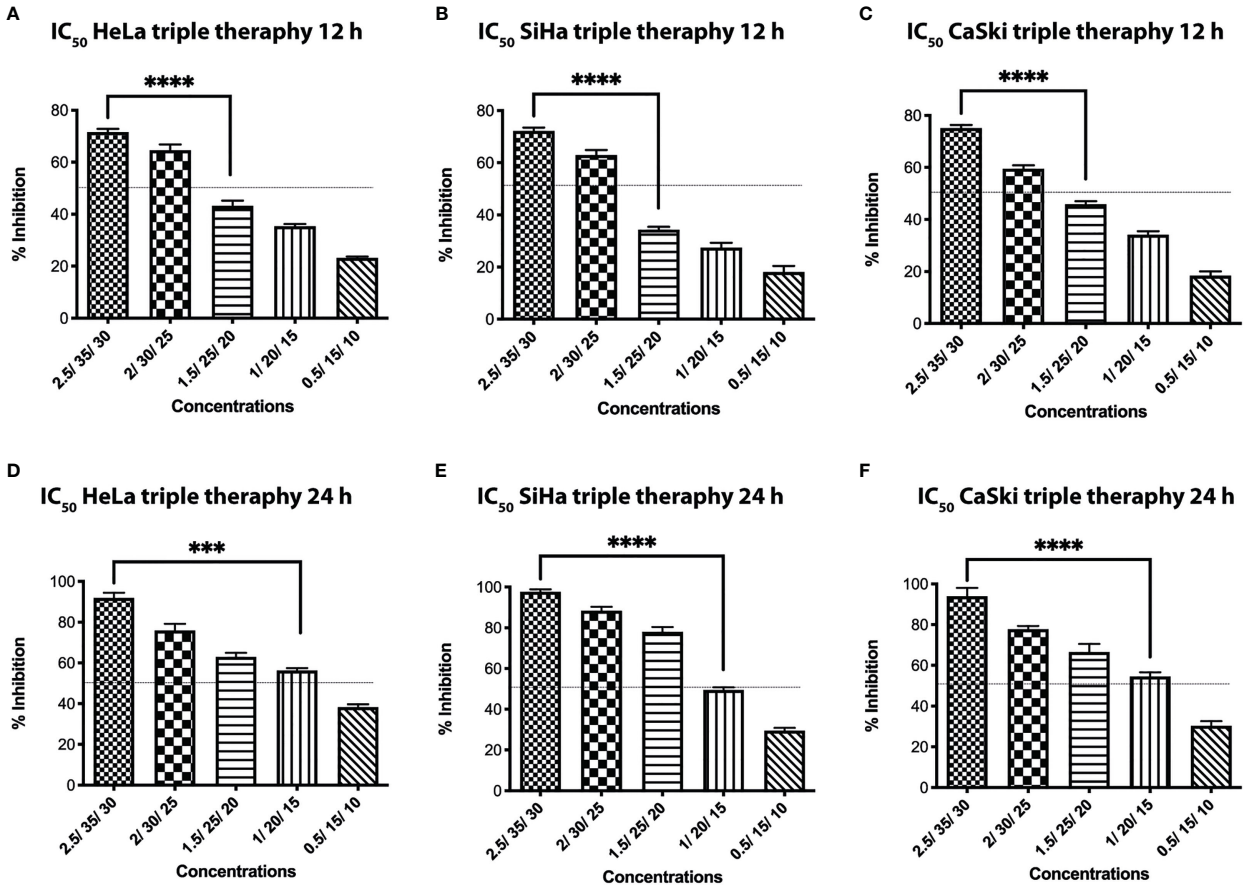

FIGURE 1
Inhibitory concentration of the TT at 12 **(A–C)** and 24 h **(D–F)** against Hela, SiHa, and CaSki cervical cancer cell lines. For all panels, *P* values were determined by the ANOVA test; ***P ≤ 0.001 ****P ≤ 0.0001.

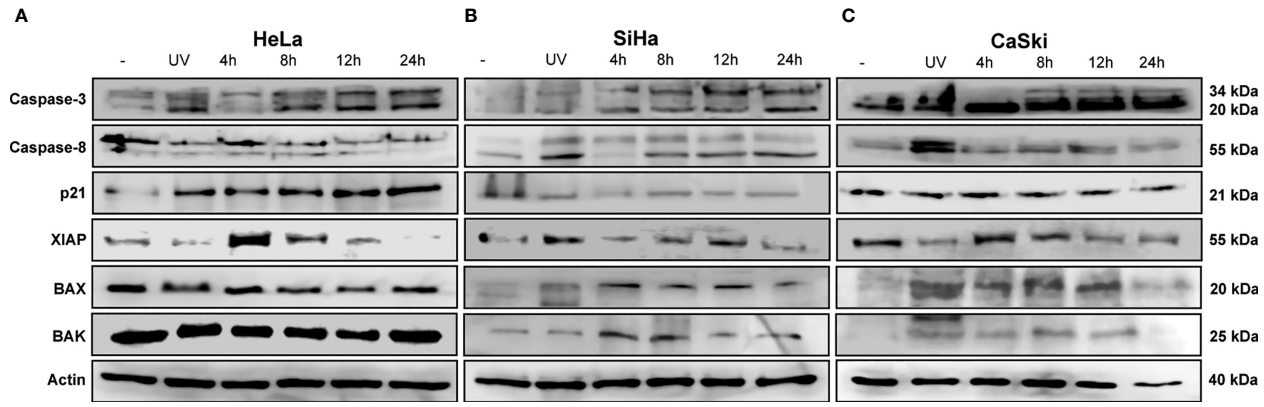

FIGURE 2
TT-induced intrinsic apoptosis by cleavage of caspase 3. **(A)** HeLa, **(B)** SiHa, and **(C)** CaSki CC cell lines. All cells were treated with the TT at 4, 8, 12, and 24 (h) UV radiation (positive control). The blots are a representative figure of at least three independent experiments.

Detection of BAX and BAK increased in the first hours of stimulation, although detection decreased after 24 h.

These findings together with the microarray assay and the Western blotting are complementary to each other. Information validates the proapoptotic proteins activated by the TT through caspase 3.

3.3 Early and late apoptoses are stimulated by the TT

The death of cervical cancer cells through the apoptotic pathway was analyzed by flow cytometry using the Annexin V/IP kit and the IC_{50} values previously mentioned. The TT produced late apoptosis in the three CC cell lines, above 60%, observed in the dot plots (Figure 4, right columns) compared with controls. In HeLa, the percentage of cells in apoptosis was 85.1% and 73.8% in 12 and 24 h, respectively. In SiHa, the apoptosis population corresponded to 76.6% and 84.4% in 12 and 24 h, respectively, whereas in CaSki late apoptosis was observed in 62.7% in 12 h and 54.1% in 24 h. Apoptosis induction by UV radiation over 50% was observed only in HeLa.

In summary, the TT requires 12 h to induce apoptosis in more than 60% of the three CC cell lines, keeping high percentages until 24 h over the positive control.

3.4 Morphological analysis revealed apoptotic bodies and DNA fragmentation due to the TT

Apoptosis is complex and implies many morphological changes for the cell, for example, membrane permeability, chromatin condensation, and cell shrinkage. The DNA fragmentation produced by the TT was visualized by confocal microscopy using the TUNEL assay. Figures 5A, B show the images of the cells taken after 12 and 24 h of TT stimulus. The formation of micronuclei, small extranuclear bodies that originate from fragments of chromatids and/or chromosomes that are left behind in the anaphase of dividing cells and are not included in the main nucleus during the telophase, is observed in TUNEL and MERGE marked with green. Likewise, DNA condensation is observed at the periphery of the nuclear membrane, forming a growing structure, whereas in the negative control, no DNA fragmentation is observed (Figure 5B MERGE).

In Figure 5B, for the three cell lines and the positive control (UV) in TUNEL and MERGE pictures, observed in green, the formation of apoptotic bodies and detection of fragmented DNA throughout the cell, characteristics of late apoptosis, is observed. Results are in congruence with the Annexin V/IP assay.

3.5 Triggering of intrinsic apoptosis is required for inhibition of the mTOR signaling pathway by triple therapy in cervical cancer cells

The master regulator, mTOR, plays a fundamental role in cell-cycle regulation, proliferation, apoptosis, and autophagy. To investigate the role of mTOR in triple therapy-induced apoptosis and autophagy, inhibition of mTOR and the substrate S6k was examined by Western blotting assay using phosphorylated antibodies. As shown in Figure 6, treatment with the triple therapy decreased the levels of phosphorylated mTOR and S6K in HeLa, SiHa, and CaSki cells. Our results displayed that the induction of intrinsic apoptosis through caspase-3 activation might be inhibiting the PI3K/AKT/mTOR signaling pathway. mTOR inhibition is an attractive therapeutic target in cancer due to its intervention in cellular functions such as cell survival or cell death (43), synthesis of biomolecules (44), and cell migration (45).

3.6 The TT suppressed the migration of cervical cancer cells *in vitro* at non-cytotoxic doses

Increasing evidence suggests that the mTOR pathway also plays a critical role in the regulation of cell migration. A wound healing

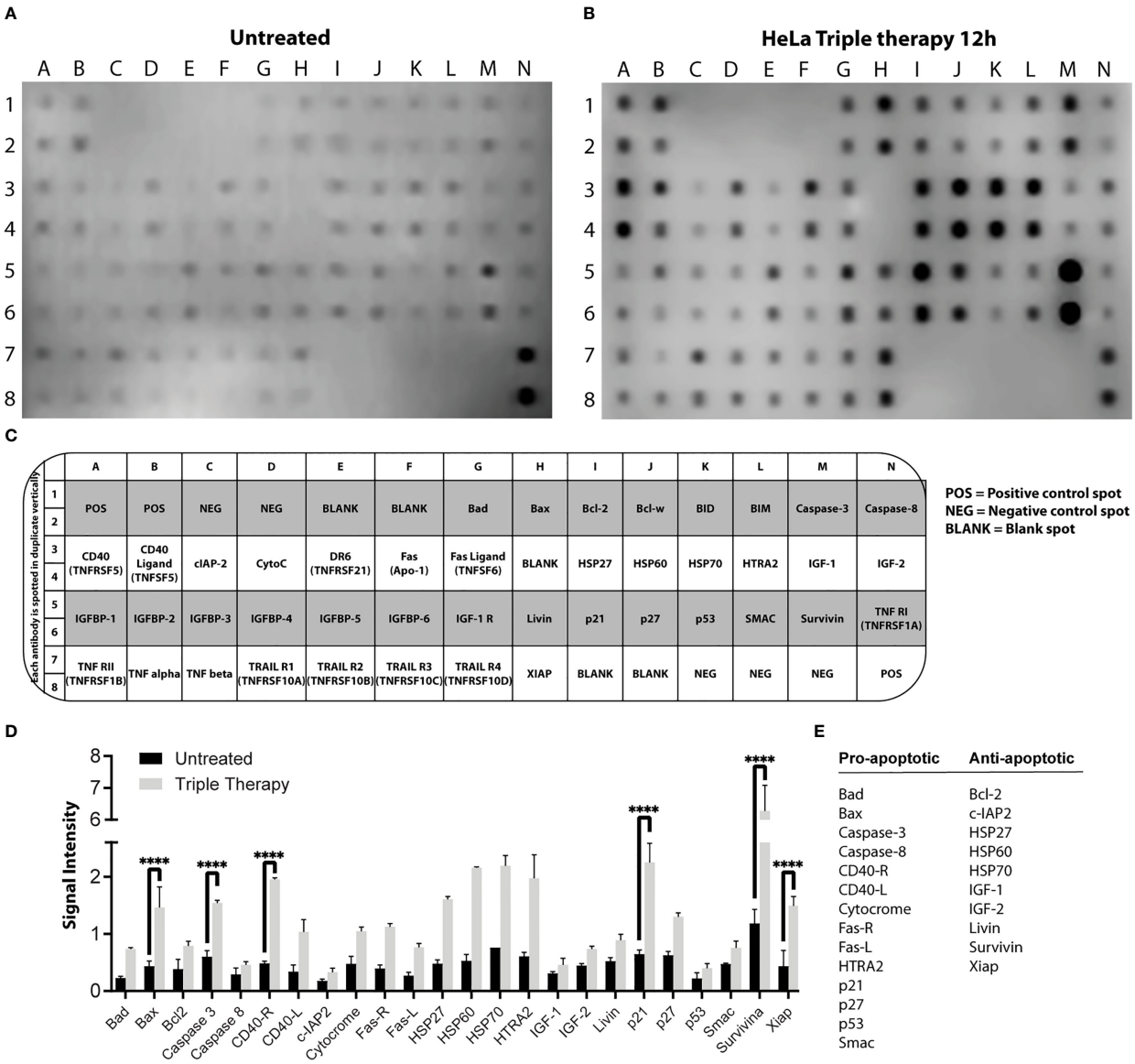

FIGURE 3
Profile of proteins involved in apoptosis in HeLa cells. Protein extracts of untreated cells **(A)** and treated cells **(B)** with the TT at 12 h of exposure. **(C)** Map array showing the location of apoptosis-related antibodies detected by the Apoptosis Kit. **(D)** Chemiluminescent intensities quantified by densitometry. A positive control was used to normalize the membrane results. **(E)** Proteins were selected and divided into two groups (pro-apoptotic or anti-apoptotic); *P* values were determined by two-way ANOVA test; ****P ≤ 0.0001.

assay was performed to test whether the triple therapy exerts an anti-migratory effect on cervical cancer cells. Cells were treated with the TT, doxorubicin, or untreated for 8, 12, and 24 h, respectively (Figure 7). Following treatment with the triple therapy for up to 24 h, cell migration was significantly inhibited, with a wound area of ~90.0% compared with the control of ~30% and doxorubicin in HeLa and CaSki ((Figure 7B). The control drug for this experiment was doxorubicin (positive control) to compare with the TT. These results suggest that the anti-migratory effects of the triple therapy may be potentially related to the induction of apoptosis and mTOR inhibition. In summary, the TT is a multitarget successful apoptosis-inducing combination.

4 Discussion

Cancer cells share several hallmarks that confer them a unique metabolism. However, the success of treatment not only depends on suppressing those characteristics but also on multifactorial events, such as sex, age, stage of disease, and response to treatment (43). The mentioned external factors establish different circumstances for treatment decisions turning the new therapeutic strategies into personal or individual medicine in the near future. In this context, our chemo design is optimistic. We propose a combination of three drugs targeting essential mechanisms of cell survival and proliferation, driving cancer cells to death in three

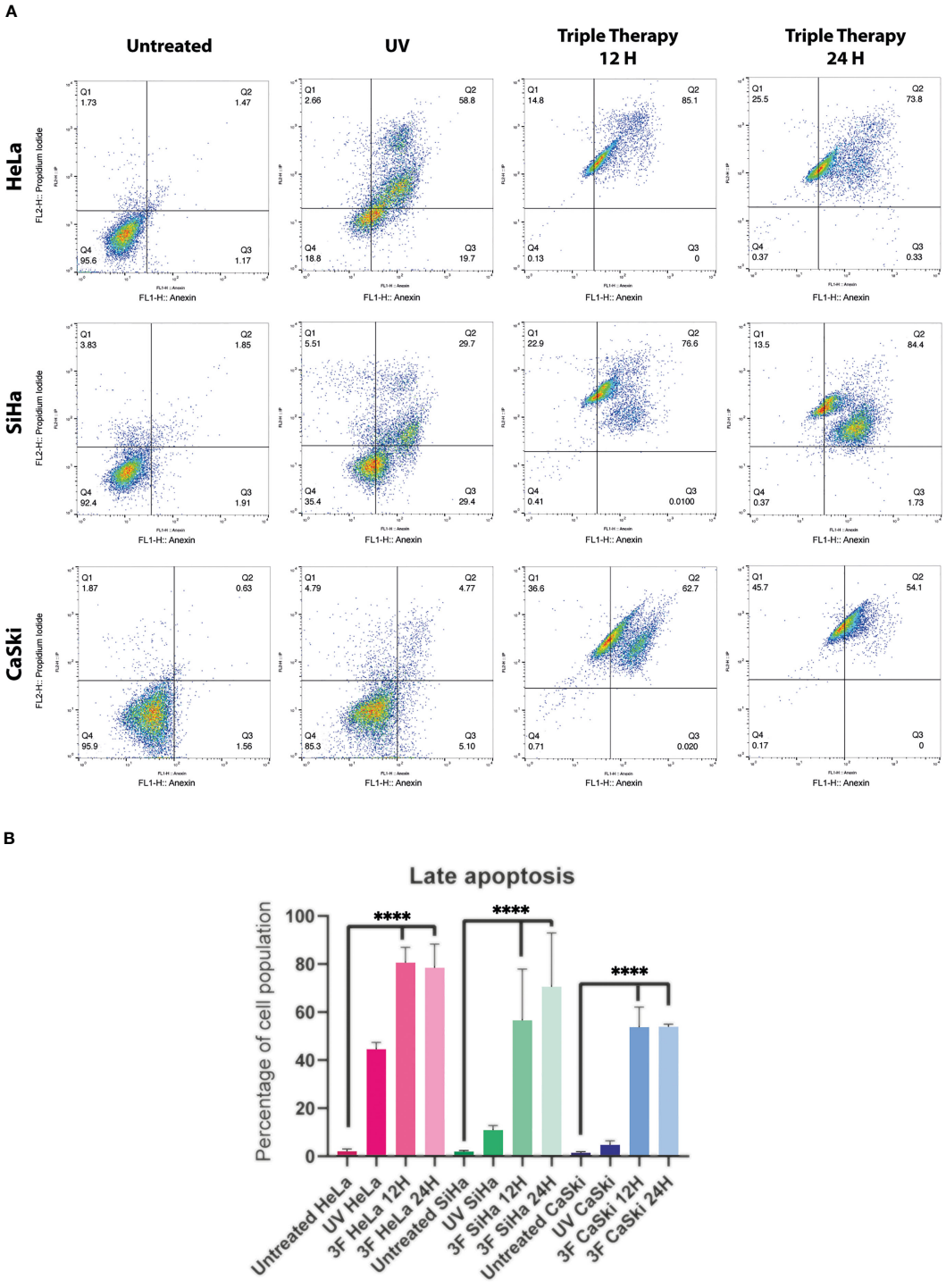

FIGURE 4
Dot plots from flow cytometry of Cervical cancer cells untreated, or treated with UV, or TT at 12 and 24 h of stimulation. **(A)** The dot plots are a representative image of at least three independent experiments. **(B)** The bar graph shows the percentage of cells undergoing apoptosis in response to triple therapy for 12 and 24 (h) *P* values were determined by ANOVA test; ****P ≤ 0.0001.

different CC cell lines. Hela cells correspond to the HPV-18 form, whereas SiHa and CaSki correspond to the HPV-16 genotype (44).

The mTOR pathway has been explored as a potential therapeutic target in cancer as it integrates two of the main signals in the regulation of cell growth activated by tyrosine kinase receptors and nutrients, including amino acids and glucose (45). One of the principal pathways leading to mTOR activation is PI3K/AKT (46), which plays an essential role in cancer progression. mTOR phosphorylates S6K, its major effector leading to protein synthesis and promoting cell survival by inhibiting the pro-apoptotic protein BAD. Furthermore, mTOR regulates autophagy characterized by the formation of autophagic vesicles and the

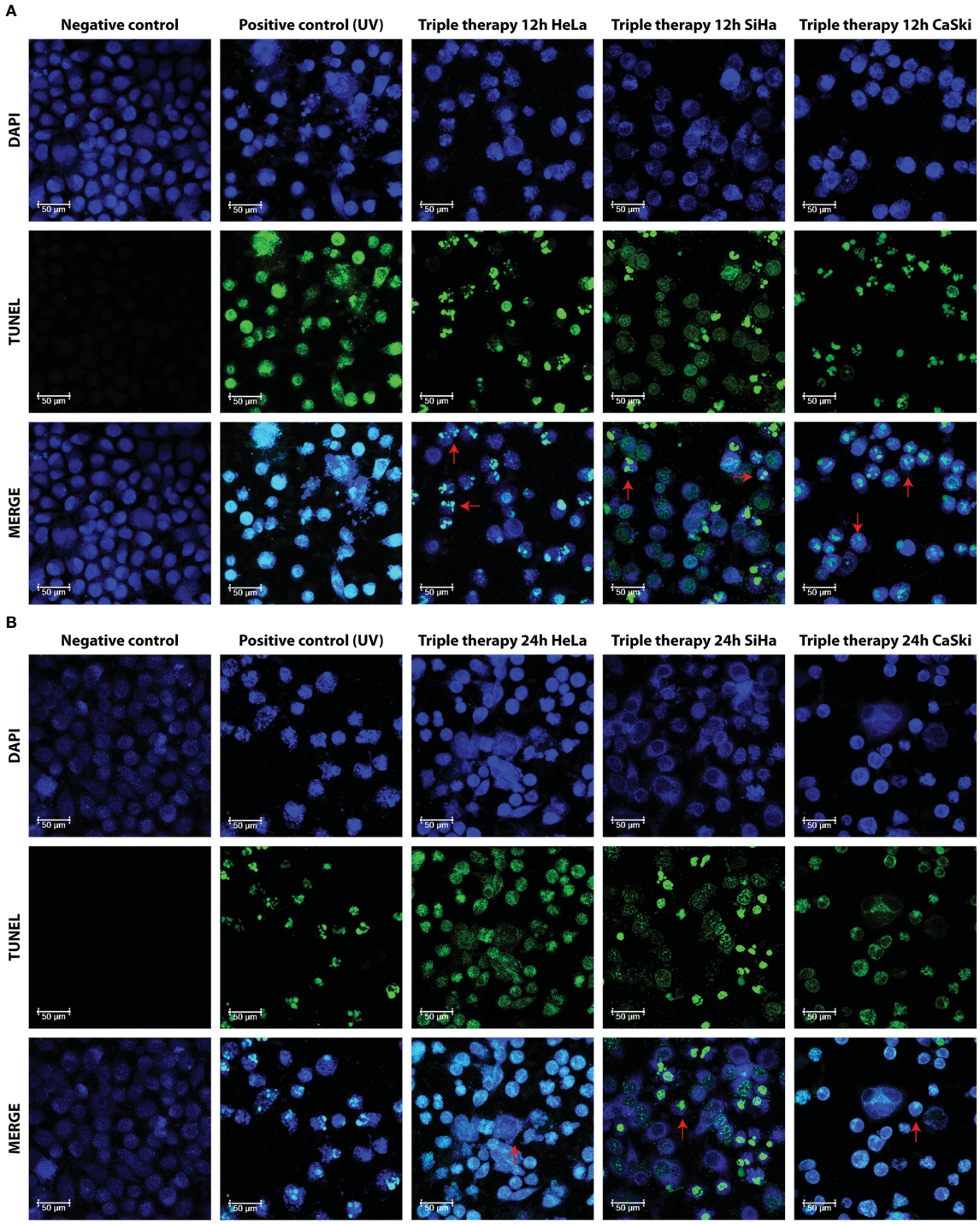

FIGURE 5
Morphological aspect of DNA fragmentation in HeLa, SiHa, and CaSki cells. Fluorescence images taken with LEICA confocal microscope at 63x with DAPI, TUNEL (dUTP cutoff marking of TUNEL deoxynucleotidyl transferase terminal), and MERGE markers in untreated cells (negative control), UV (positive control), and TT at 12 h **(A)** and 24 h **(B)** of exposure. Photos are representative of at least three independent experiments.

envelopment of organelles and proteins to recycle nutrients. Autophagy is activated mainly by the deprivation of nutrients such as glucose and amino acids. Therefore, the mTOR pathway is a sensor of the energy content of the cell, as it responds to AMP/ATP levels through AMPK, which inactivates mTOR when the AMP/ATP ratio increases. This event causes ULK1, ULK2, and Atg13 to be activated by phosphorylation leading to the initiation of autophagic vesicle conformation (47). Our findings indicate that TT involves the mTOR pathway to induce apoptosis in CC cell lines. Such an event is observed by the depletion of mTOR-activated levels when cells are stimulated with the TT (Figure 6, 12 h). According to these results and the previous ones obtained in colon

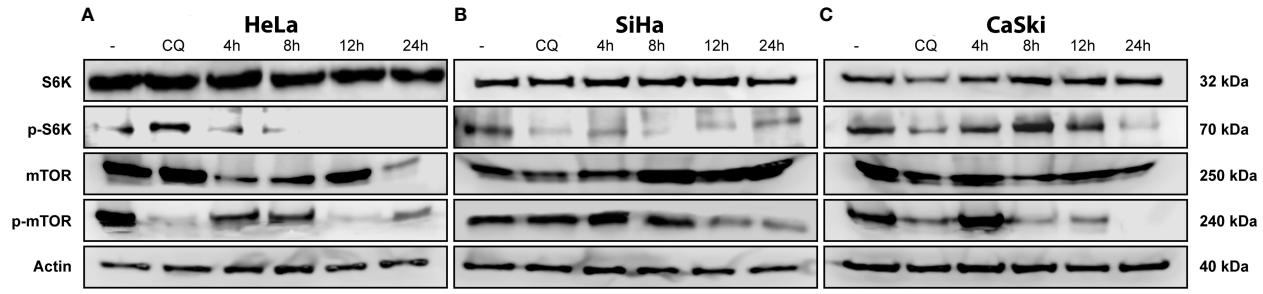

FIGURE 6
TT-induced suppression of the mTOR pathway. **(A)** HeLa, **(B)** SiHa, and **(C)** CaSki CC cell lines. All cells were treated with TT at 4, 8, 12, and 24 (h) Chloroquine (positive control). The blots are a representative figure of at least three independent experiments.

and breast cancers, we can suggest that the depletion of mTOR is due to the synergistic interaction of the drug combination. In summary, metformin induces apoptosis through inhibition of mTOR *via* AMPK activation (36, 48), sodium oxamate inhibits the lactate dehydrogenase enzyme and aerobic glycolysis (49), and doxorubicin interferes with DNA synthesis (50, 51). Each drug eventually triggers key cell pathways leading to cell death, assembling a novel and attractive therapeutic strategy for cancer treatment.

The mechanism of action of these drugs is based on the inhibition of the energy generation pathways of the tumor cell: glycolysis, the mTOR pathway, and DNA synthesis (29, 35, 39). Thus, the combined inhibition of the glycolytic pathway could lead to a complete depletion of cellular ATP and increment cell death (35, 45–49, 52). Metformin-induced activation of AMPK is associated with increased oxidative stress, cell-cycle arrest, and induction of apoptosis (53). The combination of phenformin (another biguanide) and oxamate increases the number of cells in late apoptosis in different cancer cells and increases ROS levels and DNA damage (35, 36, 45, 47–49). The mix of metformin and sodium oxamate induces cell death in 85% of cells in late apoptosis in melanoma cancer, (54) and there was a decrease in LDHA, lactate, and ATP levels (55). Our group (50) showed metformin and oxamate plus doxorubicin-induced late apoptosis, an increase of protein caspase-3, and a drop in PARP-1 in triple-negative breast cancer cells. In this study, we aimed to identify the apoptosis pathway activated by the three drugs in combination in cervical cancer. For this purpose, we performed flow cytometry, Western blot, and confocal microscopy as complementary techniques to settle the activation of apoptosis. Our results indicate that the TT induced late apoptosis (Figure 3).

The execution of intrinsic apoptosis is characterized by permeabilization of the mitochondrial outer membrane (MOMP), enabling the release of cytochrome C leading to apoptosome formation and subsequent cleavage and activation of effector caspases (3 and 7) (56); as observed with the triple-therapy treatment, there is an increase in the detection of cleaved caspase-3, but not cleavage caspase-8, which is involved in extrinsic apoptosis (57). Taken together, these data indicate that the triple therapy may trigger intrinsic apoptosis (Figure 2).

It was reported elsewhere that metformin (51) and oxamate (52, 58) induced the activation of proteins implicated in intrinsic apoptosis (59) (BAD, BAX, cytochrome-C, Apaf-1, caspase-9, caspase-3 and 7) and decreased antiapoptotic proteins such as Bcl-2 and XIAP. It has been demonstrated that in the presence of an apoptotic stimulus, mitochondrial survivin is released to the cytosol, (60) where it inhibits the activation of caspase-3 through its interaction with XIAP to continue proliferating (61); metformin decreases XIAP expression in colorectal cancer by STAT3 suppression (47).

The induction of early apoptosis is related to the activation of Bcl-2 family proteins, depolarization of mitochondria, and activation of caspases (62) and occurs approximately 30 min after the applied stimulus (63). In the case of late apoptosis, it occurs after caspase activation induces nuclear condensation and the formation of apoptotic bodies, in a time frame of 4 to 24 h depending on the stimulus (63). Our outcomes revealed that cells treated with the TT induce apoptosis by the intrinsic pathway *via* caspase 3. Based on our previous studies, this results in decreased glucose consumption, inhibition of cell growth, and proliferation signals by blocking the mTOR pathway, eventually inducing late apoptosis cell death (50, 64).

One strategy in the search for anticancer treatments is the use of drugs known to be utilized for other treatments whose mechanism of action is involved in some target of the tumor cell. This is known as drug repositioning (65, 66). Its advantages are its toxicological history, which helps in terms of safety, knowledge of collateral effects, effectiveness, and even reduction of costs. The success of the therapies will also depend on the multiple performances of the pharmacological proposal, in order to attack the tumor cell at several points simultaneously. Our research covers two main targets in cancer therapy, energy metabolism and the inhibition of cell proliferation, key steps to stop tumor growth, and subsequent invasion and metastasis.

The combination of Dox–Met–Ox is an excellent candidate for drug repositioning in cancer treatment. Together, they exerted *in vitro* apoptosis induction in cervix, colon, and breast cancer cell lines (50, 64). Moreover, their synergy showed tumor growth suppression and no accumulative or new detectable side effects *in vivo*. The drugs composing the TT are well characterized at therapeutically effective doses worthy of further study and go a step forward to clinical trials.

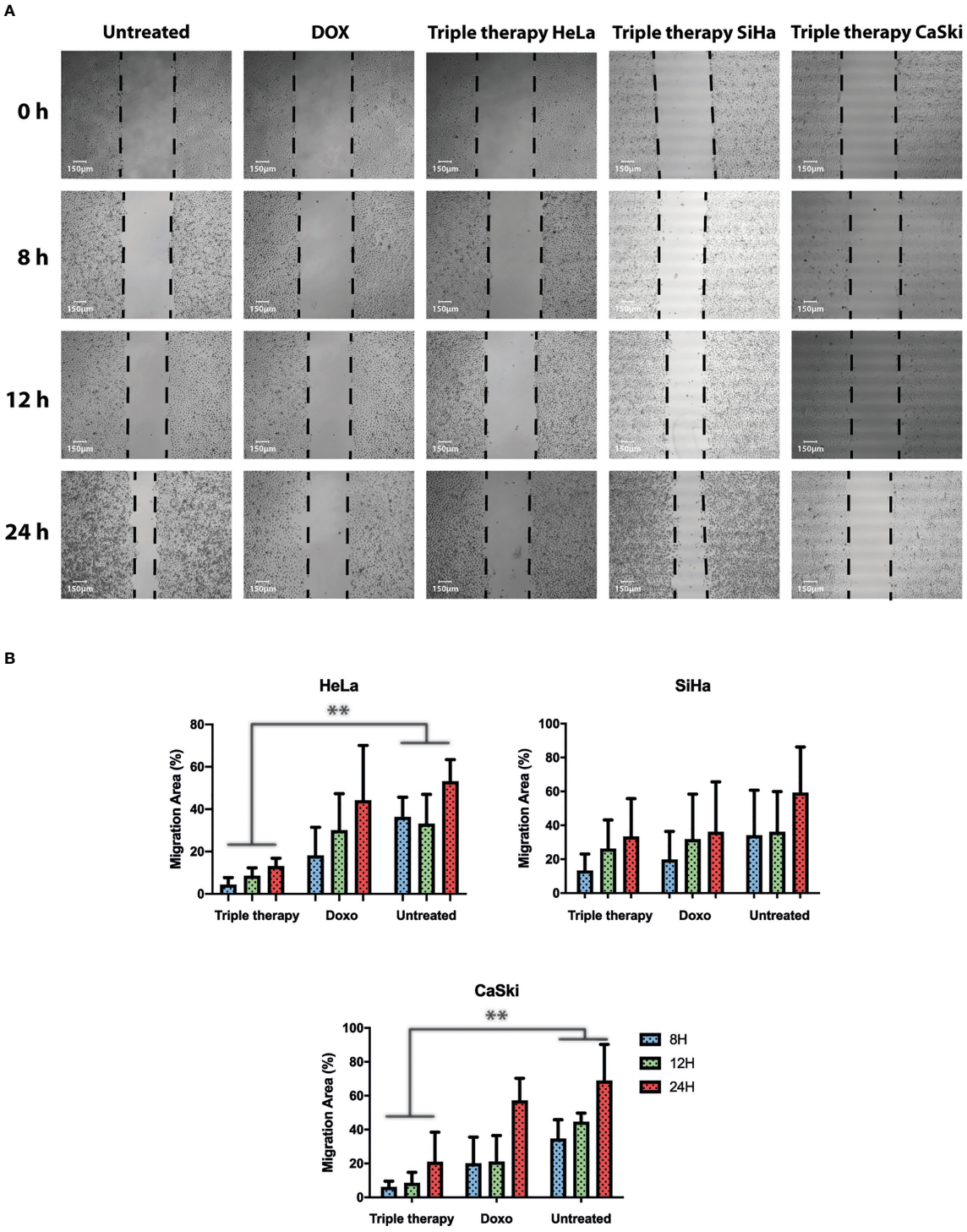

FIGURE 7
Triple therapy suppresses migration abilities in HeLa, SiHa, and CaSki cells compared with doxorubicin. A wound scratch assay was performed according to the procedure described in Materials and Methods in HeLa, SiHa, and CaSki. **(A)** Cell migration was observed at time 0 and 8, 12, and 24 h after scratching by photographs (magnification: 10×), and reduction of the initial scratch area was compared. **(B)** Quantitative analysis of the migration area was performed for HeLa, SiHa, and CaSki. All results are representative of three independent experiments. *P* values were determined by ANOVA test; **P ≤ 0.01.

All the backgrounds supporting the effectiveness and safety of metformin and oxamate, added to the metformin and doxorubicin success in the clinic, were taken together for our research group to propose them as a therapeutic option for a diverse of cancers.

Data availability statement

The original contributions presented in the study are included in the article/supplementary material. Further inquiries can be directed to the corresponding authors.

Author contributions

ID-W performed and analyzed *in vitro* experiments and participated in the discussion of the article. SS-A performed the microscopy experiments and analyzed results. CC, JP, IA and VG-C analyzed the results and NJ-H and CP-P were responsible for conceptualization, discussion, writing, and funding resources. All authors contributed to the article and approved the submitted version.

Funding

This work was supported by CONACYT, Mexico, project nos. CB-2016-285884 and UNAM/PAPIIT-IN231420.

Acknowledgments

This paper is part of the requirements for obtaining a doctoral degree at the Posgrado en Ciencias Biológicas, UNAM, of ID-W. Financing was granted by CONACYT for the scholarship no. 868414; NJ-H thanks CONACYT for the grant CB-2016-285884; C.P-P thanks UNAM/PAPIIT for the grant IN231420.

Conflict of interest

The authors declare that the research was conducted in the absence of any commercial or financial relationships that could be construed as a potential conflict of interest.

Publisher's note

References

1. Siegel RL, Miller KD, Fuchs HE, Jemal A. Cancer statistics, 2022. *CA Cancer J Clin* (2022) 72(1):7–33. doi: 10.3322/caac.21708

2. Zhang H, Kong W, Chen S, Zhao X, Luo D, Xie Y. Surgical staging of locally advanced cervical cancer: current status and research progress. *Front Oncol* (2022) 12:3277. doi: 10.3389/fonc.2022.940807

3. Anand U, Dey A, Chandel AKS, Sanyal R, Mishra A, Pandey DK, et al. Cancer chemotherapy and beyond: current status, drug candidates, associated risks and progress in targeted therapeutics. *Genes Dis* (2022). doi: 10.1016/j.gendis.2022.02.007

4. Debela DT, Muzazu SG, Heraro KD, Ndalama MT, Mesele BW, Haile DC, et al. New approaches and procedures for cancer treatment: current perspectives. *SAGE Open Med* (2021) 9:205031212110343. doi: 10.1177/20503121211034366

5. Arunachalam SS, Shetty AP, Panniyadi N, Meena C, Kumari J, Rani B, et al. Study on knowledge of chemotherapy's adverse effects and their self-care ability to manage - the cancer survivors impact. *Clin Epidemiol Glob Health* (2021) 11:100765. doi: 10.1016/j.cegh.2021.100765

6. Pichler M, Steyrer J. Cost-effectiveness analysis of the use of immunotherapy in metastatic solid tumours in Austria by applying the ESMO-magnitude of clinical benefit scale (ESMO-MCBS) version 1.1. *ESMO Open* (2021) 6(4):100198. doi: 10.1016/j.esmoop.2021.100198

7. Alfarouk KO, Stock CM, Taylor S, Walsh M, Muddathir AK, Verduzco D, et al. Resistance to cancer chemotherapy: failure in drug response from ADME to p-gp. *Cancer Cell Int* (2015) 15(1):71. doi: 10.1186/s12935-015-0221-1

8. Bukowski K, Kciuk M, Kontek R. Mechanisms of multidrug resistance in cancer chemotherapy. *Int J Mol Sci* (2020) 21(9):3233. doi: 10.3390/ijms21093233

9. Wang X, Zhang H, Chen X. Drug resistance and combating drug resistance in cancer. *Cancer Drug Res* (2019) 2(2):141–60. doi: 10.20517/cdr.2019.10

10. Das T, Anand U, Pandey SK, Ashby CR, Assaraf YG, Chen ZS, et al. Therapeutic strategies to overcome taxane resistance in cancer. *Drug Resist Update* (2021) 55:100754. doi: 10.1016/j.drup.2021.100754

11. Maeda H, Khatami M. Analyses of repeated failures in cancer therapy for solid tumors: poor tumor-selective drug delivery, low therapeutic efficacy and unsustainable costs. *Clin Transl Med* (2018) 7(1):11. doi: 10.1186/s40169-018-0185-6

12. Chen Q, Cao HZ, Zheng PS, Chen Q, Cao HZ, Zheng PS. LGR5 promotes the proliferation and tumor formation of cervical cancer cells through the wnt/β-catenin signaling pathway. *Oncotarget* (2014) 5(19):9092–105. doi: 10.18632/oncotarget.2377

13. Coronel-Hernández J, Pérez-Yépez EA, Delgado-Waldo I, Contreras-Romero C, Jacobo-Herrera N, Cantú-De León D, et al. Aberrant metabolism as inductor of epigenetic changes in breast cancer: therapeutic opportunities. *Front Oncol* (2021) 11:3895. doi: 10.3389/fonc.2021.676562

14. Pavlova NN, Thompson CB. The emerging hallmarks of cancer metabolism. *Cell Metab* (2016) 23(1):27–47. doi: 10.1016/j.cmet.2015.12.006

15. Wang ZH, Peng WB, Zhang P, Yang XP, Zhou Q. Lactate in the tumour microenvironment: from immune modulation to therapy. *EBioMedicine* (2021) 73:103627. doi: 10.1016/j.ebiom.2021.103627

16. de la Cruz-López KG, Castro-Muñoz LJ, Reyes-Hernández DO, García-Carrancá A, Manzo-Merino J. Lactate in the regulation of tumor microenvironment and therapeutic approaches. *Front Oncol* (2019) 9:1143. doi: 10.3389/fonc.2019.01143

17. Salgado-García R, Coronel-Hernández J, Delgado-Waldo I, de León DC, García-Castillo V, López-Urrutia E, et al. Negative regulation of ulk1 by microrna-106a in autophagy induced by a triple drug combination in colorectal cancer cells *in vitro*. *Genes (Basel)* (2021) 12(2):1–14. doi: 10.3390/genes12020245

18. Sharma D, Singh M, Gupta R, Kumar V, Kumar V, Rani R. Intervention on lactate in cancer: a promising approach for the development of cancer therapeutics. *Adv Cancer Biol - Metastas* (2022) 5:100058. doi: 10.1016/j.adcanc.2022.100058

19. Koundouros N, Poulogiannis G. Reprogramming of fatty acid metabolism in cancer. *Br J Cancer* (2019) 122(1):4–22. doi: 10.1038/s41416-019-0650-z

20. Jeong DW, Lee S, Chun YS. How cancer cells remodel lipid metabolism: strategies targeting transcription factors. *Lipids Health Dis* (2021) 20(1):1–19. doi: 10.1186/s12944-021-01593-8

21. Schiliro C, Firestein BL. Mechanisms of metabolic reprogramming in cancer cells supporting enhanced growth and proliferation. *Cells* (2021) 10(5):1056. doi: 10.3390/cells10051056

22. Kılınç G, Sasani H, Erbaş O. The warburg effect on cancer formation and progression. *J Exp Bas Med Sci* (2022) 3(2):090–6. doi: 10.5606/jebms.2022.1014

23. Fukushi A, Kim H, Chang YC, Kim CH. Revisited metabolic control and reprogramming cancers by means of the warburg effect in tumor cells. *Int J Mol Sci* (2022) 23(17):10037. doi: 10.3390/ijms231710037

24. Hernández-Lemus E, Martínez-García M. Pathway-based drug-repurposing schemes in cancer: the role of translational bioinformatics. *Front Oncol* (2021) 10:2996. doi: 10.3389/fonc.2020.605680

25. Kirtonia A, Gala K, Fernandes SG, Pandya G, Pandey AK, Sethi G, et al. Repurposing of drugs: an attractive pharmacological strategy for cancer therapeutics. *Semin Cancer Biol* (2021) 68:258–78. doi: 10.1016/j.semcancer.2020.04.006

26. García-Castillo V, López-Urrutia E, Villanueva-Sánchez O, Ávila-Rodríguez MA, Zentella-Dehesa A, Cortés-González C, et al. Targeting metabolic remodeling in triple negative breast cancer in a murine model. *J Cancer* (2017) 8(2):178–89. doi: 10.7150/jca.16387

27. Figueroa-González G, García-Castillo V, Coronel-Hernández J, López-Urrutia E, León-Cabrera S, Arias-Romero LE, et al. Anti-inflammatory and antitumor activity of a triple therapy for a colitis-related colorectal cancer. *J Cancer* (2016) 7(12):1632–44. doi: 10.7150/jca.13123

28. Imai A, Ichigo S, Matsunami K, Takagi H, Yasuda K. Clinical benefits of metformin in gynecologic oncology. *Oncol Lett* (2015) 10(2):577–82. doi: 10.3892/ol.2015.3262

29. Fontaine E. Metformin-induced mitochondrial complex I inhibition: facts, uncertainties, and consequences. *Front Endocrinol (Lausanne)* (2018) 9:753. doi: 10.3389/fendo.2018.00753

30. Wu H, Huang D, Zhou H, Sima X, Wu Z, Sun Y, et al. Metformin: a promising drug for human cancers. *Oncol Lett* (2022) 24(1):204. doi: 10.3892/ol.2022.13325

31. Liu Y, Zhang Y, Jia K, Dong Y, Ma W. [Corrigendum] metformin inhibits the proliferation of A431 cells by modulating the PI3K/Akt signaling pathway. *Exp Ther Med* (2022) 24(1):1–1. doi: 10.3892/etm.2022.11372/abstract

32. Shen Z, Xue D, Wang K, Zhang F, Shi J, Jia B, et al. Metformin exerts an antitumor effect by inhibiting bladder cancer cell migration and growth, and promoting apoptosis through the PI3K/AKT/mTOR pathway. *BMC Urol* (2022) 22(1):1–10. doi: 10.1186/s12894-022-01027-2

33. Zheng Y, Zhang H, Sun H. Metformin inhibits the proliferation and invasion of ovarian cancer cells by suppressing tripartite motif-containing 37-induced tumor necrosis factor receptor-associated factor 2 ubiquitination. *Cancer Sci* (2022) 113 (11):3776–86. doi: 10.1111/cas.15524

34. Xu Y, Xu T, Xiong Y, Huang J. [Metformin inhibits proliferation and promotes apoptosis of HER-2 positive breast cancer cells possibly through the hippo-YAP pathway]. *Nan Fang Yi Ke Da Xue Xue Bao* (2022) 42(5):740–6. doi: 10.12122/j.issn.1673-4254.2022.05.16

35. Zhao Z, Han F, Yang S, Wu J, Zhan W. Oxamate-mediated inhibition of lactate dehydrogenase induces protective autophagy in gastric cancer cells: involvement of the akt-mTOR signaling pathway. *Cancer Lett* (2015) 358(1):17–26. doi: 10.1016/j.canlet.2014.11.046

36. Miskimins WK, Ahn HJ, Kim JY, Ryu S, Jung YS, Choi JY. Synergistic anti-cancer effect of phenformin and oxamate. *PloS One* (2014) 9(1):85576. doi: 10.1371/journal.pone.0085576

37. Yang Y, Su D, Zhao L, Zhang D, Xu J, Wan J, et al. Different effects of LDH-a inhibition by oxamate in non-small cell lung cancer cells. *Oncotarget* (2014) 5 (23):11886–96. doi: 10.18632/oncotarget.2620

38. Zhai X, Yang Y, Wan J, Zhu R, Wu Y. Inhibition of LDH-a by oxamate induces G2/M arrest, apoptosis and increases radiosensitivity in nasopharyngeal carcinoma cells. *Oncol Rep* (2013) 30(6):2983–91. doi: 10.3892/or.2013.2735

39. van der Zanden SY, Qiao X, Neefjes J. New insights into the activities and toxicities of the old anticancer drug doxorubicin. *FEBS J* (2021) 288(21):6095–111. doi: 10.1111/febs.15583

40. Kalyanaraman B. Teaching the basics of the mechanism of doxorubicin-induced cardiotoxicity: have we been barking up the wrong tree? *Redox Biol* (2020) 29:101394. doi: 10.1016/j.redox.2019.101394

41. Micallef I, Baron B. Doxorubicin: an overview of the anti-cancer and chemoresistance mechanisms. *Ann Clin Toxicol* (2020) 3(2):1031.

42. Vichai V, Kirtikara K. Sulforhodamine b colorimetric assay for cytotoxicity screening. *Nat Protoc* (2006) 1(3):1112–6. doi: 10.1038/nprot.2006.179

43. Zhu J, Wang H, Jiang X. mTORC1 beyond anabolic metabolism: regulation of cell death. *J Cell Biol* (2022) 221(12):221. doi: 10.1083/jcb.202208103

44. Yang M, Lu Y, Piao W, Jin H. The translational regulation in mTOR pathway. *Biomolecules* (2022) 12(6):802. doi: 10.3390/biom12060802

45. Huang S, Zhou H. Role of mTOR signaling in tumor cell motility, invasion and metastasis. *Curr Protein Pept Sci* (2011) 12(1):30–42. doi: 10.2174/138920311795659407

46. Zhang C, Zhang C, Wang Q, Li Z, Lin J, Wang H. Differences in stage of cancer at diagnosis, treatment, and survival by race and ethnicity among leading cancer types. *JAMA Netw Open* (2020) 3(4):e202950–e202950. doi: 10.1001/jamanetworkopen.2020.2950

47. Meissner JD. Nucleotide sequences and further characterization of human papillomavirus DNA present in the CaSki, SiHa and HeLa cervical carcinoma cell lines. *J Gen Virol* (1999) 80(7):1725–33. doi: 10.1099/0022-1317-80-7-1725

48. Inoki K, Corradetti MN, Guan KL. Dysregulation of the TSC-mTOR pathway in human disease. *Nat Genet* (2005) 37(1):19–24. doi: 10.1038/ng1494

49. Sekulić A, Hudson CC, Homme JL, Yin P, Otterness DM, Karnitz LM, et al. A direct linkage between the phosphoinositide 3-Kinase-AKT signaling pathway and the mammalian target of rapamycin in mitogen-stimulated and transformed Cells1. *Cancer Res | Am Assoc Cancer Res* (2000) 60(13):3504–13

50. Coronel-Hernández J, Salgado-García R, Cantú-De León D, Jacobo-Herrera N, Millan-Catalan O, Delgado-Waldo I, et al. Combination of metformin, sodium oxamate and doxorubicin induces apoptosis and autophagy in colorectal cancer cells via downregulation HIF-1α. *Front Oncol* (2021) 11:594200. doi: 10.3389/fonc.2021.594200

51. Shafiei-Irannejad V, Samadi N, Yousefi B, Salehi R, Velaei K, Zarghami N. Metformin enhances doxorubicin sensitivity via inhibition of doxorubicin efflux in p-gp-overexpressing MCF-7 cells. *Chem Biol Drug Des* (2018) 91(1):269–76. doi: 10.1111/cbdd.13078

52. Wu YT, Tan HL, Huang Q, Ong CN, Shen HM. Activation of the PI3K-Akt-mTOR signaling pathway promotes necrotic cell death via suppression of autophagy. *Autophagy* (2009) 5(6):824–34. doi: 10.4161/auto.9099

53. Dowling RJO, Zakikhani M, Fantus IG, Pollak M, Sonenberg N. Metformin inhibits mammalian target of rapamycin-dependent translation initiation in breast cancer cells. *Cancer Res* (2007) 67(22):10804–12. doi: 10.1158/0008-5472.CAN-07-2310

54. Chaube B, Malvi P, Singh SV, Mohammad N, Meena AS, Bhat MK. Targeting metabolic flexibility by simultaneously inhibiting respiratory complex I and lactate generation retards melanoma progression. *Oncotarget* (2015) 6(35):37281–99. doi: 10.18632/oncotarget.6134

55. Valvona CJ, Fillmore HL. Oxamate, but not selective targeting of LDH-a, inhibits medulloblastoma cell glycolysis, growth and motility. *Brain Sci* (2018) 8 (4):56. doi: 10.3390/brainsci8040056

56. Brentnall M, Rodriguez-Menocal L, De Guevara RL, Cepero E, Boise LH. Caspase-9, caspase-3 and caspase-7 have distinct roles during intrinsic apoptosis. *BMC Cell Biol* (2013) 14(1):1–9. doi: 10.1186/1471-2121-14-32

57. Beaudouin J, Liesche C, Aschenbrenner S, Hörner M, Eils R. Caspase-8 cleaves its substrates from the plasma membrane upon CD95-induced apoptosis. *Cell Death Differ* (2013) 20(4):599–610. doi: 10.1038/cdd.2012.156

58. Park JH, Kim Yh, Park EH, Lee SJ, Kim H, Kim A, et al. Effects of metformin and phenformin on apoptosis and epithelial-mesenchymal transition in chemoresistant rectal cancer. *Cancer Sci* (2019) 110(9):2834–45. doi: 10.1111/cas.14124

59. Chen H, Sun B, Sun H, Xu L, Wu G, Tu Z, et al. Bak instead of bax plays a key role in metformin-induced apoptosis s in HCT116 cells. *Cell Death Discov* (2021) 7 (1):1–9. doi: 10.1038/s41420-021-00755-y

60. Antonio Cheung CH, Huang CC, Tsai FY, Lee JYC, Cheng SM, Chang YC, et al. Survivin – biology and potential as a therapeutic target in oncology. *Onco Targets Ther* (2013) 6:1453. doi: 10.2147/OTT.S33374

61. Lu CC, Chiang JH, Tsai FJ, Hsu YM, Juan YN, Yang JS, et al. Metformin triggers the intrinsic apoptotic response in human AGS gastric adenocarcinoma cells by activating AMPK and suppressing mTOR/AKT signalling. *Int J Oncol* (2019) 54 (4):1271–81. doi: 10.3892/ijo.2019.4704/abstract

62. Rehm M, Huber HJ, Dussmann H, Prehn JHM. Systems analysis of effector caspase activation and its control by X-linked inhibitor of apoptosis protein. *EMBO J* (2006) 25(18):4338–49. doi: 10.1038/sj.emboj.7601295

63. Altinoz MA, Ozpinar A. Oxamate targeting aggressive cancers with special emphasis to brain tumors. *Biomed Pharmacother* (2022) 147:112686. doi: 10.1016/j.biopha.2022.112686

64. Qiao T, Xiong Y, Feng Y, Guo W, Zhou Y, Zhao J, et al. Inhibition of LDH-a by oxamate enhances the efficacy of anti-PD-1 treatment in an NSCLC humanized mouse model. *Front Oncol* (2021) 11:1033. doi: 10.3389/fonc.2021.632364

65. Lei Y, Yi Y, Liu Y, Liu X, Keller ET, Qian CN, et al. Metformin targets multiple signaling pathways in cancer. *Chin J Cancer* (2017) 36(1):1–9. doi: 10.1186/s40880-017-0184-9

66. Bouche G, Gedye C, Meheus L, Pantziarka P. Drug repurposing in oncology. *Lancet Oncol* (2020) 21(12):e542. doi: 10.1016/S1470-2045(20)30561-1

frontiers | Frontiers in Oncology

TYPE Review
PUBLISHED 04 July 2023
DOI 10.3389/fonc.2023.1079041

OPEN ACCESS

EDITED BY
João Pessoa,
University of Coimbra, Portugal

REVIEWED BY
Douglas K. Graham,
Emory University, United States
Isabel Ben-Batalla,
German Cancer Research Center (DKFZ), Germany

*CORRESPONDENCE
Abbes Belkhiri
abbes.belkhiri@vanderbilt.edu

RECEIVED 24 October 2022
ACCEPTED 31 May 2023
PUBLISHED 04 July 2023

CITATION
Pidkovka N and Belkhiri A (2023) Altered expression of AXL receptor tyrosine kinase in gastrointestinal cancers: a promising therapeutic target. *Front. Oncol.* 13:1079041. doi: 10.3389/fonc.2023.1079041

Altered expression of AXL receptor tyrosine kinase in gastrointestinal cancers: a promising therapeutic target

Nataliya Pidkovka[1] and Abbes Belkhiri[2,3]*

[1]Department of Health Science, South College, Nashville, TN, United States, [2]Department of Surgery, Vanderbilt University Medical Center, Nashville, TN, United States, [3]Vanderbilt-Ingram Cancer Center, Vanderbilt University Medical Center, Nashville, TN, United States

Gastrointestinal (GI) cancers that include all cancers of the digestive tract organs are generally associated with obesity, lack of exercising, smoking, poor diet, and heavy alcohol consumption. Treatment of GI cancers typically involves surgery followed by chemotherapy and/or radiation. Unfortunately, intrinsic or acquired resistance to these therapies underscore the need for more effective targeted therapies that have been proven in other malignancies. The aggressive features of GI cancers share distinct signaling pathways that are connected to each other by the overexpression and activation of AXL receptor tyrosine kinase. Several preclinical and clinical studies involving anti-AXL antibodies and small molecule AXL kinase inhibitors to test their efficacy in solid tumors, including GI cancers, have been recently carried out. Therefore, AXL may be a promising therapeutic target for overcoming the shortcomings of standard therapies in GI cancers.

KEYWORDS

GI cancers, targeted therapy, small molecule inhibitors, anti-AXL antibodies, Gas6

Introduction

Increasing cancer risk factors linked to emerging economy and globalization have aggravated the global cancer burden with an expected 47% increase of incidence in 2040 relative to 2020 (1). The rising disease burden caused by the malignancies of the digestive system has become one of the major public health challenges. Particularly, colorectal (10%) stomach (5.6%), esophageal (3.1%), liver (8.3%), and pancreatic (4.7%) cancers are among the most diagnosed malignancies after female breast and lung cancers (11.7% and 11.4% accordingly) (1, 2). Therefore, there is a critical need for identifying reliable molecular markers and targets for gastrointestinal (GI) oncotherapies. For the last decade, AXL receptor tyrosine kinase, also known as UFO, attracted a substantial interest in cancer biology because of the progressively accumulated data demonstrating the ability of this protein to regulate cell survival, proliferation, and motility in normal and cancer tissues (3–8). The selective overexpression of AXL in GI malignancies is associated with a

poor clinical prognosis (9–11), proliferation (10, 12, 13), metastasis (14), immunosuppressive tumor microenvironment (3, 15, 16), and drug resistance (17, 18). This review provides a comprehensive update on the current research initiatives highlighting AXL as a promising therapeutic target and a novel diagnostic and prognostic marker of GI cancers. The research findings from preclinical and clinical studies on the evaluation of drugs in targeting the AXL-mediated signaling pathways in GI cancers are reviewed.

AXL function and signaling

AXL protein (100 - 140 kDa) belongs to the receptor tyrosine kinase (RTK) subfamily of transmembrane receptors TAM, which comprises TYRO3 (19), AXL (20), and MER (21–23). Initially, AXL was identified as a transforming gene in patients with chronic myelogenous leukemia (24). Later, the names AXL (from the Greek "anexelekto", meaning "uncontrolled") and UFO were given concurrently to the same cDNA encoding an RTK overexpressed in human myeloid leukemia cells (25, 26) and NIH3T3 mouse fibroblasts transfected with DNA from a patient with a chronic myeloproliferative disorder (20, 27). TAM family of RTKs is characterized by a combination of two immunoglobin-like domains and fibronectin type III domains in the extracellular (N-terminal) region. AXL also has an intracellular (C-terminal) tyrosine kinase domain, which plays an essential role in signal transduction (28). The vitamin k-dependent growth arrest-specific protein 6 (Gas6) (29) serves as a high affinity ligand for AXL (21, 30, 31). Gas6 binding to AXL primes the homodimerization of receptor with another Gas6/AXL ligand-receptor complex and autophosphorylation of three tyrosine residues (32). This set of reactions initiates the recruitment of p85 subunit of phosphoinositide-3 kinase (PI3K), phospholipase C-γ (PLCγ), or growth factor receptor–bound protein 2 (Grb2) and activate the relevant downstream signaling pathways involved in survival, proliferation, or migration (33, 34). Notably, the activation of AXL is negatively regulated by the binding of its soluble form sAXL to Gas6 (34, 35). Important physiological functions of the Gas6/AXL pathway include cell migration and survival (36), adhesion (37), and suppression of apoptosis (38) in inflammatory, endothelial, and smooth muscle cells. Additionally, the Gas6/AXL signaling plays an important role in the activation of macrophages and phagocytosis (39).

AXL expression in GI cancers (esophagus, stomach, pancreas, liver and colon)

Since genetic modifications of *AXL* gene, such as rearrangement, amplification, or mutations, are relatively rare (40, 41), the AXL functions in GI cancers are likely determined by the level of its expression. High expression of AXL has been reported in a variety of primary GI tumors and metastases and linked to poor clinical prognosis (Table 1) (11, 42–45). Invasive esophageal adenocarcinoma (EAC) frequently progresses from a premalignant condition, gastroesophageal reflux disease-associated Barrett's esophagus (BE). AXL expression is linked to adverse prognosis in EAC (11) as well as poor prognosis and distant metastases in esophageal squamous cell carcinoma (43). Particularly, serial analysis of gene expression (SAGE) indicated a significant upregulation of AXL "tags" in metachronous mucosal biopsy samples obtained from a patient progressed from BE to EAC (11). Moreover, both univariate and multivariate analyses of 92 surgically resected sections of EAC demonstrated a positive correlation of AXL overexpression with decreased median survival of the patients (11). Elevated expression of AXL and p-AXL (Y779) proteins was detected by immunoblot analysis in human EAC cell lines SK-GT-4, FLO-1, and JH-EsoAd1 as compared to normal esophageal squamous epithelial cell lines (18). Immunohistochemical (IHC) staining with anti-AXL specific antibody of tissue microarrays indicated AXL overexpression in 51.8% of EAC tumors relative to normal esophageal squamous tissue specimens (18). The results of a

TABLE 1 Overview of AXL overexpression in GI neoplasms.

GI organ/type of cancer	AXL overexpression or gene amplification	References
Barrett's esophagus/low grade dysplasia/high grade dysplasia/esophageal adenocarcinoma (EAC)	Protein (IHC), DNA (SAGE)	(11)
EAC	Protein (IHC)	(46, 47)
Esophageal squamous cell carcinoma (ESCC)	Protein (IHC)	(43)
Hepatocellular carcinoma (HCC)	Protein (IHC) Protein (WB and IHC) sAXL protein in plasma (ELISA) sAXL protein in plasma (ELISA)	(48) (44) (49) (48)
Pancreatic ductal adenocarcinoma (PDA)	Protein (IHC) Protein (IHC)	(13) (50)
Gastric cancer	mRNA (qRT-PCR), protein (IHC)	(45)
Colorectal carcinoma (CRC)	mRNA (Array), protein (IHC) mRNA (NGS), protein (IHC) DNA (FISH), protein (IHC)	(9) (42) (51)

IHC, immunohistochemistry; WB, western blotting; ELISA, enzyme-linked immunosorbent assay; qRT-PCR, quantitative real-time PCR; NGS, next generation sequencing; FISH, fluorescence in situ hybridization; sAXL, soluble AXL protein; SAGE, serial analysis of gene expression.

further IHC analysis performed on tissue microarrays including 53 human EAC and 11 normal esophageal tissues revealed that AXL as well as another potentially prooncogenic molecule non-receptor tyrosine kinase c-ABL were overexpressed in 55% and 66% of EAC samples, respectively, as compared to normal tissue specimens (46). Moreover, co-overexpression of AXL and c-ABL was detected in 49% of EAC samples (46).

High mRNA and protein expression of Gas6 and AXL has been reported in human gastric cancer cell lines and tissues (45). Notably, Gas6 expression was significantly correlated with lymph node metastases (45).

The immunohistochemical evaluation of expression of AXL protein in a panel of 99 archival pancreatic cancers revealed AXL expression in 54 out of 99 specimens (55%); and positive AXL expression in pancreatic cancer was significantly associated with lymph node metastases and a shorter median survival (12 as opposed to 18 months) as compared to AXL-negative tumor samples (50). Frequent overexpression of both molecules, Gas6 and AXL, has been detected in Pancreatic Ductal Adenocarcinoma (PDA) cells and was linked to a poor prognosis in patients with stage II PDA (13).

Additionally, high AXL mRNA and protein expression levels were associated with poor overall survival in early-stage colorectal cancer (CRC) tissues (42). Particularly, the statistical analysis of CRC microarray dataset, available through the Gene Expression Omnibus (GEO) (52), showed a significant association between high AXL mRNA expression and decreased disease-specific survival in a cohort of 177 patients diagnosed with an early-stage (stage II/III) CRC (42). Furthermore, AXL overexpression in colorectal adenocarcinoma as compared to normal colon tissues was demonstrated by IHC in tissue microarray resection specimens of primary tumors collected from 509 patients with colorectal adenocarcinoma (stage I-IV) at the National University Hospital of Singapore between 1990 and 1999 (42). Likewise, the overexpression of AXL and GAS6 was shown by IHC in 76,7% and 73.5%, respectively, in 223 human CRC specimens, while the amplification of *AXL* gene was detected by fluorescence *in situ* hybridization (FISH) in 8 out of 146 cases (5,4%) of CRC samples (51). The increased expression of AXL and GAS6 proteins was correlated with less differentiated histological grading, tumor stage and lymph nodes involvement (51). Given that majority of patients with high-risk stage II/III CRC tend to relapse (53) and progress to the advanced stages, AXL could be used as a prognostic biomarker for the distal part of GI tract.

While all known methods to evaluate AXL expression include tissue extraction, in some forms of hepatic neoplasm, it is possible to assess clinical outcome by evaluating plasma levels of soluble AXL (sAXL). It is an 85 kDa N-terminal product of extracellular ADAM metalloproteases-dependent proteolytic cleavage of AXL, which has GAS6 ligand-binding abilities and serving as a decoy receptor (26, 54, 55). This circulating sAXL has a promising potential as a specific serum marker of cirrhosis and early stages of hepatocellular carcinoma (HCC) (49). It has been documented that serum concentrations of sAXL were elevated at early (82.57 ng/mL) and later stages (114.50 ng/mL) of HCC in comparison with healthy controls (40.15 ng/mL) (49). Notably, sAXL levels were not altered in patients with chronic liver disease, liver adenomas and cholangiocarcinomas (49). These data suggest that elevated concentration of sAXL is a valuable biomarker of liver neoplastic transformation that could be noninvasively detected in plasma. In another study analyzing the diagnostic potential of this molecule, sAXL levels were evaluated in 311 HCC and 237 control serum samples collected from clinical centers in Europe and China (56). Average concentrations of sAXL were significantly higher in the serum of HCC patients (18.575 ng/mL) as compared to healthy (13.388 ng/mL) or cirrhotic (12.169 ng/mL) controls (56). Levels of sAxl remained unchanged in the serum of individuals diagnosed with primary ovarian, colorectal and breast carcinomas, or secondary colon-derived hepatic malignancies. Consequently, the soluble form of AXL was suggested as highly specific and accurate diagnostic marker for alpha-fetoprotein-negative HCC patients (56). Additionally, sAXL was proposed as a biomarker for early diagnosis of PADC based on the studies Martinez-Bosch, N. et al, 2022, which demonstrated increased sAXL levels in plasma of PDAC group as compared to healthy controls or chronic pancreatitis (CP) patients. Immunohistochemical analysis revealed higher protein expression in tissues samples obtained from PDAC and precancerous lesions as compared to CP or healthy control specimens. The immunohistochemistry data was confirmed by RNA expression analysis from TCGA database. It was noted that patients with high levels of AXL have a lower overall survival. Importantly, ROC statistical analysis of the plasma levels of sAXL, GAS6, or CA19-9 (a marker of pancreatic cancer) in two studied cohorts revealed that sAXL outperformed CA19-9 for discriminating between CP and PDAC (57). The data showing increased AXL expression in GI cancer tissues are summarized in Table 1.

The mechanisms leading to AXL overexpression are tissue-specific and may vary depending on local tissue microenvironment. Irrespective of AXL localization, the alteration of patterns of this molecule expression could be considered a hallmark of GI carcinogenesis. The specific roles of AXL in the alteration of basic cell functions in GI cancers are discussed below.

Proliferation and survival

Initial steps in carcinogenesis are associated with uncontrolled proliferation and survival of transformed or cancer stem cells (58). Gas6-AXL signaling pathway has been shown to enhance cell survival and suppress apoptosis in gastric cancer cells through activation of the AKT pathway (45). In another study, YAP-dependent cell survival and proliferation required AXL expression and activation of ERK1/2 signaling cascade in human HCC (59). Additionally, the proliferation of a metastatic HCC *in vitro* and *in vivo* was markedly suppressed by tunicamycin-induced de-glycosylation and downregulation of AXL (60).

In pancreatic ductal adenocarcinoma, the upregulation of AXL has been associated with a poor clinical prognosis and increased cell proliferation (12, 13), while stable knockdown of AXL resulted in a significant reduction in cell viability and anchorage-independent growth in pancreatic cancer cells (50). In a preclinical study,

treatment with S49076, an ATP-competitive tyrosine kinase inhibitor of MET, AXL, and FGFR1, significantly inhibited colony formation in soft agar by HCC cells overexpressing AXL and FGFR2 (61). The lack of sensitivity to S49076 in the same cell lines cultured in monolayer (61) suggests a key role of AXL in extracellular matrix anchorage-independent growth and survival. Indeed, the results of currently available preclinical and clinical studies suggest that the primary roles of AXL and other TAM RTKs may be mostly related to the mechanisms of survival, motility, and drug resistance rather than functioning as oncogenic drivers (62, 63).

Epithelial–mesenchymal transition and metastasis

The epithelial–mesenchymal transition (EMT) is a process by which epithelial cells undergo morphological and functional changes towards a mesenchymal phenotype (64). During this process of trans-differentiation, epithelial cells lose their polarity as well as cell-cell adhesion properties and acquire characteristics of mesenchymal stem cells (65). Cancer cells detach from the primary tumor location, migrate through the extracellular matrix, and intravasate into blood vessels, promoting metastases (66, 67). Importantly, residual metastatic disease from the primary tumor remains the major reason of recurrence and greater than 90% of cancer-related death (68). In cancers of the digestive system, AXL overexpression in tumors and metastases indicates adverse clinical prognosis in patients (9, 10, 42–44, 51, 69).

EMT associated with intrahepatic metastasis is a typical feature of HCC (48). Several studies in HCC have demonstrated elevated levels of AXL transcript and protein in association with EMT (48, 56, 59). For example, AXL mRNA overexpression and correlation with EMT has been documented in 28 HCC cell lines and 373 RNA-seq tissue datasets in comparison with cirrhotic and normal liver samples (70). A crucial role of AXL in transforming growth factor beta (TGF-β)-dependent HCC progression was proposed based on the studies revealing upregulation and activation of AXL in EMT-altered hepatoma cells (48). At the same time, AXL activation by Gas-6 increased TGF-β1 mRNA, while AXL knockdown dramatically reduced resistance to TGF-β-dependent growth inhibition by abrogating invasion and trans-endothelial migration of mesenchymal HCC cells (48). Notably, AXL overexpression triggered metastatic colonization of epithelial hepatoma cells *in vivo*. Immunohistochemical analysis of AXL expression in tumor tissues collected from 133 HCC patients demonstrated a correlation of increased AXL expression with advanced tumor stages, augmented vessel invasion of HCC cells, elevated risk of cancer relapse after liver transplantation, and a poor clinical prognosis (48). One of the most severe metastatic complications in HCC is portal vein tumor thrombus (PVTT). It has been shown that co-implantation of human umbilical vein endothelial cells (HUVECs) overexpressing AXL with HCC cells in xenograft nude mice and patient-derived xenograft (PDX) nude mice substantially enhanced tumor growth, hepatic metastasis, and vessel metastasis of HCC (71). These effects were suppressed by an AXL inhibitor R428, also known as BGB324 or bemcentinib (71).

Several studies suggested AXL as a potential therapeutic target in pancreatic cancer (13, 50, 72, 73). Thus, the immunohistochemical assessment of 99 pancreatic cancer specimens revealed a higher number of lymph node metastases and a shorter median survival of patients with AXL-positive tumors (12 versus 18 months) in contrast to the AXL-negative group (50). Stable knockdown of endogenous AXL in pancreatic cancer cells resulted in a significant decrease of mRNA levels of matrix metalloproteinase (MMP)-9 and EMT-associated transcription factors twist, snail, and slug (50). Moreover, AXL knockdown cells exhibited reduction in cell viability, migration, and invasion (50). The role of AXL signaling in progression and metastasis of pancreatic cancer was confirmed in a study using low-dose warfarin, a vitamin K "antagonist" to inhibit Gas6-dependent AXL activation (72). Treatment with low-dose warfarin reduced AXL-mediated human pancreatic cancer cells migration, invasiveness, and proliferation, while increasing apoptosis and sensitivity to chemotherapy. Additionally, warfarin decreased primary tumor growth and suppressed metastases in a murine model of pancreatic ductal adenocarcinoma (PDAC) (72). On a molecular level, low-dose warfarin treatment blocked TGFβ-induced expression of AXL, and markedly reduced expression levels of mesenchymal markers, Zeb1 and nuclear β-catenin in Panc-1 pancreatic epithelioid carcinoma cell line. Consistently, warfarin inhibited expression of vimentin and increased levels of E-cadherin in AXL-positive Panc-1 xenografts (72).

AXL signaling axis is also implicated in EMT of GI cancers. For instance, high levels of Gas6 and AXL mRNA and proteins were revealed in human gastric cancer cell lines and tissue samples, and Gas6 expression was significantly correlated with metastases to lymph nodes (45). The *in vitro* experiments using recombinant Gas6 and a decoy-receptor of AXL showed that activation of Gas6-AXL signaling axis leads to the inhibition of apoptosis and exacerbation of AKT-dependent survival and invasion of gastric cancer cells (45). In another study, inhibition of AXL-NF-κB signaling pathway by ursolic acid markedly inhibited cell migration and reduced the expression of mesenchymal markers and EMT-related transcription factors in gastric cancer cells and xenografts (74). In EAC cells, genetic silencing of AXL attenuated invasion, migration, and *in vivo* engraftment. Furthermore, pharmacological inhibition of AXL with small molecule agent R428 has shown similar functional effects in EAC cells (11). Our studies in EAC cell lines demonstrated that increased expression of AXL facilitates peripheral distribution of lysosomes leading to activation of cell invasion signaling cascade through the regulation of cathepsin B secretion (75). Besides, we found that these processes were caused by extracellular acidification because of AXL-induced secretion of lactate through AKT-NF-κB–dependent synthesis of lactate transporter MCT-1 (75).

Recently, dual inhibition of TGFβ and AXL signaling pathways was proposed as a novel therapy for human colorectal adenocarcinoma with mesenchymal phenotype (CMS4), a very aggressive CRC characterized by resistance to standard chemotherapies, low survival rate and high risk of recurrence (76,

77). In fact, overexpression of AXL and TGFβ receptors in CMS4 tumors correlated with higher risk of post-surgical relapse in stage II/III CRC and decreased survival (76). In CRC cell lines, treatment with the TGFβ inhibitor, galunisertib, and the AXL inhibitor, R428, markedly reduced colony formation and migration of cancer cells, and demonstrated potent anti-tumor activity in 3D spheroid cultures obtained from individuals with advanced CRC (76). Additionally, multitarget tyrosine kinase inhibitor (TKI) cabozantinib and AXL/c-MET selective inhibitor R428 both decreased AXL phosphorylation and TGFβ-induced E-cadherin expression (marker of EMT), cell viability, migration, and tumor growth in esophageal squamous cell carcinoma (ESCC) cells and xenograft models (78).

Interestingly, AXL expression was upregulated by Long non-coding RNA (lncRNA) CALIC in complex with RNA-binding protein hnRNP-L in colon cancer cells, while knockdown of either CALIC or AXL inhibited metastases *in vivo* (14). Application of AXL expression as a marker of poor prognosis and a crucial mediator of cell invasion was proposed for early-stage CRC, specifically in the adjuvant disease in the cases of unsuccessful EGFR/VEGF–targeted therapies (42).

AXL in angiogenesis

Angiogenesis is the formation of new blood vessels that often promote tumor growth and progression. AXL regulates many angiogenic activities such as proliferation and migration of vascular smooth muscle cells (VSMCs) and endothelial cells (ECs) (36), tube formation *in vitro* and angiogenesis *in vivo* (3). Vascular endothelial growth factor (VEGF) is secreted in high levels by most types of cancer cells (79). Proliferation and migration of VSMC are necessary for tumor angiogenesis (80). In fact, VSMCs express Gas6, and exogenous Gas6 promotes proliferation and migration of VSMCs (36). AXL also is expressed by tumor stromal cells, including ECs (7, 81). Knockdown of AXL or Gas6 expression markedly inhibited migration of HUVECs, while AXL overexpression enhanced cell growth and tubes formation (3). Notably, overexpression of AXL expression was observed in HCC-tumor-derived endothelial cells (TECs), although not in the tumor cells of HCC patients with portal vein tumor thrombus (PVTT) type of metastases. These data were associated with poor overall survival and disease-free survival of HCC patients with PVTT (71). Moreover, elevated expression of AXL was associated with the expression of a marker of endothelial cells CD 31 *in vitro* and *in vivo* (71).

Interestingly, Axl-null mice exhibited an impaired angiogenesis and vascular permeability in response to VEGF-A treatment (82). Therefore, it has been proposed that AXL could be one of the essential mediators of VEGF-A-dependent activation of pro-angiogenic PI3K/AKT signaling pathway (82). Accordingly, using AXL inhibitors in addition to anti-VEGF therapeutics could be an effective strategy targeting neovascularization in GI cancers.

AXL in the immune response to tumors

Inflammation is a one of the hallmarks of carcinogenesis, and it has been proven that chronic inflammation caused by autoimmune gastritis and *Helicobacter pylori* infection increases a risk of developing gastric cancer (83). In fact, more than 90% of gastric adenocarcinomas originate from epithelial cells of gastric mucosa because of chronic inflammation (83). Tumor intrinsic and immunosuppressive mechanisms contribute to conventional chemotherapy resistance (84). TAM family of RTKs, including AXL, are key regulators of immune response (85). Following their activation by Gas6 ligand – activator of all TAM family members, and Protein S ligand -activator of both MER and TYRO3, these receptors promote the resolution of inflammation by suppressing activation of cells of the innate immune system (86). Remarkably, studies on $Tyro3^{-/-}Axl^{-/-}Mer^{-/-}$ triple mutant mice (*TAM* TKOs) have demonstrated that loss of function of the three receptors, *T*yro3, *A*xl, and *M*er, dysregulates the immune system, presented by a severe lymphoproliferative disorder accompanied by a broad-spectrum autoimmune disease (39, 87). In a cancer setting, TAM receptors regulate the initiation and progression of tumorigenesis and, simultaneously, the anti-tumor functions of immune cells (85). Tumor progression is considerably affected by the tumor microenvironment (TME), comprised of all host cells and tissue components surrounding the cancer cells (88). On the other hand, programmed cell death through apoptosis maintains tissue homeostasis and prevents oncogenic transformation. Clearance of cell debris is the last stage of apoptosis. Uncleared products of this process might induce necrosis, thereby promoting inflammation and autoimmunity (89). Externalized phosphatidylserine (PS) acts as "eat-me" signal on apoptotic cells, stressed cells, exosomes, and liposomes. Importantly, endogenous ligands Gas6 and Protein S link externalized PS molecules with TAMs, activating those RTKs and promoting clearance of apoptotic cells (90, 91).

Studies on animal models have shown that TAM family receptors are involved in the clearance of apoptotic cells by macrophages and dendritic cells (DC) (92, 93). In fact, treatment with dextran sulfate sodium (DSS) salt blocked clearance of apoptotic neutrophils in the lamina propria of large intestine and promoted colitis in $Axl^{-/-}Mer^{-/-}$ double mutant mice (94). The Authors demonstrated that the observed inflammatory phenotype is associated with the knockout of *Axl* and *Mer* genes in radioresistant population of macrophages residing specifically in the intestinal tissues, while loss of Axl and Mer in the radiosensitive bone marrow–derived hematopoietic cells was not linked to exacerbated colitis (94). As such, AXL and MERTK inhibitors might induce adverse effects at the systemic level, and physiological effects of the alteration of AXL and MERTK signaling could be highly tissue-specific and depend on tumor microenvironment.

Tumor-associated macrophages are abundant in the TME and contribute to immunosuppression and tumor progression (92). In human and murine macrophage cultures, AXL activation has been shown to mediate Interferon α induction of Twist, a transcriptional

repressor of inflammatory cytokine tumor necrosis factor α (TNFα) (95). Altering AXL expression and downstream activation of Twist highlights a promising approach to control inflammation, which is the hallmark of oncogenesis. In several studies, activation of TAM receptors not only decreased severe inflammatory responses (96), but also induced efferocytosis and macrophage polarization towards a pro-tumor M2-like phenotype, accompanied by the increased production of immunosuppressive cytokines (92, 97–99). AXL induced TANK binding kinase 1 (TBK1)-NF-κB signaling pathway and innate immune suppression in the TME in pancreatic cancer (73), while inhibition of AXL with small molecule R428 enhanced immune stimulatory microenvironment (73). Immune checkpoint blockade (PD-1) is a novel popular approach in cancer immunotherapies. Unfortunately, some of the tumors are resistant to PD-1 inhibitors and considered to be immunologically "cold," because of the lack of tumor antigen-specific primed cytotoxic T cells (99). It has been shown that Sitravatinib, a broad-spectrum tyrosine kinase inhibitor (TKI) targeting MET, TAM, and members of VEGFR, platelet-derived growth factor receptor (PDGFR), and Eph families is highly effective in various cancer models, including CT1B-A5, an isogenic pancreatic cancer cell line, that could be partially attributed to altering the TME and restoring the efficacy of immune checkpoint blockade (PD-1) (99). Therefore, AXL is one of the major drivers of immune suppression in the TME. Although AXL-mediated pathway is an attractive candidate for inhibition in GI cancers to reverse the immunosuppressive TME, further investigations are needed as this therapeutic approach may cause adverse systemic effects like inflammation and autoimmunity.

AXL in resistance to anti-cancer therapies

One of the major problems of anti-cancer therapies is that many cancers are initially responsive to treatment, but ultimately develop drug resistance that may lead to an unfavorable clinical outcome (100). AXL overexpression in GI cancers has been associated with resistance to both targeted and non-targeted anti-cancer therapies. Particularly, EAC is characterized by resistance to chemotherapy and poor prognosis (18). Notably, AXL overexpression has been shown to mediate resistance to epirubicin by upregulation of c-MYC transcription *via* AKT-β-catenin signaling pathway in EAC cells (17). Additionally, AXL has been proposed as a promising therapeutic target to sensitize GI cancers to DNA-damaging chemotherapy drugs. In fact, genetic silencing of endogenous AXL abrogates cisplatin resistance through inhibition of the pro-apoptotic c-ABL/p73β signaling pathway in human EAC cells (18). AXL expression also promotes resistance to TNF-related apoptosis-inducing ligand (TRAIL) mediated by death receptor 5 (DR5) activity in EAC cells (47). Specifically, AXL and DR5 protein interaction blocks the recruitment of caspase-8 to the death-inducing signaling complex (DISC), resulting in enhanced cell survival, and decreased apoptosis. Sensitivity to TRAIL was restored in EAC cells after genetic silencing of endogenous AXL (47).

Resistance to the chemotherapy drug gemcitabine in PDAC was attributed to the function of YWHAZ/14-3-3 zeta/delta (14-3-3ζ) protein, which was isolated from monocyte-derived macrophage cultures (101). In mice bearing orthotopic PDAC xenografts, the antitumor activity of gemcitabine was significantly enhanced by pharmacological inhibition of AXL, which is a binding protein partner of 14-3-3ζ (48, 101). Therefore, it was suggested that apoptosis induced by chemotherapy might in turn activate a survival pathway through 14-3-3ζ/AXL and AKT phosphorylation cascade (101). Treatment of PDAC cells with BGB324, a selective small molecule inhibitor of AXL, promotes epithelial differentiation, stimulatory immune microenvironment, and high expression of nucleoside transporters, enhancing the response to gemcitabine (73). Of note, BGB324 treatment also improved survival and gemcitabine sensitivity in mice with advanced PDAC (73).

Based on a large body of evidence (9, 102, 103), cancer progression is frequently associated with acquired resistance to the inhibitors of EGF receptor (EGFR) mediated by the enhanced AXL expression as a bypass mechanism. For instance, increased AXL mRNA levels were found in 5 out of 7 CRC patients following anti-EGFR therapy (9). Moreover, resistance to anti-EGFR drugs accompanied by high AXL expression was demonstrated in three-dimensional CRC cell cultures derived from an AXL-positive, RAS wild-type patient after anti-EGFR treatment (9). Furthermore, AXL overexpression in CRC cell lines led to the resistance to EGFR inhibition. The role of AXL in EGFR inhibition resistance was established by analysis of AXL expression in tumor xenograft mice and in CRC patients after anti-EGFR treatment (9). Overexpression and activation of AXL upregulates PI3K/mammalian target of rapamycin (mTOR) and MAPK signaling pathways, enhancing cell survival, cell growth, invasion, and migration (104). Particularly, AXL mediates resistance to PI3Kα inhibition through activation of EGFR/PKC/mTOR cascade in head and neck (H&N) carcinomas as well in ESCC (105). The study suggested simultaneous EGFR and PI3Kα inhibition as a prospective therapeutic approach to overcome AXL-dependent resistance to PI3Kα inhibitors in patients with esophageal and H&N squamous cell carcinomas (105).

AXL plays a major role in promoting resistance to several common chemotherapeutics and targeted anti-cancer therapies. For example, treatment with AXL inhibitor S49076 markedly decreased tumor resistance to bevacizumab, a VEGF/VEGFR blocker, in a colon carcinoma xenograft model and attenuated colony formation of FGFR1/2- and AXL-positive hepatocarcinoma cells (61). In addition, cabozantinib, a dual inhibitor of MET and AXL, decreased cell growth in both *in vitro* and *in vivo* models of HER2-amplified gastric cancer with acquired resistance to afatinib, a pan-HER inhibitor (106). Studies in ESCC cell model have demonstrated a synergistic effect of combinatory treatment with HER2 inhibitor lapatinib and AXL inhibitor foretinib (43). Notably, in esophageal tissue of patients diagnosed with operable primary ESCC, the cumulative expression of AXL and HER2 was associated with unfavorable clinical outcome (43). Therefore, drug resistance to lapatinib could be potentially overcome by the inhibition of AXL.

In HCC cell lines, AXL inhibition with RNA-interference or R428 compound improved sensitivity to sorafenib associated with increased phosphorylation level of AXL (70). Elevated level of AXL expression and its activation have been implicated in the resistance to imatinib in gastrointestinal stromal tumors (GIST) (107). Since GI cancer mesenchymal cells exhibit high levels of AXL expression, this RTK is potentially a promising therapeutic target for overcoming chemoresistance and improving the efficacy of current cancer therapies.

Targeting AXL in GI cancers

With the development of personalized medicine and targeted therapy, including tyrosine kinase inhibitors, GI cancer treatment continues to progress. Preclinical studies demonstrated that small-molecule TAM inhibitors, such as R428 (73) and RXDX106 (108), display anti-cancer activity in GI organs. As AXL has been associated with various stages of carcinogenesis and the inhibition of its expression and activity demonstrated promising results, AXL-specific inhibitors are currently being evaluated in clinical studies. BGB324 (BerGenBio); also known as R428 (Rigel Pharmaceuticals), is an oral selective small molecule AXL inhibitor that is currently being investigated in phase II clinical trials of pancreatic neoplasms (Table 2). BGB324 enhanced the efficacy of gemcitabine in preclinical studies *in vivo* through the stimulation of immune cellular response, expression of nucleoside transporters and promotion of epithelial cells differentiation in PDAC (73). Additionally, BGB324 is currently being tested in clinical trials as a monotherapy and in combination with chemo-, targeted-, and immunotherapy in various cancers (acute myeloid leukemia (AML), NCT02488408; non-small cell lung cancer (NSCLC), NCT02424617, NCT02922777; melanoma, NCT02872259). Particularly, combinations with nab-paclitaxel, gemcitabine, or cisplatin have shown encouraging results of clinical activity in patients with metastatic pancreatic cancer (NCT03649321).

AVB-500 (AVB-S6-500, Batiraxcept; Aravive, Inc.) is a novel high affinity Fc-sAXL fusion protein, which acts as an AXL decoy receptor by binding Gas6 and blocking AXL signaling (109). Preclinical data demonstrated inhibition of Gas6-induced AXL and Src phosphorylation, tumor vessel density, tumor growth, and metastatic burden in renal cell carcinoma (6, 110, 111) and ovarian cancer (109, 112) in response to treatment with AVB-500. Compared with chemotherapy alone, AVB-500 in combination with carboplatin and/or paclitaxel attenuated ovarian cancer cell survival *in vitro* and tumor growth *in vivo* (112). AVB-500 is currently investigated in Phase I/II clinical trials for patients with platinum-resistant or recurrent ovarian, fallopian tube, or peritoneal cancers as a combination therapy (Clinical Trial Identification #s: NCT03639246, NCT04019288) (Table 2). Also, a Phase 1b/2 study of AVB-500 safety and efficacy as a monotherapy or in combination with cabozantinib or nivolumab in patients with advanced or metastatic clear cell renal cell carcinoma is in progress (Clinical Trial Identification # NCT04300140). Three other studies are currently active and recruiting patients for ovarian cancer, advanced urothelial carcinoma, and pancreatic adenocarcinoma to assess AVB-500 efficacy as a combination therapy either with paclitaxel, or cabozantinib, or nab-paclitaxel/gemcitabine, correspondingly (Clinical Trial Identification #s: NCT04729608, NCT04004442, NCT04983407) (113).

A promising approach using a conditionally active biologic (CAB) AXL-targeted antibody drug conjugate BA3011 CAB-AXL-ADC, BioAtla, LLC, Table 2, NCT 03425279) alone and in combination with a PD-1 inhibitor Nivolumab in patients with advanced solid tumors is currently getting tested in Phase I, and in adult and adolescent patients with advanced, refractory sarcoma is investigated in Phase II. BA3011 is a product of fusion of anti-AXL antibodies with anti-mitotic compound monomethyl auristatin E (MMAE). The binding of antibody part of BA3011 to AXL initiates intracellular translocation of antibody-drug conjugate (ADC) complex followed by the release of MMAE ultimately leading to cancer cell death. Patients with advanced solid tumors, including NSCLC, prostate cancer, and pancreatic cancer are currently recruited.

Cabozantinib (Cabometix, XL184, BMS-907351, Cabometyx™, BMS-907351) is an oral small molecule TKI that targets AXL, c-Met and VEGFR (Table 2). This inhibitor has been preclinically investigated in ESCC (78) and liver cancer (114, 115). Currently, the evaluation of cabozantinib in combination with durvalumab (anti-programmed cell death protein 1 (PD-L1) inhibitor) in patients with advanced gastroesophageal adenocarcinoma, gastric cancer, hepatocellular carcinoma, and colorectal cancer is undergoing phase I/II open label, multi-cohort trial to determine safety, tolerability, and efficacy of the treatment (Clinical Trial Identification #: NCT03539822). The investigators propose that cabozantinib in combination with checkpoint-based immunotherapeutics like durvalumab will result in synergistic effect by altering the TME. Cabozantinib has been clinically approved for patients with sorafenib-resistant HCC (116) (Clinical Trial Identification #: NCT01908426). The data from the randomized phase III CELESTIAL trial revealed a significant improvement in progression-free survival and overall survival *vs.* placebo in a cohort of patients with previously treated advanced HCC (116). The patients who were not included in CELESTIAL trial are currently enrolled in another trial evaluating the therapeutic effect of cabozantinib in the patients with HCC intolerant to sorafenib treatment or first line treatment different from sorafenib (Clinical Trial Identification #: NCT04316182, Phase II). Another trial at stage 2 is ongoing to determine the outcome of cabozantinib treatment in patients with recurrent HCC and who had received a liver transplant as a part of a previous therapy (Clinical Trial Identification #: NCT04204850). Safety and efficacy of the treatment combination of cabozantinib and atezolizumab in comparison with the standard care (treatment with sorafenib) in patients with advanced HCC, who have not received prior systemic anti-cancer treatment, is being investigated in Phase III clinical trial (NCT03755791). The clinical benefits of cabozantinib in a cohort of patients with metastatic disease or unresectable locally advanced malignancy are being assessed as a part of MegaMOST clinical study (NCT04116541).

The clinical study of SLC-391 (SignalChem Lifesciences Corporation), a novel, potent and selective small molecule inhibitor of AXL, is currently ongoing in Canada, and recruiting patients with

TABLE 2 Current clinical trials testing AXL-targeted agents in GI cancer patients.

Intervention	Primary target	Condition	Co-treatment/ comparator	Clinical trial	Identifier
BGB324	Inhibitor of AXL kinase	Pancreatic cancer	Nab-paclitaxel Gemcitabine Cisplatin	Phase 1 Phase 2	NCT03649321
AVB-500	AXL decoy soluble receptor, binds GAS6	Phase 1 Safety and Tolerability Study	Placebo	Phase 1	NCT03401528
AVB-500	AXL decoy soluble receptor, binds GAS6	Pancreatic Adenocarcinoma	Nab paclitaxel Gemcitabine	Phase 1 Phase 2	NCT04983407
BA3011	Conditionally active biologic anti-AXL antibody drug conjugate	Advanced Solid Tumor (Phase 1) Solid Tumor	PD-1 inhibitor	Phase 1 Phase 2	NCT03425279
Cabozantinib	Small molecule inhibitor of multiple receptor tyrosine kinases including MET, VEGFR 1, 2 and 3, AXL, and RET	Gastric Cancer Esophageal Adenocarcinoma Hepatocellular Carcinoma Colorectal Cancer	Durvalumab anti-(Programmed cell death protein 1 (PD-L1) inhibitor Tremelimumab	Phase 1 Phase 2	NCT03539822
Cabozantinib		Hepatocellular Carcinoma	Placebo	Phase 3	NCT01908426
Cabozantinib		Hepatocellular Carcinoma		Phase 2	NCT04316182
Cabozantinib		Hepatocellular Carcinoma Recurrent Cancer Liver Transplant		Phase 2	NCT04204850
Cabozantinib		Hepatocellular Carcinoma	Sorafenib Atezolizumab	Phase 3	NCT03755791
Cabozantinib		Malignant Solid Tumor		Phase 2	NCT04116541
SLC-391	Inhibitor of AXL	Solid Tumor		Phase 1	NCT03990454
TP-0903	Inhibitor of AXL	Advanced Solid Tumors EGFR Positive Non-small Cell Lung Cancer Colorectal Carcinoma Recurrent Ovarian Carcinoma BRAF-Mutated Melanoma		Phase 1	NCT02608268
Warfarin	Inhibits AXL activation, Vitamin K agonist	Pancreatic Cancer		Withdrawn	NCT03536208
MGCD516	c-Kit, PDGFRα/β, TAM, VEGF	Advanced Cancer		Phase 1	NCT02219711
BPI-9016M	Inhibitor of MET/AXL kinases.	Solid tumors		Phase 1	NCT02478866
Crizotinib	a small molecule directed to vascular endothelial growth factor receptors, MET and AXL	Hematologic Cancers Solid Tumors Metastatic Cancer		Phase 2	NCT02034981
INCB081776	Inhibitor of AXL and Mer that blocks TAM	Advanced Solid Tumors	INCMGA00012	Phase 1	NCT03522142

solid tumors to determine safety and tolerability of the drug (NCT03990454). Notably, the clinical outcome of SLC-391 in combination with the anti-PD-1 therapy pembrolizumab (Keytruda®) will be evaluated in SKYLITE trial, a phase II study for patients with NSCLC carried by Merck (MSD) and British Columbia-based SignalChem Lifesciences. TP-0903 (Sumitomo Dainippon Pharma Oncology, Inc), a novel oral inhibitor of AXL kinase that reverses the mesenchymal cancer phenotype, is currently investigated in Phases 1a/1b clinical trial for advanced solid tumors (Clinical Trial Identification #: NCT02729298). Commonly used

anticoagulant Warfarin prevents the Gas6 interaction with externalized phosphatidylserine on the surface of apoptotic cells and cell debris through inhibition of vitamin K-dependent gamma-carboxylation of the γ-carboxyglutamic acid-rich (Gla) domain of Gas6 (117). A preclinical study reported that low-dose warfarin blocks the progression and spread of pancreatic cancer (72). A Phase I study of the effect of escalating doses of Warfarin on circulating biomarkers of AXL pathways (phosphoGas6 and sAXL) in patients with pancreatic adenocarcinoma (Table 2, Clinical Trial Identification #: NCT03536208) was initiated in 2019, but the study was withdrawn in 2021 because of lack of accrual.

MGCD516 (Sitravatinib, Mirati Therapeutics Inc.) is a small molecule spectrum selective TKI of several closely related receptor tyrosine kinases, including TAM and members of the VEGFR, PDGFR, DDR2, TRK and Eph families (118, 119). Anti-tumorigenic and anti-angiogenic activities of MGCD516 have been demonstrated in preclinical models of soft tissue sarcoma (119) and metastatic models of anti-angiogenic therapy resistance (118). Additionally, MGCD516 treatment enhances the immune checkpoint blockade by lowering the number of tumor-associated immunosuppressive myeloid cells and expanding the populations of CD4+ T cells and proliferating CD8+ T cells in the TME (99). MGCD516 therapy is currently investigated in patients with advanced solid tumors (Table 2, Clinical Trial Identification #: NCT02219711).

BPI-9016M (Betta Pharmaceuticals Co., Ltd.), is a novel highly potent dual-target inhibitor of c-Met/AXL. Preclinical studies in a lung adenocarcinoma model demonstrated strong activity of BPI-9016M *in vitro* and *in vivo* against c-Met/AXL kinases and their downstream pathways, leading to reduced tumor cell growth, migration, and invasion (120). A clinical trial at Phase I (NCT02478866) is currently assessing pharmacokinetics, safety, and anti-tumor activity of the inhibitor in patients with advanced solid tumors (121). Crizotinib (XALKORI®, PF-02341066, Pfizer Inc.) is a multitargeted, ATP-competitive, small molecule and orally available tyrosine kinase inhibitor that inhibits c-Met, AXL, ALK, and Ron (113). Preclinically, this compound reduced cell growth and induced apoptosis in human gastric carcinoma cells (122). Additionally, crizotinib in combination with mitomycin C increased apoptosis in CRC (123). A Phase II clinical trial is ongoing for patients with hematologic cancers, solid tumors, and metastatic cancer to determine the efficacy and the safety of crizotinib in 23 cohorts of patients with identified activating molecular alterations in the crizotinib target genes (Table 2, Clinical Trial Identification #: NCT02034981). Overall, there are 168 clinical studies associated with crizotinib in the ClinicalTrials.gov database. INCB081776 as a monotherapy or in combination with INCMGA00012 is undergoing Phase I trial for the safety and tolerability, pharmacokinetics, pharmacodynamics, and early clinical activity in patients with advanced solid tumors (Clinical Trial Identification #: NCT03522142). AXL-targeted therapies either as particular agents or in combination with conventional chemotherapy or other small molecule inhibitors have a promising opportunity to increase the survival rate of cancer patients. Nonetheless, more studies of AXL signaling pathways and physiological effects of their alteration are essential to identify the specific cohorts of patients who would be more responsive to the treatments with fewer adverse effects.

Chimeric antigen receptor (CAR)-T cell therapy targeting the B-cell antigen CD19 has proven clinically very successful in hematologic cancers [Clinical Trial Identification #: NCT02435849, NCT02445248, and NCT02348216 (124, 125)]. However, the development of CAR-T cell therapies for solid tumors has been slow because of the unique challenges associated with tumor microenvironment (126, 127). Preclinical studies indicated that CAR-T cell therapy targeting AXL

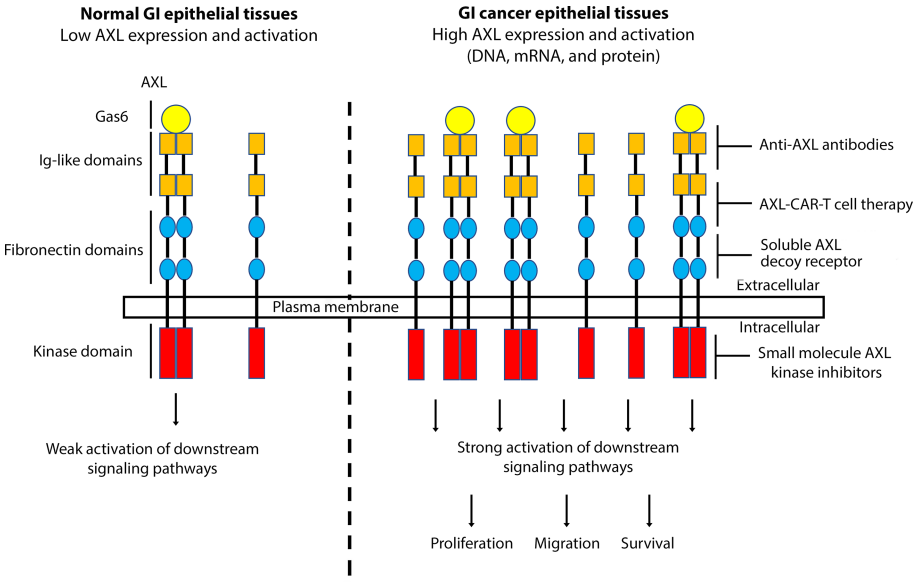

FIGURE 1
A schematic representation depicting the role of AXL overexpression and activation in GI cancers. Overexpression of AXL, induced by DNA amplification or high mRNA and protein levels, in GI epithelial tissues leads to strong activation of downstream signaling pathways, promoting cell proliferation, migration, and survival, hallmarks of GI carcinogenesis. Targeting AXL with specific monoclonal antibodies, small molecule kinase inhibitors, soluble AXL decoy receptor, or CAR-T cell therapy could be effective as a targeted therapeutic approach in GI cancers.

induced *in vitro* cytotoxicity in triple negative breast cancer cells (TNBC) and reduced tumor growth in a TNBC xenograft mouse model (128). Preclinical and clinical studies are needed to investigate AXL-CAR-T cell therapy approach in GI cancers with high AXL expression.

Conclusions and future perspectives

Collectively and based on the current literature, AXL has been associated with GI cancer development and progression and its inhibition provides a novel therapeutic approach in the fight against GI cancers (Figure 1). Targeting AXL alone or with other TAM receptor tyrosine kinases could stimulate antitumor immunity, reduce cancer cell survival, enhance chemosensitivity and markedly attenuate metastatic tumor burden (129, 130). AXL might potentially become a valuable therapeutic target in GI cancers, and targeted anti-AXL therapies could further improve the standard first line of therapies with the objective to improve the prognosis and clinical outcome in patients with GI cancers or other AXL-expressing tumors.

Author contributions

NP, writing and conception of the manuscript. AB, editing the manuscript and securing the funding. All authors contributed to the article and approved the submitted version.

Funding

This work was supported by the National Cancer Institute of the National Institutes of Health under Award Number RO1CA193219 and Vanderbilt-Ingram Cancer Center (VICC) Specialized Project of Research Excellence (SPORE) in GI cancer (P50CA95103). The content is solely the responsibility of the authors and does not necessarily represent the official views of the National Institutes of Health and Vanderbilt University Medical Center.

Conflict of interest

The authors declare that the research was conducted in the absence of any commercial or financial relationships that could be construed as a potential conflict of interest.

Publisher's note

References

1. Sung H, Ferlay J, Siegel RL, Laversanne M, Soerjomataram I, Jemal A, et al. Global cancer statistics 2020: GLOBOCAN estimates of incidence and mortality worldwide for 36 cancers in 185 countries. *CA Cancer J Clin* (2021) 71(3):209–49. doi: 10.3322/caac.21660

2. (WHO), W.H.O. *Global health estimates 2020: deaths by cause, age, sex, by country and by region 2000-2019* (2020). WHO (Accessed December 11, 2020).

3. Holland SJ, Powell MJ, Franci C, Chan EW, Friera AM, Atchison RE, et al. Multiple roles for the receptor tyrosine kinase axl in tumor formation. *Cancer Res* (2005) 65(20):9294–303. doi: 10.1158/0008-5472.CAN-05-0993

4. Holland SJ, Pan A, Franci C, Hu Y, Chang B, Li W, et al. R428, a selective small molecule inhibitor of axl kinase, blocks tumor spread and prolongs survival in models of metastatic breast cancer. *Cancer Res* (2010) 70(4):1544–54. doi: 10.1158/0008-5472.CAN-09-2997

5. Onken J, Vajkoczy P, Torka R, Hempt C, Patsouris V, Heppner FL, et al. Phospho-AXL is widely expressed in glioblastoma and associated with significant shorter overall survival. *Oncotarget* (2017) 8(31):50403–14. doi: 10.18632/oncotarget.18468

6. Rankin EB, Fuh KC, Castellini L, Viswanathan K, Finger EC, Diep AN, et al. Direct regulation of GAS6/AXL signaling by HIF promotes renal metastasis through SRC and MET. *Proc Natl Acad Sci U.S.A.* (2014) 111(37):13373–8. doi: 10.1073/pnas.1404848111

7. Tanaka M, Siemann DW. Axl signaling is an important mediator of tumor angiogenesis. *Oncotarget* (2019) 10(30):2887–98. doi: 10.18632/oncotarget.26882

8. Tanaka M, Siemann DW. Gas6/Axl signaling pathway in the tumor immune microenvironment. *Cancers (Basel)* (2020) 12(7):1850. doi: 10.3390/cancers12071850

9. Cardone C, Blauensteiner B, Moreno-Viedma V, Martini G, Simeon V, Vitiello PP, et al. AXL is a predictor of poor survival and of resistance to anti-EGFR therapy in RAS wild-type metastatic colorectal cancer. *Eur J Cancer* (2020) 138:1–10. doi: 10.1016/j.ejca.2020.07.010

10. He L, Lei Y, Hou J, Wu J, Lv G. Implications of the receptor tyrosine kinase axl in gastric cancer progression. *Onco Targets Ther* (2020) 13:5901–11. doi: 10.2147/OTT.S257606

11. Hector A, Montgomery EA, Karikari C, Canto M, Dunbar KB, Wang JS, et al. The axl receptor tyrosine kinase is an adverse prognostic factor and a therapeutic target in esophageal adenocarcinoma. *Cancer Biol Ther* (2010) 10(10):1009–18. doi: 10.4161/cbt.10.10.13248

12. Bae CA, Ham IH, Oh HJ, Lee D, Woo J, Son SY, et al. Inhibiting the GAS6/AXL axis suppresses tumor progression by blocking the interaction between cancer-associated fibroblasts and cancer cells in gastric carcinoma. *Gastric Cancer* (2020) 23(5):824–36. doi: 10.1007/s10120-020-01066-4

13. Song X, Wang H, Logsdon CD, Rashid A, Fleming JB, Abbruzzese JL, et al. Overexpression of receptor tyrosine kinase axl promotes tumor cell invasion and survival in pancreatic ductal adenocarcinoma. *Cancer* (2011) 117(4):734–43. doi: 10.1002/cncr.25483

14. Kawasaki Y, Miyamoto M, Oda T, Matsumura K, Negishi L, Nakato R, et al. The novel lncRNA CALIC upregulates AXL to promote colon cancer metastasis. *EMBO Rep* (2019) 20(8):e47052. doi: 10.15252/embr.201847052

15. Davra V, Kumar S, Geng K, Calianese D, Mehta D, Gadiyar V, et al. Axl and mertk receptors cooperate to promote breast cancer progression by combined oncogenic signaling and evasion of host antitumor immunity. *Cancer Res* (2021) 81(3):698–712. doi: 10.1158/0008-5472.CAN-20-2066

16. Rothlin CV, Ghosh S, Zuniga EI, Oldstone MB, Lemke G. TAM receptors are pleiotropic inhibitors of the innate immune response. *Cell* (2007) 131(6):1124–36. doi: 10.1016/j.cell.2007.10.034

17. Hong J, Maacha S, Belkhiri A. Transcriptional upregulation of c-MYC by AXL confers epirubicin resistance in esophageal adenocarcinoma. *Mol Oncol* (2018) 12(12):2191–208. doi: 10.1002/1878-0261.12395

18. Hong J, Peng D, Chen Z, Sehdev V, Belkhiri A. ABL regulation by AXL promotes cisplatin resistance in esophageal cancer. *Cancer Res* (2013) 73(1):331–40. doi: 10.1158/0008-5472.CAN-12-3151

19. Polvi A, Armstrong E, Lai C, Lemke G, Huebner K, Spritz RA, et al. The human TYRO3 gene and pseudogene are located in chromosome 15q14-q25. *Gene* (1993) 134(2):289–93. doi: 10.1016/0378-1119(93)90109-G

20. Janssen JW, Schulz AS, Steenvoorden AC, Schmidberger M, Strehl S, Ambros PF, et al. A novel putative tyrosine kinase receptor with oncogenic potential. *Oncogene* (1991) 6(11):2113–20.

21. Nagata K, Ohashi K, Nakano T, Arita H, Zong C, Hanafusa H, et al. Identification of the product of growth arrest-specific gene 6 as a common ligand for axl, sky, and mer receptor tyrosine kinases. *J Biol Chem* (1996) 271(47):30022–7. doi: 10.1074/jbc.271.47.30022

22. Antony J, Huang RY. AXL-driven EMT state as a targetable conduit in cancer. *Cancer Res* (2017) 77(14):3725–32. doi: 10.1158/0008-5472.CAN-17-0392

23. Uehara H, Shacter E. Auto-oxidation and oligomerization of protein s on the apoptotic cell surface is required for mer tyrosine kinase-mediated phagocytosis of apoptotic cells. *J Immunol* (2008) 180(4):2522–30. doi: 10.4049/jimmunol.180.4.2522

24. Liu E, Hjelle B, Bishop JM. Transforming genes in chronic myelogenous leukemia. *Proc Natl Acad Sci U.S.A.* (1988) 85(6):1952–6. doi: 10.1073/pnas.85.6.1952

25. Neubauer A, Fiebeler A, Graham DK, O'Bryan JP, Schmidt CA, Barckow P, et al. Expression of axl, a transforming receptor tyrosine kinase, in normal and malignant hematopoiesis. *Blood* (1994) 84(6):1931–41. doi: 10.1182/blood.V84.6.1931.1931

26. O'Bryan JP, Frye RA, Cogswell PC, Neubauer A, Kitch B, Prokop C, et al. Axl, a transforming gene isolated from primary human myeloid leukemia cells, encodes a novel receptor tyrosine kinase. *Mol Cell Biol* (1991) 11(10):5016–31. doi: 10.1128/mcb.11.10.5016

27. Gay CM, Balaji K, Byers LA. Giving AXL the axe: targeting AXL in human malignancy. *Br J Cancer* (2017) 116(4):415–23. doi: 10.1038/bjc.2016.428

28. Korshunov VA. Axl-dependent signalling: a clinical update. *Clin Sci (Lond)* (2012) 122(8):361–8. doi: 10.1042/CS20110411

29. Manfioletti G, Brancolini C, Avanzi G, Schneider C. The protein encoded by a growth arrest-specific gene (gas6) is a new member of the vitamin K-dependent proteins related to protein s, a negative coregulator in the blood coagulation cascade. *Mol Cell Biol* (1993) 13(8):4976–85. doi: 10.1128/mcb.13.8.4976

30. Stitt TN, Conn G, Gore M, Lai C, Bruno J, Radziejewski C, et al. The anticoagulation factor protein s and its relative, Gas6, are ligands for the tyro 3/Axl family of receptor tyrosine kinases. *Cell* (1995) 80(4):661–70. doi: 10.1016/0092-8674(95)90520-0

31. Varnum BC, Young C, Elliott G, Garcia A, Bartley TD, Fridell YW, et al. Axl receptor tyrosine kinase stimulated by the vitamin K-dependent protein encoded by growth-arrest-specific gene 6. *Nature* (1995) 373(6515):623–6. doi: 10.1038/373623a0

32. Sasaki T, Knyazev PG, Clout NJ, Cheburkin Y, Gohring W, Ullrich A, et al. Structural basis for Gas6-axl signalling. *EMBO J* (2006) 25(1):80–7. doi: 10.1038/sj.emboj.7600912

33. Braunger J, Schleithoff L, Schulz AS, Kessler H, Lammers R, Ullrich A, et al. Intracellular signaling of the Ufo/Axl receptor tyrosine kinase is mediated mainly by a multi-substrate docking-site. *Oncogene* (1997) 14(22):2619–31. doi: 10.1038/sj.onc.1201123

34. Scaltriti M, Elkabets M, Baselga J. Molecular pathways: AXL, a membrane receptor mediator of resistance to therapy. *Clin Cancer Res* (2016) 22(6):1313–7. doi: 10.1158/1078-0432.CCR-15-1458

35. Ekman C, Stenhoff J, Dahlback B. Gas6 is complexed to the soluble tyrosine kinase receptor axl in human blood. *J Thromb Haemost* (2010) 8(4):838–44. doi: 10.1111/j.1538-7836.2010.03752.x

36. Fridell YW, Villa J Jr., Attar EC, Liu ET. GAS6 induces axl-mediated chemotaxis of vascular smooth muscle cells. *J Biol Chem* (1998) 273(12):7123–6. doi: 10.1074/jbc.273.12.7123

37. McCloskey P, Fridell YW, Attar E, Villa J, Jin Y, Varnum B, et al. GAS6 mediates adhesion of cells expressing the receptor tyrosine kinase axl. *J Biol Chem* (1997) 272(37):23285–91. doi: 10.1074/jbc.272.37.23285

38. Lee WP, Liao Y, Robinson D, Kung HJ, Liu ET, Hung MC. Axl-gas6 interaction counteracts E1A-mediated cell growth suppression and proapoptotic activity. *Mol Cell Biol* (1999) 19(12):8075–82. doi: 10.1128/MCB.19.12.8075

39. Lemke G, Lu Q. Macrophage regulation by tyro 3 family receptors. *Curr Opin Immunol* (2003) 15(1):31–6. doi: 10.1016/S0952-7915(02)00016-X

40. Bailey MH, Tokheim C, Porta-Pardo E, Sengupta S, Bertrand D, Weerasinghe A, et al. Comprehensive characterization of cancer driver genes and mutations. *Cell* (2018) 174(4):1034–5. doi: 10.1016/j.cell.2018.07.034

41. Gao J, Aksoy BA, Dogrusoz U, Dresdner G, Gross B, Sumer SO, et al. Integrative analysis of complex cancer genomics and clinical profiles using the cBioPortal. *Sci Signal* (2013) 6(269):pl1. doi: 10.1126/scisignal.2004088

42. Dunne PD, McArt DG, Blayney JK, Kalimutho M, Greer S, Wang T, et al. AXL is a key regulator of inherent and chemotherapy-induced invasion and predicts a poor clinical outcome in early-stage colon cancer. *Clin Cancer Res* (2014) 20(1):164–75. doi: 10.1158/1078-0432.CCR-13-1354

43. Hsieh MS, Yang PW, Wong LF, Lee JM. The AXL receptor tyrosine kinase is associated with adverse prognosis and distant metastasis in esophageal squamous cell carcinoma. *Oncotarget* (2016) 7(24):36956–70. doi: 10.18632/oncotarget.9231

44. Liu J, Wang K, Yan Z, Xia Y, Li J, Shi L, et al. Axl expression stratifies patients with poor prognosis after hepatectomy for hepatocellular carcinoma. *PloS One* (2016) 11(5):e0154767. doi: 10.1371/journal.pone.0154767

45. Sawabu T, Seno H, Kawashima T, Fukuda A, Uenoyama Y, Kawada M, et al. Growth arrest-specific gene 6 and axl signaling enhances gastric cancer cell survival *via* akt pathway. *Mol Carcinog* (2007) 46(2):155–64. doi: 10.1002/mc.20211

46. Hong J, Abid F, Phillips S, Salaria SN, Revetta FL, Peng D, et al. Co-Overexpression of AXL and c-ABL predicts a poor prognosis in esophageal adenocarcinoma and promotes cancer cell survival. *J Cancer* (2020) 11(20):5867–79. doi: 10.7150/jca.47318

47. Hong J, Belkhiri A. AXL mediates TRAIL resistance in esophageal adenocarcinoma. *Neoplasia* (2013) 15(3):296–304. doi: 10.1593/neo.122044

48. Reichel P, Dengler M, van Zijl F, Huber H, Fuhrlinger JG., Reichl C, et al. Axl activates autocrine transforming growth factor-beta signaling in hepatocellular carcinoma. *Hepatology* (2015) 61(3):930–41. doi: 10.1002/hep.27492

49. Dengler M, Staufer K, Huber H, Stauber R, Bantel H, Weiss KH, et al. Soluble axl is an accurate biomarker of cirrhosis and hepatocellular carcinoma development: results from a large scale multicenter analysis. *Oncotarget* (2017) 8(28):46234–48. doi: 10.18632/oncotarget.17598

50. Koorstra JB, Karikari CA, Feldmann G, Bisht S, Rojas PL, Offerhaus GJ, et al. The axl receptor tyrosine kinase confers an adverse prognostic influence in pancreatic cancer and represents a new therapeutic target. *Cancer Biol Ther* (2009) 8(7):618–26. doi: 10.4161/cbt.8.7.7923

51. Martinelli E, Martini G, Cardone C, Troiani T, Liguori G, Vitagliano D, et al. AXL is an oncotarget in human colorectal cancer. *Oncotarget* (2015) 6(27):23281–96. doi: 10.18632/oncotarget.3962

52. Barrett T, Troup DB, Wilhite SE, Ledoux P, Evangelista C, Kim IF, et al. NCBI GEO: archive for functional genomics data sets–10 years on. *Nucleic Acids Res* (2011) 39(Database issue):D1005–10. doi: 10.1093/nar/gkq1184

53. Bockelman C, Engelmann BE, Kaprio T, Hansen TF, Glimelius B. Risk of recurrence in patients with colon cancer stage II and III: a systematic review and meta-analysis of recent literature. *Acta Oncol* (2015) 54(1):5–16. doi: 10.3109/0284186X.2014.975839

54. Orme JJ, Du Y, Vanarsa K, Mayeux J, Li L, Mutwally A, et al. Heightened cleavage of axl receptor tyrosine kinase by ADAM metalloproteases may contribute to disease pathogenesis in SLE. *Clin Immunol* (2016) 169:58–68. doi: 10.1016/j.clim.2016.05.011

55. Miller MA, Oudin MJ, Sullivan RJ, Wang SJ, Meyer AS, Im H, et al. Reduced proteolytic shedding of receptor tyrosine kinases is a post-translational mechanism of kinase inhibitor resistance. *Cancer Discovery* (2016) 6(4):382–99. doi: 10.1158/2159-8290.CD-15-0933

56. Reichl P, Fang M, Starlinger P, Staufer K, Nenutil R, Muller P, et al. Multicenter analysis of soluble axl reveals diagnostic value for very early stage hepatocellular carcinoma. *Int J Cancer* (2015) 137(2):385–94. doi: 10.1002/ijc.29394

57. Martinez-Bosch N, Cristobal H, Iglesias M, Gironella M, Barranco L, Visa L, et al. Soluble AXL is a novel blood marker for early detection of pancreatic ductal adenocarcinoma and differential diagnosis from chronic pancreatitis. *EBioMedicine* (2022) 75:103797. doi: 10.1016/j.ebiom.2021.103797

58. Feitelson MA, Arzumanyan A, Kulathinal RJ, Blain SW, Holcombe RF, Mahajna J, et al. Sustained proliferation in cancer: mechanisms and novel therapeutic targets. *Semin Cancer Biol* (2015) 35 Suppl:S25–54. doi: 10.1016/j.semcancer.2015.02.006

59. Xu MZ, Chan SW, Liu AM, Wong KF, Fan ST, Chen J, et al. AXL receptor kinase is a mediator of YAP-dependent oncogenic functions in hepatocellular carcinoma. *Oncogene* (2011) 30(10):1229–40. doi: 10.1038/onc.2010.504

60. Li J, Jia L, Ma ZH, Ma QH, Yang XH, Zhao YF. Axl glycosylation mediates tumor cell proliferation, invasion and lymphatic metastasis in murine hepatocellular carcinoma. *World J Gastroenterol* (2012) 18(38):5369–76. doi: 10.3748/wjg.v18.i38.5369

61. Burbridge MF, Bossard CJ, Saunier C, Fejes I, Bruno A, Leonce S, et al. S49076 is a novel kinase inhibitor of MET, AXL, and FGFR with strong preclinical activity alone and in association with bevacizumab. *Mol Cancer Ther* (2013) 12(9):1749–62. doi: 10.1158/1535-7163.MCT-13-0075

62. Graham DK, DeRyckere D, Davies KD, Earp HS. The TAM family: phosphatidylserine sensing receptor tyrosine kinases gone awry in cancer. *Nat Rev Cancer* (2014) 14(12):769–85. doi: 10.1038/nrc3847

63. Li Y, Ye X, Tan C, Hongo JA, Zha J, Liu J, et al. Axl as a potential therapeutic target in cancer: role of axl in tumor growth, metastasis and angiogenesis. *Oncogene* (2009) 28(39):3442–55. doi: 10.1038/onc.2009.212

64. Hay ED. An overview of epithelio-mesenchymal transformation. *Acta Anat (Basel)* (1995) 154(1):8–20. doi: 10.1159/000147748

65. Babaei G, Aziz SG, Jaghi NZZ. EMT, cancer stem cells and autophagy; the three main axes of metastasis. *BioMed Pharmacother* (2021) 133:110909. doi: 10.1016/j.biopha.2020.110909

66. Gjerdrum C, Tiron C, Hoiby T, Stefansson I, Haugen H, Sandal T, et al. Axl is an essential epithelial-to-mesenchymal transition-induced regulator of breast cancer metastasis and patient survival. *Proc Natl Acad Sci USA* (2010) 107(3):1124–9. doi: 10.1073/pnas.0909333107

67. Nieto MA, Huang RY, Jackson RA, Thiery JP. Emt: 2016. *Cell* (2016) 166(1):21–45. doi: 10.1016/j.cell.2016.06.028

68. Ganesh K, Massague J. Targeting metastatic cancer. *Nat Med* (2021) 27(1):34–44. doi: 10.1038/s41591-020-01195-4

69. Niu Z-S, Niu X-J, Wang W-H. Role of the receptor tyrosine kinase axl in hepatocellular carcinoma and its clinical relevance. *Future Oncol* (2019) 15(6):653–62. doi: 10.2217/fon-2018-0528

70. Pinato DJ, Brown MW, Trousil S, Aboagye EO, Beaumont J, Zhang H, et al. Integrated analysis of multiple receptor tyrosine kinases identifies axl as a therapeutic

target and mediator of resistance to sorafenib in hepatocellular carcinoma. *Br J Cancer* (2019) 120(5):512–21. doi: 10.1038/s41416-018-0373-6

71. Chai ZT, Zhang XP, Ao JY, Zhu XD, Wu MC, Lau WY, et al. AXL overexpression in tumor-derived endothelial cells promotes vessel metastasis in patients with hepatocellular carcinoma. *Front Oncol* (2021) 11:650963. doi: 10.3389/fonc.2021.650963

72. Kirane A, Ludwig KF, Sorrelle N, Haaland G, Sandal T, Ranaweera R, et al. Warfarin blocks Gas6-mediated axl activation required for pancreatic cancer epithelial plasticity and metastasis. *Cancer Res* (2015) 75(18):3699–705. doi: 10.1158/0008-5472.CAN-14-2887-T

73. Ludwig KF, Du W, Sorrelle NB, Wnuk-Lipinska K, Topalovski M, Toombs JE, et al. Small-molecule inhibition of axl targets tumor immune suppression and enhances chemotherapy in pancreatic cancer. *Cancer Res* (2018) 78(1):246–55. doi: 10.1158/0008-5472.CAN-17-1973

74. Li J, Dai C, Shen L. Ursolic acid inhibits epithelial-mesenchymal transition through the Axl/NF-kappaB pathway in gastric cancer cells. *Evid Based Complement Alternat Med* (2019) 2019:2474805. doi: 10.1155/2019/2474805

75. Maacha S, Hong J, von Lersner A, Zijlstra A, Belkhiri A. AXL mediates esophageal adenocarcinoma cell invasion through regulation of extracellular acidification and lysosome trafficking. *Neoplasia* (2018) 20(10):1008–22. doi: 10.1016/j.neo.2018.08.005

76. Ciardiello D, Blauensteiner B, Matrone N, Belli V, Mohr T, Vitiello PP, et al. Dual inhibition of TGFbeta and AXL as a novel therapy for human colorectal adenocarcinoma with mesenchymal phenotype. *Med Oncol* (2021) 38(3):24. doi: 10.1007/s12032-021-01464-3

77. Van der Jeught K, Xu HC, Li YJ, Lu XB, Ji G. Drug resistance and new therapies in colorectal cancer. *World J Gastroenterol* (2018) 24(34):3834–48. doi: 10.3748/wjg.v24.i34.3834

78. Yang PW, Liu YC, Chang YH, Lin CC, Huang PM, Hua KT, et al. Cabozantinib (XL184) and R428 (BGB324) inhibit the growth of esophageal squamous cell carcinoma (ESCC). *Front Oncol* (2019) 9:1138. doi: 10.3389/fonc.2019.01138

79. Grepin R, Pages G. Molecular mechanisms of resistance to tumour anti-angiogenic strategies. *J Oncol 2010.* (2010) p:835680. doi: 10.1155/2010/835680

80. Owens GK. Molecular control of vascular smooth muscle cell differentiation and phenotypic plasticity. *Novartis Found Symp* (2007) 283:174–91; discussion 191-3, 238-41. doi: 10.1002/9780470319413.ch14

81. Fedeli C, Torriani G, Galan-Navarro C, Moraz ML, Moreno H, Gerold G, et al. Axl can serve as entry factor for lassa virus depending on the functional glycosylation of dystroglycan. *J Virol* (2018) 92(5). doi: 10.1128/JVI.01613-17

82. Ruan GX, Kazlauskas A. Axl is essential for VEGF-a-dependent activation of PI3K/Akt. *EMBO J* (2012) 31(7):1692–703. doi: 10.1038/emboj.2012.21

83. Bockerstett KA, DiPaolo RJ. Regulation of gastric carcinogenesis by inflammatory cytokines. *Cell Mol Gastroenterol Hepatol* (2017) 4(1):47–53. doi: 10.1016/j.jcmgh.2017.03.005

84. Zitvogel L, Kepp O, Kroemer G. Immune parameters affecting the efficacy of chemotherapeutic regimens. *Nat Rev Clin Oncol* (2011) 8(3):151–60. doi: 10.1038/nrclinonc.2010.223

85. Paolino M, Penninger JM. The role of TAM family receptors in immune cell function: implications for cancer therapy. *Cancers (Basel)* (2016) 8(10):97. doi: 10.3390/cancers8100097

86. Caraux A, Lu Q, Fernandez N, Riou S, Di Santo JP, Raulet DH, et al. Natural killer cell differentiation driven by Tyro3 receptor tyrosine kinases. *Nat Immunol* (2006) 7(7):747–54. doi: 10.1038/ni1353

87. Lu Q, Lemke G. Homeostatic regulation of the immune system by receptor tyrosine kinases of the tyro 3 family. *Science* (2001) 293(5528):306–11. doi: 10.1126/science.1061663

88. Valkenburg KC, de Groot AE, Pienta KJ. Targeting the tumour stroma to improve cancer therapy. *Nat Rev Clin Oncol* (2018) 15(6):366–81. doi: 10.1038/s41571-018-0007-1

89. Hochreiter-Hufford A, Ravichandran KS. Clearing the dead: apoptotic cell sensing, recognition, engulfment, and digestion. *Cold Spring Harb Perspect Biol* (2013) 5(1):a008748. doi: 10.1101/cshperspect.a008748

90. Kasikara C, Davra V, Calianese D, Geng K, Spires TE, Quigley M, et al. Pan-TAM tyrosine kinase inhibitor BMS-777607 enhances anti-PD-1 mAb efficacy in a murine model of triple-negative breast cancer. *Cancer Res* (2019) 79(10):2669–83. doi: 10.1158/0008-5472.CAN-18-2614

91. Kasikara C, Kumar S, Kimani S, Tsou WI, Geng K, Davra V, et al. Phosphatidylserine sensing by TAM receptors regulates AKT-dependent chemoresistance and PD-L1 expression. *Mol Cancer Res* (2017) 15(6):753–64. doi: 10.1158/1541-7786.MCR-16-0350

92. Myers KV, Amend SR, Pienta KJ. Targeting Tyro3, axl and MerTK (TAM receptors): implications for macrophages in the tumor microenvironment. *Mol Cancer* (2019) 18(1):94. doi: 10.1186/s12943-019-1022-2

93. Seitz HM, Camenisch TD, Lemke G, Earp HS, Matsushima GK. Macrophages and dendritic cells use different Axl/Mertk/Tyro3 receptors in clearance of apoptotic cells. *J Immunol* (2007) 178(9):5635–42. doi: 10.4049/jimmunol.178.9.5635

94. Bosurgi L, Bernink JH, Delgado Cuevas V, Gagliani N, Joannas L, Schmid ET, et al. Paradoxical role of the proto-oncogene axl and mer receptor tyrosine kinases in colon cancer. *Proc Natl Acad Sci USA* (2013) 110(32):13091–6. doi: 10.1073/pnas.1302507110

95. Sharif MN, Sosic D, Rothlin CV, Kelly E, Lemke G, Olson EN, et al. Twist mediates suppression of inflammation by type I IFNs and axl. *J Exp Med* (2006) 203 (8):1891–901. doi: 10.1084/jem.20051725

96. Alciato F, Sainaghi PP, Sola D, Castello L, Avanzi GC. TNF-alpha, IL-6, and IL-1 expression is inhibited by GAS6 in monocytes/macrophages. *J Leukoc Biol* (2010) 87 (5):869–75. doi: 10.1189/jlb.0909610

97. Kim SY, Lim EJ, Yoon YS, Ahn YH, Park EM, Kim HS, et al. Liver X receptor and STAT1 cooperate downstream of Gas6/Mer to induce anti-inflammatory arginase 2 expression in macrophages. *Sci Rep* (2016) 6:29673. doi: 10.1038/srep29673

98. Shen Y, Cui X, Rong Y, Zhang Z, Xiao L, Zhou T, et al. Exogenous Gas6 attenuates silica-induced inflammation on differentiated THP-1 macrophages. *Environ Toxicol Pharmacol* (2016) 45:222–6. doi: 10.1016/j.etap.2016.05.029

99. Du W, Huang H, Sorrelle N, Brekken RA. Sitravatinib potentiates immune checkpoint blockade in refractory cancer models. *JCI Insight* (2018) 3(21):e124184. doi: 10.1172/jci.insight.124184

100. Engelman JA, Settleman J. Acquired resistance to tyrosine kinase inhibitors during cancer therapy. *Curr Opin Genet Dev* (2008) 18(1):73–9. doi: 10.1016/j.gde.2008.01.004

101. D'Errico G, Alonso-Nocelo M, Vallespinos M, Hermann PC, Alcala S, Garcia CP, et al. Tumor-associated macrophage-secreted 14-3-3zeta signals *via* AXL to promote pancreatic cancer chemoresistance. *Oncogene* (2019) 38(27):5469–85. doi: 10.1038/s41388-019-0803-9

102. Park K, Chang GC, Curigliano G, Lim WT, Soo RA, Molina-Vila MA, et al. Phase I results of S49076 plus gefitinib in patients with EGFR TKI-resistant non-small cell lung cancer harbouring MET/AXL dysregulation. *Lung Cancer* (2021) 155:127–35. doi: 10.1016/j.lungcan.2021.03.012

103. Zhang Z, Lee JC, Lin L, Olivas V, Au V, LaFramboise T, et al. Activation of the AXL kinase causes resistance to EGFR-targeted therapy in lung cancer. *Nat Genet* (2012) 44(8):852–60. doi: 10.1038/ng.2330

104. Verma A, Warner SL, Vankayalapati H, Bearss DJ, Sharma S. Targeting axl and mer kinases in cancer. *Mol Cancer Ther* (2011) 10(10):1763–73. doi: 10.1158/1535-7163.MCT-11-0116

105. Elkabets M, Pazarentzos E, Juric D, Sheng Q, Pelossof RA, Brook S, et al. AXL mediates resistance to PI3Kalpha inhibition by activating the EGFR/PKC/mTOR axis in head and neck and esophageal squamous cell carcinomas. *Cancer Cell* (2015) 27 (4):533–46. doi: 10.1016/j.ccell.2015.03.010

106. Yoshioka T, Shien K, Takeda T, Takahashi Y, Kurihara E, Ogoshi Y, et al. Acquired resistance mechanisms to afatinib in HER2-amplified gastric cancer cells. *Cancer Sci* (2019) 110(8):2549–57. doi: 10.1111/cas.14089

107. Mahadevan D, Cooke L, Riley C, Swart R, Simons B, Della Croce K, et al. A novel tyrosine kinase switch is a mechanism of imatinib resistance in gastrointestinal stromal tumors. *Oncogene* (2007) 26(27):3909–19. doi: 10.1038/sj.onc.1210173

108. Kim JE, Kim Y, Li G, Kim ST, Kim K, Park SH, et al. MerTK inhibition by RXDX-106 in MerTK activated gastric cancer cell lines. *Oncotarget* (2017) 8 (62):105727–34. doi: 10.18632/oncotarget.22394

109. Fuh KC, Bookman MA, Liu JF, Coleman RL, Herzog TJ, Thaker PH, et al. Phase 1b study of AVB-500 in combination with paclitaxel or pegylated liposomal doxorubicin platinum-resistant recurrent ovarian cancer. *Gynecol Oncol* (2021) 163 (2):254–61. doi: 10.1016/j.ygyno.2021.08.020

110. Rankin EB, Giaccia AJ. The receptor tyrosine kinase AXL in cancer progression. *Cancers (Basel)* (2016) 8(11):103. doi: 10.3390/cancers8110103

111. Xiao Y, Zhao H, Tian L, Nolley R, Diep AN, Ernst A, et al. S100A10 is a critical mediator of GAS6/AXL-induced angiogenesis in renal cell carcinoma. *Cancer Res* (2019) 79(22):5758–68. doi: 10.1158/0008-5472.CAN-19-1366

112. Mullen MM, Lomonosova E, Toboni MD, Oplt A, Cybulla E, Blachut B, et al. GAS6/AXL inhibition enhances ovarian cancer sensitivity to chemotherapy and PARP inhibition through increased DNA damage and enhanced replication stress. *Mol Cancer Res* (2022) 20(2):265–79.. doi: 10.1158/1541-7786.MCR-21-0302

113. Tanaka M, Siemann DW. Therapeutic targeting of the Gas6/Axl signaling pathway in cancer. *Int J Mol Sci* (2021) 22(18):9953. doi: 10.3390/ijms22189953

114. Wang DD, Chen Y, Chen ZB, Yan FJ, Dai XY, Ying MD, et al. CT-707, a novel FAK inhibitor, synergizes with cabozantinib to suppress hepatocellular carcinoma by blocking cabozantinib-induced FAK activation. *Mol Cancer Ther* (2016) 15(12):2916–25. doi: 10.1158/1535-7163.MCT-16-0282

115. Xiang QF, Zhang DM, Wang JN, Zhang HW, Zheng ZY, Yu DC, et al. Cabozantinib reverses multidrug resistance of human hepatoma HepG2/adr cells by modulating the function of p-glycoprotein. *Liver Int* (2015) 35(3):1010–23. doi: 10.1111/liv.12524

116. Abou-Alfa GK, Meyer T, Cheng AL, El-Khoueiry AB, Rimassa L, Ryoo BY, et al. Cabozantinib in patients with advanced and progressing hepatocellular carcinoma. *N Engl J Med* (2018) 379(1):54–63. doi: 10.1056/NEJMoa1717002

117. Lew ED, Oh J, Burrola PG, Lax I, Zagorska A, Traves PG, et al. Differential TAM receptor-ligand-phospholipid interactions delimit differential TAM bioactivities. *Elife* (2014) 3:9953. doi: 10.7554/eLife.03385

118. Dolan M, Mastri M, Tracz A, Christensen JG, Chatta G, Ebos JML. Enhanced efficacy of sitravatinib in metastatic models of antiangiogenic therapy resistance. *PloS One* (2019) 14(8):e0220101. doi: 10.1371/journal.pone.0220101

119. Patwardhan PP, Ivy KS, Musi E, de Stanchina E, Schwartz GK. Significant blockade of multiple receptor tyrosine kinases by MGCD516 (Sitravatinib), a novel small molecule inhibitor, shows potent anti-tumor activity in preclinical models of sarcoma. *Oncotarget* (2016) 7(4):4093–109. doi: 10.18632/oncotarget.6547

120. Zhang P, Li S, Lv C, Si J, Xiong Y, Ding L, et al. BPI-9016M, a c-met inhibitor, suppresses tumor cell growth, migration and invasion of lung adenocarcinoma *via* miR203-DKK1. *Theranostics* (2018) 8(21):5890–902. doi: 10.7150/thno.27667

121. Hu X, Zheng X, Yang S, Wang L, Hao X, Cui X, et al. First-in-human phase I study of BPI-9016M, a dual MET/Axl inhibitor, in patients with non-small cell lung cancer. *J Hematol Oncol* (2020) 13(1):6. doi: 10.1186/s13045-019-0834-2

122. Zou HY, Li Q, Lee JH, Arango ME, McDonnell SR, Yamazaki S, et al. An orally available small-molecule inhibitor of c-met, PF-2341066, exhibits cytoreductive antitumor efficacy through antiproliferative and antiangiogenic mechanisms. *Cancer Res* (2007) 67(9):4408–17. doi: 10.1158/0008-5472.CAN-06-4443

123. Lev A, Deihimi S, Shagisultanova E, Xiu J, Lulla AR, Dicker DT, et al. Preclinical rationale for combination of crizotinib with mitomycin c for the treatment of advanced colorectal cancer. *Cancer Biol Ther* (2017) 18(9):694–704. doi: 10.1080/15384047.2017.1364323

124. June CH, O'Connor RS, Kawalekar OU, Ghassemi S, Milone MC. CAR T cell immunotherapy for human cancer. *Science* (2018) 359(6382):1361–5. doi: 10.1126/science.aar6711

125. Yang X, Wang GX, Zhou JF. CAR T cell therapy for hematological malignancies. *Curr Med Sci* (2019) 39(6):874–82. doi: 10.1007/s11596-019-2118-z

126. Bagley SJ, O'Rourke DM. Clinical investigation of CAR T cells for solid tumors: lessons learned and future directions. *Pharmacol Ther* (2020) 205:107419. doi: 10.1016/j.pharmthera.2019.107419

127. Dees S, Ganesan R, Singh S, Grewal IS. Emerging CAR-T cell therapy for the treatment of triple-negative breast cancer. *Mol Cancer Ther* (2020) 19(12):2409–21. doi: 10.1158/1535-7163.MCT-20-0385

128. Wei J, Sun H, Zhang A, Wu X, Li Y, Liu J, et al. A novel AXL chimeric antigen receptor endows T cells with anti-tumor effects against triple negative breast cancers. *Cell Immunol* (2018) 331:49–58. doi: 10.1016/j.cellimm.2018.05.004

129. Khalaf N, El-Serag HB, Abrams HR, Thrift AP. Burden of pancreatic cancer: from epidemiology to practice. *Clin Gastroenterol Hepatol* (2021) 19(5):876–84. doi: 10.1016/j.cgh.2020.02.054

130. Maitra A, Hruban RH. Pancreatic cancer. *Annu Rev Pathol* (2008) 3:157–88. doi: 10.1146/annurev.pathmechdis.3.121806.154305

Frontiers in Oncology

Advances knowledge of carcinogenesis and tumor progression for better treatment and management

The third most-cited oncology journal, which highlights research in carcinogenesis and tumor progression, bridging the gap between basic research and applications to imrpove diagnosis, therapeutics and management strategies.

Discover the latest Research Topics

See more →

Frontiers

Avenue du Tribunal-Fédéral 34
1005 Lausanne, Switzerland
frontiersin.org

Contact us

+41 (0)21 510 17 00
frontiersin.org/about/contact